

# ***THE RIDE COMFORT VS. HANDLING COMPROMISE FOR OFF-ROAD VEHICLES***

by

**PIETER SCHALK ELS**

Submitted in partial fulfilment of the requirements for the degree

**Philosophiae Doctor (Mechanical Engineering)**

in the

FACULTY OF ENGINEERING, THE BUILT ENVIRONMENT AND INFORMATION  
TECHNOLOGY (EBIT)

UNIVERSITY OF PRETORIA  
Pretoria

July 2006

## THESIS SUMMARY

**Title:** The Ride Comfort *vs.* Handling Compromise for Off-Road Vehicles

**Author:** PIETER SCHALK ELS

**Supervisor:** Prof. N.J. Theron

**Department:** Mechanical and Aeronautical Engineering, University of Pretoria

**Degree:** Philosophiae Doctor (Mechanical Engineering)

This thesis examines the classic ride comfort *vs.* handling compromise when designing a vehicle suspension system. A controllable suspension system, that can, through the use of suitable control algorithms, eliminate this compromise, is proposed and implemented.

It is a well known fact that if a vehicle suspension system is designed for best ride comfort, then handling performance will suffer and vice versa. This is especially true for the class of vehicle that need to perform well both on- and off-road such as Sports Utility Vehicles (SUV's) and wheeled military vehicles. These vehicles form the focus of this investigation.

The ride comfort and handling of a Land Rover Defender 110 Sports Utility Vehicle is investigated using mathematical modelling and field tests. The full vehicle, non-linear mathematical model, built in MSC ADAMS software, is verified against test data, with favourable correlation between modelled and measured results. The model is subsequently modified to incorporate hydropneumatic springs and used to obtain optimised spring and damper characteristics for ride comfort and handling respectively. Ride comfort is optimised by minimising vertical acceleration when driving in a straight line over a rough, off-road terrain profile. Handling is optimised by minimising the body roll angle through a double lane change manoeuvre. It is found that these optimised results are at opposite corners of the design space, *i.e.* ride comfort requires a soft suspension while handling requires a stiff suspension. It is shown that the ride comfort *vs.* handling compromise can only be eliminated by having an active suspension system, or a controllable suspension system that can switch between a soft and a stiff spring, as well as low and high damping. This switching must occur rapidly and automatically without driver intervention.

A prototype **4 State Semi-active Suspension System (4S<sub>4</sub>)** is designed, manufactured, tested and modelled mathematically. This system enables switching between low and high damping, as well as between soft and stiff springs in less than 100 milliseconds.

A control strategy to switch the suspension system between the “ride” mode and the “handling” mode is proposed, implemented on a test vehicle and evaluated during vehicle tests over various on- and off-road terrains and for various handling manoeuvres. The control strategy is found to be simple and cost effective to implement and works extremely well. Improvements of the order of 50% can be achieved for both ride comfort and handling.

## SAMEVATTING VAN PROEFSKRIF

- Titel:** Die Ritgemak vs. Hantering Kompromie vir Veldvoertuie
- Outeur:** PIETER SCHALK ELS
- Studieleier:** Prof. N.J. Theron
- Departement:** Meganiese en Lugvaartkundige Ingenieurswese  
Universiteit van Pretoria
- Graad:** PhD in Ingenieurswese (Meganiese Ingenieurswese)

In hierdie proefskrif word die klassieke kompromie wat getref moet word tussen ritgemak en hantering, tydens die ontwerp van 'n voertuig suspensiestelsel ondersoek. 'n Beheerbare suspensiestelsel, wat die kompromie kan elimineer deur gebruik te maak van toepaslike beheeralgoritmes, word voorgestel en geïmplementeer.

Dit is 'n bekende feit dat, wanneer die karakteristieke van 'n voertuigsuspensiestelsel ontwerp word vir die beste moontlike ritgemak, die hantering nie na wense is nie, en ook omgekeerd. Dit is veral waar vir 'n spesifieke kategorie van voertuie, soos veldvoertuie en militêre wielvoertuie, wat oor goeie ritgemak en hantering, beide op paaie en in die veld, moet beskik. Die fokus van die huidige studie val op hierdie kategorie voertuie.

Die ritgemak en hantering van 'n Land Rover Defender 110 veldvoertuig is ondersoek deur gebruik te maak van wiskundige modellering en veldtoetse. Die volvoertuig, nie-linéêre wiskundige model, soos ontwikkel met behulp van MSC ADAMS sagteware, is geverifieer teen eksperimentele data en goeie korrelasie is verkry. Die model is verander ten einde 'n hidropneumatiese veer-en-demperstelsel te inkorporeer en verder gebruik om optimale veer- en demperkarakteristieke vir onderskeidelik ritgemak en hantering te verkry. Ritgemak is geoptimeer deur in 'n reguit lyn oor 'n rowwe veldterreinprofiel te ry, terwyl hantering geoptimeer is deur 'n dubbelbaanveranderingsmaneuver uit te voer. Die resultaat is dat die geoptimeerde karakteristieke op die twee uiterstes van die ontwerpgebied lê. Beste ritgemak benodig 'n sagte suspensie terwyl beste hantering 'n harde suspensie benodig. Daar word aangedui dat die ritgemak vs. hantering kompromie slegs elimineer kan word deur gebruik van 'n aktiewe suspensiestelsel, of 'n beheerbare suspensiestelsel wat kan skakel tussen 'n sagte en stywe veer, asook hoë en lae demping. Dié oorskakeling moet vinnig en outomaties geskied sonder enige ingryping van die voertuigbestuurder.

'n Prototipe 4 Stadium Semi-aktiewe Suspensie Stelsel (4S<sub>4</sub>) is ontwerp, vervaardig, getoets en wiskundig gemodelleer. Die stelsel skakel tussen hoë en lae demping, asook tussen 'n stywe en sagte veer binne 100 millisekondes.

'n Beheerstrategie wat die suspensiestelsel skakel tussen die "ritgemak" en "hantering" modes is voorgestel, op 'n toetsvoertuig geïmplementeer en evalueer tydens voertuigtoetse oor verskeie pad- en veldry toestande, asook tydens omrol- en hanteringstoetse. Die beheerstrategie is koste-effektief en maklik om te implementeer en werk besonder goed. Verbeterings in die orde van 50% kan behaal word vir beide ritgemak en hantering.

---

---

## ***ACKNOWLEDGEMENTS***

---

---

The research has been made possible through the generous support and sponsorship of the U.S. Government through its European Research Office of the U.S. Army under Contracts N68171-01-M-5852, N62558-02-M-6372 and N62558-04-P-6004.

Optimisation related investigations were performed under the auspices of the Multi-disciplinary Design Optimisation Group (MDOG) of the Department of Mechanical and Aeronautical Engineering at the University of Pretoria.

A special word of thanks to the following people who contributed in various ways to the project:

- Dr. F.B. Hoogterp and Mr. Bill Mackie, US Army Tank Automotive Command (TACOM)
- Dr. Sam Sampath – European Research Office of the US Army
- Prof. N.J. Theron and Dr. Petro Uys (University of Pretoria)
- Mr. Michael Thoresson, Mr. Werner Misselhorn, Mr. Karl Voigt, Mr. R. Bester and Mr. B.P. Uys (My dedicated post-graduate students)
- Mr Gareth Thomas from Ford Motor Company (Land Rover) South Africa
- My parents without whose continual support and motivation this project would not have been possible

Soli Deo Gloria

---



---

## **TABLE OF CONTENTS**

---

Thesis summary	ii
Samevatting van proefskrif	iii
<b>ACKNOWLEDGEMENTS</b>	<b>iv</b>
<b>LIST OF SYMBOLS</b>	<b>x</b>
<b>LIST OF ABBREVIATIONS</b>	<b>xiii</b>
<b>LIST OF FIGURES</b>	<b>xviii</b>
<b>LIST OF TABLES</b>	<b>xxvii</b>
<b>1. INTRODUCTION</b>	<b>1.1</b>
1.1 Vehicle models	1.2
1.2 Controllable suspension system classification	1.3
1.3 Semi-active springs	1.6
1.4 Current applications of controllable suspension systems	1.7
1.5 Global viewpoints	1.8
1.6 Problem statement	1.11
<b>2. THE RIDE COMFORT VS. HANDLING COMPROMISE</b>	<b>2.1</b>
2.1 Literature	2.1
2.1.1 Ride comfort	2.1
2.1.2 Handling, rollover and stability	2.3
2.1.2.1 Literature survey on handling, rollover and stability	2.5
2.1.2.2 Handling tests	2.11
2.1.2.3 Experimental investigation of handling	2.11
2.1.2.4 Results of experimental investigation	2.12
2.1.2.5 Conclusion from the handling investigation	2.15
2.1.3 Ride comfort vs. handling	2.16

2.2	Case Study 1: Landmine protected vehicle	2.18
2.2.1	Vehicle model	2.19
2.2.2	Terrain inputs	2.19
2.2.3	Results	2.20
2.2.4	Conclusions from Case Study 1	2.25
2.3	Case Study 2: Land Rover Defender 110	2.25
2.3.1	Vehicle model	2.25
2.3.2	Definition of “design space”	2.26
2.3.3	Simulation results	2.27
2.3.3.1	Ride comfort	2.27
2.3.3.2	Handling	2.28
2.3.3.3	Combined ride comfort and handling	2.28
2.3.4	Conclusion from Case Study 2	2.28
2.3.5	Follow-up work by Uys, Els and Thoresson	2.30
2.4	Validated vehicle model	2.32
2.4.1	Geometric parameters	2.32
2.4.2	Mass properties	2.32
2.4.3	Spring and damper characteristics	2.32
2.4.4	Tyre characteristics	2.32
2.4.5	ADAMS full vehicle model	2.32
2.4.6	Baseline vehicle tests	2.33
2.4.6.1	Instrumentation	2.35
2.4.6.2	Tests	2.35
2.4.7	Correlation between ADAMS model and test results	2.37
2.4.7.1	Transient response (APG track)	2.37
2.4.7.2	Handling (ISO 3888 double lane change)	2.37
2.4.8	Simulation results	2.41
2.5	Conclusion	2.42
<b>3.</b>	<b>POSSIBLE SOLUTIONS TO THE RIDE COMFORT VS. HANDLING COMPROMISE</b>	<b>3.1</b>
3.1	Published literature surveys on controllable suspension systems	3.1
3.2	Controllable suspension system hardware	3.2
3.2.1	Semi-active dampers	3.2
3.2.1.1	Magneto-Rheological (MR) fluids	3.2
3.2.1.2	Hydraulic bypass system	3.3
3.2.2	Semi-active springs	3.6
3.2.2.1	Air springs	3.6
3.2.2.2	Hydropneumatic springs	3.7
3.2.2.3	Other semi-active spring concepts	3.8
3.2.3	Active suspension systems	3.9
3.2.3.1	Electric actuators	3.9
3.2.3.2	Hydraulic actuators	3.9

3.3	Control techniques and algorithms	3.10
3.3.1	Combination of input and reaction driven strategies	3.10
3.3.2	Linear optimal, skyhook and on-off control	3.12
3.3.3	Neural networks and Fuzzy logic	3.16
3.3.4	$H_{\infty}$ control	3.16
3.3.5	Proportional Derivative (PD) control	3.16
3.3.6	Preview control	3.16
3.3.7	Model following	3.17
3.3.8	Frequency domain analysis	3.17
3.3.9	“Relative” control	3.18
3.3.10	Traditional controller design on the s-plane	3.18
3.3.11	Minimum product (MP) strategy	3.18
3.3.12	Roll and pitch velocity	3.19
3.3.13	Resistance control	3.19
3.3.14	Mechanical control	3.19
3.3.15	Steepest gradient method	3.19
3.3.16	Use of estimators and observers	3.19
3.3.17	Control of handling	3.19
3.3.18	Control of rollover	3.20
3.3.19	Ride height adjustment	3.20
3.3.20	Comparison of semi-active control strategies for ride comfort improvement	3.20
3.4	Conclusion	3.21
3.5	Proposed solutions to the ride comfort <i>vs.</i> handling compromise	3.23
<b>4.</b>	<b>THE FOUR-STATE SEMI-ACTIVE SUSPENSION SYSTEM (4S<sub>4</sub>)</b>	<b>4.1</b>
4.1	Literature	4.1
4.1.1	Hydropneumatic springs	4.1
4.1.2	Variable spring concepts	4.2
4.1.3	Hydraulic semi-active dampers	4.2
4.2	4S <sub>4</sub> Working principle	4.2
4.3	Design requirements	4.4
4.4	Space envelope	4.6
4.5	Detail design of 4S <sub>4</sub>	4.6
4.6	Manufacturing of 4S <sub>4</sub> prototypes	4.9
4.7	Testing and characterisation of the 4S <sub>4</sub>	4.9
4.7.1	Gas charging procedure	4.15
4.7.2	Bulk modulus	4.21
4.7.3	Thermal time constant	4.22
4.7.4	Spring characteristics	4.24

4.7.5	Damping characteristics	4.25
4.7.6	Valve response times	4.30
4.7.7	Friction	4.30
4.8	Mathematical model	4.33
4.8.1	Modelling philosophy	4.33
4.8.2	Pressure dependent valve switching	4.36
4.8.3	Pressure drop over dampers and valves	4.37
4.8.4	Flow and pressure calculation	4.37
4.8.5	Implementation in SIMULINK®	4.40
4.8.6	Validation of the mathematical model	4.40
4.9	Conclusion	4.54
<b>5.</b>	<b>THE RIDE COMFORT VS. HANDLING DECISION</b>	<b>5.1</b>
5.1	Literature	5.1
5.2	Suggested concepts for making the “ride comfort vs. handling decision”	5.11
5.3	Easily measurable parameters	5.11
5.4	Experimental work on baseline vehicle	5.12
5.5	Evaluation of concepts	5.13
5.5.1	Frequency domain analysis	5.16
5.5.2	Lateral vs. vertical acceleration	5.16
5.5.3	Lateral vs. vertical acceleration - modified	5.22
5.5.4	Steering angle vs. speed	5.22
5.5.5	Disadvantages of proposed concepts	5.24
5.6	Novel strategies proposed	5.28
5.6.1	“Relative roll angle” calculated from suspension deflection	5.28
5.6.2	Running RMS vertical acceleration vs. lateral acceleration	5.28
5.7	Conclusion	5.35
<b>6.</b>	<b>VEHICLE IMPLEMENTATION</b>	<b>6.1</b>
6.1	Installation of 4S <sub>4</sub> hardware on test vehicle	6.1
6.2	Control electronics	6.6
6.3	Steady state handling	6.8
6.4	Dynamic handling	6.12



6.5	Ride comfort	6.18
6.6	Mountain pass driving	6.21
6.7	City and highway driving	6.21
6.8	Conclusions	6.21
<b>7.</b>	<b>CONCLUSIONS AND RECOMMENDATIONS</b>	<b>7.1</b>
7.1	Conclusions	7.1
7.1.1	The ride comfort <i>vs.</i> handling compromise	7.2
7.1.2	Possible solutions to the ride comfort <i>vs.</i> handling compromise	7.3
7.1.3	The four-state semi-active suspension system (4S <sub>4</sub> )	7.3
7.1.4	The ride comfort <i>vs.</i> handling decision	7.3
7.1.5	Vehicle implementation	7.4
7.1.6	Final comments	7.4
7.2.	Recommendations	7.4
7.2.1	The ride comfort <i>vs.</i> handling compromise	7.4
7.2.2	Possible solutions to the ride comfort <i>vs.</i> handling compromise	7.5
7.2.3	The four-state semi-active suspension system (4S <sub>4</sub> )	7.5
7.2.4	The ride comfort <i>vs.</i> handling decision	7.5
7.2.5	Vehicle implementation	7.6
7.2.6	Additional possibilities	7.6
	<b>BIBLIOGRAPHY / REFERENCES</b>	<b>BR.1</b>
	<b>APPENDIX A: HANDLING CRITERIA</b>	<b>A.1</b>

---



---

## ***LIST OF SYMBOLS***

---

### **ENGLISH SYMBOLS:**

$A$	Area [ $m^2$ ]
$a_y$	Lateral acceleration [ $m/s^2$ ]
$c_v$	Specific heat at constant volume [ $J/kg.K$ ]
$C$	Damping coefficient [ $Ns/m$ ]
$C_{\alpha f}$	Cornering stiffness of front tyres [ $N/^\circ$ ]
$C_{\alpha r}$	Cornering stiffness of rear tyres [ $N/^\circ$ ]
$f$	Fraction
$f_n$	Natural frequency [Hz]
$g$	Gravitational constant = 9.81 [ $m/s^2$ ]
$h_1$	Distance from centre of gravity to roll axis [m]
$i$	Index for accumulator or valve to be used ( <i>e.g.</i> $i=1$ : small accumulator, $i=2$ : large accumulator)
$k_s$	Spring stiffness [ $N/m$ ]
$k_t$	Tyre stiffness [ $N/m$ ]
$K_{\phi f}$	Front suspension roll stiffness [ $N/rad$ ]
$K_{\phi r}$	Rear suspension roll stiffness [ $N/rad$ ]
$l_f$	Horizontal distance from front axle to centre of gravity [m]
$l_r$	Horizontal distance from rear axle to centre of gravity [m]
$M$	Sprung mass [kg]

$m$	Unsprung mass or mass of gas [kg]
$P$	Pressure [Pa]
$P_{\text{accui}}$	Pressure in accumulator $i$ [Pa]
$P_{\text{begin}}$	Pressure before valve opens [MPa]
$P_{\text{end}}$	Pressure after valve is fully open [MPa]
$p$	Steering Factor
$P_1$	Pressure in small accumulator [Pa]
$P_2$	Main strut pressure [Pa]
$P_3$	Pressure between valve 2 and valves 3 and 4 [Pa]
$P_4$	Pressure in large accumulator [Pa]
$q$	Flow rate [ $\text{m}^3/\text{s}$ ]
$R$	Universal gas constant [J/kg.K]
$T$	Temperature [K]
$V$	Volt [V]
$V$	Volume [ $\text{m}^3$ ]
$V_1$	Valve 1 – damper bypass valve on small accumulator
$V_2$	Valve 2 – damper bypass valve on large accumulator
$V_3$	Valve 3 – Spring valve
$V_4$	Valve 4 – Spring valve
$v$	Specific volume [ $\text{m}^3/\text{kg}$ ]
$W$	Vehicle weight [N]
$W_b$	British Standard BS 6841 vertical acceleration filter
$W_f$	British Standard BS 6841 motion sickness filter
$x$	Relative suspension displacement [m]
$\dot{x}$	Relative suspension velocity [m/s]
$Y_e$	Lateral position error [m]

**GREEK SYMBOLS:**

$\varphi$	Roll angle [rad]
$\beta$	Bulk modulus of fluid [Pa]
$\Delta$	Difference
$\tau$	Thermal time constant [s]
$\omega$	Circular frequency [rad/s]

---

---

## ***LIST OF ABBREVIATIONS***

---

---

### **A**

AAP	Average Absorbed Power
ABC	Active Body Control (Mercedes Benz)
ABS	Antilock Braking System
ADAMS	Automatic Dynamic Analysis of Mechanical Systems (Computer software)
ADC	Adaptive Damping Control
ADD	Acceleration Driven Damper
APG	Aberdeen Proving Ground
ARC	Active Roll Control
AWD	All Wheel Drive

### **B**

BS	British Standard
BWR	Benedict-Webb-Rubin

### **C**

CATS	Computer Active Technology Suspension (Jaguar)
CAN	Controller Area Network
cg	Centre of gravity
CDC	Continuous Damping Control (Opel)

CUV	Crossover Utility Vehicle
CVRSS	Continuously Variable Road Sensing Suspension (Cadillac)

## **D**

DADS	Dynamic Analysis and Design System (Computer software)
DC	Direct Current
DFT	Discrete Fourier Transform
DHS	Dynamic Handling System
DIO	Digital Input Output
DRC	Dynamic Ride Control (Audi)
DSP	Digital Signal Processor
DWT	Draw Wire Transducer

## **E**

EAS	Electronic Air Suspension (Volkswagen / Continental)
ECS	Electronic Controlled Suspension (Mitsubishi)
ER	Electro-Rheological
ERM	Electro-Rheological Magnetic

## **F**

FFT	Fast Fourier Transform
Four-C	Continuously Controllable Chassis Concept (Volvo)

## **G**

GA	Genetic Algorithm
GM	General Motors
GPS	Global Positioning System

## H

HiL	Hardware-in-the-loop
HMMWV	High Mobility Multi-purpose Wheeled Vehicle
HP	Horse Power
HVOF	High Velocity Oxygen Fuel

## I

ICS	In Cylinder Sensor
ISO	International Standards Organization

## L

LDV	Light Delivery Vehicle
LQO	Linear Quadratic Optimal
LVDT	Linear Variable Differential Transformer

## M

MISO	Multiple Input Single Output
MM	Mini Module
MP	Minimum Product
MR	Magneto-Rheological
MTTB	Mobility Technology Test Bed

## N

N	Number of points
NAND	Inverted AND gate
NATO	North Atlantic Treaty Organisation
NHTSA	National Highway Traffic Safety Administration (USA)

NRMM NATO Reference Mobility Model

## **P**

PC Personal Computer

PD Proportional Derivative

PID Proportional Integral Derivative

PSD Power Spectral Density

## **R**

ReS Control strategy proposed by Rakheja and Sankar

RMS Root Mean Square

RRMS Running Root Mean Square

## **S**

SSF Static Stability Factor

SSRT Steady State Rollover Threshold

SUV Sports Utility Vehicle

SVFB State Variable FeedBack

## **T**

TACOM Tank-automotive and Armaments Command of the US Army

TARDEC Tank-Automotive Research, Development and Engineering Center of the US Army

TRW Automotive Component Manufacturer

## **U**

USB Universal Serial Bus



**V**

VDI Verein Deutscher Ingenieure (Association of German Engineers)

VDV Vibration Dose Value

VW Volkswagen

**Z**

ZF German component manufacturer

**Other**

4S<sub>4</sub> 4 State Semi-active Suspension System

2WS Two wheel steer

4WS Four wheel steer

---



---

## ***LIST OF FIGURES***

---

### **CHAPTER 1 – INTRODUCTION**

<b>Figure 1.1</b>	- ¼ Car suspension system	1.2
<b>Figure 1.2</b>	- Flow diagram of present study	1.13

### **CHAPTER 2 – THE RIDE COMFORT VS. HANDLING COMPROMISE**

<b>Figure 2.1</b>	- Test vehicle	2.2
<b>Figure 2.2</b>	- Handling classification according to Harty (2005)	2.4
<b>Figure 2.3</b>	- Ride and Handling track	2.13
<b>Figure 2.4</b>	- Dynamic handling track – light vehicles	2.14
<b>Figure 2.5</b>	- Suspension design space according to Holdman and Holle (1999)	2.17
<b>Figure 2.6</b>	- Photograph of vehicle used in simulation	2.19
<b>Figure 2.7</b>	- Improvement in weighted RMS vertical acceleration (ride comfort – linear spring)	2.22
<b>Figure 2.8</b>	- Improvement in pitch velocity (linear spring)	2.23
<b>Figure 2.9</b>	- Improvement in roll angle (linear spring)	2.23
<b>Figure 2.10</b>	- Improvement in roll velocity (linear spring)	2.24
<b>Figure 2.11</b>	- Land Rover Defender 110 vehicle	2.26
<b>Figure 2.12</b>	- Results of ride comfort analysis	2.29
<b>Figure 2.13</b>	- Results of handling analysis	2.29

<b>Figure 2.14</b>	- Combined ride comfort and handling	2.30
<b>Figure 2.15</b>	- Path followed by Dynamic-Q	2.31
<b>Figure 2.16</b>	- Tyre side-force <i>vs.</i> slip angle characteristic	2.33
<b>Figure 2.17</b>	- Front suspension layout	2.34
<b>Figure 2.18</b>	- Front suspension schematic	2.34
<b>Figure 2.19</b>	- Rear suspension layout	2.36
<b>Figure 2.20</b>	- Rear suspension schematic	2.36
<b>Figure 2.21</b>	- Belgian paving	2.37
<b>Figure 2.22</b>	- “APG” Bump	2.38
<b>Figure 2.23</b>	- Constant radius test	2.38
<b>Figure 2.24</b>	- Severe double lane change manoeuvre	2.39
<b>Figure 2.25</b>	- Rough track	2.39
<b>Figure 2.26</b>	- Rough track	2.40
<b>Figure 2.27</b>	- Model validation results for passing over 100 mm APG bump at 25 km/h	2.41
<b>Figure 2.28</b>	- Model validation results for a double lane change manoeuvre at 65 km/h	2.42
<b>Figure 2.29</b>	- Ride comfort <i>vs.</i> gas volume and damping	2.43
<b>Figure 2.30</b>	- Definition of handling objective function	2.43
<b>Figure 2.31</b>	- Roll angle <i>vs.</i> gas volume and damping	2.44
<b>Figure 2.32</b>	- Roll velocity <i>vs.</i> gas volume and damping	2.44

### **CHAPTER 3 – POSSIBLE SOLUTIONS TO THE RIDE COMFORT *VS.* HANDLING COMPROMISE**

<b>Figure 3.1</b>	- Hydraulic two-state semi-active damper with bypass valve	3.3
<b>Figure 3.2</b>	- Semi-active damper developed by Nell (1993)	3.4
<b>Figure 3.3</b>	- Semi-active rotary damper developed by Els and Holman (1999)	3.5
<b>Figure 3.4</b>	- Operator controlled variable spring as proposed by Eberle and Steele (1975)	3.8

## CHAPTER 4 – THE FOUR-STATE SEMI-ACTIVE SUSPENSION SYSTEM (4S<sub>4</sub>)

<b>Figure 4.1</b>	- 4S <sub>4</sub> circuit diagram	4.3
<b>Figure 4.2</b>	- Relative suspension velocity over Gerotek Rough track	4.5
<b>Figure 4.3</b>	- Pressure drop vs. flow rate for SV10-24 valve (Anon, 1998)	4.7
<b>Figure 4.4</b>	- Operating range for SV10-24 valve (Anon, 1998)	4.7
<b>Figure 4.5</b>	- Baseline left front suspension layout	4.8
<b>Figure 4.6</b>	- Baseline left rear suspension layout	4.8
<b>Figure 4.7</b>	- 4S <sub>4</sub> Suspension schematic diagram	4.10
<b>Figure 4.8</b>	- 4S <sub>4</sub> suspension system – exterior view	4.11
<b>Figure 4.9</b>	- 4S <sub>4</sub> suspension system – cross sectional view	4.12
<b>Figure 4.10</b>	- Front suspension layout with 4S <sub>4</sub> unit fitted	4.13
<b>Figure 4.11</b>	- Rear suspension layout with 4S <sub>4</sub> unit fitted	4.13
<b>Figure 4.12</b>	- 4S <sub>4</sub> Prototype 2	4.14
<b>Figure 4.13</b>	- 4S <sub>4</sub> Prototype 2 (left) compared to Prototype 1 (right)	4.15
<b>Figure 4.14</b>	- 4S <sub>4</sub> Prototype 2 on test rig	4.16
<b>Figure 4.15</b>	- 4S <sub>4</sub> Prototype 2 on test rig	4.17
<b>Figure 4.16</b>	- 4S <sub>4</sub> Prototype 2 on test rig	4.18
<b>Figure 4.17</b>	- 4S <sub>4</sub> Prototype 2 on test rig	4.19
<b>Figure 4.18</b>	- 4S <sub>4</sub> Strut mounting to test rig	4.20
<b>Figure 4.19</b>	- Measured bulk modulus	4.23
<b>Figure 4.20</b>	- Determination of thermal time constant	4.24
<b>Figure 4.21</b>	- Soft spring characteristic	4.25
<b>Figure 4.22</b>	- Stiff spring characteristic	4.27
<b>Figure 4.23</b>	- Soft and stiff spring characteristics	4.27
<b>Figure 4.24</b>	- Pressure drop over valve 1	4.28

<b>Figure 4.25</b>	- Curve fits on pressure drop data	4.28
<b>Figure 4.26</b>	- Pressure drop over valve 3 (single valve vs. 2 valves in parallel)	4.29
<b>Figure 4.27</b>	- Damper characteristics for Prototype 2	4.29
<b>Figure 4.28</b>	- Explanation of valve response time definitions	4.31
<b>Figure 4.29</b>	- Valve response time for Prototype 1	4.32
<b>Figure 4.30</b>	- Valve response time for Prototype 2	4.32
<b>Figure 4.31</b>	- Hysteresis problem on Prototype 1	4.33
<b>Figure 4.32</b>	- Effect of friction on soft spring at low speeds	4.34
<b>Figure 4.33</b>	- Effect of friction on soft spring at high speeds	4.34
<b>Figure 4.34</b>	- Effect of friction on stiff spring at low speeds	4.35
<b>Figure 4.35</b>	- Effect of friction on stiff spring at high speeds	4.35
<b>Figure 4.36</b>	- Measured input and output: stiff spring and low damping at low speed	4.42
<b>Figure 4.37</b>	- Comparison between measured and calculated values of $P_1$ and $P_2$ : stiff spring and low damping at low speed	4.43
<b>Figure 4.38</b>	- Comparison between measured and calculated force-displacement curve: stiff spring and low damping at low speed	4.43
<b>Figure 4.39</b>	- Measured input and output: stiff spring and low damping at high speed	4.44
<b>Figure 4.40</b>	- Comparison between measured and calculated values of $P_1$ and $P_2$ : stiff spring and low damping at high speed	4.45
<b>Figure 4.41</b>	- Comparison between measured and calculated force-displacement curve: stiff spring and low damping at high speed	4.45
<b>Figure 4.42</b>	- Measured input and output: stiff spring and low damping at high speed, larger displacement stroke	4.46
<b>Figure 4.43</b>	- Comparison between measured and calculated values of $P_1$ and $P_2$ : stiff spring and low damping at high speed, larger displacement stroke	4.46
<b>Figure 4.44</b>	- Comparison between measured and calculated force-displacement curve: stiff spring and low damping at high speed, larger displacement stroke	4.47
<b>Figure 4.45</b>	- Measured input and output: stiff spring and high damping at high speed	4.48
<b>Figure 4.46</b>	- Comparison between measured and calculated values of $P_1$ and $P_2$ : stiff spring and high damping at high speed	4.49

<b>Figure 4.47</b>	- Comparison between measured and calculated force-displacement curve: stiff spring and high damping at high speed	4.49
<b>Figure 4.48</b>	- Measured input and output: soft spring and low damping at low speed	4.50
<b>Figure 4.49</b>	- Comparison between measured and calculated values of $P_1$ and $P_4$ : soft spring and damping at low speed	4.50
<b>Figure 4.50</b>	- Comparison between measured and calculated values of $P_2$ and $P_3$ : soft spring and low damping at low speed	4.51
<b>Figure 4.51</b>	- Comparison between measured and calculated force-displacement curve: soft spring and low damping at low speed	4.51
<b>Figure 4.52</b>	- Measured input and output: soft spring and low damping at high speed	4.52
<b>Figure 4.53</b>	- Comparison between measured and calculated values of $P_1$ and $P_4$ : soft spring and low damping at high speed	4.52
<b>Figure 4.54</b>	- Comparison between measured and calculated values of $P_2$ and $P_3$ : soft spring and low damping at high speed	4.53
<b>Figure 4.55</b>	- Comparison between measured and calculated force-displacement curve: soft spring and low damping at high speed	4.53
<b>Figure 4.56</b>	- Measured input and output, and valve 3 switch signal: incremental compression test with low damping	4.55
<b>Figure 4.57</b>	- Comparison between measured and calculated values of $P_1$ and $P_4$ : incremental compression test with low damping	4.55
<b>Figure 4.58</b>	- Comparison between measured and calculated values of $P_2$ and $P_3$ : incremental compression test with low damping	4.56
<b>Figure 4.59</b>	- Comparison between measured and calculated force-displacement curve: incremental compression test	4.56

## CHAPTER 5 – THE RIDE COMFORT VS. HANDLING DECISION

<b>Figure 5.1</b>	- The ride comfort vs. handling decision	5.2
<b>Figure 5.2</b>	- TRW's active roll control system according to Böcker and Neuking (2001)	5.6
<b>Figure 5.3</b>	- Steering wheel angle vs. vehicle speed	5.8
<b>Figure 5.4</b>	- Steering wheel rotation speed vs. vehicle speed	5.9
<b>Figure 5.5</b>	- Dive and squat vs. vehicle speed	5.9
<b>Figure 5.6</b>	- Accelerator pedal press rate vs. vehicle speed	5.10
<b>Figure 5.7</b>	- Accelerator pedal release rate vs. vehicle speed	5.10
<b>Figure 5.8</b>	- City and highway driving route	5.14
<b>Figure 5.9</b>	- Fishhook test	5.14

<b>Figure 5.10</b>	- Gerotek rough track top 800 m	5.15
<b>Figure 5.11</b>	- Gerotek Ride and handling track	5.15
<b>Figure 5.12</b>	- Double lane change test	5.15
<b>Figure 5.13</b>	- FFT magnitude of vertical body acceleration (left and right rear)	5.17
<b>Figure 5.14</b>	- FFT magnitude of body lateral acceleration (left front and left rear)	5.17
<b>Figure 5.15</b>	- FFT magnitudes of body roll, yaw and pitch velocity	5.18
<b>Figure 5.16</b>	- FFT magnitude of relative suspension displacement (all four wheels)	5.18
<b>Figure 5.17</b>	- FFT magnitude of steering displacement and kingpin steering angle	5.19
<b>Figure 5.18</b>	- FFT magnitude of relative suspension velocity (all four wheels)	5.19
<b>Figure 5.19</b>	- FFT magnitude of steering velocity	5.20
<b>Figure 5.20</b>	- Strategy proposed by Nell (1993) as applied to city driving	5.21
<b>Figure 5.21</b>	- Strategy proposed by Nell (1993) as applied to the rollover test	5.21
<b>Figure 5.22</b>	- Modified lateral vs. longitudinal acceleration for highway driving	5.23
<b>Figure 5.23</b>	- Modified lateral vs. longitudinal acceleration for rollover test	5.23
<b>Figure 5.24</b>	- Steering limits vs. vehicle speed measured during three tests	5.24
<b>Figure 5.25</b>	- Steer angle vs. speed implemented for city driving	5.25
<b>Figure 5.26</b>	- Steer angle vs. speed implemented for highway driving	5.25
<b>Figure 5.27</b>	- Steer angle vs. speed implemented for off-road driving	5.26
<b>Figure 5.28</b>	- Steer angle vs. speed implemented for mountain pass driving	5.26
<b>Figure 5.29</b>	- Steer angle vs. speed implemented for handling test	5.27
<b>Figure 5.30</b>	- Steer angle vs. speed implemented for rollover test	5.27
<b>Figure 5.31</b>	- Relative roll angle strategy for city driving	5.29
<b>Figure 5.32</b>	- Relative roll angle strategy for highway driving	5.29
<b>Figure 5.33</b>	- Relative roll angle strategy for off-road driving	5.30
<b>Figure 5.34</b>	- Relative roll angle strategy for mountain pass driving	5.30

<b>Figure 5.35</b>	- Relative roll angle strategy for handling	5.31
<b>Figure 5.36</b>	- Relative roll angle strategy for rollover	5.31
<b>Figure 5.37</b>	- RRMS strategy for city driving	5.32
<b>Figure 5.38</b>	- RRMS strategy for highway driving	5.32
<b>Figure 5.39</b>	- RRMS strategy for off-road driving	5.33
<b>Figure 5.40</b>	- RRMS strategy for mountain pass	5.33
<b>Figure 5.41</b>	- RRMS strategy for handling test	5.34
<b>Figure 5.42</b>	- RRMS strategy for rollover test	5.34
<b>Figure 5.43</b>	- Effect of number of points in the RRMS on switching	5.36
<b>Figure 5.44</b>	- Effect of number of points in the RRMS on the switching delay	5.36
<b>Figure 5.45</b>	- Effect of number of points in the RRMS on time spent in “handling” mode	5.37

## **CHAPTER 6 – VEHICLE IMPLEMENTATION**

<b>Figure 6.1</b>	- Right rear suspension fitted to chassis – front view	6.2
<b>Figure 6.2</b>	- Right rear suspension fitted to chassis – inside view	6.3
<b>Figure 6.3</b>	- Right front and right rear suspension fitted to chassis	6.3
<b>Figure 6.4</b>	- Right rear suspension fitted to test vehicle – side view	6.4
<b>Figure 6.5</b>	- Right front suspension fitted to test vehicle – side view	6.5
<b>Figure 6.6</b>	- Assembled hydraulic power pack	6.6
<b>Figure 6.7</b>	- Control manifold for ride height adjustment	6.7
<b>Figure 6.8</b>	- Piping, wiring and electronics	6.7
<b>Figure 6.9</b>	- Control computer schematic	6.9
<b>Figure 6.10</b>	- Constant radius test results	6.10
<b>Figure 6.11</b>	- Relative roll angle front – effect of ride height	6.10
<b>Figure 6.12</b>	- Relative roll angle front – effect of stiffness	6.11



<b>Figure 6.13</b>	- Relative roll angle rear – effect of ride height	6.11
<b>Figure 6.14</b>	- Relative roll angle rear – effect of stiffness	6.12
<b>Figure 6.15</b>	- Body roll with 4S <sub>4</sub> settings compared to baseline at 58 km/h	6.14
<b>Figure 6.16</b>	- Effect of ride height on body roll at 58 km/h	6.14
<b>Figure 6.17</b>	- RRMS control at 61 km/h	6.15
<b>Figure 6.18</b>	- RRMS control at 74 km/h	6.15
<b>Figure 6.19</b>	- RRMS control at 75 km/h	6.16
<b>Figure 6.20</b>	- RRMS control at 83 km/h	6.16
<b>Figure 6.21</b>	- RRMS control at 84 km/h	6.17
<b>Figure 6.22</b>	- RRMS control compared to “handling mode” at 70 km/h	6.17
<b>Figure 6.23</b>	- RRMS control compared to “handling mode” at 82 km/h	6.19
<b>Figure 6.24</b>	- Body roll for “handling mode” at different speeds	6.19
<b>Figure 6.25</b>	- Body roll for RRMS control at different speeds	6.20
<b>Figure 6.26</b>	- RRMS control over Belgian paving at 74 km/h	6.20
<b>Figure 6.27</b>	- Ride comfort of RRMS control compared to “ride mode”	6.21
<b>Figure 6.28</b>	- RRMS control during mountain pass driving	6.22
<b>Figure 6.29</b>	- City driving	6.22
<b>Figure 6.30</b>	- Highway driving	6.23

## APPENDIX A: HANDLING CRITERIA

<b>Figure A-1</b>	- Performance related to driver A – Golf 4 GTI on ride and handling track	A.2
<b>Figure A-2</b>	- Performance related to driver B – Golf 4 GTI on ride and handling track	A.2
<b>Figure A-3</b>	- Roll angle histograms for drivers A and B – Golf 4 GTI on ride and handling track	A.3
<b>Figure A-4</b>	- Lateral acceleration histogram for drivers A and B – Golf 4 GTI on ride and handling track	A.3
<b>Figure A-5</b>	- Lateral acceleration, yaw rate and roll angle performance of a Ford Courier on a dynamic handling track	A.4

<b>Figure A-6</b>	- Lateral acceleration, yaw rate and roll angle performance of a Ford Courier on a ride and handling track	A.4
<b>Figure A-7</b>	- Lateral acceleration histogram for a Ford Courier on a dynamic handling track	A.5
<b>Figure A-8</b>	- Roll angle histogram for a Ford Courier on a dynamic handling track	A.5
<b>Figure A-9</b>	- Lateral acceleration histogram of a Ford Courier on a ride and handling track	A.6
<b>Figure A-10</b>	- Roll angle histogram of a Ford Courier on a ride and handling track	A.6
<b>Figure A-11</b>	- Lateral acceleration, yaw rate and roll angle performance of a VW Golf 4 GTI on a dynamic handling track	A.7
<b>Figure A-12</b>	- Lateral acceleration, yaw rate and roll angle performance of a VW Golf 4 GTI on a ride and handling track	A.7
<b>Figure A-13</b>	- Lateral acceleration histogram for a VW Golf 4 GTI on a dynamic handling track	A.8
<b>Figure A-14</b>	- Roll angle histogram for a VW Golf 4 GTI on a dynamic handling track	A.8
<b>Figure A-15</b>	- Lateral acceleration histogram for a VW Golf 4 GTI on a ride and handling track	A.9
<b>Figure A-16</b>	- Roll angle histogram for a VW Golf 4 GTI on a ride and handling track	A.9
<b>Figure A-17</b>	- Lateral acceleration and yaw rate performance of a Land Rover Defender 110 on a ride and handling track (roll angle data not available)	A.10
<b>Figure A-18</b>	- Lateral acceleration histogram for a Land Rover Defender 110 on a ride and handling track	A.10

---

---

## ***LIST OF TABLES***

---

### **CHAPTER 1 – INTRODUCTION**

<b>Table 1.1</b> - Classification of suspension systems	1.4
<b>Table 1.2</b> - Applications of controllable suspension systems	1.8

### **CHAPTER 2 – THE RIDE COMFORT VS. HANDLING COMPROMISE**

<b>Table 2.1</b> - Summary of measurements	2.12
<b>Table 2.2</b> - Limiting parameter values (all vehicles and all drivers)	2.15
<b>Table 2.3</b> - Calculated spring stiffness for linear spring	2.20
<b>Table 2.4</b> - Natural frequencies for hydropneumatic spring	2.21
<b>Table 2.5</b> - Summary of the DADS simulation model	2.27
<b>Table 2.6</b> - Summary of results by Thoresson (2003)	2.31
<b>Table 2.7</b> - Instrumentation used for baseline vehicle tests	2.35

### **CHAPTER 3 – POSSIBLE SOLUTIONS TO THE RIDE COMFORT VS. HANDLING COMPROMISE**

<b>Table 3.1</b> - Control ideas evaluated by Voigt (2006)	3.22
--	------

### **CHAPTER 4 – THE FOUR-STATE SEMI-ACTIVE SUSPENSION SYSTEM (4S<sub>4</sub>)**

<b>Table 4.1</b> - Thermal time constants	4.23
---	------

## CHAPTER 5 – THE RIDE COMFORT VS. HANDLING DECISION

<b>Table 5.1</b> - Predictive control as implemented by Hirose <i>et. al.</i> (1988)	5.4
<b>Table 5.2</b> - Tracking control as implemented by Hirose <i>et. al.</i> (1988)	5.4
<b>Table 5.3</b> - Strategy used by Mizuguchi <i>et. al.</i> (1984)	5.4
<b>Table 5.4</b> - Candidate ideas for assisting with the “ride vs. handling” decision	5.11
<b>Table 5.5</b> - Directly measurable parameters	5.12
<b>Table 5.6</b> - Parameters that can be easily calculated from measurements	5.12
<b>Table 5.7</b> - Chosen tests and test routes	5.13

## CHAPTER 6 – VEHICLE IMPLEMENTATION

<b>Table 6.1</b> - Comparison between baseline and 4S <sub>4</sub> relative roll angles through double lane change at 57 to 61 km/h	6.13
---	------

---

## ***INTRODUCTION***

---

The main aim of a vehicle's suspension system is to isolate the occupants from external terrain induced disturbances, while still allowing the average driver to maintain control over the vehicle and drive it safely. The design of vehicle suspension systems always involves a compromise between ride comfort and handling. For good ride comfort a compliant suspension system is normally required, while good handling demands a stiff suspension system to control body roll.

With a normal passive suspension system, the characteristics of the springs and dampers are fixed at the design stage and cannot be changed afterwards. By using controllable springs and dampers, the suspension characteristics can be changed while the vehicle is moving. It therefore becomes possible to have soft settings for good ride comfort whilst traveling in a straight line on a good road, while the suspension characteristics can be changed to a hard setting moments later to give good handling when the vehicle has to change direction as required for lane changing or even accident avoidance. Settings can also be adjusted based on the terrain roughness. With limited suspension travel available, increased terrain roughness might require an increase in spring stiffness to prevent bump-stop contact and therefore improve ride comfort.

The problem becomes even more severe when the operational requirements of a vehicle are in conflict with the suspension design. On most off-road vehicles high ground clearance is required to enable crossing obstacles. Large suspension travel is also required to keep all wheels in contact with the ground in order to maintain traction. Even load distribution amongst the different wheels improves traction but requires soft springs. A problem however arises when these vehicles have to be operated at high speeds on smooth roads. The high center of gravity, large suspension travel and soft springs create an inherent handling and stability problem making these vehicles prone to rollover.

A satisfactory solution cannot be obtained with a passive suspension system, but controllable suspension systems have the potential to reduce or even eliminate the ride comfort vs. handling compromise. The type of controllable suspension system that is the topic of the current research, can significantly improve the situation by having a choice of two discrete spring characteristics, as well as two discrete damper characteristics. The system also features ride height adjustment capabilities giving control over ground clearance and center of gravity height. This means that the suspension can be switched to a setting optimized for off-road use (ride comfort and traction). Another setting, optimized for high-speed on-road use, is available under conditions where good handling is required. To obtain maximum benefit, switchover must occur automatically without driver intervention. This being the main challenge that needs to be addressed before these

systems can be successfully applied to vehicles: the “*ride comfort vs. handling decision*”.

The rest of this chapter gives background on several relevant topics such as vehicle models, classification of controllable suspension systems, hydropneumatic springs, production and concept applications of controllable suspension systems and global viewpoints. The chapter closes with the problem statement and hypothesis.

### 1.1 Vehicle models

It can be argued that the simplest model of a car suspension system that is really useful is the  $\frac{1}{4}$  car representation as indicated in Figure 1.1. Here the vehicle body is represented by the sprung mass  $M$ . The suspension, wheels and tyres are lumped as an unsprung mass,  $m$ . The unsprung mass is connected to the sprung mass via a spring and damper and to the road input via the tyre, normally represented only by a spring. Tyre damping is usually small and therefore often neglected in  $\frac{1}{4}$  car analyses. Suspension kinematics is ignored and the two masses are only allowed vertical translation.

If the spring, damper and tyre characteristics are linear, the analysis can be performed in either the frequency domain or the time domain. Non-linear characteristics however require time domain analysis where a weighted root mean square (RMS) value of the sprung mass acceleration is normally used as a measure of ride comfort.

This model can be useful to obtain first order values of spring and damper characteristics required to meet a ride comfort specification. Although many authors attempt to get an indication of handling by looking at the tyre force variations, this is an extreme oversimplification of the handling phenomena (Miller 1988b). Handling is much more complicated to simulate or measure on a vehicle, not least because it is very dependent on the human driver. Human driver preferences and characteristics vary widely making subjective vs. objective comparison of vehicle handling troublesome.

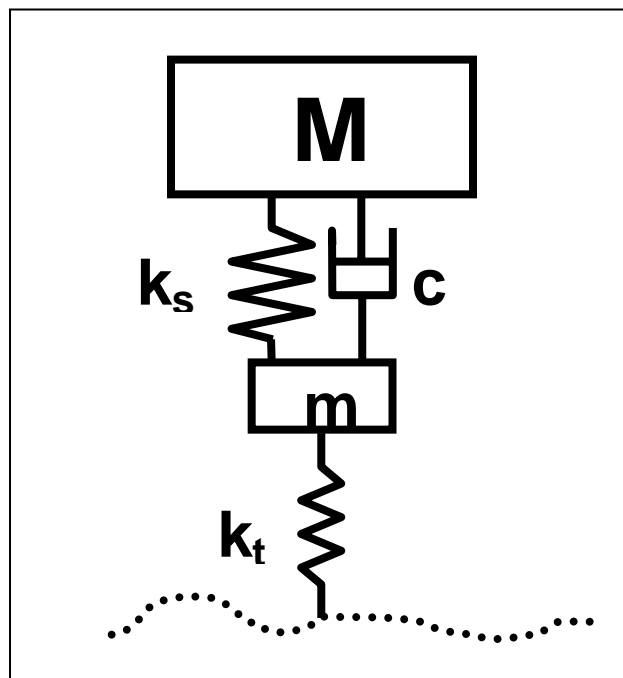


**Figure 1.1** –  $\frac{1}{4}$  Car suspension system

The  $\frac{1}{4}$  car model can be expanded to a  $\frac{1}{2}$  car model considering either roll or pitch motion, resulting in a model with four degrees of freedom. The next logical step is a full car model with seven degrees of freedom taking roll, pitch and vertical movement into account. This type of model usually still ignores suspension kinematics and only allows for vertical translation of the unsprung mass. However, to obtain useful results for handling, longitudinal and lateral translations need to be added.

Throughout the present study, use is made of a non-linear full vehicle model. The model is developed using the ADAMS multi-body dynamics code (**Anon, 2002**). The model includes suspension kinematics, a non-linear tyre model and a human driver model. Simulation is performed over real off-road terrain profiles. The model is validated against vehicle test results and the full details are discussed in Chapter 2.

## 1.2 Controllable suspension system classification

Before continuing it is necessary to discuss the main categories of controllable suspension systems. Confusion has been created by the inconsequent use of the terms adaptive, semi-active and active suspension systems. Suspension systems are classified for the purpose of the current study as given in Table 1. This classification is based on that proposed by **Decker et.al. (1988)**. **Williams (1994)** also gives a description of various concepts.

All the controllable systems have physical limits imposed on them. Maximum force, displacement, velocity and response times are usually limited by the hardware.

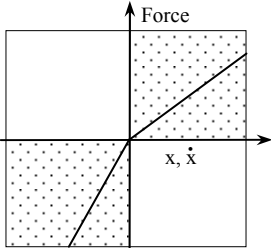
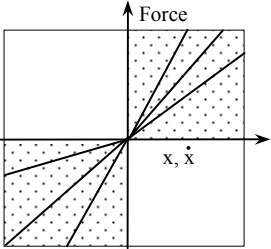
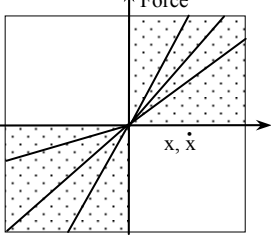
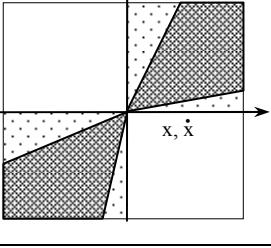
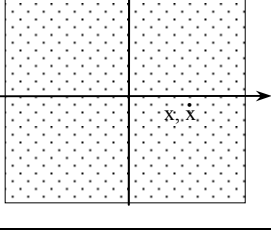
*Passive* suspension systems are very well known and still used on the vast majority of new vehicles. Passive implies that the force-displacement and force-velocity characteristics of the suspension system remain fixed at the design values throughout the useful life of the components. Some degradation in performance usually takes place due to wear and fatigue, but the characteristics cannot be modified without replacing or manually adjusting components. Adjustable dampers that can be switched between different characteristics using simple tools such as a screwdriver also fall in this category.

*Adaptive* systems can usually change certain characteristics slowly to adapt to changes in vehicle load, speed or other operating conditions. These changes may take a few seconds or a few minutes to have an effect. Self-levelling is the best-known example. **Buchholz (2003b)** describes the ZF Sachs Nivomat mono tube damper with self-levelling feature. Self-levelling is accomplished by using the energy that is generated by relative movement between the vehicle body and suspension whilst moving. To accomplish levelling, typically 1.6 to 2.4 km of driving is required. Adding an electric pump will eliminate the need to drive the vehicle to accomplish self-levelling. The Nivomat system boasts two features that normal air levelling systems lack, namely a load dependent spring rate (which controls the ride frequency), and load dependent damping (which provides control for additional mass/payload in rebound). The conventional Nivomat system first appeared in the US market in 1996, fitted to a Chrysler vehicle.

*Semi-active* systems are classified as systems where the characteristics can be changed rapidly (typically in less than 100 milliseconds). These systems can still only store energy (springs) or dissipate energy (dampers). The most common example is the semi-active damper where the damper force-velocity characteristic can be varied either between

certain pre-defined discrete values (*e.g.* hard and soft), or continuously between a certain minimum and maximum boundary.

**Table 1.1** – Classification of suspension systems

Class	Forces	Actuating times	Energy requirements
<b>Passive</b>  Characteristics fixed at design stage		-	-
<b>Adaptive</b>  Characteristics can change slowly		Longer than characteristic periods of oscillation	Low
<b>Semi-active: Discreet</b>  Characteristics can change quickly between certain discrete values		Shorter than characteristic periods of oscillation	Low
<b>Semi-active: Continuous</b>  Characteristics can change quickly and continuously between certain limits		Shorter than characteristic periods of oscillation	Low
<b>Active</b>  Characteristics can change quickly and continuously between certain limits		Shorter than characteristic periods of oscillation	High

According to **Harty (2003)**, “the next step beyond current successful damper designs that switch between two or a few more discrete calibrations – allows ‘step-less’ damper characteristic modifications but represents a relatively new production technology. Adjusting damper characteristics does not alter fundamental handling balance, although it



can modify transient events (*e.g.* turn-in) by phasing damper switching front to rear and/or side to side. Benefits include significant ride enhancements for a given level of handling performance and the potential for control of transient effects using more sophisticated algorithms than currently employed. However, handling balance cannot be continuously altered.” The Magnetic Ride Control dampers on the Cadillac XLR are a production example. This system employs magneto-rheological (MR) fluid and can continuously vary damping at speeds approaching 1 millisecond.

The working principles of semi-active dampers can be divided into two main categories namely: hydraulic dampers with bypass valves, and dampers employing magneto-rheological fluids.

The Ohlins dampers fitted by Volvo amongst others, as well as the semi-active dampers used in the present study are basically normal hydraulic dampers fitted with a valve that can bypass the damper orifices. This bypass valve can have anything from two states (open and closed) to being continuously variable.

Lord Corporation is one of the world leaders in the development and manufacture of magneto-rheological fluids. New fluids have been developed in response to improvements in MR technology driven by high volume production (**Ponticel 2002**). Both hydrocarbon oil and water-based products are available. The viscosity of MR fluids is dependent on the magnetic field applied. MR materials can change from a fluid to a near-solid state within milliseconds when applying a magnetic field. System design is simple and control power requirements are low. MR fluids are used in various applications, including automobile dampers and seat suspension systems.

Delphi and Lord Corporation co-developed the MR fluid used in the Cadillac Seville STS dampers (**Jost 2002b**). The MR fluid consists of iron particles suspended in a synthetic hydrocarbon base fluid specifically developed for shock absorber application. In the “off” state the MR fluid is not magnetized and the iron articles are dispersed randomly. When applying a magnetic field, the iron particles align into fibrous structures, changing the fluid rheology in the “on” state and thus the damping properties. The damping fluid can change from a mineral oil type consistency (low damping forces) to a jelly-like substance (high damping) within one millisecond.

**Active suspensions** usually replace springs and dampers with fast hydraulic, pneumatic or electric actuators. A soft spring is often used in parallel with the actuator to reduce power consumption by carrying the static wheel load. Active systems are still in the prototype stage and suffer from high power demands and cost. Active suspension has the ability to add significant amounts of energy to the system.

**Low-bandwidth active** suspensions can only control primary suspension modes and front/rear roll moment balance at frequencies typically below 5 Hz. The Mercedes-Benz Active Body Control (ABC) system is a current production example. Low-bandwidth active suspension systems can offer ride benefits for a given level of handling performance. The cost can also be considerably less compared to higher bandwidth solutions (**Harty 2003**).

**Full-bandwidth active** suspensions can provide control up to 25 Hz. High-bandwidth examples offer control of handling as well as body dynamics and thus theoretically

improved performance compared to low-bandwidth systems. Several successful motor sport applications and research vehicles, notably from Lotus, exists but no production examples are known. The high bandwidth requires expensive hydraulic systems. High forces and displacements means that power consumption is also high (**Harty 2003**).

Active suspension control using a linear electromagnetic actuator is described by **Buckner *et.al.* (2000)**. The actuator is installed in parallel with a soft spring supporting the static load. The application is for a high mobility off-road military vehicle (HMMWV). **Decker *et.al.* (1988)** also describes a magnetic spring in parallel with the conventional steel spring.

A recent variation on the theme of controllable suspension systems is active or semi-active roll control. **Kim and Park (2004)** describe an electrically actuated active roll control system. This system uses an electric actuator acting on the vehicle's anti-rollbar. The addition of a variable damper is also investigated. Several control strategies are investigated with simulation and hardware-in-the-loop (HiL) testing. The system is said to be effective in spite of the limited bandwidth of the actuator. "Active anti-rollbars for warp control on one or both axles provide some of the platform-levelling benefits of low-band active suspension plus the ability to alter the handling balance continuously". A production system is implemented on the 2004 model year BMW 7 Series. Handling benefits by being continuously adjustable from passive understeer to oversteer. The technology has minimal package and power requirements, and is lower cost than even low-band active suspensions. Disadvantages are the lack of pitch control and absolute authority for roll control, unless both front and rear bars are used.

### 1.3 Semi-active springs

The two viable options considered for creating semi-active springs are either hydropneumatic or air springs. Although the rest of this document will refer to hydropneumatic springs, the same principles can be applied to air springs – the main difference being the working pressure. Hydropneumatic springs have been applied to military vehicles for many years. The most well known applications in passenger cars are by Citroën (**Nastasić & Jahn, 2005**). The spring force in a hydropneumatic suspension system is generated by compressing a gas in a closed container. The spring characteristic is non-linear and governed by gas laws. For low speed excitation, the spring characteristic can be approximated by isothermal compression, while for very high speeds, adiabatic compression yields more accurate results. Care must be taken when the ideal gas approach is used, as this results in significant errors for the typical pressures found in hydropneumatic suspension systems.

Different models can be used to predict the spring characteristic of hydropneumatic springs. A thermal time constant model is used by **Els (1993)**, **Els & Grobbelaar (1993)** and **Els & Grobbelaar (1999)**. They take heat transfer effects and non-ideal gas behaviour into account. Another modelling technique is to use an anelastic model consisting of two parallel springs, one of which is in series with a damper. This approach is described by **Kornhauser (1994)** and **Giliomee, Els and Van Niekerk (2005)** amongst others.

#### 1.4 Current applications of controllable suspension systems

Citroën is considered to be the pioneers in the application of controllable suspension systems to passenger cars. The working principles of the different **Citroën** hydropneumatic suspension systems are described in considerable detail by **Nastasić and Jahn (2005)**. All models since the introduction of the **Citroën DS** at the **1955** Paris Motor Show are described. This includes Hydractive I (first used on the Citroën XM), Hydractive II (launched in 1993), Activa (used on some Citroën Xantia models), Hydractive 3 and Hydractive 3+ (introduced on the C5).

The number of commercial applications of controllable suspension systems in production cars is increasing rapidly. Most applications are however still limited to top of the range models where the cost penalty can be easily justified. An example is Continuous Damping Control (CDC), as developed by ZF Sachs. CDC was launched in 2001 as optional equipment on cars such as the **BMW 7 Series** and **Ferrari Modena** and is now available as optional equipment on the new **(2004) Opel Astra (Jost 2004)**. The total number of CDC equipped vehicles on the road was expected to rise to 225 000 in 2005 (**Anon, 2004**).

For the present study, application of controllable suspension systems to off-road vehicles is of special interest. **Land Rover** implemented a cross-linked electronic air suspension system on the 2003 model year Range Rover (**Mayne 2002**). The system joins the left front and right front air springs via an electronically controlled valve. The same happens on the rear suspension. When the valve is open, roll stiffness is dramatically reduced as air flows between the left and right suspension system to equalise the pressure. This results in low variation between wheel load left and right. The effect is less rocking on rough terrain and better traction, because all wheels maintain effective ground contact. If the valve is closed, the left and right suspension systems are isolated from each other – the setting used for on-road driving. An electronic control unit, that uses vehicle speed and suspension displacements as inputs, determines valve switching. The system is also fitted with automatic load levelling and ride height control.

**Volkswagen's SUV, the Touareg**, is fitted with air suspension and adjustable damping (**Birch 2002b**). Manual adjustment of four different suspension height levels and three different damper settings is provided. On-road ride height varies automatically according to vehicle speed. Ground clearance is reduced from 215 mm to 190 mm above 125 km/h although the driver can manually set other levels. Above 180 km/h the ride height is automatically reduced to 180 mm.

The **SmarTruck II**, developed for the U.S. Army Tank-Automotive and Armaments Command's National Automotive Centre, is based on a Chevrolet Silverado 2500 pickup. It features a heavy-duty adjustable air suspension system (**Buchholz 2003a**).

A summary of current production and prototype applications of controllable suspension systems to light vehicles is given in Table 1.2. Features include adjustment of ground clearance, ride height control to compensate for load changes and selectability of different modes e.g. "Sport" or "Comfort". This summary does not intend to be complete, but rather aims to give the reader an overview of the typical applications of controllable suspension systems.

**Table 1.2 – Applications of controllable suspension systems**

Manufacturer	Reference	Spring					Class		Damper		Class			Acronym
		Active anti-roll bar	Air	Hydropneumatic	Ride height control	Load levelling	Passive	Adaptive	Hydraulic	Magneto-rheologic (MR)	Passive	Adaptive	Semi-Active: Discrete	
Audi A6 (2004)	Birch 2004a	X					X							
Audi A8, 2003	Birch 2002a; Birch 2002c	X		X	X	X	X	X					X	
Audi All-Road Quattro	Jost 2002a; Jost 2005	X		X	X	X	X						X	Electronic Air Suspension (EAS)
Audi Le Mans Concept, 2003	Birch 2003b								X				X	Audi Magnetic Ride Technology
Audi RS6	Birch 2002c							X					X	Dynamic ride control (DRC)
Bentley Continental, 2003	Birch 2003d	X											X	
BMW 7-series (2001) opt. equip.	Gehm 2004						X	X					X	CDC (Continuous Damping Control)
Cadillac Seville STS, Post mid 2002	Jost 2002b; Alexander 2003					X	X	X					X	MagneRide (Delphi)
Cadillac Seville STS, Pre mid 2002	Jost 2002b													Continuously Variable Road Sensing Suspension (CVRSS)
Chrysler Pacifica, 2003	Gehm 2003			X	X									
Citroën	Nastasić and Jahn 2005			X	X	X	X	X		X				Hydractive 3
Citroën Activa 2 Concept, 1990	Birch <i>et.al.</i> 1990	X		X				X						
Citroën C5	Nastasić and Jahn 2005			X	X	X	X	X		X				Hydractive 3+
Citroën C-Airlounge Concept, 2003	Birch 2003b			X										Hydractive 3
Citroën DS, 1955	Nastasić and Jahn 2005			X	X	X	X	X		X				
Citroën Xantia	Nastasić and Jahn 2005	X		X	X	X	X	X		X				Activa
Citroën XM	Nastasić and Jahn 2005			X	X	X	X	X		X				Hydractive 1
Citroën Xsara Dynactive	Birch 1999			X	X	X								Hydractive 3
Citroën, 1993	Nastasić and Jahn 2005			X	X	X	X	X		X				Hydractive II
Ferrari 306, 2003	Carney 2003a						X	X					?	?
Ferrari Modena (2001) opt. equip.	Gehm 2004						X	X					X	CDC (Continuous Damping Control)
Ford Visos Concept, 2003	Birch 2003b												X	
Jaguar XJ, 2003	Birch 2003c	X												Computer Actives Technology Suspension (CATS)
Jeep Grand Cherokee	Carney 2004b	X												DHS (Dynamic Handling System)
Lamborghini Gallardo, 2003	Birch 2003d						X	X			X			
Land Rover Range Rover, 2003	Mayne 2002	X	X	X	X		X	X		X				
Maserati Quattroporte, 2004	Carney 2003b						X	X					X	“Skyhook”
Maserati Spyder, 2002	Kelly 2001; Carney 2003b						X	X					X	“Skyhook”
Mercedes Benz A-class (2004)	Birch 2004b							X			X			
Opel Astra, 2004	Jost 2004						X	X					X	Continuous Damping Control (CDC); ISDPlus
Opel Insignia Concept, 2003	Birch 2003b			X			X							
Toyota Soarer, 1986	Hirose <i>et.al.</i> 1988		X	X	X		X	X			X			
US Army SmarTruck II, 2003	Buchholz 2003a		X				X							
Volkswagen Phaeton, 2002	Jost 2002a; Jost 2005	X		X	X		X						X	Electronic Air Suspension (EAS)
Volkswagen Touareg SUV, 2004	Birch 2002b		X	X	X		X					3		
Volvo S60R and V70R, 2003	Weissler 2003						X	X					X	Continuously Controlled Chassis Concept (four-C)
Number of applications		4	8	9	15	15	7	16	20	2	7	3	3	12

It is clear that the application of controllable suspension systems is quickly gaining ground in new passenger cars. Current fitment is to top-end road vehicles only. Current systems are mostly semi-active dampers and/or ride height control. A few applications of active anti-rollbars are also noted. Switching between various gas volumes have been employed by Citroën and Land Rover. Fully active systems have only been realized on prototypes. The developments by Lotus (**Wright, 2001**) are especially notable.

### 1.5 Global viewpoints

The viewpoints of several global experts in the vehicle suspension field are now discussed to determine general trends and forecasts.

Vertical load modification systems (*e.g.* springs and dampers) have a direct influence on handling (**Harty 2003**). The scope for these systems to improve handling and stability is dependent on the relationship between the vertical force applied to the tyre and the corresponding lateral and longitudinal forces generated by the tyre.

According to **Harty (2003)** ride comfort can be significantly improved using adaptive damper control. Stability can be influenced to a limited extent by damper control, because the damper can only have an influence during transients. Stability is currently improved by using brake-based systems. Brake-based systems are proven in the market. Active anti-rollbar technology can be used to good effect. The other candidate is variable geometry active suspension, but packaging problems and bandwidth issues hamper progress.

Many of the current technical obstacles centre on sensing difficulties. Reliable sensing of friction coefficient between the tyre and road is a problem. The body slip angle of the vehicle also poses problems with many attempts focussed on calculating slip angle using state estimators and techniques such as Kalman filtering to retrieve robust estimates from noisy data.

**Land Rover's Director of Product Development, Steve Ross**, comments on the use of advanced technology as follows: "However, for us, technology is used to enhance both off- and on-road capabilities. Technology is a means to an end in achieving greater safety, security and refinement" (**Birch 2001a**). Range Rover's computer-controlled air suspension, which can vary vehicle height on and off road, is an added safety element, lowering the centre of gravity (cg) when necessary, according to Ross.

**Birch (2003a)** summarized comments from several European industry experts on the topic of integration of electronically controlled chassis and suspension systems.

**Hugh Kemp, Engineering Director of International Automotive Technology Business at Prodrive** regards continuously variable dampers as having the potential to offer most of the benefits promised by active suspension but at a "more realistic price". Prodrive favours mechanical variable orifice technology. Electronic control will also allow a single damper specification to be used across a vast range of vehicles.

**Michael Paul, Main Board Executive Director, Research and Development at ZF**, agrees that there are great opportunities for more intelligent single components. "The new BMW 7 Series has an intelligent stabilizer system and electronically adjustable dampers. As for fully active suspension, I would be very hesitant; it requires a lot of power, which opposes the target of reducing fuel consumption", he said.

"... for cost reasons, air springs and particularly active body control (ABC) will remain in 'privileged' market sectors" according to **Hans-Joachim Schöpf, Executive Vice President for Development, Mercedes Car Group**.

**Nevio di Giusto, Head of Product Development, Fiat/Lancia Business unit**, believes that any worthwhile project deserves a good chassis. "In the short term, I cannot envisage a well-designed chassis not using electronic control" he said.

**Clive Hickman, Managing Director of Ricardo Vehicle Engineering**, regards the integration of chassis electronics as a significant challenge, with the development of air-

springs, roll control, adaptive steering and damping systems complementing antilock, traction and stability programs.

**Roberto Fedeli, who is responsible for the development of all Ferrari development platforms**, says that electronic systems should help the driver in some types of conditions and support safety. On normal road and normal climatic conditions, electronics must not mask the driver's enjoyment of driving the car. He considers this to be a tuning problem that depends on the control algorithms used.

**Buchholz (2003c)** looks at chassis developments for trucks and SUV's from a North American perspective and interviews experts in the field. **Scott Bailey, Director of Engineering for Energy and Chassis Systems at Delphi Corporation** says: "With advanced technologies, [we] can all but eliminate ride and handling compromises". Volvo became a first-to-market application example via the 2003 XC90 SUV's active Roll Stability Control System, which was co-developed by Ford Motor Company and Continental Teves. Gyroscopic sensors are used to determine roll speed and roll angle. The system uses the braking and traction control systems to prevent rollover. Bailey also comments on trucks: "It's an entirely different dynamic at play when you're dealing with a pickup truck versus a passenger car. A truck can be partially loaded, or fully loaded, and is often towing something. Any of those conditions can significantly change the mass of the vehicle, which means the dynamic models have to change. You have to get much smarter about the different models that are at play to improve upon the control schemes. The result is a much more sophisticated modelling requirement". **Bob Walker, Engineering Director of Suspension and Exhaust Product Development for Visteon Corporation** says programs at several companies include the concept of an "active corner" suspension. One particular active four-corner suspension system involves "inducing force into the suspension system – typically to a shock absorber or strut – so it can counteract the energy when the vehicle pitches in a particular direction", says Walker. **Aly Badawy, TRW Automotive Vice President of Steering, Linkage, and Suspension Engineering** expects a production intent vehicle using the "active corner" concept to be ready by 2008, but production will be dependent on the development of 42 Volt technology, which he sees as "a must for an active corner".

In another article on chassis integration from a North American perspective by **Alexander (2004b)**, **Aly Badawy, TRW Automotive Vice President of Steering, Linkage, and Suspension Engineering** states that rollover avoidance and mitigation is getting a lot of attention but there is no single technology to make a vehicle safe from rollover. Active roll control (ARC) is under development and about to go into production. Active damping control (ADC) is similar but allows for control of different sides of the vehicle. The key to improvements is to integrate all systems. "Fundamentally, the industry all has the same technology". Sensing and control technology is the key to having the best product.

**Delphi** has **MagneRide** in production that uses magneto-rheological fluid. Delphi's active stabilizer comes in two variations namely a single channel and a two-channel version. It operates hydraulically but an electric version is under development according to **Brian Murray, Manager of Delphi's Innovation Center in Brighton, MI**.

It is clear that many industry specialists see the development of controllable suspension systems as one of the trends that will increase in future.

## 1.6 Problem statement

Controllable suspension systems have been implemented successfully in the case of top-end passenger cars and is seen by industry specialists as the development trend of the future. A void exists within the scope of vehicles that require good off-road capability (high ground clearance, large suspension travel and soft springs), but also good handling and stability on smooth roads at high speeds (low center of gravity and stiff springs). Military wheeled vehicles, Sports Utility Vehicles (SUV's) and Crossover utility vehicles (CUV's) all fall within this category.

The following hypotheses are made:

- i) Ride comfort and handling have opposing requirements in terms of spring and damper characteristics.
- ii) Suspension requirements for off-road use differ substantially from requirements for high-speed on- road use.
- iii) A set of passive spring and damper characteristics, called the “ride comfort characteristic” can be obtained that will optimise ride comfort over prescribed off-road terrains at prescribed speeds. Additional improvements might be possible by using “control” but is not considered for the purposes of this thesis.
- iv) A set of passive spring and damper characteristics, called the “handling characteristic”, can be obtained that will optimise handling for prescribed high-speed manoeuvres on good roads. Additional improvements might be possible using “control” but is not considered for the purposes of this thesis.
- v) Advanced suspension system hardware that can switch between the passive “ride comfort” and “handling” spring and damper characteristics, can be feasibly implemented. Response time must be quick enough to enable control of the sprung mass natural frequencies.
- vi) A robust decision can be made whether “ride comfort” or “handling” is required for the prevailing conditions.

Chapters 2 to 6 of this thesis will investigate the validity of these hypotheses.

Fully active suspension systems have been explicitly eliminated for the purposes of the current study due to prohibitive cost as well as power requirements during off-road driving (although both power requirements and cost can be improved).

The purpose of this research is to design, develop, manufacture and test an advanced suspension system that can eliminate the ride comfort *vs.* handling compromise for vehicles that require good off-road capability, but also good handling and stability on smooth roads at high speeds. The resulting suspension hardware is tested and characterized to obtain all the parameters required for mathematical modeling.

A Land Rover Defender 110 vehicle was chosen as the platform for simulation and testing of the controllable suspension concept proposed in the present study. The Land Rover Defender is still considered by many, not least the marketing division, to be the “best 4x4x4” but the design is now dated. Although the vehicle behaves very well off-road, the on-road handling is less than desirable due to the soft suspension with large suspension travel and the high centre of mass. The vehicle, with its ladder frame chassis

and boxy styling, makes it relatively easy to change suspension components and suspension mounting points. The vehicle is also fitted with coil springs. This means that all the axle-locating functions are performed by suspension links (e.g. leading arms, trailing arms, Panhard rods *etc.*) and not the springs, as is the case on many other vehicles in this class fitted with leaf springs. These factors combine to make the Land Rover Defender the ideal platform to test the controllable suspension concept.

In order to investigate the feasibility of the proposed suspension system, the project consists of nine tasks namely:

- i) Develop a full vehicle dynamics simulation model to predict ride comfort and handling.
- ii) Validate the vehicle dynamics simulation model.
- iii) Determine the required suspension characteristics for the “best” ride comfort and “best” handling respectively, using the vehicle dynamics model.
- iv) Design a prototype suspension system capable of producing the required characteristics.
- v) Manufacture the prototype suspension system according to the design.
- vi) Test and characterise the prototype suspension system to determine feasibility and conformance to specification.
- vii) Develop a mathematical model of the prototype suspension system that can be incorporated into the vehicle dynamics model.
- viii) Develop a decision making methodology that can be used to switch the suspension system between ride comfort and handling modes. From now on this will be called the “ride *vs.* handling decision”. The ride *vs.* handling decision constitutes the main challenge for the successful implementation of the controllable suspension system proposed in this study and is therefore seen as the major contribution of the present study.
- ix) Fit the prototype suspension system to a test vehicle, implement the ride *vs.* handling strategy and validate the strategy using vehicle tests.

The nine steps listed are represented graphically in Figure 1.2. The chapter in this thesis where each step is further discussed is indicated below each block.

In Chapter 2, a validated, non-linear full vehicle model is used to investigate the “optimal” characteristics for both ride comfort and handling. The conflicts between these requirements are investigated and analysed using simulation.

The focus of Chapter 3 is on possible controllable suspension solutions to the ride *vs.* handling compromise. A possible solution is formulated and investigated in greater detail in Chapter 4 where the design, manufacturing, testing and mathematical modelling of the proposed prototype system is described.

Chapter 5 looks at the crucial “ride comfort” *vs.* “handling” decision. Test data for different driving conditions is analysed and different decision-making ideas investigated. Vehicle implementation of the proposed hardware as well as the decision-making strategy and final test results are discussed in Chapter 6.



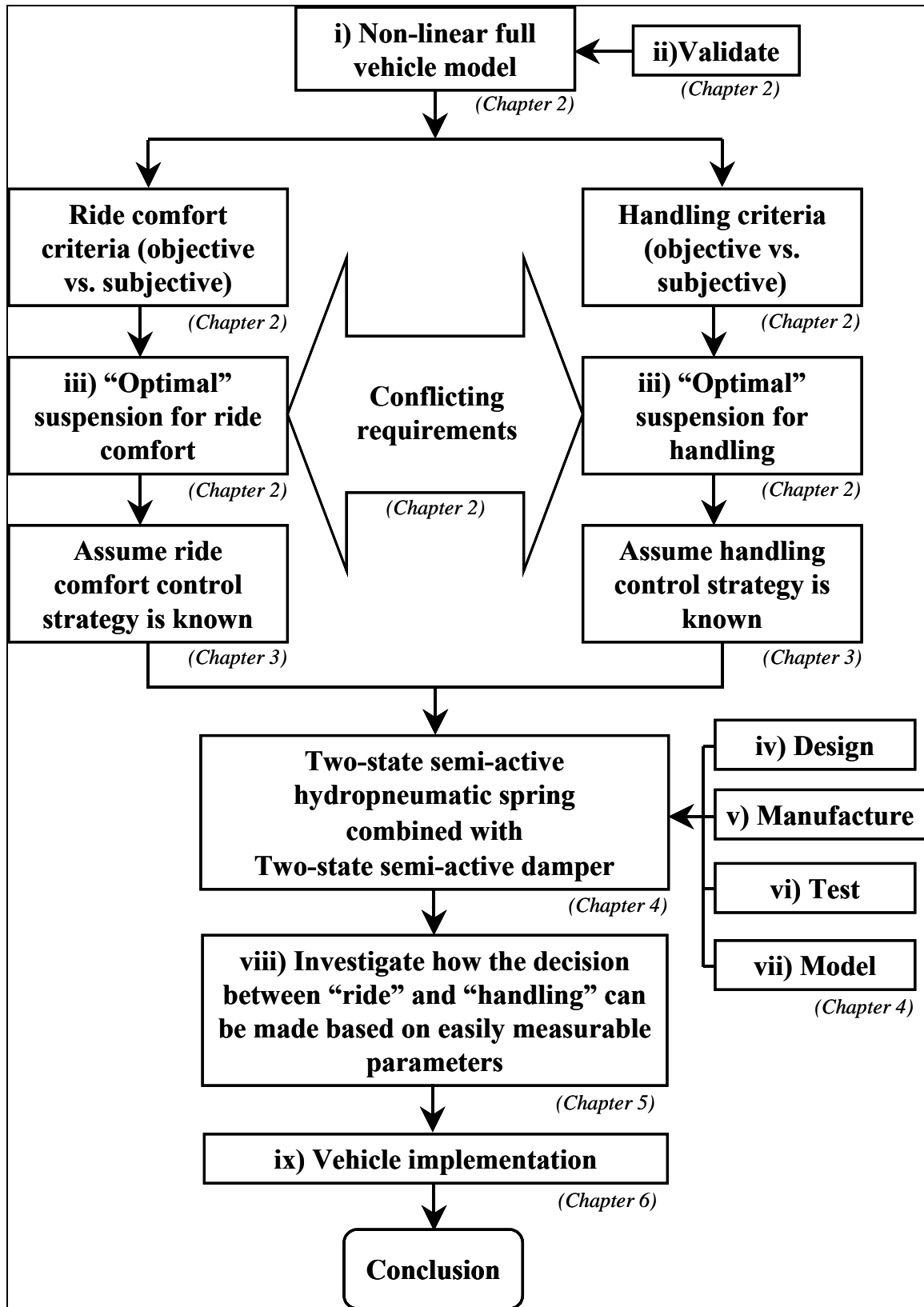


Figure 1.2 - Flow diagram of present study

---

---

## ***THE RIDE COMFORT VS. HANDLING COMPROMISE***

---

---

It is commonly accepted that vehicles with soft suspension systems generally provide very good ride comfort at the expense of handling. Most sports cars suffer from the opposite symptoms in that a firm suspension system offers excellent handling up to very high speeds but then the ride comfort is often described as harsh or rough. It is apparent that the design of a passive suspension system always involves a compromise between ride comfort and handling.

In this chapter the ride comfort *vs.* handling compromise is investigated by means of two case studies. The case studies are presented after analyses of literature on the subject.

The chapter concludes with the development and experimental validation of an ADAMS model of a Land Rover Defender 110 vehicle. The ADAMS model is used to determine spring and damper characteristics optimised for ride comfort and handling respectively.

### **2.1 Literature**

In order to analyse the ride comfort *vs.* handling compromise, it is important to define the concepts of “ride comfort” and “handling” separately. In general “ride comfort” is associated with the vertical dynamics of the vehicle, primarily caused by road input excitation. “Handling” is usually associated with the lateral, yaw and roll degrees of freedom that are primarily a result of steering inputs by the driver.

In the remainder of this study, ride comfort is associated with vehicle dynamics caused by road excitation. Handling is associated with vehicle dynamics due to steering inputs by the driver.

#### **2.1.1 Ride comfort**

Ride comfort is described by **Harty (2003)** as follows: “Ride comfort is a frequency-weighted measure of vertical acceleration, together with subjective assessments of harshness over lateral features and other secondary behaviours”.

Four methods to objectively evaluate ride comfort (also referred to as human response to vibration) are used throughout the world today. The ISO 2631 standard (**International Standards Organisation, 1997**) is used mainly in Europe and the British Standard BS 6841 (**British Standards Institution, 1987**) in the United Kingdom. Germany and Austria use VDI 2057 (**Hohl, 1984**) while Average Absorbed Power or AAP (**Pradko &**

Lee, 1966) is used by the United States of America and by NATO in the NATO Reference Mobility Model (NRMM). This presents two questions namely: (i) which method is most suitable for the evaluation of off-road vehicle ride comfort, and (ii) how does the results differ if different methods are used.

The correlation between objective methods for determining ride comfort and subjective comments from crew driving in vehicles was investigated by Els (2005). For objective measurements, the ISO 2631, BS 6841, AAP and VDI 2057 methods were used. The emphasis was on the ride comfort of military vehicles operated under off-road conditions over typical terrains.

An experiment was devised in which a 14-ton, 4x4 mine protected military vehicle (see Figure 2.1) was driven over seven different terrains, using various vehicle speeds and tyre pressures. The terrains were chosen to be representative of typical operating conditions in Southern Africa and excite significant amounts of body roll, pitch and yaw motion. Seven groups, consisting of 9 people each, were used for determining subjective comments using a questionnaire, while simultaneously recording acceleration data required for objective analysis at 11 positions in the vehicle.



**Figure 2.1** - Test vehicle

The resulting sets of measured data were converted into objective ride comfort values according to the ISO 2631, BS 6841, AAP and VDI 2057 methods. The unweighted values were also used for comparative purposes. Objective values were calculated for all the relevant parameters and measurement positions and compared to subjective ratings.

It is concluded by Els (2005) that any of the four methods under consideration, namely ISO 2631, BS 6841, AAP and VDI 2057, could be used to objectively determine ride

comfort for the vehicles and terrains of importance for the study. The vertical acceleration measurements give the best, and in fact the only reliable correlation and should be used in all cases. The RMS values are sufficient for ISO 2631, BS 6841 and unweighted values. Correlation for roll, pitch and yaw acceleration with subjective values is poor and not useful.

According to **Murphy (1984)**, a 6-Watt limit is normally assumed to be sustainable while values as high as 12 Watts can be sustained only for a short period of time. It was found by **Els (2005)** that a subjective response of 50% agrees with the 6 Watt AAP limit. Els reports the corresponding limit for the other methods to be 2.0 m/s<sup>2</sup> RMS (according to ISO 2631 - rated as “very uncomfortable” according to Table 9 and Annex C in **International Standards Organisation, 1997**). Limits of 2.8 m/s<sup>2</sup> for the unweighted RMS values, 1.8 m/s<sup>2</sup> RMS for BS 6841, a VDI 2057 value of 88 and a 4-hour vibration dose value (VDV) of 26 m/s<sup>1.75</sup> were also found. The 4-hour VDV of 26 m/s<sup>1.75</sup> is significantly higher than the VDV of 15 normally assumed to be the guideline.

Terrain inputs used for measuring or simulating ride comfort are usually described as a kind of Gaussian random or white noise input, often band limited to the frequency range of interest (**Karnopp, 1968**). The power spectral density (PSD or roughness number) approach is also used (**International Standards Organisation, 1995; Gillespie, 1992; Cebon 1999**). Very few studies use physically measured road profile data as input, because of the difficulties in accurately measuring the profile of rough roads. Discrete obstacles and sinusoidal inputs are also used.

### 2.1.2 Handling, rollover and stability

Simulation of vehicle handling is virtually non-existent in literature when analysing advanced suspension concepts. In isolated cases, handling is evaluated using step inputs and evaluating transient response.

Figure 2.2 provides a graphical representation of the broader term “handling” as described by **Harty (2005)**. Harty defines handling using this representation as the percentage of the available friction or the maximum achievable lateral acceleration utilised by the vehicle-driver combination. At values lower than the linearity limit, everybody can control the vehicle and avoid accidents. At values higher than the friction limit, control over the vehicle is physically impossible and even the most experienced driver in the best handling vehicle will lose control. He states several reasons why intervention by electronic stability enhancement systems is required namely:

- Most drivers’ “in-head” model of the vehicle is based on linearity and zero phase lags.
- Most drivers have no experience of significant loss of linearity.
- Most drivers have no experience of phase lag in yaw/sideslip resonance.
- When the vehicle departs from linearity, the population is very variable in its ability to retain control of the car.
- There is a group of events where crashes occur even though the vehicle was not exceeding the friction limit due to the driver’s lack of control skill.
- For road cars we need to match the car to the skill of the population.
- For motor sport we can calibrate the car to the individual driver’s skill level.

Harty sees the task of the vehicle designer as having two components namely: to raise the absolute friction limit and to raise the linearity limit. These simplistic statements ignore some problems namely:

- is the distance between the friction limit and the linearity limit a function of the population only and not the car?
- are we allowing some people to have crashes at higher speeds than they could previously have had?

**Harty (2005)** also compares several advanced methods for improving vehicle handling. These methods include active front steering, rear wheel steering, brake-based stability control as well as front / rear torque distribution. No mention is made of semi-active suspension control.

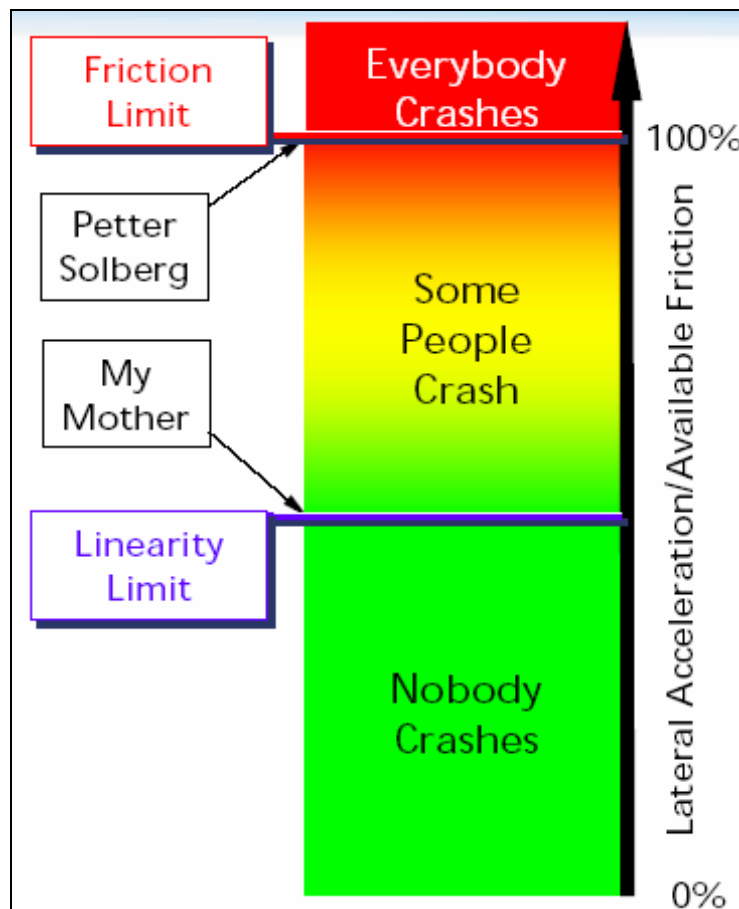


**Figure 2.2** – Handling classification according to **Harty (2005)**

While human response to vibration (ride comfort) has been extensively researched, a single, unambiguous objective criterion for handling has eluded the vehicle science community despite numerous studies pertaining to the topic. As **Vlk (1985)** notes with respect to truck-trailer devices: "It is most desirable to define evaluation criteria for the handling performance of vehicle combinations, both for steady state and transient driving behaviour".

For this reason a study was performed in order to establish relationships that can be used to objectively quantify vehicle handling (**Uys, Els & Thoresson, 2006**). The idea was to

identify parameters that can be used to specify handling and that can be used as the objective function in suspension optimisation studies. Literature on the topic will now be reviewed, followed by test results for three different vehicles and four different drivers.

### 2.1.2.1 Literature survey on handling, rollover and stability

**Horiuchi et al. (1989)** determined that drivers focus attention on yaw angle rather than on lateral position error,  $Y_e$ , for steering a two-wheel active steering vehicle (2WS). For a four-wheel steer (4WS) vehicle,  $Y_e$  becomes more important. Handling (steer response) is measured in terms of *yaw rate* and *lateral acceleration* for handling characteristics of four wheel active steering vehicles over a full manoeuvring range of lateral and longitudinal accelerations (**Masato, 1989**).

**Sharp and Pan (1991)** comment that a vehicle that exhibits no body roll in general has better steering behaviour than one that rolls.

**Crolla et al. (1998)** obtained data using the ISO defined steady state, step input (J-turn) and impulse steer tests (**International Standards Organisation, 1982 and 1988**). Metrics used for their subjective/objective driver-handling correlations include: peak *lateral acceleration* response time, peak road wheel *steer angle* and road wheel *steer angle response time*, and peak *steering angle torque* and *steering angle torque response time*. The authors conclude that frequency response results (lateral acceleration gain, yaw gain, steering gain, steering phase) are of greater value in assessing vehicle response than has to date been proven to be the case. These metrics, along with the change in sideslip with respect to the change in lateral acceleration, were rated by drivers as uniform and unequivocal indicators of steering response required. From an investigation on the correlation between the different metrics, the authors found that, over smooth roads, the degree of *roll angle* correlates with lateral acceleration gain; yaw gain and peak roll rate and response. The degree of roll angle in transient cornering correlates with lateral acceleration phase and yaw rate in a J-turn and steady state roll angle at  $2 \text{ m/s}^2$ . Controllability during a single lane change correlated with the J-turn yaw rate response at  $2 \text{ m/s}^2$  lateral acceleration (**Crolla et al., 1998**).

From these studies it can be concluded that the degree of roll angle is indicative of the lateral acceleration and yaw rate, which are both effective inputs for driver response. Lateral transient response to step input is a frequently adopted measure for assessing handling characteristics according to **Reichardt (1991)**.

Since rollover is to an extent related to handling, although handling capability and rollover aptitude is not similar, rollover considerations as deduced from the National Highway Traffic Safety Administration (NHTSA) survey were investigated (**National Highway Traffic Safety Administration, 2000**). In a proposed rulemaking exercise NHTSA was considering a safety standard “that would specify minimum performance requirements for the resistance of vehicles to rollover in simulations of extreme driving conditions”. The conclusion was that “vehicle rollover response is dominated by the vehicle’s rigid body geometry with dynamic contributions from suspension effects.” Analysis of 100 000 single-vehicle rollover crashes eventually focused on two static measurements: tilt table angle (the angle at which a vehicle will begin to tip off a gradually tilted platform) and critical sliding velocity (the minimum velocity needed to trip a vehicle which is sliding sideways) – both measurements address situations in which

a vehicle encounters something that trips it into rollover (a curb, soft dirt, the tyre rim digging into the pavement). Taking safety objectives into account, the following vehicle stability metrics were considered as having a potentially significant role in rollover: centre of gravity height, static stability factor, tilt table ratio, side pull ratio, wheelbase, critical sliding velocity, rollover prevention metric, braking stability metric and percentage of total weight on the rear axle (**National Highway Traffic Safety Administration, 2000**).

The following aspects were considered by NHTSA for rollover rating:

- a) **Static stability factor (SSF):** This is the present static rollover rating calculated by taking half a vehicle's track width divided by its centre of gravity height.
- b) **J-turn & Fish hook manoeuvres:** In order to inform the public about a vehicle's stability with specific reference to rollover, NHTSA has chosen the J-turn and the fishhook manoeuvre to rate a vehicle's performance. "They are the limit manoeuvre tests that NHTSA found to have the highest levels of objectivity, repeatability and discriminatory capability." The intention is that "vehicles will be tested in two load conditions, using the J-turn at up to 97 km/h and the fish hook manoeuvre at up to 80 km/h". "Light load conditions will be provided by the test driver who will be the test vehicle's sole occupant. Heavy load conditions will be created by adding a 79.5 kg mannequin to each rear seating position". "The dynamic manoeuvre test performance will be used to rate resistance to untripped rollovers on a qualitative scale such as A - for no tip-ups, B - for tip-up in one manoeuvre, C - for tip-ups in two manoeuvres *etc.*" (**National Highway Traffic Safety Administration, 2000**) "The reverse steer of the fishhook manoeuvre will be timed to coincide with the maximum roll angle to create an objective 'worst case' for all vehicles regardless of differences in resonant roll frequency".

In response to NHTSA's request for development of a dynamic test for rollover resistance (**National Highway Traffic Safety Administration, 2000**), the following limiting values for good rollover resistance were mentioned by General Motors: a) quasi-static centrifuge test tip-up threshold of at least 0.9g; b) maximum lateral acceleration in a circular driving manoeuvre of at least 0.6g; and c) a stability margin (a)-(b) at least 0.2g or 1.5/wheelbase [units in m<sup>2</sup>]. GM estimated that a centrifuge measurement of 0.9g would correspond to a SSF of 1.06. NHTSA however, estimated the centrifuge measurement as corresponding closer to a SSF of 1.00, based on comparisons with tilt table tests with an allowance for the vertical load error inherent with the tilt table. Ford (**National Highway Traffic Safety Administration, 2000**) suggested lane change manoeuvres producing a maximum lateral acceleration of 0.7g.

In the same survey NHTSA posed the question: Should measures of vehicle handling be reported so that consumers can be aware of possible trade-offs? What indicators of vehicle handling would be appropriate to measure, and how should this consumer information be reported? The following responses are documented:

- a) **Steady state lateral acceleration and lateral transient response:** Nissan recommended that NHTSA measure handling rather than rollover resistance, on the basis that the fishhook test may be too severe for the purposes of consumer information, and that Nissan had no data regarding the correlation of fishhook test

performance to real-world crashes. It suggested a steady state lateral acceleration test and a lateral transient response test.

**b) The following comments based on ISO 3888 Part 2 (International Standards Organisation, 2002) were made:**

- Optimised cornering capability and “limit condition performance”.  
Daimler-Chrysler addressed the question directly by stating that its recommended ISO 3888 PART 2 test does not give incentives for negative trade-offs, but rather encourages optimised cornering capability and “limit condition performance” by giving lower ratings for “bad handling”. In its recommendation of the ISO 3888 PART 2 test, Continental-Tyres actually described it as a handling test.
- Entry speed and peak-to-peak yaw rate.  
Toyota suggested using the ISO 3888 PART 2 test as a handling test with both entry speed and peak-to-peak yaw rate as performance criteria. The peak-to-peak yaw rate would reflect on the yaw stability of the vehicle.
- Centrifuge and steady state lateral acceleration tests.  
General Motors also recommended the centrifuge test, but suggested combining its results with a driving test of steady state maximum lateral acceleration to create a stability margin and set a lower limit for handling. In addition to static and dynamic rollover resistance tests, a steady state lateral acceleration test on a ski pad and “track-type tests to assess the vehicle’s controllability, response and grip” is also recommended.
- Evaluation of double lane change  
Daimler-Chrysler, Mitsubishi, Volkswagen, BMW and Continental-Tyres recommended the ISO 3888 PART 2 closed-loop tight double lane change test as the best dynamic rollover test, but also described it as a handling test. Toyota, University of Michigan Transport Research Institute, Nissan, Volkswagen and Ford recommend a separate handling test distinct from the rollover rating with particular emphasis on yaw stability and Electronic Stability Control.
- Double lane change vs. fishhook and J-turn.  
Although all rollover resistance manoeuvres are influenced by both a vehicle’s handling characteristics and its resistance to tip-up, it appears that handling dominates the double lane change manoeuvres but is less important for the J-Turn and Fishhook manoeuvres. The double lane change manoeuvres are better for studying emergency vehicle handling than rollover resistance. Clean runs of the CU and ISO 3888 tests are not limit manoeuvres in the sense of the J-Turn and Fishhook because they cannot measure tip-up after the vehicle’s direction control is lost. One way to characterize manoeuvres is by the number of major steering movements they involve. The J-Turn has just one major steering movement, the initial steer. A Fishhook has two major steering movements, the initial steer and the counter steer. A double lane change has four major steering movements, the initial lane change steer, the second lane change steer, the recovery steer, and the stabilization steer, plus some minor steering movements. These additional major steering movements increase the influence of handling for Double Lane Change results compared to J-Turn and Fishhook manoeuvres.
- Highest clean run.



NHTSA comments: "double lane change manoeuvres scored on the basis of highest "clean" run speed had no value as dynamic tests of rollover resistance". For a sample of test vehicles, there was actually an inverse relationship between double lane change speed scores and the incidence of tip-up in more severe manoeuvres that induced tip-up. The test vehicle that tipped-up the most often in other manoeuvres and at a consistently lower tip-up speed than other test vehicles, would be rated the best vehicle for rollover resistance by ISO 3888 Part 2 double lane change on the basis of maximum clean run speed. These tests measure a type of handling performance but do not measure rollover resistance".

**Holdmann & Holle (1999)** use effective dynamic wheel loads as a measure of driving safety. By taking into account the RMS values of the dynamic loads, a hard damper system assures driving comfort as well as driving safety up to 4 Hz. A soft damper system assures good results for both at frequencies from 4 to 8 Hz. At higher frequencies, a soft damper minimises body movement and a hard damper minimises dynamic wheel loads. They state that different damping systems have a very small effect on lateral dynamics.

**Choi et. al. (2001)** indicate pitch motion and roll angle as measures of steering stability in the evaluation a semi-active Electro Rheological suspension system.

For experimental comparison of passive, semi-active on/off and semi-active continuous suspensions, **Ivers and Miller (1989)** use RMS tyre contact force as an indication of wheel hop and road holding capability.

**Data and Frigero (2002)** note that it is possible to obtain valid objective indications of vehicle handling behaviour by comparing subjective evaluations by drivers of steady state circular tests, step steering wheel input and double lane change with objective parameters. This resulted in the following objective parameters being proposed as representative of vehicle behaviour:

- Lateral acceleration versus steering wheel angle,
- Yaw velocity versus steering wheel angle,
- Lateral acceleration versus yaw velocity,
- Roll angle versus lateral acceleration and
- Sideslip angle versus steering wheel angle.

Parameters, which are considered functions of lateral acceleration, are standardised with respect to steering wheel activity, which is strongly influenced by driver activity. The objective parameters representative of vehicle behaviour are the values of the regression lines and their angular coefficients at 0.4 g lateral acceleration. It was found that there is no correlation between a single partial rating and a single objective indicator. Linear combinations of the objective indicators were used to find a maximum regression coefficient. This resulted in a series of equations called partial indices that predict a subjective rating, given objective parameters as input. From this paper the most important parameters related to handling performance are **roll angle**, **lateral acceleration** and **roll velocity**, which are related to steering wheel angle, yaw velocity and lateral acceleration.

In its presentation of rollover propensity testing of light vehicles (**Forkenbrock and Garrot, 2001**), NHTSA suggests measuring steering wheel angle during a simple step steer test, a J-turn and a fishhook turn; measuring dynamic weight transfer during a

double lane change and measuring the roll rate for a steering rate of 1000 °/s in a J-turn and for 720 °/s during a fish hook turn.

In his studies of the onset of rollover, **Dahlberg (2000)** states that for the detection of instability the most frequently used method is in-vehicle measurement of lateral acceleration, followed by comparison to the steady state rollover threshold (SSRT) where the accelerometer is mounted on the front axle. SSRT is considered the maximum value of lateral acceleration that the vehicle may resist during steady state driving not to roll over. It is a sufficient but not necessary requirement for rollover to occur. The static stability factor (SSF) =  $\frac{1}{2}$  (average front and rear track width) divided by total centre of gravity (cg) height, is a first order approximation to SSRT. It is the least conservative estimation of rollover propensity and thus predicts a higher threshold. SSRT becomes smaller as more flexibility is introduced in the analysis (suspension compliance, lateral shift of cg, flexibility of tyres, chassis and frame flexibility). Another approach, taking roll and roll moment into account in addition to lateral acceleration, gives a better understanding of individual axle roll resistance. From such information it can be determined that the vehicle can roll over when the lateral acceleration is larger than the value corresponding to wheel lift. Rollover does not take place during steady state driving, but during transient manoeuvres. SSRT is a best-case measure of roll stability, whereas a worst-case measure is needed. Therefore the Dynamic Rollover Threshold is defined being the minimum absolute peak value of lateral acceleration of all manoeuvres bringing the vehicle to rollover. This defines a worst-case measure of roll stability. It is a necessary but not sufficient condition for rollover.

**Garrot et. al. (2001)** describe experiments to determine untripped rollover propensity. Different categories of vehicles are used – passenger cars, light delivery vehicles, vans and sport utility vehicles. Vehicle characterisation is done by means of manoeuvres designed to determine fundamental handling properties. For vehicles with relative higher rollover propensity, measures are designed to produce two-wheel lift off. Vehicle characterisation manoeuvres include: pulse steer, sinusoidal sweep, slowly increasing steer and slowly increasing speed (at constant steering angle up to 0.7 g lateral acceleration). Rollover propensity is determined from the following manoeuvres: J-turn, J-turn with pulse braking, a Fishhook manoeuvre using a fixed 270 degree initial steering input, a Fish hook manoeuvre using an initial steering angle 7.5 times the overall steering ratio of a given vehicle and resonant steer. They relate the degree of lift off (minor, moderate, major) and vehicle manoeuvring steer score, to rollover stability metrics (SSF, tilt table ratio and critical sliding velocity).

**Uffelmann (1983)** relates handling to the steering factor,  $p$ , calculated using the following equation:

$$p = \frac{C_{af}l_f}{C_{ar}l_r} \tag{2.1}$$

where:

- $C_{af}$  is the cornering stiffness of the front tyres,
- $C_{ar}$  is the cornering stiffness of the rear tyres,
- $l_f$  is the distance from the front axle to the centre of gravity and
- $l_r$  is the distance from the rear axle to the centre of gravity.

The limit of handling instability is considered at the point of a level tangent of the steering wheel angle versus the acceleration graph. Uffelmann considers performance

characteristics for quasi-steady-state cornering and braking. He shows that for a passenger car the ratio  $p$  and steering wheel angle increase sharply for a lateral acceleration around  $5 \text{ m/s}^2$  for braking at  $1 \text{ m/s}^2$  and between 4 and  $5 \text{ m/s}^2$  for braking between 2 and  $4 \text{ m/s}^2$  where the limit of adhesion is approached. These limits are dependent on braking balance and load conditions.

**El-Gindy and Mikulcik (1993)** indicates that yaw rate gain (ratio of yaw rate to steering angle) increases with increasing speed. The sensitivity of yaw rate gain to steering input frequency increases with increasing speed, but the sensitivity to an increase in speed, decreases as speed increases. The effect of mass, moment of inertia, front and rear cornering stiffness and location of centre of gravity is also addressed. They conclude that the strongest parameter on the yaw rate gain is the location of the centre of gravity. The cornering stiffness of the front wheels has a more pronounced effect than the rear cornering stiffness.

**Starkey (1993)** derives yaw rate and sideslip frequency response for a highway vehicle from a yaw-plane handling model valid in the linear range.

Suspension technology capable of reconciling handling, stability and ride comfort has been designed by Toyota Motor Company. The front and rear suspension settings react to the lateral force input to the tyres (**Kizu et. al. 1989**).

In order to objectively evaluate handling performance, **Harada (1997)** derives stability criteria for typical lane change cases and running against cross winds, applying a linear preview control model to the driver and a bicycle model of the vehicle. The performance index is composed of the weighted mean square values of state variables such as the course deviation, steering correction angle, yaw velocity and lateral velocity. Stability criteria consist of the steering control gain and steering time constant, which are obtained numerically for a closed loop system by the Hurwitz criteria.

In his survey of the handling performance of truck-trailer vehicles, **Vlk (1985)** mentions the following criteria that were used: lateral stability and movement, Hurwitz criterion for stability, yaw angle, lateral displacements in tyre road contact paths, lateral play at the hitch, side amplitude of trailer, frequency of trailer yaw oscillations, yaw rate gain, lateral axle deviation, side slip angle, overturning risk, lateral acceleration, change of wheel vertical loads, longitudinal tyre slip and cornering forces as a result of directional response due to braking. He also mentions experiments by Zhukov who ascertained that the roll rotation of a trailer was accompanied by a lateral displacement of both truck and trailer from their direct path. The most outstanding correlation found was between trailer roll and yaw.

**EL-Gindy and Ilosvai (1983)** mention a study of Yim *et. al.* that indicated that the slip-ratio of the front wheels relative to that of the rear wheels correlated with stability. El-Gindy investigated lane change and braking manoeuvres on dry and wet asphalt and uses lateral acceleration, yaw rate, lateral displacement and heading angle to determine stability.

It is apparent from this survey that measurement of vehicle handling is not a clear-cut matter. The aim of the survey was to determine whether a metric existed that could be used to decide when a switch over from a soft to a hard suspension setting and vice versa

should occur. It should also be such that it can be used to optimise the suspension settings. It is concluded from the information presented here that no such unambiguous metric is apparent. Different authors use a variety of different metrics. There are, however, some parameters that are worth considering. For example, the use of roll angle is frequently encountered. These frequently encountered parameters were used to direct the experimental investigation discussed in paragraph 2.1.2.3.

### 2.1.2.2 Handling tests

Handling tests can be divided into two main categories namely steady state handling tests and dynamic handling tests (also called transient response tests).

The most widely used steady state handling test is the constant radius test, where the vehicle is driven around a circle with constant radius (*e.g.* a dry skid pan). The most important parameters that need to be measured are steering wheel angle and lateral acceleration. The test starts at the lowest speed the vehicle can drive smoothly. Speed is gradually increased until the constant radius cannot be safely maintained. A graph of lateral acceleration against vehicle speed is used to determine whether the vehicle exhibits oversteer (negative gradient), understeer (positive gradient) or neutral steer (zero gradient) behaviour (**Gillespie, 1992**). Variations on this test method are the constant steering angle test (where speed and radius changes) and the constant speed test (where steering angle and radius changes).

Dynamic handling tests can be either closed loop where a human driver tries to steer the vehicle through a prescribed path, or open loop where the steering angle *vs.* time is prescribed. Closed loop tests include the severe double lane change test (ISO 3888-1, **International Standards Organisation, 1999**), obstacle avoidance test (ISO 3888-2, **International Standards Organisation, 2002**) and “Moose” or “Elk” test (**Birch, 1998**). Open loop tests can be performed either by an experienced test driver or a computer controlled steering robot. These include the J-turn (**Garrot *et. al.*, 2001**), Fishhook (**Garrot *et. al.*, 2001**), step steer and pulse steer tests (ISO 7401, **International Standards Organisation, 1988**).

### 2.1.2.3 Experimental investigation of handling

In previous simulation studies by **Els and Uys (2003)** it was shown that measurements of roll angle could be used for optimisation of suspension settings. **Choi *et. al.* (2001)**, **Data & Frigero (2002)** and **Crolla *et. al.* (1998)** also refer to roll angle as a measure of handling, as does the NHTSA survey and **Vlk (1985)** (see section 2.1.2.1). Other parameters that have prominence in handling quality measurements are lateral acceleration, dynamic weight transfer, roll rate, maximum entry speed to a clean run on a double lane change and peak to peak yaw rate. Since dynamic weight transfer is very dependent on the tyre model used in simulations and direct measurement poses complications, this property is disregarded. For suspension control it is argued that in general drivers do not drive vehicles at their performance limits, since they are not trained to do so. Preferably parameters should be sought that can be measured during regular off-road driving, on highways and over mountain passes requiring greater handling skills. Also, experience with the optimisation of suspension settings for both handling and comfort, has indicated that convergence to an optimum can readily be obtained if optimisation is first performed with respect to handling and then with respect to ride

comfort, with boundaries set on the handling parameters (**Els and Uys, 2003**). These limits of secure handling, as experienced by drivers, have not been quantified as in the case of comfort (see paragraph. 2.1.1).

With this background, an experiment was designed in which three vehicles were test driven by four drivers. The vehicles consisted of a Ford Courier LDV, a Volkswagen Golf 1 Chico and a Volkswagen Golf 4 GTI. The drivers included a man in his twenties, a woman in her forties, a man in his thirties and one in his forties. The vehicles were equipped with accelerometers, displacement sensors, roll angle sensors and equipment to measure speed. The measurements taken are indicated in Table 2.1. Measurements were taken on two tracks at the Gerotek Test Facility outside Pretoria in South Africa: a ride and handling track and a dynamic handling track for light vehicles. A single run on a rough track representing off-road conditions was also performed. These tests are considered preliminary to establish a procedure and base of comparison for future tests that may also include a constant radius and double lane change test and will be supported by a larger number of drivers.

**Table 2.1** - Summary of measurements

Instrument	Position	Measurement
Accelerometer	Front centre	Lateral acceleration
		Longitudinal acceleration
		Vertical acceleration
Accelerometer	Right rear	Lateral acceleration
		Longitudinal acceleration
		Vertical acceleration
Accelerometer	Left rear	Lateral acceleration
		Longitudinal acceleration
		Vertical acceleration
Angle sensor		Roll angle
		Yaw angle
Gyro		Roll rate
		Yaw rate
		Pitch rate
Displacement		Steering wheel angle
Speed sensor		Longitudinal speed

The Ride and Handling Track, of which a plan view is indicated in Figure 2.3, was designed to evaluate the ride and handling characteristics and driveline endurance of wheeled vehicles. The track is 4.2 km long and has 13 left turns and 15 right turns. The maximum gradient on the low mobility course used for the tests is 15%.

The Dynamic Handling Track for light vehicles, indicated in Figure 2.4, was designed to evaluate the high speed handling characteristics of light vehicles. The track is 1.68 km long (excluding the spiral curve) and has an asphalt surface. The coefficient of friction is 0.7 Scrim (average). The track consists of a wave curve, trapezium curve, spiral curve as well as a kink/hairpin combination.

#### 2.1.2.4 Results of experimental investigation

The results of the experimental investigation into the development of handling criteria will be discussed in more detail (**Uys, Els and Thoreson, 2006**). All measured data was filtered with a 4 Hz low-pass filter so that only low frequency dynamics were observed. The 4 Hz limit was also used because that is the specified frequency response limit of the

roll angle sensors used. Due to the large number of graphs, the graphs are given in Appendix A and only the main conclusions are represented here. Figures A-1 to A-4 in Appendix A refer to dynamic handling performance of a Volkswagen Golf 4 GTI as related to two different drivers. Figures A-5 to A-16 are concerned with the performance of the different vehicles, considering all the drivers, in order to obtain a global impression of vehicle performance on both the dynamic handling and ride and handling tracks. Only the results of the Courier and GTI are shown since these indicated the lowest and highest performance levels. Figures A-17 and A-18 show some results of tests performed on a Land Rover Defender 110. Unfortunately, roll angle sensors were not installed on the Land Rover. The Land Rover data is included to determine if the same trends as those observed for the other vehicle tests apply. The figures relate lateral acceleration, yaw rate and vehicle speed.

Figures A-1 and A-2 indicate measurements for the VW Golf 4 GTI on the ride and handling track for two different drivers. The trends in the relationships of longitudinal acceleration vs. lateral acceleration, yaw rate vs. roll angle, yaw rate vs. lateral acceleration and roll angle vs. lateral acceleration, are the same. This has been verified for the other drivers as well. The limiting values do however differ. For example the upper limit of the lateral acceleration is significantly higher for driver A than for driver B.

The same trends are also observed for different vehicles on different tracks, although the absolute values differ (compare Figures A-5, A-6, A-11, A-12 and A-17).

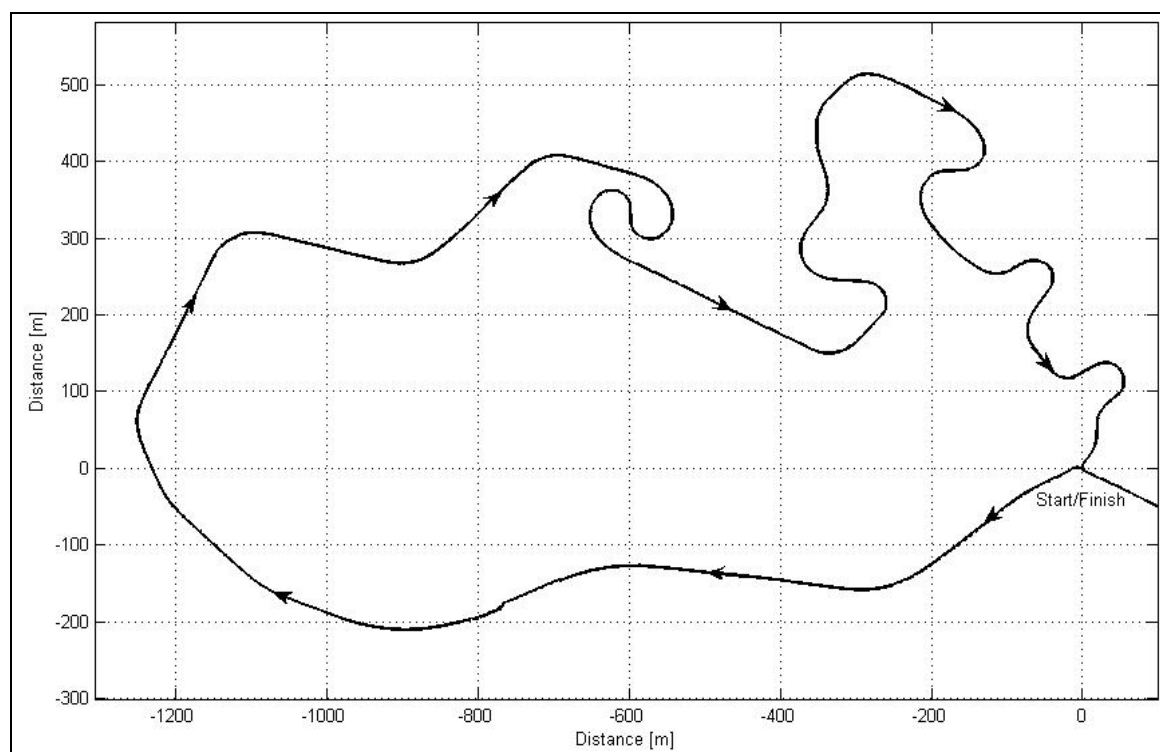


**Figure 2.3** – Ride and Handling track

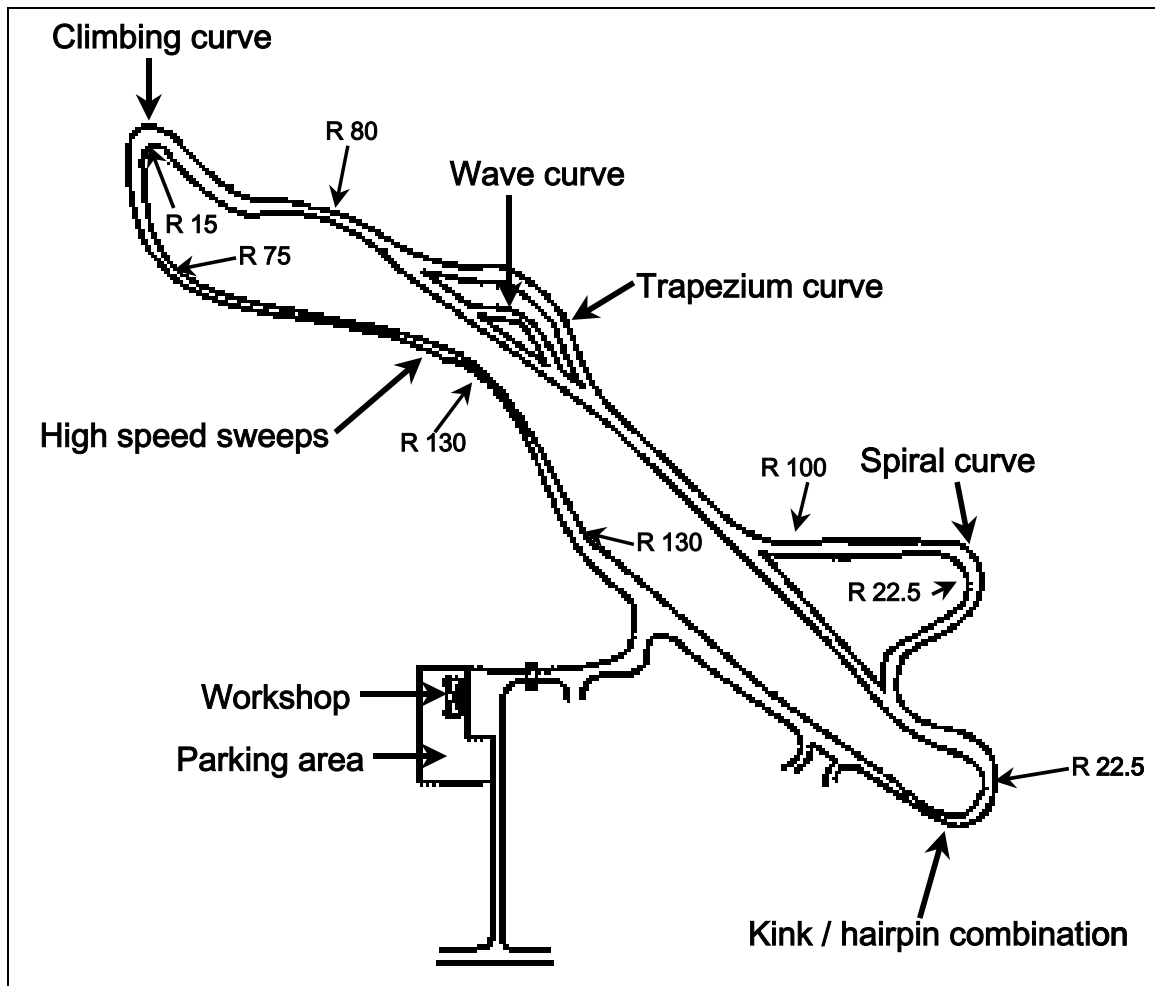


**Figure 2.4** – Dynamic handling track – light vehicles

Referring to the yaw rate vs. roll angle, yaw rate vs. lateral acceleration and roll angle vs. lateral acceleration graphs in Figures A-1 and A-2, linear dependency is observed. The linear dependency amongst the indicated parameters holds true for:

- i) Different drivers (Figure A-1 compared to A-2),
- ii) Different vehicles (Figure A-5 compared to Figure A-11 and Figure A-6 compared to Figure A-12, refer also to Figure A-17 for yaw rate vs. lateral acceleration)
- iii) Different test tracks (Compare Figures A-5 and A-6 and Figures A-11 and A-12).

Differences in gradients amongst the vehicles can be attributed to differences in suspension roll stiffness. This effectively means that the same levels of lateral acceleration can result in different roll angles for different vehicles, depending on spring, damper and anti-rollbar characteristics as well as other vehicle parameters such as suspension kinematics, centre of gravity height *etc.* This is especially true for off-road vehicles with high centres of gravity that will normally roll over before the limits of tyre side force are reached. In these vehicles, body roll and rollover propensity is more important than the ultimate lateral acceleration that can be generated by the tyre forces.

The limiting hyperbolic tendency between lateral acceleration and vehicle speed is apparent from Figures A-5, A-6, A-11 and A-12 (see “envelope in figures), confirming the applicability of the handling control based on these limits (**Hirose et. al. 1988**).

The non-linear tendency between yaw rate and lateral acceleration for the Ford Courier on the dynamic handling track (Figure A-5), is attributed to side-slip of the rear wheels, since the vehicle exhibits considerable understeer behaviour that goes into limit oversteer.

Limited test results that were available for a Land Rover Defender 110 were also analysed (Figures A-17 and A-18) and similar trends were observed.

The lateral acceleration and roll angle histograms (Figures A-3, A-4, A-7 to A-10, A-13 to A-16 and A-18) indicate more clearly the limits in lateral acceleration and roll angle achieved on the various tracks by the different vehicles and drivers. It is clear from Figures A-3 and A-4 that driver A spent more time at the vehicle limits, while driver B kept within safer boundaries.

The difference in limiting values for the different vehicles, drivers and tracks can also be observed. The limits are thus related to the track, driver and vehicle properties. More noise is observed on the ride and handling track than on the dynamic track. The irregular surface and bumps induce more high frequency motion.

No relation similar to that observed for yaw rate, lateral acceleration and roll angle is observed for roll rate.

The limiting values relating to the tracks on which the tests were performed are listed in Table 2.2.

**Table 2.2** - Limiting parameter values (all vehicles and all drivers)

Parameter	Ride and handling track	Dynamic handling track
Roll angle [°]	-3.5 to +3.5	-2 to +2
Lateral acceleration front centre [g]	-1.4 to +1.0	-1 to +0.7
Roll rate [°/s]	-32 to +32	-10 to +15
Yaw rate [°/s]	-35 to +35	-32 to +35
Steering angle [°]	-60 to +130	-48 to +48
Vehicle speed [km/h]	0 to 120	0 to 100
Longitudinal acceleration [g]	-0.8 to +0.4	-0.1 to +0.5

Lateral acceleration is often considered by analysts as a measure of handling performance. The observed relationship between lateral acceleration and roll angle can be verified by considering the moment distribution of a total vehicle about the roll axis during steady state cornering (Gillespie, 1992):

$$\phi = \frac{Wh_1/g}{K_{\phi f} + K_{\phi r} - Wh_1} a_y, \tag{2.2}$$

*i.e.* linear dependence determined by the roll stiffness.

Here  $a_y$  is the lateral acceleration,  $K_{\phi f}$  is the front roll stiffness of the suspension,  $K_{\phi r}$  the rear roll stiffness,  $W$  the weight and  $h_1$  the distance from centre of gravity to the roll axis.

### 2.1.2.5 Conclusion from the handling investigation

A linear relationship between lateral acceleration and roll angle has been observed in the case of all drivers of different vehicles on a ride and handling as well as a dynamic handling track. The range of values of roll angle observed for the tracks referred, is between  $-3.5^\circ$  and  $3.5^\circ$ . The same levels of lateral acceleration result in different roll angles for different vehicles, depending on vehicle parameters. This is especially true for



off-road vehicles with high centres of gravity that will normally roll over before the limits of tyre side force are reached. In these vehicles, body roll and rollover propensity is more important than the ultimate lateral acceleration that can be generated by the tyre forces.

Although the maximum lateral acceleration that can be achieved by a vehicle during, *e.g.* a constant radius test, can be used as a measure of handling, at lower speeds the lateral acceleration will only be a function of the vehicle speed and the radius of the turn, and not of the vehicle suspension or tyre characteristics. Suspension and tyre characteristics will however influence the over- or understeer behaviour. If a vehicle was tested through *e.g.* a double lane change or constant radius test, at a speed below the maximum capability of the vehicle, the lateral acceleration will be essentially the same for a wide range of suspension characteristics, but the body roll angle will differ significantly.

The tests conducted strongly suggest that roll angle is a suitable metric to measure the effect of suspension stiffness and damping on vehicle stability during handling tests. From previous results it is known that roll angle is also suitable for the optimisation of suspension settings given a prescribed road and manoeuvre. If levels of acceptable roll angle can be determined, this metric can be used as criterion to ascertain the moment of switchover for a semi-active suspension. Whether the value of the roll angle is a sufficient indicator to determine suspension settings on rough roads, remains to be verified.

Although this study with four drivers and three vehicles is definitely not exhaustive, and does not include off-road vehicles driven over rough terrain, it substantiates the use of body roll angle as a measure of vehicle stability during handling tests. This result is sufficient for the requirements of this study. Future research should include tests on a larger number of vehicles and include more drivers to determine the limits of acceptable roll angle.

### 2.1.3 Ride comfort vs. handling

According to **Harty (2003)**, controllable suspension systems must be designed to deliver improvements in ride comfort, handling and stability. These characteristics are to some extent in conflict with each other. It is also important that controllable systems give the maximum benefit for the smallest possible actuation forces or energy requirements.

**Karnopp (1983)** states that for ride comfort, the suspension should isolate the body from high frequency road inputs. At lower frequencies the body and wheel should closely follow the vertical inputs from the road to improve handling. Resonance of the body and wheel should be controlled, so that these disturbances are not excessively amplified and so that wheel hop and loss of wheel contact with the ground can be avoided. The suspension must also control forces due to change in payload, forces from braking and cornering and aerodynamic forces.

**Wallentowitz and Holdman (1997)** conclude that two spring stages are sufficient to overcome the compromise associated with passive systems. A soft spring is required to optimise ride comfort while a stiff spring is only used during cornering and braking when the soft spring will result in unacceptable body roll and pitch.

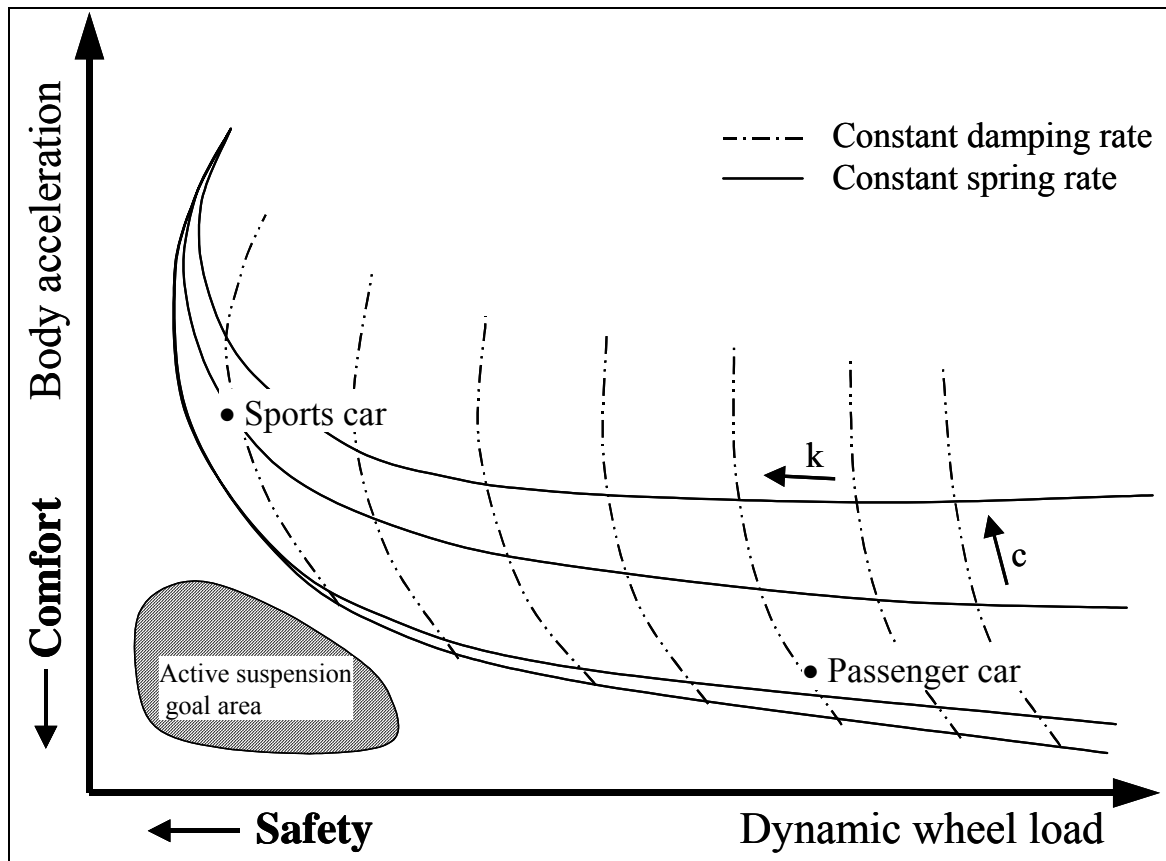


Figure 2.5 - Suspension design space according to Holdman and Holle (1999)

Holdman and Holle (1999) investigate the possibilities to improve ride comfort and handling of a 3.5-ton delivery vehicle. They illustrate the compromise in terms of the graph given in Figure 2.5. Any passive system will only resemble one point on this graph and is thus always a compromise between comfort and safety. They use three different damping curves namely soft (2/3 of standard), standard and hard (1.5 times standard) and investigate various skyhook-derived strategies. They find that for the passive damper, damping should be high at frequencies below 4 Hz to ensure comfort and safety. Between 4 and 8 Hz, low damping gives best results for both comfort and safety. Above 8 Hz a soft damper improves comfort, but a hard damper improves safety (minimizes the dynamic wheel load). Different damping systems have a small effect on lateral dynamics (handling). Additional forces need to be applied between the body and the wheel as a function of lateral acceleration to reduce body roll angle.

Karnopp and Margolis (1984) discuss the effects of a change in spring and damper rates on the transfer function of a single degree of freedom suspension system. It is said that changing the damping alone is not a very efficient way of stiffening or softening a suspension system. Changing the spring stiffness changes the natural frequency of the system but the asymptotic attenuation at higher frequencies stays the same. The study concludes that a system containing variable spring and damper rates can be very advantageous in improving ride comfort.

A vehicle suspension system must be designed to provide adequate damping over a range of driving conditions *e.g.* smooth and rough roads, laden and unladen conditions as well as good ride comfort and handling according to Hine and Pearce (1988). This leads to

the well-known conflict between the maximum use of suspension working space for best ride comfort and the need to provide sufficient displacement for all road conditions and road surfaces. Their proposed solution is a two- or three-state semi-active damper with ride height control.

According to **Ikenaga et. al. (2000)**, vehicle suspension system performance is typically rated by its ability to provide improved road handling and improved passenger comfort. Automobile suspension systems using passive components can only offer a compromise between these two conflicting criteria by providing fixed spring and damper characteristics. Sports cars usually have stiff, harsh suspensions with poor comfort while luxury cars offer good ride but poor handling. This compromise has existed since the development of the first automobiles in the late 1800's.

**Nell (1993)** states that suspension design involves a compromise between two conflicting requirements. To ensure good support of the vehicle body, stability, handling and side wind stability a stiff suspension is required. Good vibration and shock isolation on the other hand requires a soft suspension. Soft suspension characteristics suffer drawbacks e.g. when the suspension working space is limited, frequent bump stop contact can occur. Large static position changes due to variations in vehicle load can also be a problem.

Many investigators therefore agree that ride comfort and handling requirements are often in conflict with each other. The two case studies that will be presented now analyses the spring and damper characteristics required for optimum ride comfort and handling stability as applicable to off-road vehicles.

## 2.2 Case study 1: Landmine protected vehicle

**Els & Van Niekerk, (1999)** perform evaluation of the ride comfort and handling of a heavy off-road military vehicle using DADS (Dynamic Analysis and Design System) software. The vehicle used for simulation is a 12-ton 4x4 military vehicle, designed for off-road use over very rough terrain. A photograph of the vehicle is shown in Figure 2.6.

The three-dimensional, multiple degree of freedom, non-linear DADS simulation model consists of 11 rigid bodies (vehicle body, 4 wheels, front axle, rear axle, ground, 2 front hubs and steering pivot). The wheels and hubs are connected to the axles using 7 revolute joints while axle locating rods and steering links are modelled using 10 spherical-spherical joints. Force elements consist of non-linear dampers, springs (linear and hydropneumatic, depending on simulation), bump stops, as well as a generic non-linear tyre model.

The resulting model has 66 degrees of freedom but after adding joints, constraints and a driver model, 14 unconstrained degrees of freedom remain. These consist of the vehicle body displacements (lateral, longitudinal, vertical, roll, pitch and yaw), wheels (rotation), front axle (vertical, roll) and rear axle (vertical, roll). Non-linear spring, damper, bump stop and tyre characteristics are used. The vehicle is steered over a predetermined course by a simple driver model that estimates the lateral position error based on the yaw angle of the vehicle body at the current time step and the desired lateral position at the driver preview time of 0.6 seconds. The driver model is implemented using amplifiers, summers and input elements.



**Figure 2.6** - Photograph of vehicle used in simulation

### 2.2.1 Vehicle model

To make provision for controlling the semi-active spring-damper system in future simulation work, the DADS model is exported for use in Matlab/Simulink by defining plant inputs and outputs. By doing this, the complete non-linear DADS model is included as an S-function and solved in Simulink. In this case, the DADS model provides relative spring displacements, damper velocities and other parameters needed as inputs to the control algorithm. Simulink then calculates the spring and damper forces according to the control strategy and outputs these forces to the DADS model.

### 2.2.2 Terrain inputs

In this study, typical rough terrain inputs, such as a Belgian paving track, were used. Instead of performing only the normal straight line ride comfort simulation, the vehicle is also steered over the terrain in order to try and follow a predetermined course. A typical double lane change manoeuvre was performed over the Belgian paving.

### 2.2.3 Results

Simulation was performed with different spring and damper characteristics in order to complete a sensitivity analysis. A severe double lane change manoeuvre, performed over Belgian paving at a vehicle speed of 60 km/h, was chosen as representative of high speed off-road driving on gravel roads and tracks. The speed of 60 km/h is close to the maximum double lane change speed achievable with the particular vehicle on a level paved surface.

As the simulation included ride comfort, stability and handling, interpretation of the results are difficult and it is necessary to define certain performance criteria. For ride comfort, the vertical acceleration at the vehicle body's centre of gravity was filtered using the BS 6841  $W_b$  filter and the RMS value determined. Motion sickness dose values were determined in a similar fashion using the motion sickness or  $W_f$  filter. When driving in off-road conditions, body roll and pitch usually give the first indication that the vehicle speed is excessive. Furthermore, it is more difficult to brace the human body against roll and pitch motion than is the case for yaw or vertical motion. Stability and handling were therefore evaluated using the RMS roll angle, RMS roll velocity and RMS pitch velocity of the vehicle body.

Two suspension configurations were simulated namely linear springs (see Table 2.3 for the stiffness and static deflection) as well as non-linear hydropneumatic springs (see Table 2.4). In both cases the damper force ratios (damper force normalised to the baseline damper force at any specific damper speed) were varied between 0.001 and 3. For both linear and hydropneumatic springs, 9 different spring and 12 different damper characteristics were simulated, giving a total of 108 simulation runs. The simulation results are presented as contour plots (Figures 2.7 to 2.10) where the horizontal axis represents the damper force ratio and the vertical axis the natural frequency (or stiffness) of the suspension system. The contours represent the percentage improvement in the respective values relative to that of the baseline suspension (damper force ratio of 1 and natural frequency of 1.2 Hz). The left hand bottom corners of the graphs (low spring and damper rates) have no contour lines since the suspension is so soft that the vehicle could not perform the double lane change manoeuvre and rollover occurred. Figures 2.7 to 2.10 represent the results for the linear springs but the trends are very similar for the hydropneumatic springs.

**Table 2.3** - Calculated spring stiffness for linear spring

Natural Frequency [Hz]	Required spring stiffness [N/m]	Static deflection [m]
0.6	33 034	0.668
0.8	60 276	0.366
1.0	97 486	0.226
1.2	146 671	0.151
1.4	210 800	0.105
1.6	294 324	0.075
1.8	404 095	0.055
2.0	551 123	0.040
3.0	3 985 988	0.0055

**Table 2.4** - Natural frequencies for hydropneumatic spring

Static Gas Volume [Litre]	Natural Frequency [Hz]	Stiffness in Static Position [N/m]
0.3	1.51	255 100
0.5	1.20	146 280
0.6	1.10	120 550
0.8	0.96	89 200
1.0	0.86	70 780
1.3	0.76	54 050
1.6	0.69	43 710
2.0	0.62	34 830
3.0	0.50	23 100

Figure 2.7 indicates the relationship between natural frequency (spring stiffness) and damper force ratio on the ride comfort for the linear spring configuration. A maximum improvement of 55% is reached at a natural frequency of 1 Hz and damper force ratio of 0.2. The percentage improvement is calculated using Equation 2.3.

$$\% \text{ improvement} = \frac{(\text{baseline value} - \text{new value})}{\text{baseline value}} * 100 \tag{2.3}$$

The trend indicates that further improvements in ride comfort may be possible at lower natural frequencies, but that the vehicle becomes unstable and rolls due to the handling manoeuvre. The best spring characteristic for ride comfort is therefore as low as can be tolerated from a stability and handling perspective. Although a reduction in damper force ratio improves ride comfort, a certain minimum damping level is required.

A maximum improvement of 51% in the motion sickness dose value (not indicated) was achieved for the lowest natural frequency and highest damper force ratio. The motion sickness dose value was however much less sensitive to the damping value than to the natural frequency. It was expected that the motion sickness dose value should increase with a reduction in suspension natural frequency, but apparently this is offset by the improved isolation performance of the lower natural frequency suspension.

Figure 2.8 indicates that a maximum pitch velocity improvement of 11% is achievable at a damper force ratio of 0.7 and natural frequency of 1.2 Hz. This is in close correlation to the ride comfort optimum although the improvement is not very significant in magnitude compared to the ride comfort improvement of 55%.

A maximum improvement of 77% in roll angle (Figure 2.9) is achieved at a suspension natural frequency of 3 Hz. The roll angle improvement is insensitive to the damper force ratio as can be expected. The optimal characteristics for roll velocity (improvement of 32%) are achieved at a suspension natural frequency of 2 Hz and damper force ratio of 1.8 (see Figure 2.10). Both roll angle and roll velocity are therefore reduced by higher spring and damper characteristics although the trends indicate that there is little improvement after the spring and damper characteristics have been doubled from the base-line values. This is due to the increase in tyre deflection that occurs as the spring stiffness is increased.

All the graphs shown are for the linear suspension configuration mainly due to the wider range of suspension natural frequencies that could be indicated. All the tendencies are however similar for the non-linear hydropneumatic suspension system.

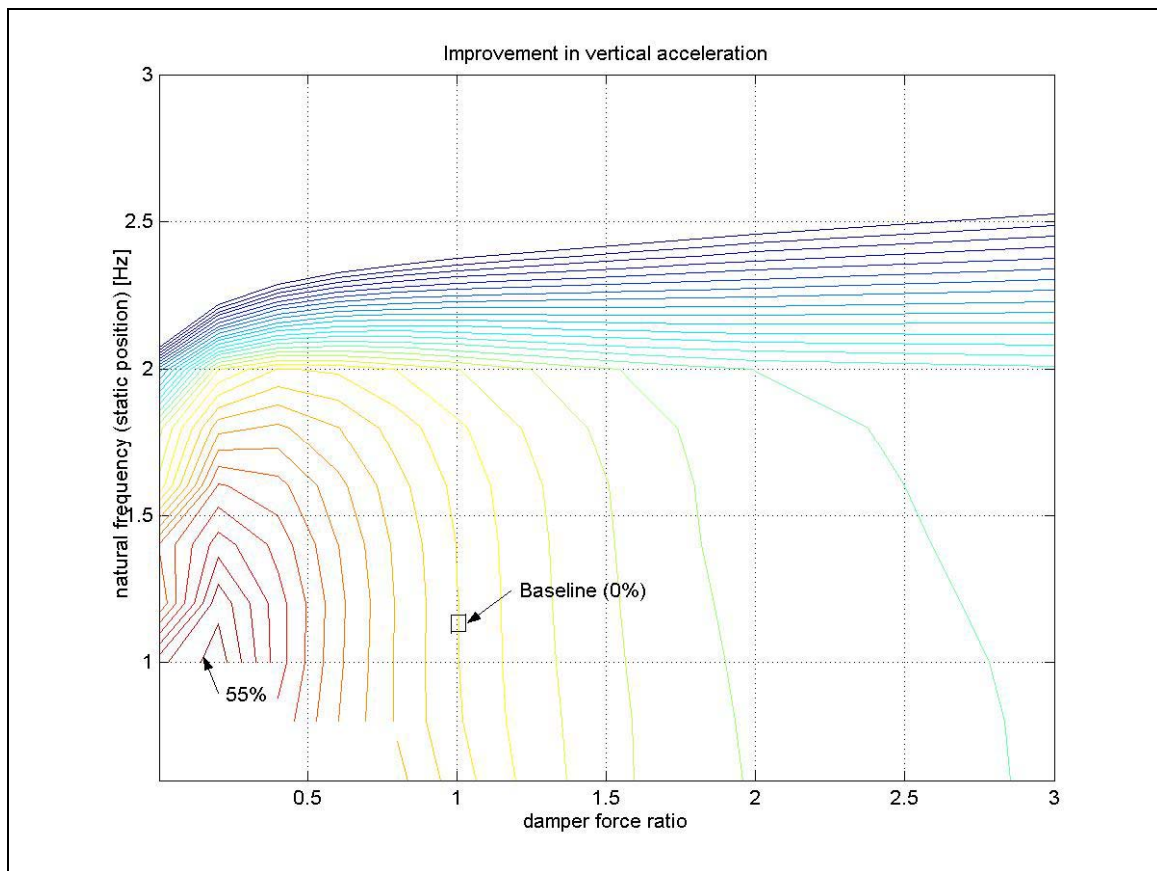


**Figure 2.7** - Improvement in weighted RMS vertical acceleration (ride comfort – linear spring)

The expected conclusion is made that ride comfort requires opposite characteristics to handling and stability. The suspension resulting in the best ride comfort, leads to rollover. This fact gives a good motivation for the use of a semi-active spring-damper system to improve both ride comfort and handling. The semi-active spring-damper system has to be designed with natural frequencies of approximately 0.6 and 2 Hz respectively while damper force ratios of 0.2-0.5 and 2.0 are required. It must be emphasised that these characteristics are for the passive suspension case only and may change when research on control strategies is continued. The results are also only valid as long as terrain inputs do not result in contact with the bump-stops. When bump-stop contact occurs, stiffer suspension may result in improved ride comfort. The semi-active hydropneumatic spring-damper system can however adapt to these circumstances if a suitable control strategy is employed. Valve dynamics and response times may also affect the results.

Although the simulation results indicate optimal values for the spring and damper characteristics, these characteristics may not always be obtainable on a practical vehicle suspension system because of certain physical constraints.

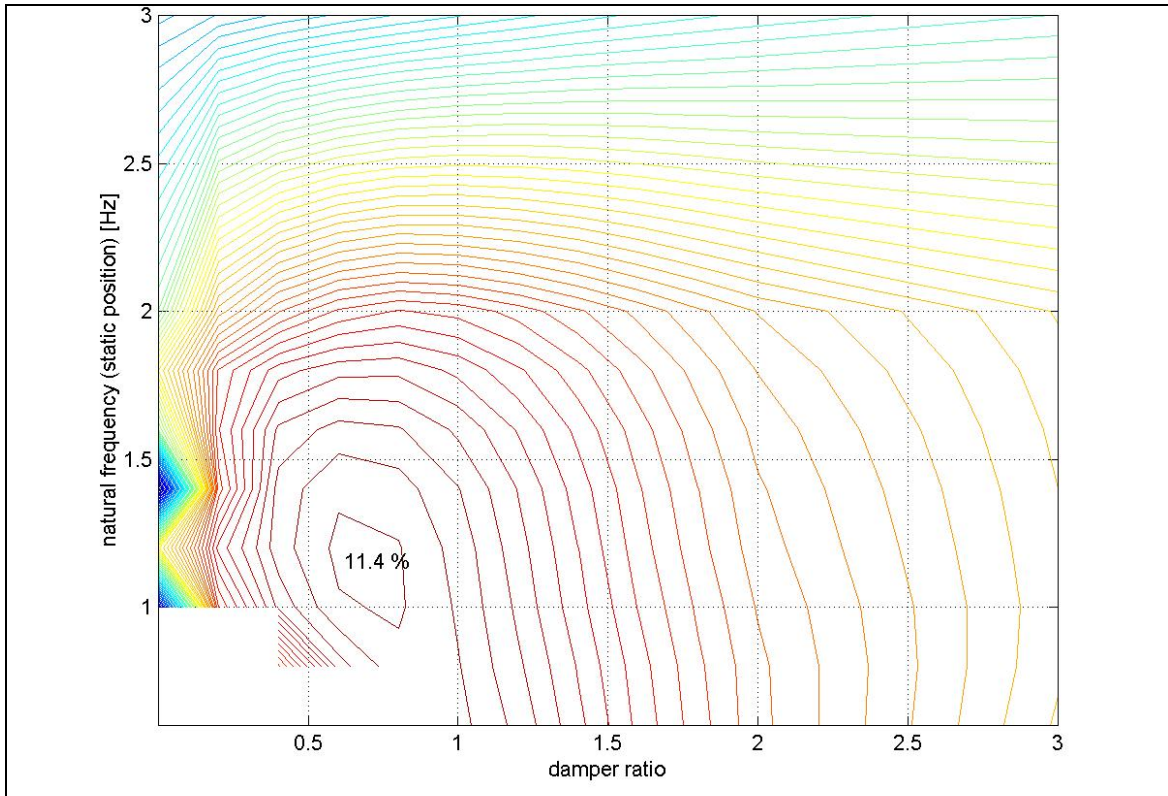


**Figure 2.8** - Improvement in pitch velocity (linear spring)

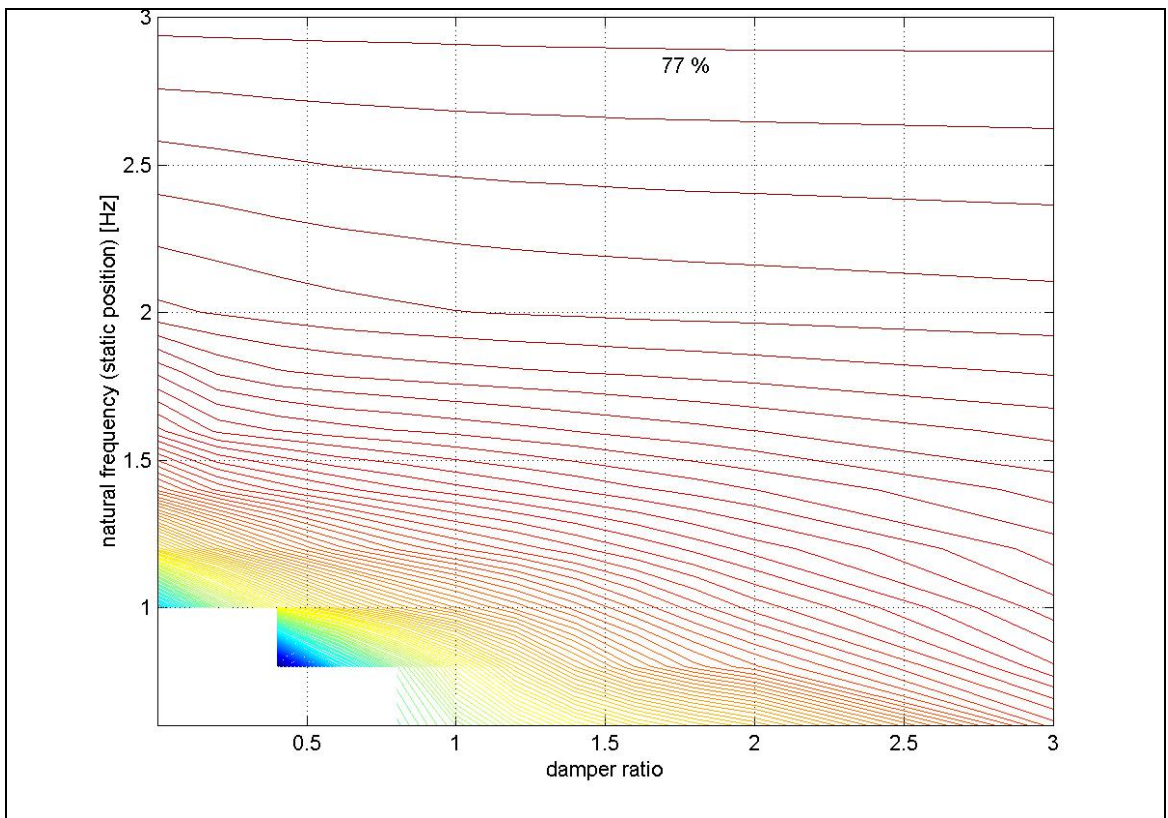


**Figure 2.9** - Improvement in roll angle (linear spring)



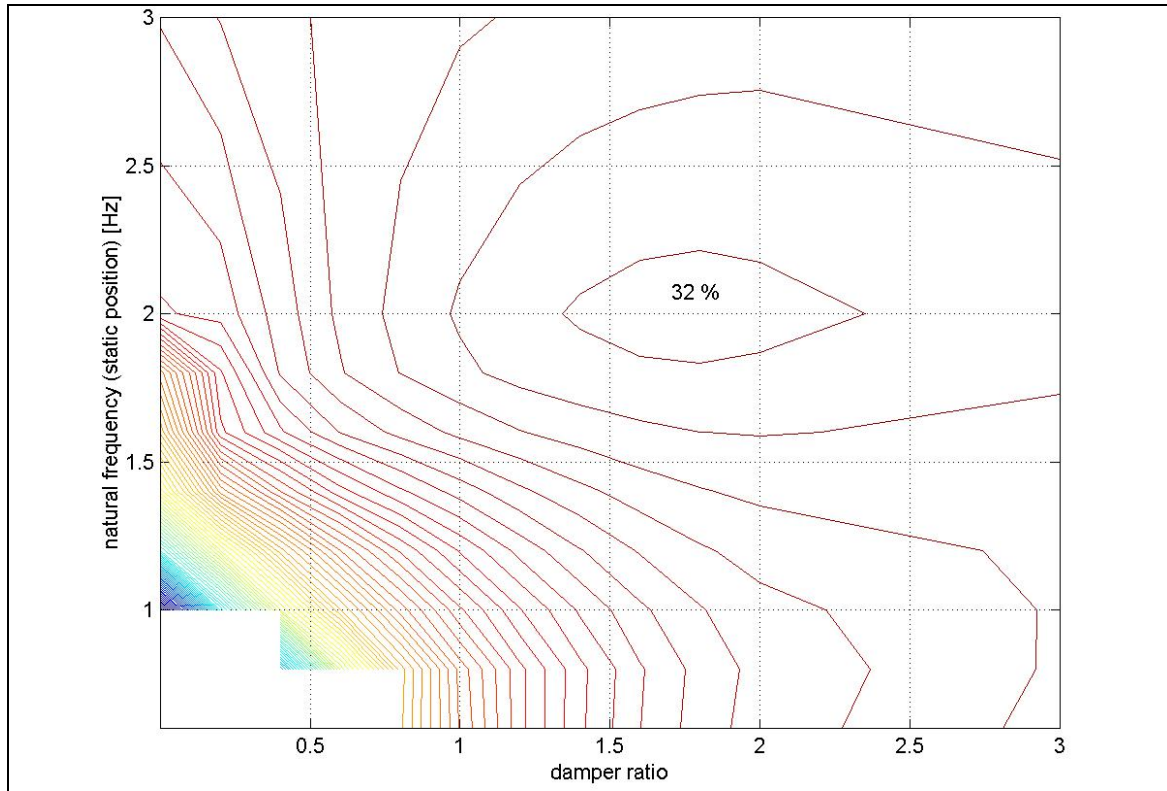


**Figure 2.10** - Improvement in roll velocity (linear spring)

The maximum rebound damper force is limited by the pressure difference across the damper. When the pressure difference becomes so large that the pressure in the hydraulic strut approaches zero, then cavitation will occur. The oil will boil and apart from the physical damage that may result, the damper force will stay constant. The minimum damper characteristic on the other hand is limited by the flow loss through the channels and hydraulic valves.

The sprung mass natural frequency of a quarter car suspension system is calculated by approximation according to equation 2.4.

$$f_n = \frac{1}{2\pi} \sqrt{\frac{k_s \cdot k_t}{k_s + k_t} \cdot \frac{1}{M}} \quad (2.4)$$

- Where  $f_n$  = Sprung mass natural frequency [Hz]
- $k_s$  = Spring stiffness [N/m]
- $k_t$  = Tyre stiffness [N/m]
- $M$  = Sprung mass [kg]

For the vehicle under consideration,  $k_t = 1\,000\,000$  N/m and  $M = 2\,250$  kg. Table 2.3 indicates the required linear spring stiffness and static deflection for different natural frequencies.

It is evident that in order to obtain a natural frequency of 3 Hz, the spring stiffness must be four times higher than the tyre stiffness while the static deflection of the spring is only 5.5 mm. This implies that the tyre will deflect significantly, negating the effect of the stiff

spring. On the other hand, the static deflection of 0.668 m, required for a 0.6 Hz natural frequency, is also unreasonable.

Similar limitations are applicable to the hydropneumatic spring except that the spring stiffness used for calculation of the natural frequency is linearised through the static suspension position. Table 2.4 indicates the natural frequencies calculated for different static gas volumes. An accumulator of 2 or 3 litre capacity is bulky and it is doubtful whether this will fit into the space envelope normally available on a vehicle.

### 2.2.4 Conclusions from Case Study 1

The results indicated that for best ride comfort, the damper force ratio should be between 20 and 50% of the baseline value and the natural frequency should be in the region of 0.6 Hz. For optimal stability and handling, the natural frequency should be around 2 Hz and the damper force ratio double the baseline value. These characteristics will be used as the starting point for determining the best “on” and “off” characteristics for a controlled, two-stage semi-active hydropneumatic spring and damper system. It should however be noted that these values may differ for other vehicle speeds, terrain inputs or handling manoeuvres. The values might also be vehicle-specific.

## 2.3 Case Study 2: Land Rover Defender 110

A Land Rover Defender 110 vehicle was chosen for case study 2 as well as for the rest of the research discussed in this thesis. This vehicle is ideal due to the following reasons:

- i) A used vehicle in good condition could be obtained at an affordable price.
- ii) The vehicle has a good reputation for its off-road capability.
- iii) It is a “low technology” vehicle that greatly simplifies the required modifications.
- iv) The vehicle has a ladder frame chassis that makes it possible to easily modify mounting points for fitting a controllable suspension system.
- v) The design is square and boxy resulting in enough space in the wheel arches.
- vi) It is easy to mount different springs and dampers to the vehicle.
- vii) Considerable improvements in handling can be obtained.
- viii) The vehicle has a high center of gravity that should highlight the improvements offered by a controllable suspension system.
- ix) The vehicle is fitted with coil springs. The suspension is already located by links and bars, *i.e.* spring and damper characteristics can be changed without changing kinematics. The springs and dampers also perform no axle locating functions.

### 2.3.1 Vehicle model

In order to simulate the ride comfort and handling of the vehicle, a first order DADS simulation model, based on a combination of measured and estimated parameters for a Land Rover Defender 110 sports utility vehicle (see Figure 2.11), was developed. A second, more detailed model was later developed and is discussed in paragraph 2.4.



**Figure 2.11** - Land Rover Defender 110 vehicle

The DADS model has 81 degrees of freedom, but after adding joints, constraints and a driver model, 14 unconstrained degrees of freedom remain. These consist of the vehicle body displacements (lateral, longitudinal, vertical, roll, pitch and yaw), wheel rotations, front axle vertical displacement and roll and rear axle vertical displacement and roll. Non-linear spring, damper, bump stop and tyre characteristics are used. The vehicle is steered over a predetermined course by a simple driver model which estimates the lateral positional error based on the yaw angle of the vehicle body at the current time step and the desired lateral position at a specified driver preview time. The driver model is implemented using amplifiers, summers and input elements. The basic components of the DADS model are summarized in Table 2.5.

### 2.3.2 Definition of “design space”

The upper limit of spring stiffness is limited by the tyre stiffness. If the spring stiffness becomes too high, the tyre stiffness will become dominant, negating the effect of the stiff spring. As tyre deflection increases, the lateral force capability will decrease as the tyre’s lateral stiffness decreases. The lower limit of the spring stiffness is limited by two factors namely motion sickness and restricted suspension movement (“rattle space”). If the spring stiffness is so low that the suspension natural frequency is well below 1 Hz, the incidence of motion sickness in the vehicle will increase. A softer spring will also require more travel than a stiff spring over the same terrain roughness.

The upper limit for damper force in rebound is the cavitation of the oil when the pressure in the damper drops to the vapour pressure of the oil. There is no physical limit to compression damping, although the effect of the bulk modulus will increase and mechanical buckling of the damper rod may arise. The lower limit for damping is determined by the flow losses through the damper valves, valve block channels as well as friction.

The coil springs on the baseline suspension were replaced with hydropneumatic springs where the spring stiffness is determined by the gas volume in the static position. Static gas volumes were varied between 0.01 litres and 3.0 litres. This gives a range of spring stiffness from about 10 to 0.1 times that of the baseline coil spring stiffness. To simplify the damper characteristics, the baseline damper force was scaled with a constant factor that varied between 0.5 (i.e., softer than baseline) up to 3 (3 times higher than baseline). Simulations were performed for 7 damper characteristics and 10 spring characteristics within these ranges, giving a total of 70 simulation runs.

**Table 2.5** – Summary of the DADS simulation model

Model entities	Components	Quantity
Rigid bodies (13)	Vehicle body	2
	Wheels	4
	Front axle	1
	Rear axle	1
	Ground (fixed in space)	1
	Front hubs (left & right)	2
	Anti-rollbars	2
Revolute joints (9)	Front wheels to front hubs	2
	Front hubs to front axle	2
	Rear wheels to rear axle	2
	Body torsional stiffness	1
	Anti-rollbar left and right	2
Spherical-spherical joints (5)	Axle locating and push-pull rods, steering links	5
Revolute-revolute joint (1)	Radius rod	1
Revolute-spherical joints (2)	A-arm rear	1
	Panhard rod front	1
Constraints (2)	Steering control input	1
	Forward speed	1
Force elements (18)	Non-linear dampers	4
	Springs (choice of hydropneumatic and coil springs)	4
	Bump stops	4
	Generic tyres	4
	Body torsional stiffness spring	1
	Anti-rollbar stiffness	1
Control elements (9)	Amplifiers	2
	Summers	2
	Inputs	2
	Steering angle limiter	1
	Output torques left and right	2
Initial conditions (1)	Vehicle forward speed	1

### 2.3.3 Simulation results

The DADS model was used to predict ride comfort and handling of the vehicle with different combinations of spring and damper characteristics. Simulation results were used to determine first order indications of the “best” soft and hard characteristics for both spring and damper.

#### 2.3.3.1 Ride comfort

Ride comfort was simulated over a typical off-road terrain (Belgian paving block course) at a vehicle speed of 60 km/h. Ride comfort was evaluated using the vertical acceleration at the driver position (right front) as well as the left rear passenger position. The vertical acceleration was weighted using the British Standard BS 6841  $W_b$  weighting filter and

calculating a weighted root mean square (RMS) value. A three-dimensional plot of weighted RMS acceleration vs. spring static gas volume and damper scale factor, for the driver's seat position, is indicated in Figure 2.12.

The lowest acceleration levels (best ride comfort) are obtained with low damping (damper scale factor of 0.8) and soft springs (static gas volume > 0.5 litres). Motion sickness values do however increase with very soft springs (not shown).

### **2.3.3.2 Handling**

Handling was simulated by performing a severe double lane change manoeuvre at a speed of 60 km/h for the same values of spring and damper characteristics used for ride comfort analysis. Maximum body roll angle was used as the evaluation parameter of handling and stability. Figure 2.13 indicates the results of the handling simulations. The smallest body roll angle is achieved with the stiffest spring (static gas volume of 0.01 litre) while the roll angle is insensitive to the damper scale factor as could be expected. The "best" suspension is therefore given by the highest possible spring stiffness. The areas where there are no data points on the graph are where the vehicle could not complete the lane change without rolling over.

### **2.3.3.3 Combined ride comfort and handling**

The investigation was further extended by looking at a scenario where ride comfort and handling were simultaneously required. For this analysis, a double lane change was performed over the Belgian paving. The result is indicated in Figure 2.14. The infeasible area where the vehicle rolls over is now significantly enlarged. The suspension design is forced towards higher spring stiffness to keep the vehicle safe, at the expense of ride comfort.

### **2.3.4 Conclusion from Case Study 2**

It is concluded that for best ride comfort, a soft suspension is needed and for best handling a stiff suspension is needed. This is in line with general design rules and was the motivation for initializing this research project. The simulation results do however indicate that for the hard suspension setting, a static gas volume of 0.1 litre and damping scale factor of between 2 and 3 is suitable and for the soft suspension setting, a gas volume of greater than 0.5 litre and a damping scale factor of 0.8 will be suitable first order values for the design. The high damper characteristic used in the design of the suspension system will therefore be between 2 and 3 times the baseline values, while the low damping should be less than 0.8 times the baseline value.

This also confirms the results obtained for case study 1.

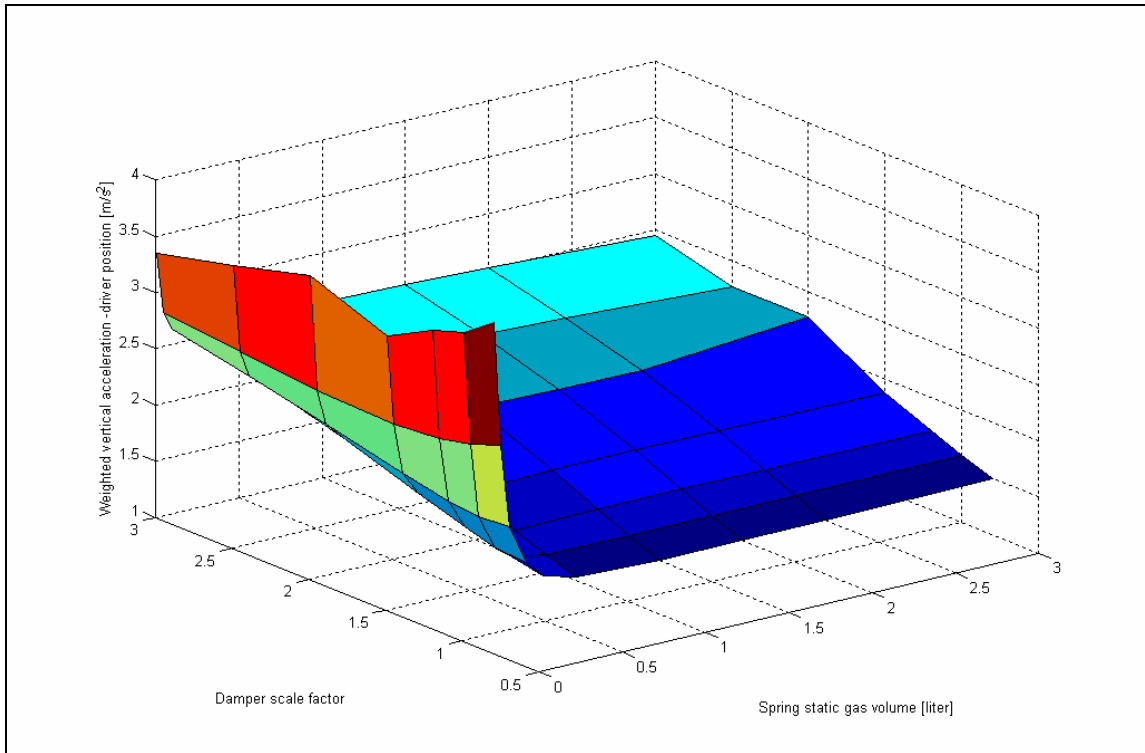


Figure 2.12 - Results of ride comfort analysis

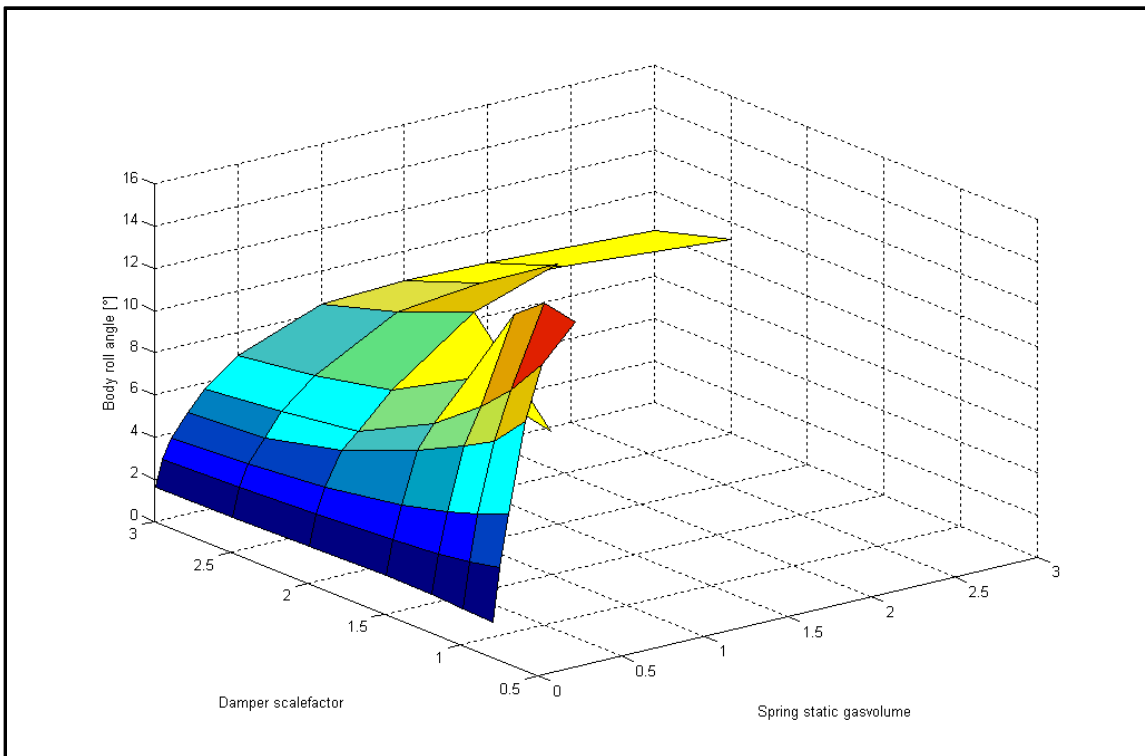


Figure 2.13 – Results of handling analysis

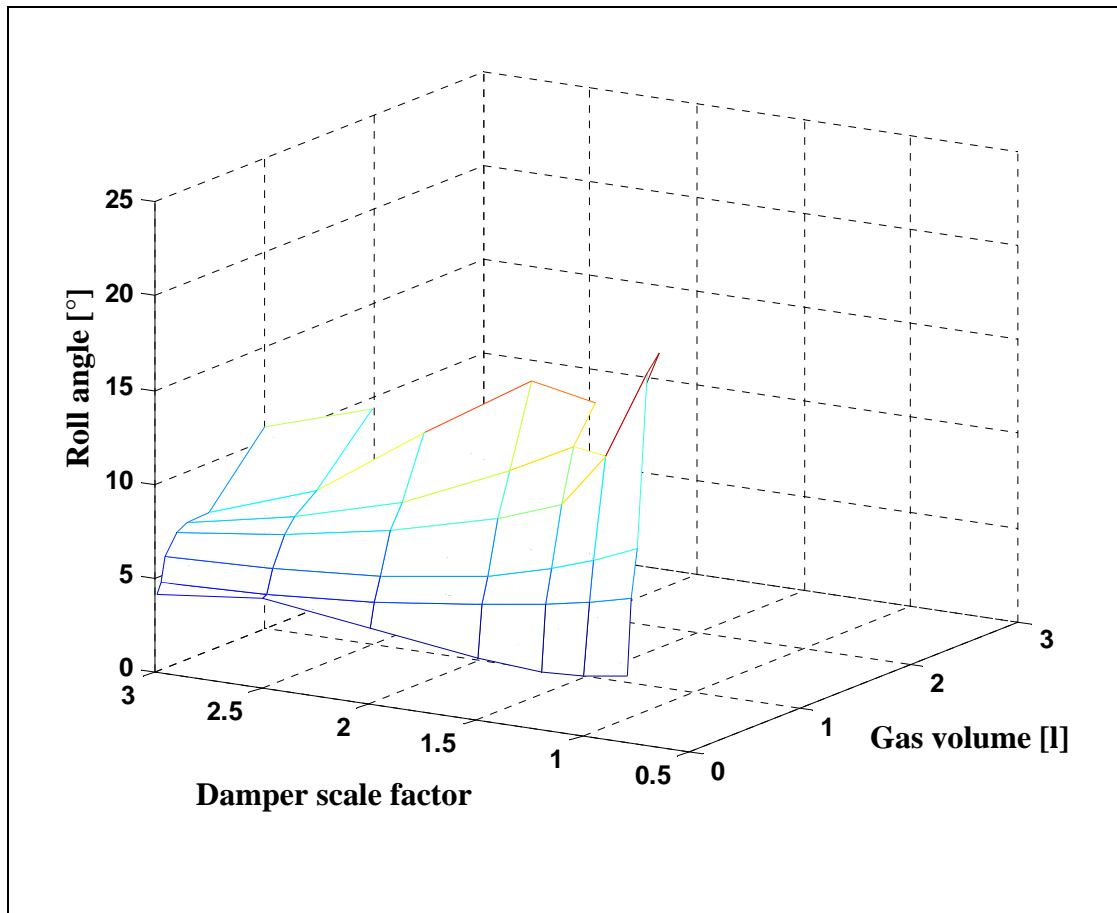


Figure 2.14 – Combined ride comfort and handling

### 2.3.5 Follow-up work by Uys, Els & Thoresson

In case study 2, simulations were performed for 7 damper characteristics and 10 spring characteristics within specified ranges, giving a total of 70 simulation runs. Ride comfort simulation was only performed for one terrain profile at one speed. Handling was also simulated only for one handling manoeuvre (the double lane change) at one vehicle speed. This process was performed manually. The next logical step was to investigate the applicability of mathematical optimization techniques to the problem in an attempt to decrease the number of required simulation runs. This should enable the simulation of more terrain profiles at various speeds, as well as a more in-depth look at handling.

**Els and Uys (2003)** optimise the handling of a vehicle, equipped with a hydropneumatic spring-damper suspension system, in conjunction with ride comfort. This is seen as a challenge due to the fact that the suspension characteristics determining ride comfort and handling respectively tend to oppose one another. The complexity and non-linearity of the dynamics of suspension systems impose further difficulty. Furthermore the suspension characteristics imply a large number of variables. The Dynamic-Q gradient-based optimisation method is used in conjunction with the dynamics simulation code DADS. Dynamic-Q is a robust and reliable algorithm particularly suitable for solving engineering optimisation problems. It applies an existing dynamic trajectory optimisation algorithm to successive spherical quadratic approximate sub-problems and can be used when analytical functions are not available and only discrete function values can be obtained via numerical simulation of engineering processes.

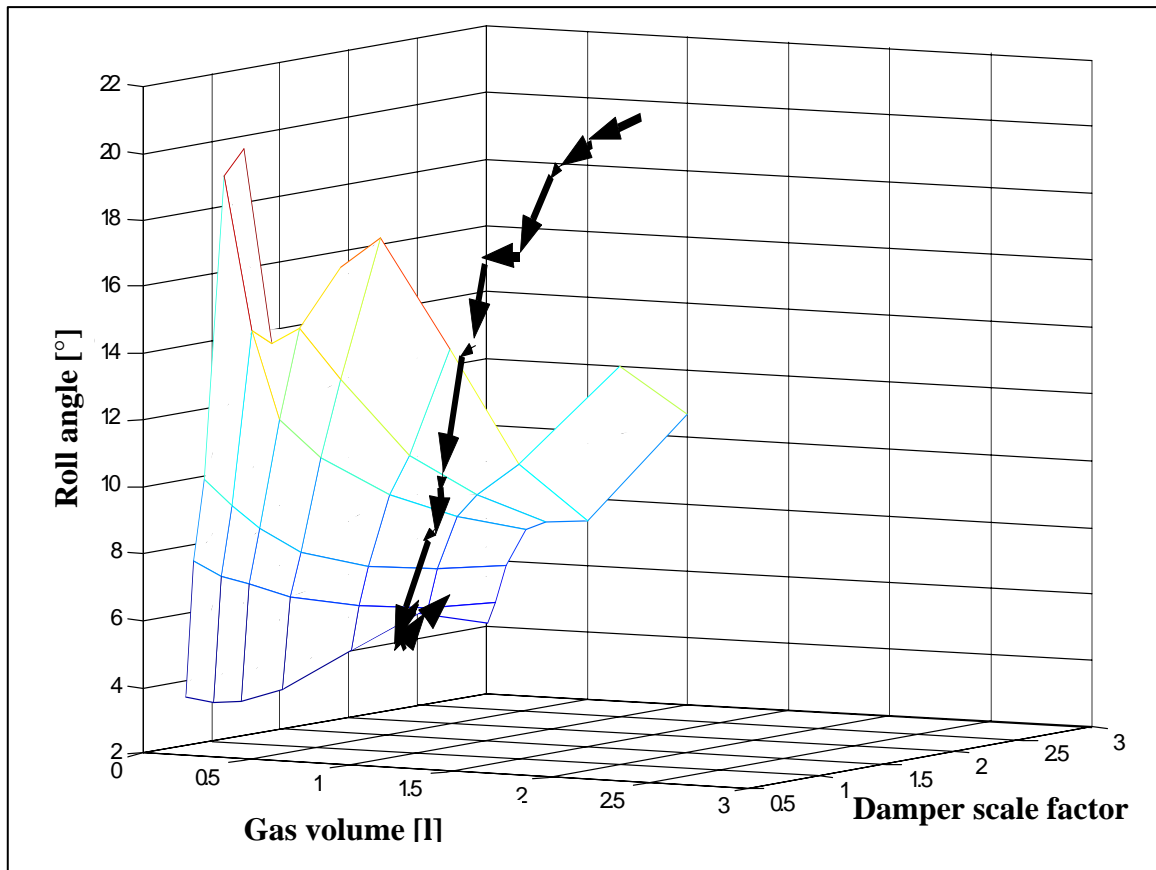


Figure 2.15 - Path followed by Dynamic-Q

The purpose of the investigation by Els and Uys was to determine whether the Dynamic-Q method is suitable for optimising the design of a vehicle suspension system modelled in DADS. Optimisation of the spring and damper characteristic was performed to obtain the best characteristics for handling on a smooth road, best characteristics for ride comfort while driving in a straight line and best characteristics for ride comfort and handling combined (performing a handling manoeuvre on a rough road).

Thoreson (2003) builds on the work by Els and Uys (2003) and performs mathematical optimisation on a Land Rover Defender 110 vehicle looking at ride comfort and handling separately (Els *et. al.*, 2003). His results are summarized in Table 2.6.

Table 2.6 – Summary of results by Thoreson (2003)

	Handling		Ride Comfort	
	Damper scale factor	Spring static gas volume [l]	Damper scale factor	Spring static gas volume [l]
Two design variables	1.35 to 1.99	0.05 (lower limit)	0.11 to 0.37	1.44 to 3.0
Four design variables	1.5 to 3 front 1.44 to 3 rear	0.1 (lower limit) front and rear	0.18 to 0.48 front 0.1 to 0.35 rear	1.32 to 2.08 front 1.6 to 2.18 rear
Seven design variables	Low speed damping must be high	0.1 (lower limit)	Low speed damping must be high	1.07 to 2.18

For the two design variable case, the spring static gas volume and damper scale factor were used as design variables. These factors were kept the same for both the front and



rear suspensions. In the four design variable case, the scale factors for the front and rear suspension was allowed to differ. For the seven design variable case, the gas volume and damper characteristics were kept the same front and rear, but the damper was now approximated by a piecewise linear spline, altering low and high speed damping separately.

For handling, all the cases required the stiffest spring allowed and damping that is between 35% and 300% higher than the baseline damping. Ride comfort required soft springs and damping that is lower than the baseline damping.

## 2.4 Validated vehicle model

The encouraging results obtained from case study 2 justified the development of an improved vehicle model that could be used to predict absolute values and not only trends as was the case with the first model. The fidelity of this model had to be good enough to accurately predict both ride comfort and handling. This model had to be combined with a model of the controllable suspension system and control system later in the project.

### 2.4.1 Geometric parameters

The majority of geometric parameters were obtained by physical measurement on a vehicle, although some critical measurements were obtained from available drawings.

### 2.4.2 Mass properties

Mass properties were obtained from physical measurements on a vehicle. The determination of the centre of gravity position, as well as estimation of the roll, pitch and yaw mass moments of inertia are described by *Uys et. al. (2005)*.

### 2.4.3 Spring and damper characteristics

Spring, damper and bump-stop characteristics were obtained by removing the components from the test vehicle and determining force-displacement and force-velocity relationships respectively using Schenck Hydropulse test equipment.

### 2.4.4 Tyre characteristics

Tyre side-force vs. slip angle characteristics were obtained from measurements using a two-wheeled tyre tester towed behind a vehicle. The measured data was converted to the coefficients required for the MSC ADAMS Pacjeka '89 tyre model. The tyres side-force vs. slip angle characteristics are indicated in Figure 2.16.

### 2.4.5 ADAMS full vehicle model

#### i) Front suspension

Figure 2.17 indicates the layout of the front suspension system. The rigid axle is located longitudinally by leading arms connected to the vehicle body with rubber bushes. The stiffness of these bushes was measured and included in the ADAMS model. Lateral location of the axle is via a Panhard rod. The baseline vehicle is fitted with coil springs,

translational dampers concentric with the coil springs and rubber bump stops. A steering angle driver is applied directly to the kingpin with a steering link connecting the left and right wheels. All other steering geometry is ignored in the model. The connections between the different components are indicated in Figure 2.18. To take the torsional stiffness of the ladder chassis into account, the vehicle body is modelled as two bodies connected to each other with a revolute joint along the roll axis and a torsional spring.

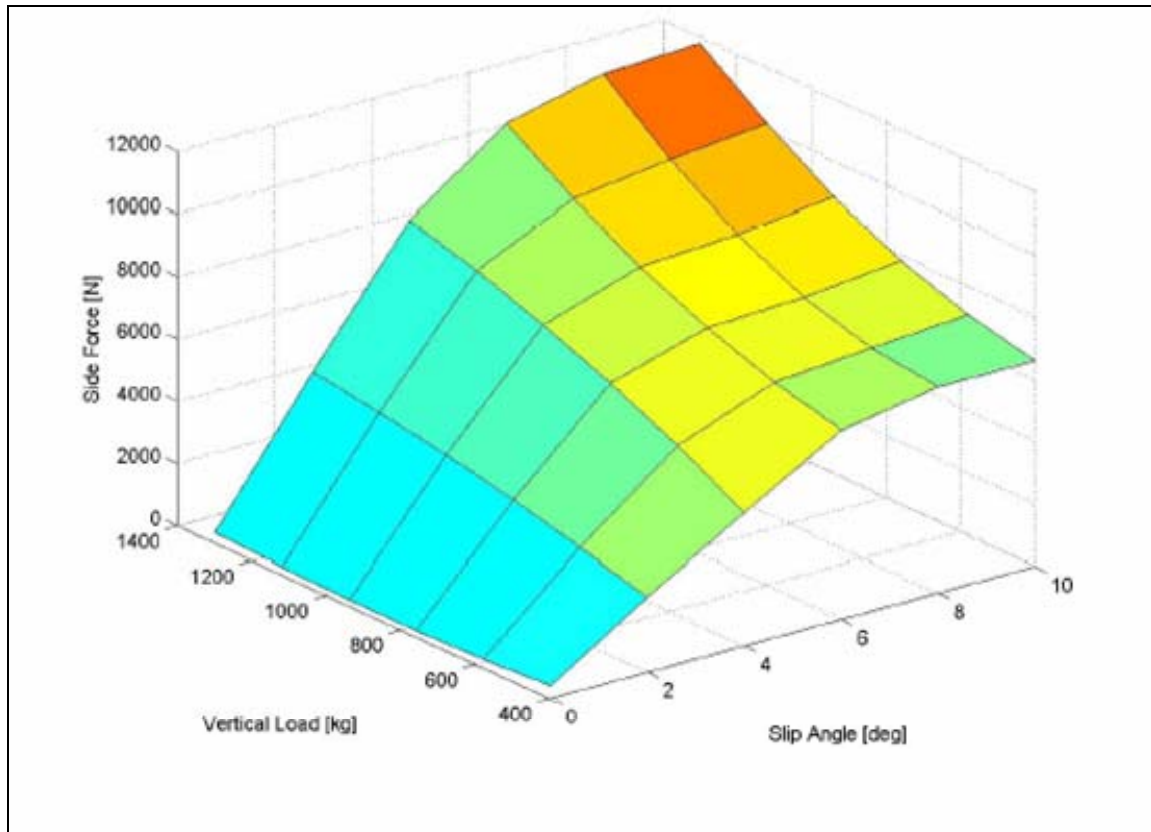


**Figure 2.16** - Tyre side-force vs. slip angle characteristic

ii) Rear suspension

The rear suspension consists of a rigid axle with trailing arms, an A-arm, coil springs, translational dampers mounted at an angle outside coil springs and rubber bump stops. The basic layout is indicated in Figure 2.19. An anti-rollbar is fitted to the rear suspension. The stiffness of the trailing arm rubber bushes is included in the ADAMS model. The schematic layout of the rear suspension is indicated in Figure 2.20.

**2.4.6 Baseline vehicle tests**

A Land Rover Defender 110 SUV was obtained locally for testing purposes. The aim of the baseline vehicle tests was to validate the ADAMS model of the vehicle. Tests were performed at the Gerotek Vehicle Test Facility West of Pretoria.

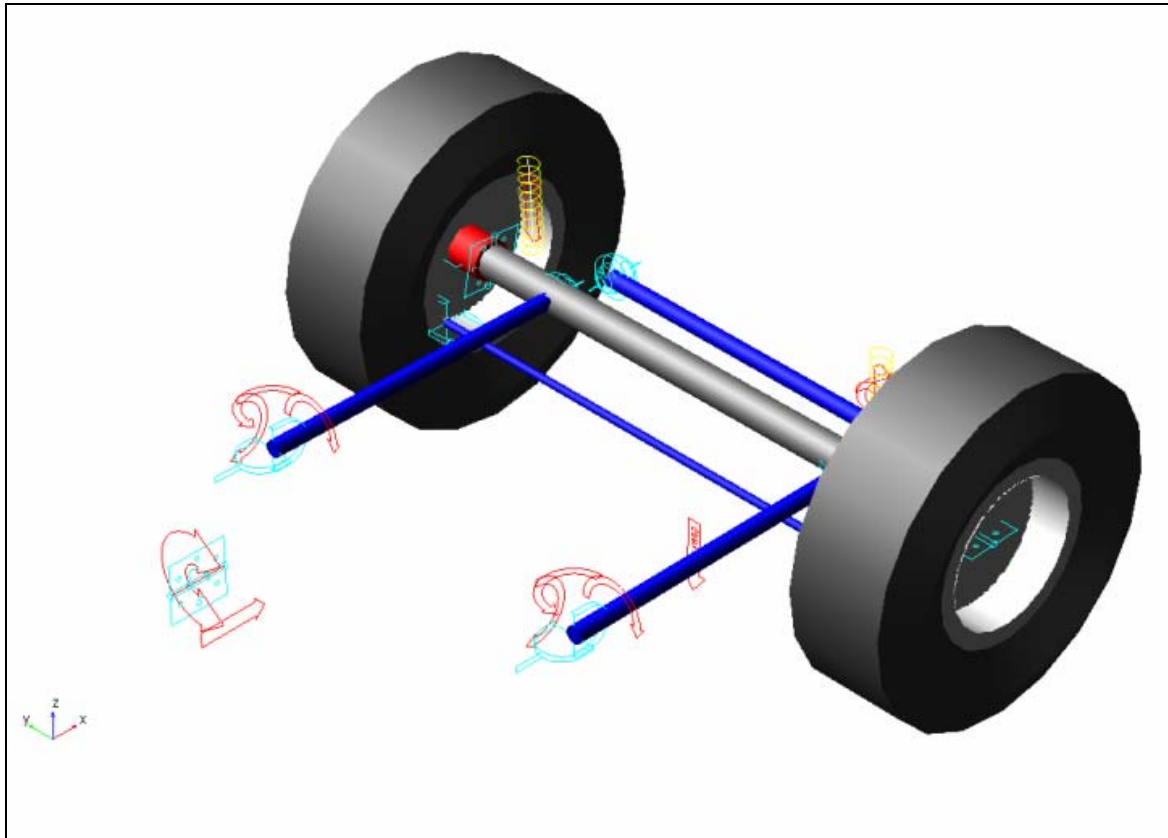


Figure 2.17 – Front suspension layout

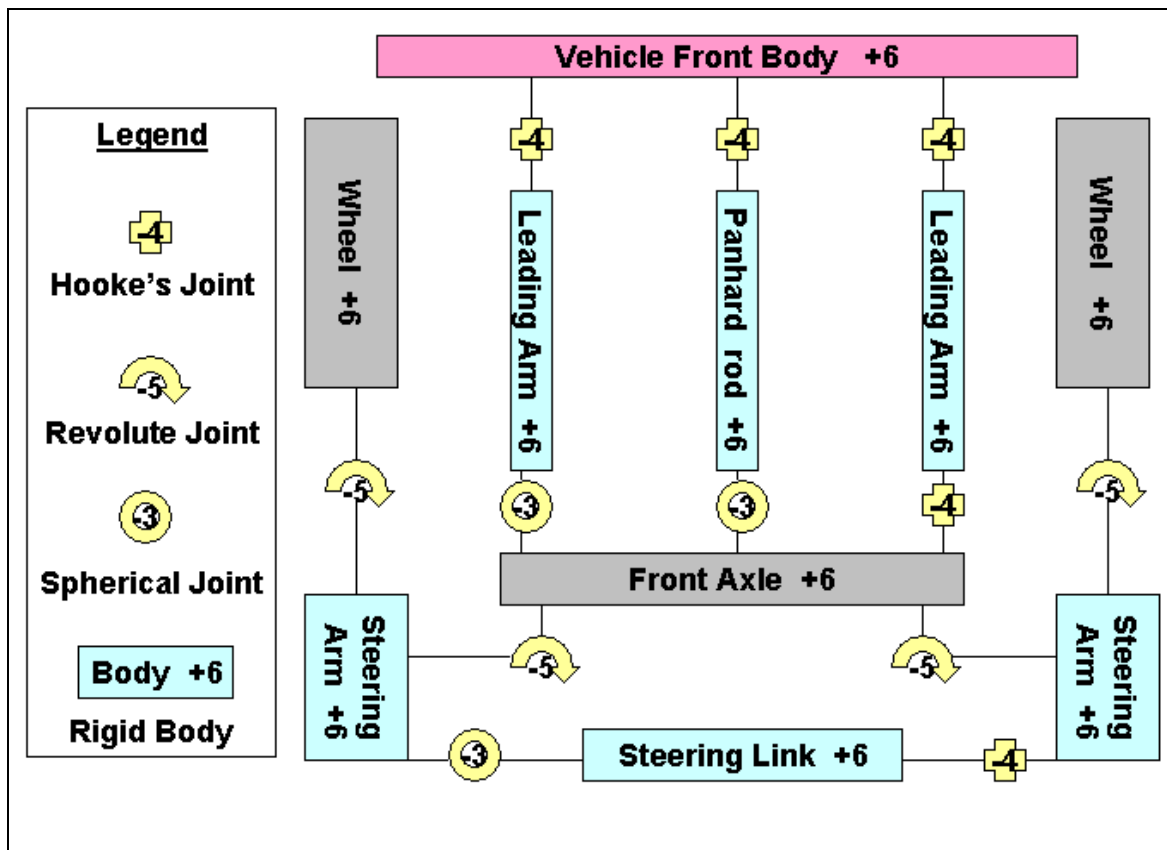


Figure 2.18 – Front suspension schematic

### 2.4.6.1 Instrumentation

The instrumentation used for the baseline tests, as well as measurement positions, is indicated in Table 2.7.

**Table 2.7** – Instrumentation used for baseline vehicle tests

No	Parameter	Position	Equipment
1	Vehicle speed	Roof	VBOX GPS
2	Relative displacement	Left front suspension	Penny&Giles rope displacement transducer
3	Relative displacement	Right front suspension	Penny&Giles rope displacement transducer
4	Relative displacement	Left rear suspension	DWT rope displacement transducer
5	Relative displacement	Right rear suspension	DWT rope displacement transducer
6	Roll velocity	Vehicle body between front seats	Solid state gyro
7	Yaw velocity	Vehicle body between front seats (close to cg)	Solid state gyro
8	Relative displacement	Steering arm between axle and body	Penny&Giles rope displacement transducer
9	Acceleration	Left front lateral	Solid state accelerometer $\pm 4g$ range
10	Acceleration	Right rear vertical	Solid state accelerometer $\pm 4g$ range
11	Acceleration	Left rear lateral	Solid state accelerometer $\pm 4g$ range
12	Acceleration	Left rear vertical	Solid state accelerometer $\pm 4g$ range
13	Pitch velocity	Vehicle body between front seats	Solid state gyro
14	Kingpin steer angle	Kingpin	Potensiometer
15	Wheel speed	Left rear wheel	Turck Banner optical speed sensor
16	Driveshaft speed	Gearbox output rear	Turck Banner optical speed sensor

### 2.4.6.2 Tests

The vehicle was evaluated for ride comfort over repeatable test tracks of various roughnesses at known, repeatable and representative speeds. Weighted root mean square vertical accelerations were used to quantify ride comfort. Figure 2.21 indicates the vehicle on the Belgian paving track during testing. Tests also included single discrete obstacles (locally known as an “APG” bump) as indicated in Figure 2.22. Vehicle handling was evaluated using a constant radius test (Figure 2.23) as well as a severe double lane change manoeuvre (Figure 2.24).

Additional tests over typical off-road terrain were performed on the Gerotek rough track (Figures 2.25 and 2.26) where a combination of ride comfort and handling is required. The rough track consists of natural terrain features embedded in concrete to give repeatability.

Test procedures and terrains were chosen to ensure repeatability. Vehicle speed was kept constant by driving the diesel engine against its governor. This is important, as the baseline test results will be used later to quantify the improvements offered by the controllable suspension system.

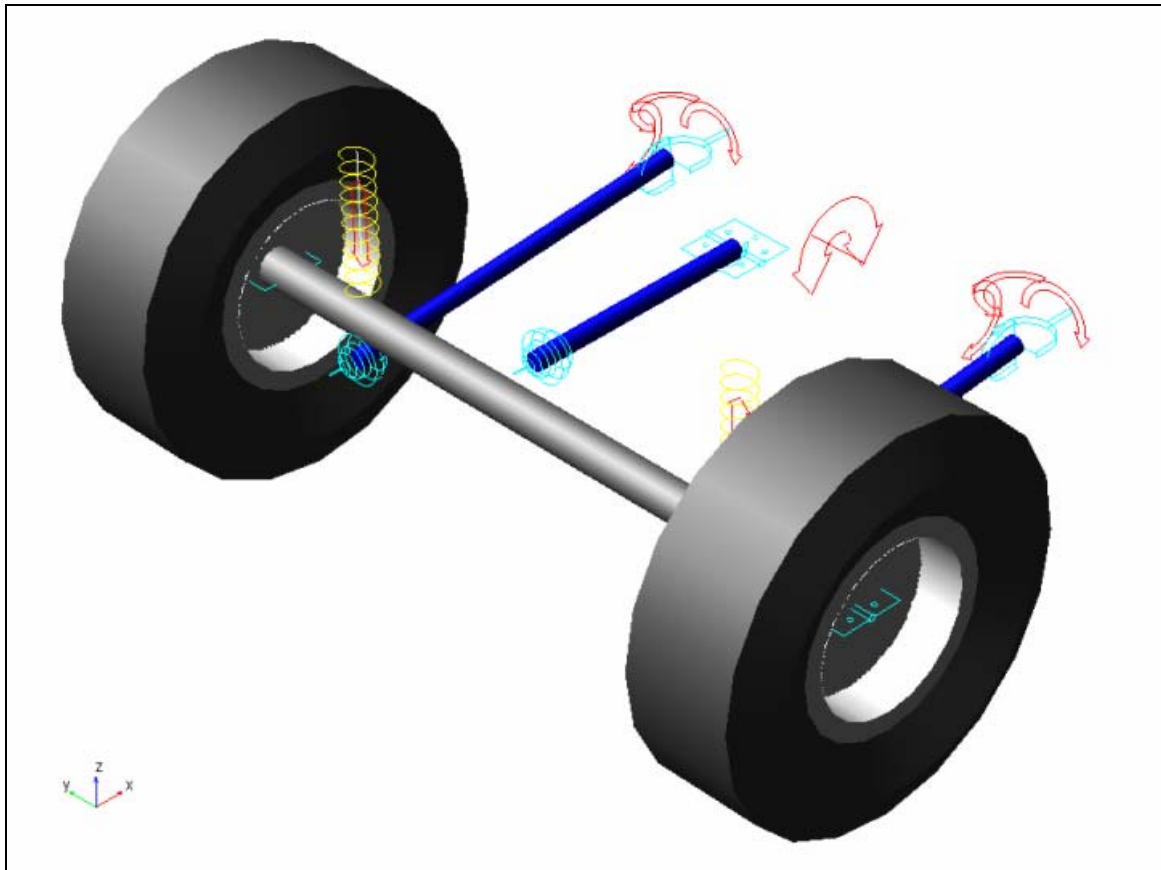


Figure 2.19 – Rear suspension layout

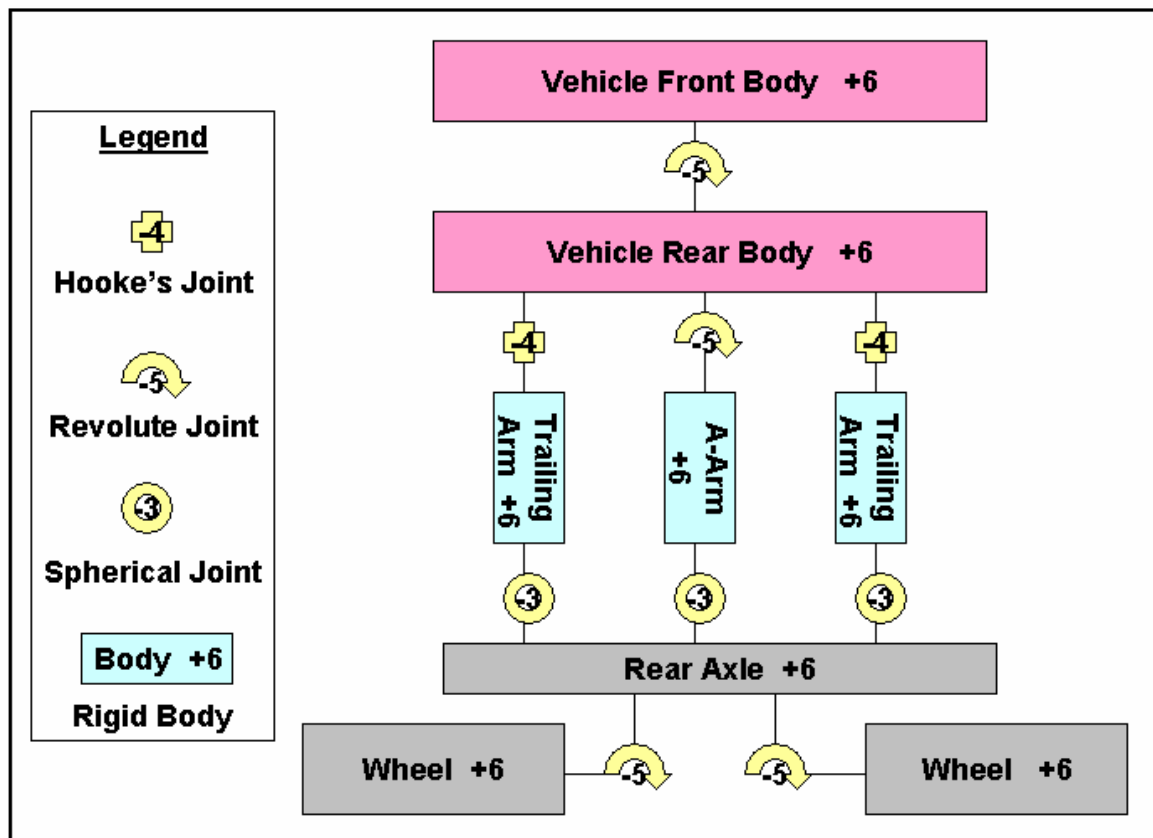


Figure 2.20 – Rear suspension schematic



**Figure 2.21** - Belgian paving

#### **2.4.7 Correlation between ADAMS model and test results**

To validate the ADAMS model, simulation results were compared to measured results for two different tests namely the APG bump, and the ISO 3888 double lane change test.

##### **2.4.7.1 Transient response (APG track)**

The APG track was chosen to validate the vertical and pitch dynamics of the vehicle. The road input profile is easily measured and included in a simulation model. Figure 2.27 indicates the correlation obtained between the measured and simulated results. Correlation is indicated for pitch velocity, spring displacement right front (rf), spring displacement rear left (rl), steering displacement as well as front and rear vertical accelerations. Correlation for vertical accelerations is especially good which is important because vertical acceleration is a direct measure of ride comfort. The model is thus considered validated for ride comfort simulation.

##### **2.4.7.2 Handling (ISO 3888 Double lane change)**

Figure 2.28 indicates the correlation achieved for a double lane manoeuvre performed at 65 km/h. The speed for the baseline vehicle tests varied between 61 and 65 km/h. The steering input, as measured during baseline testing, was used to drive the vehicle and not the driver model. The graphs therefore represent the dynamic reaction of the vehicle to the same input conditions as during testing. Correlation is very good for all the measured parameters. The model is thus considered validated for handling simulation.



**Figure 2.22** - “APG” Bump



**Figure 2.23** - Constant radius test



**Figure 2.24** - Severe double lane change manoeuvre



**Figure 2.25** - Rough track





**Figure 2.26** - Rough track

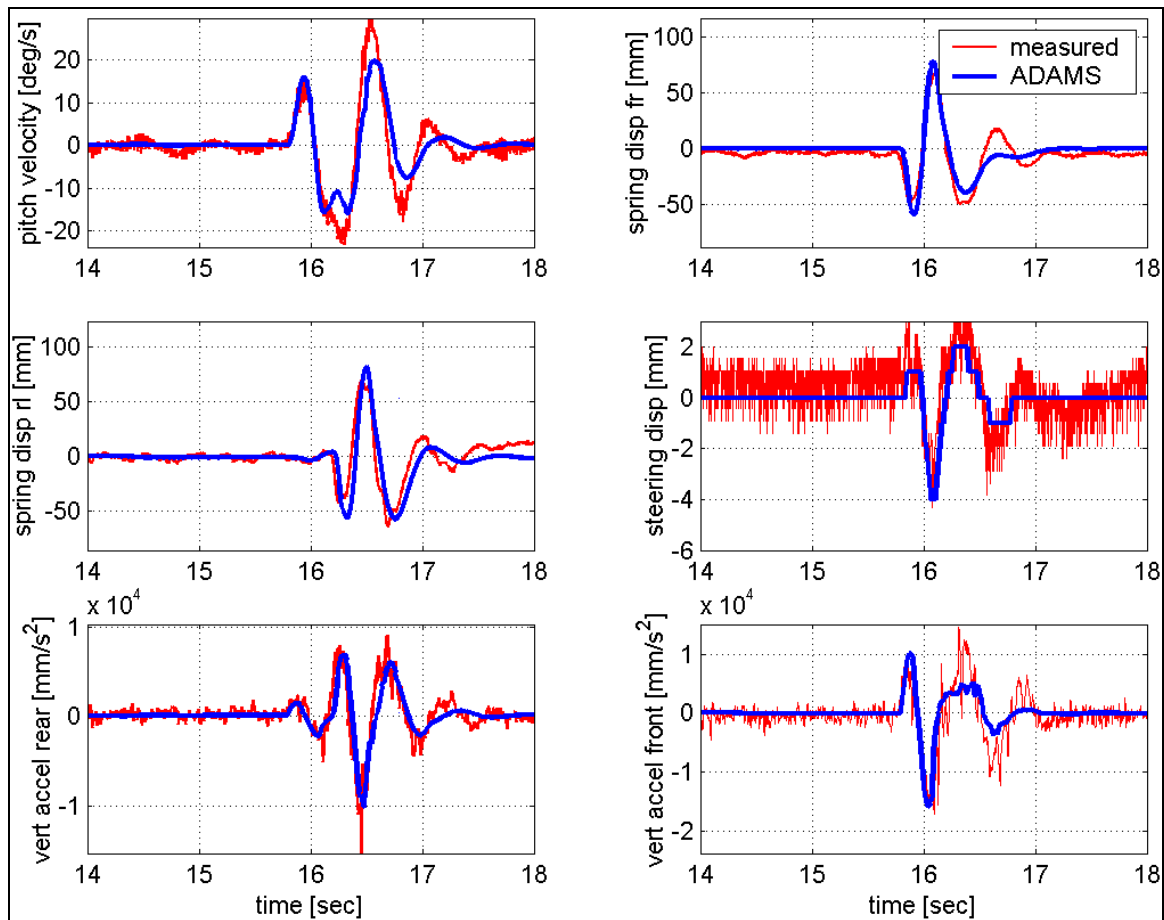


**Figure 2.27** - Model validation results for passing over 100 mm APG bump at 25 km/h

### 2.4.8 Simulation results

The validated ADAMS model was modified by replacing the coil springs with hydropneumatic springs. As before the static gas volume was varied between 0.1 and 1 litre while the damper scale factor was varied between 0.5 and 3. The effect of spring and damper characteristics on ride comfort over the Belgian paving is indicated in Figure 2.29. The conclusion is made that for best ride comfort, the damping scale factor must be as low as possible and the static gas volume as large as possible although the improvement is negligible for gas volumes higher than 0.5 litre. For handling, a double lane change manoeuvre was again performed. In this case both the body roll angle and body roll velocity was used as a measure of handling and stability. Figure 2.30 indicates that the maximum body roll angle at the first valley, and maximum roll velocity at the first peak was used.

Figure 2.31 indicates the maximum roll angle as a function of static gas volume and damper scale factor. The lowest maximum roll angle (best handling) is obtained with a static gas volume of 0.1 litre and a damper scale factor of 3. The maximum roll velocity (Figure 2.32) is more sensitive to the damper scale factor. This result was expected, as damping force is velocity dependant while spring force is displacement dependant. The results however point to a damper scale factor of 3.

All these results indicate that the optimum characteristics for ride comfort and handling are at opposite corners of the design space. For good ride comfort, low damping and a soft spring is required. A damper scale factor of less than 0.5 and a static gas volume of 0.5 litre or more will give the best ride comfort. For best handling, a static gas volume of 0.1 litre and damper scale factor of 3 is required.

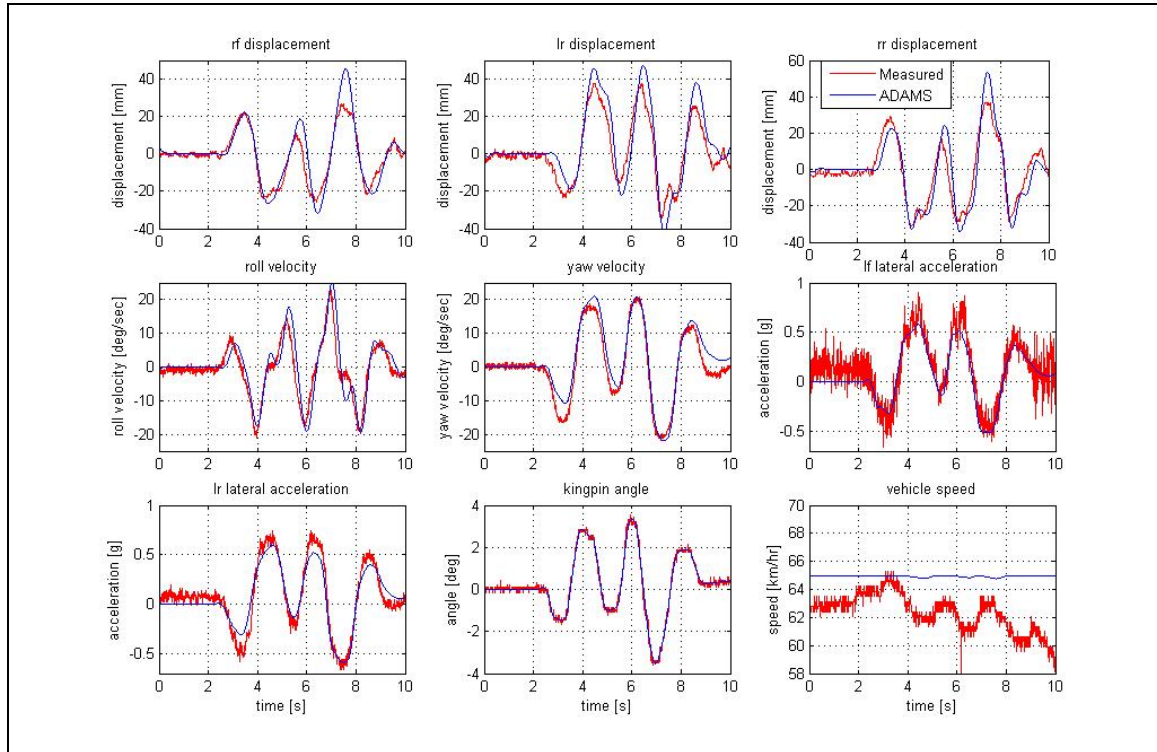


**Figure 2.28** – Model validation results for a double lane change manoeuvre at 65km/h

## 2.5 Conclusion

The following is concluded based on the evidence presented in this chapter:

- a) A passive suspension system is a compromise between ride comfort and handling as the respective requirements for ride comfort and handling are at opposite ends of the design space.
- b) To eliminate the ride comfort vs. handling compromise, two discrete spring characteristics are required namely:
  - A stiff spring for best handling (0.1 litre static gas volume for hydropneumatic spring in the case of the test vehicle)
  - A soft spring for best ride comfort (>0.5 litre static gas volume for hydropneumatic spring in the case of the test vehicle).
- c) To eliminate the ride vs. handling compromise, two discrete damper characteristics are required namely:
  - High damping for best handling (greater than double baseline damping value)
  - Low damping for best ride comfort (less than ½ the baseline damping value).

- d) The capability to switch between the two spring and the two damper characteristics is required.
- e) A control strategy that can switch between “ride comfort” mode and “handling” mode in a safe and predictable way is of critical importance.

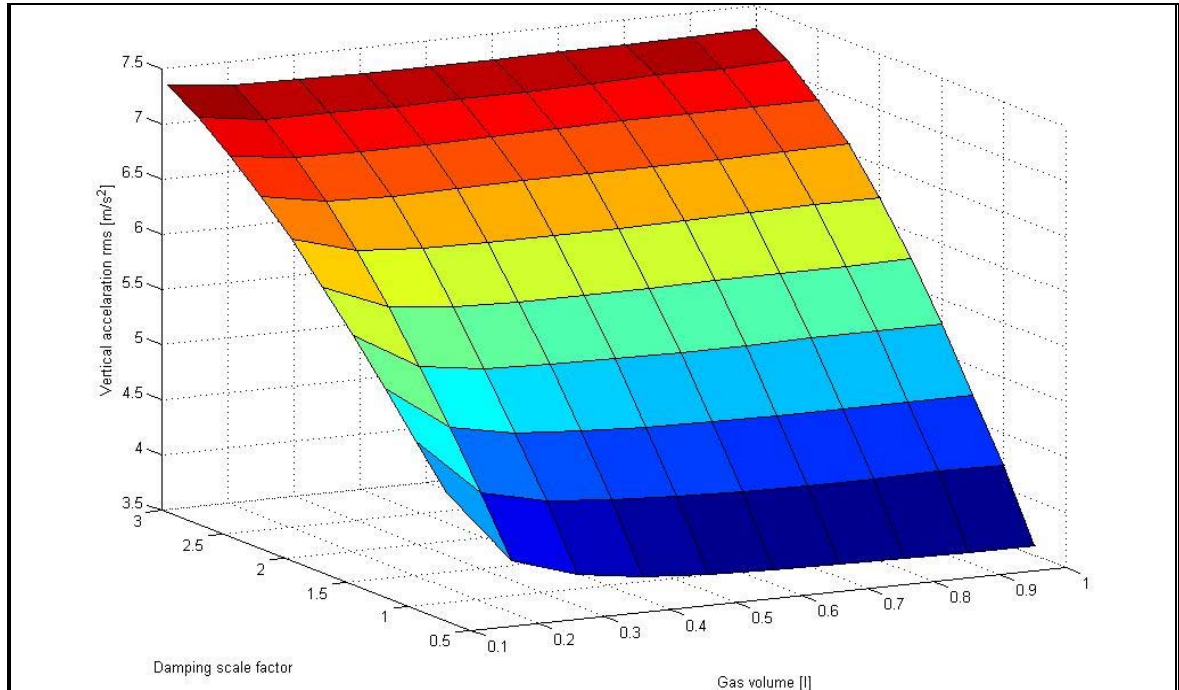


**Figure 2.29** – Ride comfort vs. gas volume and damping

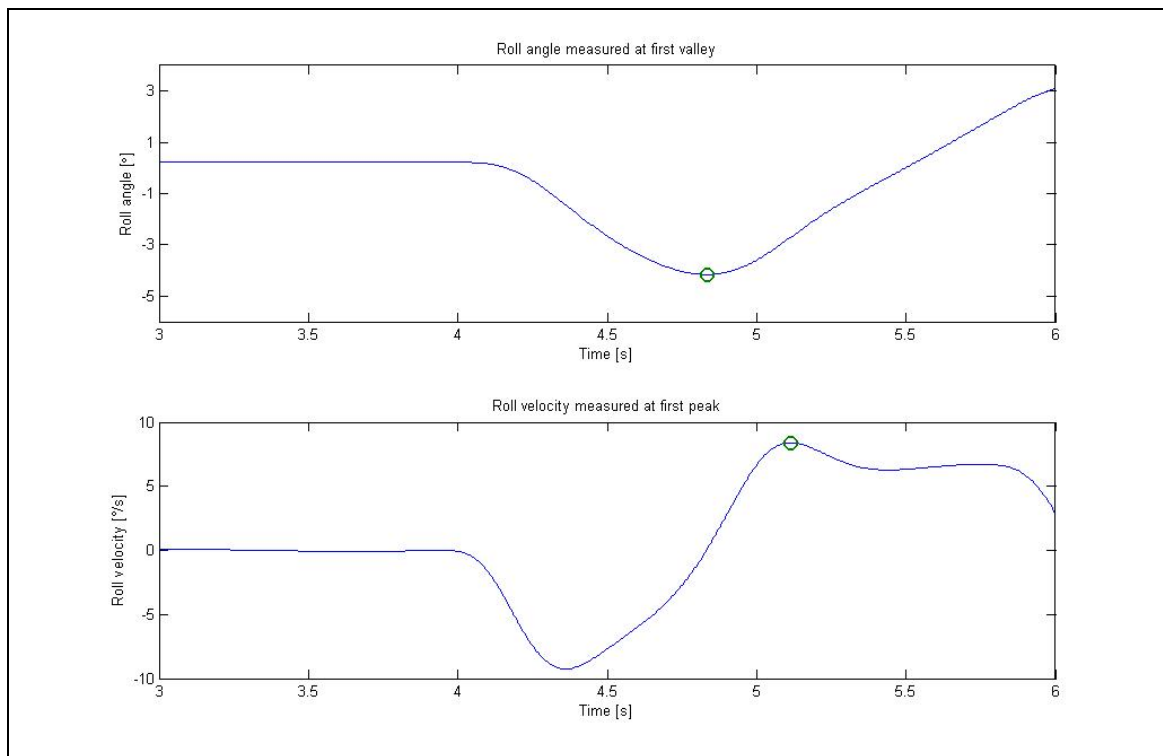


**Figure 2.30** - Definition of handling objective function

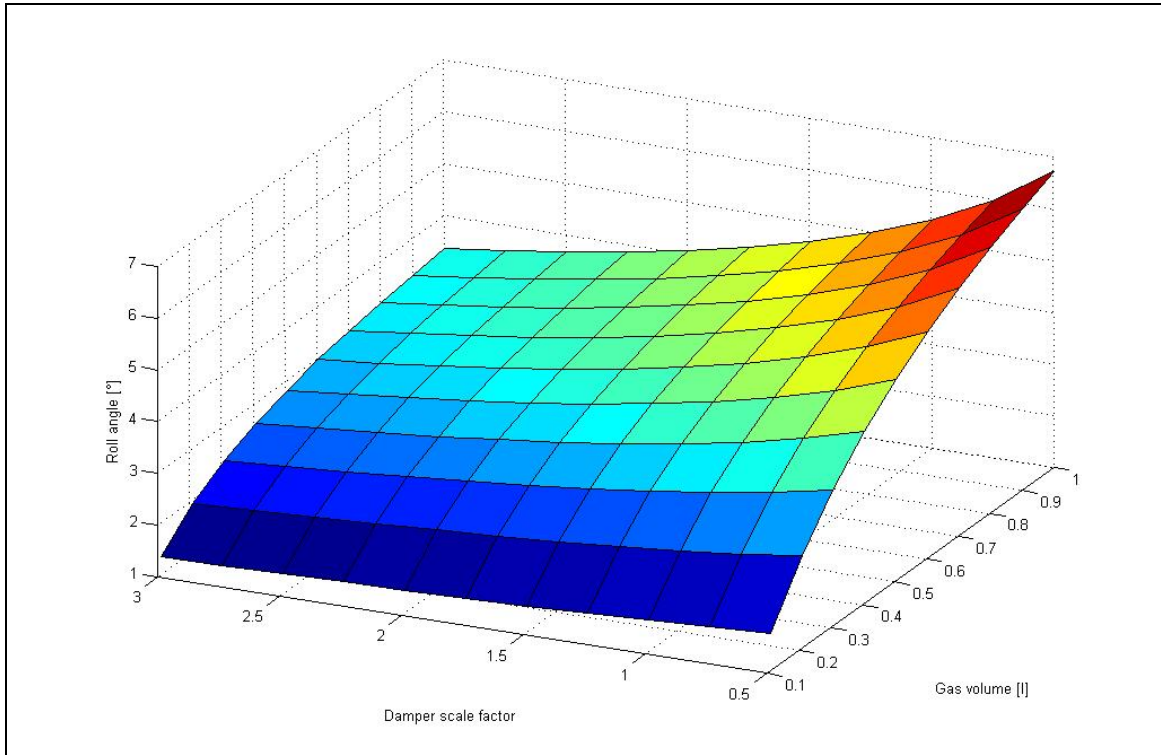


Figure 2.31 – Roll angle vs. gas volume and damping

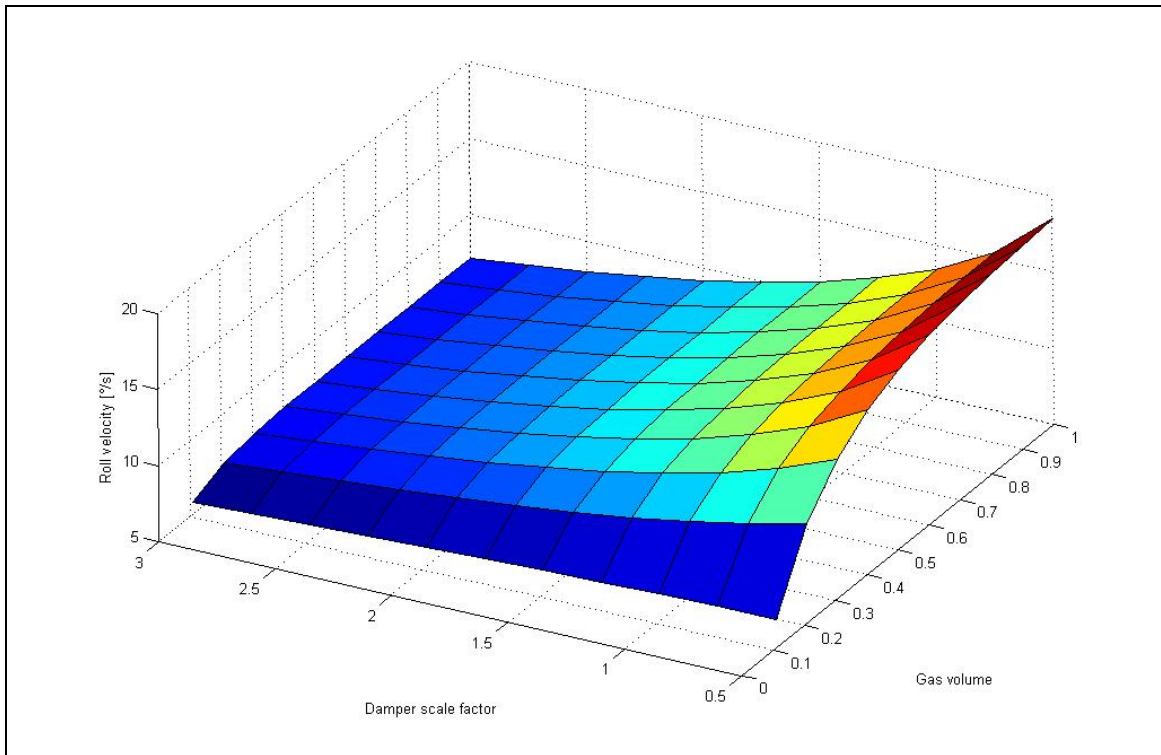


Figure 2.32 – Roll velocity vs. gas volume and damping

---

---

## ***POSSIBLE SOLUTIONS TO THE RIDE COMFORT VS. HANDLING COMPROMISE***

---

---

Possible concepts for the improvement or elimination of the ride comfort *vs.* handling compromise are investigated in this chapter. Current literature is reviewed, firstly to determine possible hardware concepts for controllable suspension systems and secondly to obtain a global view of the technical requirements involved in the development and implementation of control methodologies. Fully active suspension systems are not considered mainly due to their large power requirements, especially when applied to heavy off-road vehicles. For this reason, the literature review is therefore not concerned with fully active suspension systems in particular, but instead focuses on semi-active and adaptive systems where spring and damper characteristics can be changed either continuously or switched between different discrete characteristics. Some active suspension concepts and control methods are however discussed, as many of these might be adapted to semi-active suspension systems. In some cases it might be possible to control a semi-active damper with the same strategy as a fully active suspension system, but it will only dissipate energy as no energy can be supplied. The damper will therefore be switched to the low damping state when energy supply is demanded by the control system. Active suspension systems dissipate energy for a large amount of the time in any case and semi-active dampers can therefore often approach the results obtainable with fully active systems.

After briefly discussing published literature on advanced suspension systems, this chapter deals more thoroughly with the subjects of semi-active dampers, semi-active springs and active suspension systems, followed by control techniques and algorithms. The chapter closes with a proposed controllable suspension solution to the ride comfort *vs.* handling compromise.

### **3.1 Published literature surveys on controllable suspension systems**

Six published literature surveys concerning advanced suspension systems were found. Although these surveys do not provide sufficient detail on each topic to be really useful for the purposes of the current study, they provide a valuable source of references and a general overview on the specific subject.

**Tomizuka and Hedrick (1995)** discuss advanced control methods for automotive applications in general and include a paragraph on suspension systems. Various control methods are mentioned for fully active systems as well as semi-active dampers. No mention is made of the existence or control of controllable spring systems.

**Sharp and Crolla (1987)** discuss suspension system design in general and include aspects such as road surfaces, tyres, vehicle models and performance criteria. Passive, active, semi-active and slow active suspension systems are also included in the survey. Mention is made of slow active (3 Hz bandwidth) controllable pneumatic and hydropneumatic systems.

Active suspensions for ground transport vehicles are reviewed by **Hedrick and Wormley (1975)**. The article does not include semi-active suspension systems and no mention is made of semi-active or variable springs.

The application of neural networks and fuzzy logic to vehicle systems is reviewed by **Ghazi Zadeh, Fahim and El-Gindy (1997)**. An introduction to neural networks and fuzzy logic is given. The techniques have been applied to active and semi-active suspension systems by various authors.

**Elbeheiry et. al. (1995b)** give a classified bibliography of advanced ground vehicle suspension systems. A reference list of 71 papers concerned with semi-active suspensions and 58 papers concerned with adaptive, actively damped and load-levelling suspensions is given but not discussed.

Applications of optimal control techniques to the design of active suspension systems are surveyed by **Hrovat (1997)**. The main emphasis of the survey is on Linear Quadratic Optimal (LQO) control and active suspension systems, but related subjects such as semi-active suspensions and related control topics are also discussed. Some 256 papers are included in the list of references.

## **3.2 Controllable suspension system hardware**

Vehicle suspension system configurations vary over a wide spectrum. The most important variations on the theme will now be discussed.

### **3.2.1 Semi-active dampers**

Semi-active dampers vary from two-state (on/off) to continuously variable. Both linear and non-linear damper characteristics are considered. The majority of semi-active dampers are based on either magneto-rheological (MR) fluids or hydraulic dampers with controllable valves.

#### **3.2.1.1 Magneto-Rheological (MR) fluids**

A Magneto-rheological (MR) fluid is used as the damping medium inside a hydraulic damper and replaces the conventional damper oil. A MR fluid is a dense suspension of micrometer-sized magnetisable particles in a carrier fluid that solidify to a pasty consistency in the presence of a magnetic field (**Lord Corporation, 2005; Ouellette, 2005**). When the magnetic field is removed the fluid returns to its liquid state. Altering the strength of the applied magnetic field will proportionally control the consistency or yield strength of the fluid and therefore the pressure required to force the fluid through a magnetized orifice. MR fluids offer a very fast response time (order of 10 milliseconds) and have been commercially applied in continuously variable semi-active dampers (see

**Lord Corporation 2005** for a description of MagneRide as fitted to some General Motors products).

Researchers at the Advanced Vehicle Dynamics Laboratory at Virginia Polytechnic Institute and State University used controllable MR dampers to control the roll dynamics of a Ford Expedition SUV. Results of vehicle tests indicated that a velocity based skyhook control, augmented with steering wheel feedback, outperformed the passive stock dampers (**Simon, 2001**).

### 3.2.1.2 Hydraulic bypass system

Semi-active dampers based on the by-pass principle use a hydraulic valve (mostly electrically operated) in parallel with a conventional damper orifice and valve assembly. A two-stage (open-closed) valve is indicated in Figure 3.1. If the bypass valve is closed, all the flow goes through the conventional damper orifice and valve assembly, giving high damping or the “on” characteristic. If the bypass valve is open, most of the flow will pass through the bypass valve due to the lower flow resistance. This results in the low damping or “off” characteristic. During valve switching some transient response will result between the “on” and “off” characteristics. The bypass valve can have several discrete stages, or it can be a servo valve giving continuously variable damping characteristics.

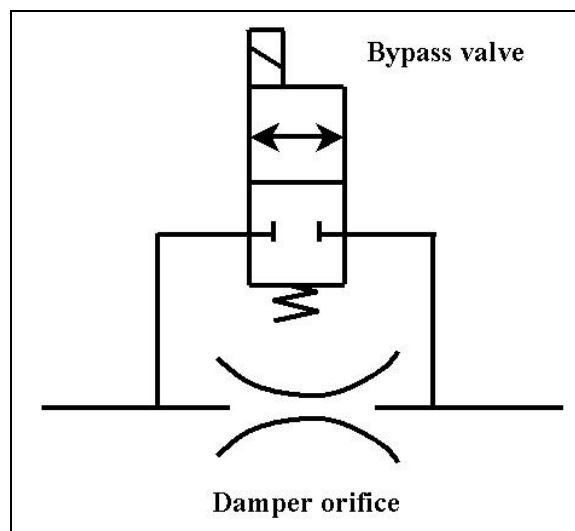


**Figure 3.1** - Hydraulic two-state semi-active damper with bypass valve

The choice of valve is based on the pressure drop and flow rate characteristic, as well as the required response time.

Examples of two-state semi-active dampers, using the bypass valve principle, are discussed by **Nell (1993)** and **Nell and Steyn (1994)**. A picture of their first prototype can be seen in Figure 3.2 with the bypass valve indicated. This damper was designed for a maximum flow rate of 1000 l/min, a static wheel load of 3 ton and a response time in the region of 50 milliseconds. The largest semi-active damper for a wheeled vehicle, developed by **Els and Holman (1999)**, is indicated in Figure 3.3. This damper has a maximum damping torque of 150 kN.m and was used on a 46-ton 6x6 vehicle. These dampers are all applied to off-road military vehicles.



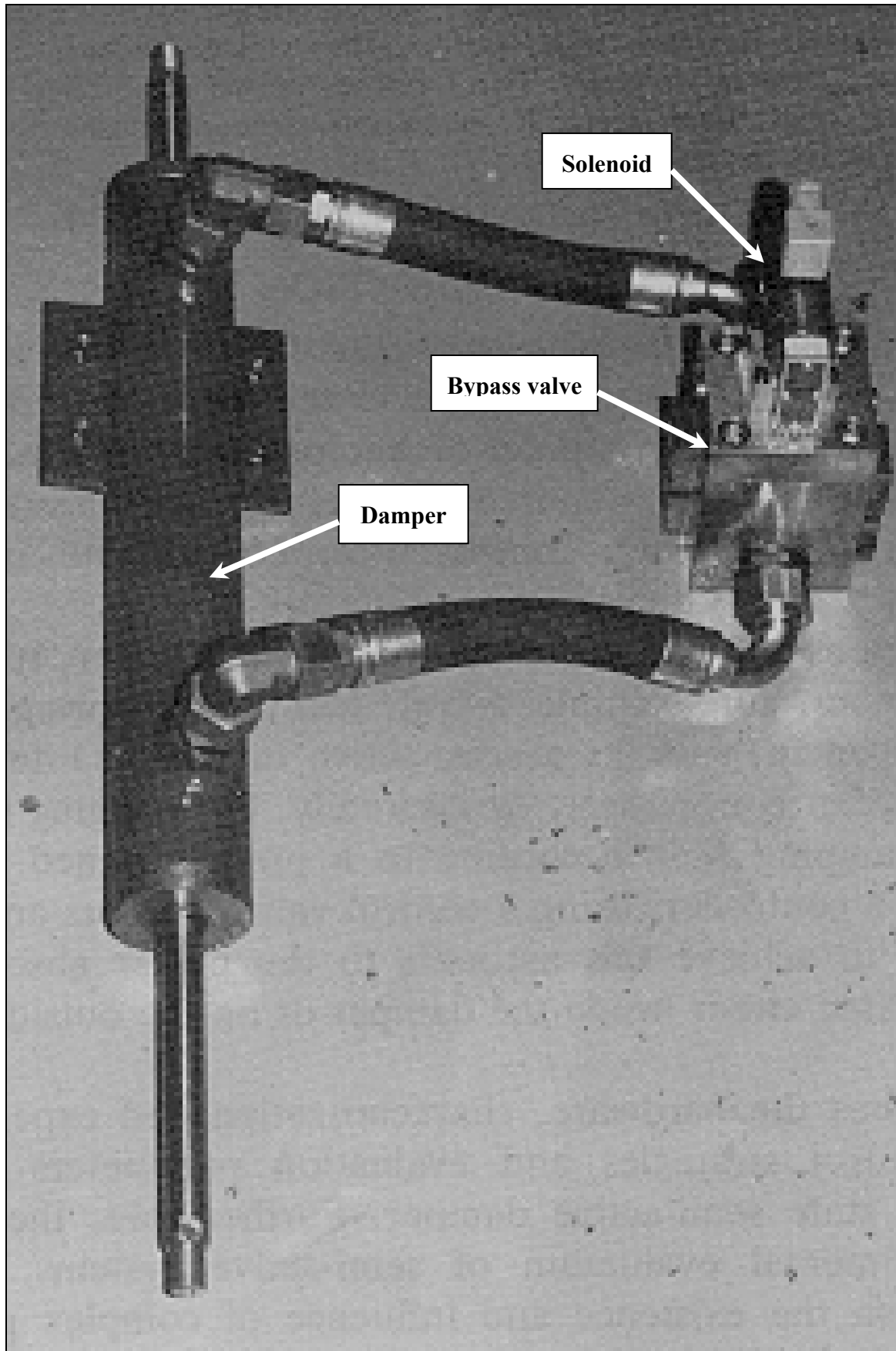


**Figure 3.2** – Semi-active damper developed by Nell (1993)

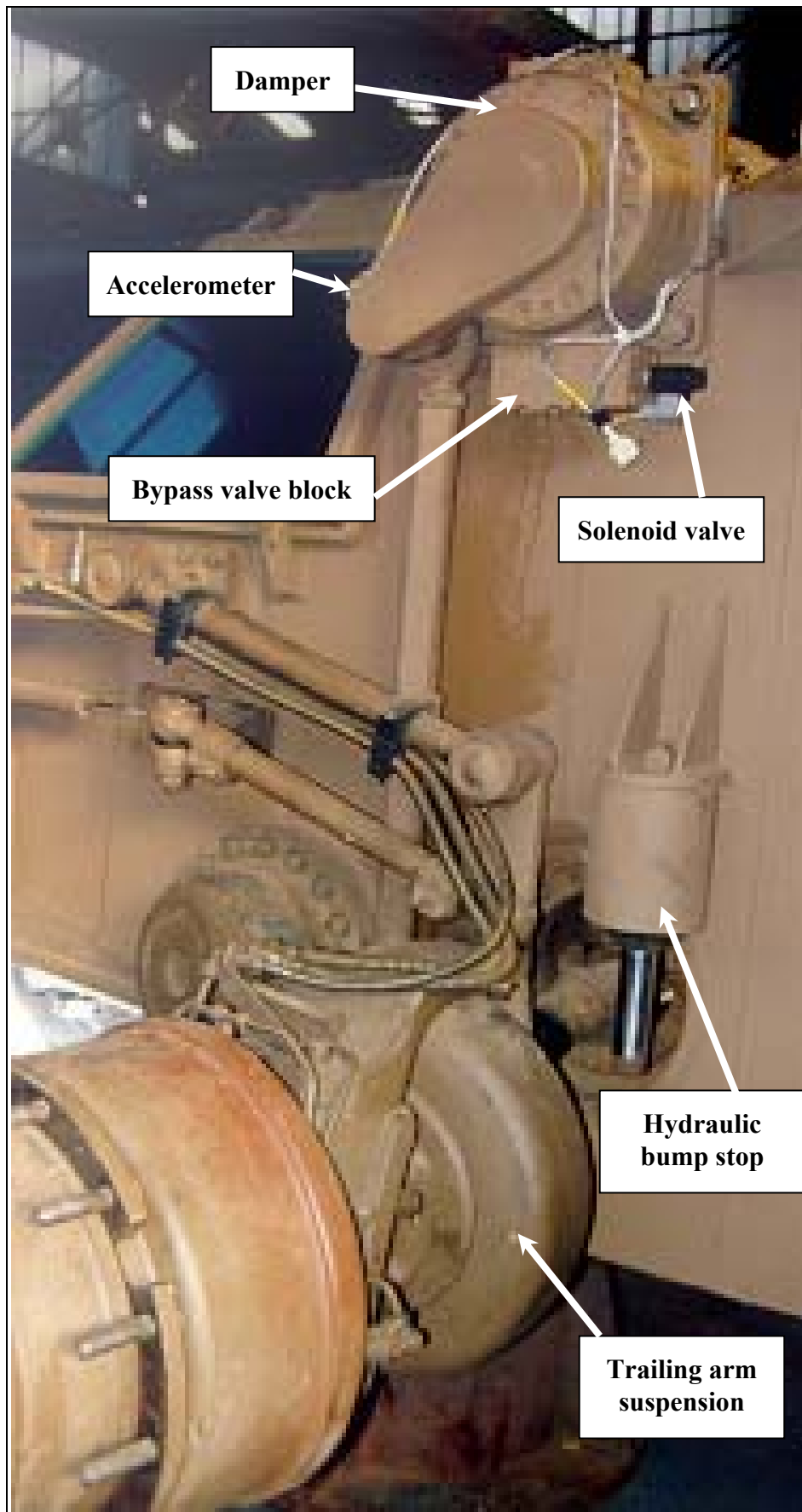


Figure 3.3 - Semi-active rotary damper developed by Els and Holman (1999)

### 3.2.2 Semi-active springs

Semi-active springs are based on either air or hydropneumatic springs that are mostly non-linear due to their operating principles. Hydropneumatic and air springs frequently incorporate some kind of slow active ride height correcting device. Cases also exist where an air spring is combined with a normal passive coil spring.

#### 3.2.2.1 Air springs

**Decker, Schramm and Kallenbach (1988)** describe a prototype adjustable air spring developed by BOSCH, where the spring characteristic can be changed between several values by fast (25 milliseconds) switching of different air volumes. The adjustable spring is used in conjunction with a fast (4 milliseconds) semi-active damper. Very limited simulation results are included. A closed loop control strategy, of which no details are provided, is used to switch both the spring and damper during simulation. An improvement potential of 36% in ride comfort is obtainable from simulation results. The skyhook control strategy as proposed by Karnopp is also investigated although no further details are presented. No experimental work concerning evaluation of control strategies is presented.

An industrialised version of a semi-active suspension developed by Armstrong is discussed by **Hine and Pearce (1988)**. A two or three state adjustable damper is combined with an air or oleo-pneumatic spring that is said to offer both height and spring rate control. It is not clear how the spring rate is changed but it appears as if the spring rate changes because of the ride height adjustment. The oleo-pneumatic damper can be pressurised to a maximum pressure of 200 bar (20 MPa) supplied by an oil pump. The unit is fitted with an external reservoir. The control strategy can be separated into five components namely ride, handling, acceleration, deceleration (dive), ride frequency control and vehicle levelling (if required). The system is commercially applied to the 1986 GM Corvette (5.7 litre) and Ford Granada 2.8 Ghia.

**Pollard (1983)** describes a fully active air actuator fitted to a railway couch. Where most conventional air suspensions have an auxiliary reservoir to provide the desirable spring and damping characteristics, the air pump actuator replaces the fixed volume reservoir with one of continuously variable volume. An electric motor is attached to the diaphragm via a nut and a lead screw. Operating the lead screw can change the volume. A prototype has been tested with good success and power consumption is found to be low.

A performance air suspension developed by Bridgestone/Firestone is described by **Alexander (2004a)**. The system is cockpit adjustable by the driver. Ride height can be lowered to improve handling or increased to improve ground clearance. Spring rate may also be reduced to improve isolation or increased for handling. The spring rate can be changed either with, or independent of height. Roll stiffness distribution between front and rear can seemingly also be altered.

The suspension system used on the 1986 model Toyota Soarer is described by **Hirose et al. (1988)**. This system changes both spring and damper characteristics using direct current electric motors. The air spring uses main and supplementary air chambers connected by a disc valve to change the gas volume and therefore the spring characteristic. Height control is also implemented for which air pressure is supplied by a

compressor. System response time is 70 milliseconds. The spring and damper rates are changed simultaneously by a single electric motor. The four struts on the vehicle are also controlled together. Vehicle speed, throttle position, steering angle, height and other factors related to vehicle attitude are used to determine the suspension state.

An Electronic Controlled Suspension (ECS) as fitted to the 1984 Mitsubishi Galant is discussed by **Mizuguchi et. al. (1984)**. A two-stage spring is constructed using an air spring in parallel with a conventional metal coil spring. The air spring consists of two chambers connected by a valve. The valve is closed to activate the stiff spring rate. Vehicle speed, steering wheel speed, sprung mass acceleration, throttle speed and suspension stroke are used as control parameters. A methodology to determine the spring and damper rate for the two-state suspension systems is described. The suspension is either set to “off” (soft spring and soft damper) or “on” (hard spring and damper). The normal suspension state is soft for good ride comfort but is switched to hard for high vehicle speeds or during handling manoeuvres.

**Karnopp and Margolis (1984)** discuss the effects of a change in spring and damper rates on the transfer function of a single degree of freedom suspension system. It is said that changing the damping alone is not a very good way of stiffening or softening a suspension system. A system with two air volumes separated by control valves is proposed that enables both the spring and damper rates to be adjusted. Air can also be slowly added to or subtracted from the air volume to enable ride height adjustment. The proposed system can be adaptively controlled using brake and steering inputs as well as angular acceleration. Manual overrides can be included to suit personal preference.

**Wallentowitz and Holdman (1997)** give a frequency domain analysis of the effect of spring and damper constants on the transfer function of the suspension. It is concluded that two spring stages are sufficient to overcome the compromise associated with passive systems. The two-stage spring can be realised in hardware by using two air springs connected by a pipe and orifice arrangement. The orifice is designed so that the second air spring is effectively closed off at suspension frequencies higher than 5 Hz. A valve in series with the orifice can be closed to achieve a high spring rate during handling manoeuvres. No hardware seems to be available. The study is theoretical only and includes a suggestion for a possible control strategy based on the frequency response of a quarter car system.

### **3.2.2.2 Hydropneumatic springs**

Citroën has been applying hydropneumatic suspension systems to their passenger cars for many years. **Nastasić and Jahn (2005)** describe the suspension systems fitted to different models in detail. On the XM model, both the front and rear suspensions consist of three spheres (bladder accumulators) and four dampers. The system can be switched to a low spring and low damping state (3 spheres and 4 dampers) or high spring and high damping rate (2 spheres and 2 dampers). The system reacts in less than 50 milliseconds and is computer controlled. Inputs to the controller include the angle and angular speed of the steering wheel, speed of movement of the accelerator pedal, braking effort, rotation of the front anti-rollbar and vehicle speed. A switch on the centre console enables the driver to permanently select the high spring and damper state. Another system fitted to Citroën’s Activa 2 research prototype car is described by **Birch, Yamaguchi and Demmler (1990)**. The system is an upgrade of that used for the XM and adds an active anti-roll system that

can double the roll stiffness almost instantly to counter body roll. Roll control is implemented by adding a fourth sphere and a roll control strategy. Roll is reduced when this fourth sphere is disconnected from the system. The system absorbs less than 0.375 kW through a fast corner and double that amount for violent emergency avoidance action.

One of the oldest references found for a switchable hydropneumatic spring system is that described by **Eberle and Steele (1975)**. Their system is indicated in Figure 3.4 and was intended as an operator controlled system. The operator could choose the spring constant to suit the vehicle speed and the type of terrain by opening or closing two valves. Four discrete characteristics are possible namely rigid, firm, medium and soft depending on valves 1 and 2. The placing of the damping units in the branches to the accumulators permits matching of the damping to the selected spring constant.

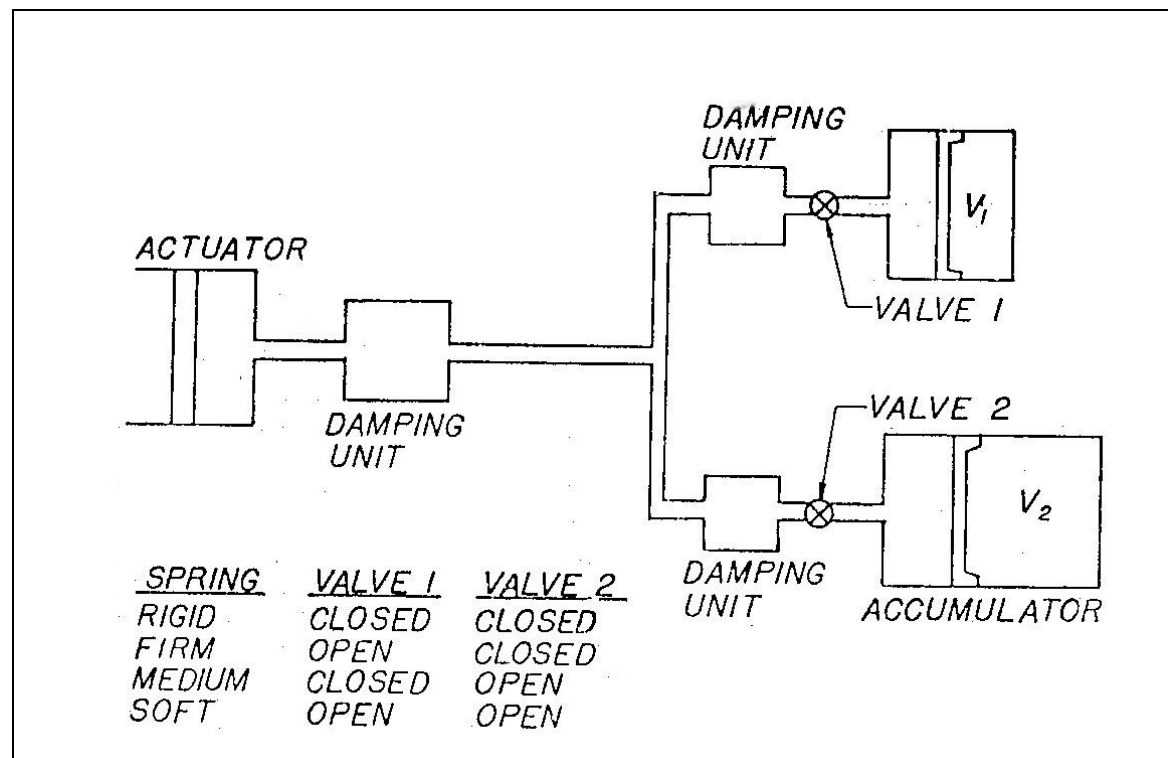


**Figure 3.4** – Operator controlled variable spring as proposed by **Eberle and Steele (1975)**

### 3.2.2.3 Other semi-active spring concepts

Semi-active springs may be realized using other methods *e.g.*:

- Metal springs in combination with air or hydropneumatic springs
- Accumulators with adjustable volume *e.g.* lead screw connected to an electric motor
- Compressible fluid suspension systems
- Piezo-electric actuators
- Smart materials

These ideas were not given further consideration for the purposes of the present study.

### 3.2.3 Active suspension systems

Active suspension systems have been applied to off-road vehicles with limited success. Apart from the high cost, power requirements and bandwidth restrictions seem to be the major obstacles. Both electric and hydraulic actuators have been used.

#### 3.2.3.1 Electric actuators

The design of an electromagnetic linear actuator for active suspension application is described by **Weeks et. al. (1999)** and **Buckner et. al. (2000)**. The actuator consists of an electric motor driving a rack-and-pinion. The actuator was designed to be used in parallel with an air spring that carries the static wheel load. The actuator was designed for retrofit to a high mobility multi-purpose wheeled vehicle (HMMWV). It produces a maximum force of 8896 N, a stroke of 127 mm and a maximum velocity of 1 m/s. The performance of the actuator was evaluated on a quarter-car test rig and found to meet and even exceed the design specifications. Very reasonable peak power requirements of about 12 kW were recorded during some rig tests.

Bose Corporation developed a prototype linear magnetic actuator that was installed at each wheel of a vehicle in a modified McPherson strut configuration (**Anon, 2005b**). A belt-driven alternator and a 12 Volt battery power the system. It is said to improve both comfort and handling and eliminates the need for anti-rollbars. No quantification of performance improvements or power requirements is given.

#### 3.2.3.2 Hydraulic actuators

Lotus was one of the pioneers of hydraulic fully-active suspension systems. A concise summary of the development of the Lotus active suspension system is given by **Wright (2001)**. The technology was initially developed for use in Formula 1 and quickly banned. It was used later in various prototype applications to passenger cars as well as military vehicles (both wheeled and tracked).

Scientists in the Tactical Vehicle Section of the Canadian Army built an active suspension prototype based on the Iltis truck (**Anon, 2005a**). The test vehicle has been in operation since 1995 at the Royal Military College at Kingston, Ontario for its training and testing programmes. The system uses Moog-Lotus servo-controlled actuators with a 20 Hz system response. Power requirements are low (5-10 HP) over moderate cross-country terrain. Vertical acceleration of the driver is reduced by 10% over discrete bumps while slalom speed is increased by 20%. The driver is said to feel increased control with reduced steering effort while rollover is less likely to occur.

Researchers at the University of California (Berkeley) have been involved in research on the control of fully active, hydraulic suspension systems for many years (**Hedrick and Wormley, 1975 and Hedrick et.al. 1994**).

### 3.3 Control techniques and algorithms

It seems that the possibilities concerning control strategies are limitless although the majority of papers use the “Skyhook” strategy proposed by **Karnopp et. al. (1974)** that was derived using Linear Quadratic Optimal (LQO) control theory. Other methods include neural networks, fuzzy logic,  $H_\infty$  and PD control. Preview control is often considered.

Control strategies can broadly be classified in two main categories namely **input driven** and **reaction driven** strategies. The control parameters for **input driven strategies** usually consist of parameters such as vehicle speed, steering angle and brake pressure. These strategies therefore react on inputs from the driver or vehicle before the dynamics of the vehicle changes. **Reaction driven strategies** react to the vehicle’s dynamic reaction due to terrain roughness or driver input. Take as an example a vehicle driving in a straight line, when the driver gives a sudden step input on the steering wheel in order to avoid an accident. An **input driven** strategy might use steering angle as input and switch the dampers to the high damping state as soon as the steering angle or steering velocity exceeds a predetermined level, while a **reaction driven** strategy might use lateral acceleration or yaw rate as input and the dampers will only be switched to the high damping state after the tyres developed enough side force so that the vehicle will turn. In this instance it can be seen that the input driven strategy will respond earlier.

Further discrimination must also be made between the terms **adaptive**, **semi-active** and **active** suspension systems. These terms, as they are used in this study, are defined in Table 1.1. **Adaptive control** on the other hand is used for systems where the controller gains are changed (adapted) according to certain measured parameters i.e. wheel acceleration as a measure of terrain roughness.

#### 3.3.1 Combination of input and reaction driven strategies

**Hine and Pearce (1988)** discuss a strategy for obtaining optimum ride comfort and handling control. The control strategy is separated into six components namely ride, handling, acceleration, deceleration (dive) as well as ride frequency control and vehicle levelling (if required). **Ride control** is initiated by the relative wheel to body displacement in combination with the vehicle speed. For any particular speed, displacement limits are established, outside of which the damper is switched to a higher level. This enables maximum use of available suspension working space while keeping the damper in the soft state for most of the time. The steering sensor together with the speed sensor is used to determine when dampers should be switched to a higher state to improve **handling**. Dampers are also switched to a higher state during **acceleration** and **deceleration** caused by throttle and brake applications. **Levelling** is effected by measurement of relative suspension displacement and compensates for mass and aerodynamic load changes. It is said that significant improvements in ride comfort have been achieved while handling is also improved. The system is commercialised and put into production on the GM Corvette (1986) and Ford Granada 2.8 Ghia.

The hydractive suspension introduced by Citroën in its XM passenger car, and featured in various other Citroën models, is described by **Nastasić and Jahn (2005)**. The angle and angular rate of the steering wheel are used together with the car’s speed and the suspension is switched to firm whenever certain threshold values are exceeded to enable

**handling** control. The speed of movement of the throttle, as well as braking effort is measured and the suspension switched to the firm state when thresholds are exceeded to enable **acceleration** and **braking** control. **Roll** and **yaw** control is achieved by measuring the rotation angle of the front anti-rollbar. Adoption of this control strategy ensures that the system always works in advance of the dynamic reaction of the car (*i.e.* input driven control). This anticipation is said to be of particular advantage during fast driving on winding roads where it reduces body movement and greatly enhances road holding and handling, providing the driver with a unique sensation of control. The system is taken one step further in the Activa 2 concept car (**Birch *et. al.*, 1990**) by the introduction of an additional roll control program.

**Mizuguchi *et. al.* (1984)** discuss the control system fitted to the Mitsubishi Galant. Control inputs include steering wheel speed, lateral, longitudinal and vertical acceleration, vehicle speed and suspension stroke. Test results indicate a significant improvement in ride comfort, handling and stability. A very similar system is fitted to the Toyota Soarer (**Hirose *et. al.* 1988**). A driver's selector switch is also included. The system includes control for anti-dive, anti-roll, anti-squat, anti-bump, response to speed and response to rough road. Very good ride comfort and stability are achieved while vehicle attitude changes are remarkably reduced.

**Wallentowitz and Holdman (1997)** investigate the effect of different spring and damper characteristics. They suggest that vehicle velocity and steering wheel angle be used to switch the suspension to the hard characteristics during ambitious driving situations. Otherwise damper software analyses the excitation frequency and load based on a quarter car model and switches the damper accordingly. No validation is given.

**Hennecke and Ziegler (1988)** discuss a three-state variable damping system fitted to the BMW 635 CSi. Sensors used include steering wheel angle, loading condition, travelling speed, brake pressure, throttle position and vertical body acceleration.

**Poyser (1987)** describes a system designed by Armstrong incorporating a ride levelling hydropneumatic spring and a 3-stage controllable damper. Steering wheel angle, vehicle speed, body roll angle, and suspension travel are used to switch the dampers. For ride comfort control the dampers are switched to the intermediate and high states when certain pre-set limits (vehicle speed dependant) are reached.

**Pinkos *et. al.* (1993)** investigates the feasibility of a continuously variable semi-active Electro-Rheological Magnetic (ERM) fluid damper through mathematical analysis, computer simulation and actual vehicle testing. The control strategy employed is based on adaptive gain control and vector summation of weighted sensor measurements. Each corner of the vehicle is treated independently, but the total control output is calculated from information on vehicle behaviour. Separate calculations are produced for ride comfort, roll, dive, squat, pitch, heave and yaw. The vector summation of these calculations produces an output signal to each damper. Algorithm calculations are prioritised based on safety related vehicle behaviour *i.e.* any calculations related to vehicle handling are completed first. Thirteen sensors are used namely vehicle speed, braking and acceleration, vertical accelerometers on the sprung mass, angular position between the body and the wheel, lateral acceleration and absolute steering wheel position. Both analogue (hardware) and digital (software) filters are employed. Quarter car and half



car models are examined while full-scale vehicle tests are also performed. Good theoretical and experimental results are obtained.

### **3.3.2 Linear optimal, skyhook and on-off control**

These three control methods are discussed together because skyhook control was derived using linear optimal control theory and is used for a continuously variable damper. The on-off strategy is a simplification of the skyhook strategy, adapted for a two stage (on-off) semi-active damper.

**Krasnicki (1981)** investigates the “skyhook” damping principle applied to a two-stage (on-off) semi-active damper.

**Karnopp (1990)** points out that optimal control systems generally require the feedback of all state variables while passive vibration control elements generate forces related to only a subset of the system state variables. A quarter car model is used for simulation (four state variables). Modern control theory suggests that the suspension force should consist of a weighted sum of any four suitable state variables such as positions and velocities. An optimum linear active system can thus be designed using Linear Quadratic Gaussian control theory. According to the author, several other researchers report very similar results. These control methods result in significantly better control of the body (sprung mass) natural frequency. Partial state feedback is also shown to offer nearly the same results as full state feedback. It is concluded that as far as body movement due to terrain inputs is concerned, semi-active systems can approach the performance of fully active systems with state variable feedback. It is however necessary to know the sprung mass absolute velocity in order to apply state variable feedback control. (This cannot easily be measured and might not be practical for vehicle implementation. It might not even be possible to accurately estimate (see **Hedrick et. al., 1994**))

**Sharp and Hassan (1987)** study two alternative forms of control law. A quarter car model is used for simulation. The semi-active damper is assumed to be capable of producing a force that is a linear combination of state variables as long as such a force opposes the relative motion of the damper. Otherwise it is set to produce no force. The control laws are derived using stochastic linear optimal control theory. The constants used in the control laws are obtained by minimising a performance index using two weighting parameters, one for dynamic tyre load variations and the other for suspension working space. The results given are for only one road surface roughness and one vehicle speed but cover a range of suspension working space. It is concluded that semi-active damping can improve ride comfort significantly but that the constants in the control laws must be adapted according to the terrain roughness (or available suspension working space). It is suggested that this adaptation of the coefficients can be achieved by keeping a running average of the relative suspension displacement or monitoring the number of bump stop contacts. The maximum use must be made of the available suspension travel while hitting the bump stops must be avoided.

**Margolis (1982a)** uses a vehicle model that includes the heave (vertical) and pitching motions of a vehicle. Controllers are designed for the fully active case and then modified to be semi-active. Two control strategies are investigated namely the familiar “skyhook” control (feedback of body absolute velocity and relative damper velocity) as well as complete state variable feedback (SVFB). It is concluded that SVFB and “skyhook”

control both give excellent results compared to that of the passive system. Results are not sufficiently strong in favour of SVFB to justify the increased complexity of measuring all four state variables.

**Margolis (1982b)** presents the expected response of a simple vehicle (single degree of freedom) fitted with an active and semi-active suspension when the control system is presented with non-ideal feedback information. The control strategies evaluated need feedback of the absolute velocity of the sprung mass. Determination of this velocity is quite difficult in a realistic environment where the vehicle has many degrees of freedom, for example roll, pitch, yaw and heave. This problem is intensified because all measurements are corrupted by noise. The absolute velocity can be determined by integrating an accelerometer signal by analog or digital means. It is however very difficult to produce a drift free pure integrator. A low pass filter is used instead of a pure integrator with a break frequency much lower than the frequency of interest. This is also very difficult to realise because huge capacitor and resistor values are needed. Furthermore the long time constants involved give rise to DC drift. The DC drift is exaggerated by the fact that an accelerometer that can measure at the very low frequencies is also sensitive to vehicle orientation (for example driving up a long incline). This necessitates the inclusion of a high pass filter to eliminate the DC drift or steady state bias. The high pass filter suffers from the same drawback of an extremely low break frequency. It is indicated that the provision of acceleration feedback can provide some compensation for the non-ideal velocity measurement. Significant improvements over the passive system are still achieved although degraded by non-ideal velocity measurements.

**Nell and Steyn (1994)** discuss the experimental evaluation of a two-state semi-active damper for off-road vehicles. Three control strategies available from literature are tested. The first strategy used is the on-off strategy proposed by Karnopp (see **Rakheja and Sankar, 1985**) that switches the damper according to the sign of the product of absolute body velocity and relative damper velocity. The second strategy uses absolute body acceleration and relative damper velocity. The third strategy proposed by **Rakheja and Sankar (1985)** uses the product of relative damper displacement and relative damper velocity. Unweighted RMS values of body acceleration, relative displacement and velocity, absolute velocity and force indicate that the biggest improvement is achieved using acceleration feedback followed by relative displacement and velocity (Rakheja and Sankar). The on-off strategy proposed by Karnopp returns unsatisfactory results without any significant improvements.

Experimental verification of theoretical work is discussed by **Rajamani and Hedrick (1991)**. A full-scale half-car suspension test rig is used to evaluate semi-active dampers. High bandwidth (10 ms) 12 state semi-active dampers as well as low bandwidth 3-state dampers are used. Conventional on-off, optimal on-off, optimal multi-state control and a robust form of multi-state control are implemented and compared to predicted results. Good correlation between predicted and measured results is achieved. The semi-active suspension is found to behave as well as the best of all passive states at every frequency.

**Lizell (1988)** describes semi-active damper hardware and software that is tested in the laboratory and on a vehicle. The aim of the control strategy employed is to switch the two-stage damper to the high damping state in the region of the body resonance and wheel hop frequencies, while the soft state is used for all other frequencies. This is said to improve both handling and ride comfort throughout the frequency range. Damping of the

body resonance frequency is controlled using the Karnopp strategy. The wheel hop frequency is controlled by calculating a discrete Fourier transform (DFT) around the wheel hop frequency. The value obtained is compared to a threshold level to determine damper switching. The damper is switched to the low damping state under all other conditions. The absolute body velocity is determined from integrating an acceleration signal after analog low-pass filtering. A digital high pass filter is implemented and drift in the integration process is controlled by “leakage”. Preliminary test data is promising.

**Ivers and Miller (1989)** compare experimental results obtained from a quarter car test rig with simulation data. A semi-active damper with 25 discrete states is used. The control algorithms used are based on the simple analogy of the skyhook damper. Absolute body velocity is determined by pseudo-integrating an acceleration signal. Three cases are investigated namely passive, two stage (on-off) semi-active and continuous (25 stages) semi-active control. Test results confirm the trends indicated by simulation, but there are discrepancies due to the fact that valve response times, time delays in the control system, hysteresis, friction in the test rig and non-linear damper characteristics are ignored in the simulation.

**Miller and Nobles (1988)** describes the development and testing of a semi-active suspension on an M551 military tank. The article gives a good overview of the development history of controllable suspension systems and presents the basic theory concerned with optimal control, resulting in the skyhook damper and on-off strategy. The on-off strategy is implemented for vehicle trials. The determination of absolute velocity is considered a challenge and is estimated (pseudo integrated) by filtering an accelerometer signal. The valve configuration in the damper is designed so as to eliminate the need to measure relative velocity. The control system therefore only has absolute velocity as input while valve logic takes care of the rest. Vehicle testing is performed on a 10-axis vertical road simulator. Average absorbed power was used as evaluation parameter and indicated a measured performance gain between 13 and 43% depending on vehicle speed.

**Miller (1988a)** investigates the effect of hardware limitations on an on-off semi-active suspension using a single degree of freedom simulation model and the familiar on-off control strategy. The effects of non-zero off-state damping, valve dynamics and digital filter dynamics (used to determine the absolute velocity) are investigated. Results indicate that the off-state damping ratio should be less than 0.2. Valve response times should be less than 14 milliseconds and sampling time less than 4 milliseconds. Digital filters should have a break frequency of approximately 0.1 Hz and a damping ratio of between 0.3 and 1.0.

**Temple and Hoogterp (1992)** describe simulation and vehicle test results obtained for the Mobility Technology Test Bed (MTTB) vehicle. The adaptive dampers employ an on-off strategy based on hull and damper dynamics. The damper is turned on only when it will help to reduce the pitch and roll velocities. Whenever the anticipated jounce or rebound damping would tend to increase the hull pitch and roll velocities, the dampers are switched to the low damping state. No further details of the control strategy or implementation thereof are given. Nearly a 1000 mobility and agility tests were conducted on 10 vehicle configurations, all indicating noteworthy improvements in ride comfort, reaction to discrete obstacles, reductions in body roll and reductions in pitching.

**Besinger, Cebon and Cole (1991)** tests an on-off semi-active damper in a hardware-in-the-loop (HiL) test setup where a quarter car model is solved by computer simulation while the damper force is measured directly in real time from the experimental setup. On-off skyhook control is implemented.

**Hrovat and Margolis (1981)** describe an experimental heave model of a tracked air cushion vehicle incorporating an on-off semi-active damper. The control is performed using a simple analog circuit with operation amplifiers and NAND gates implementing the on-off strategy. Sinusoidal ground inputs in the range of 2 to 5.5 Hz are used. Results indicate that significant improvements can be realised using semi-active damping compared to passive damping. Absolute and relative damper velocities are obtained by analog differentiation of displacements measured by LVDT's. It is not possible to implement this strategy in a real vehicle application.

**Soliman *et. al.* (1996a and 1996b)** extend previous work (where linear stochastic optimal control theory was used to formulate a limited state feedback scheme) to include adaptive control based on a gain scheduling approach. Results are determined theoretically and experimentally using a quarter car model and test rig. Two strategies are investigated using RMS wheel acceleration and RMS of the suspension working space (relative displacement) respectively. Road surfaces of varying roughness are generated using Gaussian random distributions and a road roughness number. Based on linear optimal control theory, the absolute displacements and velocities of the wheel and body are still required. A look-up table is used to determine the "optimum" gains for the specific road input conditions as measured by the sensors. Theoretical and experimental results indicate that the scheme based on the RMS vertical acceleration results in the highest improvements in body acceleration, suspension working space and dynamic tyre loads.

**Abd El-Tawwab and Crolla (1996)** include component limitations in the theoretical and experimental investigation of a three state semi-active damper in a quarter car model and test rig. The ideal actuator force is determined from optimal control theory and involves feedback of absolute displacements and velocities for both the sprung and unsprung mass, each associated with a control gain. The gains are determined using a gradient search method. A random road input and a constant vehicle speed of 20 m/s is used. Results indicate an improvement of between 13 and 17% for sprung mass acceleration and 7 to 8% for dynamic tyre load.

**Lieh (1996)** studies the application of velocity feedback active suspension systems. No results are presented.

**Petek *et. al.* (1995)** performs vehicle tests using fast, continuously variable, electro-rheological (ER) dampers. A modified skyhook algorithm is implemented which include roll, pitch and heave motion. Accelerometers and LVDT's are used to determine body acceleration and relative displacement respectively. Accelerations are integrated (to obtain absolute roll, pitch and heave velocities) and relative displacements differentiated to obtain relative velocities. Four gain constants are used to determine the relative importance of roll, pitch and heave motion. Test results indicate significant improvements in ride comfort and stability compared to the standard passive suspension.

### 3.3.3 Neural networks and Fuzzy logic

An extensive literature survey on the applications of fuzzy logic and neural networks to vehicle systems, including suspension control, is given by **Ghazi Zadeh *et. al.* (1997)**.

**Chou *et. al.* (1998)** present a new control scheme referred to as the grey-fuzzy control method that consists of two parts namely the grey predictors and the fuzzy logic controller. The system is said to be able to control excessive tyre deflection and improve ride comfort. The Taguchi method is employed to search for the optimal control parameters and the results, obtained by computer simulation of a quarter car model, is said to be satisfactory.

**Hashiyama *et. al.* (1995)** presents a new method to generate fuzzy controllers through the use of a genetic algorithm (GA). Appropriate combinations of input variables, number of fuzzy rules and parameters for membership functions are determined automatically through the GA operations. A fuzzified version of Karnop's law of suspension control was incorporated as the initial fuzzy rules. These initial rules are not modified by the GA but the GA with a new local improvement mechanism is applied to find additional fuzzy rules for better performance. The performance index is improved but no comparisons are given to the passive suspension performance.

**Yoshimura *et. al.* (1997)** presents a semi-active suspension controlled by fuzzy reasoning. The input variables to the fuzzy control rules are the suspension travel and its derivative. The aim is to minimise body vertical and roll acceleration at the centre of gravity under the constraints of suspension travel and tyre deflection. A half car simulation model is used. Simulation results show that the proposed system is very effective in improving the vertical and rotary accelerations of the vehicle body as well as tyre deflections.

### 3.3.4 $H_{\infty}$ control

**Palmeri *et. al.* (1995)** describes the application of  $H_{\infty}$  optimal control theory to the design of a fully active suspension system for an experimental Lancia Thema sedan car. The system functions as a Multiple Input Single Output (MISO) regulator with hub acceleration, actuator force and actuator position as inputs. The  $H_{\infty}$  control strategy has been chosen to take advantage of the possibility to design a competitive MISO controller as well as exploit robust disturbance rejection which the  $H_{\infty}$  theory grants. Each corner of the vehicle is modelled as a seventh order state-space model. The  $H_{\infty}$  regulator is a model-based compensator, which means that it contains the system's state-space model that is observed and the control compensates for the error. Vehicle tests on a laboratory test setup indicate that  $H_{\infty}$  performs significantly better at all speeds than the skyhook baseline, especially at low frequencies around the body roll frequency.

### 3.3.5 Proportional Derivative (PD) control

**Esmailzadeh (1979)** uses a linear model of a suspension system employing a pneumatic isolator and a three-way servo valve. Simulation is performed on an analogue computer and compared to experimental measurements of a quarter car model. Proportional and derivative feedback control is used.

### 3.3.6 Preview control

Currently no feasible mass production preview sensors are available for suspension control purposes and even if such sensors become available in the near future, it is doubtful whether they will be of much use on off-road vehicles travelling over rough, vegetation covered and deformable terrain. Preview control is not discussed in depth due to this reason.

**Soliman and Crolla (1996b)** investigate the use of preview or “look-ahead” information for semi-active damper systems using a quarter car theoretical model. The system is said to achieve the same performance as a fully active system without preview.

**Youn (1991)** derives a preview control strategy using optimal control theory with jerk included in the performance index. Simulation is performed using a two-degree of freedom quarter car model. The proposed control method is said to improve handling and ride comfort simultaneously. The jerk controller can determine the damping coefficient or spring stiffness of the semi-active system.

**Crolla and Abdel-Hady (1991)** investigates the effect of wheelbase preview (i.e. that the rear suspension input is just a delayed version of the input at the front) on the performance of semi-active and fully active suspension systems. A continuous semi-active damper is used which is modelled as having a maximum and minimum damping constant. Damper response time is modelled as a first order time lag. A simple full vehicle model with vertical, pitch and roll degrees of freedom is used for simulation. The control law is based on full state feedback. The conclusion is drawn that semi-active systems with wheelbase preview can perform better than fully active systems without wheelbase preview.

### 3.3.7 Model following

**Pollard (1983)** adopts a strategy first developed for a maglev train, to control the active suspension of a normal train. The control system consists of two complementary parts. At low frequencies the vehicle must follow the tracks and displacements must be maintained within certain limits. The actuator is then controlled so as to minimise relative displacements over the secondary suspension. At high frequencies, the acceleration of the body is fed back to the control system and the system tries to minimise acceleration. The control system is said to model the ideal suspension while the actuator tries to correct the error. The bounce and pitch modes of the body are controlled separately.

### 3.3.8 Frequency domain analysis

**Hamilton (1985)** proposes to use a Discrete Fourier Transform (DFT) to calculate the magnitude of vibration levels in different frequency bands in order to control body resonances.

**Kojima et. al. (1991)** implement a frequency detection method that changes the dampers to high damping when suspension inputs are predominantly in the low frequency range. Low damping is used for suspension movements that are predominantly in the high frequency range. It is found that the low frequency region is accompanied by large suspension stroke variation and large variations in distance between the vehicle body and

ground while damping force variation ratio and bounce down acceleration is small. The magnitude of these parameters is reversed in the high frequency region, enabling discrimination between frequency ranges on the basis of the amplitude of these parameters. A relative position sensor measures suspension movement and piezo-electric ceramic sensor is used to detect the damping force variation ratio. The suspension movement sensor does not have an absolute neutral position signal but determines the neutral position by compensation with learning control. Additional sensors, for example vehicle speed, steering, brake application and throttle angle are also used.

### 3.3.9 “Relative” control

**Rakheja and Sankar (1985)** and **Alanoly and Sankar (1987)** present an “original” control strategy employing only directly measurable variables in vehicle applications. A continuously modulated damper is controlled using only relative damper displacement and relative velocity as feedback signals. A condition function based on the sign of the product of relative velocity and relative displacement determines whether the high (on) or low (off) damping state have to be used. The origin of, or reasoning behind, this strategy appears to be determined from a thought experiment. There is very little variation between this scheme and the “skyhook” damping algorithm. Performance approaching that of a fully active suspension system is achieved from simulation results on a single degree of freedom system. This system avoids the problem of measuring the sprung mass absolute velocity, that is said to be a near impossible task, and has never been implemented on a vehicle (at the time of writing). The same strategy is proposed by **Jolly and Miller (1989)** and is termed “relative control”. It is developed by means of intuitive reasoning. Relative control is found to perform better than the passive system but slightly worse than skyhook control. At high frequencies, relative control gives results very similar to skyhook damping, but at low frequencies, relative control performs worse than the passive system. It is likely that relative control will provide better performance in applications where most of the disturbance energy is transmitted at higher frequencies.

### 3.3.10 Traditional controller design on the s-plane

**Hall and Gill (1987)** depart from the approach of using optimal control theory. Instead they try to relate the position of the closed loop poles of the system on the s-plane to the poles of a well-designed “skyhook” system. Not much success is achieved with this method. The authors then revert to scanning of the s-plane in order to find optimum pole locations. It is concluded that, although the transmissibility indicates significant improvements, the phase relationships need to be taken into account.

### 3.3.11 Minimum product (MP) strategy

**Nell and Steyn (1998)** develop an alternative control strategy (called the minimum product or MP strategy) for semi-active dampers on off-road vehicles that takes into account the pitch and roll degrees of freedom. The strategy selects a combination of damper settings (all dampers on vehicle taken into account) that minimises roll and/or pitch acceleration. Both simulation and experimental results, that indicate that this strategy performs better over off-road terrain in comparison with both the passive and on-off skyhook systems, are given. The damper state that will give the lowest acceleration in the present direction of movement, or the highest acceleration in the opposite direction, is selected. Input variables to the control system are relative velocity of each damper as well

as the roll and pitch accelerations of the vehicle body (calculated from three vertical acceleration measurements by assuming that the vehicle body is rigid).

### 3.3.12 Roll and pitch velocity

**Salemka and Beck (1975)** formulate and test a strategy based on the roll and pitch velocities of the vehicle body. Terrain parameters, for example the relative amount of roll and pitch velocities and vertical acceleration generated by the terrain, severely influence the success of any control strategy.

### 3.3.13 Resistance control

**Fodor and Redfield (1996)** implement resistance control semi-active damping on a 1/30th-scale quarter car test rig. Test results are compared to simulation results and good correlation is found.

### 3.3.14 Mechanical control

**Speckhart and Harrison (1968)** perform an analytical and experimental investigation of a hydraulic damper having internal inertially controlled valves. The valve is purely mechanical and no “control system” is used. The system claims to improve ride comfort by reducing jerk. System performance is evaluated by simulation and laboratory testing of a two degree of freedom system.

### 3.3.15 Steepest gradient method

**Tseng and Hedrick (1994)** investigate the optimal semi-active suspension that will minimise a deterministic quadratic performance index. The optimal control law is a time-varying solution that involves three related Riccati equations. The constant Riccati equation (so-called “clipped optimal” solution) is not optimal. They develop a new semi-active algorithm called the “steepest gradient” algorithm. Performance is shown to be superior to that of the “clipped optimal” solution.

### 3.3.16 Use of estimators and observers

**Hedrick *et. al.* (1994)** propose a new method for designing observers for automotive suspensions. The methodology guarantees exponentially convergent state estimation using easily accessible and inexpensive measurements. It is also demonstrated that the sprung mass absolute velocity cannot be estimated in an exponentially stable manner with such measurements. The estimation error is merely bounded and would not converge to zero. Results are verified on the Berkely Active Suspension Test Rig with excellent results. The sprung mass velocity is, however, not estimated, but determined by integrating the body acceleration after passing it through a high pass filter.

### 3.3.17 Control of handling

No literature proposing any control strategies for specifically improving vehicle handling was found. In cases where handling is considered, it seems that the authors opted for the stiffest possible setting when encountering handling manoeuvres.



### 3.3.18 Control of rollover

A genetic algorithm predictor for vehicle rollover was developed by **Trent and Greene (2002)**. They modelled a 1997 model Jeep Cherokee SUV. Their preliminary results indicate rollover prediction of 400 milliseconds in advance of the actual event. They suggest that this early warning could be used to prevent rollover by activating other vehicle systems such as differential braking or suspension control.

### 3.3.19 Ride height adjustment

A decrease in ride height is generally beneficial for handling as the centre of gravity height will be decreased. This improves the static stability factor (SSF) and should therefore reduce the rollover propensity of the vehicle. Care should however be taken not to change the suspension geometry in a manner that will adversely affect the handling. On the other hand an increase in ride height might benefit ride comfort over rough terrain because suspension travel in bump will be increased, thereby reducing the number of bump-stop contacts. In many vehicles, the ability to maintain constant ride height independent of load is a major advantage, without necessarily adding the capability to increase or decrease ride height. The success of ride height control can be judged by its numerous commercial applications.

### 3.3.20 Comparison of semi-active control strategies for ride comfort improvement

**Voigt (2006)** studied several control strategies proposed in literature during the last 20 years with the objective of improving ride comfort. The study focussed on on-off control ideas. The aim of the study was to develop and implement an appropriate ride comfort control strategy for a 4-state semi-active hydropneumatic suspension system, consisting of a two-state semi-active hydropneumatic spring and a two-state semi-active damper.

Simulation models of both  $\frac{1}{4}$  car and  $\frac{1}{2}$  car (pitch and bounce) vehicles were developed in Simulink. Typical values for a Land Rover Defender 110 SUV were used in the models. The suspension model developed by **Theron and Els (2005)**, as described in paragraph 4.8, was used in the simulation. Hardware-in-the-loop (HiL) testing of a prototype suspension system was also performed using the techniques developed by **Misselhorn, Theron and Els (2006)**. The suspension used in the HiL test rig was Prototype 2 discussed in chapter 4 of the present study. Simulation results and HiL results were found to correlate very well (within 10%). In order to simulate ride comfort for both on- and off-road conditions, road inputs included:

- i) sine waves with frequencies between 0 and 30 Hz and amplitudes of 0.001 to 0.015 m.
- ii) Belgian paving (Figure 2.21)
- iii) APG bump (Figure 2.22)
- iv) typical random road profiles ranging from a “smooth runway” to a “ploughed field” generated from road roughness information obtained from literature.

The following control ideas were evaluated:

- i) ADD – Acceleration driven damper as proposed by **Silane et. al. (2004)**. This proposed strategy is the same as the strategy proposed by **Holsher and Huang (1991)**.

- ii) Skyhook – The familiar skyhook damper strategy proposed by **Karnopp et al. (1973)**.
- iii) ReS – The strategy proposed by **Rakheja and Sankar (1985)**.
- iv) MP – The minimum product strategy proposed by **Nell (1993)**.

Table 3.1 indicates all the proposed ideas that were evaluated. No useful semi-active spring control ideas were found. The springs were controlled using appropriately modified versions of the damper control ideas. As a comparison, the passive “ride comfort” mode (soft spring and low damping) of the semi-active hydropneumatic spring-damper system was also simulated.

Simulation results indicated that “Spring ADD” performed marginally better than the passive “ride comfort” mode. No control strategy was able to outperform the passive “ride comfort” mode by more than 2%, which is within expected simulation error. The “ride comfort” mode outperformed all control strategies for all HiL tests.

Voigt also investigated why the skyhook strategy performed unsatisfactory. The non-linearity of the system affects performance. Skyhook performs well at low frequencies but performance deteriorates at higher frequencies. This indicates that the valve response time is too slow. Better ride comfort is also achieved by controlling the spring rather than the damper.

The effect of limited suspension working space was also addressed by including bump stops in the model. This had the biggest effect on the ride comfort of the passive suspension. Again the “ride comfort” mode performed the best of all the possibilities. It seems that the suspension system under consideration exhibits the same useful characteristic of the twin-accumulator system described by **Abd El-Tawwab (1997)** amongst others. Due to the dampers between the accumulators, the large accumulator is progressively “sealed off” by the increased flow through the damper, *i.e.* spring stiffness increases automatically when terrain gets rougher (higher flow rate of oil) thereby eliminating bumpstop contact. This change is not discrete but happens gradually in relationship to the suspension velocity.

It is concluded from **Voigt’s** study that it is not possible to improve ride comfort to any worthwhile extent by controlling the spring and damper characteristics when the characteristics have been optimised for ride comfort.

A similar study for handling has not yet been performed.

### 3.4 Conclusion

The following conclusions are made with respect to possible solutions for the ride comfort vs. handling compromise:

- i) The ride comfort vs. handling compromise can be eliminated using active suspension systems. These systems are very expensive and require significant amounts of engine power. This option is disregarded for these reasons.
- ii) Semi-active suspension systems have the potential to approximate the performance of fully active systems, but at a considerable reduction in cost and complexity.

**Table 3.1** – Control strategies evaluated by Voigt (2006)

Control Strategy Description	Damper Strategy	Damper	Spring strategy	Spring
ADD	$\ddot{x}_1(\dot{x}_1 - \dot{x}_2) > 0$ $\ddot{x}_1(\dot{x}_1 - \dot{x}_2) < 0$	Hard Soft	Soft spring	
Skyhook	$\dot{x}_1(\dot{x}_1 - \dot{x}_2) > 0$ $\dot{x}_1(\dot{x}_1 - \dot{x}_2) < 0$	Hard Soft	Soft spring	
ReS	$(\dot{x}_1 - \dot{x}_2)(x_1 - x_2) < 0$ $(\dot{x}_1 - \dot{x}_2)(x_1 - x_2) > 0$	Hard Soft	Soft spring	
Spring ADD	Hard damping		$\ddot{x}_1(\dot{x}_1 - \dot{x}_2) > 0$ $\ddot{x}_1(\dot{x}_1 - \dot{x}_2) < 0$	Hard Soft
Spring Skyhook1	Hard damping		$\dot{x}_1(\dot{x}_1 - \dot{x}_2) < 0$ $\dot{x}_1(\dot{x}_1 - \dot{x}_2) > 0$	Hard Soft
Spring Skyhook2	Hard damping		$x_1(x_1 - x_2) < 0$ $x_1(x_1 - x_2) > 0$	Hard Soft
Spring Skyhook3	Hard damping		$\ddot{x}_1(x_1 - x_2) > 0$ $\ddot{x}_1(x_1 - x_2) < 0$	Hard Soft
Spring ReS	Hard damping		$(\dot{x}_1 - \dot{x}_2)(x_1 - x_2) > 0$ $(\dot{x}_1 - \dot{x}_2)(x_1 - x_2) < 0$	Hard Soft
Combo ADD1	$\ddot{x}_1(\dot{x}_1 - \dot{x}_2) > 0$ $\ddot{x}_1(\dot{x}_1 - \dot{x}_2) < 0$	Hard Soft	$\ddot{x}_1(\dot{x}_1 - \dot{x}_2) > 0$ $\ddot{x}_1(\dot{x}_1 - \dot{x}_2) < 0$	Hard Soft
Combo ADD2	$\ddot{x}_1(\dot{x}_1 - \dot{x}_2) > 0$ $\ddot{x}_1(\dot{x}_1 - \dot{x}_2) < 0$	Hard Soft	$\ddot{x}_1(x_1 - x_2) > 0$ $\ddot{x}_1(x_1 - x_2) < 0$	Hard Soft
Combo ADD3	$\ddot{x}_1(\dot{x}_1 - \dot{x}_2) > 0$ $\ddot{x}_1(\dot{x}_1 - \dot{x}_2) < 0$	Hard Soft	$x_1(x_1 - x_2) < 0$ $x_1(x_1 - x_2) > 0$	Hard Soft
Combo Skyhook1	$\dot{x}_1(\dot{x}_1 - \dot{x}_2) > 0$ $\dot{x}_1(\dot{x}_1 - \dot{x}_2) < 0$	Hard Soft	$\dot{x}_1(\dot{x}_1 - \dot{x}_2) > 0$ $\dot{x}_1(\dot{x}_1 - \dot{x}_2) < 0$	Hard Soft
Combo Skyhook2	$\dot{x}_1(\dot{x}_1 - \dot{x}_2) > 0$ $\dot{x}_1(\dot{x}_1 - \dot{x}_2) < 0$	Hard Soft	$x_1(x_1 - x_2) < 0$ $x_1(x_1 - x_2) > 0$	Hard Soft
Combo Skyhook3	$\dot{x}_1(\dot{x}_1 - \dot{x}_2) > 0$ $\dot{x}_1(\dot{x}_1 - \dot{x}_2) < 0$	Hard Soft	$\dot{x}_1(x_1 - x_2) > 0$ $\dot{x}_1(x_1 - x_2) < 0$	Hard Soft
Combo ReS1	$(\dot{x}_1 - \dot{x}_2)(x_1 - x_2) < 0$ $(\dot{x}_1 - \dot{x}_2)(x_1 - x_2) > 0$	Hard Soft	$(\dot{x}_1 - \dot{x}_2)(x_1 - x_2) > 0$ $(\dot{x}_1 - \dot{x}_2)(x_1 - x_2) < 0$	Hard Soft
Combo ReS2	$(\dot{x}_1 - \dot{x}_2)(x_1 - x_2) < 0$ $(\dot{x}_1 - \dot{x}_2)(x_1 - x_2) > 0$	Hard Soft	$\dot{x}_1(x_1 - x_2) < 0$ $\dot{x}_1(x_1 - x_2) > 0$	Hard Soft
Combo KP	$\ddot{z}_w \cdot \ddot{z}_{b(2)} < \ddot{z}_w \cdot \ddot{z}_{b(1)}$ $\ddot{z}_w \cdot \ddot{z}_{b(2)} > \ddot{z}_w \cdot \ddot{z}_{b(1)}$	Hard Soft	$\ddot{z}_w \cdot \ddot{z}_{b(2)} < \ddot{z}_w \cdot \ddot{z}_{b(1)}$ $\ddot{z}_w \cdot \ddot{z}_{b(2)} > \ddot{z}_w \cdot \ddot{z}_{b(1)}$	Hard Soft

- iii) There are two viable concepts for a semi-active damper namely: Magneto-rheological (MR) fluids and hydraulic dampers with bypass valves. Designs can be continuously variable or discrete.
- iv) There are basically two viable concepts for a semi-active spring namely air springs and hydropneumatic springs.
- v) As far as control is concerned, a myriad of possibilities exist. All ideas can however not be easily implemented in the vehicle *e.g.* measurement of absolute body velocity for full-state feedback.
- vi) Ride height adjustment is widely used and offers many possibilities.
- vii) Reaction speed needs to be taken into account to determine potential system performance.
- viii) Very little literature exists on semi-active springs.
- ix) Most control ideas are developed using  $\frac{1}{4}$  car linear models that do not sufficiently represent actual vehicle dynamics.
- x) Very limited hardware has been implemented and documented.
- xi) Almost no work has been performed on off-road vehicles.
- xii) The majority of studies focus on ride comfort, and handling is often neglected.
- xiii) Preview is a popular research topic, although hardware implementation is problematic.

### **3.5 Proposed solutions to the ride comfort vs. handling compromise**

Based on the ideas and research described in chapters 2 and 3, the proposed solution to the “ride comfort vs. handling compromise” is to use a twin accumulator hydropneumatic (two-state) spring combined with an on-off (two-state) semi-active hydraulic damper (achieved with a by-pass valve), based loosely on idea by **Eberle and Steele (1975)**. Although more than two spring and/or damper characteristics can be incorporated, two is considered sufficient based on the simulation results presented in Chapter 2.

Based on the results, presented by **Voigt (2006)**, for ride comfort control, and assuming that the same trends will be found for handling, if studied, the best practical solution would be no “control” other than switching between the “ride comfort” and “handling” modes. The pre-requisite is however that a successful ride comfort vs. handling decision-making strategy can be developed that will automatically switch between the “ride comfort” and “handling” modes. The switching must be safe and quick enough to prevent accidents, using only easily measurable parameters.

The proposed suspension system will now be called the **4-State Semi-active Suspension System** or **4S<sub>4</sub>**.

---

---

## ***THE FOUR-STATE SEMI-ACTIVE SUSPENSION SYSTEM (4S<sub>4</sub>)***

---

---

The development of a prototype 4-State Semi-active Suspension System (4S<sub>4</sub>) is described in this chapter. Literature appropriate to the development of the suspension system, and the working principle of the system is discussed. Two prototype suspension systems (from now on referred to as Prototype 1 and Prototype 2 respectively) were designed, manufactured, tested on a laboratory test rig and modelled mathematically.

After determination of the space envelope on the proposed test vehicle, Prototype 1 was designed and manufactured by Hytec, a specialist hydraulic equipment manufacturer. Prototype 1 suffered from several drawbacks that necessitated a redesign. Prototype 2 is an in-house design and solved all the problems experienced on Prototype 1.

Detailed test results for Prototype 2 are discussed and interpreted. Test results for Prototype 1 are only discussed where necessary to motivate some of the decisions made during development of Prototype 2. Test results include spring and damper characteristics as well as several parameters required for mathematical modelling of the suspension system. These parameters include the bulk modulus of the oil, thermal time constant of the accumulators, valve response times and pressure drops over the valves.

### **4.1 Literature**

#### **4.1.1 Hydropneumatic springs**

Hydropneumatic springs are often modelled as polytropic gas compression processes. With the assumption that the ideal gas law is applicable, this approach gives satisfactory first order results. The static spring force can be calculated accurately using isothermal compression. The dynamic force is however time and temperature dependent and requires a more advanced model to achieve accurate results.

A detailed hydropneumatic spring model is developed and validated by **Els (1993)** and **Els and Grobbelaar (1993)**. This model is based on the solution of the energy equation of a gas in a closed container and therefore takes time- and temperature dependency of the spring characteristic into account. It is based on a thermal time constant approach and uses the Benedict-Webb-Rubin (BWR) equation for real gas behaviour (**Cooper and Goldfrank, 1976**). The model is verified against experimental results and good correlation is achieved between measured and predicted spring characteristics. The model is further developed to include heat transfer effects from the damper that is usually an

integral part of a hydropneumatic suspension system (**Els and Grobbelaar, 1999**). This model was used to predict the  $4S_4$  spring characteristics in paragraph 4.8.

Another approach that can be used to model hydropneumatic springs is by making use of the so-called anelastic model (**Kornhauser, 1994** and **Giliomee *et. al*, 2005**).

#### 4.1.2 Variable spring concepts

The concept of making a semi-active spring using accumulators is not new. The fundamental idea was proposed by **Eberle and Steele (1975)** as discussed in par 3.2.2.2. **Decker *et. al*. (1988)** also implemented an air spring with various discrete volumes that can be switched. The design was made for a passenger car, but no quantitative results or design guidelines are given.

A passive twin-accumulator suspension system is proposed by **Abd El-Tawwab (1997)**. Two accumulators are connected via an orifice. As the flow rate of oil in the system increases, damping through the orifices increases thereby resulting in different amounts of fluid flowing into each accumulator. This results in a speed or frequency dependant spring characteristic. The  $4S_4$  system incorporates this capability as a function of its design.

First attempts by the candidate to develop a two-state semi-active spring combined with a two-state semi-active damper are discussed by **Giliomee and Els (1998)**. The design was for a heavy off-road wheeled vehicle with a static wheel load of 3 000 kg. Experimental results included testing the system in a single degree of freedom test rig using various control methods. Initial results were very promising and warranted further development of the  $4S_4$  system.

#### 4.1.3 Hydraulic semi-active dampers

Semi-active dampers have been applied widely in prototypes and production vehicles. The work of **Nell (1993)**, **Nell and Steyn (1994, 1998 and 2003)** as well as **Els and Holman (1999)** is of particular significance to the development of the  $4S_4$  due to the applications to heavy off-road military vehicles. The applications varied from two-state translational semi-active dampers for a 12-ton 4x4 vehicle up to a two-state semi-active rotary damper for a 46-ton self-propelled gun. In all these cases simulation results are validated using vehicle tests with prototype dampers and control systems fitted. The results are generally very satisfactory.

All these dampers operate on the bypass valve principle and have valve response times of between 40 and 200 milliseconds. Large flow rates of up to 1000 l/min can be accommodated with acceptable pressure drops over the valves.

## 4.2 $4S_4$ Working principle

The concept behind the  $4S_4$  system is to achieve switching between two discrete spring characteristics, and between two discrete damper characteristics. The high and low characteristics for both spring and damper are possible by alternate channeling of hydraulic fluid with solenoid valves. The basic circuit diagram of the proposed suspension system is given in Figure 4.1. The strut is fixed between the vehicle body and

the unsprung mass, replacing both the spring and damper. The strut is connected to two accumulators via the control valves and hydraulic damper valves. The two-state hydropneumatic spring can also be used on its own in parallel with an additional semi-active damper *e.g.* a continuously variable MR fluid based damper, but then some of the elegance and packaging possibilities of the 4S<sub>4</sub> unit will be sacrificed.

The low spring rate is achieved by compressing the combined volume of gas in the two accumulators. By sealing off accumulator 2 with valve 3, a smaller gas volume is compressed and a higher spring rate is achieved. Spring rates can be individually tailored by changing the two gas volumes. For low damping, the hydraulic dampers (dampers 1 and 2) are short circuited by opening the bypass valves (valves 1 and 2). For high damping these valves are closed and the hydraulic fluid is forced through the dampers resulting in high damping force. The proposed system therefore achieves its aim to provide switching between two discrete spring characteristics, as well as switching between two discrete damper characteristics using solenoid valves.

The concept can easily be extended to more spring characteristics by adding more accumulators and valves. The two-state dampers can also be upgraded by fitting proportional or servo valves, thereby achieving continuously variable semi-active damping. Although these improvements are possible, they will add considerable complexity and cost and are therefore not considered at present. Adding or extracting oil from the unit results in ride height adjustment.

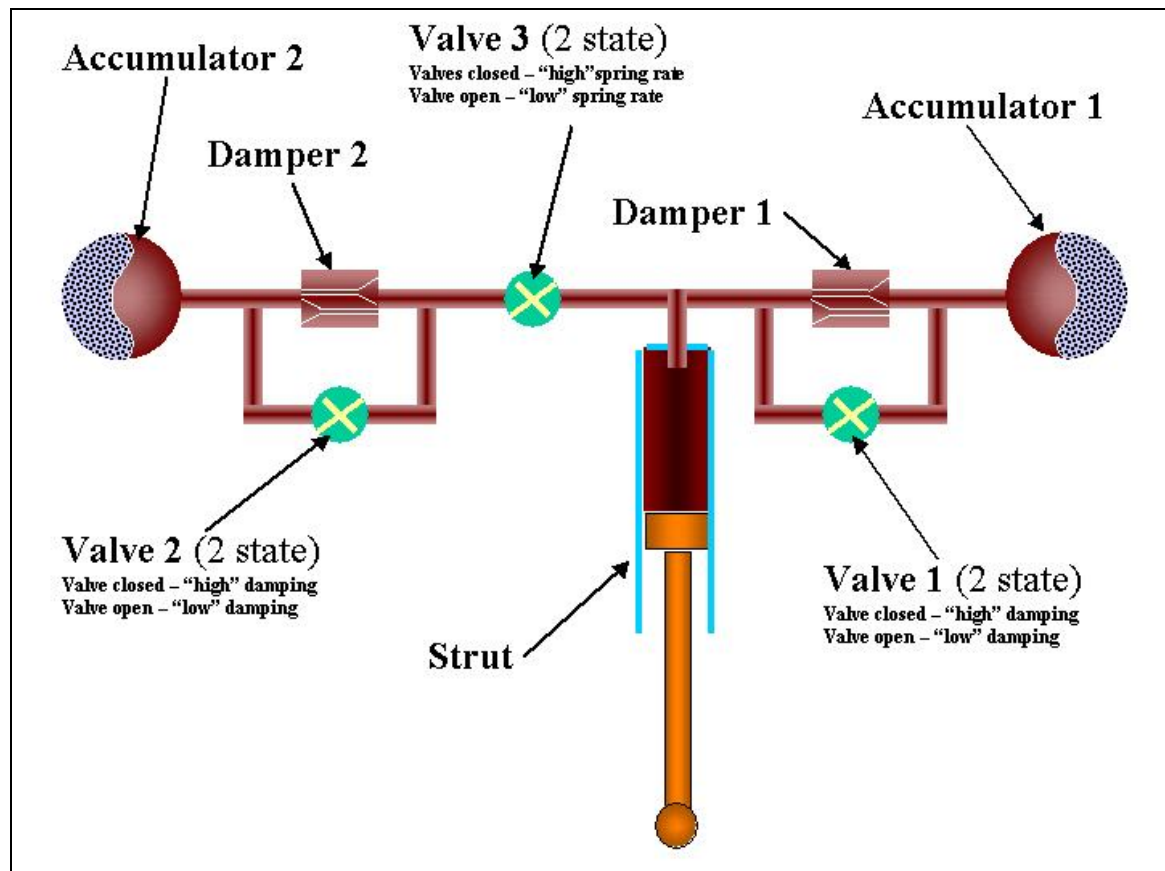


**Figure 4.1** – 4S<sub>4</sub> circuit diagram

### 4.3 Design requirements

Before designing the new suspension system, it is necessary to obtain the specifications for the existing baseline system in terms of wheel load, maximum suspension deflection and space envelope available.

The maximum static vertical wheel load for the fully laden Land Rover Defender 110 test vehicle is 800 kg and occurs on the rear wheels. The prototype suspension system is therefore designed for a static load of 8000 N and a dynamic load of 40 000 N (five times the static wheel load). Provision is made for a total suspension travel of 300 mm (maximum compression to maximum rebound). The baseline rear suspension system has a total travel of 290 mm (170 mm compression and 120 mm rebound). The required suspension characteristics for the springs and dampers are obtained from the analysis in chapter 2. Gas volumes of 0.1 litre (Accumulator 1) and 0.4 litre (Accumulator 2) are used as design values. Provision is made for fitment of a wide range of available hydraulic damper packs so that the damper characteristics can be fine-tuned before final vehicle implementation. To enable the use of standard hydraulic seals, valves and fittings, the system is designed not to exceed a maximum pressure of 20 MPa. A maximum relative suspension velocity of 2 m/s is assumed to be sufficient for extreme events. This was determined from simulation results as well as measurements on the baseline vehicle. It is envisaged that the suspension system must be able to control the body's natural frequencies in the region of one to two Hz. This requires a valve reaction of 10 to 20 Hz or 50 to 100 milliseconds. This was also found to be the case by **Nell (1993)** and **Nell and Steyn (1994)**.

The main design specifications for the prototype controllable suspension system are summarized as follows:

- i) Suspension travel of 300 mm (same as for baseline suspension)
- ii) Soft suspension static gas volume of 0.5 litre
- iii) Hard suspension static gas volume of 0.1 litre
- iv) Maximum system pressure at full bump of 20 MPa
- v) Maximum relative suspension velocity of 2 m/s
- vi) Maximum suspension force of 40 kN (5x static force)
- vii) Valve response time of the order of 50 milliseconds
- viii) Must fit into available space envelope without major modifications to vehicle
- ix) Low damper characteristic < 0.5 of baseline value
- x) High damper characteristics between 2 and 3 times the baseline value

These specifications are for the rear suspension and represent the worst-case scenario. The only changes required for fitment of the prototype to the front suspension of the Land Rover 110, is to reduce the total suspension travel to 250 mm.

The piston diameter required to give a maximum pressure of 20 MPa at 40 kN is 50.5 mm. A piston diameter of 50 mm will be used for the design of the prototype. Figure 4.2 indicates the relative suspension velocity over the left rear spring of a standard Land Rover Defender 110 when driven on the Gerotek Test Facility's rough track. This velocity was calculated by differentiating the measured relative displacement. The maximum extreme event velocity over this type of terrain at representative speeds is 2 m/s. The 50 mm piston diameter will therefore result in a flow rate of 236 litre/min at 2 m/s relative suspension velocity.



Selection of an appropriate valve was based on the response time of 50 milliseconds, maximum system pressure of 20 MPa and maximum extreme event flow rate of 236 litre/min. Choice and availability of valves is problematic as a valve with a fast switching time is required. Standard valves, available off-the-shelf, can meet either the flow or the time response requirements, but not both. For this flow rate requirement logic element valves operated by a pilot solenoid valves are usually employed (Nell (1993), Nell and Steyn (1994), Janse van Rensburg, Steyn and Els (2002), Els and Holman (1999)). This solution is bulky and expensive, and above all results in response times that are strongly pressure dependent and very slow at small pressure differences. The design has therefore been modified to use two smaller, fast switching valves in parallel to handle the required flow and meet the switching time requirement.

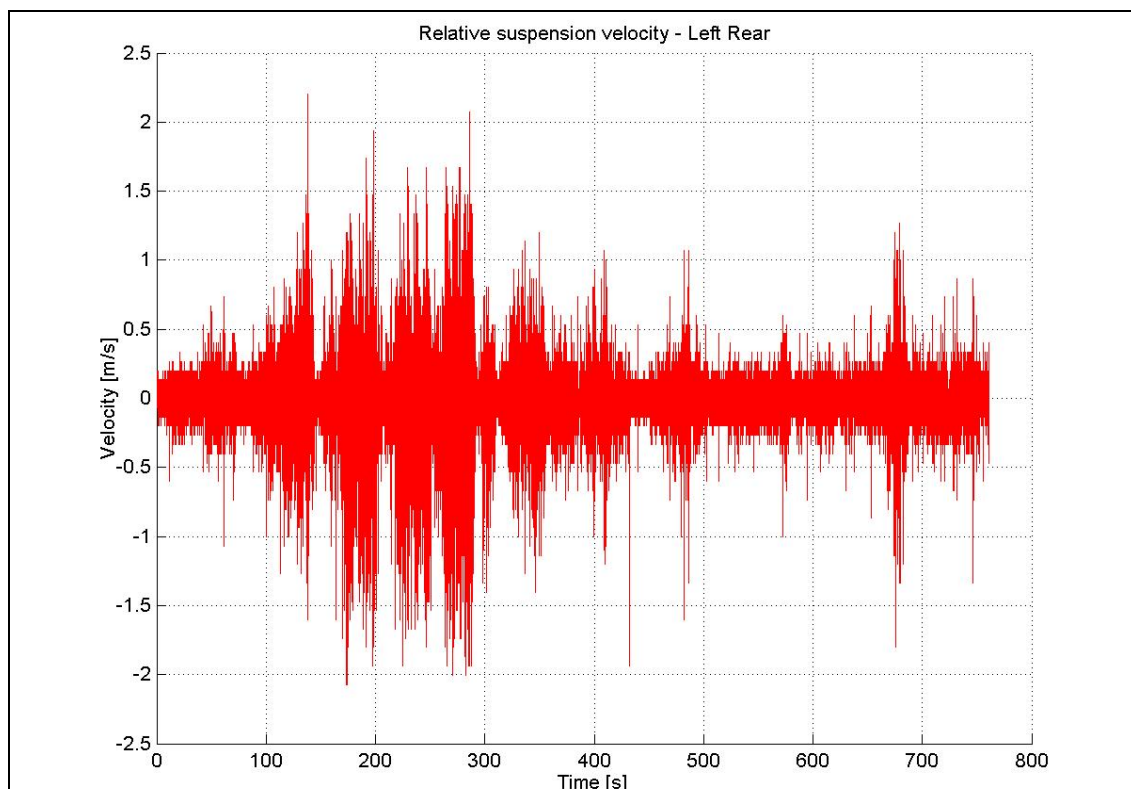


**Figure 4.2** – Relative suspension velocity over Gerotek Rough track

The valve selected for the current application is the SV10-24 2-way normally closed spool valve from HydraForce (Anon, 1998). This valve has previously been characterized for a different project at the University of Pretoria and information on response times and pressure drops are available (De Wet, 2000). The valve is actuated by a solenoid that is available in different voltage ratings. The response time (initial delay) is quoted to be 30 milliseconds when energised (i.e. opening) and 25 milliseconds when de-energised (i.e. closing). This is the time from the switch signal to the first indication of the change of state, called the initial delay (see par 4.7.6 for definitions). This response time is quoted at a flow rate of 80% of the nominal flow rate when the valve is fully open. The valve is designed for a maximum operating pressure of 20.1 MPa and proof pressure of 35 MPa. The valve can handle a flow of 113.6 litre/min at a pressure of 6.9 MPa and 37.9 litre/min at 20.7 MPa (see Figures 4.3 and 4.4). When valve 3 in the proposed concept (see Figure 4.1) is open, the flow will be split between accumulators 1 and 2 but with the higher portion of the flow going into the bigger accumulator 2. The expected flow is however

still higher than the maximum capacity of the valve. It was therefore decided to use two valves in parallel for V<sub>3</sub>.

Eight standard Land Rover Defender rear dampers were stripped, the damper packs removed and mounted in the 4S<sub>4</sub> units (two damper packs per unit). Due to the difference in bore size, and thus flow rate, as well as the pressure difference now acting on a larger area, use of the standard damper packs resulted in the required hard damper characteristics (see discussion in paragraph 4.7.5 and Figure 4.27).

#### 4.4 Space envelope

The space envelope available for the new suspension was determined by physical measurement on a Land Rover Defender 110 vehicle. The controllable suspension system, with the required characteristics, has to fit in the space envelope. The left front and left rear axle portions and wheel well details were measured and modelled in Solid Edge for this purpose as indicated in Figures 4.5 and 4.6.

#### 4.5 Detail design of 4S<sub>4</sub>

The height of the space envelope is the major restricting parameter, followed by the distance between the fenders and the inside of the wheel arches. Length should not pose any limitations, as the full tyre diameter is available. To comply with the height restriction, the two accumulators are mounted to the front and rear of the main strut respectively as indicated in Figure 4.7. The strut is connected to the two accumulators via a valve block. All the control valves, hydraulic damper valves, control ports and channels are accommodated inside the valve block. Piston accumulators are used mainly for two reasons:

- i) It can be made long and thin compared to bladder accumulators, thereby resulting in more freedom of packaging
- ii) The gas volume can be controlled much more precisely (see paragraph 4.7.1 – charging of unit).

The choice as far as sealing arrangements are concerned is between sealing in the cylinder bore and sealing on the piston rod. The rod sealing arrangement was chosen instead of the more conventional cylinder sealing because it was much easier to finish the rod to the correct tolerances and surface finish required than the cylinder bore. The options considered for surface coatings at this stage is the normal hard chroming as well as a tungsten-carbide-cobalt coating applied with a high velocity oxygen fuel (HVOF) process. The latter is very resistant to flaking and has extremely good wear resistance. For both Prototypes 1 and 2, the tungsten-carbide-cobalt coating was used because it is suggested for the application by one of the world's biggest seal manufacturers, Greene Tweede. After coating the rod was ground and superfinished with diamond tape to obtain a hard, corrosion resistant component with the required surface finish to ensure durability and low friction. During the design phase, attention was given to minimise friction and stick-slip. Standard seals from the Busak and Shamban catalogue (**Anon, 2005d**) were used throughout the design of the 4S<sub>4</sub>. A Turcon AQ Seal 5 and two Glydring wear rings were used on the floating pistons in the accumulators. The main cylinder pressure was sealed

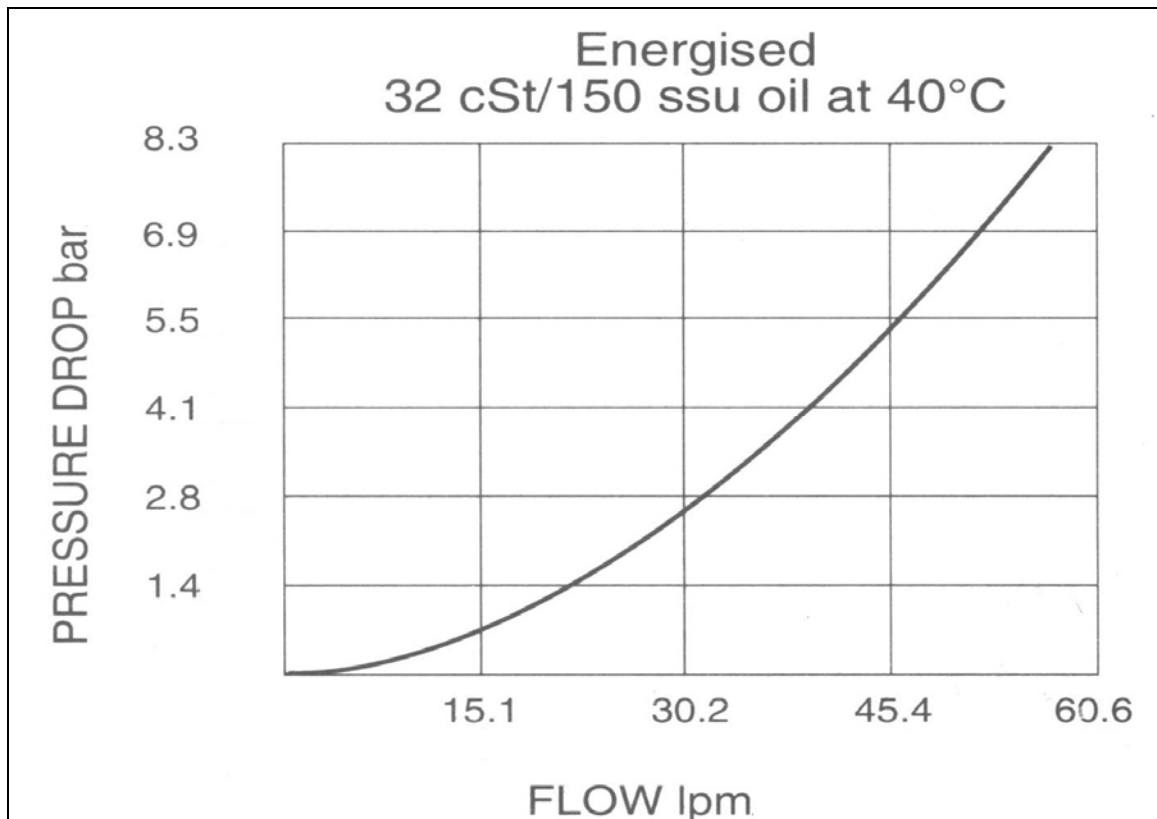


Figure 4.3 – Pressure drop vs. flow rate for SV10-24 valve (Anon, 1998)

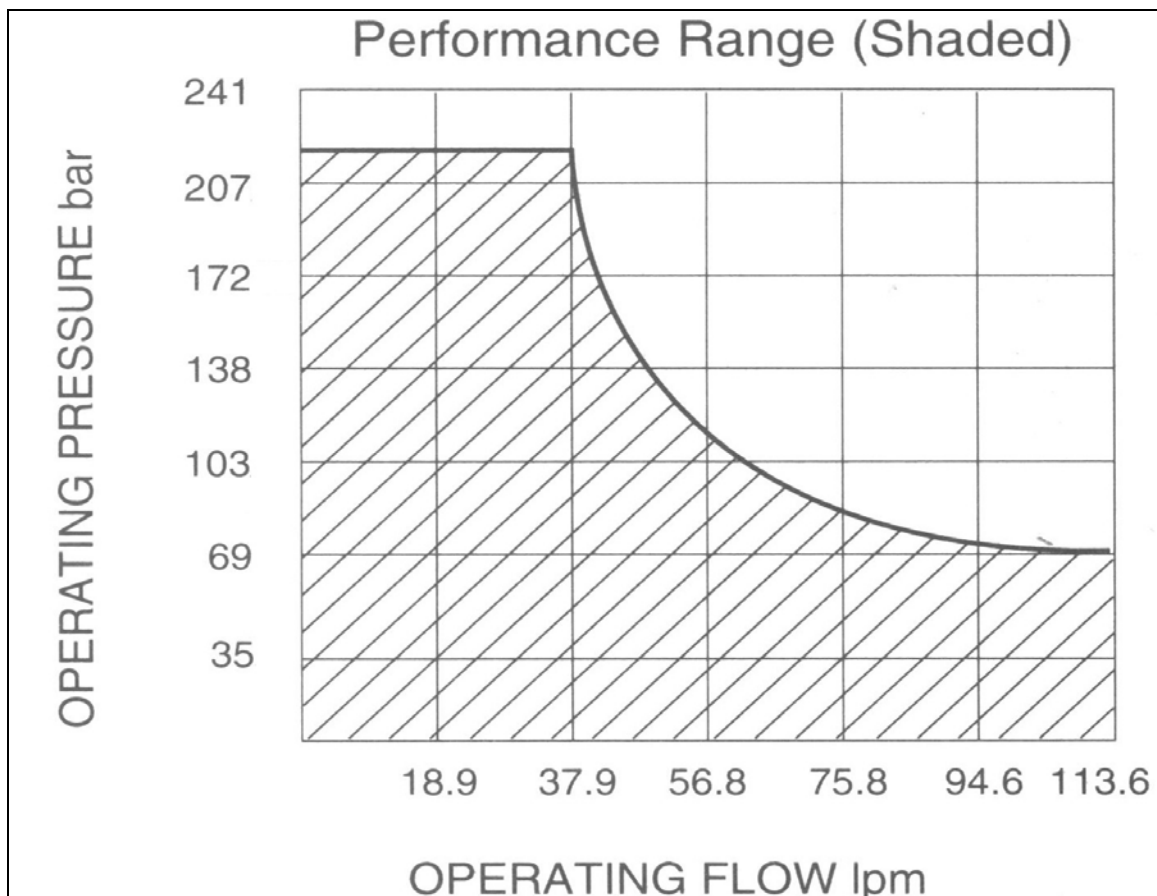
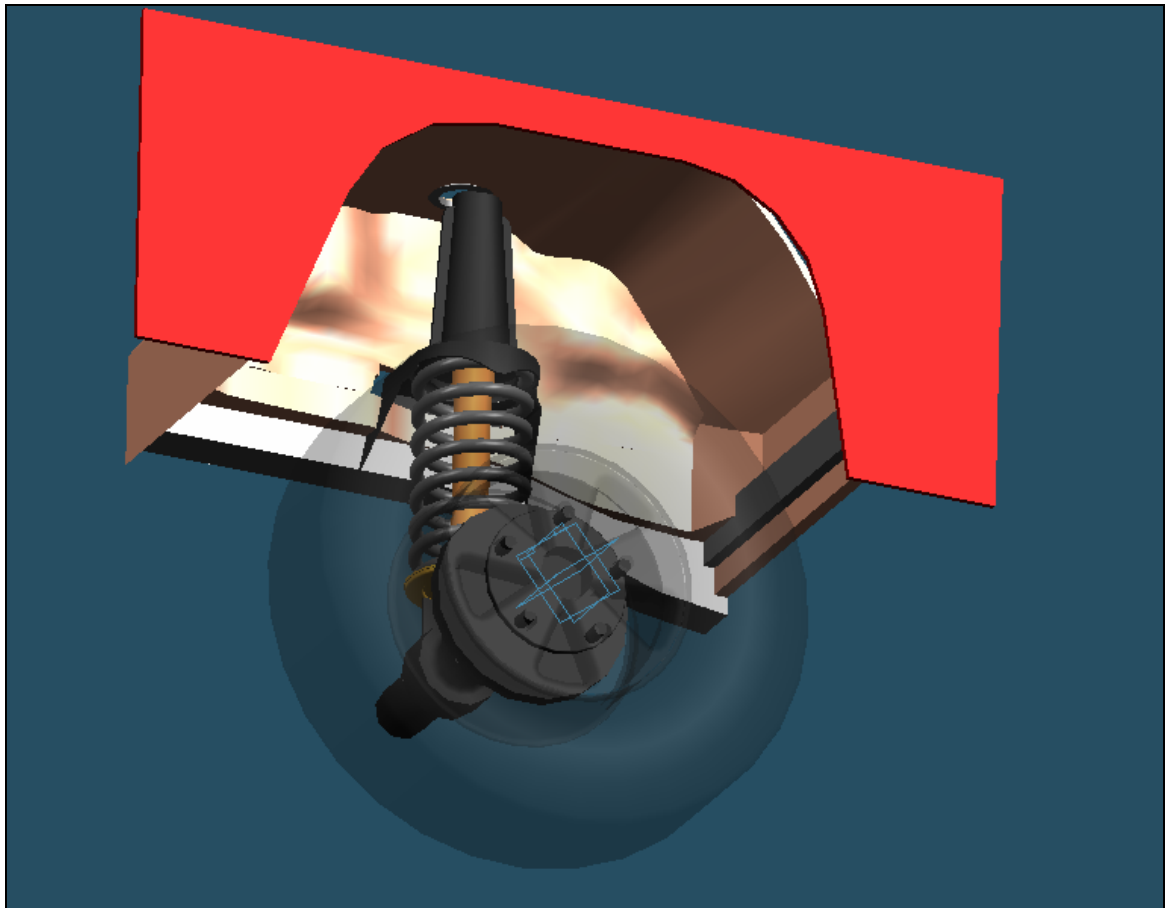
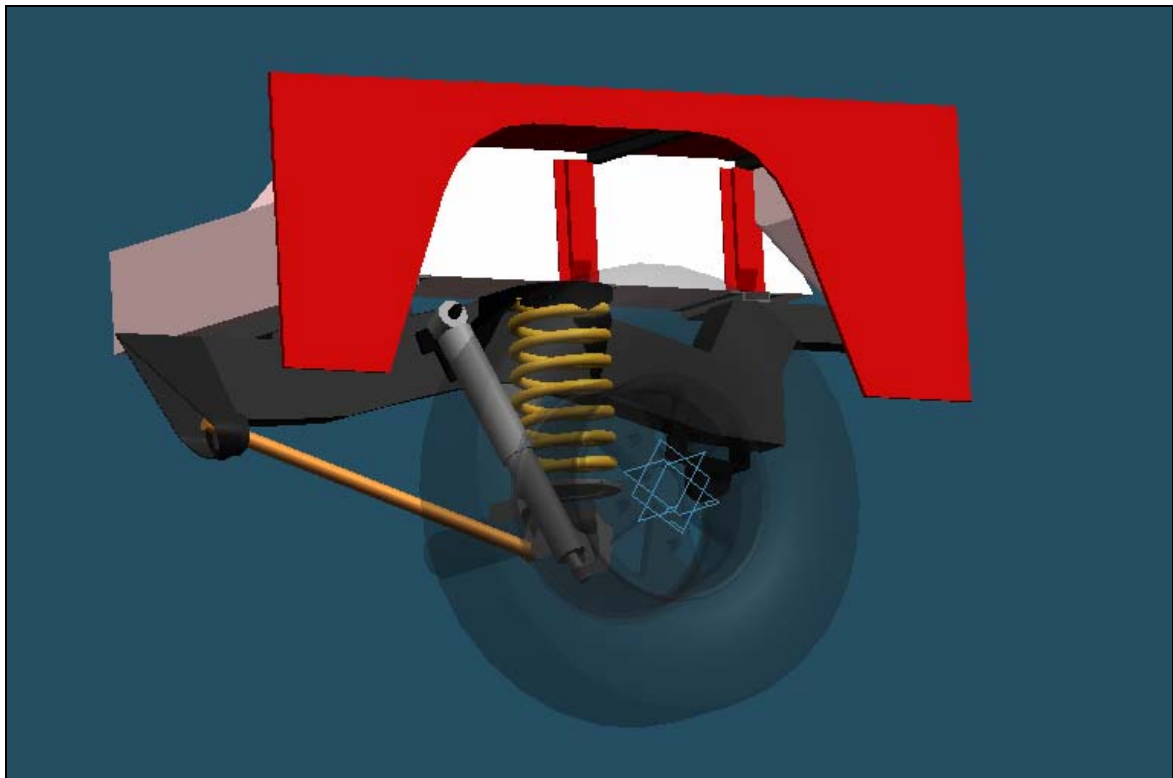


Figure 4.4 – Operating range for SV10-24 valve (Anon, 1998)



**Figure 4.5** - Baseline left front suspension layout



**Figure 4.6** - Baseline left rear suspension layout

using a rod sealing arrangement with a triple seal system consisting of a TURCON STEPSEAL 2K, TURCON RIMSEAL and TURCON EXCLUDER 2 rod scraper.

During testing of the first prototype suspension system the force characteristics exhibited very high frictional behavior (hysteresis). This was traced to the off-center mounting arrangement on the first prototype that subjected the cylinder to a moment loading and caused high seal friction. The mounting arrangement on Prototype 2 was changed to be concentric with the cylinder. The new mounting arrangement eliminated the hysteresis encountered on the first prototype (see par 4.7.7. under test results).

On the prototype, provision is made for four pressure transducers (P<sub>1</sub> to P<sub>4</sub>) to measure pressures in the system.

Two views of the Prototype 2 controllable suspension system are provided in Figures 4.8 and 4.9. Figure 4.8 shows an exterior side view and Figure 4.9 indicates a cross-sectional view. The suspension system is mounted to the axle and the chassis by means of a spherical bearing used axially. The spherical bearing, although normally intended for radial forces, is appropriately sized to handle the axial load. This bearing is used to ensure pure axial force loading on the suspension system and eliminates any moment loading.

Figures 4.10 and 4.11 depict the 4S<sub>4</sub> unit fitted to the vehicle at the front and rear respectively.

It is concluded that the suspension system can be fitted in the available space although small changes to the vehicle may be required. The new suspension system is narrower than the coil spring and this may result in more interior space in the vehicle.

#### **4.6 Manufacturing of 4S<sub>4</sub> prototypes**

The Prototype 2 controllable suspension system was manufactured according to detail design drawings. A photograph of the assembled unit is given in Figure 4.12. Figure 4.13 compares Prototype 2 to Prototype 1. Prototype 2 is considerably smaller than Prototype 1 in overall size and weight. Valve positions have been optimised to reduce size. The valve block requires very few external blanking plugs compared to the first prototype. The weight of the unit was reduced from 59 kg for Prototype 1 to 40 kg for Prototype 2. The mounting arrangement to the vehicle chassis has been modified considerably to remove the moment loading. On Prototype 2, the weight includes all the mounting brackets to the vehicle, while on Prototype 1 mounting brackets are not included in the quoted weight.

#### **4.7 Testing and characterisation of the 4S<sub>4</sub>**

The 4S<sub>4</sub> Prototype 2 suspension was characterized on a test rig to obtain all the spring and damper characteristics as well as valve response times. A series of basic reliability tests were also performed to validate the choice of hydraulic seals and valves. The test rig consisted of a purpose designed test frame and a 100 kN SCHENCK hydropulse actuator (see Figures 4.14 to 4.18). The prototype suspension unit was instrumented with four pressure transducers to determine dynamic system pressures, with actuator force and actuator displacement also being measured. The switching signal to the valves was recorded for determining the valve response times. A linear potentiometer was installed on valve 3 to measure the valve plunger displacement.

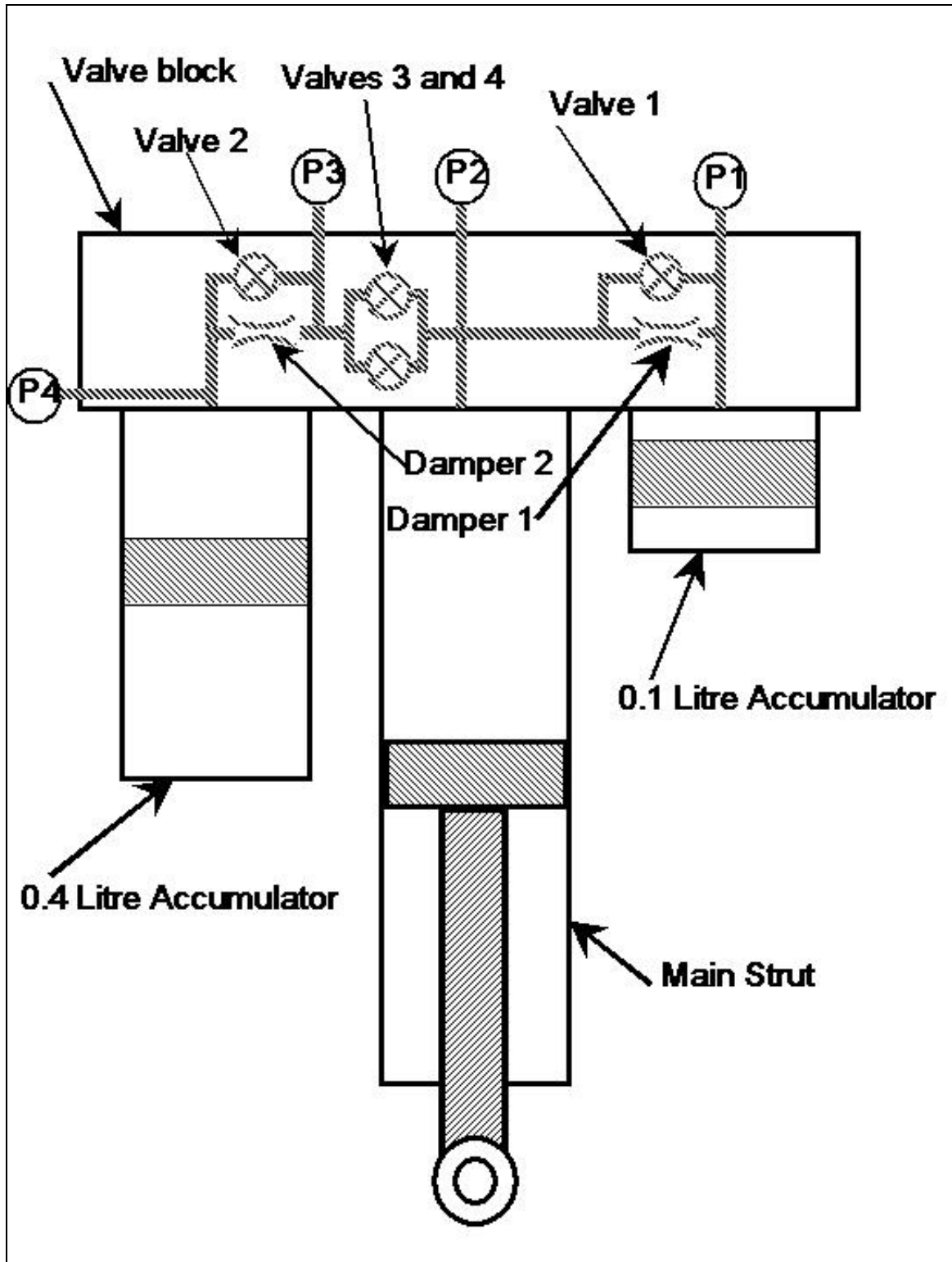
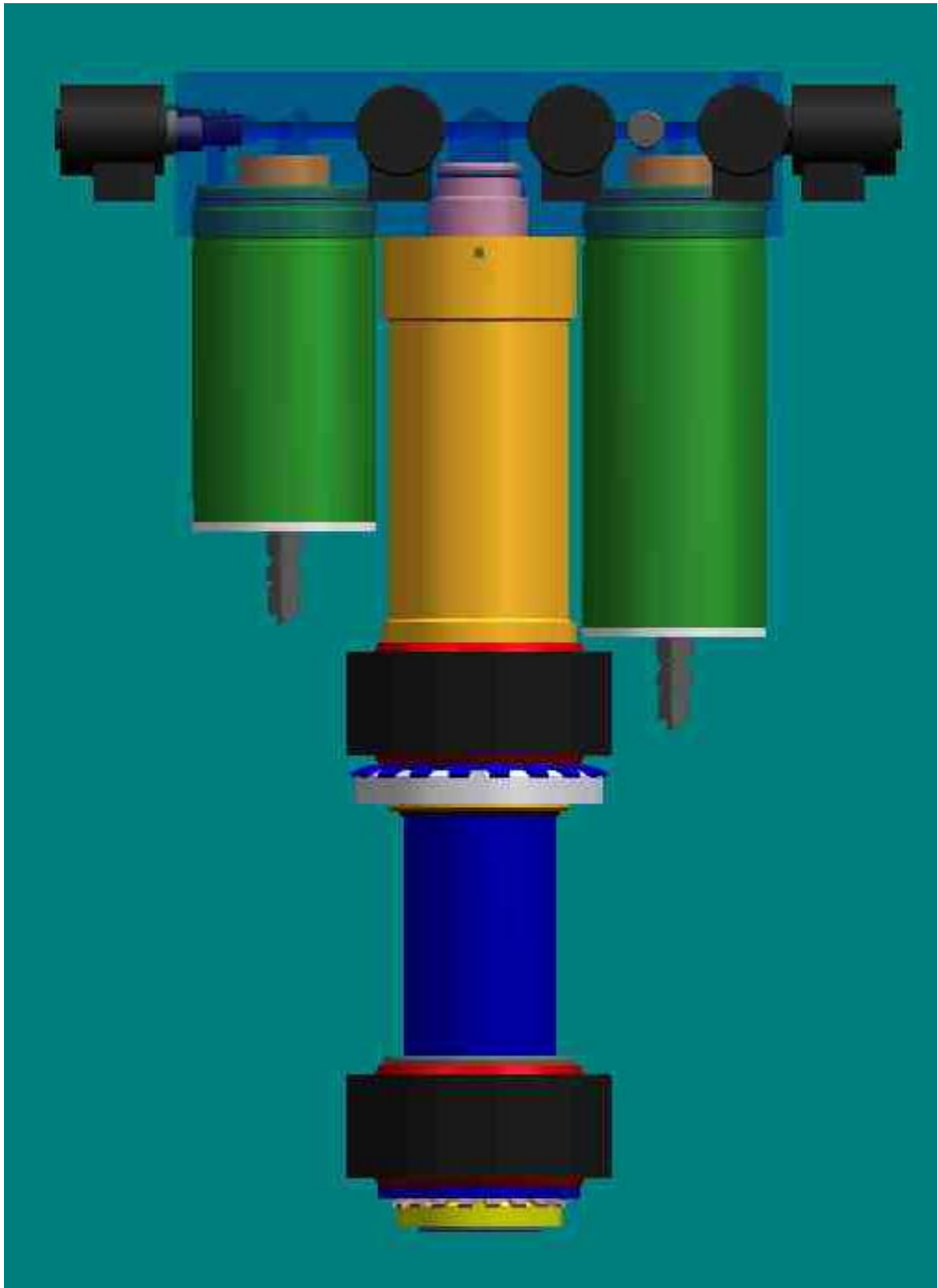


Figure 4.7 –  $4s_4$  suspension schematic diagram



**Figure 4.8** –  $4S_4$  suspension system – exterior view

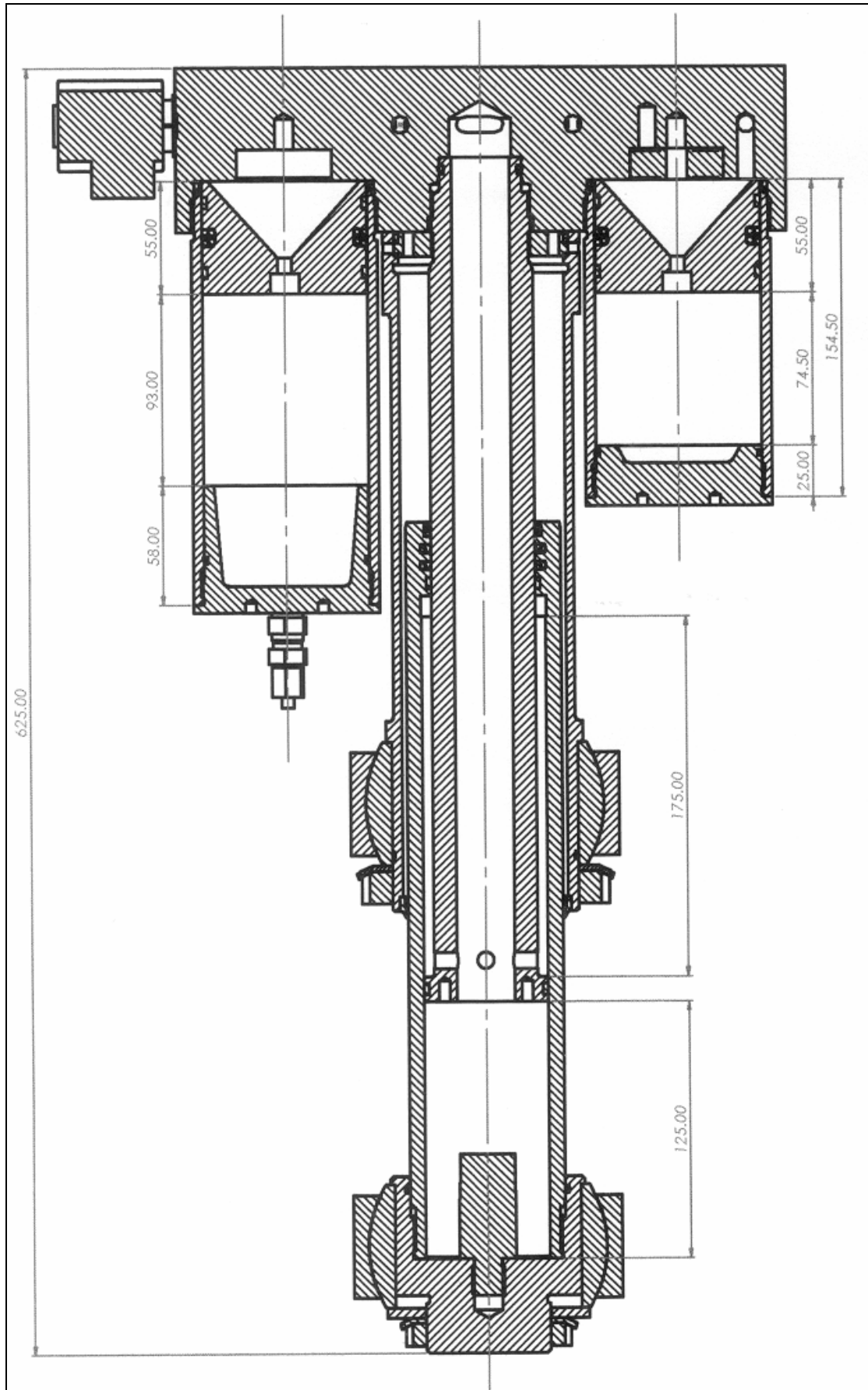


Figure 4.9 –  $4s_4$  suspension system – cross sectional view



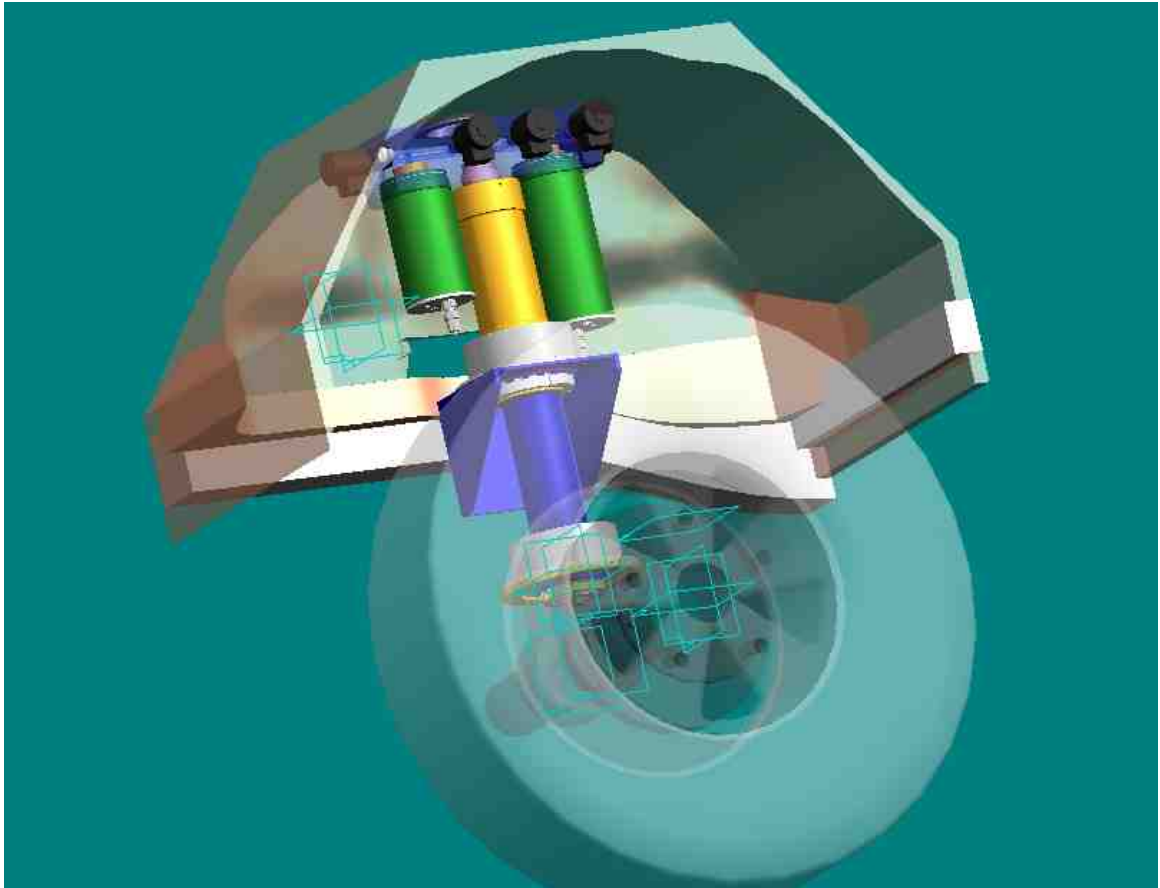


Figure 4.10 - Front suspension layout with  $4S_4$  unit fitted

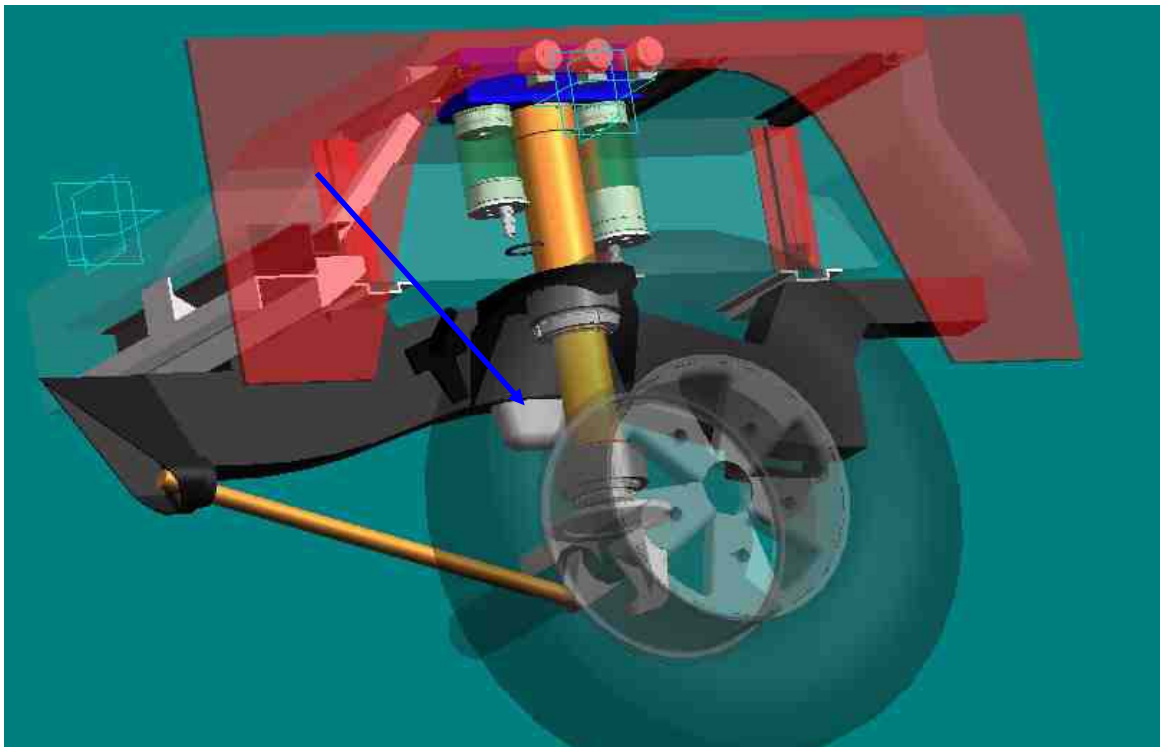


Figure 4.11 – Rear suspension layout with  $4S_4$  unit fitted

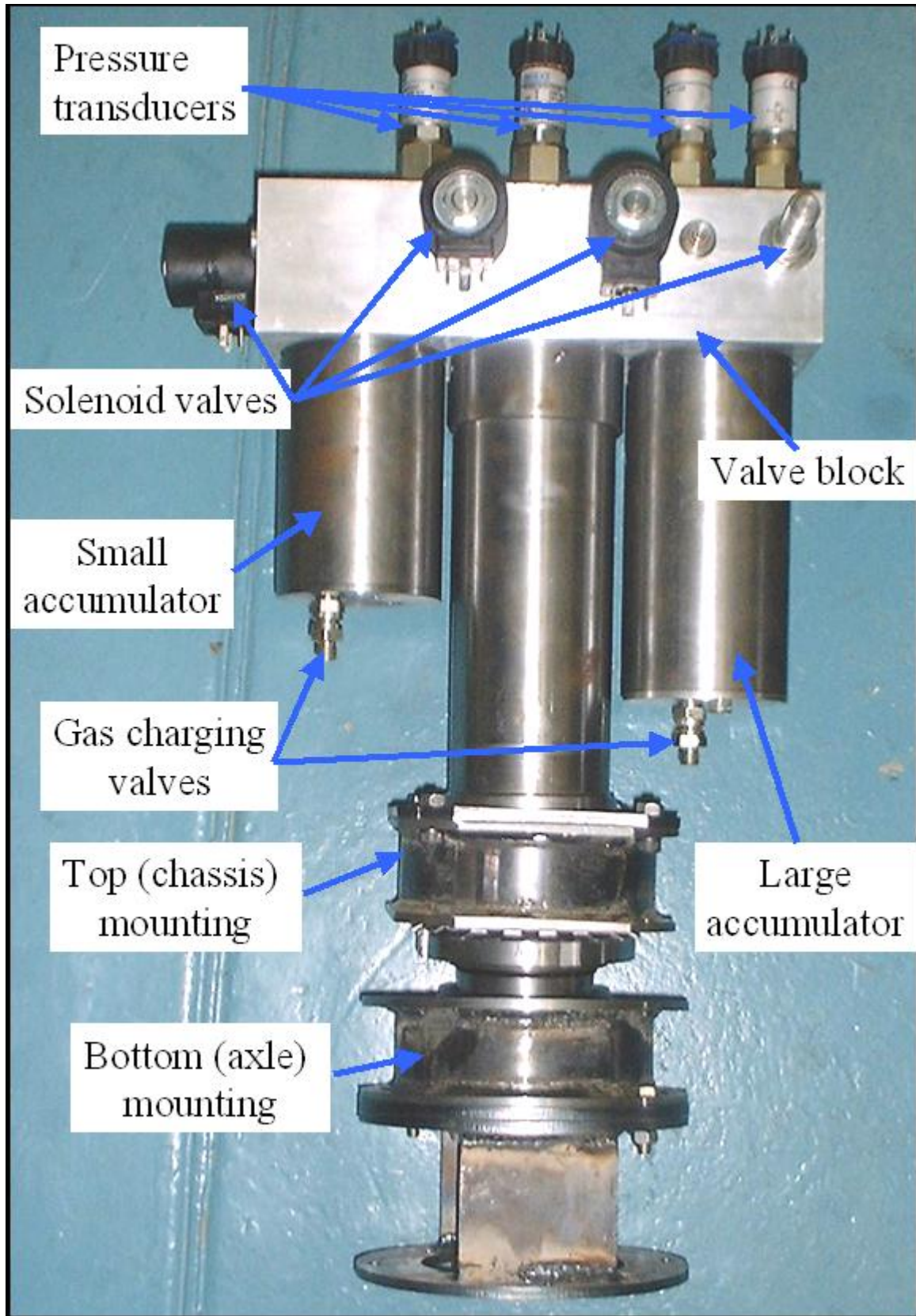


Figure 4.12 – 4S<sub>4</sub> Prototype 2



**Figure 4.13** - 4S<sub>4</sub> Prototype 2 (left) compared to Prototype 1 (right)

#### **4.7.1 Gas charging procedure**

The spring characteristics are completely dependant on the volume of gas in each accumulator. It is therefore imperative that the gas charging procedure described below be strictly observed otherwise the spring characteristics will be in error.

- i) During assembly of the suspension unit, both floating pistons must be pushed in until they touch the valve block.
- ii) Move the piston rod to the maximum extended (rebound) position.
- iii) Open all solenoid valves by connecting them to a suitable power supply.
- iv) Fill the strut completely with oil. Tilt the strut slowly in different directions in an attempt to get rid of trapped air. If the unit seems to be full, let it stand for a few hours and top up frequently with oil. Slowly tilt the unit during each filling attempt. The unit should take at least 1.6 litres of Aeroshell Fluid 41.
- v) Disconnect power to the valves.

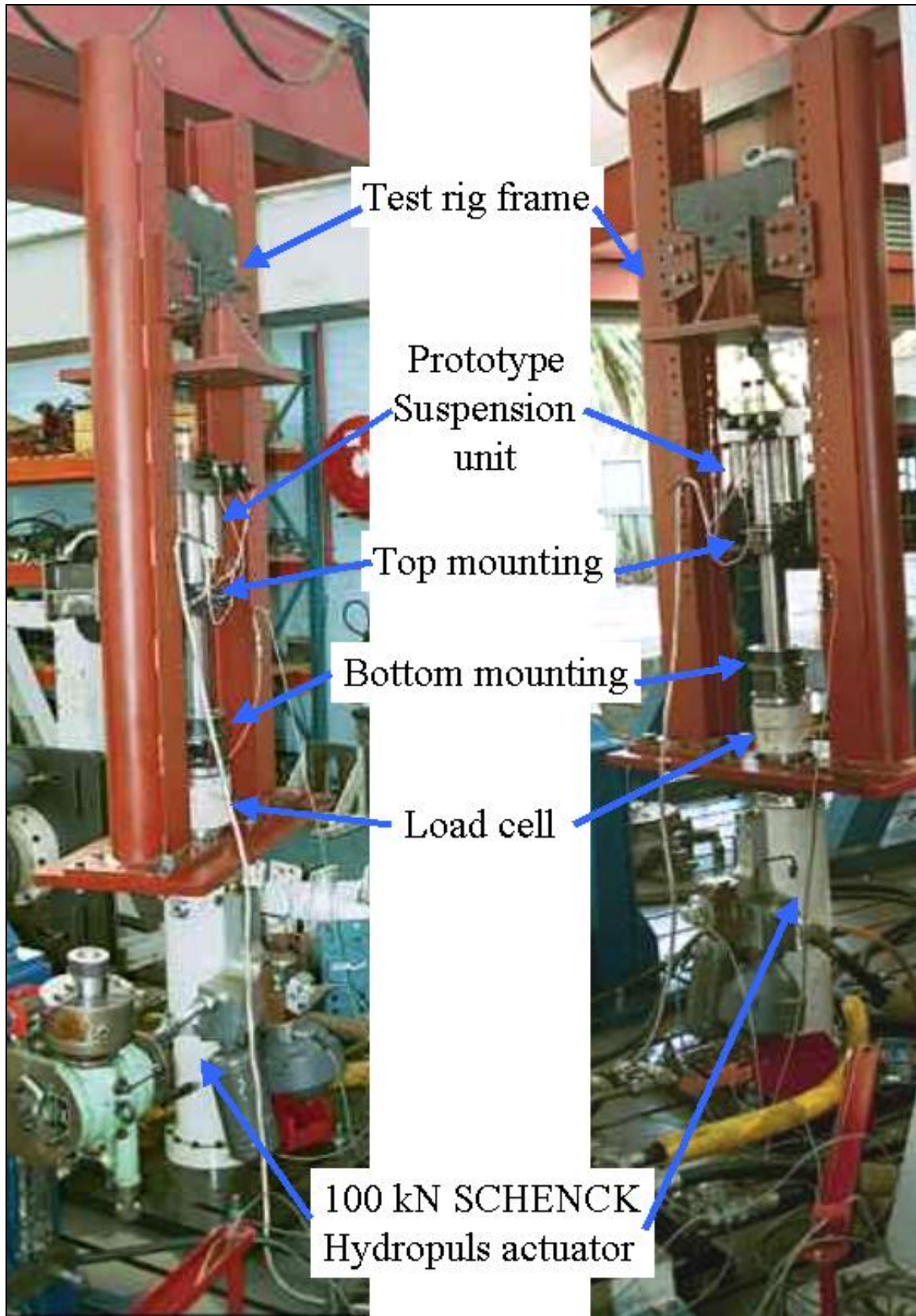


Figure 4.14 -  $4S_4$  Prototype 2 on test rig

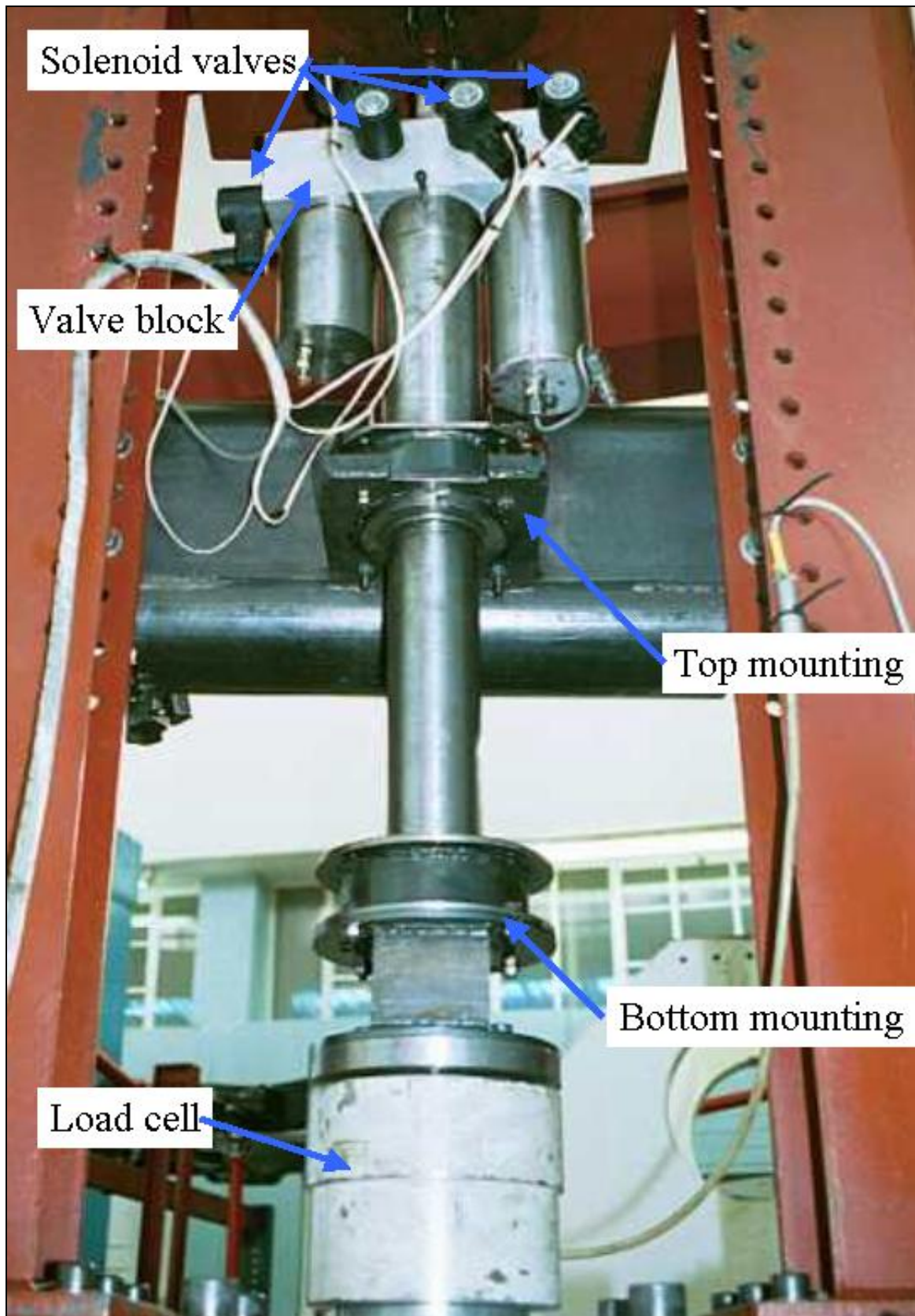


Figure 4.15 -  $4s_4$  Prototype 2 on test rig

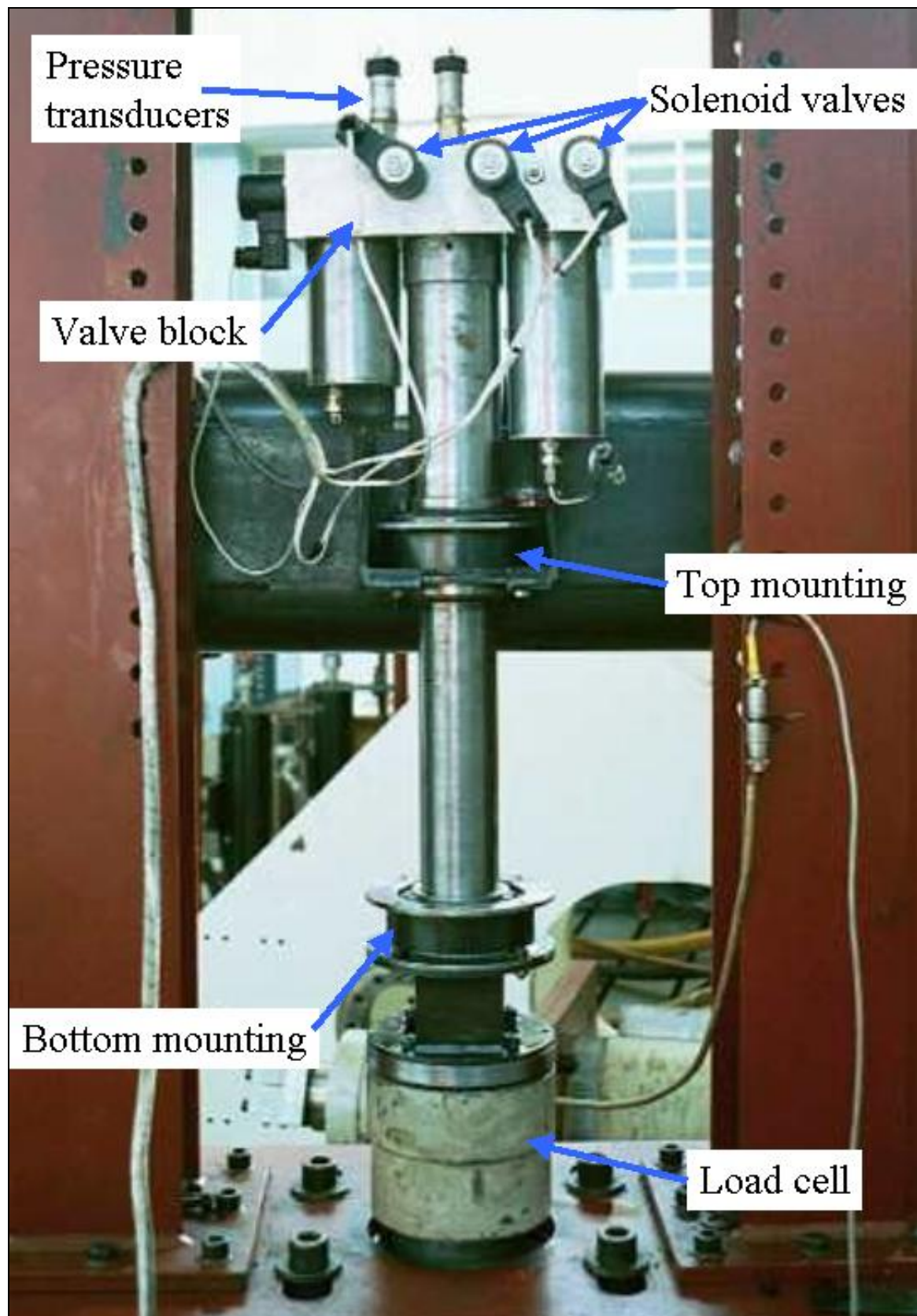


Figure 4.16 -  $4S_4$  Prototype 2 on test rig

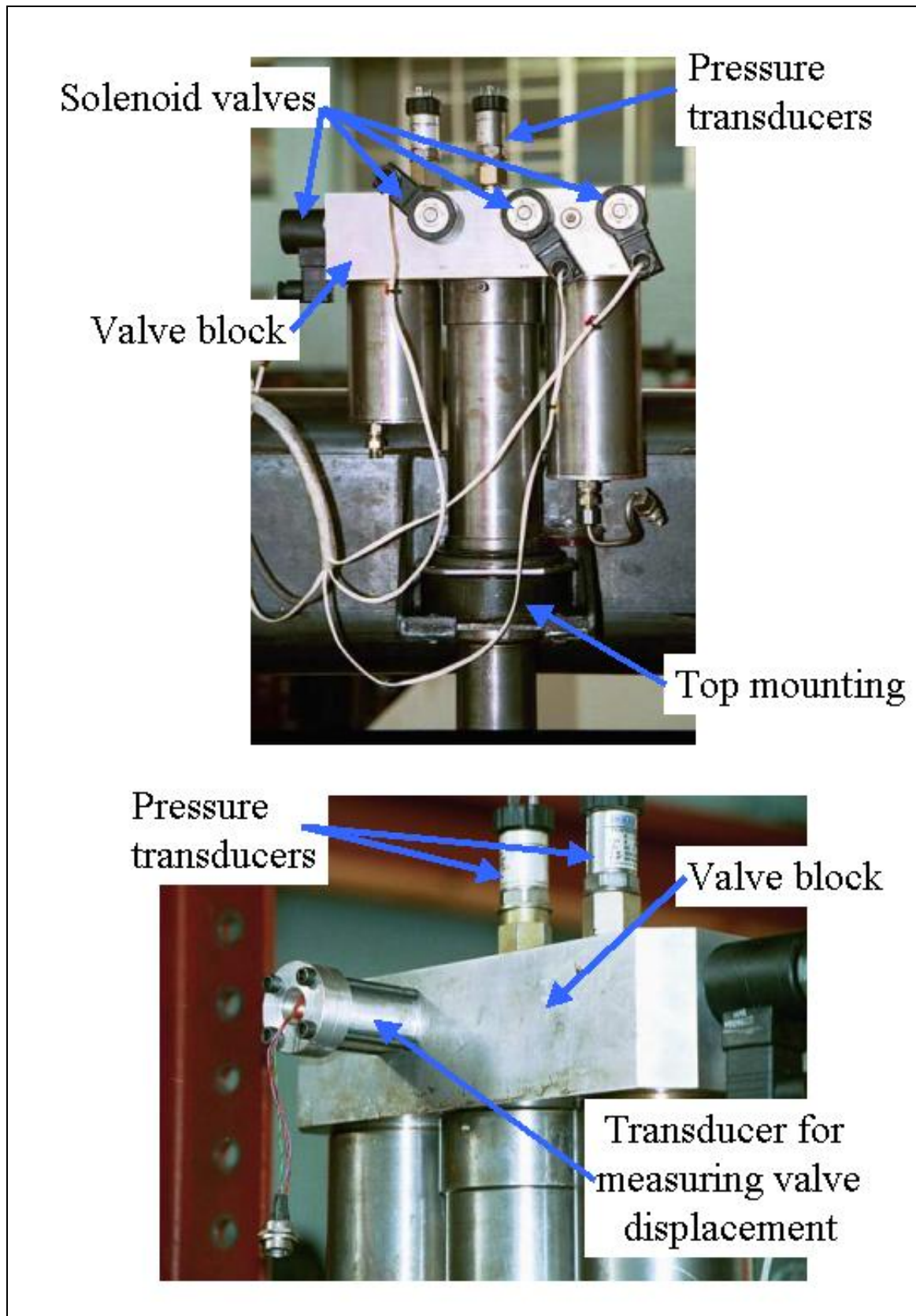


Figure 4.17 - 4S<sub>4</sub> Prototype 2 on test rig

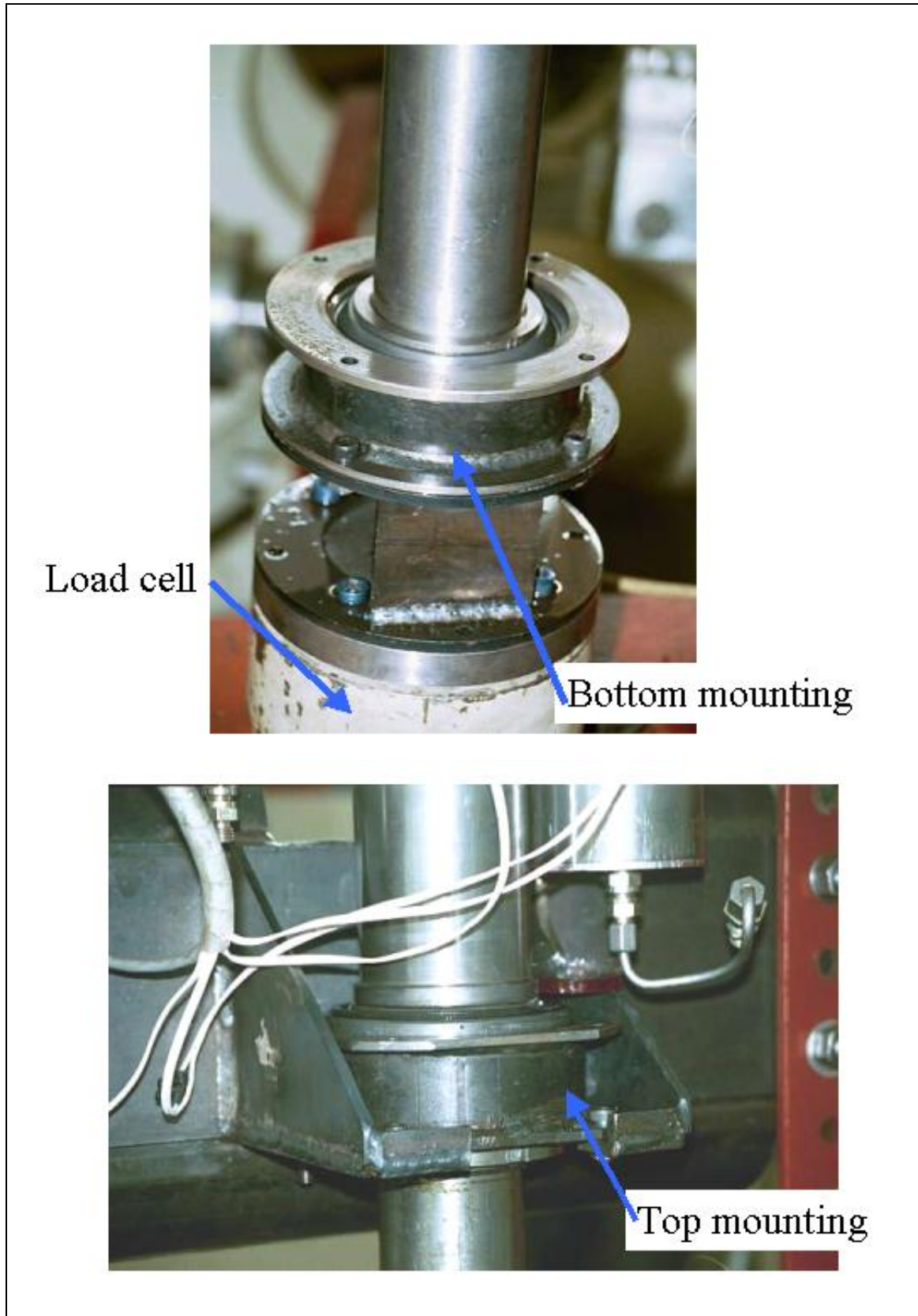


Figure 4.18 -  $4S_4$  strut mounting to test rig



- vi) Install the unit in the test rig.
- vii) Reconnect the valves and apply power so that all the valves are open.
- viii) Remove the M8 cap screws used to bleed off gas from the accumulators from the accumulator end caps.
- ix) Slowly compress the unit to the maximum compression (bump) position, noting the force on the load cell whilst doing so.
- x) If the force on the load cell starts increasing rapidly before maximum compression is reached, investigate the problem before continuing.
- xi) When maximum compression is reached, measure the distance between the accumulator end caps and the floating piston through the gas bleed hole with a vernier. This distance should be 29 mm for the small (0.1 litre) accumulator and 62 mm for the big (0.4 litre) accumulator. The cavities in the accumulator end caps have been designed to result in the correct gas volumes in the maximum compressed positions when the floating pistons are resting against the end caps.
- xii) If any of these two distances are greater than indicated, there is not enough oil in the strut. If this is the case, remove the highest blanking plug on the valve block. Extend the strut by about 10 mm. Fill the strut with more oil. Repeat steps (ix) to (xii) until the strut is filled completely. If there is too much oil in the strut, the excess can be drained off by removing the highest blanking plug and compressing the strut fully.
- xiii) Once filled with oil, charging the accumulators with Nitrogen gas can begin.
- xiv) Close the valves.
- xv) Replace the gas bleed valve on the small (0.1 litre) accumulator.
- xvi) Load gas into the small accumulator (about 1 MPa maximum).
- xvii) Extend the strut by a distance of 40.8 mm by moving the actuator downwards.
- xviii) Load more gas into the small accumulator until the required static spring force is reached on the actuator. For all the tests in this chapter, the accumulator was loaded to 7.8 kN (or 4 MPa). This should be done slowly to allow the gas to reach equilibrium temperature.
- xix) Open all valves.
- xx) Replace the gas bleed valve on the big (0.4 litre) accumulator.
- xxi) Load some gas into the big accumulator.
- xxii) Extend the strut by a further distance of 119.2 mm by moving the actuator downwards. This represents a total movement of 160 mm downwards.
- xxiii) Load more gas into the big accumulator until the required static spring force is reached on the actuator. For all the tests in this chapter, the accumulator was loaded to 7.8 kN (or 4 MPa). This should be done slowly to allow the gas to reach equilibrium temperature.
- xxiv) Check to make sure that there are no gas or oil leaks.
- xxv) The unit is now ready for testing or vehicle installation.

#### **4.7.2 Bulk modulus**

Normally in hydraulic applications, the oil is assumed to be incompressible. In hydropneumatic suspension systems, ignoring the compressibility of the oil can result in significant errors. The compressibility effect is aggravated by the fact that there is always air present in the oil. Air is entrapped in the oil during filling due to mixing and diffusion. Air also gets trapped in channels in the valve block, behind seals and o-rings and in the

valves. One possible way of reducing this problem might be to remove air by using a vacuum pump. The current method of filling the unit is to pour oil slowly into the strut, giving enough time for air to escape. The strut is also moved slowly in all directions in an attempt to remove all the trapped air. This procedure may take several hours before all air bubbles disappear and even then there is a good possibility of air still trapped in the system. The total volume of oil required to fill the rear strut using this method was measured to be 1.6 litres.

The bulk modulus of the fluid is given by:

$$\beta = \frac{\Delta P}{\left(\frac{\Delta V}{V}\right)} \quad (4.1)$$

where:

- $\beta$  = Bulk modulus of the fluid [Pa]
- $\Delta P$  = change in pressure of the fluid between two conditions [Pa]
- $\Delta V$  = change in volume of the fluid between the same two conditions [m<sup>3</sup>]
- $V$  = total volume of fluid in the system at atmospheric pressure [m<sup>3</sup>]

To determine the bulk modulus of the oil in the strut, the accumulators are blocked with steel spacers so that the accumulator pistons cannot move (no gas in accumulators). The strut is then compressed slowly whilst the force and relative displacement is measured. Force and displacement is converted to pressure and volume by using the piston area (see Figure 4.19). The pressure initially stays almost constant until the spacers in the accumulators start compressing. At this point the accumulators become solid and only the oil is compressed. This assumes that the strut itself is incompressible which is a good assumption in this case.

The value for the bulk modulus measured on the strut is 1.368 GPa as shown in Figure 4.19. This compares favourably with typical values of bulk modulus of 1.4 GPa for hydraulic oil (**Poley, 2005**).

### 4.7.3 Thermal time constant

The thermal time constant is a measure of the heat transfer coefficient between a gas in a closed container and its surroundings (**Els and Grobbelaar, 1993**). In the case of the hydropneumatic suspension system, it is determined experimentally by displacing the strut with a step input displacement at the highest possible velocity. During the step, the gas is compressed adiabatically (i.e. there is no time for heat transfer between the gas and its surroundings). The temperature will rise and then slowly return to the ambient value. On the other hand, in the case of a rebound step input, the gas will expand. The temperature will drop first and then rise to the ambient value. The time required for the temperature to change by 63%, between the initial value (immediately after the step) and final ambient value, is defined as the thermal time constant ( $\tau$ ).

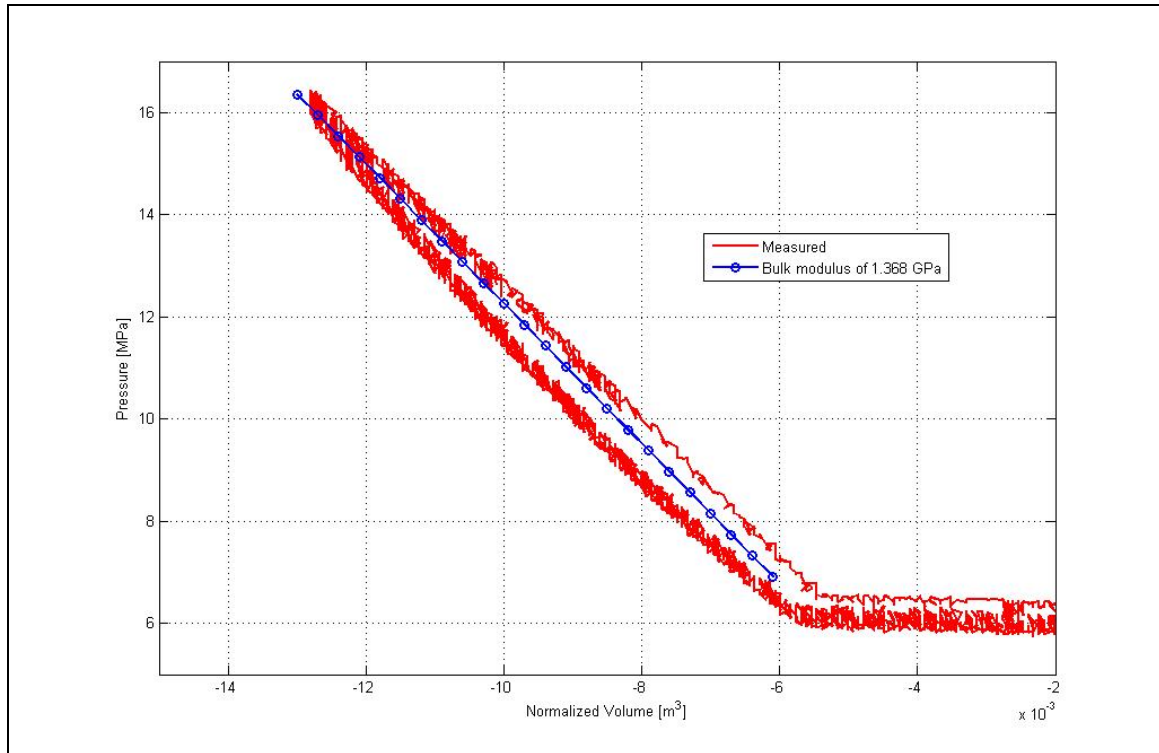


**Figure 4.19** - Measured bulk modulus

Strictly speaking the thermal time constant is defined in terms of temperature. Measuring temperature fluctuation accurately at high speed is very difficult. If the ideal gas assumption is valid, then the time constant can be obtained from pressure or force measurements. The pressure in the strut is measured *vs.* time as indicated in Figure 4.20. The strut must be kept stationary both before and after the high-speed step input. The thermal time constant was measured with no damper packs in the system (i.e. free flow dampers). The experimentally determined thermal time constants for Prototype 2 are shown in Table 4.1 for three different test conditions. The values given for the soft spring are the combined time constant for both accumulators, while the stiff spring results are for the small accumulator only. The thermal time constants for compression and rebound compare well for each test, but the values depend significantly on the displacement of the step. **Els (1993)** however indicates that the analyses is fairly insensitive to the value of the thermal time constant and differences as large as 30% still result in acceptable predictions.

**Table 4.1** – Thermal time constants

File name	Spring setting	Size of step input [mm]	P <sub>begin</sub> [MPa]	P <sub>end</sub> [MPa]	ΔP [MPa]	63% point [MPa]	τ [s]
TYD1 - Compression	Soft	25	5.07	4.91	0.16	4.97	10.1
TYD1 - Rebound	Soft	25	4.30	4.45	0.15	4.39	9.9
TYD2 - Compression	Soft	50	5.99	5.55	0.44	5.71	7.1
TYD2 - Rebound	Soft	50	4.11	4.42	0.31	4.31	7.1
TYD3 - Compression	Stiff	25	8.83	6.57	2.26	7.41	4.8
TYD3 - Rebound	Stiff	25	3.43	4.23	0.80	3.93	4.85

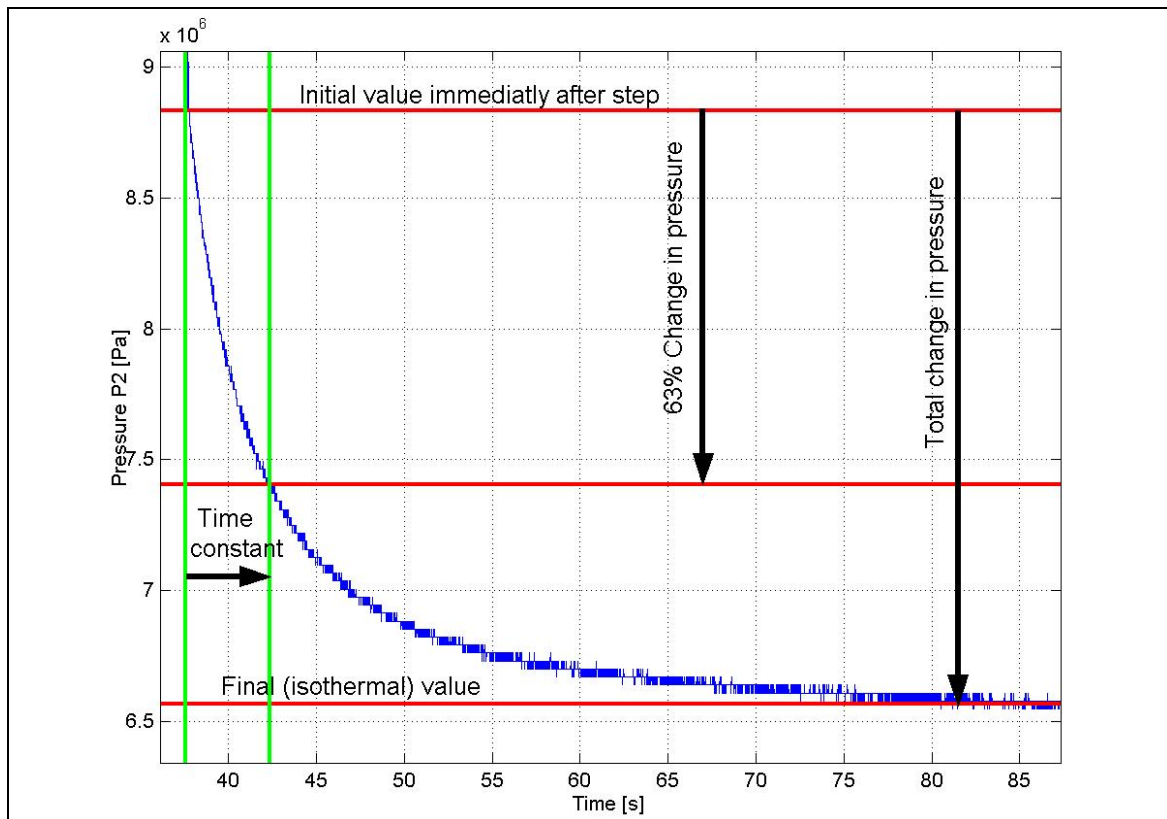


**Figure 4.20** - Determination of thermal time constant

#### 4.7.4 Spring characteristics

The two spring characteristics are determined by displacing the actuator slowly with a triangular wave input displacement with a frequency of 0.001 Hz or a period (duration) of 1000 s. This means that the strut is first compressed from the static position to maximum compression at a constant speed. The strut is then extended to the maximum rebound position, again at constant speed and finally returned to the static position at constant speed. This sequence is repeated for typically three cycles, although the graphs in the rest of this chapter only show data for typically one cycle. Figure 4.21 displays the soft spring characteristic measured for one complete compression and rebound cycle lasting 300 seconds. The measured value is compared to the predicted isothermal spring characteristic calculated for a static gas volume of 0.5 litres. Excellent correlation is observed. The small hysteresis loop in the measured characteristic can be attributed to heat transfer between the gas and the surroundings. This effect is well documented by **Els (1993)**. Other possible contributing factors are seal friction and hysteresis in the test frame.

Figure 4.22 indicates the stiff spring characteristic measured for a complete compression and rebound cycle. The displacement cycle starts in the static position, compresses the spring to -62 mm, extends the spring to +75 mm, compresses the spring again to -62 mm and then returns to the static position. This cycle lasts 1000 seconds. The measured value is again compared to the predicted isothermal spring characteristic, but in this case there is a significant discrepancy between measured and predicted results. The hysteresis loop in the measured characteristic can again be attributed to heat transfer between the gas and the surroundings, friction and hysteresis in the test frame. Further investigation indicated that the discrepancy in the stiff spring characteristic could partly be attributed to the

compressibility of the oil (usually deemed negligible). Figure 4.23 indicates a straight line corresponding to the bulk modulus of 1.368 GPa determined in paragraph 4.7.2. The compressibility is significant for the stiff spring characteristics and needs to be taken into account during spring calculations. The figure also indicates the very good correlation achieved when the spring characteristic is corrected using the bulk modulus. The correlation is however achieved with a static gas volume of 0.13 litres and not the 0.1 litres expected. Several sets of tests were performed on Prototype 2 where the damper configuration was changed. This meant that the unit had to be discharged and recharged every time. At the beginning of each new test series, the spring characteristics were measured. Significant variations in actual gas volume were found when measured characteristics were compared to predicted values. This re-iterates the fact that the oil filling and gas charging procedures are extremely important and still needs improvement to limit the errors due to static gas volume discrepancies.

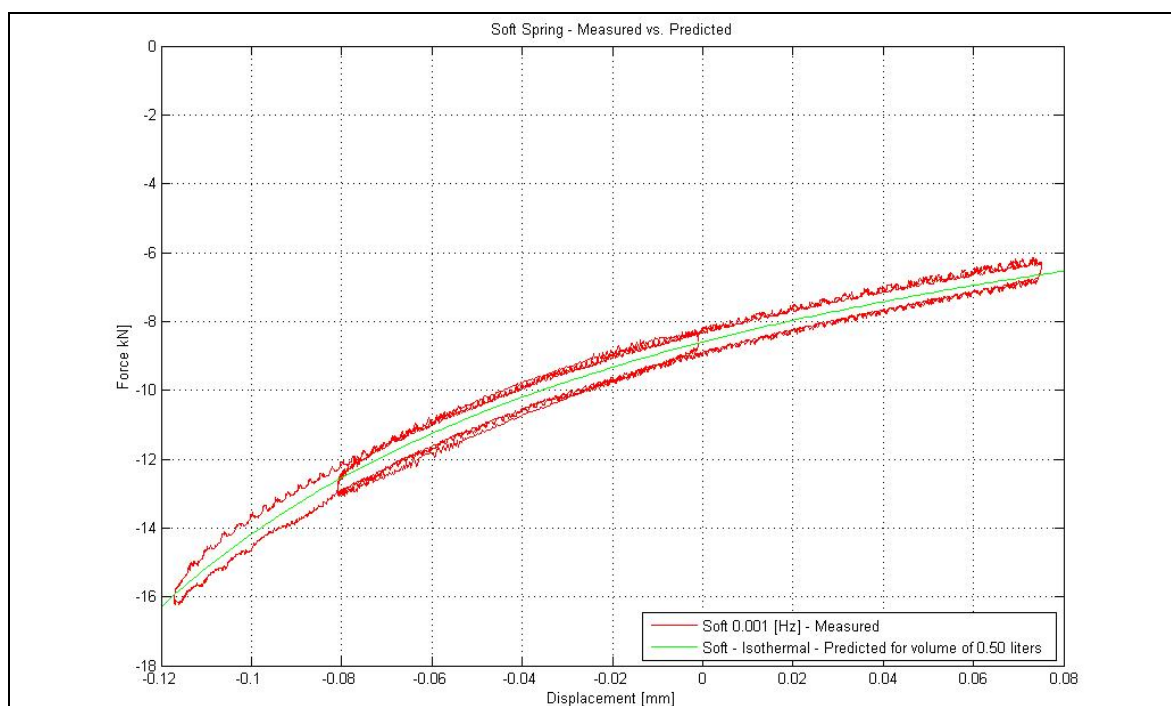


**Figure 4.21** - Soft spring characteristic

Figure 4.23 indicates measured isothermal characteristics for both the soft and stiff springs.

#### 4.7.5 Damping characteristics

The hydraulic damper characteristics of the suspension unit consists of different components, the most important of which are:

- i) Pressure drops over valve block channels and ports
- ii) Pressure drops over valves (partially and fully open)
- iii) Pressure drops over hydraulic damper packs

These pressure drops are dependent on the flow rate through the various components. Measuring these characteristics on the prototype is very difficult because of all the

possible combinations and the fact that it is very difficult to isolate specific components to determine their individual contributions. In most instances it is impossible to measure or calculate the flow through a specific component as the flow is often split between the damper, the bypass valve, and the two accumulators. For these reasons the discussion that follows does not attempt to give exact values for individual components, but rather to give a better understanding of all the interactions and the orders of magnitude. This explains why most of the graphs indicate pressure drops against strut speed and not flow.

By closing off the large accumulator with valve 3 (see Figure 4.7), all the flow is forced into the small accumulator. The flow into the small accumulator can now be calculated by multiplying the speed with the piston area. Figure 4.24 indicates four different lines for the pressure difference ( $P_1 - P_2$ ) against flow. The data for “Valve block channel only” was measured on Prototype 2 with no damper packs installed in the unit, i.e. the only flow resistance was that of the valve block. “Valve block channel and valve” was measured with solid damper packs in the unit, i.e. with all oil flowing through the valve. Also indicated is the data measured by **De Wet (2000)** under steady state conditions on a hydraulic test bench, and the valve manufacturer’s specification. All these values correlate exceptionally well, especially if taken into account the variation in test conditions and hydraulic oil used. Curve fits through the data are indicated in Figure 4.25. As expected the pressure drop is proportional to the square of the flow rate. Values for both flow directions are also very similar. These curve fits can be used in the mathematical model.

Figure 4.26 indicates the effect of a single valve in the  $V_3$  position as well as for two identical valves in parallel. It is clear that the concept of two valves in parallel works very well as the pressure drop is significantly reduced. The ratio between the two graphs is not exactly a factor of two due to the fact that the ports and channels connecting the two valves in parallel are not identical.

The most important damper characteristic, as far as vehicle dynamics is concerned, is the force velocity relationship of the high damping and low damping characteristics respectively as measured using a triangular wave displacement input at various frequencies. Figure 4.27 indicates this relationship for the stiff spring with low damping ( $V_3$  closed and  $V_1$  open), stiff spring with high damping ( $V_3$  and  $V_1$  closed) as well as the soft spring with low damping (all valves open). The damper packs in the strut were sourced from standard Land Rover rear dampers. Also indicated on the graph is the baseline Land Rover Defender 110 rear damper characteristic, correctly scaled for the new application as explained below. The baseline graph is included as an indication of what could theoretically be expected in the case of the stiff spring with high damping. The baseline graph is scaled because the standard piston diameter is 35 mm and the piston diameter on Prototype 2 is 50 mm. For the same linear velocity, the flow in Prototype 2 will be higher than that on the baseline Land Rover damper by a factor of  $(0.050)^2 / (0.035)^2$  or 2.04. The force on Prototype 2 will also be higher than the force on the baseline Land Rover damper for the same pressure difference across the damper pack, also by a factor of 2.04. The Land Rover damper characteristic can therefore be scaled for Prototype 2 by multiplying the force by 2.04 and dividing the velocity by 2.04. It can be seen from Figure 4.27 that there is some discrepancy between the expected and measured characteristics. In the low speed region the Prototype 2 forces are lower than expected. This is attributed to leakage past the o-ring seals that mount the damper packs into the

cavity of Prototype 2. At higher speeds the Prototype 2 damping force is higher. This can be expected due to the extra flow losses through the valve block ports and channels.

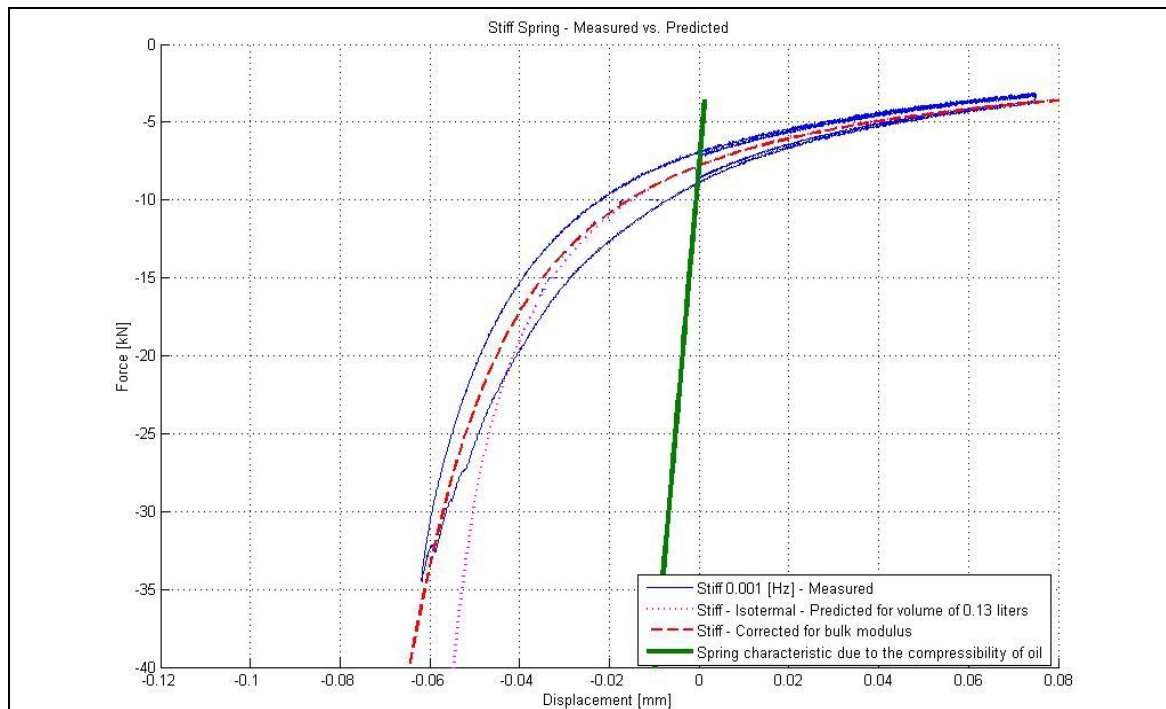


Figure 4.22 - Stiff spring characteristic

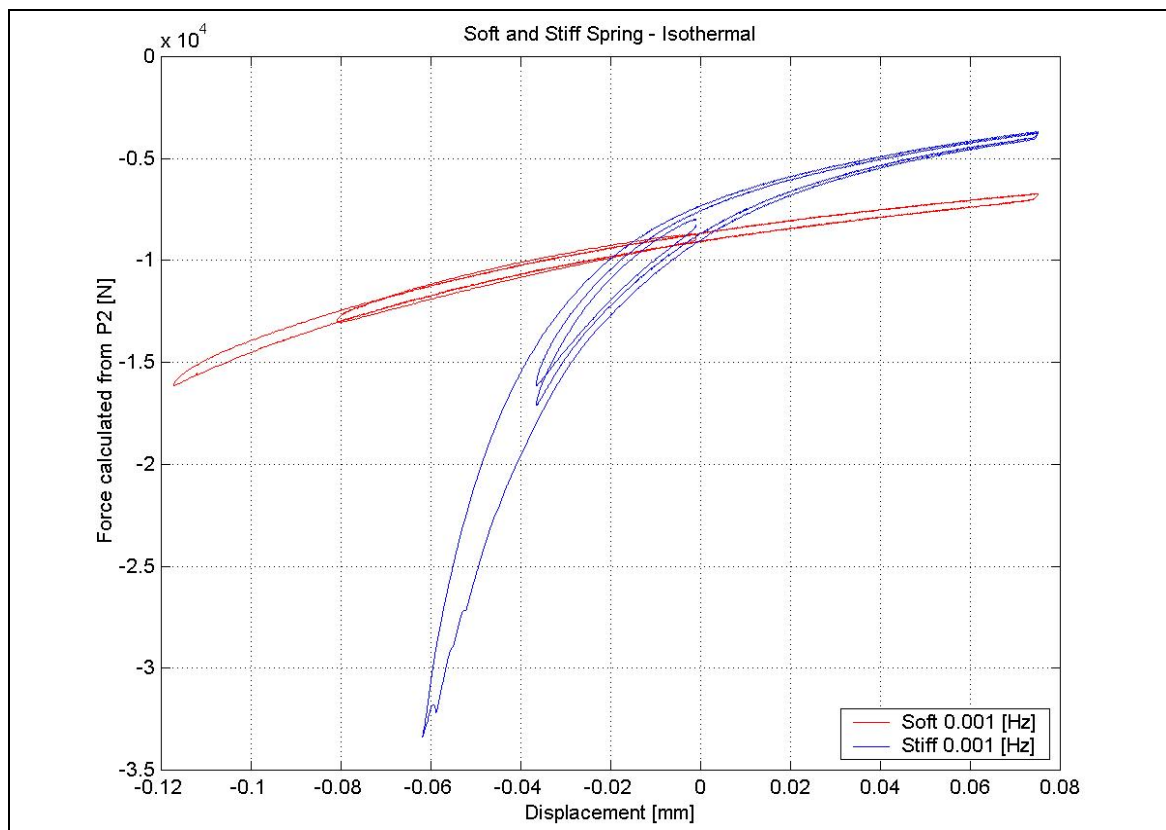


Figure 4.23 - Soft and stiff spring characteristics

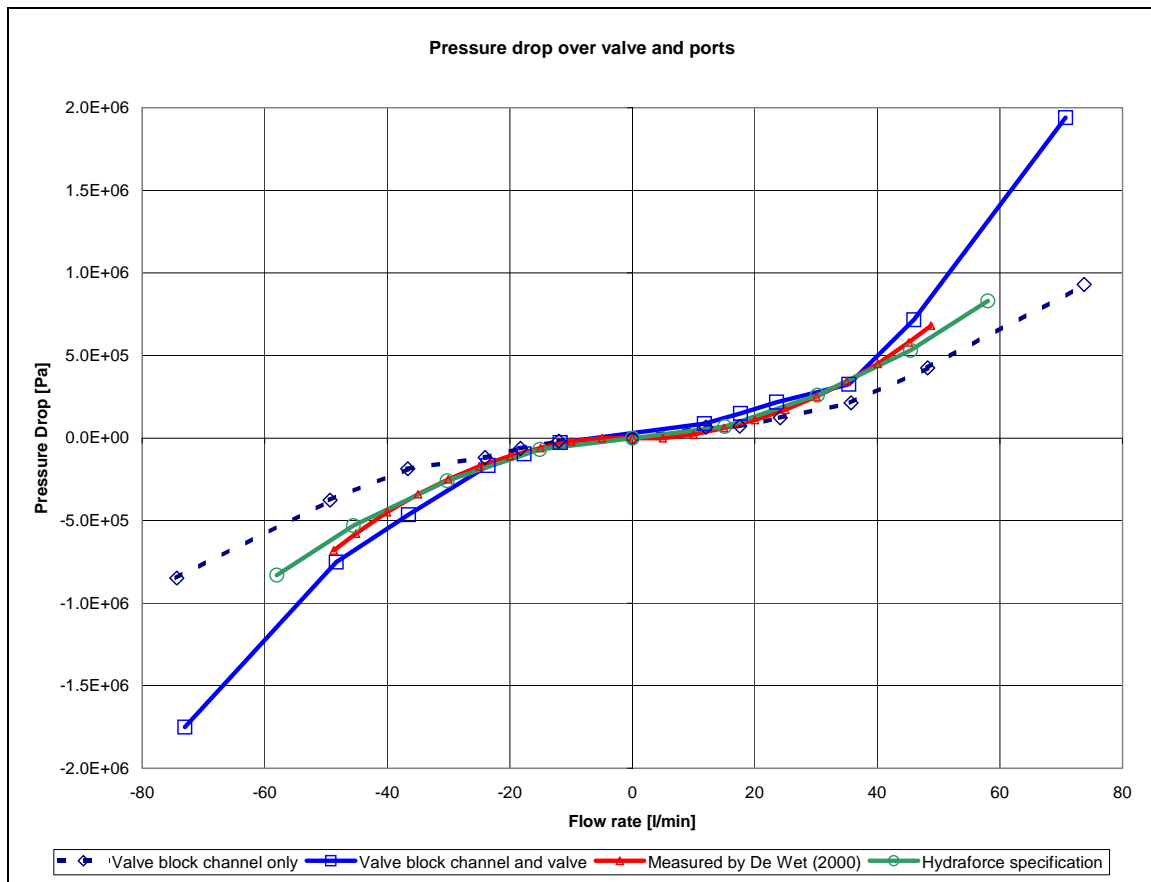


Figure 4.24 - Pressure drop over valve 1

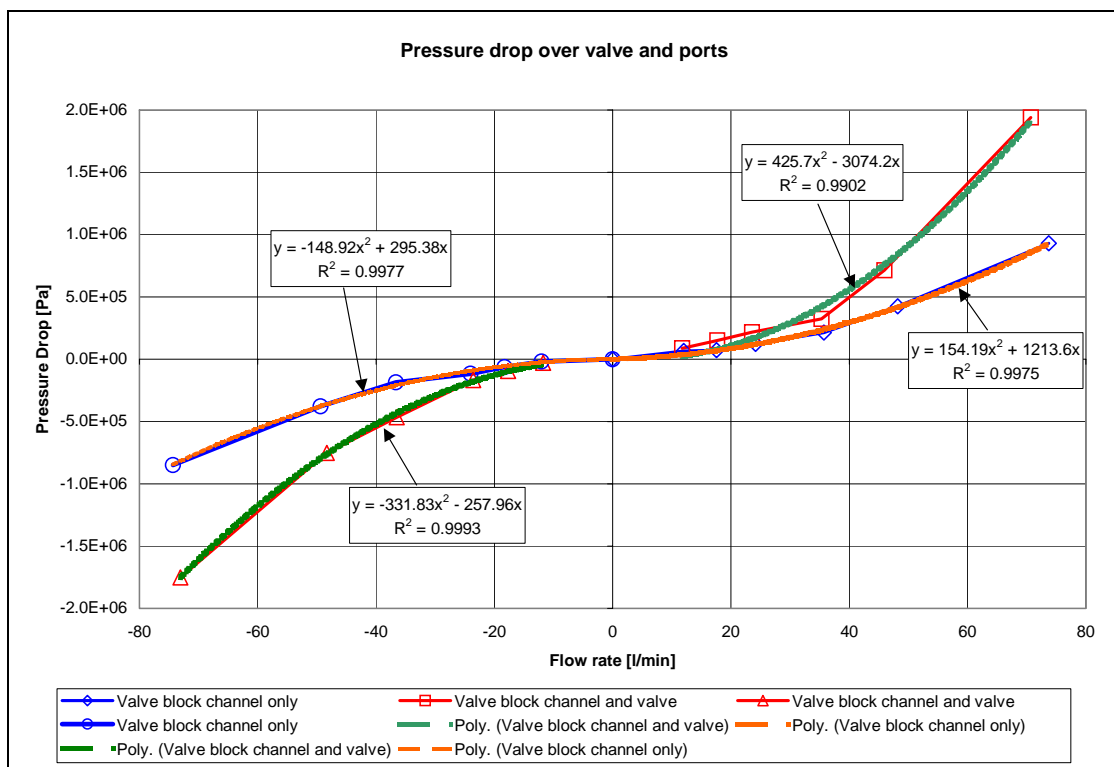


Figure 4.25 - Curve fits on pressure drop data



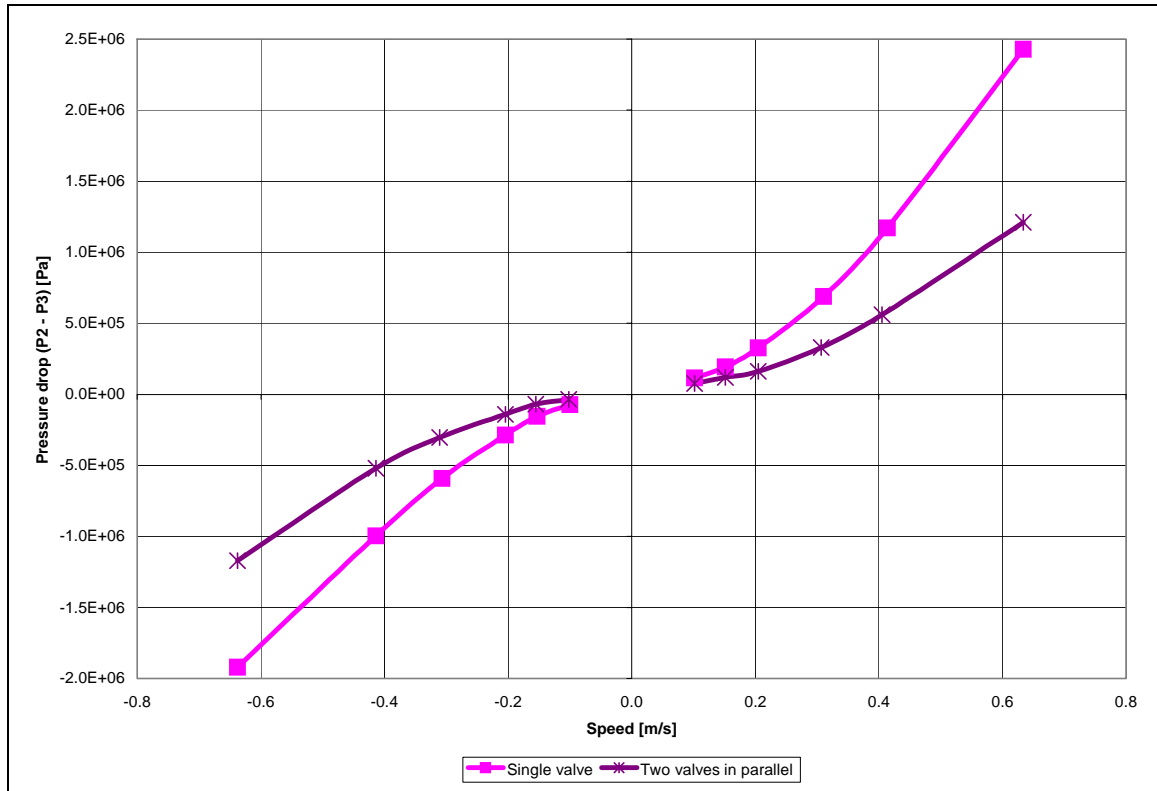


Figure 4.26 - Pressure drop over valve 3 (single valve vs. 2 valves in parallel)

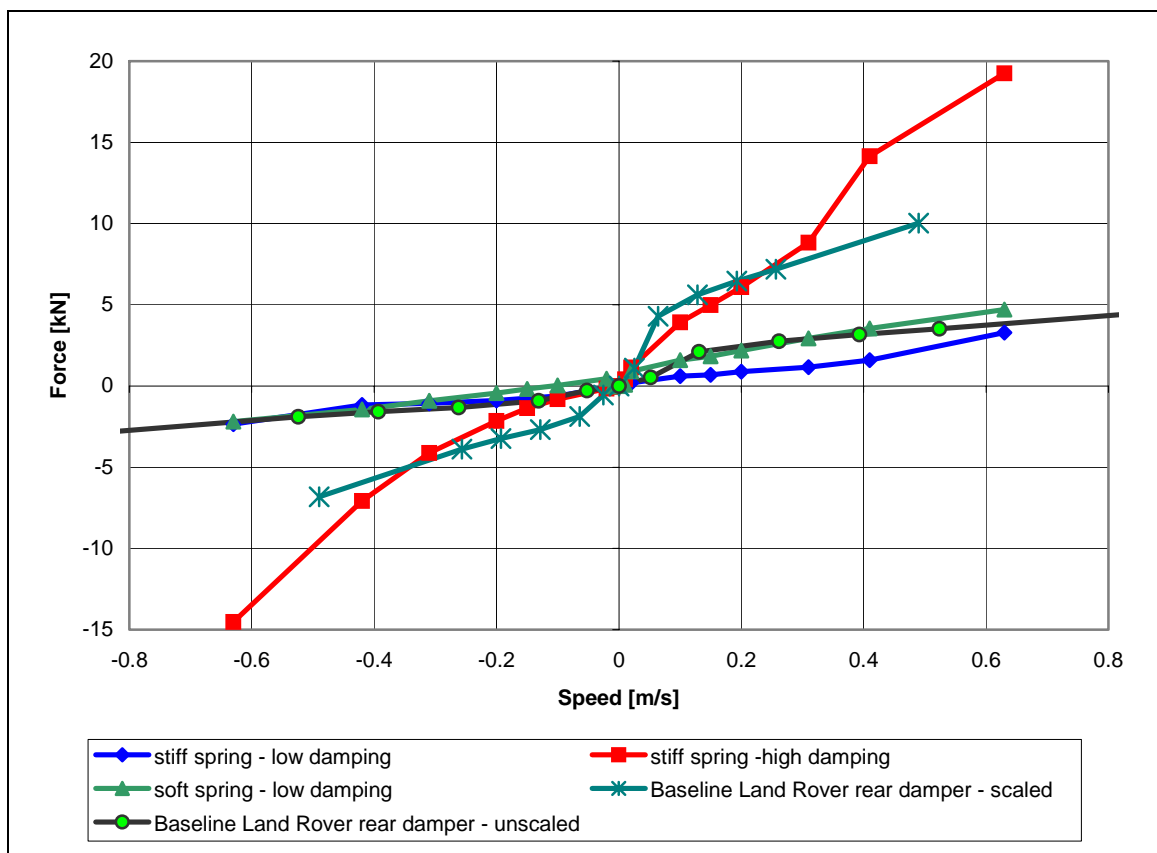


Figure 4.27 - Damper characteristics for Prototype 2

#### 4.7.6 Valve response times

Valve response times are very important for predicting the transient response of the system to valve switching. A typical trend of pressure drop over the valve vs. time is shown in Figure 4.28. The solenoid switching signal is indicated on the same graph. To obtain the valve response time, the initial pressure difference (before switching) and the final pressure difference (after the transient response has died away) is determined. Two values (represented by horizontal lines) are calculated representing a 5% change and a 95% change in pressure difference respectively. This is done in order to define the switching points more precisely as the exact moment where the change occurs is very difficult to determine. The time from the solenoid switching signal to the 5% change point is defined as the initial delay. This is the time required for the solenoid to build up enough force so that the valve plunger starts moving. The time between the 5% and 95% point is defined as the transient response time of the valve and represents the time required from the initial plunger movement until the valve is fully open. The total valve response time is the sum of the initial delay and the transient response time as indicated in Figure 4.28.

The valve response times were measured for all 4 four valves. The damper orifices were blocked so that all the flow was channelled through the valves. The valve response time was measured by closing the respective valve, compressing the strut until the required pressure difference was obtained, and then opening the valve. This resulted in flow through the valve until the pressure in the system stabilized. The procedure was repeated in the opposite direction, e.g. closing the valve and extending the strut before opening the valve.

Figures 4.29 and 4.30 give the valve response time (initial delay, transient response time and total response time) as a function of pressure drop across the valve for Prototypes 1 and 2 respectively. Prototypes 1 and 2 were both fitted with the same valves, although Prototype 1 used 24 Volt solenoids. This was changed to 12 Volt solenoids on Prototype 2 to be compatible with the test vehicle's electrical system.

The valve response time is to some extent dependant on the system (**Janse van Rensburg, Steyn and Els (2002)**). All four valves in Prototype 2 are fitted in different positions in the valve block with the result that the channels to these valves are all different. Valve response times are also dependent on the pressure difference across the valve as can be seen in the figure. The valve response time varies from 40 to 100 milliseconds over the pressure range of interest and is acceptable for the current application.

#### 4.7.7 Friction

The isothermal spring characteristic was determined by slowly compressing the spring through its operating range whilst recording force, displacement and pressure. Figure 4.31 indicates the spring force against spring displacement for the soft spring on Prototype 1. Two curves are shown namely the force measured by the load cell, and the force calculated from the pressure data. The measured force shows unacceptable levels of hysteresis, while the force calculated from the pressure measurement gives the expected characteristic.

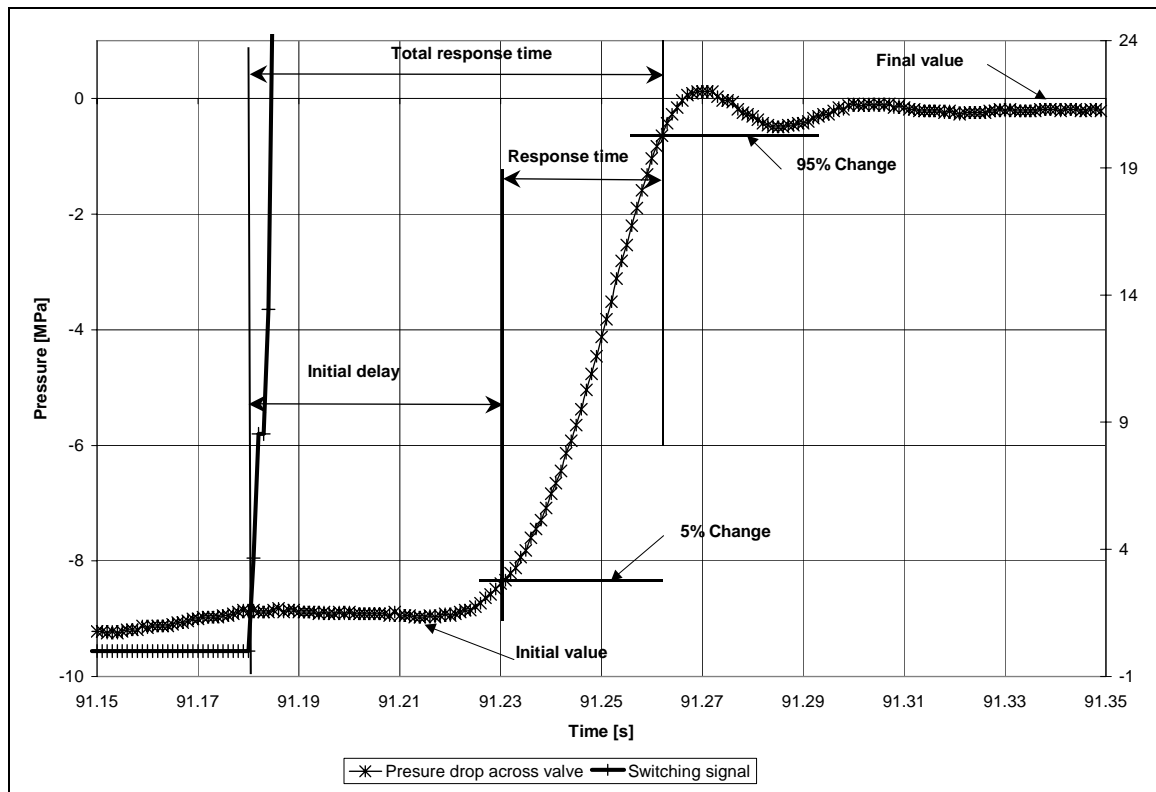


**Figure 4.28** - Explanation of valve response time definitions

During initial assembly of the unit, it was found that the main cylinder could be moved easily by hand, while the accumulator pistons had to be moved using compressed air. There was no way to move the accumulator pistons by hand. The hysteresis was therefore attributed to seal friction (stick-slip) in the accumulator seals. After considerable research, two new accumulator pistons were designed and manufactured using wear rings combined with a state-of-the-art accumulator seal (Turcon AQ Seal5) with negligible stick slip. The original design used a fairly basic seal layout with a double o-ring and back-up ring system.

After testing the more advanced sealing concept in the suspension system, it was found that the hysteresis had improved only marginally. Careful investigation traced the problem to the bending moment applied to the main cylinder due to the offset of the chassis mounting arrangement used on Prototype 1. This results in a high side force between the main cylinder and the piston, causing unacceptable friction and wear.

Figures 4.32 to 4.35 illustrate that friction in Prototype 2 is very low and should not cause any serious problems. Friction may however degrade the vibration isolation of the system for small road inputs.

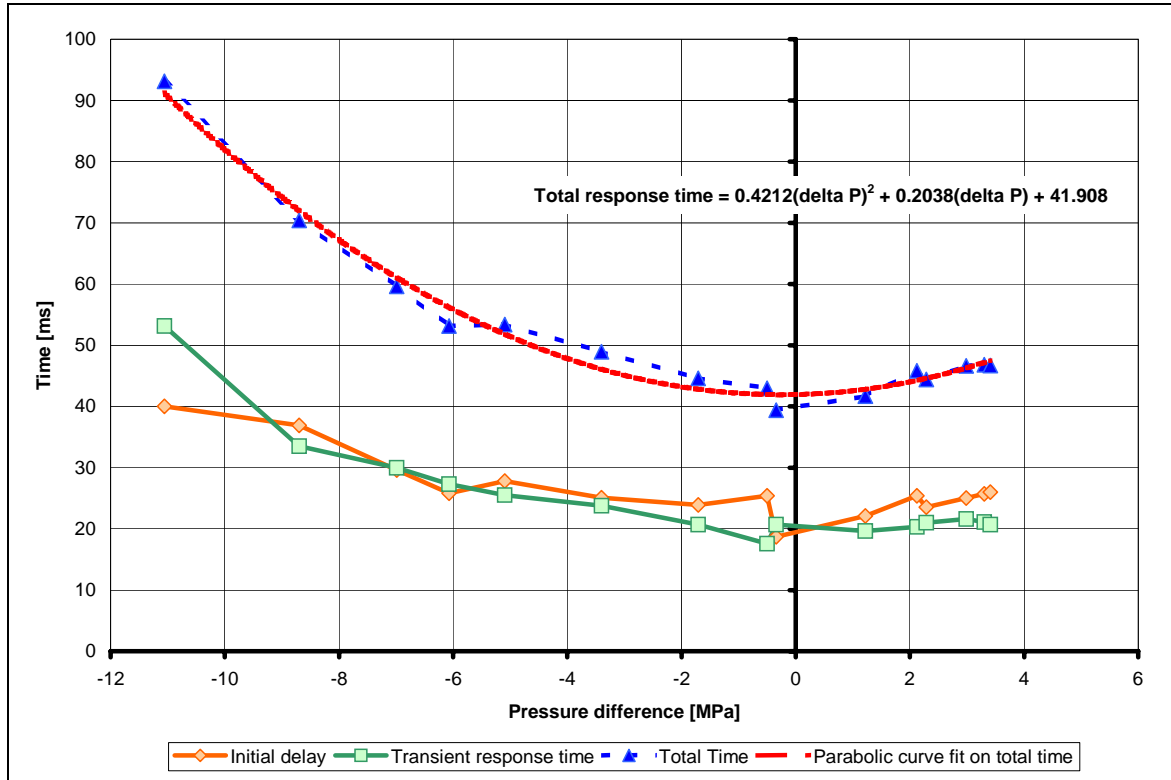


Figure 4.29 - Valve response time for Prototype 1

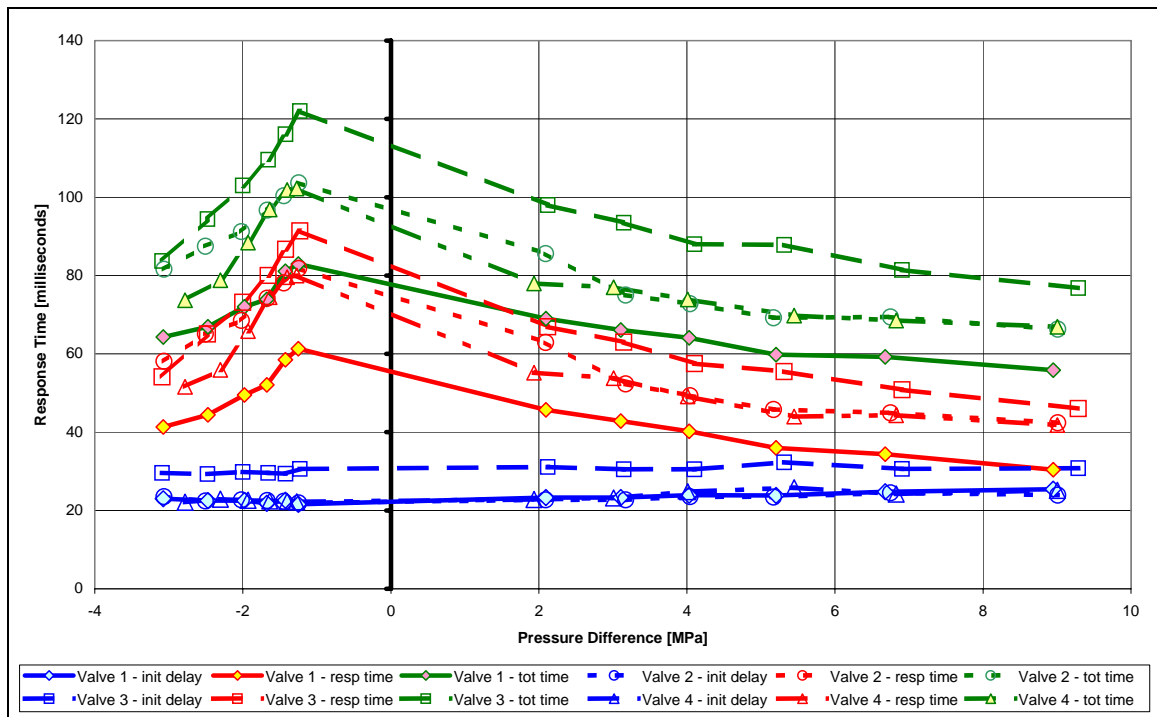


Figure 4.30 - Valve response time for Prototype 2

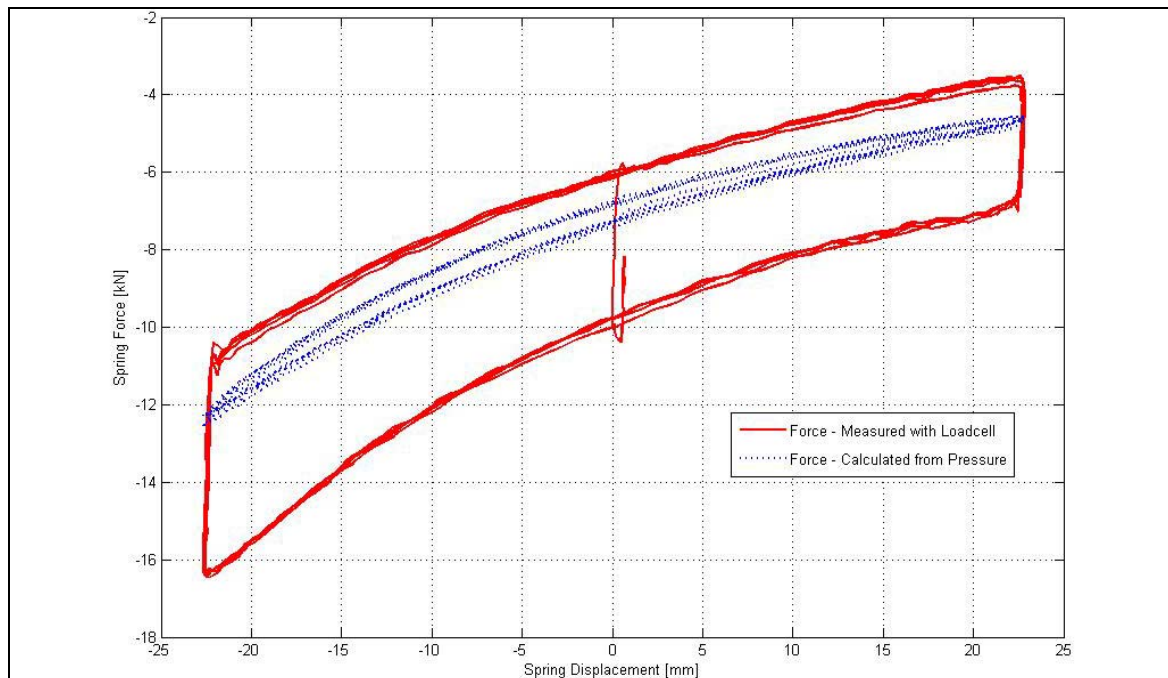


Figure 4.31 - Hysteresis problem on Prototype 1

## 4.8 Mathematical model

A SIMULINK<sup>®</sup> model of the suspension unit was developed by **Theron (Theron and Els, 2005)**. This model takes the deflection rate of the suspension unit as input and employs simple fluid dynamics theory in an iterative manner to calculate the flow rates from each accumulator to the cylinder. Iteration takes place until pressure balance in the parallel branches is established. The model then calculates the pressure in the two accumulators by solving the energy equation for an ideal gas in an enclosed container (**Els and Grobbelaar, 1993**) and time integrating the flow rates to determine the gas volumes in the two accumulators. The model renders the dynamic force generated by the suspension unit as output.

Physical tests have been performed on Prototype 2, where the spring characteristics, damper characteristics and valve dynamics have been measured. These tests were described in previous paragraphs. Generally, good correlation exists between the results of the SIMULINK<sup>®</sup> model and the experimental data measured in the laboratory on the prototype suspension unit. A number of aspects, where the model or the quantification of its parameters needs improvement, were identified.

The aim was to develop a mathematical model that can be used in vehicle dynamic simulations and to investigate suitable control strategies for semi-active switching of the spring and damper.

### 4.8.1 Modelling philosophy

In developing a mathematical model, a tension force in the unit is considered positive, while a compressive force is negative. Any extension of the unit relative to a reference state is considered as a positive (relative) displacement and compression of the unit as

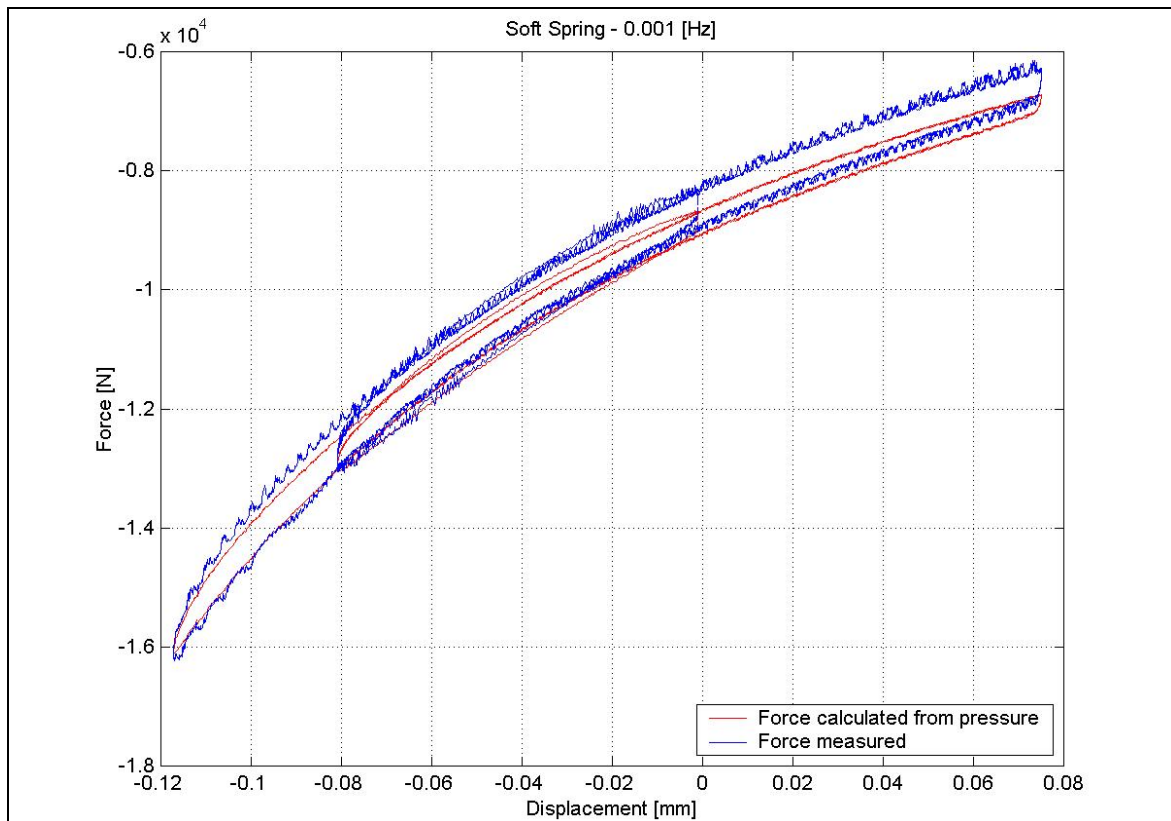


Figure 4.32 - Effect of friction on soft spring at low speeds

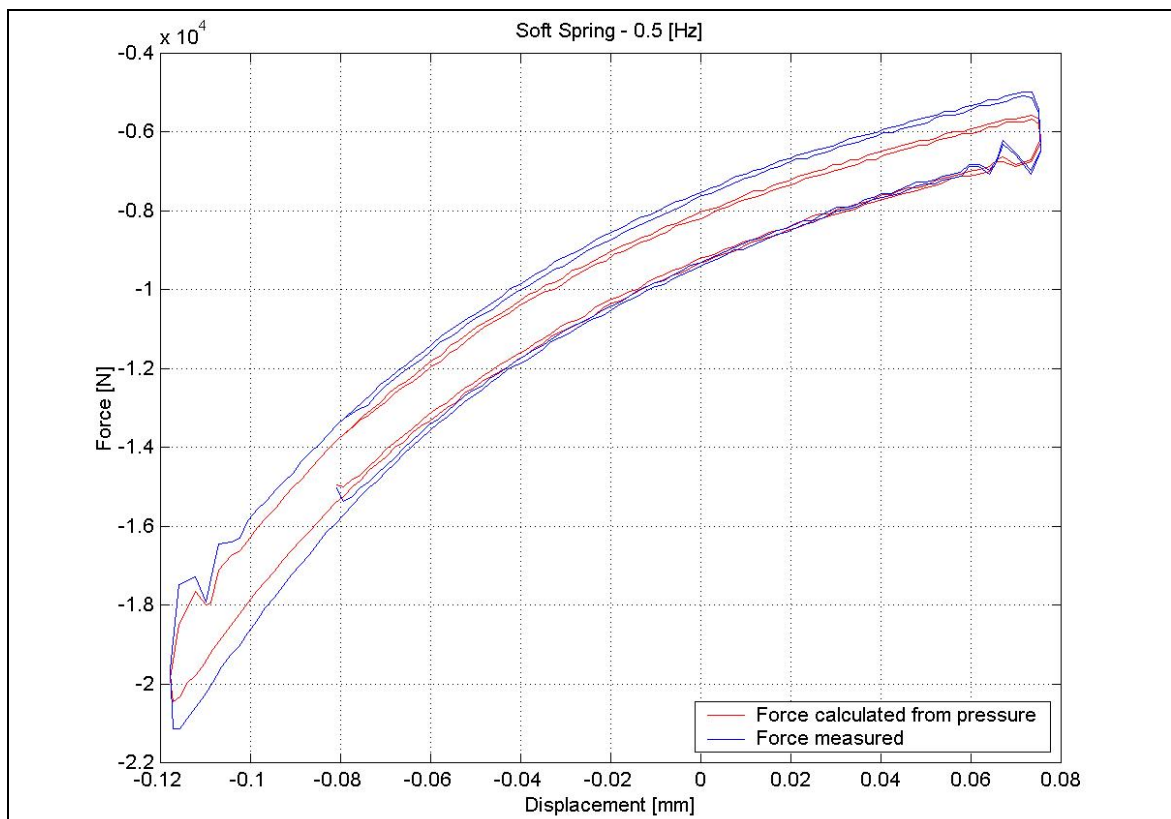
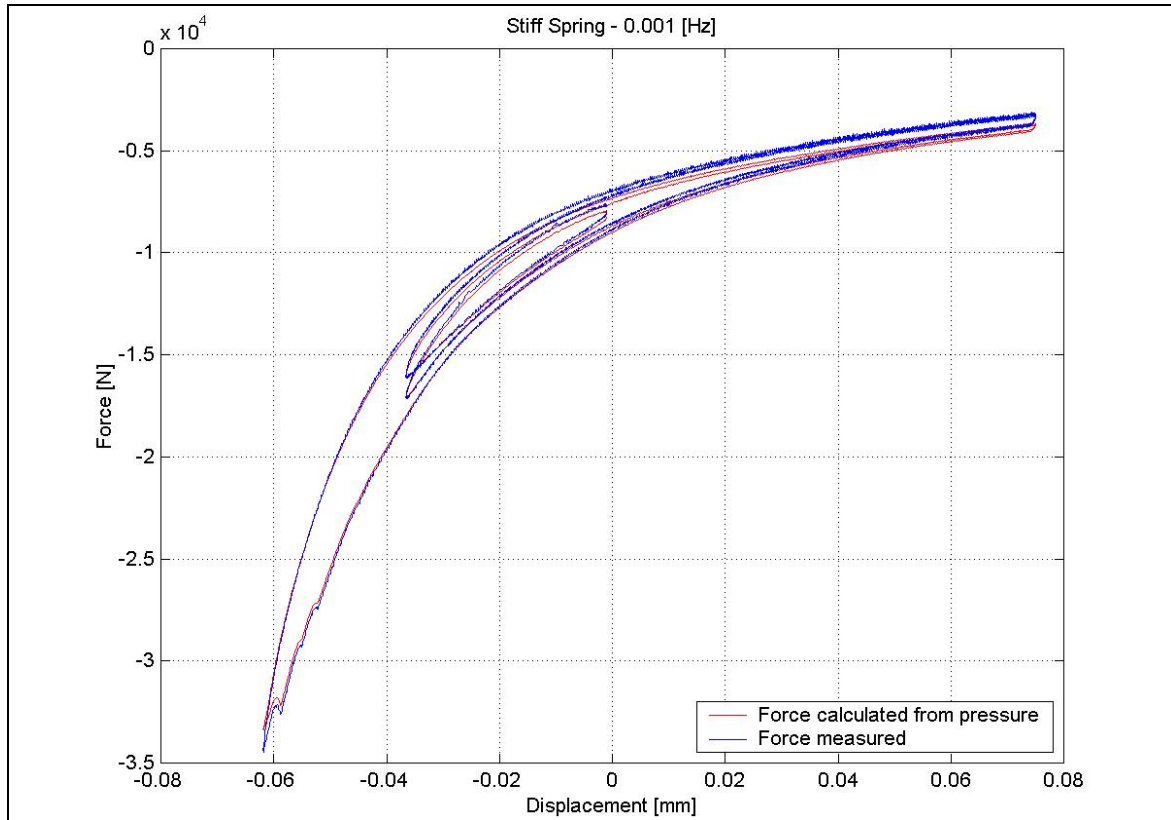
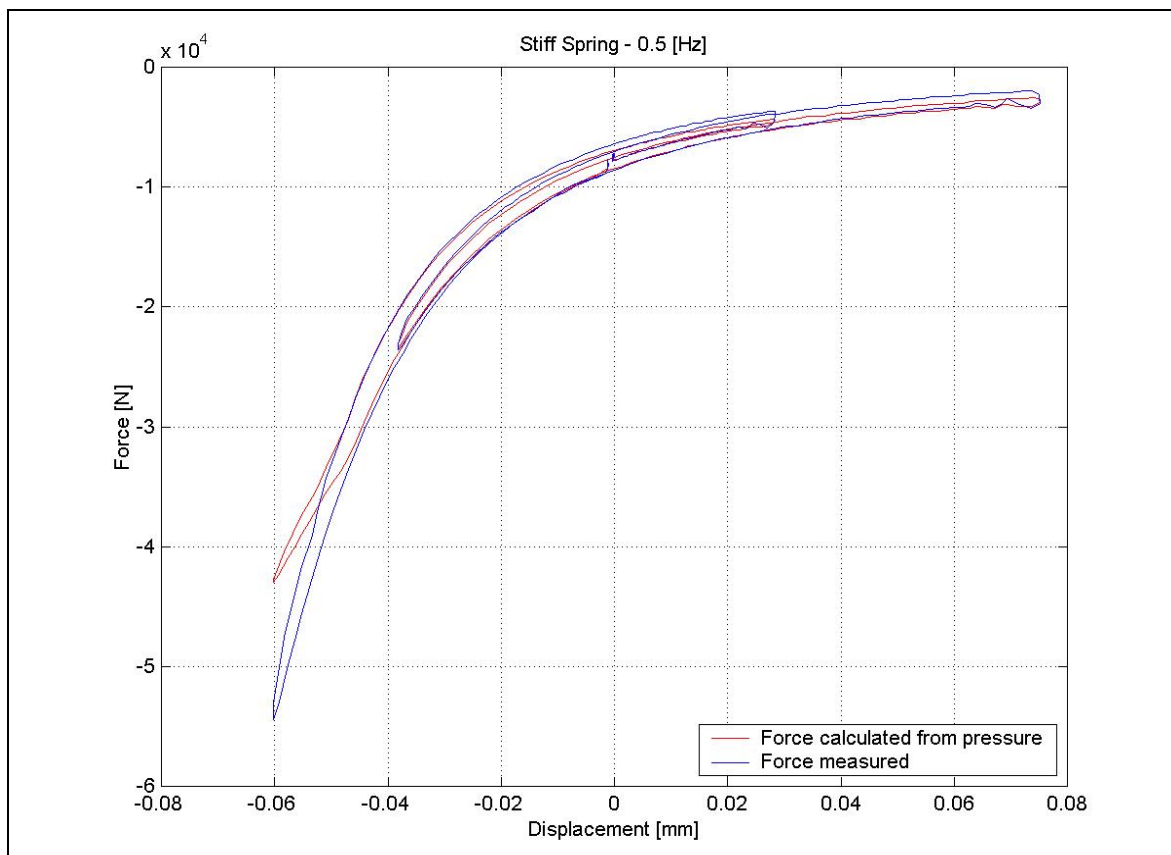


Figure 4.33 - Effect of friction on soft spring at high speeds



**Figure 4.34** - Effect of friction on stiff spring at low speeds



**Figure 4.35** - Effect of friction on stiff spring at high speeds

negative displacement. An extensional speed is considered positive and a compression speed as negative.

For the purposes of vehicle dynamics simulation a mathematical model of this unit is required that calculates the combined spring-damper force for a certain set of valve settings and a given state of displacement and speed. One may therefore consider the force of the suspension unit as the output of the model and the valve settings of the three valves and the displacement and speed of the unit as the inputs to the model, where the model calculates the output for given inputs. This calculation is typically performed within a time step in a simulation run and is repeated for each time step.

The working principle of the suspension unit is discussed in paragraph 4.2. Figure 4.7 indicates the various pressures, dampers and valves in the suspension system. The output force of the unit is essentially directly related to the pressure  $P_2$  in the main strut cylinder. This pressure depends on the pressures in the two accumulators, the flow through and corresponding pressure drops over the two dampers with corresponding channels and the valve switching. The pressure in the accumulators depends on the volume of oil in the accumulators, which is related to the displacement of the suspension unit and the state of valve 3. An alternative way of looking at the volume of oil in the accumulators is to realise that this is determined by the flow history, i.e., these volumes may be determined by integrating the flow rates in the two main branches of the system. Using this approach makes the mathematical model independent of the displacement of the unit as an input. This is indeed the approach that was used in modelling the unit. The input to the model of the suspension unit is therefore, in addition to the three valve switch signals, only the extensional speed  $\dot{x}$  of the unit. From this the volume flow rate  $q = A\dot{x}$  into the main strut cylinder, of cross sectional area  $A$ , can directly be calculated. The flow rates in the two branches are taken as  $q_i$ ,  $i = 1, 2$ , for the branch associated with accumulator  $i$ , positive in the direction from the accumulator towards the main strut.

#### 4.8.2 Pressure dependent valve switching

It is assumed that the electric signals with which the various valves are switched changes instantaneously from low to high values, or vice versa. When this happens, valve and other dynamics prevent immediate pressure and flow changes. These dynamic effects are not currently modelled mathematically, but are taken into account empirically. The valve response time was defined and determined in paragraph 4.7.6 (Figures 4.29 and 4.30). The parabolic curve indicated in Figure 4.29 (although determined for Prototype 1) was subsequently employed in the mathematical model with respect to all three valves and for both prototypes.

Wherever the state of the valve is taken into account in the model, a fraction  $f_i$  between zero and one is used, where the subscript  $i = 1, 2, 3$  indicates the valve number. For switching on the valve (electric signal going from low to high, valve going from closed to open)  $f_i = 0$  before the electrical signal switches,  $f_i = 0.05$  at half the valve response time after the electrical signal switches,  $f_i = 0.95$  at the valve response time and  $f_i = 1$  after 1.5 times the valve response time. In between these time points a piecewise cubic Hermite interpolation is used to calculate the fraction. For switching off the valve the same type of interpolation is used on the reversed sequence.



### 4.8.3 Pressure drop over dampers and valves

Due to the complexity of possible dampers that may be used in the suspension unit, it was decided to use table look-up techniques to get the pressure drop over the damper for a given flow rate through the damper. Quite often the pressure-flow characteristics display significant hysteresis. For now the table look-up procedure employed does not provide for possible hysteresis. The pressure drop over the damper was measured, with the by-pass valve both open and closed, for various positive and negative flow rates in a practically realistic range. This measured data was used to establish a high damping and a low damping damper curve, corresponding to the by-pass valve being closed and open, respectively. These curves are used in the table look-up procedure for both dampers 1 and 2, since they currently are identical and their by-pass valves are also identical. The fact that the internal passages in the valve block for the two dampers at this time are not identical is neglected in the model.

For a certain flow rate  $q_i$  the pressure drop over damper  $i$  with  $i = 1, 2$ , is calculated as  $\Delta P_{di} = f_i \Delta P_{doi} + (1 - f_i) \Delta P_{dci}$ , where  $\Delta P_{dci}$  is the pressure drop interpolated at  $q_i$  from the high damping graph of damper  $i$ , while  $\Delta P_{doi}$  is the pressure drop interpolated at  $q_i$  from the low damping graph of damper  $i$ .

When valve 3 is fully open ( $f_3 = 1$ ), the pressure drop over valve 3,  $\Delta P_{v3}$ , is calculated using an experimentally determined loss factor and the flow  $q_2$ . When the valve is opening ( $0 < f_3 < 1$ ,  $f_3$  increasing), a value  $\Delta P_{v3o}$  is calculated in exactly the same way as  $\Delta P_{v3}$  above, but the actual pressure drop over the valve is taken as  $\Delta P_{v3} = f_3 \Delta P_{v3o} + (1 - f_3) \Delta P_{v3i}$ , where  $\Delta P_{v3i}$  is the pressure drop over the valve before the switching started. When the valve is closing ( $0 < f_3 < 1$ ,  $f_3$  decreasing), on the other hand, the actual pressure drop over the valve is taken as  $\Delta P_{v3} = f_3 \Delta P_{v3o} + (1 - f_3) \Delta P_{v3e}$ , where  $\Delta P_{v3e}$  is the pressure drop over the valve calculated for the scenario where all variables are at their current values except  $q = q_1$  and  $q_2 = 0$ , i.e., as if valve 3 is fully closed.

### 4.8.4 Flow and pressure calculation

The mathematical model is essentially based on the assumption that the hydraulic fluid is incompressible. In the simulation, however, the compressibility of the fluid is taken into account as a refining correction in the calculation of the gas volumes in the accumulators. This correction is based on the various major volumes of fluid in the system, each at its respective pressure, and the bulk modulus of the hydraulic fluid (see paragraph 4.7.2).

Whenever valve 3 is closed, the system can be modelled as a third order non-linear state space system; otherwise a fourth order non-linear state space system with an algebraic constraint is obtained. These two alternative situations will now be considered separately.

**i) Valve 3 closed**

When valve 3 is closed,  $q = q_1$  and  $q_2 = 0$ , due to the assumed incompressibility of the hydraulic fluid. Let the volume of gas in accumulator  $i$  be  $V_{gi}$ . The rate of change in the gas volume in accumulator 1 is

$$\dot{V}_{g1} = q_1 \cdot \quad (4.2)$$

The pressure  $P_{accui}$  in the accumulator  $i$  is calculated using the ideal gas law

$$P_{accui} = m_i R T_i / V_{gi} = R T_i / v_i \quad (4.3)$$

where:  $m_i$  is the mass of gas with which the accumulator is charged,  $R = 296.797$  is the gas constant for Nitrogen,  $v_i = V_{gi} / m_i$  is the specific volume and  $T_i$  is the absolute temperature of the gas in the accumulator. ( $P_{accui} = P_1$  for accumulator 1 and  $P_{accui} = P_4$  for accumulator 2.)  $T_i$  is calculated by solving the following differential equation, as suggested by **Els (1993)** and **Els and Grobbelaar (1993)**:

$$\dot{T}_i = \frac{T_{i0} - T_i}{\tau_i} - \frac{T_i}{c_v} \left( \frac{\partial P_{accui}}{\partial T_i} \right)_v \dot{v}_i \quad (4.4)$$

where  $T_{i0}$  is the initial gas temperature, in this taken as the ambient temperature,  $\tau_i$  is the thermal time constant of the accumulator and  $c_v$  is the specific heat at constant volume of the gas. The thermal time constant is taken at experimentally determined values of 4.8 seconds for both accumulators (see paragraph 4.7.3). Calculating the gas temperature in this way means that if the gas is suddenly compressed, the model calculates the pressure rise along an adiabatic compression curve, while the temperature rises. However, if the gas is subsequently allowed to cool down, the model allows the pressure to drop to the value indicated by the isothermal compression curve.

From equation (4.3) it follows that

$$\frac{\partial P_{accui}}{\partial T_i} = \frac{R}{v_i} \quad (4.5)$$

Substituting this in equation (4.4) renders

$$\dot{T}_i = \frac{T_{i0} - T_i}{\tau_i} - \frac{T_i R}{c_v V_{gi}} q_i = f_{Ti}(T_i, V_{gi}, q_i) \quad (4.6)$$

where the  $f_{Ti}(T_i, V_{gi}, q_i)$  on the right hand side indicates that  $\dot{T}_i$  is a function of the variables  $T_i$ ,  $q_i$  and  $V_{gi}$ . Equation (4.6) is non-linear due to the appearance of the product of these variables.

Since  $q_2 = 0$ , there is no change in the gas volume in accumulator 2. The pressure in this accumulator may however still change, as the gas temperature may change. The third order system is thus defined by the three differential equations, equation (4.2) and equation (4.6) for  $i = 1, 2$ . Within a simulation time step, in addition to these three differential equations, various other variables are calculated (for example, the accumulator pressures with equation (4.3)). There are, however, no algebraic equations that need to be solved simultaneously with the three differential equations, and the solution is therefore fairly straightforward.

Once  $q_1$  for the current time step has been calculated, the pressure  $P_2$  in the main strut cylinder is calculated by calculating  $\Delta P_{d1}$  as described in section 4.8.3 above, and then  $P_2 = P_1 - \Delta P_{d1}$ . With  $P_2$  known the output of the model is simply calculated by multiplying this pressure with the negative of the main strut cross sectional area.

**ii) Valve 3 open, opening or closing.**

When valve 3 is partially or fully opened, the flow rate  $q_2$  is no longer zero. Due to the assumed incompressibility of the hydraulic fluid,  $q = q_1 + q_2$ . The rate of change in gas volume in accumulator 1 is still given by equation (4.2), while the rate of change in the gas volume in accumulator 2 is

$$\begin{aligned}\dot{V}_{g2} &= q_2 \\ &= q - q_1\end{aligned}\tag{4.7}$$

In this case, however, an additional algebraic equation needs to be solved simultaneously with the differential equations. This equation may be considered as a constraint that needs to be satisfied, namely that the pressure  $P_2$  in the main strut cylinder calculated along two different paths must be the same. Let  $P_{21}$  be the pressure in the main strut cylinder, calculated along the branch connecting this to accumulator 1 as outlined in section 4.8.4(i) above (which for a given flow rate  $q_1$  is also valid in this case).  $P_{21}$  is therefore a function of the flow rate  $q_1$  and the pressure  $P_1$ . The pressure  $P_1$ , by equation (4.3), is a function of  $T_1$  and  $V_{g1}$ . Therefore  $P_{21} = P_{21}(q_1, T_1, V_{g1})$ . In a similar way the pressure  $P_{22}$  in the main strut cylinder, calculated along the branch connecting this to accumulator 2, may be calculated, by first calculating  $\Delta P_{d2}$  and  $\Delta P_{v3}$  at flow rate  $q_2 = q - q_1$ , as described in section 4.8.3 above. Then,  $P_3 = P_4 - \Delta P_{d2}$  and  $P_{22} = P_3 - \Delta P_{v3}$ . The pressure  $P_4$  is a function of  $T_2$  and  $V_{g2}$ , therefore,  $P_{22} = P_{22}(q, q_1, T_2, V_{g2})$ . The algebraic constraint may then be written as:

$$0 = P_{21}(q_1, T_1, V_{g1}) - P_{22}(q, q_1, T_2, V_{g2}) .\tag{4.8}$$

Also, whereas equation (4.6) is still valid for accumulator 1, for accumulator 2 the flow rate  $q_2$  needs to be substituted with  $q - q_1$ , so that the system dynamics may be summarized in the following non-linear state space representation:

$$\begin{bmatrix} 1 & 0 & 0 & 0 & 0 \\ 0 & 1 & 0 & 0 & 0 \\ 0 & 0 & 1 & 0 & 0 \\ 0 & 0 & 0 & 1 & 0 \\ 0 & 0 & 0 & 0 & 0 \end{bmatrix} \begin{bmatrix} \dot{T}_1 \\ \dot{T}_2 \\ \dot{V}_{g1} \\ \dot{V}_{g2} \\ \dot{q}_1 \end{bmatrix} = \begin{bmatrix} f_{T1}(T_1, V_{g1}, q_1) \\ f_{T2}(T_2, V_{g2}, q, q_1) \\ q_1 \\ q - q_1 \\ P_{21}(q_1, T_1, V_{g1}) - P_{22}(q, q_1, T_2, V_{g2}) \end{bmatrix},\tag{4.9}$$

with input variable  $q$  and state variables  $T_1, T_2, V_{g1}, V_{g2}$  and  $q_1$ . The flow rate  $q_1$  is not truly a state variable, but it is convenient to consider it as such in order to write the four differential equations and the algebraic constraint in a single equation as above.

The matrix on the left of equation (4.9) is often called a mass matrix. This equation is an example of a so-called differential-algebraic equation, as the mass matrix is singular. This singularity is clearly caused by the algebraic constraint.

#### 4.8.5 Implementation in SIMULINK<sup>®</sup>

As mentioned above, the aim of this research was to develop a mathematical model of the suspension unit, to be used in vehicle dynamic simulations. It was decided earlier to use the ADAMS<sup>®</sup> program for the vehicle dynamics simulation. A very convenient way to interface a mathematical model like that of the suspension unit as described above with an ADAMS model of a larger system (in this case the vehicle and its suspension system components other than the suspension units) is to implement the mathematical model in the SIMULINK environment. ADAMS can be linked to MATLAB<sup>®</sup> SIMULINK sub-programs. For this reason the mathematical model was implemented in SIMULINK.

MATLAB provides a solution scheme for differential-algebraic equations and as a consequence SIMULINK has the ability to model algebraic constraints. Solution of the differential-algebraic equation, equation (4.9), using this functionality has been unsuccessful thus far. The mathematical model was however implemented successfully in SIMULINK by, within each time step, first calculating the valve fractions  $f_i, i = 1,2,3$ , based on the pressure drops over the valves at the end of the previous time step and then enforcing the algebraic constraint using a Newton-Raphson type iteration to find the values of  $q_1, q_2, P_2$  and  $P_3$ . After these values have been calculated,  $T_1, T_2, V_{g1}$  and  $V_{g2}$  are calculated by solving the four first order differential equations contained in equation (4.9). Lastly  $P_1$  and  $P_4$  are calculated using equation (4.3). During the Newton-Raphson type iteration the values of  $P_1$  and  $P_4$  at the end of the previous time step are used. This iteration is performed in a MATLAB s-function that is called by the SIMULINK program. Once  $P_2$  is calculated, the output force of the suspension unit for the current time step may be calculated as  $F = -P_2A$  and the program may move on to the next time step. It should be noted that the friction between the piston and the cylinder walls and the piston rod and its bushing is neglected in the calculation of  $F$ .

#### 4.8.6 Validation of the mathematical model

The model of the suspension unit has been validated by comparing its predicted force output with forces measured on the Prototype 2 unit in a SCHENCK Hydropulse hydrodynamic testing machine under displacement control.

During testing on the hydrodynamic testing machine, the displacement feedback signal and resulting force as measured with a load cell were recorded. In addition to these two signals, the signals from the four pressure transducers measuring pressures  $P_1$  to  $P_4$  and the electric command signals for switching the valves were also recorded. All these signals were filtered to prevent aliasing, digitised and stored on disc.

Comparing the load cell force and the pressure  $P_2$  measurements clearly showed that the error made in the model by neglecting the friction on the sliding parts of the unit and taking the output force of the unit as  $-P_2A$ , is not insignificant but generally quite small. There is a second reason, other than friction, for the difference between the load cell force and  $-P_2A$ , especially in situations of oscillation at high frequency. During vehicle simulation, the inertial properties of the piston and piston rod should be combined with those of the unsprung mass, so that the associated dynamic effects are taken into account by the ADAMS model, rather than the SIMULINK model. The output of the SIMULINK model should therefore be the suspension unit output force before the inertial effect of the piston and piston rod has been taken into account. The load cell, however, measures the suspension unit net output force after accelerating this mass. It is therefore prudent, in the comparison of the mathematical model with the measured results, to compare the output of the model in terms of measured and calculated  $-P_2A$  values. In the discussion that follows all reference to measured force should be understood to mean force calculated from the measured pressure  $P_2$  and thus neglects friction.

Since the mathematical model does not accept a displacement time history as input, but rather the extensional speed time history, the measured displacement signal first had to be differentiated with respect to time. It was always possible to bring the displacement signal back to its initial value at the end of a test run. The differentiation was therefore performed by transforming the whole displacement time history of a test run to the frequency domain using a Fast Fourier Transform (FFT), then multiplying the resultant double sided complex spectrum with  $j\omega$ , setting all values corresponding to frequencies above a chosen low pass filter cut-off frequency and below the negative of this cut-off frequency to zero and lastly back transforming the signal to the time domain using the inverse FFT. (In this  $j = \sqrt{-1}$  and  $\omega$  is the circular frequency.) This procedure not only performs the differentiation but also realizes a low pass filter with very sharp cut-off properties and no magnitude and phase distortion below the cut-off frequency. During vehicle simulation this differentiation of the displacement is not required, since the ADAMS model directly calculates the required speeds.

To first test the spring properties without the influence of the dampers the suspension unit was cycled through a triangular wave displacement at low speed, as indicated in Figure 4.36. This figure also shows the output force of the suspension unit, as calculated from the measured pressure  $P_2$ , for the case of stiff spring and low damping properties. Figure 4.37 shows the comparison between the measured and SIMULINK calculated time histories for this case, for the pressure in the active accumulator,  $P_1$ , and the main strut,  $P_2$ . Even though the nominal gas volume of accumulator 1 at the static wheel load was designed to be 0.1 litres, during this simulation it was adjusted to 0.135 litres, in order to obtain what was considered an acceptable correlation between the measured and calculated results. This adjustment is to some extent justified due to the fact that the volume calculation during design did not take into account some small cavities and screw thread inside the accumulator, and it was also determined that it is rather difficult to fill the suspension unit with oil without trapping small pockets of air inside the unit. The volume of accumulator 1 could have been adjusted to an even higher value, to get an even closer correlation between the measured and calculated results at the peak at 100 seconds in Figure 4.37, but there also was evidence that valve 3 was prone to leak at a high

pressure differential, which may have caused a reduced pressure during the measurement. The force-displacement graph obtained during the test that produced Figure 4.37 is shown in Figure 4.38, once again comparing the measured and calculated results. This test was repeated with a high damping setting and essentially the same results were obtained, as expected, since the very slow speed renders very small damping.

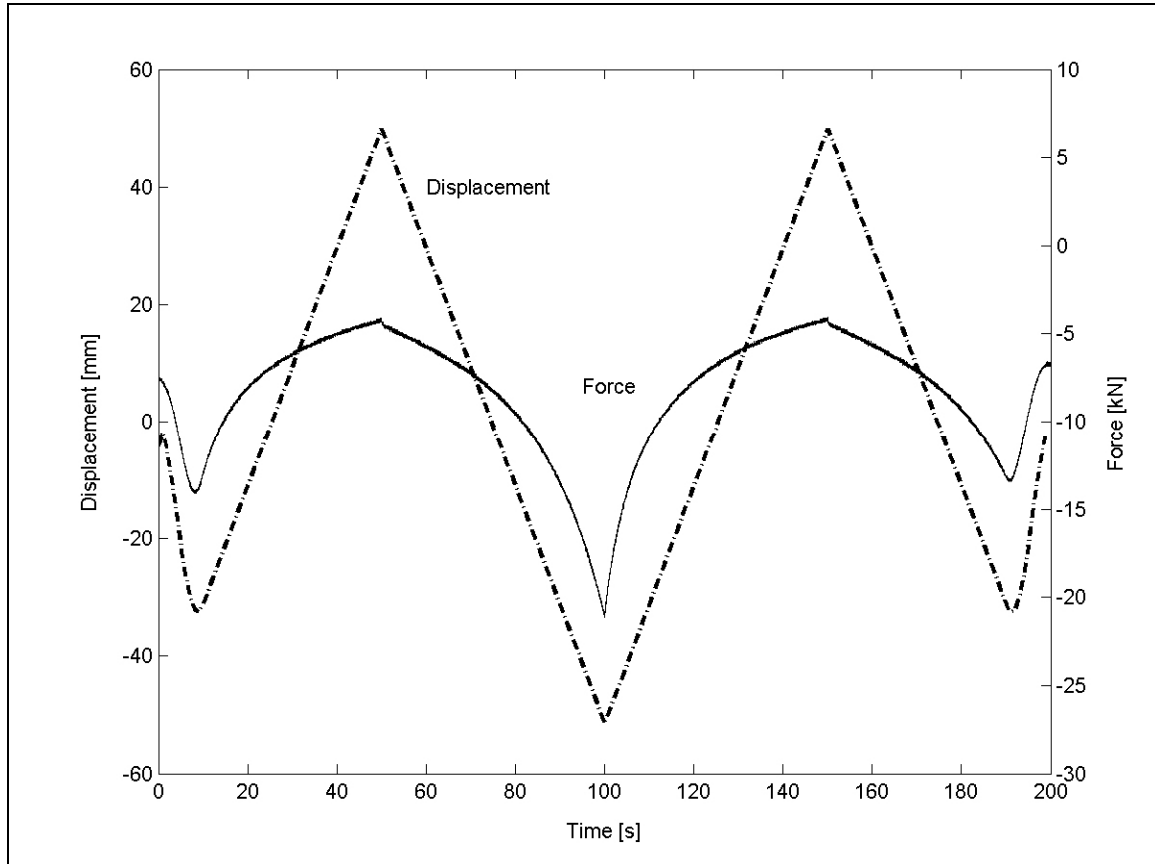


**Figure 4.36** – Measured input and output: stiff spring and low damping at low speed

Next a similar test was conducted but at considerably higher speeds, to generate a significant damping effect. The input displacement and output force for a stiff spring and low damping setting is shown in Figure 4.39. The comparison between the measured and calculated time histories for this case, for  $P_1$  and  $P_2$ , are shown in Figure 4.40 and the force-displacement graph obtained during this test in Figure 4.41. The correlation between measurement and calculation displayed in Figure 4.40 is generally good, except at the high-pressure peaks. The calculated force-displacement graph shows an interesting figure eight shape, which was not observed in the measurement nor any other simulation result. When evaluating the force-displacement graphs generated by the simulation, one needs to bear in mind that the model does not yet provide for hysteresis in the damping properties. This may account for the strange curve calculated and displayed in Figure 4.41.

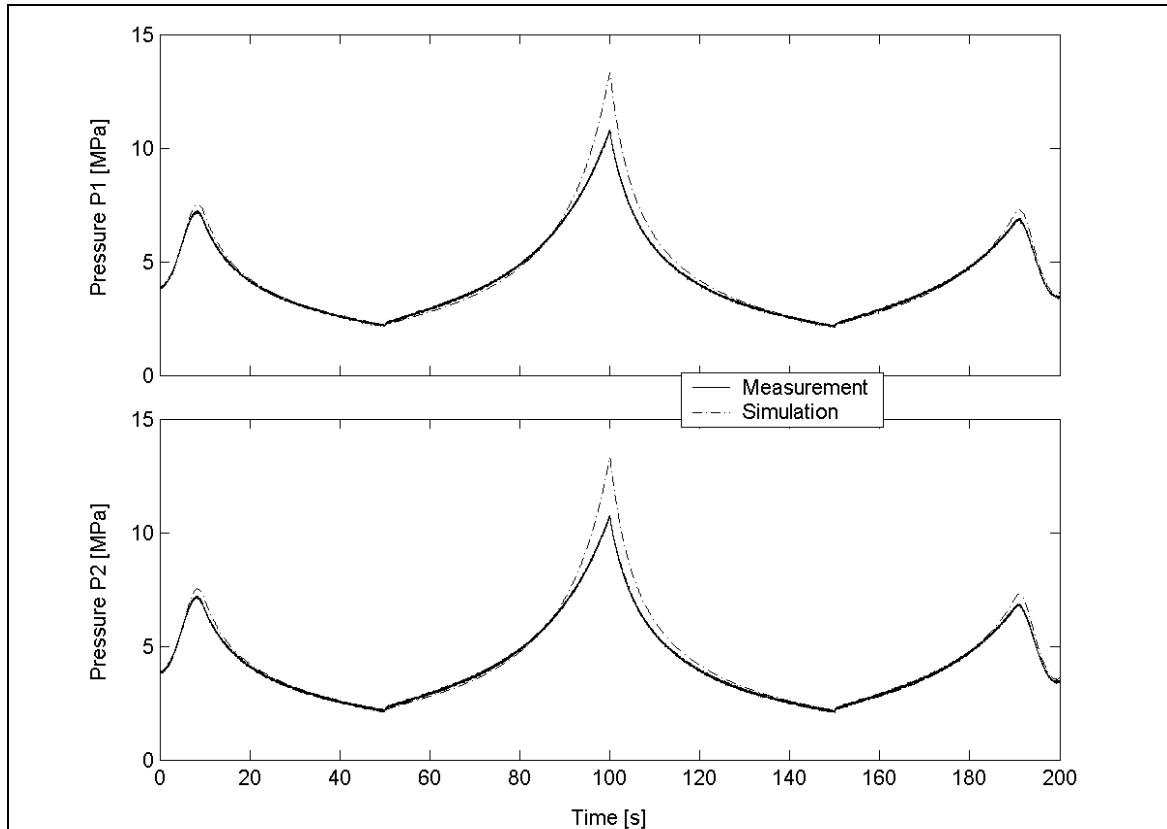


**Figure 4.37** – Comparison between measured and calculated values of  $P_1$  and  $P_2$ : stiff spring and low damping at low speed

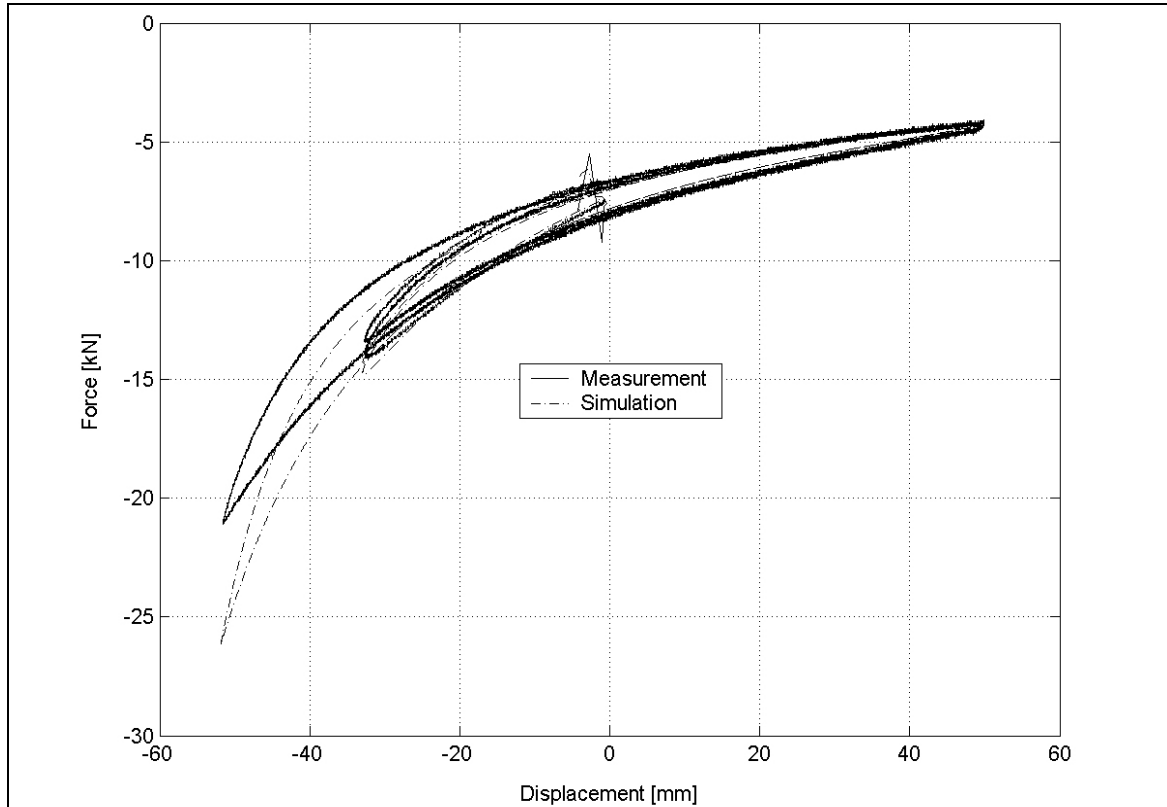


**Figure 4.38** – Comparison between measured and calculated force-displacement curve: stiff spring and low damping at low speed

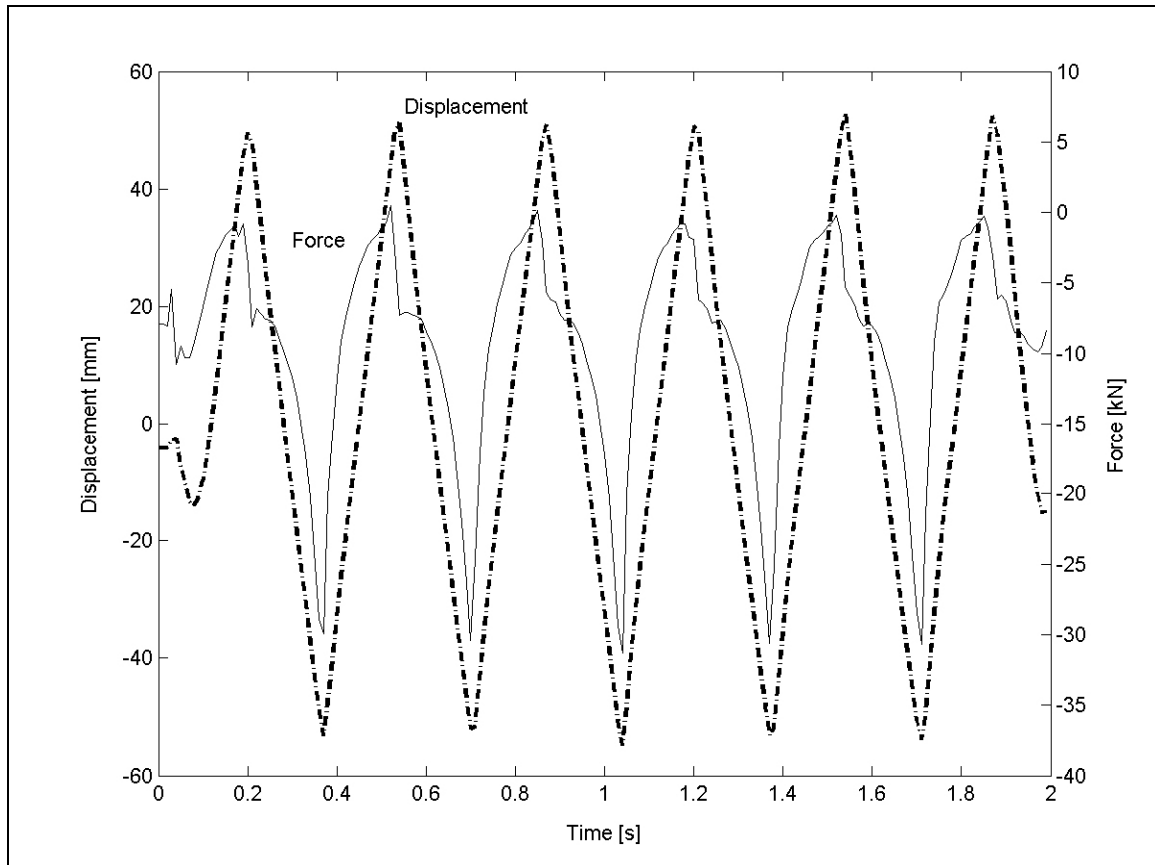


**Figure 4.39** – Measured input and output: stiff spring and low damping at high speed

A third stiff spring low damping test was performed at a slightly lower speed but a higher displacement stroke, as indicated in Figure 4.42. The comparison between the measured and calculated time histories for this case, for  $P_1$  and  $P_2$ , are shown in Figure 4.43 and the force-displacement graph obtained during this test in Figure 4.44. The simulation indeed indicated significantly higher pressures to accompany the higher displacement input, but the measured pressures failed to reach the high values as expected. The clear kink in the measured force-displacement graph in Figure 4.44 near  $-50$  mm displacement is seen as a clear indication of leakage, at high differential pressure, through valve 3.

Next the same kind of test as shown in Figure 4.39 was performed, only now with high damping (i.e., high stiffness and high damping, triangular displacement excitation at high speed). The input displacement and measured force time histories are shown in Figure 4.45. It is clear that the output force is clipped at about zero Newton, and the reason for this is that the pressure cannot drop very far below zero Pascal (atmospheric pressure) because at lower pressures the oil starts to boil preventing further pressure drop. In any case, the pressure cannot drop below zero absolute, which would correspond to a positive output force of merely 196 N. The time histories of the pressures  $P_1$  and  $P_2$  are shown in Figure 4.46. The SIMULINK model has been constructed such that pressure  $P_2$  will only drop to zero. It is seen that while  $P_2$  is dropping, the model follows the measurement quite well into the saturation at zero. The model, however, recovers from this more quickly than the actual physical unit. This causes the calculated pressure to start rising significantly earlier on the compression stroke than the measured pressure. After a



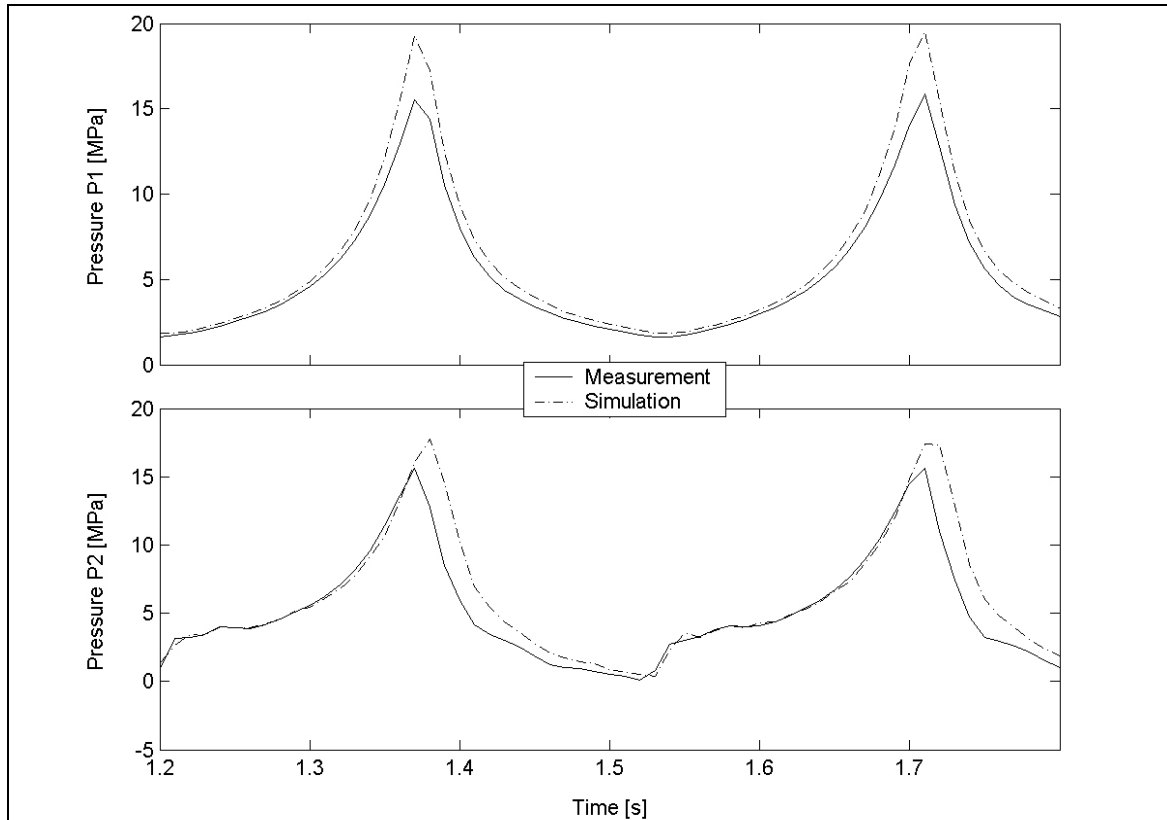


**Figure 4.40** – Comparison between measured and calculated values of  $P_1$  and  $P_2$ : stiff spring and low damping at high speed

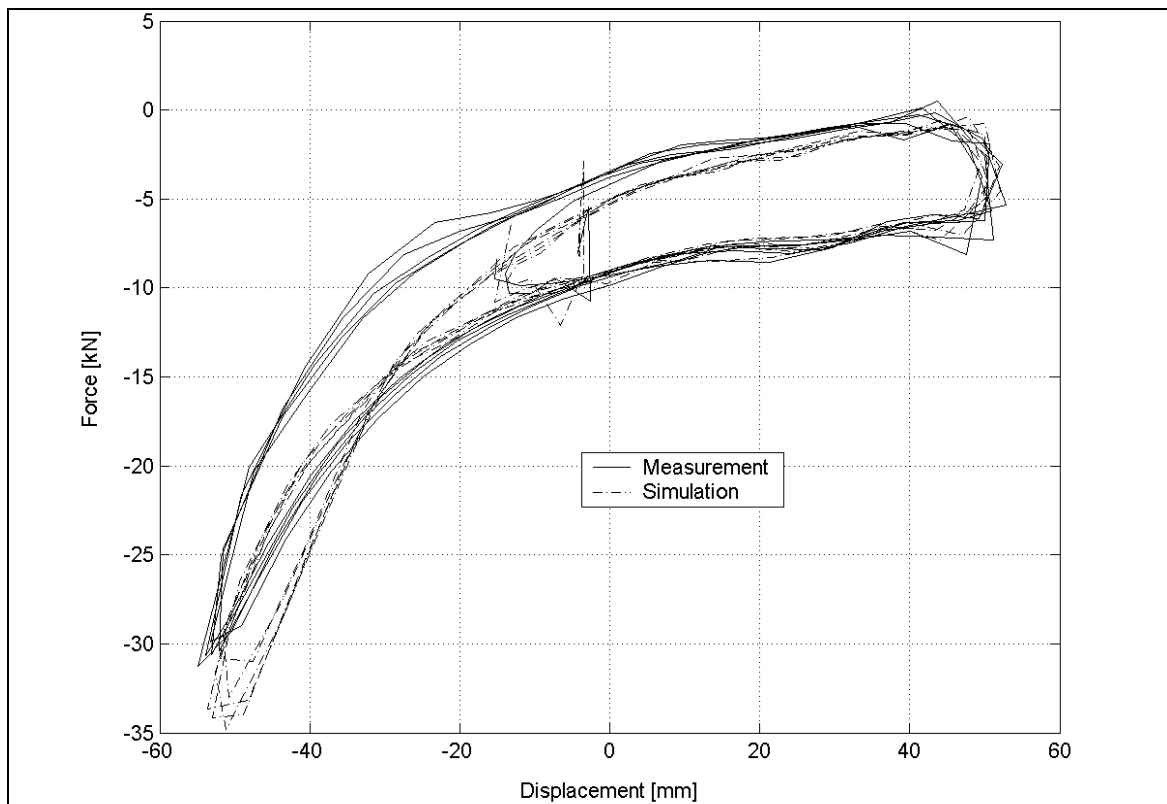


**Figure 4.41** – Comparison between measured and calculated force-displacement curve: stiff spring and low damping at high speed

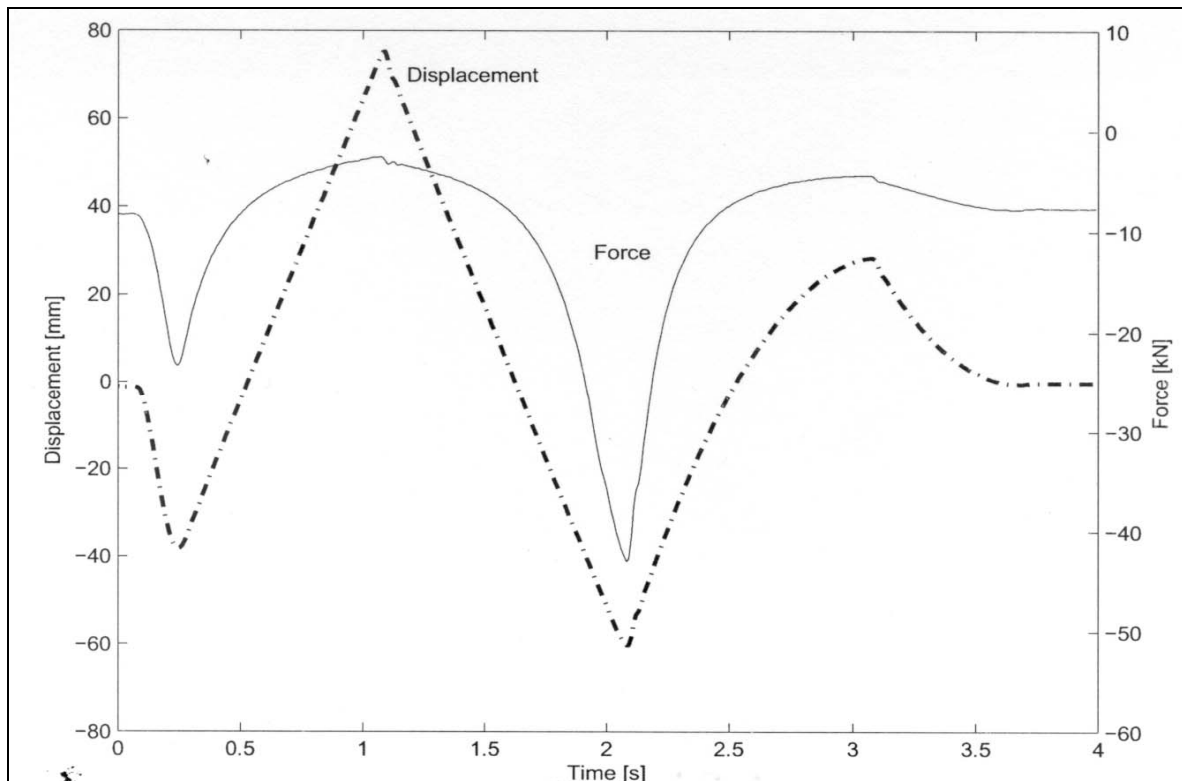


**Figure 4.42** – Measured input and output: stiff spring and low damping at high speed, larger displacement stroke

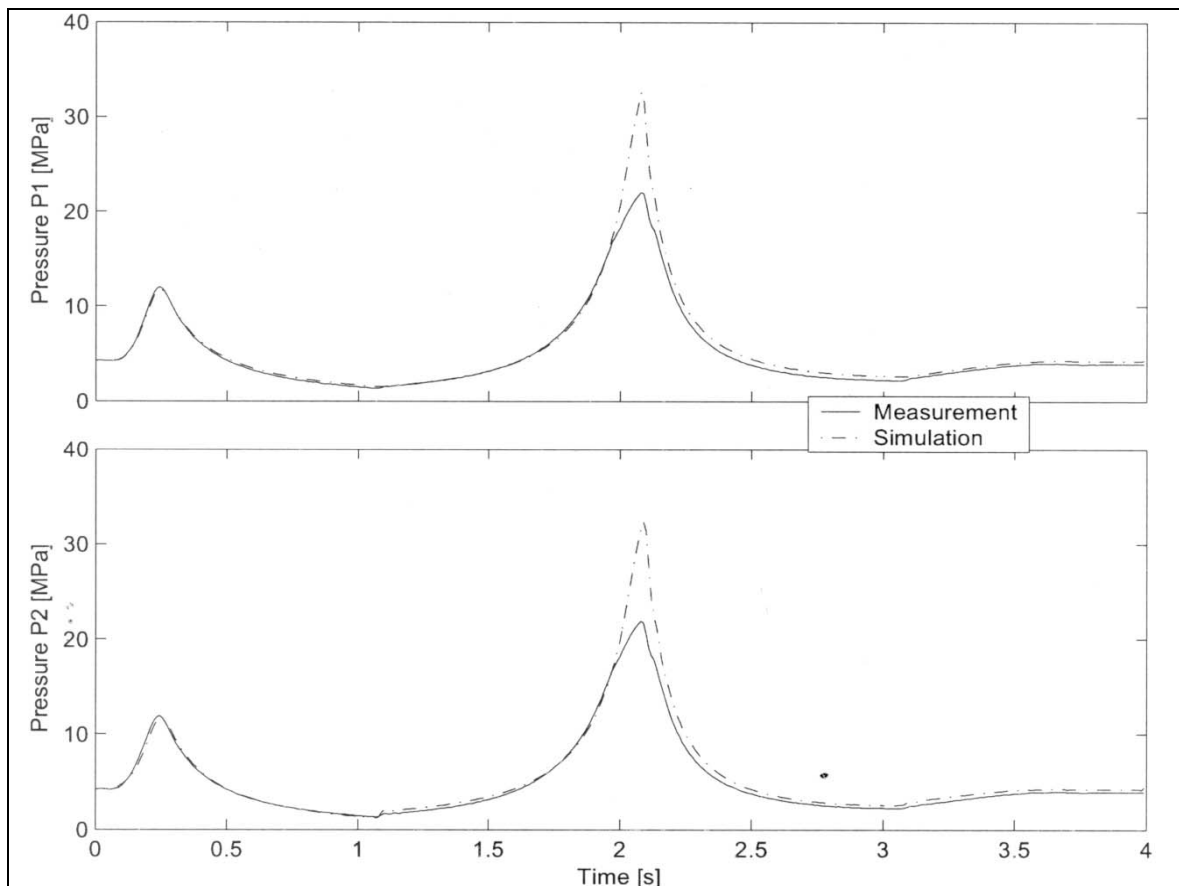


**Figure 4.43** – Comparison between measured and calculated values of  $P_1$  and  $P_2$ : stiff spring and low damping at high speed, larger displacement stroke

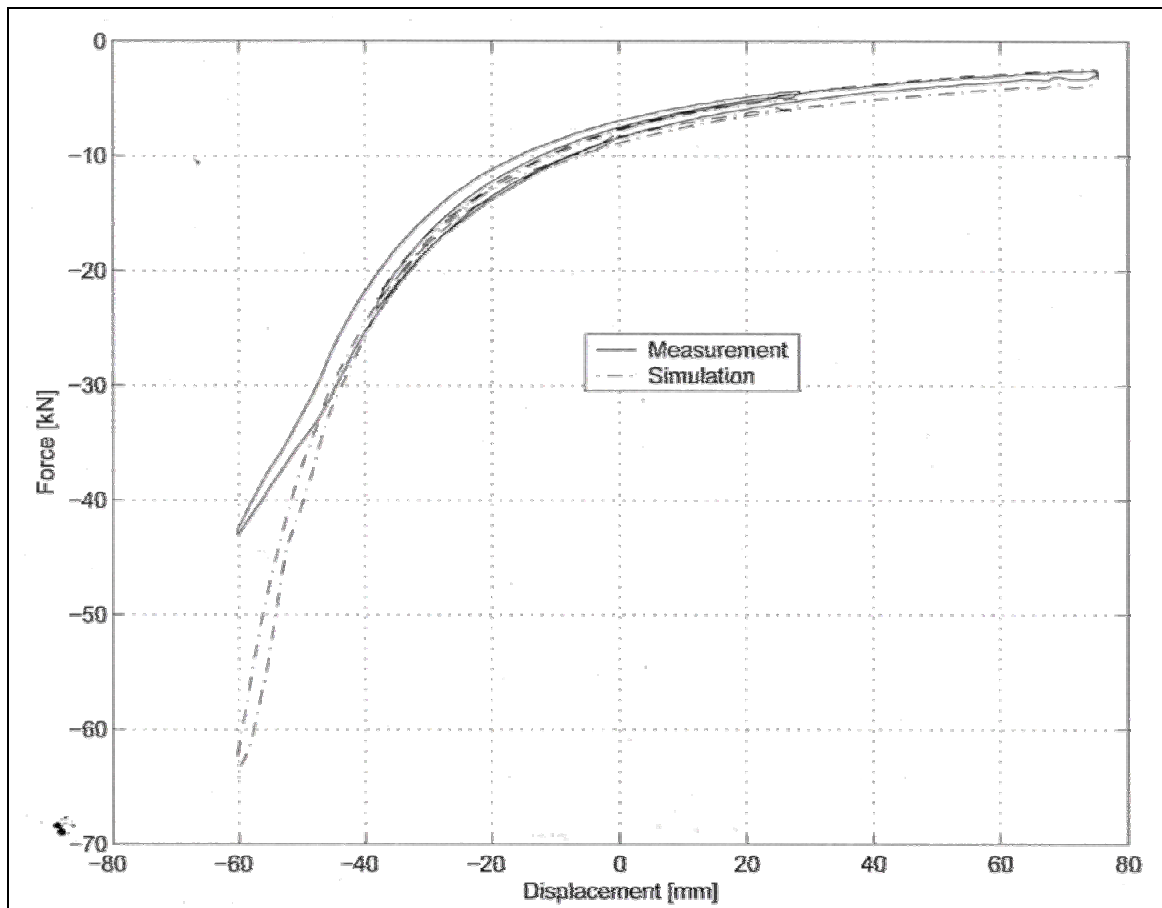


**Figure 4.44** – Comparison between measured and calculated force-displacement curve: stiff spring and low damping at high speed, larger displacement stroke

delay, the calculation and the measurement meet up again with good correlation until this is repeated in the next cycle. One possible explanation for this delay is that in the physical unit some boiling of the oil at low pressure occurs, a phenomenon that is not provided for in the SIMULINK model. Oil vapour caused by boiling and suspended in the oil is expected to cause a delay in pressure rise on compression. In this case, during the low-pressure part of the  $P_1$  cycle, the correlation between simulation and measurement is not as good as observed in the results discussed earlier. This may be related to the suspected boiling of the oil. The poor correlation in both the  $P_1$  and  $P_2$  results is not of serious concern, as the situation where the suspension unit is subjected to a prescribed high speed rebound that can cause  $P_2$  to drop to zero, even though easy to create on a test bench, is highly unlikely with the unit installed in a vehicle, even under rough road conditions. There is simply no downwards pull on the wheel available to cause such a condition. The force-displacement graph generated for this test is shown in Figure 4.47.

Whereas all the results discussed above pertain to stiff spring scenarios, with valve 3 closed, the more complicated part of the model corresponds to the soft spring scenario. Figure 4.48 shows input displacement and output force measured for a soft spring and low damping case, at low speed. Figure 4.49 shows the comparison of the measured and calculated time histories of the two accumulator pressures  $P_1$  and  $P_4$ , while Figure 4.50 shows the same for the pressures  $P_2$  and  $P_3$ . The force-displacement curve is shown in

Figure 4.51. In this case the gas volumes of accumulator 1 and 2 during the simulation were taken as 0.135 and 0.4 litres, respectively. Correlation is generally acceptable.

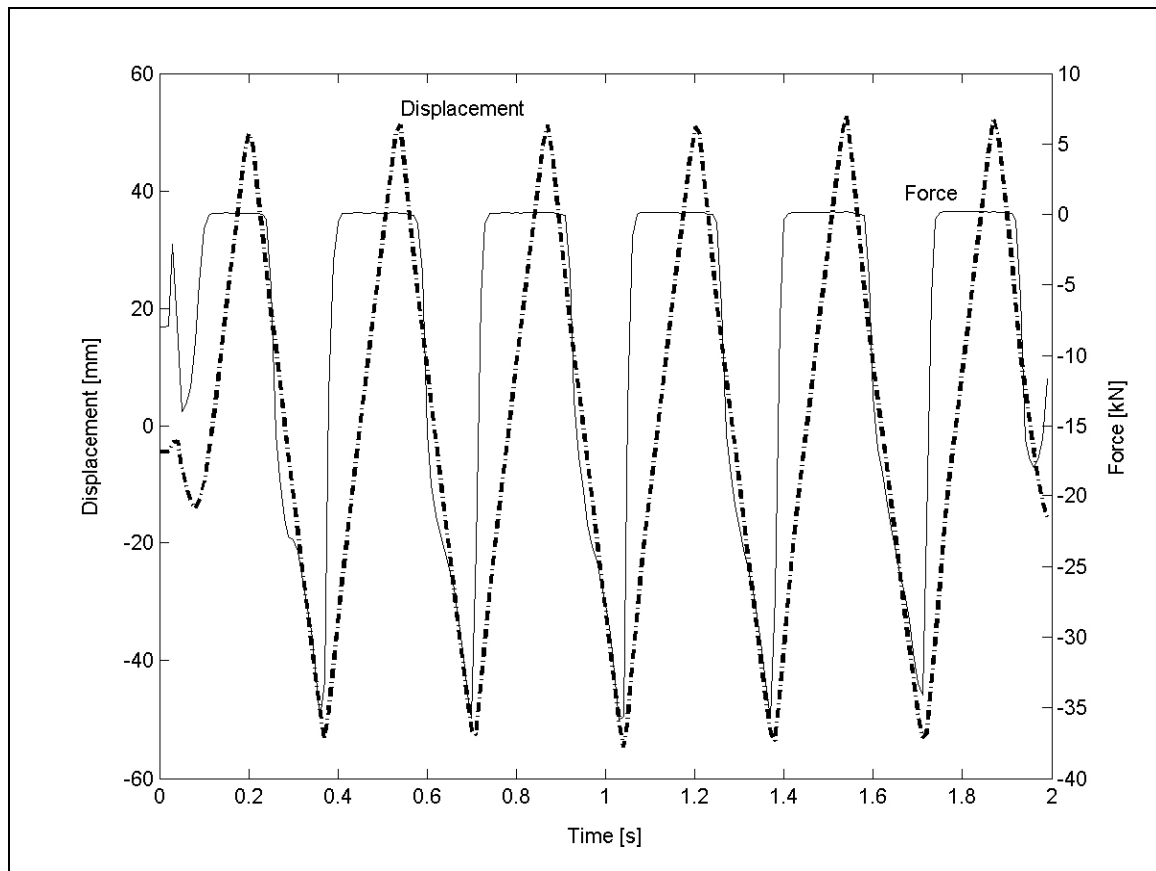


**Figure 4.45** – Measured input and output: stiff spring and high damping at high speed

Next the above test was repeated at high speed, the displacement input and measured force output shown in Figure 4.52. The comparison of the measured and calculated time histories of  $P_1$  and  $P_4$  for this case is shown in Figure 4.53 and that of  $P_2$  and  $P_3$  in Figure 4.54, with the force-displacement curve in Figure 4.55. Once again the correlation is generally acceptable.

Lastly, a test was performed on the suspension unit wherein it was compressed some distance in the stiff spring mode, then kept at this displacement for a while, after which valve 3 was opened and the pressures in the system allowed to equalize. Valve 3 was then closed again and the unit was then further compressed. This was repeated twice after which the unit was extended in a similar stepwise manner. This procedure, referred to herein as the incremental compression test, is well illustrated in Figure 4.56, which shows the time histories of the input displacement, the measured output force and the switch signal for valve 3. The switch signal is not plotted against a specific scale; it merely indicates when the valve is open (high) or closed (low). This whole test was conducted with a low damping setting. The measured and calculated time histories of the pressure in the two accumulators are shown in Figure 4.57, while the time histories of  $P_2$  and  $P_3$  are shown in Figure 4.58. In this case the gas volumes of accumulator 1 and 2 during the simulation were taken as 0.111 and 0.4 litres, respectively. The change in the volume of accumulator 1 may be justified by the fact that the suspension unit was emptied of both gas and oil, and then refilled, between this test and the test described earlier. With these

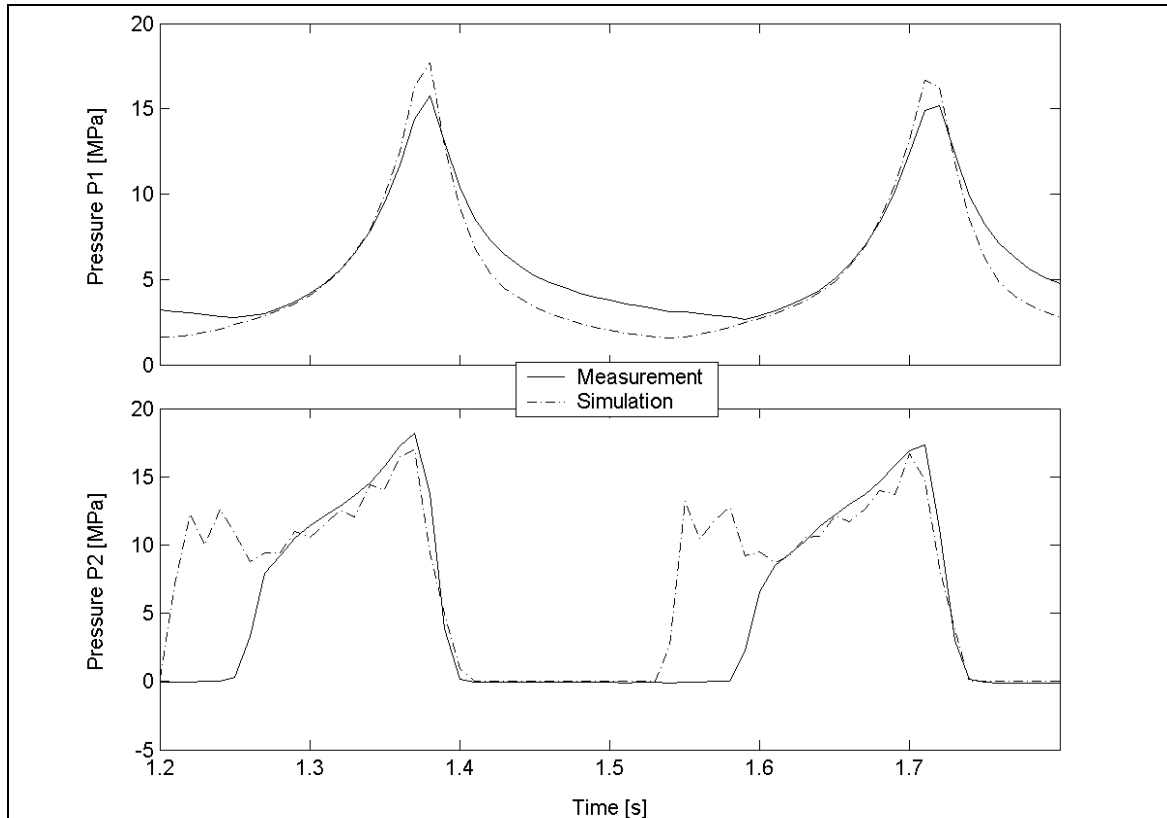


**Figure 4.46** - Comparison between measured and calculated values of  $P_1$  and  $P_2$ : stiff spring and high damping at high speed

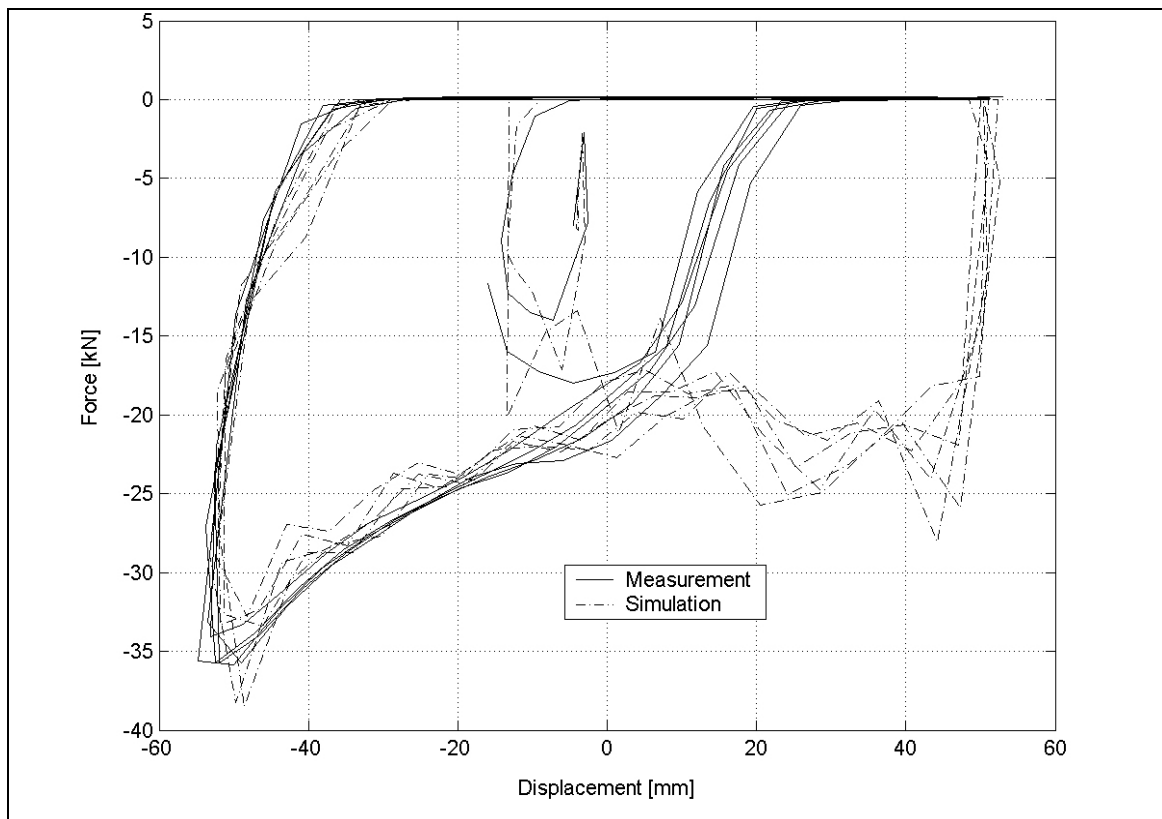


**Figure 4.47** – Comparison between measured and calculated force-displacement curve: stiff spring and high damping at high speed

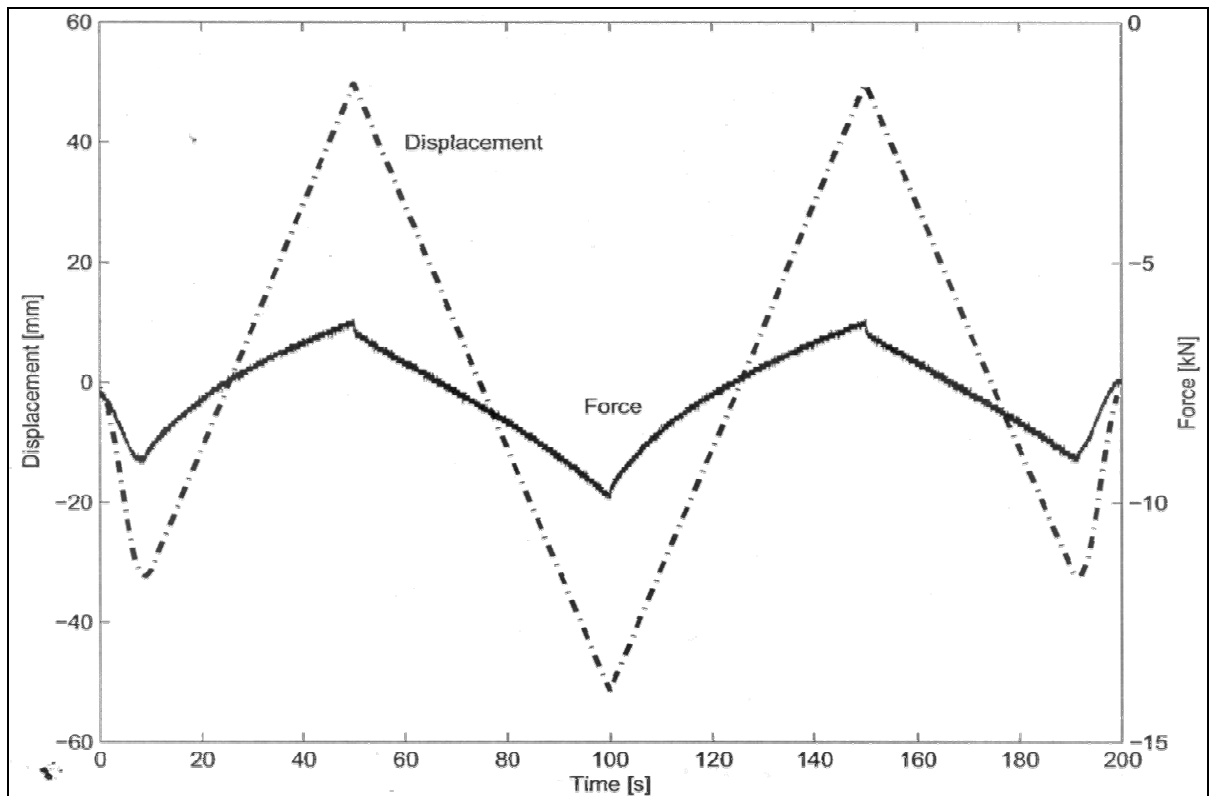


**Figure 4.48** - Measured input and output: soft spring and low damping at low speed

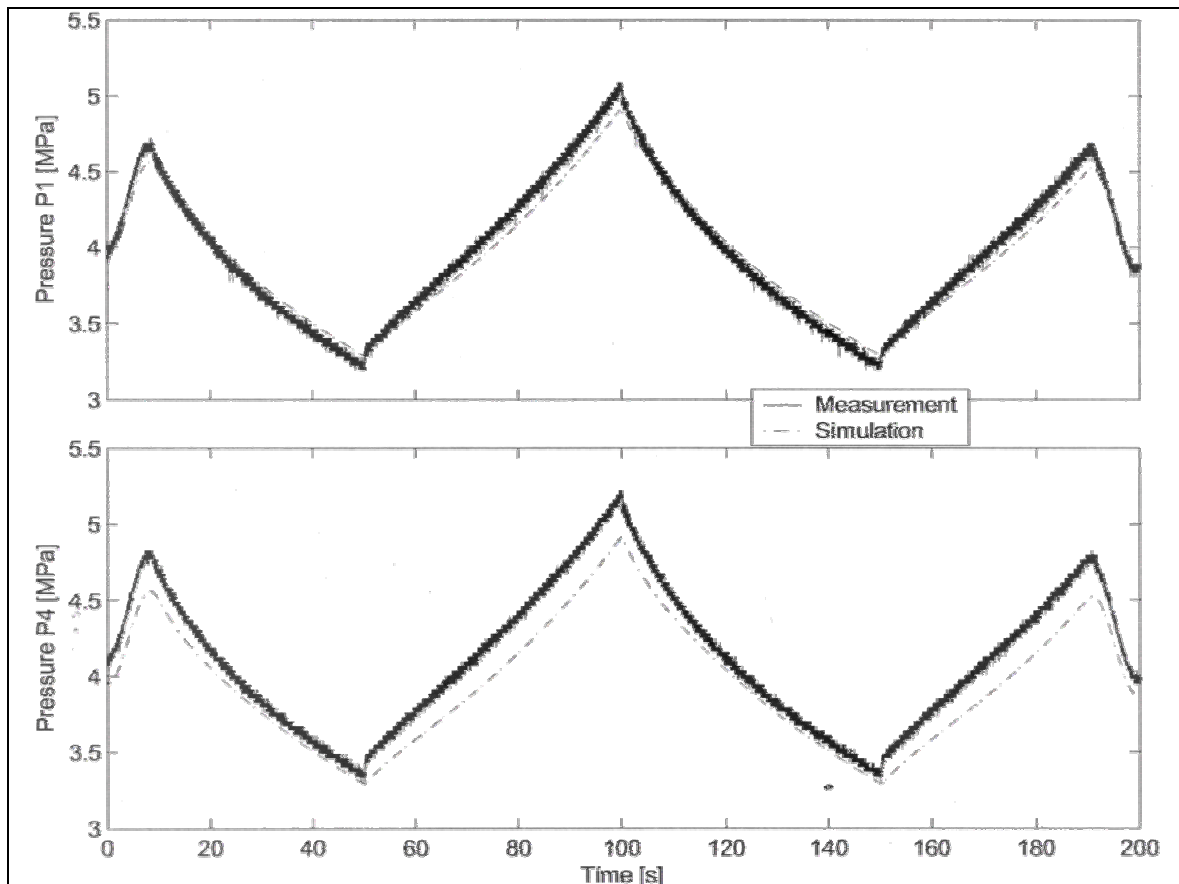


**Figure 4.49** – Comparison between measured and calculated values of  $P_1$  and  $P_4$ : soft spring and damping at low speed

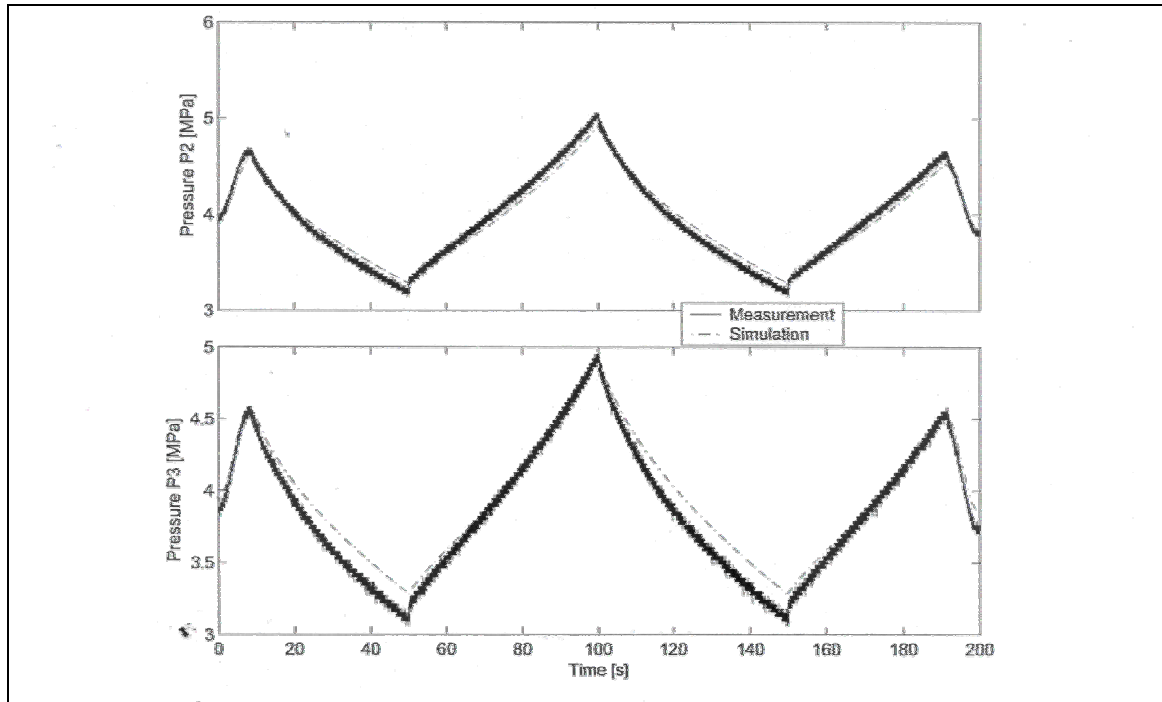


**Figure 4.50** – Comparison between measured and calculated values of  $P_2$  and  $P_3$ : soft spring and low damping at low speed

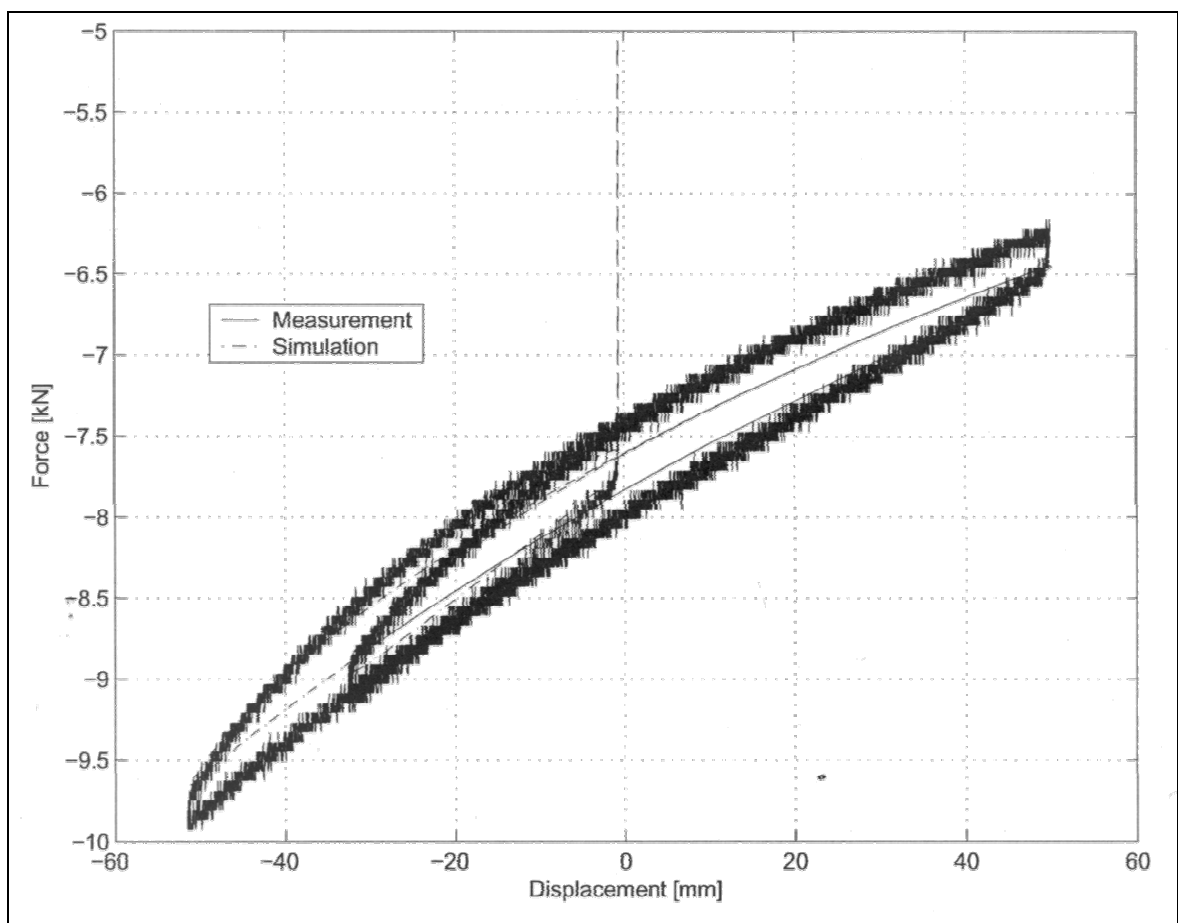


**Figure 4.51** - Comparison between measured and calculated force-displacement curve: soft spring and low damping at low speed

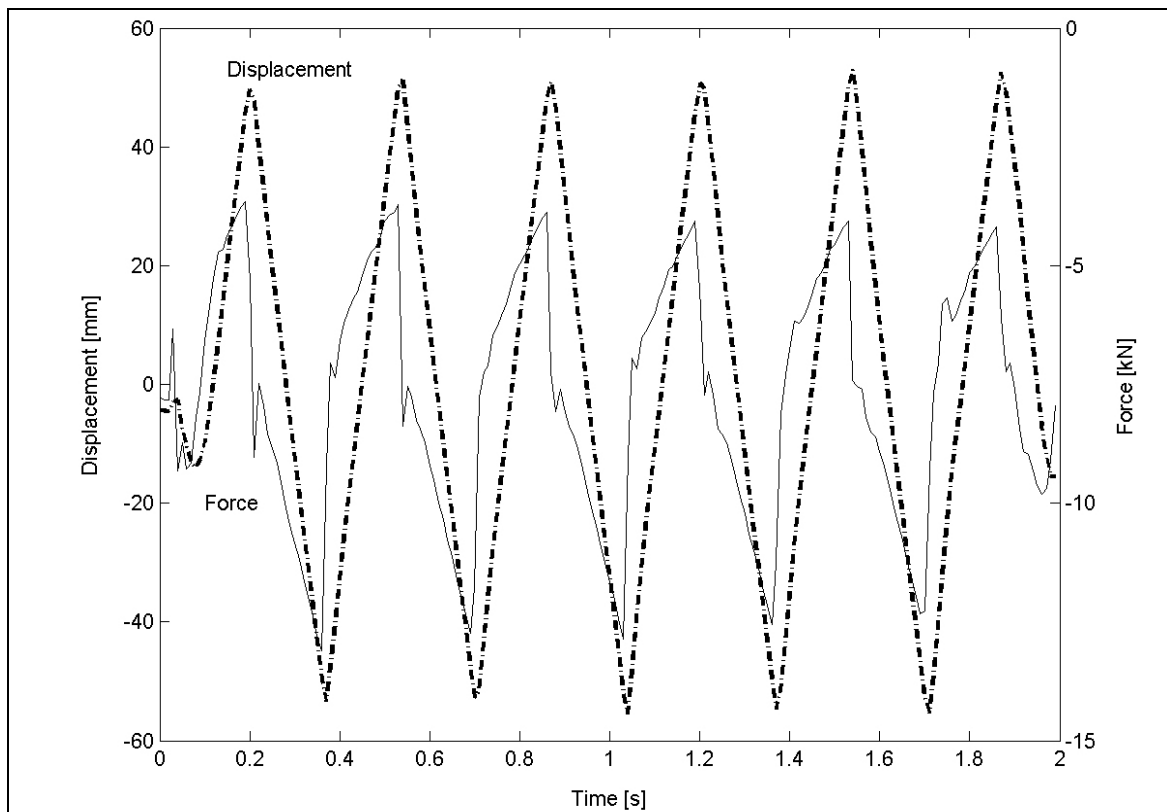


**Figure 4.52** - Measured input and output: soft spring and low damping at high speed

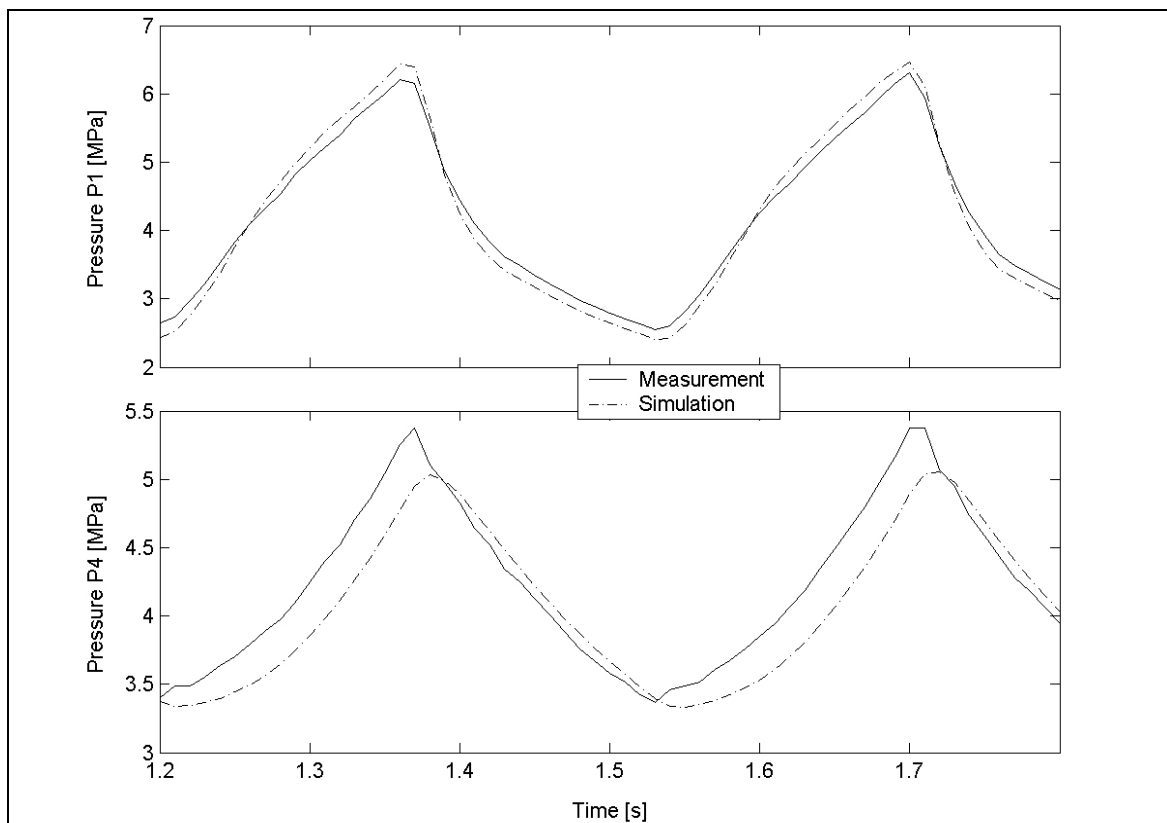


**Figure 4.53** – Comparison between measured and calculated values of  $P_1$  and  $P_4$ : soft spring and low damping at high speed



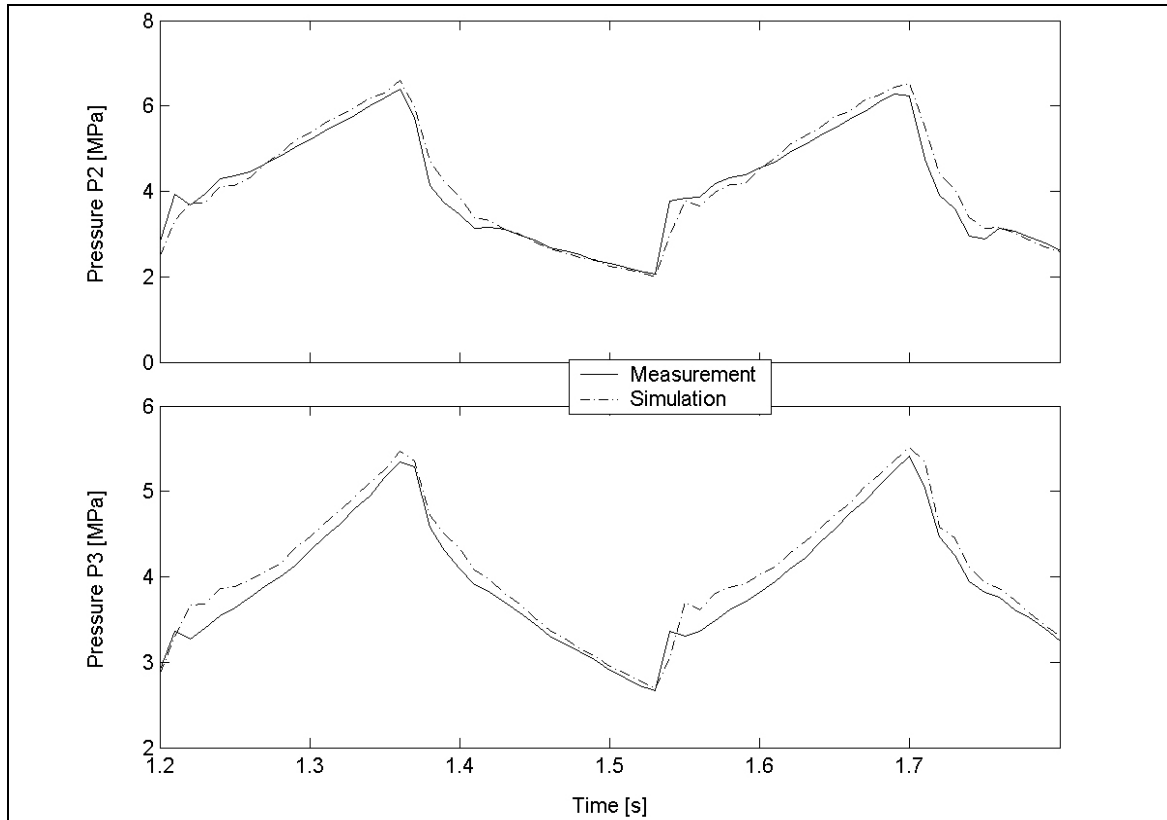


**Figure 4.54** – Comparison between measured and calculated values of  $P_2$  and  $P_3$ : soft spring and low damping at high speed

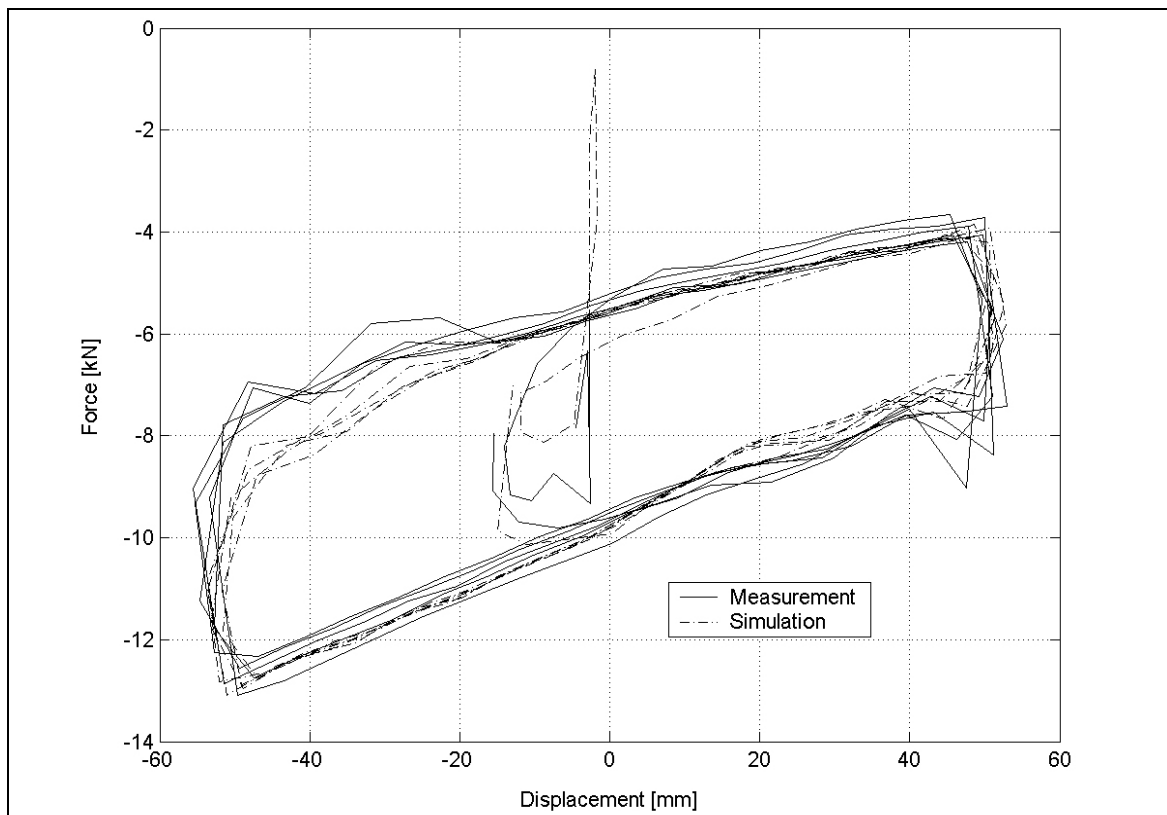


**Figure 4.55** – Comparison between measured and calculated force-displacement curve: soft spring and low damping at high speed

settings, the only correlation that does not seem good is that between the measured and calculated time histories of  $P_4$ . It should however be realized that while valve 3 is closed,  $P_3$  and  $P_4$  should practically be identical, as there is no flow through damper 2 or its by-pass valve. If the measured values of  $P_4$  and  $P_3$  from Figures 4.49 and 4.50 are compared, during the first second, when valve 3 is indeed closed, it is seen that the  $P_4$  pressure transducer reads a pressure slightly higher than the  $P_3$  transducer, by the same amount as the difference in the measured and calculated  $P_4$  values in Figure 4.57. If based on this observation it is assumed that an offset was present in the  $P_4$  measurement, the correlation between the measurement and the simulation result may be considered as very good. The measured and calculated force-displacement graphs for this test are shown in Figure 4.59. This figure also shows a very good correlation between measurement and simulation.

It is also worth noting that the slow drop in pressure  $P_1$  right after achieving the local peaks at the end of the compression strokes in Figure 4.57, just before valve 3 is opened, is predicted quite well by the model. Since the displacement input does not vary in this period, it is evident that the cooling of gas in accumulator 1 causes this pressure drop. This effect is captured adequately in the model by the use of equation (4.4).

Since the displacement of the suspension unit is not taken as an input in the mathematical model, it is necessary to check that the displacement of the unit that would be mandated by the solution of the differential equations like equation (4.2) does in fact correspond to the actual displacement experienced by the unit. During all the tests described in this section this was in fact checked and the correlation was exceptionally good. At this time it is proposed that a similar check should be incorporated in an implementation of the SIMULINK model within an ADAMS simulation of vehicle dynamics.

To date no measurement was done to specifically validate the way that the pressure dependent valve switching was implemented in the mathematical model.

## 4.9 Conclusion

A prototype four-state semi-active hydropneumatic spring-damper system (4S<sub>4</sub>) has been designed, manufactured, characterised on a test rig and modelled mathematically.

The design meets all the initial specifications and can be fitted to the proposed test vehicle without major modifications to the test vehicle.

The manufactured prototypes (Prototypes 1 and 2) have been extensively tested and characterised on a SCHENCK hydropulse actuator. Although several problems have been identified on Prototype 1, these have been addressed and eliminated on Prototype 2. Prototype 2 meets all the dynamic requirements.

A mathematical model of the suspension unit was developed and implemented in SIMULINK. Agreement between the model predictions and the measurements was generally good. Some aspects where the model or the quantifying of its parameters need improvement were identified. In particular, the tests to date clearly identified the need for an accurate method of quantifying the mass of gas loaded into the two accumulators.

Further work will be done on testing the model within simulations of a full vehicle equipped with these suspension units.

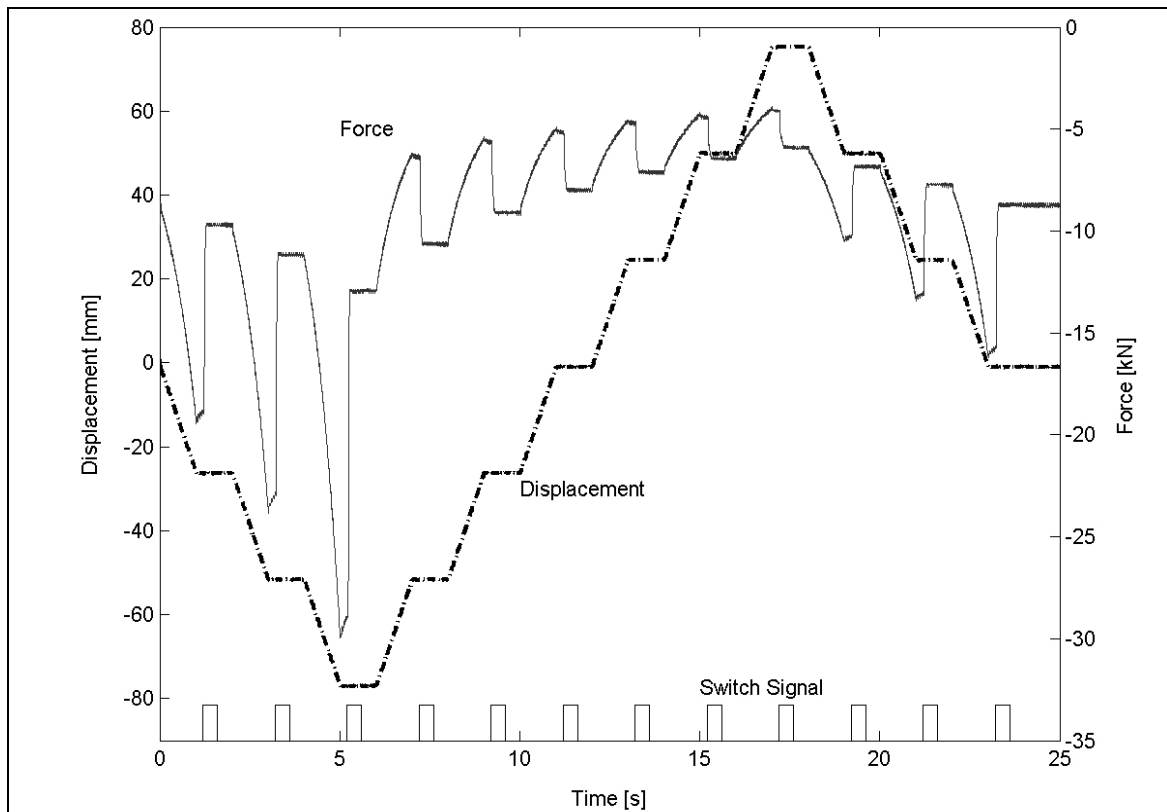


**Figure 4.56** – Measured input and output, and valve 3 switch signal: incremental compression test with low damping

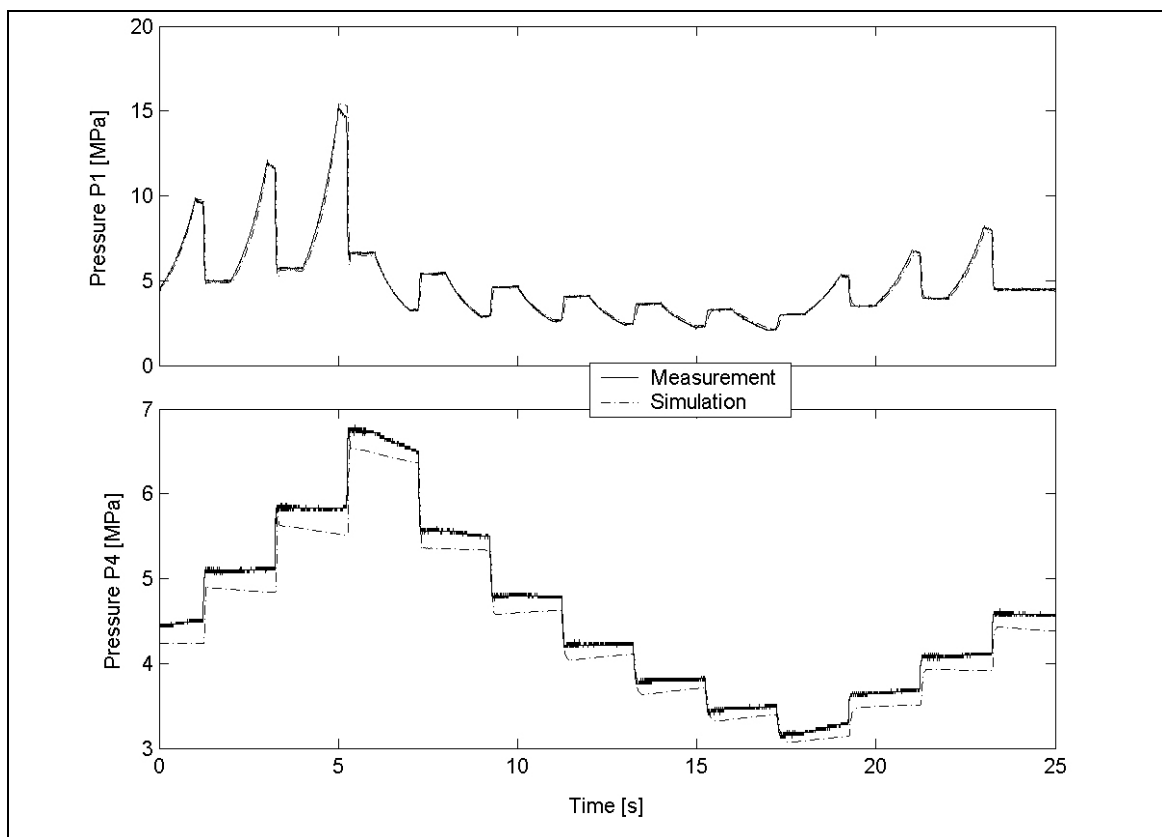


**Figure 4.57** – Comparison between measured and calculated values of  $P_1$  and  $P_4$ : incremental compression test with low damping

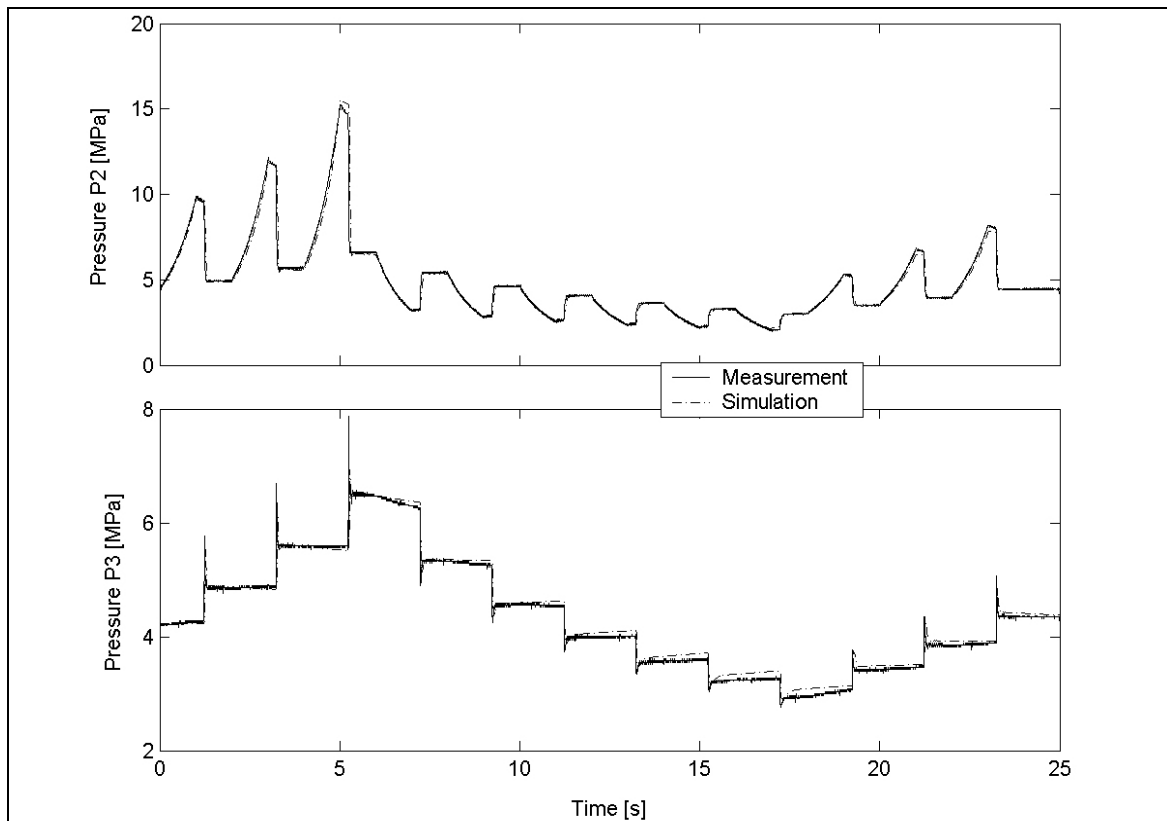


**Figure 4.58** – Comparison between measured and calculated values of  $P_2$  and  $P_3$ : incremental compression test with low damping

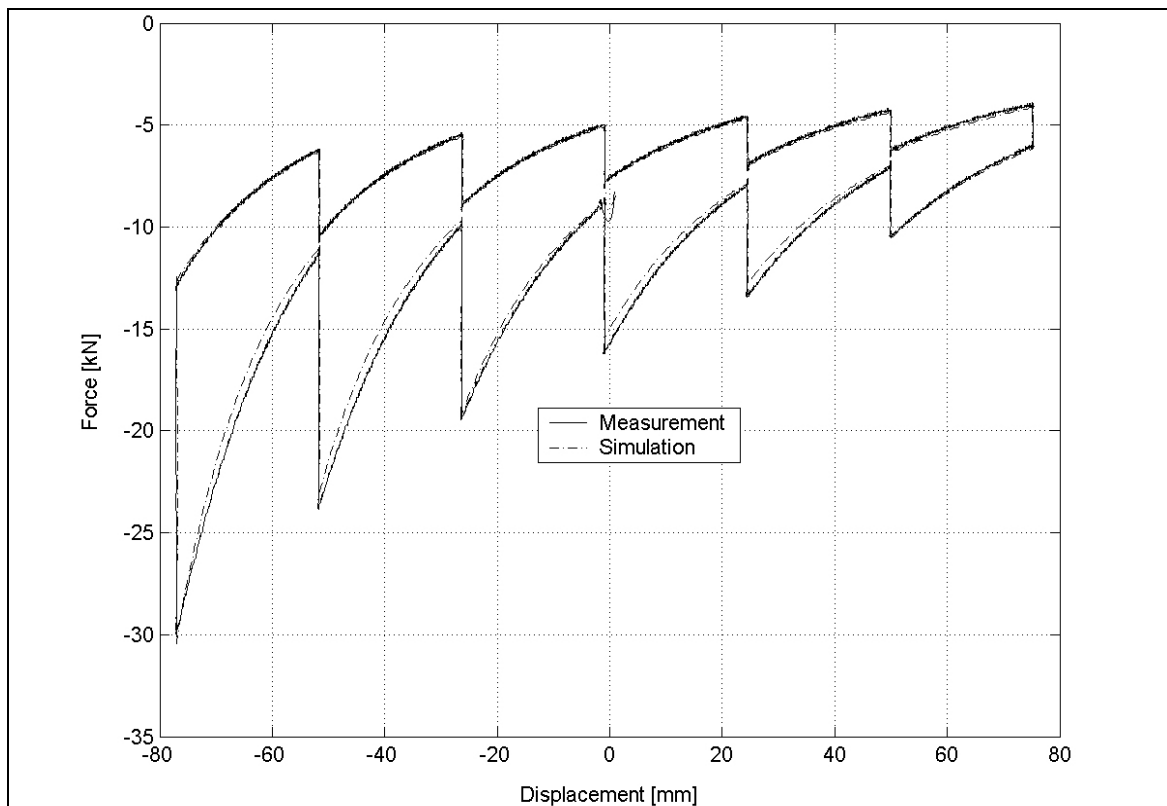


**Figure 4.59** – Comparison between measured and calculated force-displacement curve: incremental compression test

---

---

### ***THE RIDE COMFORT VS. HANDLING DECISION***

---

---

This chapter describes and analyses various methodologies that can be used to make the decision whether the suspension should be set to “ride comfort mode” or “handling mode”. This is referred to as the “**ride comfort vs. handling decision**”. It does not attempt to discuss or investigate possible control strategies for ride comfort and/or handling respectively. It rather assumes that these characteristics and control methods are known, *i.e.* that a set of “optimal” suspension characteristics and/or control laws exist for both ride comfort and handling. These two sets of conditions are in conflict as described in chapter 2. The importance of the ride comfort *vs.* handling decision cannot be overemphasized, as it is a safety critical decision. If the suspension system for example switches to the “ride comfort” mode during a severe handling or accident avoidance manoeuvre, the consequences might be severe and loss of control or rollover might result.

For the purposes of this study, the 4S<sub>4</sub> will be switched to the soft spring and low damping characteristics when ride comfort is required and will switch to high damping and the stiff spring when handling is required. The effects of ride height on ride comfort and handling is excluded from the analysis. All the analyses will be made with the suspension set to the same ride height as the baseline suspension system. Effects caused by acceleration (*e.g.* squat) or braking (*e.g.* dive) are neglected at present. Figure 5.1 indicates where the ride comfort *vs.* handling decision fits into the study.

The aim of the present chapter is to find a strategy that uses parameters that can be measured directly, or otherwise easily calculated from direct measurements. This excludes the use of state estimators, integrators and artificial intelligence techniques such as neural networks.

No literature was found that is directly applicable to the ride comfort *vs.* handling decision as applied to off-road vehicles or controllable springs, although some of the concepts proposed by different authors are worth exploring and will be discussed now.

#### **5.1 Literature**

**Stone and Cebon (2002)** investigate semi-active roll control of a heavy vehicle. They make use of a system where an anti-rollbar is connected to the vehicle body with hydraulic cylinders providing switchable roll stiffness. The anti-rollbar can either be “free” (*i.e.* transmit little force) or “locked” (*i.e.* provides high roll stiffness). The low roll stiffness is intended for use when the lateral forces on the vehicle are small, thus providing good ride comfort. When large lateral forces are present, the system is switched

to higher roll stiffness to improve handling. The vertical bounce stiffness of the suspension system is therefore unaffected. Although only a preliminary analysis is performed, the authors differentiate between a case where the lateral acceleration builds up slowly (general driving) and a case where rapid increases in lateral acceleration takes place (avoidance manoeuvres). For a rapid increase in lateral acceleration, using a **lateral acceleration threshold as control input** seems reasonable if control system delays are small. For the case of a slowly increasing lateral acceleration, a more sophisticated control strategy (*e.g.* one that uses steering inputs) might be beneficial.

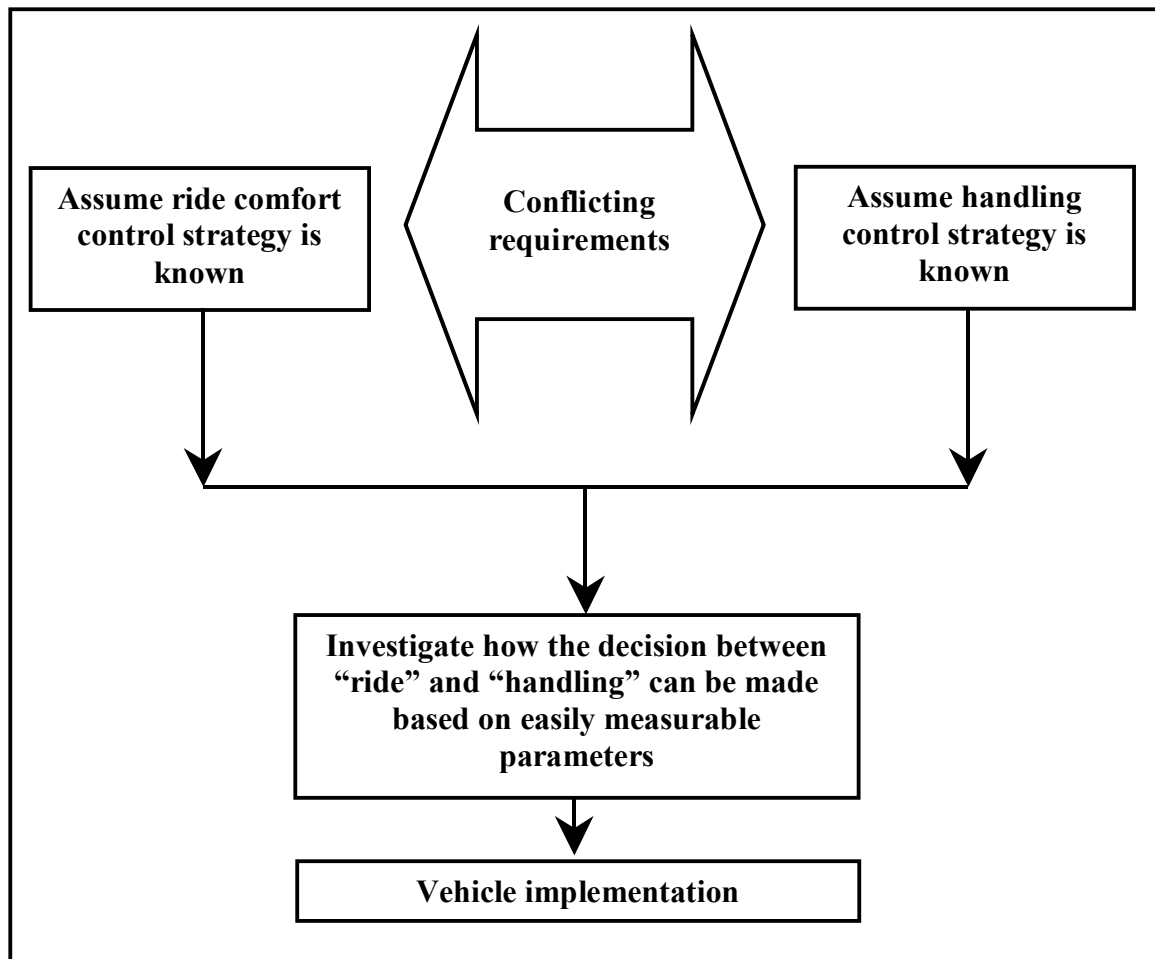


**Figure 5.1** - The ride comfort vs. handling decision

**Jost (2002a)** describes the Continental Teve's four-corner air suspension with continuously variable semi-active damper control fitted to the Volkswagen Phaeton. The system adjusts damping force on each wheel within 10 to 15 milliseconds and automatically adjusts vehicle height. The system uses wheel acceleration sensors on the shock absorbers as well as body movement sensors (two at the front and one at the rear). Other inputs include data from the engine management, brake and electronic stability control systems. The system can recognise when the driver is steering into a curve. The driver can select between four fixed damper settings ranging from soft to sporty or firm. The control system will however temporarily override these settings when handling manoeuvres are encountered.

**Nell (1993)** and **Nell and Steyn (1998)** develop a general strategy for the control of two-state semi-active dampers in an off-road vehicle suspension system. Nell focussed on a

full vehicle model taking all degrees of freedom into account instead of looking at each wheel separately. He defines suspension control as a “decision making” problem. The damper is switched to the high damping state whenever handling is required and controlled using a “minimum product” strategy whenever ride comfort takes preference. Roll movement over rough terrain is caused by suspension forces whereas lateral acceleration causes roll movement during handling manoeuvres on smooth roads. The ride comfort vs. handling strategy needs to differentiate between these two conditions. Nell measures and compares lateral and vertical acceleration on the centre of the (rigid) front axle. If this lateral acceleration is greater than the vertical acceleration, the handling mode (all dampers switched to high damping) is selected; otherwise the “minimum product” strategy is used to improve ride comfort.

**Nell and Steyn (2003)** apply the same basic idea to another off-road vehicle, in this case using measurements from two solid-state gyroscopes and two accelerometers as inputs to the control system. The control strategy is said to be a derivative of the method proposed by **Nell and Steyn (1998)**. It switches the two-state semi-active dampers to the conditions that will provide the highest accelerations opposing the motion of the sprung mass, or the lowest acceleration in the same direction. The relative damper velocities and absolute sprung mass velocity are no longer required. Handling is improved over the baseline vehicle by changing the “on” characteristic of the semi-active damper.

**Darling and Hickson (1998)** investigate the effect of an active anti-rollbar on the handling of a vehicle. They aim for a “flat” ride *e.g.* no body roll. They state that, although steering angle and vehicle speed can be used as control inputs, this relationship can vary significantly due to differences in tyre-road friction. They therefore make use of a lateral accelerometer mounted on the vehicle body in front of the centre of mass to measure a combination of lateral and yaw acceleration. A simple PID controller was implemented and the gains were optimised by a process of trial and error vehicle tests.

An electronic modulated air suspension system, as fitted to the 1986 Toyota Soarer is described by **Hirose et. al. (1988)**. The system is said to control spring rate, damping force and height with a response time of 70 milliseconds. There are three control steps namely: i) detection of vehicle travelling conditions, ii) classification of travelling conditions into one of several preset patterns, iii) adjust suspension parameters according to selected pattern. Sensors include three height sensors (left front, right front and left rear), steering angle sensor, throttle position, stop lamp switch and mode select switch. Vehicle height is detected in 16 steps between maximum and minimum height. Vehicle height is lowered if the vehicle speed exceeds 90 km/h and only increased again once vehicle speed drops to below 60 km/h resulting in a hysteresis of 30 km/h. On rough roads, height is increased above 40 km/h and only decreased again below 25 km/h to eliminate bump stop contact. Rough road conditions are detected by the left front wheel displacement using an observation duration of 0.5 seconds (half the sprung mass natural period). If the displacement measured during the observation duration exceeds a reference value four times in succession, ride height is increased. The detection period for changing ride height is 20 seconds to eliminate frequent ride height changes due to cornering for example. Spring and damper rates are changed simultaneously on all four wheels. Control of spring and damper settings are performed by either predictive control (see Table 5.1) or tracking control (see Table 5.2)

**Table 5.1** – Predictive control as implemented by **Hirose *et. al.* (1988)**

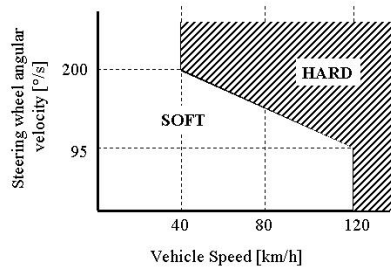
Situation	Sensor	Purpose
Anti-dive	Speed sensor Stop lamp switch	Suspension is changed to harder setting to restrict attitude change before the attitude change begins
Anti-roll	Speed sensor Steering sensor	
Anti-squat	Speed sensor Throttle position sensor	
Anti-bump	Speed sensor Height sensor	Irregularity of roads is detected by vertical movement of the front wheels and suspension is changed softer before the rear wheels pass through the detected irregularity to reduce shock

**Table 5.2** - Tracking control as implemented by **Hirose *et. al.* (1988)**

Situation	Sensor	Purpose
Response to speed	Speed sensor	Suspension is set harder to improve travelling stability at high speed cruising. Since speed change is gradual, tracking control has satisfactory effect
Response to rough road	Speed sensor Height sensor	Suspension is set harder to restrict pitching and bouncing on rough road

A very similar system, fitted by Mitsubishi, is described by **Mizuguchi *et. al.* (1984)**. The suspension consists of air springs used in conjunction with coil springs and semi-active dampers. Sensors for vehicle speed, steering wheel angular speed, sprung mass acceleration (lateral, longitudinal and vertical), throttle speed and suspension stroke is used. Apart from ride height control, the suspension system can be switched from soft to hard quickly whenever any of the conditions in Table 5.3 are satisfied. The hard setting increases spring stiffness by approximately 50% and damping by 150%. The soft state is restored after 2 seconds in the hard state.

**Table 5.3** – Strategy used by **Mizuguchi *et. al.* (1984)**

Case	Item	Sensor	Conditions
1	Vehicle speed	Vehicle speed	Soft to hard above 120 km/h Hard to soft below 110 km/h 10 km/h hysteresis
2	Steering speed	Steering wheel angular velocity	
3	Sprung mass acceleration	Acceleration sensor	Longitudinal acceleration: over 0.3g Lateral acceleration: over 0.5g Vertical acceleration: over 1g
4	Throttle speed	Throttle position sensor	Throttle wire moving speed: *over 0.25 m/s when accelerating *over 0.5 m/s when decelerating (with vehicle speed $\geq$ 3 km/h)
5	Front suspension displacement	Displacement sensor	Highest and lowest positions



**Wallentowitz and Holdmann (1997)** propose a frequency based control algorithm that generates high damping only when the vehicle is excited in the vicinity of the natural frequencies. They also propose a strategy where the vertical movement of each wheel is controlled individually, but with an overlying controller for roll and pitch movements. The spring must be switched to the stiff mode during braking and cornering to reduce roll and pitch angles. The soft spring is said to be only beneficial for frequencies lower than 5 Hz. No simulation or test results are given for the proposed controller.

Armstrong Patents Company Limited of York developed a practical intelligent damping system described by **Hine and Pearce (1988)**. The system consists of two or three state adaptive dampers combined with an auxiliary air spring to provide ride height control. Measurements indicate that reducing the damper setting below standard greatly improves vibration isolation at frequencies above 2 Hz, while higher than normal settings reduces the amount of motion around 1 Hz (roll *etc.*) The aim of the control strategy is to keep the damper in the lowest setting as long as possible and only switch to higher levels when required. Switching typically takes place in 12 milliseconds. The system has sensors for suspension movement, steering wheel angular velocity, vehicle speed, brake application and wheel or body acceleration. The control strategy is separated into a number of components namely:

- i) Ride: Ride control is initiated by the relative suspension displacement and vehicle speed using displacement maps. If the displacement exceeds a pre-programmed limit for the specific vehicle speed, higher damping will be selected. For returning to the lower damper setting, the valves have been designed to delay until the pressure is below a preset limit to reduce hydraulic noise.
- ii) Handling (including roll control): Handling is detected based on steering wheel speed and vehicle speed. Roll information, obtained from the suspension displacement sensors, is then used to switch back to the lower damper settings shortly after the vehicle returns to the level position.
- iii) Acceleration: Information from the vehicle speed sensor is used to determine the acceleration. Damper rate is increased when acceleration exceeds a pre-defined level.
- iv) Deceleration (Dive): Information from the brake and speed sensors is used to immediately switch the dampers to the hard setting. The system returns to the softer setting once the longitudinal acceleration drops to below a preset level.
- v) Ride frequency control and vehicle levelling: Levelling compensates for changes in payload and aerodynamics.

The system was implemented on a 1986 model GM Corvette (5.7 litre) as well as a Ford Granada 2.8 Ghia. The improvements in ride comfort and handling is however not quantified.

An active suspension control approach that consists of an inner loop that rejects terrain disturbances, an outer loop that stabilises heave, pitch and roll response and an input decoupling transformation that blends the inner and outer control loops is proposed by **Ikenaga *et. al.* (2000)**. The ride control loop isolates the car body from uneven terrain while the attitude control loop maintains load levelling and load distribution during handling manoeuvres. Skyhook damping (the term used to describe the feedback of absolute sprung mass heave, pitch and roll velocities) improves heave, pitch and roll accelerations at all frequencies below the wheel frequency.

**Truscott (1994)** develops a composite controller for a high bandwidth (35 Hz) fully active suspension system. Only simulation results for a linear quarter car suspension system are presented. The proposed composite controller consists of two controllers operating together, but over different frequency ranges. The first controller cancels out low frequency dynamic loads experienced during cornering and braking, keeping the vehicle level. This controller operates at frequencies below 5 Hz. The second controller isolates the car from high frequency terrain induced vibration and operates at frequencies above 5 Hz. The vibration controller is fully adaptive and auto-tunes the system according to varying payload, tyre stiffness and varying road frequency spectrum. The 5 Hz frequency was chosen to be between the sprung mass and wheel-hop frequencies.

**Trent and Greene (2002)** propose a model-based genetic algorithm predictor to estimate the potential for rollover. The tyre deflection that will result in vehicle rollover approximately 50 time steps in future is calculated assuming all other operating conditions such as vehicle speed remain constant. Advanced rollover warning of 400 milliseconds may be possible, giving enough time for an intelligent suspension system or stability control (differential braking) system to react and decrease the rollover propensity.

Active roll control, as developed by TRW, is discussed by **Böcker and Neuking (2001)**. The system uses hydraulic cylinders fitted to the anti-rollbars. Figure 5.2 indicates the functioning of the control system schematically. Sensors include steering angle, lateral acceleration, hydraulic system pressure and vehicle speed.

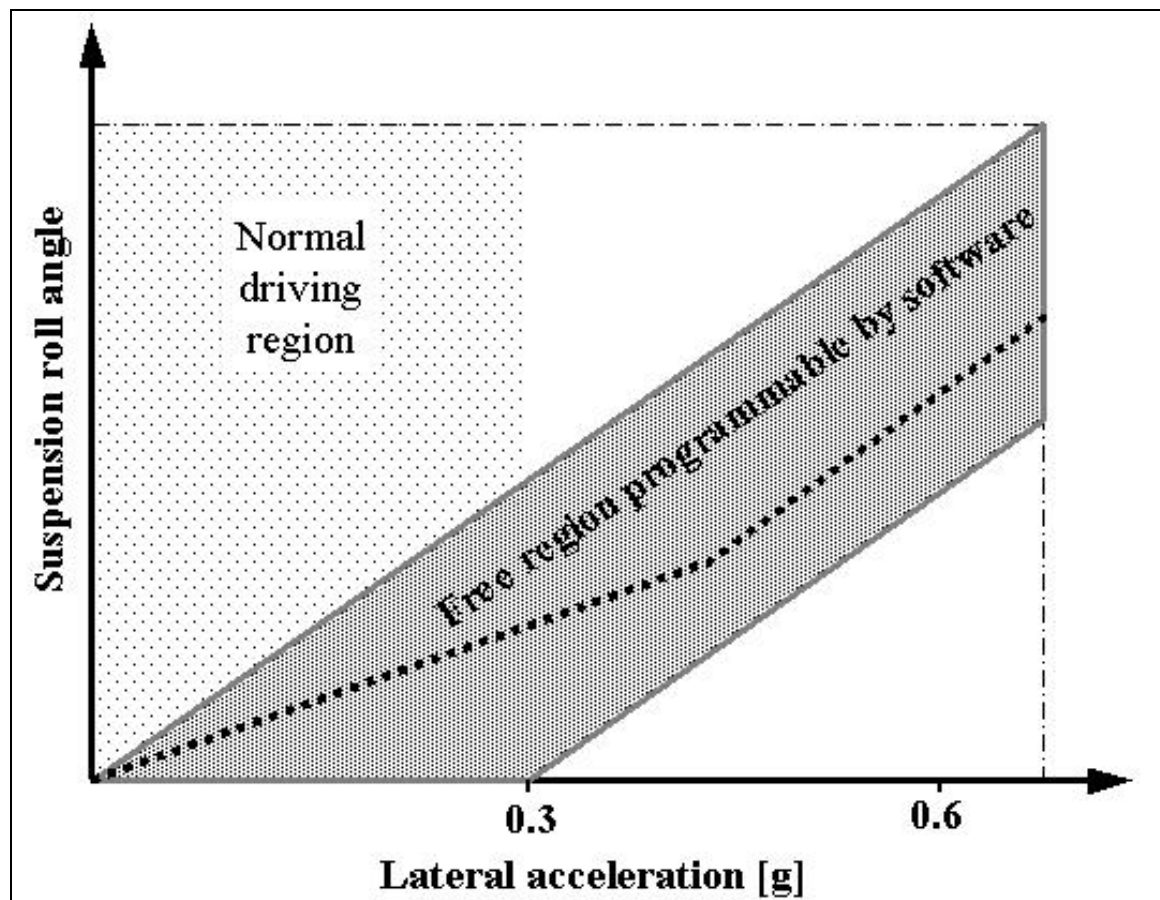


**Figure 5.2** – TRW’s active roll control system according to **Böcker and Neuking (2001)**

**Hamilton (1985)** defines many general aspects for the theoretical operation of controllable suspension systems. No simulation or test results are given although prototype hardware was available. The proposed system consists of the following components:

- i) *Ideal damping device*: must instantly provide the damping force required by the computer independent of suspension position or velocity.
- ii) *Ideal energy storage device*: must be capable of changing its energy storage capacity to a value demanded by the computer.
- iii) *Ideal computer controller*: must have all the necessary inputs to calculate all required parameters.

The ideal theory of operation also consists of many aspects namely:

- i) *Optimised ride comfort*: requires a very soft spring and virtually no damping force. Some force is required to control the kinetic energy of the wheel.
- ii) *Cornering*: The centrifugal force on the vehicle's centre of gravity causes a torque on the sprung mass, about the roll centre, that can be counteracted by the damping device by applying equal forces in the opposite direction.
- iii) *Ideal pitch control*: Attempt to maintain a level ride during acceleration or braking by looking at the change in pitch height.
- iv) *Ideal level ride control*: This is required to compensate for substantial variations in the loading condition of the vehicle. Height control can also be used to decrease the frontal area of the vehicle during high speed driving or to increase ride height over rough terrain.
- v) *Ideal roll control*: e.g. on a mountain road. Can be based on the difference in height between the sprung mass and the road surface on the left and right hand side of the car.
- vi) *Ideal natural frequency control*: Observe the two primary natural frequencies (sprung and unsprung mass) using a Discrete Fourier Transform (DFT) and control each one of them separately.
- vii) *Ideal high amplitude or high velocity control*: Road inputs that exceed the dynamic range of the suspension require forces to be applied to the sprung mass to move it up and over the obstacle. The magnitude of these forces should be such that the suspension movement limits are never exceeded.

Not all forces acting on the sprung mass can be totally eliminated. The system should aim to minimise them while optimally controlling vehicle movements within the suspension working space. There are many counteracting forces that are required simultaneously and these must be superimposed to control all the dynamics simultaneously.

The concept is to apply these forces when required and keep them as small as possible to ensure good ride comfort. The author states that only relative suspension movements need to be measured as all the other required parameters can easily be calculated from these.

The Mercedes-Benz Active Body Control (ABC) is described by **Birch (1999)**. The system was introduced on the CL Coupe and adapts both spring and damper characteristics to prevailing conditions. A hydraulic system (called a "plunger") acts on the coil spring to change the preload on the spring. The stiffness remains unchanged. The hydraulic system acts up to a frequency of 5 Hz thereby improving vehicle response to long wavelength road inputs as well as during braking and cornering. Anti-rollbars are not

necessary and the system is also self-levelling. The driver can select sport and comfort settings.

A detailed description of the Citroën Hydractive I, II and III is beyond the scope of this text, but is described in substantial detail by **Nastasić and Jahn (2005)**. The control principles employed are however relevant to the ride vs. handling decision. The basic idea is to map different vehicle parameters against vehicle speed. Figure 5.3 indicates the steering wheel angle threshold as a function of vehicle speed. The suspension is switched to the handling mode whenever the measured steering wheel angle exceeds the threshold at a certain speed. The driver can select one of two different threshold levels by selecting a “normal” or “sport” mode with a switch. The steering wheel velocity threshold (Figure 5.4) exhibits a similar trend and operates on the same principle. At low vehicle speeds, large steering wheel angles and velocities are allowed *e.g.* during parking manoeuvres. As the vehicle speed increases the threshold levels become smaller, resulting in faster reaction times.

Body dive and squat (Figure 5.5) is determined by measuring the relative displacement of the front and rear suspension respectively. Threshold levels also decrease as vehicle speed increases. The accelerator pedal press and release rate is also used (Figures 5.6 and 5.7) to reduce squat and pitch during hard acceleration. Slow release of the accelerator pedal indicates that the driver desires to reduce speed gradually whilst a sudden release will often be followed by hard braking to quickly reduce speed. Dive and squat effects are further ignored for the present study.

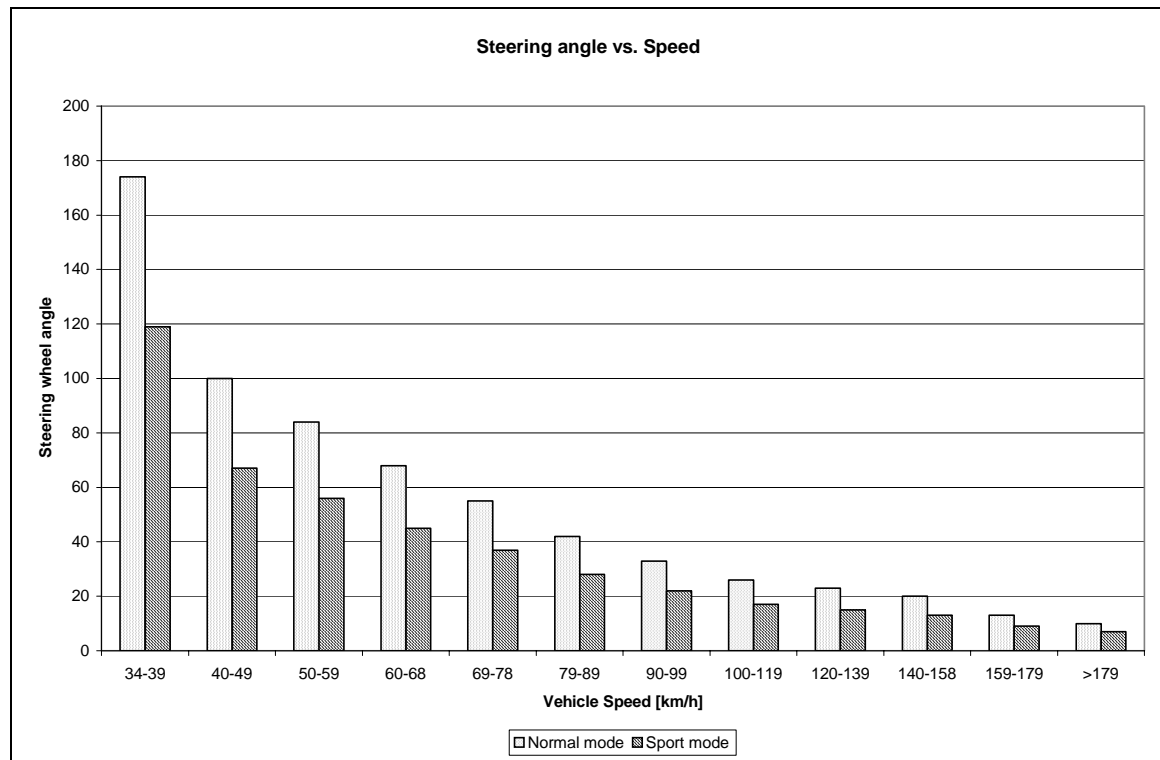


**Figure 5.3** – Steering wheel angle vs. vehicle speed

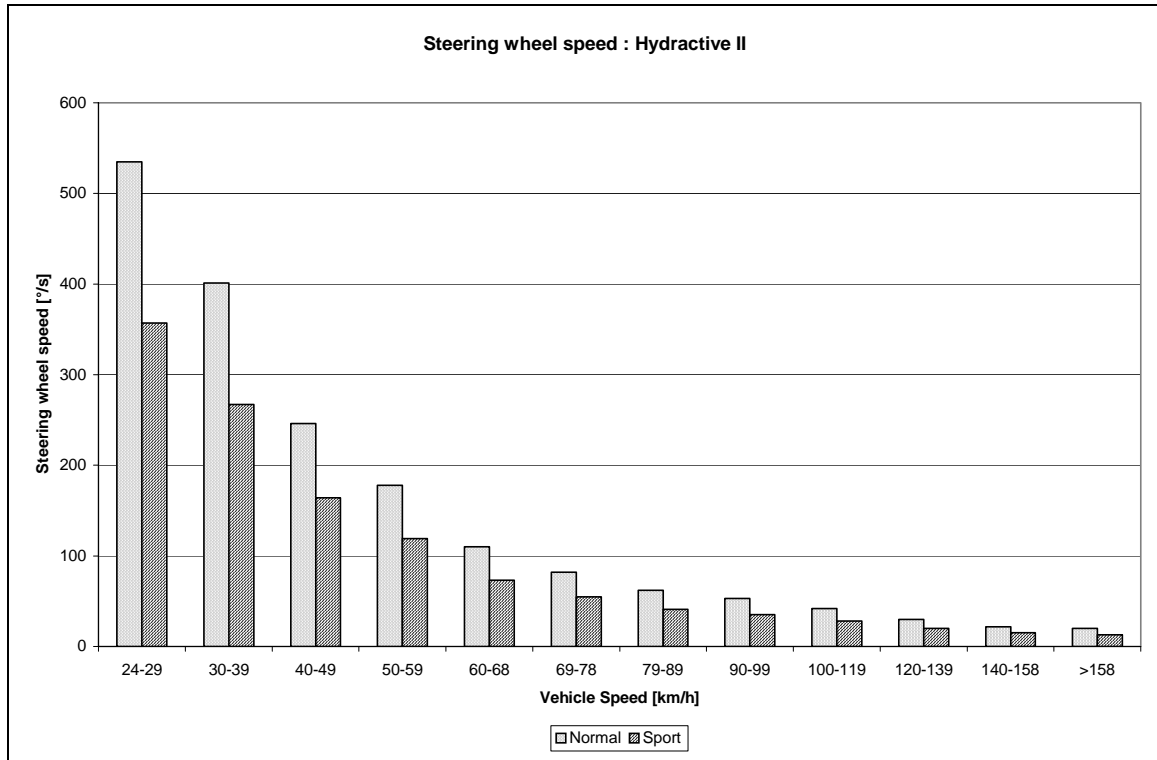


Figure 5.4 – Steering wheel rotation speed vs. vehicle speed

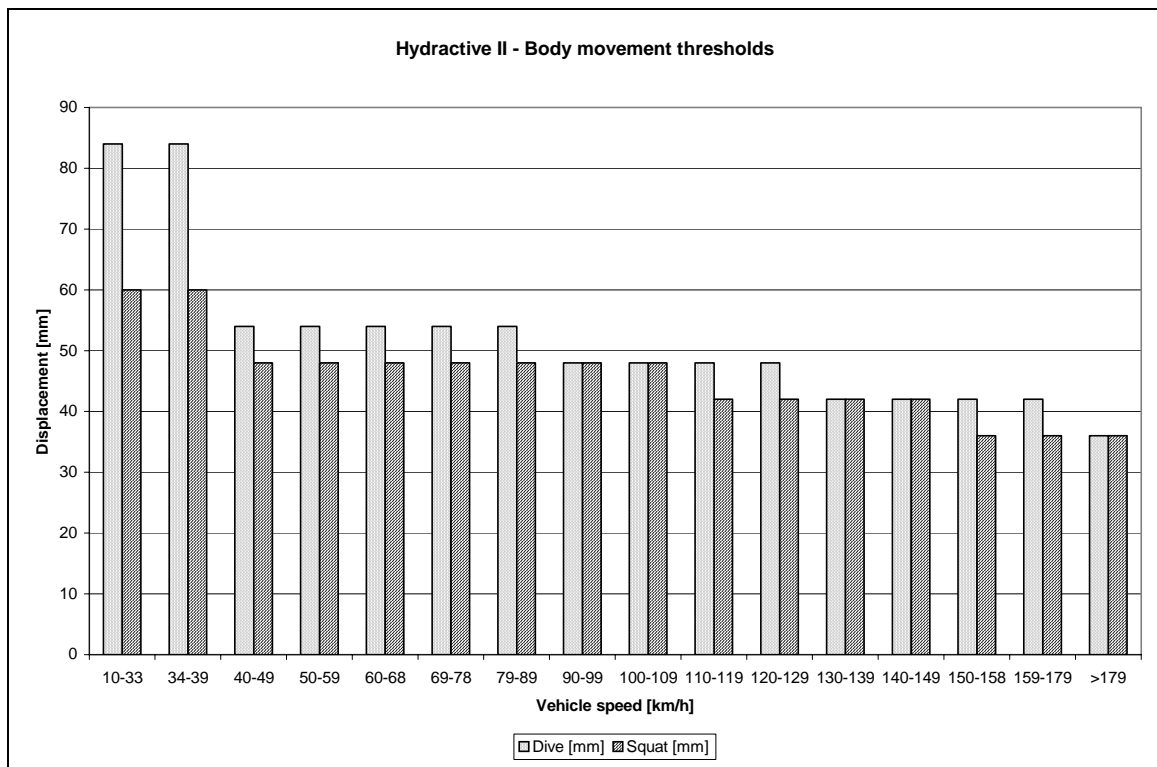


Figure 5.5 – Dive and squat vs. vehicle speed

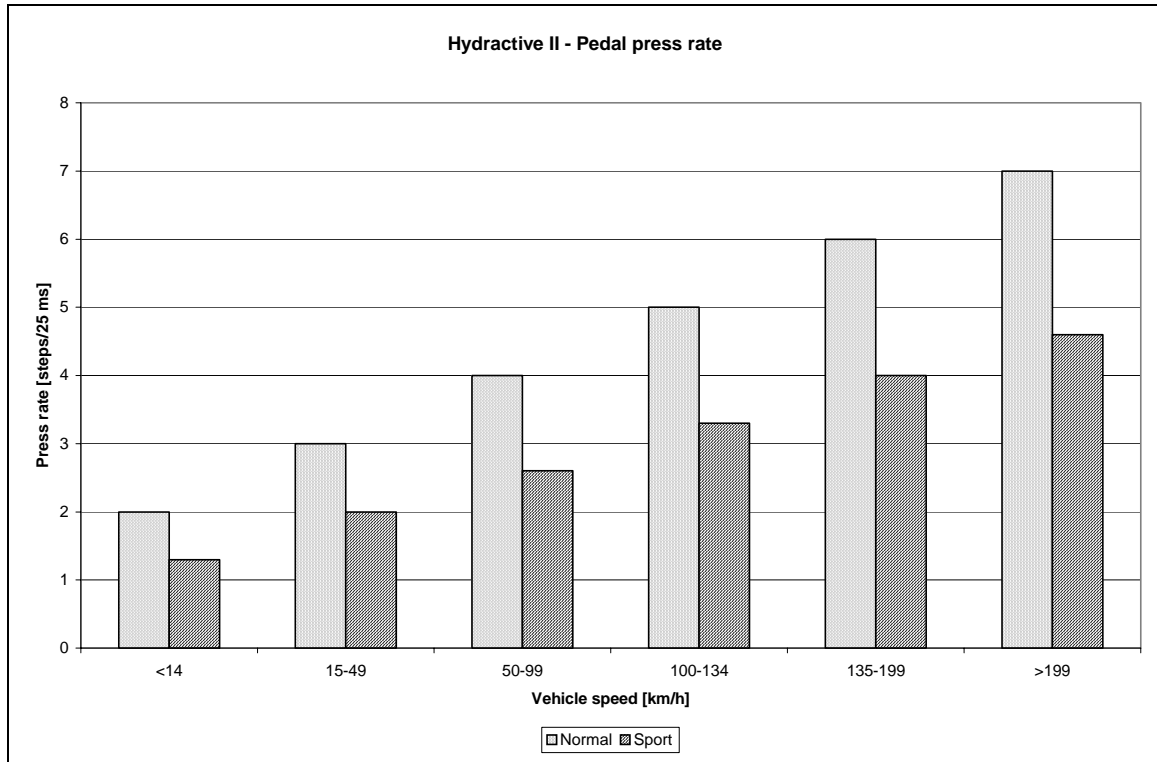


Figure 5.6 – Accelerator pedal press rate vs. vehicle speed

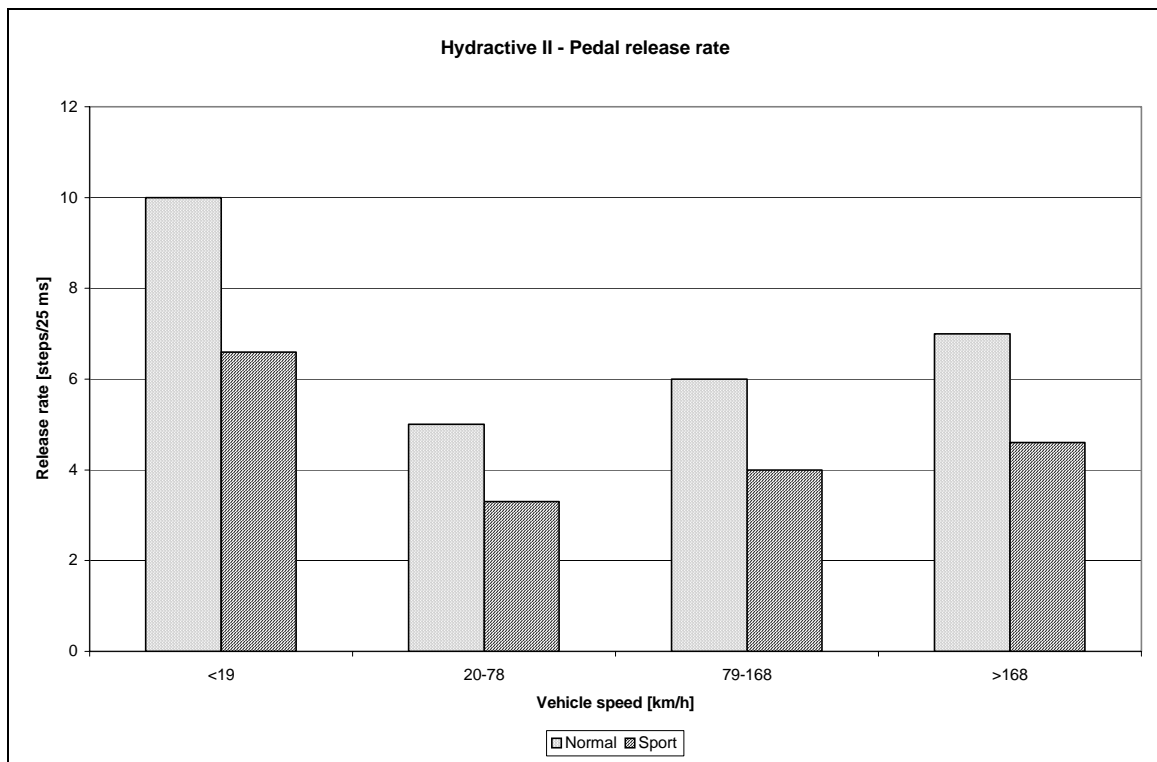


Figure 5.7 - Accelerator pedal release rate vs. vehicle speed

Interactive vehicle dynamics control on the 2000 Ford Focus is discussed by Broge (1999). Although not controlling the suspension system of the car, the general concept may be applicable to the current study. Several parameters measured on the vehicle are

compared to a dynamic handling map stored in the on-board computer. When any vehicle parameter deviates from the stored map, corrective action is taken by reducing engine power and braking appropriate wheels. Sensors include individual wheel speeds, steering wheel movement, yaw rate sensors and lateral accelerometers.

## 5.2 Suggested concepts for making the “ride comfort vs. handling decision”

From the literature discussed in paragraph 5.1, several concepts have been identified to assist in making the “ride comfort vs. handling decision”. These concepts are listed in Table 5.4 and will be investigated further in paragraph 5.5. It is important to note that the majority of the applications discussed so far are related to road vehicles. Substantial differences might be required for off-road driving.

**Table 5.4** – Suggested concepts for assisting with the “ride vs. handling” decision

Concept no.	Measurement parameters	Reference
1	Frequency analysis of acceleration	Wallentowitz and Holdman (1997) Truscott (1994)
2	Lateral acceleration vs. vertical acceleration	Nell (1993) Nell and Steyn (1998)
3	Steering angle vs. speed	Hirose <i>et. al.</i> (1988) Hine and Pearce (1988) Nastasic and Jahn (2005) Broge (1999)
4	Pitch and roll velocity / acceleration	Nell and Steyn (2003)
5	Height, throttle position, brake application, mode select switch	Hirose <i>et. al.</i> (1988) Hine and Pearce (1988) Nastasic and Jahn (2005) Broge (1999)
6	Lateral acceleration	Stone and Cebon (2002) Daling and Hickson (1998)

## 5.3 Easily measurable parameters

At the outset of this study, the decision was made to try and find a strategy that uses parameters that can be measured directly, or otherwise easily calculated from direct measurements. This therefore excludes the use of state estimators, integrators and artificial intelligence techniques such as neural networks. This decision was made based on several factors namely:

- This is the first study focussed on the “ride comfort vs. handling decision” for off-road vehicles
- No previous concepts or algorithms seem to exist
- Attempting to keep it as simple as possible and only as complicated as necessary
- The current focus is on a more fundamental understanding of the issues involved
- It is important to keep the cost of the sensors and control system within the project budget
- The “controller” to be used was a personal computer based system with an analog to digital converter card and a digital input-output card fitted. This excluded the use of digital signal processing (DSP) cards.

The parameters identified to be easily and directly measurable are listed in Table 5.5 while Table 5.6 lists parameters that can be easily calculated from the directly measured parameters. Displacement measurements can be differentiated with respect to time to give

velocities. Although differentiation tends to add high-frequency noise, we are primarily interested in the low-frequency content of the velocity and good results can be achieved using simple mathematics and low-pass filters. Integration is also possible in theory, but creates many obstacles in practice due to the effect of drift. Small offsets in the zero reading of a sensor (*e.g.* accelerometer) can cause the integrated value to quickly drift to the limits. Because we are primarily interested in the low-frequency content, it is very difficult to control drift by for example high-pass filtering. The signal offsets are often influenced by effects such as change in temperature or attitude changes of the vehicle body due to varying load and road conditions. Absolute body movements can presently only be calculated by integrating acceleration signals twice. Absolute body movements are thus not easily measured directly, or calculated, and are therefore excluded at present.

**Table 5.5** – Directly measurable parameters

No	Parameter	Position	Equipment
1	Vehicle speed	Roof	Global positioning system (GPS)
2	Relative displacement	Every suspension position	Rope displacement transducer
3	Angular velocity (roll, yaw, pitch)	Vehicle body	Solid state gyroscope
4	Relative displacement	Steering arm between axle and body	Rope displacement transducer
5	Acceleration	Vehicle body	Solid state accelerometer $\pm 4g$ range
6	Kingpin steer angle	Kingpin	Potensiometer
7	Wheel speed	Any wheel	Optical speed sensor
8	Driveshaft speed	Gearbox output rear	Optical speed sensor

**Table 5.6** – Parameters that can be easily calculated from measurements

No	Parameter
1	Relative suspension velocities
2	Relative angles between vehicle body and suspension components
3	Relative angular velocities
4	Angular accelerations

#### 5.4 Experimental work on baseline vehicle

A test sequence, consisting of six different test routes and manoeuvres, was devised to be representative of the Land Rover Defender 110 vehicle's typical application profile. Tests were performed at representative speeds. For city and highway driving, tests were performed in and around the city of Pretoria. All other tests were performed at the Gerotek Vehicle Test Facility West of Pretoria. The legal speed limit was adhered to on all public roads. For off-road driving, the speed was determined by the driver's judgement of ride comfort while on the mountain pass the speed was limited either by vehicle performance on the steep uphill slopes or by handling around the corners. For the handling and rollover tests the speed constraint was the vehicle's handling combined with the driver's ability. The chosen test routes are summarised in Table 5.7 with the plan layouts of the test routes and tracks indicated in Figures 5.8 to 5.12.

It was also postulated that an objective vehicle parameter (*e.g.* lateral acceleration) might be correlated with an objective human physiologic parameter (*e.g.* heart rate or blood pressure). A series of tests were performed where heart rate and blood pressure was measured for both driver and passengers in attempt to obtain a correlation between vehicle parameters and change in heart rate. A total of 85 test subjects were used for the



physiological measurements. Although very interesting trends were noticed, no correlation could be found between the measured physiological parameters and vehicle parameters.

**Table 5.7** – Chosen tests and test routes

Test	Driving conditions	Test route	Driver	Duration [s]	Figure
1	City driving	Start: corner Dely & High (point 2) End: corner Rigel & Buffelsdrift (point 3)	Normal	704	5.8
2	Highway driving	Start: Fountains circle (point 4) End: corner Lynnwood & Kiepersol (point 5)	Normal	783	5.8
3	Off-road	Top 800m of Gerotek Rough Track	Normal	166	5.10
4	Mountain pass	Gerotek Ride & Handling Track - clockwise	Experienced	268	5.11
5	Handling	ISO 3888 Severe double lane change test	Experienced	13.4	5.12
6	Rollover	Fishhook rollover simulation test	Driving robot	7.1	5.9

## 5.5 Evaluation of concepts

The concepts identified in paragraph 5.2, and summarised in Table 5.4, will now be implemented on the test data measured on the baseline vehicle and evaluated. Although this approach is not strictly correct since the vehicle dynamics will change when the suspension settings change, this method is expected to illustrate trends and provide a first order evaluation of feasibility.

Only the first three concepts listed in Table 5.4 were investigated in more detail. Concept 4 is a “ride comfort” strategy while concept 5 focuses on the effect of longitudinal forces (*e.g.* due to acceleration or braking) on the vehicle and therefore not ride comfort or handling. Concept 6 is a “handling” strategy and ignores ride comfort.

At this point, the controllable suspension system is assumed to function as a two-state system that can be switched between a “ride comfort mode” and a “handling mode”.

Several requirements were set for evaluating the feasibility of a control strategy. These requirements are:

- Switching should not be too frequent, *e.g.* the strategy should not “hunt” between the “ride comfort” and “handling” settings
- The strategy should work for all six chosen tests without manual driver intervention.
- The strategy should rather err towards the “handling” mode.
- For both the handling test and the rollover test, the system should switch to the “handling mode” as quickly as possible, and remain in the “handling mode” for the duration of the manoeuvre. Ideally the “handling mode” should be selected before the start of the manoeuvre, but this is not possible without some kind of preview.
- During off-road driving, the system should remain in “ride comfort” mode for most of the time.

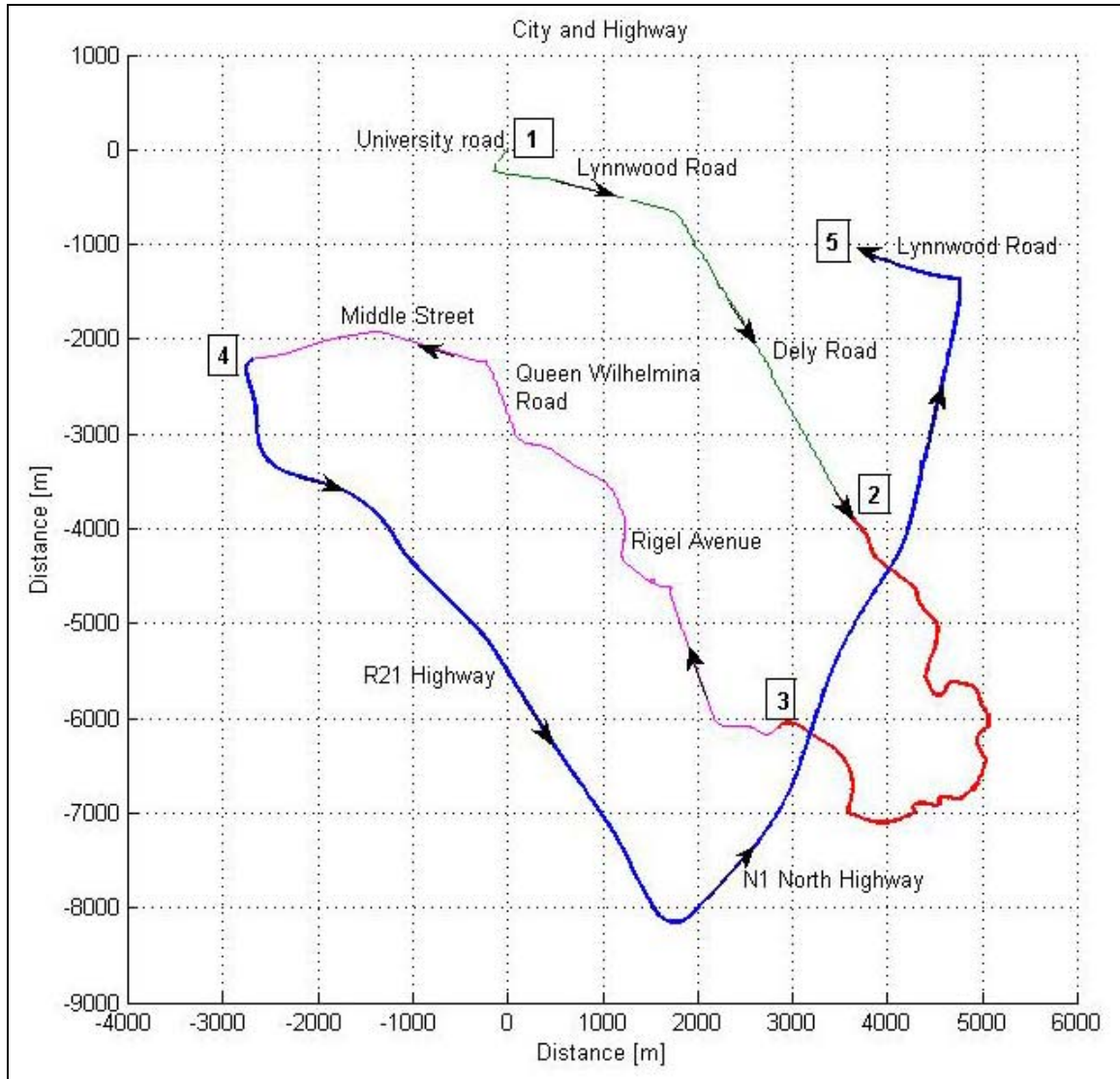


Figure 5.8 – City and highway driving route

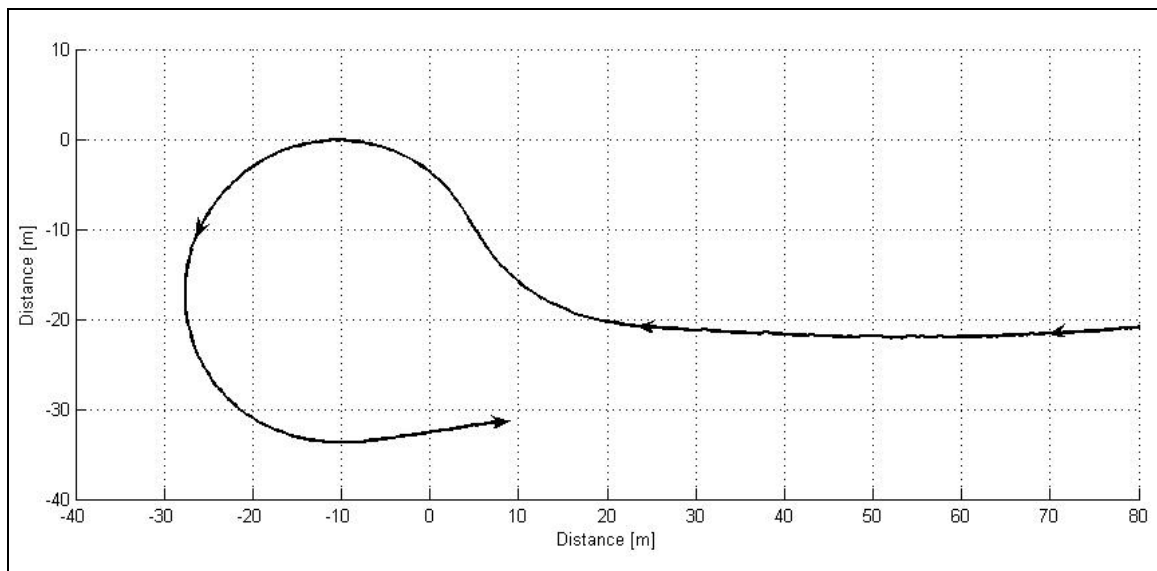


Figure 5.9 – Fishhook test

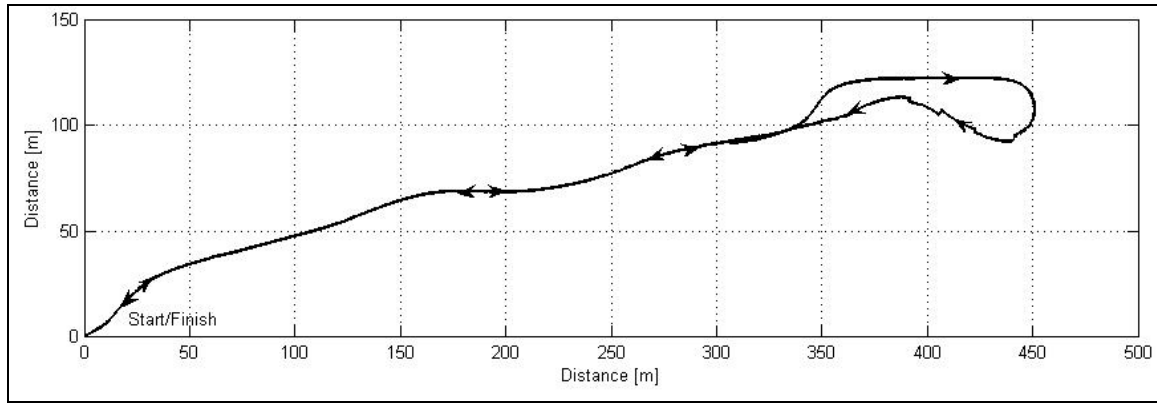


Figure 5.10 – Gerotek rough track top 800 m

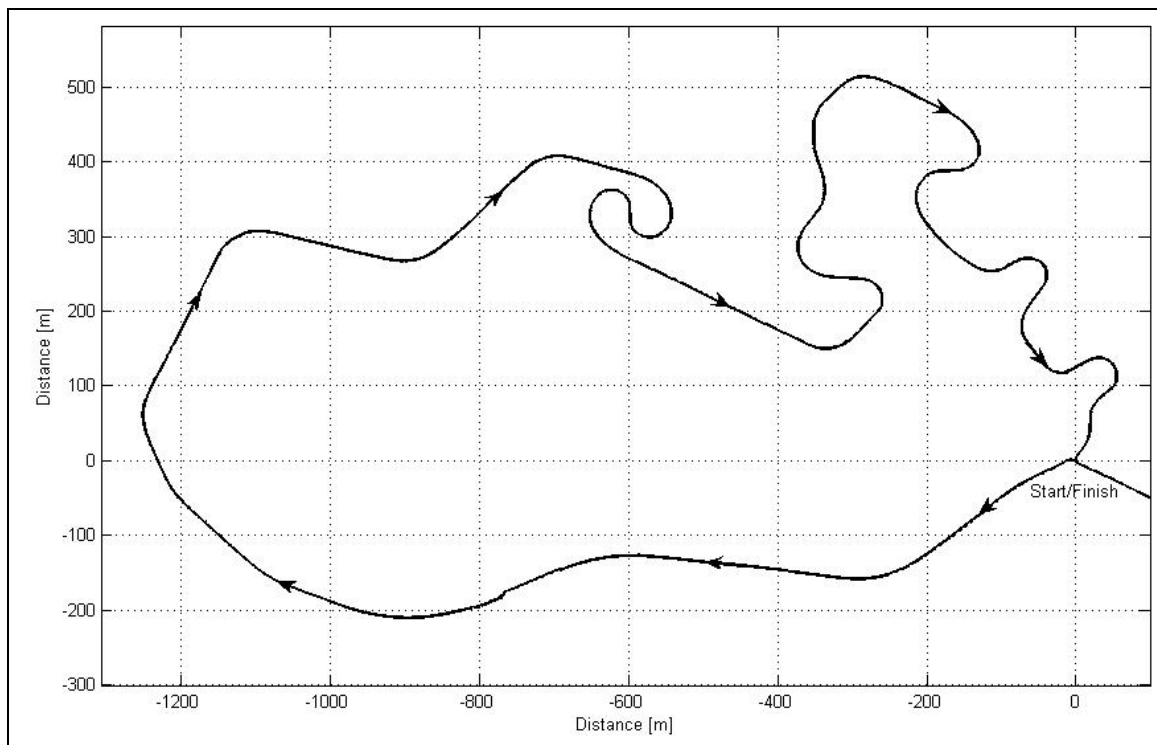


Figure 5.11 – Gerotek Ride and handling track

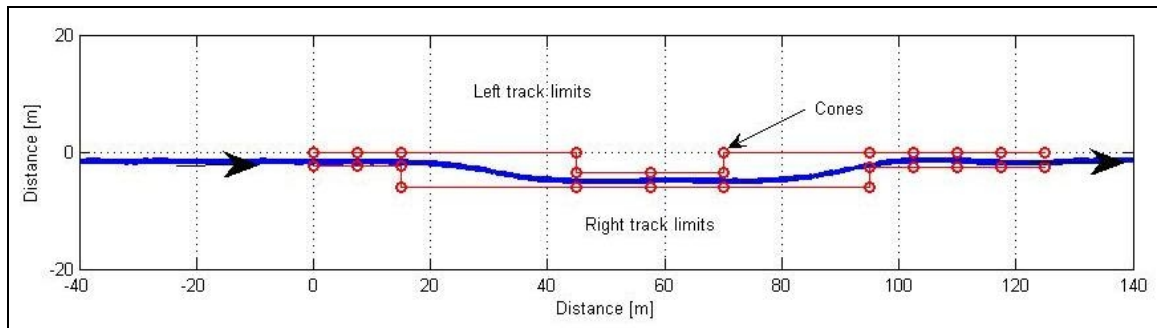


Figure 5.12 – Double lane change test

### 5.5.1 Frequency domain analysis

The first concept implemented is frequency domain analysis proposed by **Wallentowitz and Holdman (1997)** as well as **Truscott (1994)**. To determine whether this concept is feasible, FFT magnitudes were calculated for measurements over the six predefined tests. Each measurement was divided into bins of 1024 data points each with no overlapping. The FFT magnitudes were calculated for each bin of 1024 points, and then averaged for all the bins of the specific measurement at each frequency. Figure 5.13 indicates the average FFT magnitudes for the left rear and right rear vertical accelerations measured on the vehicle body. All six superimposed graphs indicate the same two peaks at 2 Hz (Body natural frequency) and 12 Hz (wheel hop frequency), although the magnitudes differ for the different terrains.

Figure 5.14 indicates that only very low frequencies can be detected by looking at the lateral acceleration. Trends are similar for all six tests. Roll, yaw and pitch velocities are indicated in Figure 5.15. The off-road track causes significant activity around 2 Hz that is absent in the other tests. Yaw velocity is restricted to low frequencies while the pitch natural frequency can be seen to be around 2 Hz for all six terrains. Relative suspension displacements (Figure 5.16) indicates the body natural frequency around 2 Hz. This is only really noticeable on the off-road test. The FFT magnitudes of the steering displacement and kingpin steering angle are indicated in Figure 5.17. All activity takes place at very low frequencies.

FFT magnitudes of relative suspension velocities are indicated in Figure 5.18. The relative velocity was obtained by differentiating the relative displacement in the time domain and then calculating the FFT. Again the frequency at 2 Hz is prominent with activity from about 1 Hz to 12 Hz. Trends do however look the same for all terrains.

The FFT magnitudes of the steering velocities, calculated by first differentiating the steering displacements in the time domain, are indicated in Figure 5.19. Figure 5.19(b) indicates the FFT magnitude of the steering velocity at the kingpin. Figure 5.19(a) indicates the steering velocity calculated from the measured displacement between the vehicle body and the steering link going to the wheels. The steering velocity clearly indicates activity around 8 to 10 Hz when driving off-road and through the mountain pass that is not present on the kingpin steering velocity. This is attributed to bump and roll steer as well as the kinematic effects resulting from the Panhard rod.

Although the frequency domain analysis provides valuable insight into the various excitation and natural frequencies, it is concluded that “ride vs. handling” cannot be detected from the frequency analysis. The same frequencies are excited regardless of terrain types, manoeuvres and speeds.

### 5.5.2 Lateral vs. vertical acceleration

The next strategy that was investigated is the one proposed by **Nell (1993)** and **Nell and Steyn (1998)**. They compare lateral and vertical acceleration as measured on the rigid front axle of a heavy off-road military vehicle. The semi-active dampers on their test vehicle is switched to “hard” when the lateral acceleration is higher than the vertical

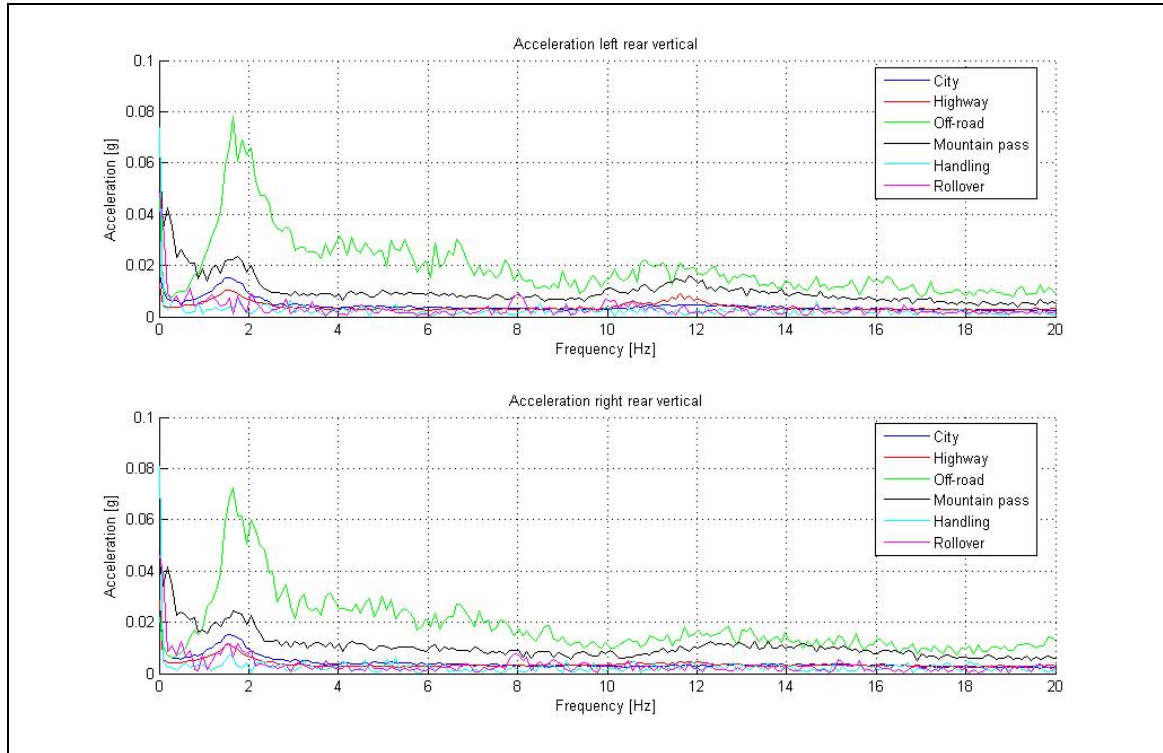


Figure 5.13 – FFT magnitude of vertical body acceleration (left and right rear)

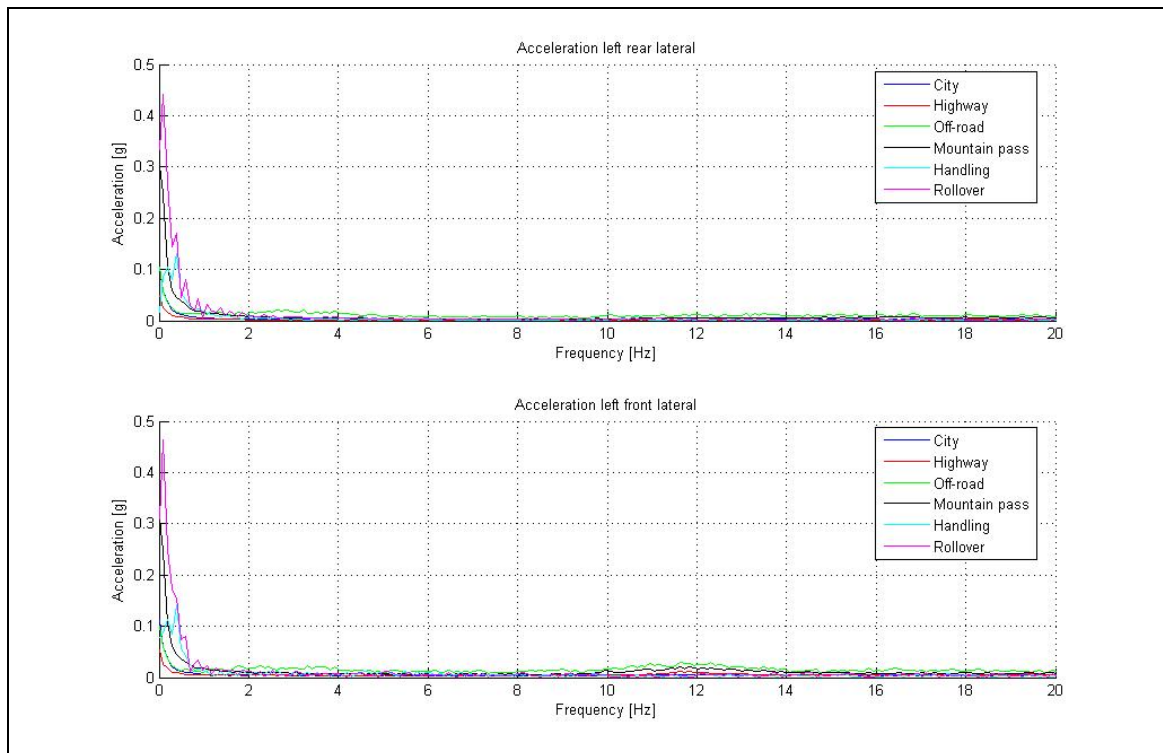


Figure 5.14 – FFT magnitude of body lateral acceleration (left front and left rear)

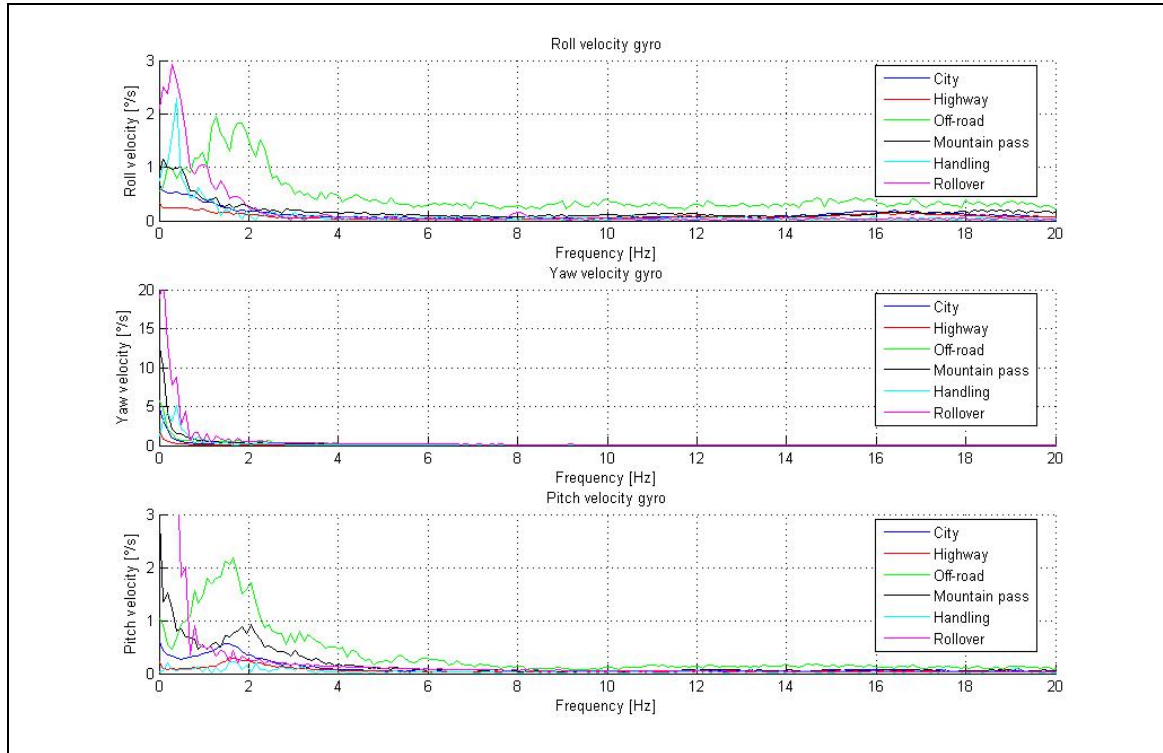


Figure 5.15 – FFT magnitudes of body roll, yaw and pitch velocity

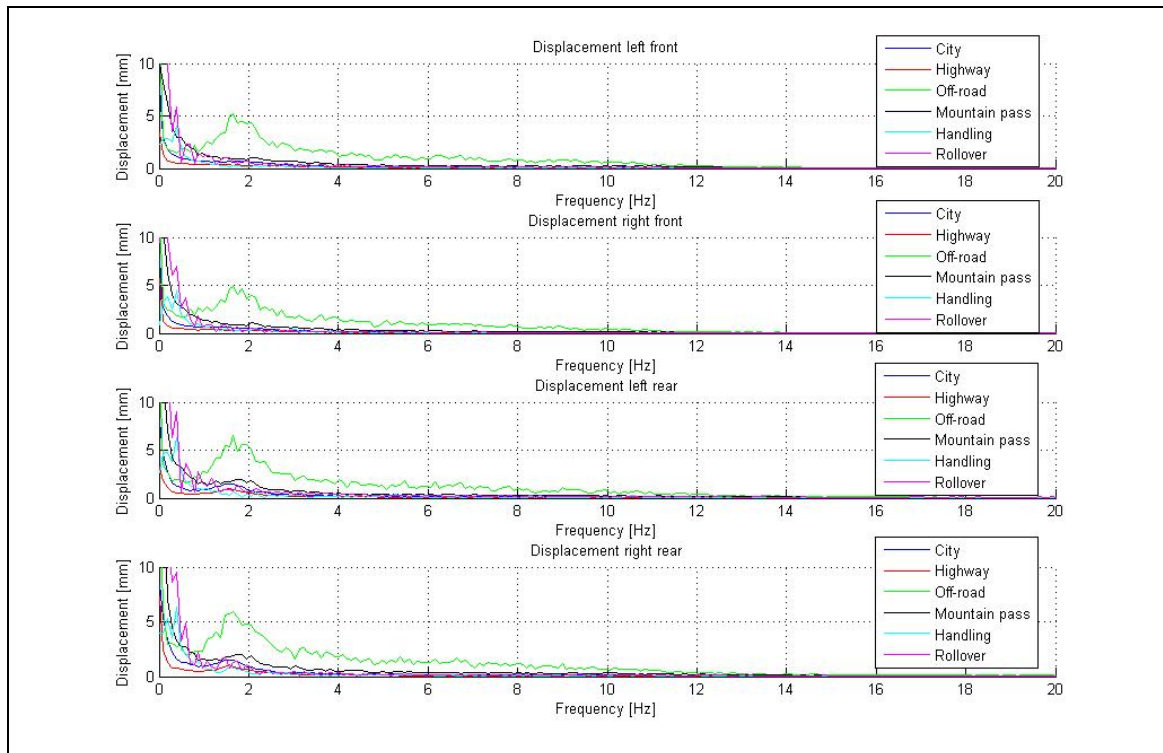


Figure 5.16 – FFT magnitude of relative suspension displacement (all four wheels)

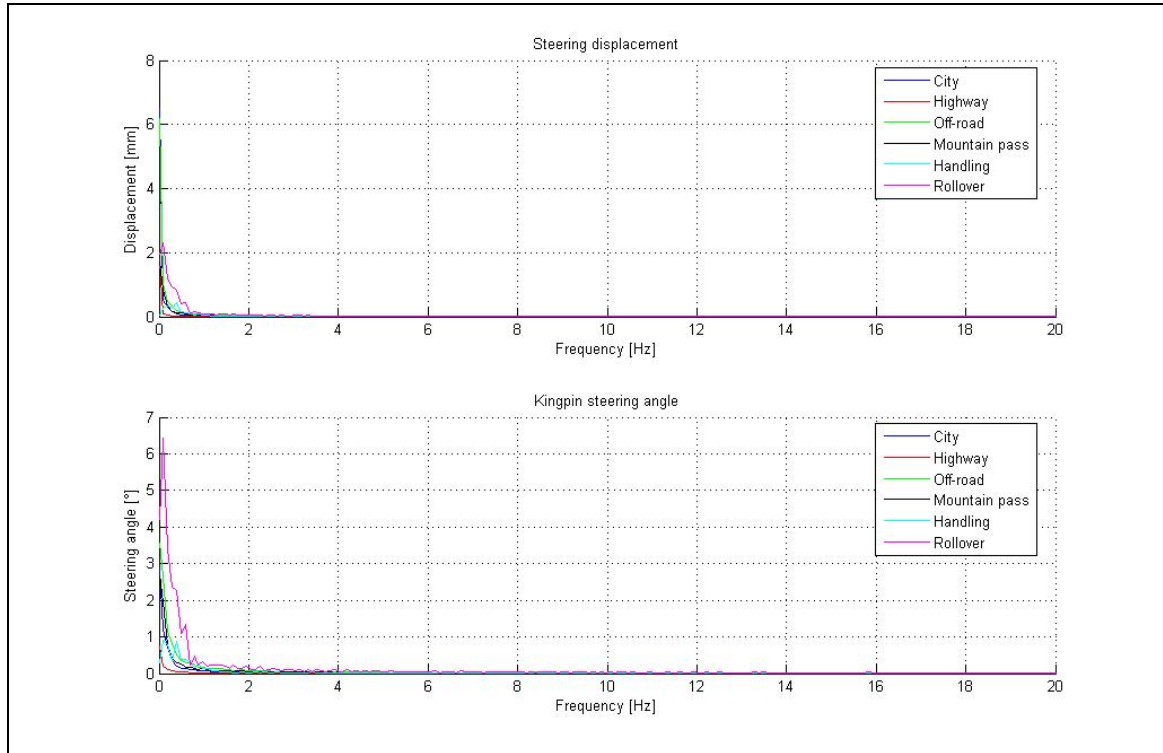


Figure 5.17 – FFT magnitude of steering displacement and kingpin steering angle

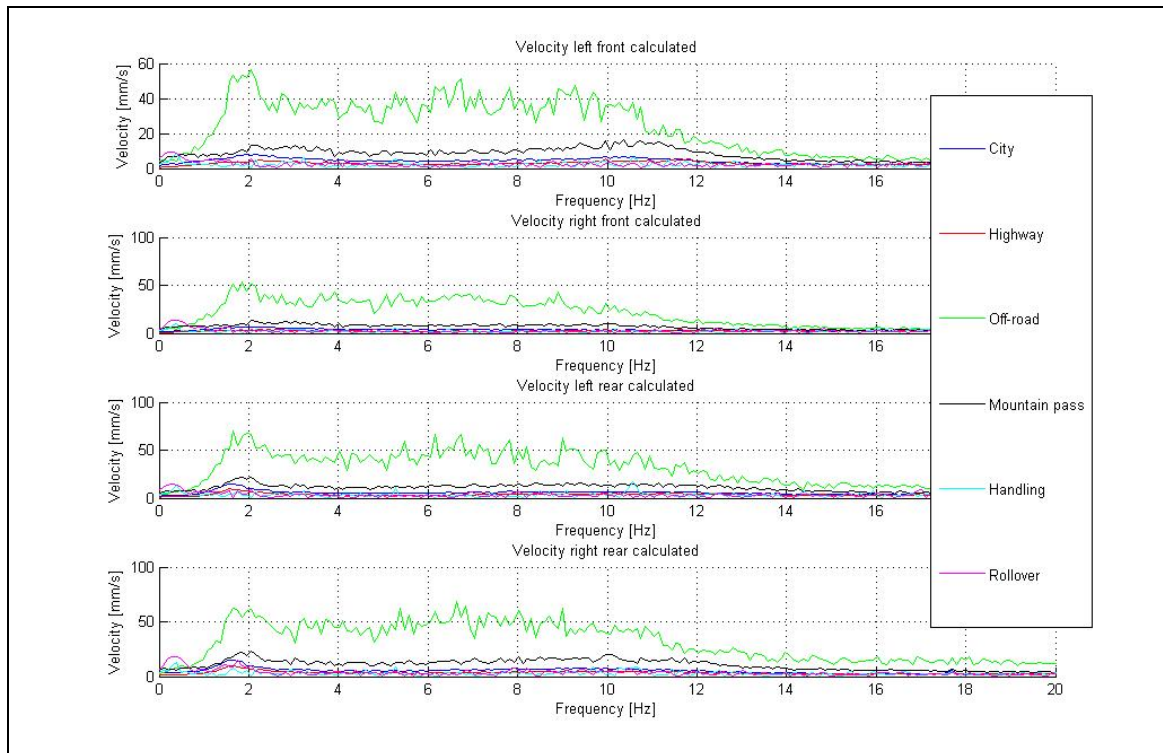
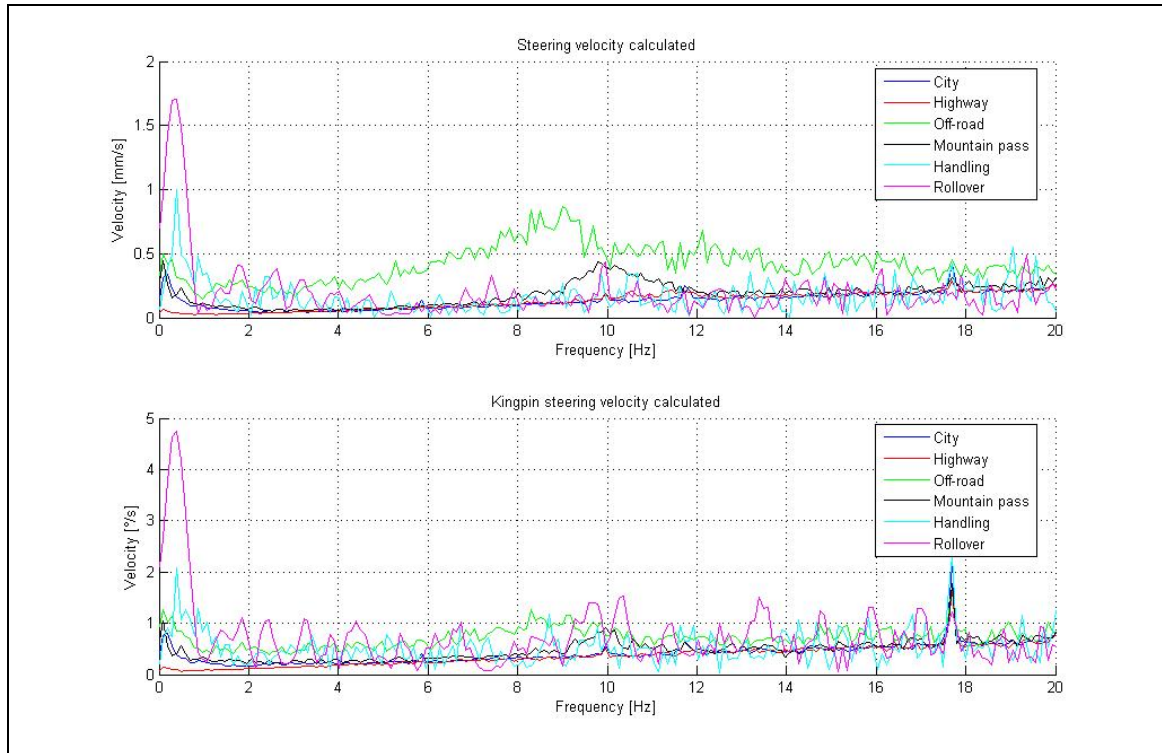


Figure 5.18 – FFT magnitude of relative suspension velocity (all four wheels)



**Figure 5.19** – FFT magnitude of steering velocity

acceleration and to the “ride comfort” mode when vertical acceleration is higher than lateral acceleration.

Figure 5.20 indicates the result of this analysis when applied to our measurements during city driving. Figure 5.20(a) indicates vertical and lateral accelerations measured on the left rear of the vehicle while Figure 5.20(b) indicates the suspension switching. A value of “0” in Figure 5.20(b) indicates “ride” mode while a value of “1” indicates “handling” mode. Switching seems spurious and random, *e.g.* between 530 and 600 seconds the vehicle is stationary, but the suspension switches all the time due to the background noise on the acceleration signals. The idling engine causes some of this noise.

Figure 5.21 indicates switching during the rollover test. It can be seen that the switching only works in one direction. The absolute values of the lateral and vertical acceleration should therefore be compared to enable correct switching. Two fundamental problems exist with the strategy as proposed by Nell namely:

- The absolute values of the accelerations should be compared
- Provision should be made for some type of dead band to prevent spurious switching when the measured values are close to zero

Nell intended the strategy to be used for accelerations on the front axle of the vehicle. The vertical acceleration on the axle is however significantly higher (can be 15 to 25g peak) than the lateral acceleration (about 1g peak). The strategy will therefore favour ride comfort, especially on rough roads. The strategy will also emphasize wheel hop frequency and not body motion due to the measuring position on the axle.



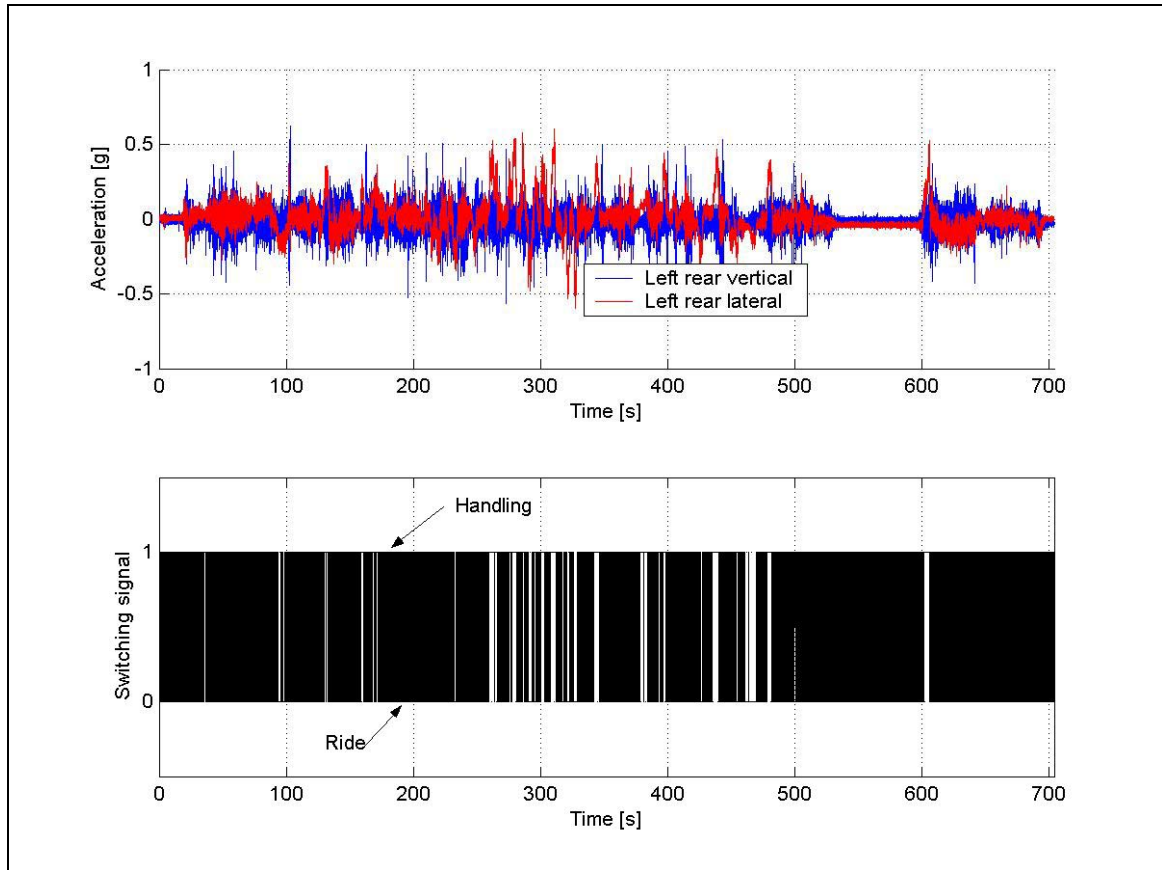


Figure 5.20 - Strategy proposed by Nell (1993) as applied to city driving

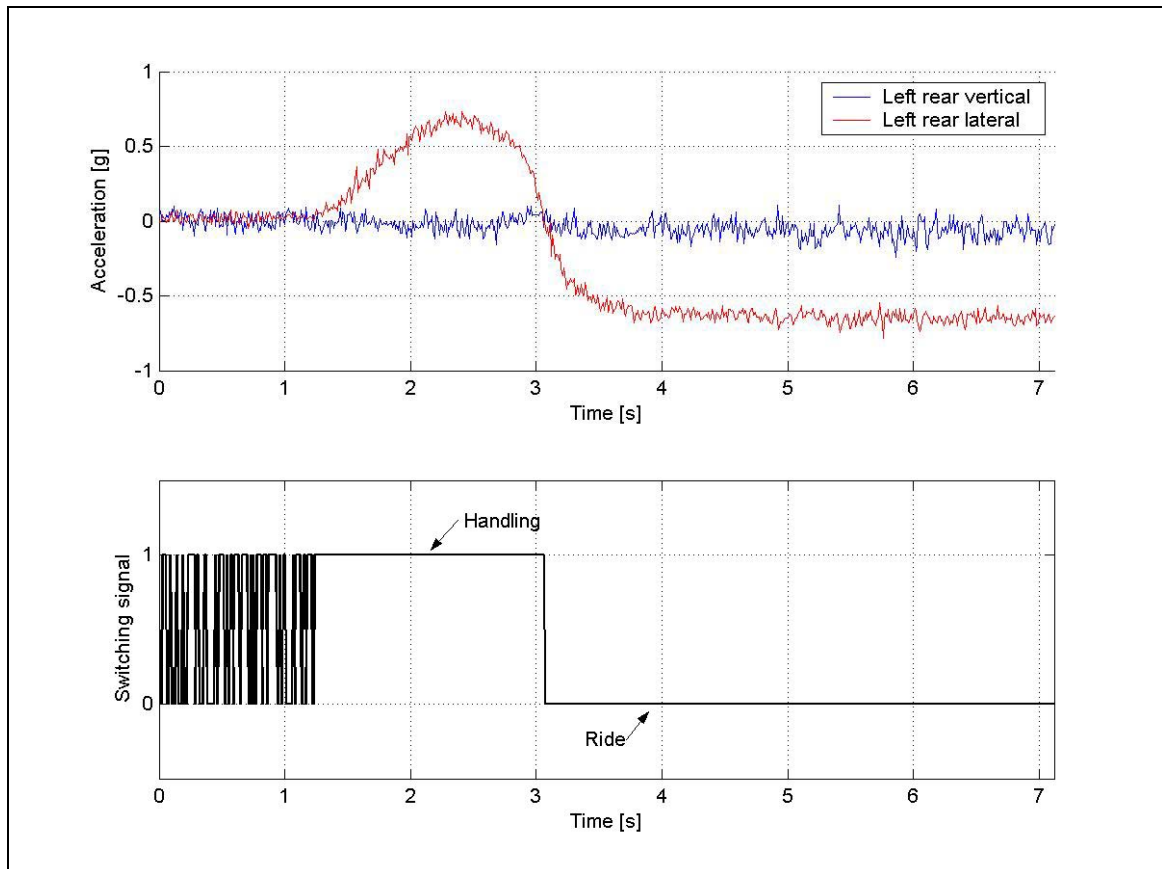


Figure 5.21 - Strategy proposed by Nell (1993) as applied to the rollover test

### 5.5.3 Lateral vs. vertical acceleration - modified

The strategy proposed in paragraph 5.5.2 is now modified in order to eliminate its drawbacks. The absolute values of the lateral and vertical accelerations on the vehicle body are used. A dead band is introduced to prevent spurious switching due to accelerometer noise and drift. The “ride” mode is always selected if the absolute lateral acceleration is less than 0.1 g. An upper limit is also included that forces switching to the “handling” mode when lateral acceleration exceeds 0.3g (see **Stone and Cebon, 2002** and **Darling and Hickson, 1998**). This however results in negligible improvement during highway driving (Figure 5.22) although the ride mode is at least selected during periods when the vehicle is stationary (*e.g.* between 650 and 700 seconds). A significant improvement is however noticed for the rollover test (Figure 5.23) where the handling mode is selected during most of the manoeuvre. The switching to the ride mode at 3.2 seconds is however problematic as this happens at a critical point in the test. The method is however an improvement on the previous case.

### 5.5.4 Steering angle vs. speed

The use of a speed dependant steering angle threshold has been applied frequently. Some examples are discussed by **Hirose *et. al.* (1988)**, **Hine and Pearce (1988)**, **Nastasic and Jahn (2005)** as well as **Broge (1999)**. The steering angle vs. speed threshold used by Citroën was indicated in Figure 5.3.

The envelope for the Land Rover was determined by plotting steering angle against vehicle speed for all the tests. The results are indicated in Figure 5.24. The circles in Figure 5.24 indicate the measured data points obtained for city driving and the solid lines indicate the limiting values determined for different terrains. These curves represent the values of steering angle that is achieved during normal driving.

The strategy itself is very easy to implement and is an “input driven” strategy *i.e.* it will react on driver input and not vehicle reaction to driver input as is the case with lateral acceleration *etc.* It should therefore also give an early warning before the vehicle reaction can be detected.

The results of this strategy as implemented on test data is shown in Figures 5.25 to 5.30. The threshold value used for all the analyses indicated in Figures 5.25 to 5.30 is 50% of the steering angle limit for city driving (solid red line in Figure 5.24) at any given vehicle speed. During city driving (Figure 5.25), off-road driving (Figure 5.27) and on the mountain pass (Figure 5.28) the strategy works well due to the large steering angles involved. During the highway tests (Figure 5.26) switching seems to occur too often due to the fact that the steering threshold is very low and measurement noise and sensor drift has a significant effect on the results.

For the handling test (Figure 5.29) and rollover test (Figure 5.30) results are not entirely satisfactory, as the suspension will be switched to the “ride” mode whenever the steering goes through the zero position. This is dangerous as the effect takes place during critical parts of the manoeuvre.

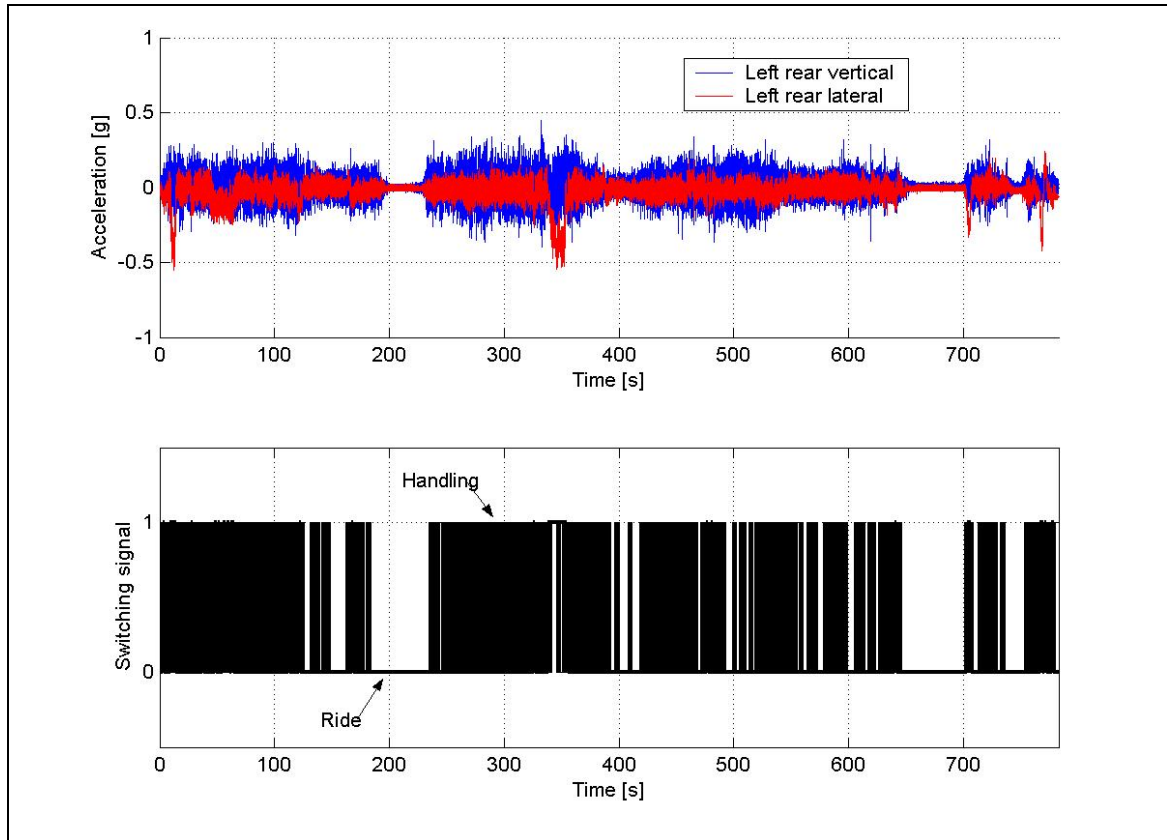


Figure 5.22 – Modified lateral vs. longitudinal acceleration for highway driving

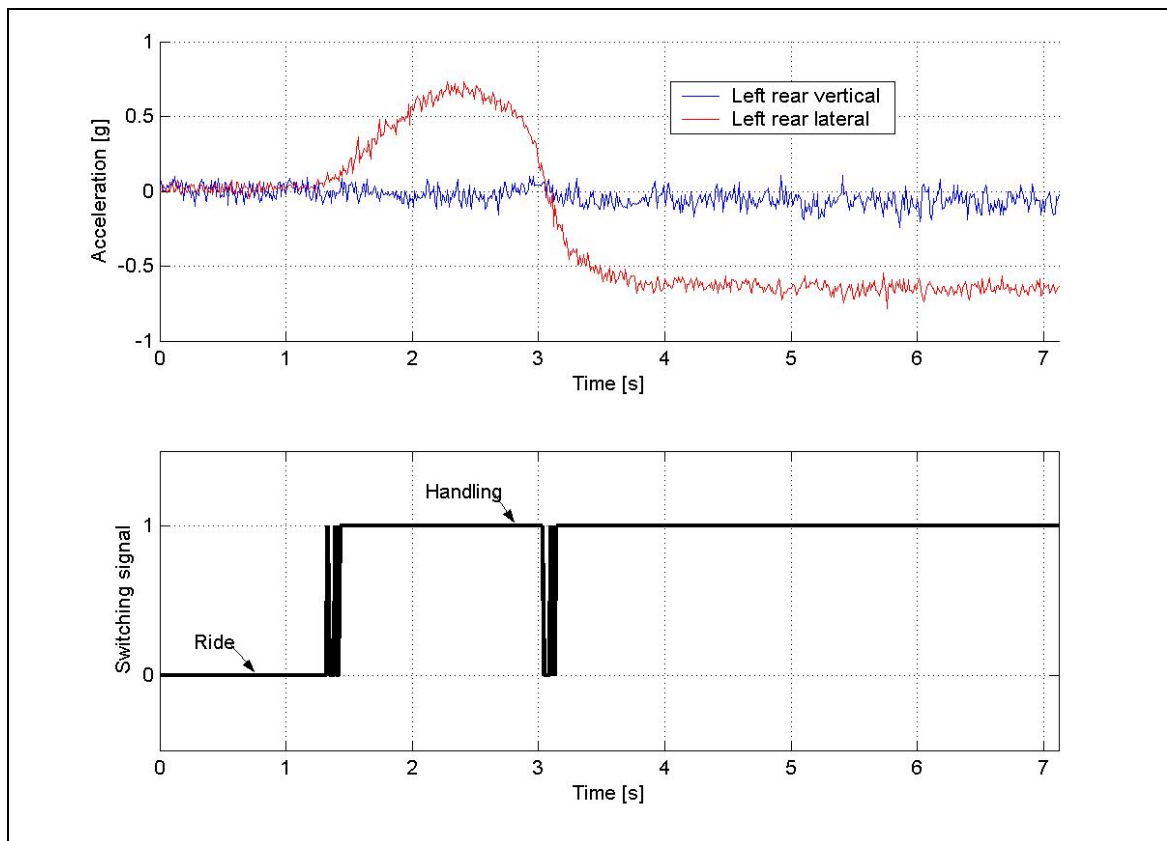
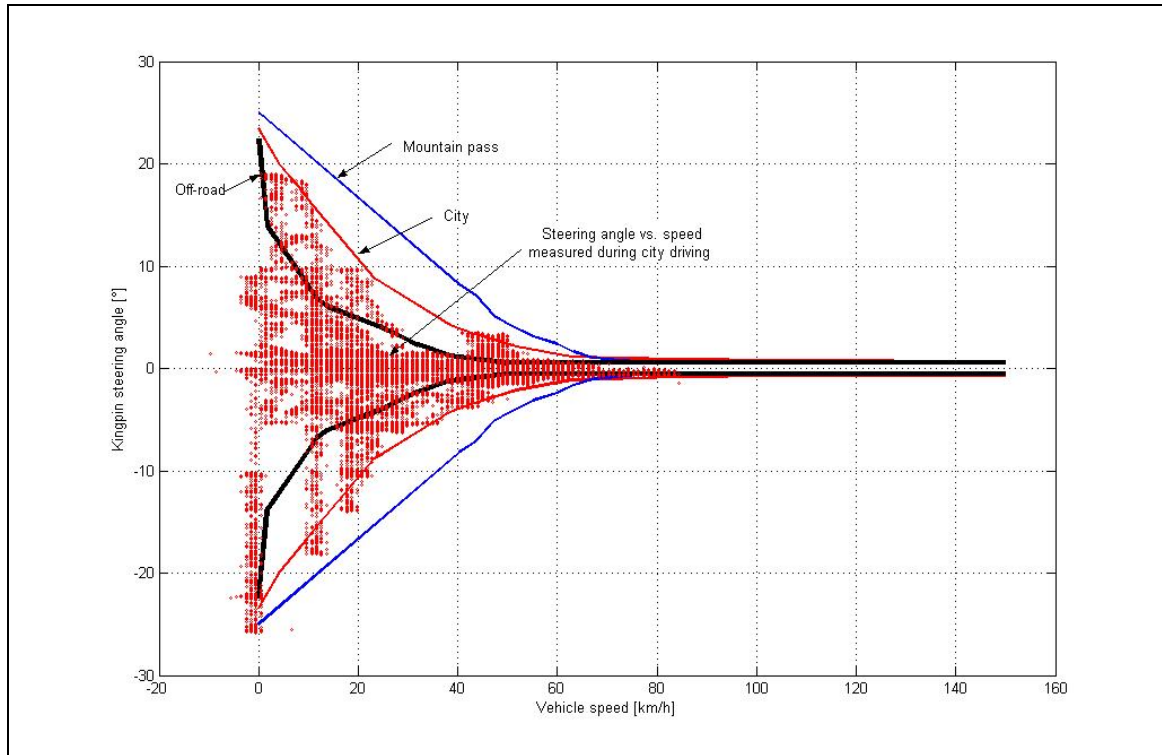


Figure 5.23 - Modified lateral vs. longitudinal acceleration for rollover test



**Figure 5.24** – Steering limits vs. vehicle speed measured during three tests

Spurious switching also sometimes occurs due to noise. This can be seen for example in the first 20 seconds of Figure 5.25 where the vehicle is stationary, but the steering wheel is turned. This problem can however be solved by using a dead band instead of a single limit.

The biggest difficulty when applying this strategy to the off-road vehicle is that the threshold values differ considerably depending on the terrain. If the terrain can be somehow “identified”, and the threshold values adapted accordingly, then the performance of the strategy can be improved. Performance for the handling and rollover tests are however only expected to improve marginally because the system will still switch to “ride mode” when the steering angle goes through the zero position.

### 5.5.5 Disadvantages of proposed concepts

All the concepts investigated up to this point suffer from the same disadvantages namely:

- i) Switching occurs too frequently
- ii) All strategies don't work properly for all conditions
- iii) Strategies that work well for on-road driving fail during off-road tests and *vice versa*

Unnecessary switching could be eliminated by applying a dead band, low pass filtering or delayed switching. It is imperative that absolute values be used.

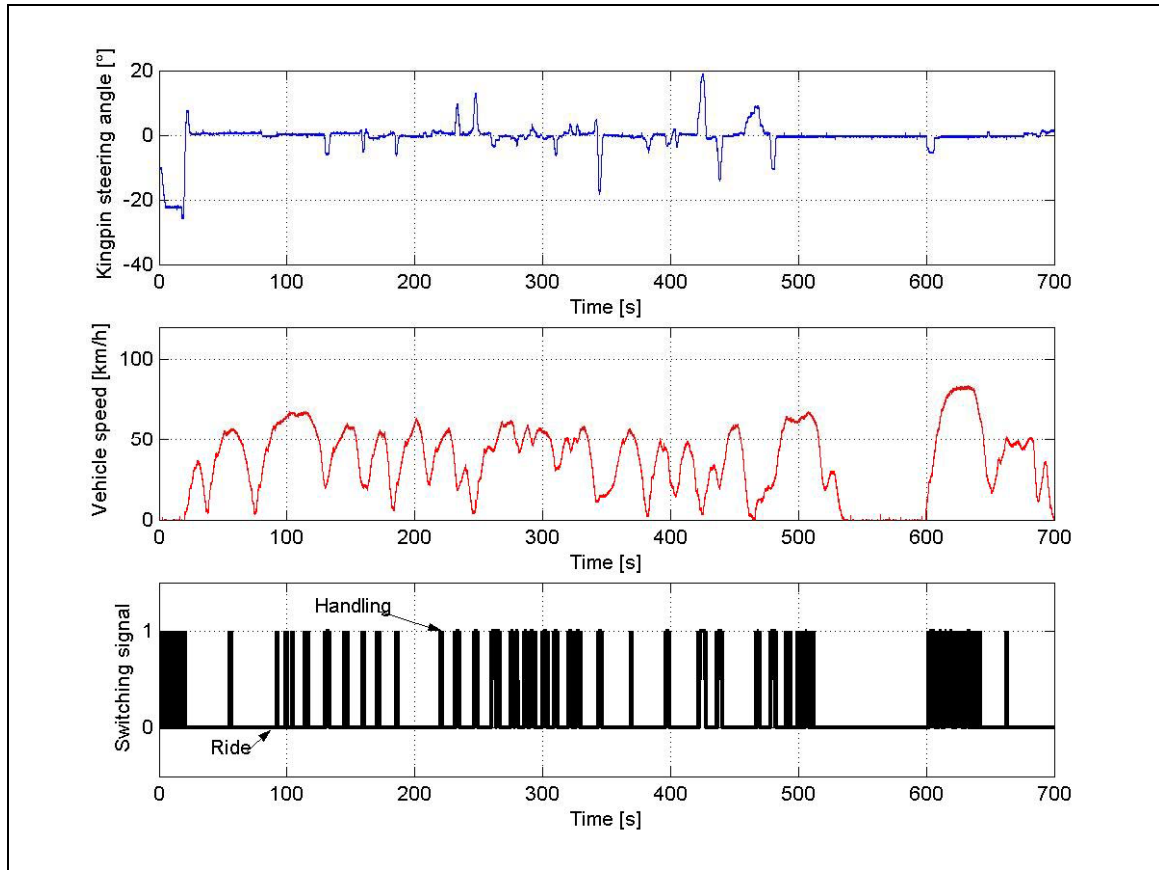


Figure 5.25 – Steer angle vs. speed implemented for city driving

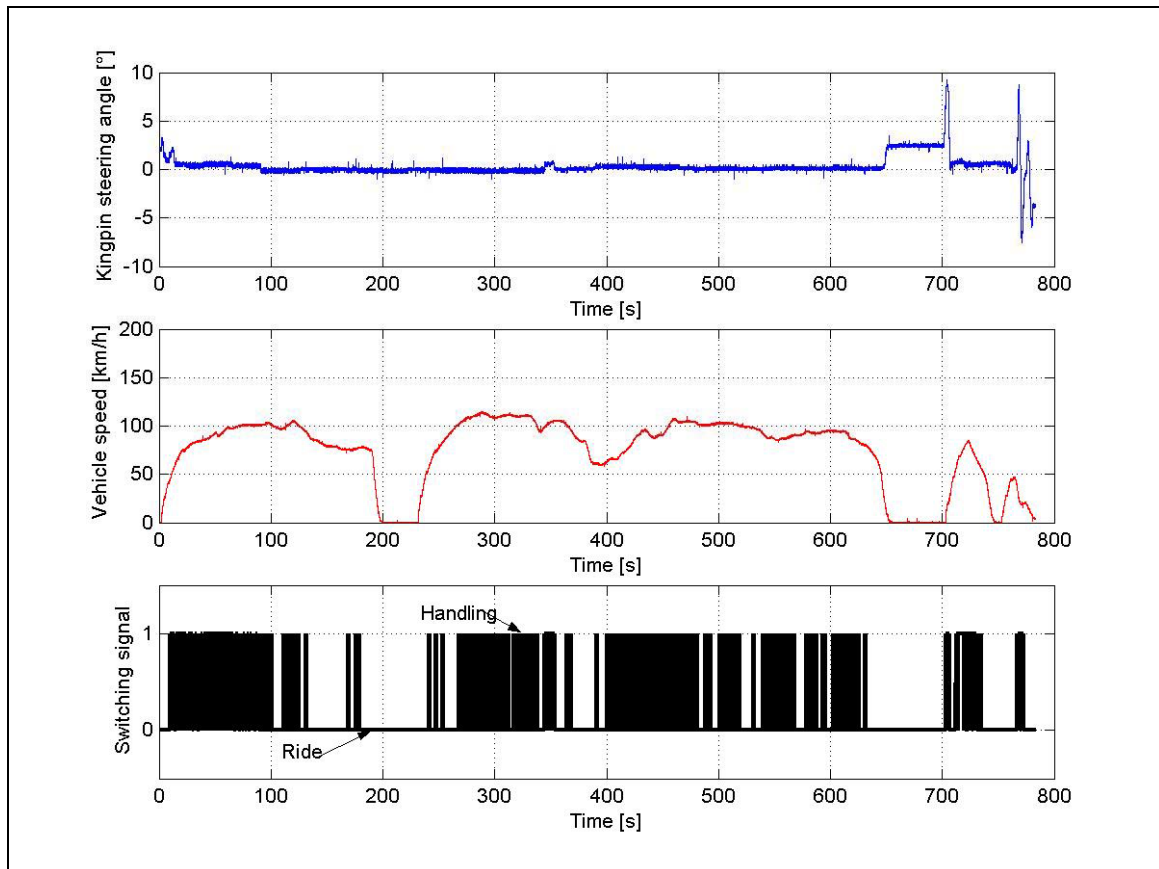


Figure 5.26 – Steer angle vs. speed implemented for highway driving

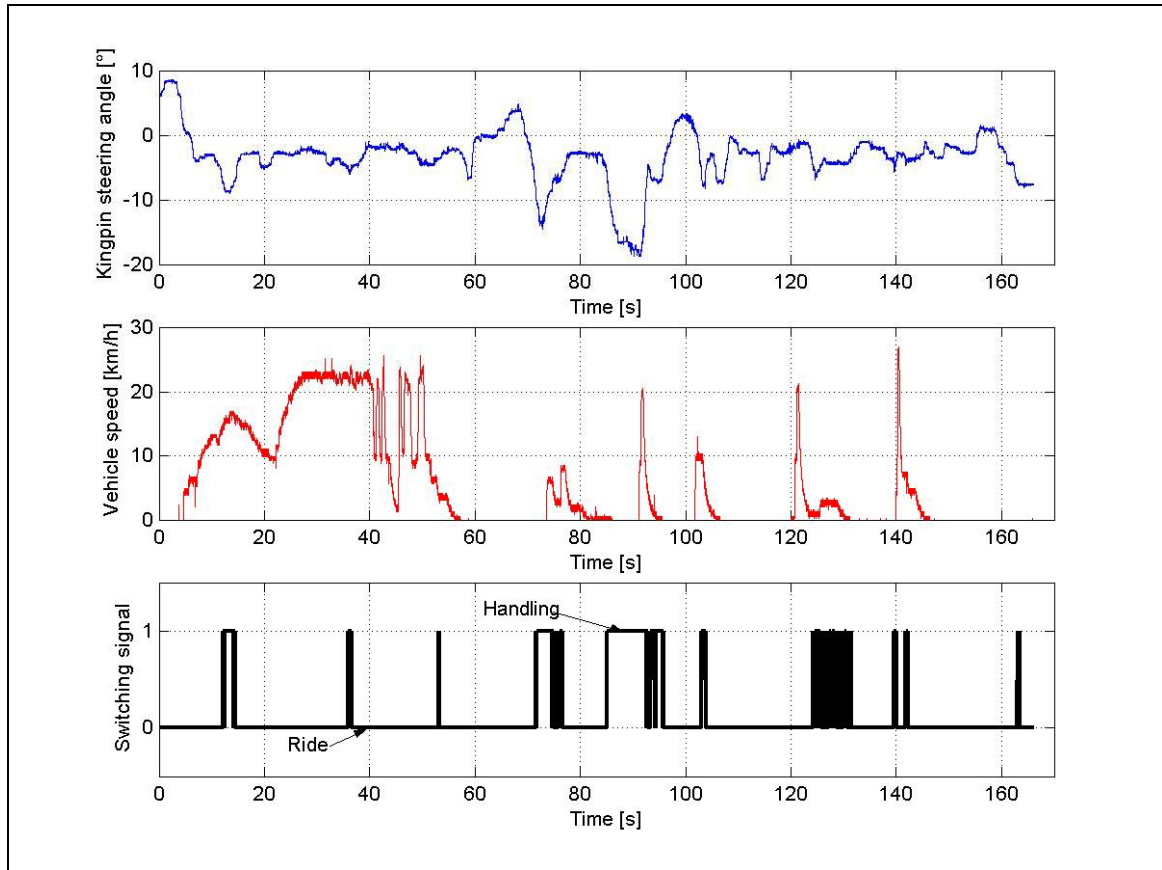


Figure 5.27 – Steer angle vs. speed implemented for off-road driving

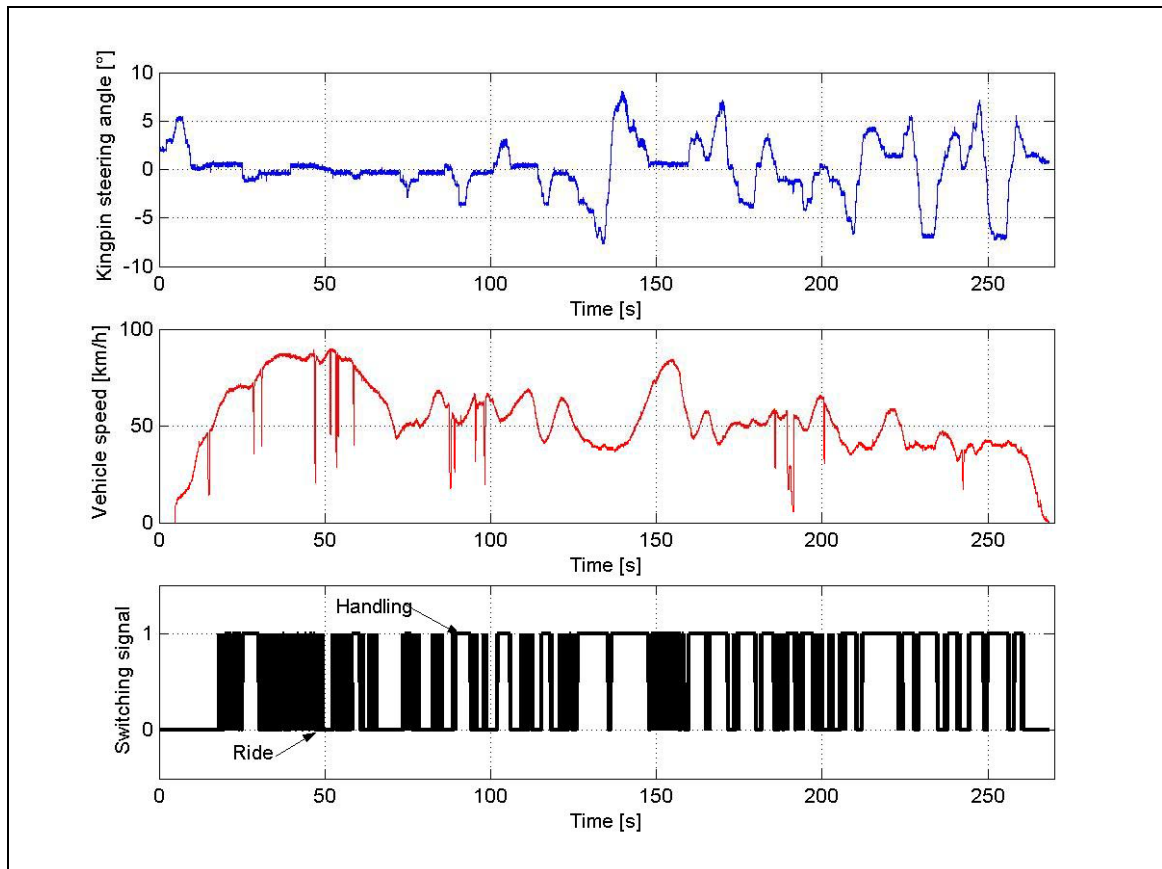


Figure 5.28 – Steer angle vs. speed implemented for mountain pass driving

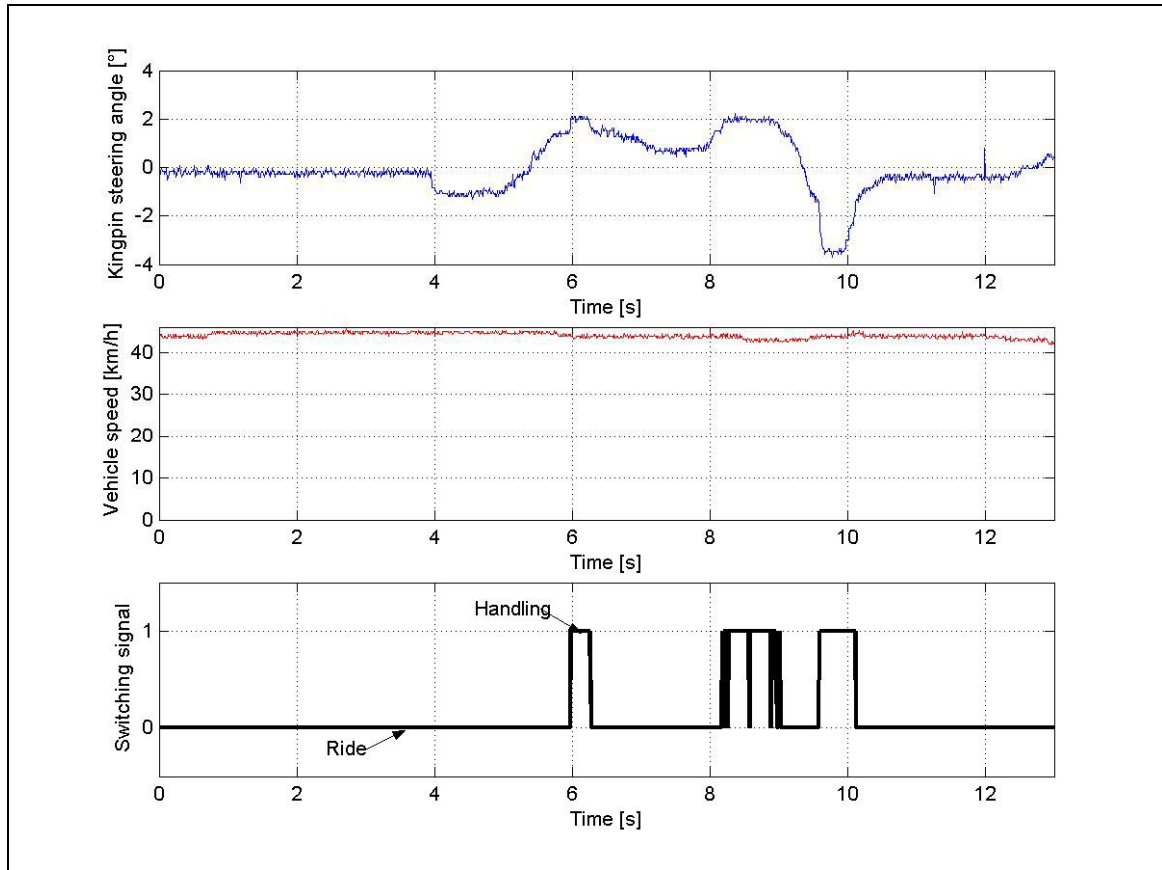


Figure 5.29 – Steer angle vs. speed implemented for handling test

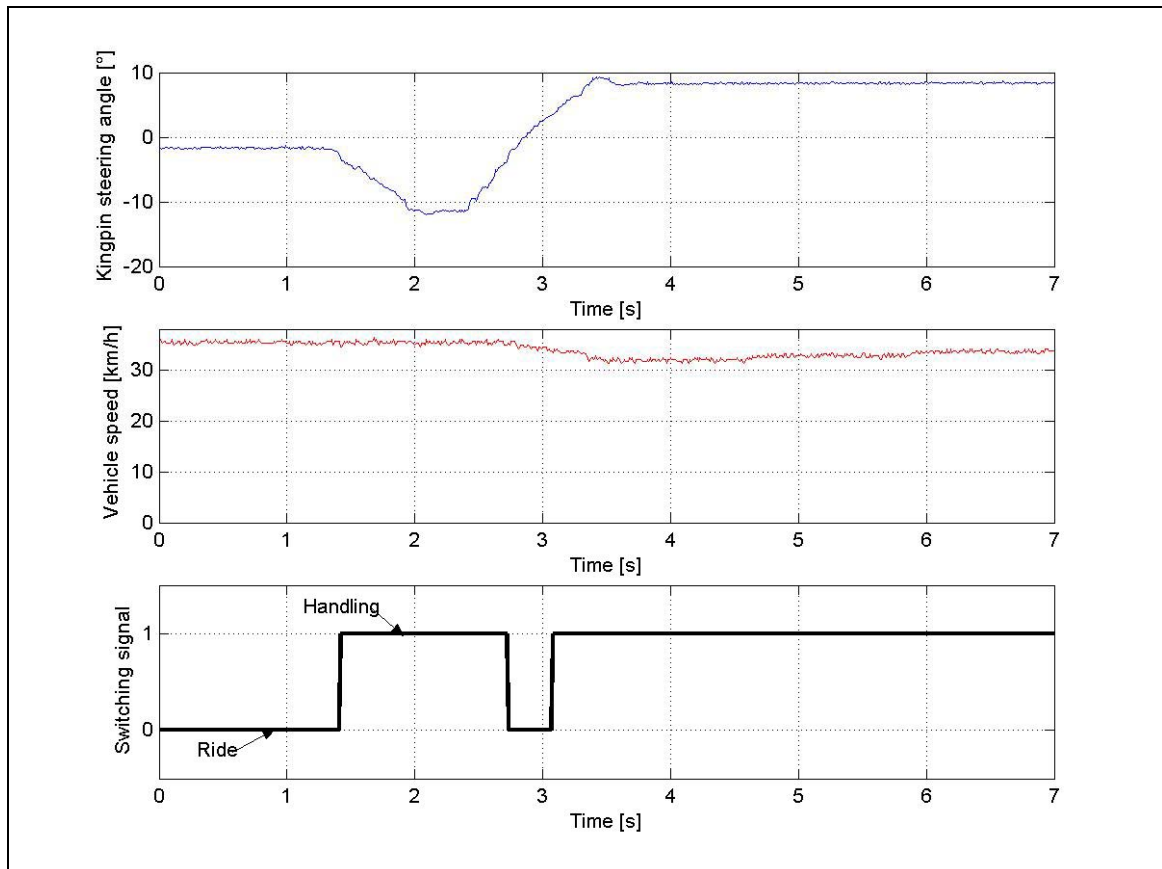


Figure 5.30 – Steer angle vs. speed implemented for rollover

## 5.6 Novel strategies proposed

To overcome the problems mentioned in paragraph 5.5.5, two additional strategies are proposed namely relative roll angle and running RMS (RRMS).

These proposed strategies will be discussed in paragraphs 5.6.1 and 5.6.2.

### 5.6.1 “Relative roll angle” calculated from suspension deflection

Roll angle was identified as a good measure of handling in paragraph 2.1.2.5. Absolute body roll angle is however very difficult to measure directly. The first proposal is to use the relative body roll angle between the vehicle body and axle, calculated using the relative suspension deflection of the left and right suspension systems. Because the body roll angle is small ( $< 5^\circ$ ), the roll angle is proportional to the difference between left and right relative displacements, divided by the distance between the left hand and right hand displacement measuring points. The difference between left and right displacements is therefore directly compared to a threshold value, without calculating the actual body roll angle. If this difference exceeds the threshold, the suspension system is switched to the handling mode. Results of this concept, applied with a threshold value of 20 mm, are indicated in Figures 5.31 to 5.36. The left front and right front relative suspension displacements were used in these calculations, but the same concept could be applied to the displacements measured for the rear axle.

The strategy works well for city driving (Figure 5.31), highway driving (Figure 5.32) and mountain pass driving (Figure 5.34). It switches to “handling” mode too frequently during off-road driving (Figure 5.33). During the handling test (Figure 5.35), the “ride” mode is selected for most of the manoeuvre. “Handling” mode is selected only at the most critical part of the test where the vehicle returns to the initial lane (between 70 and 100 meters in Figure 5.12, corresponding to between 8 and 11 seconds in Figure 5.35). This switch to “handling” mode at this critical point of the test might have disastrous effects. Although behaviour during the handling test can be improved by reducing the switching threshold of 20 mm, “ride” mode will still be selected whenever the relative roll angle crosses through the zero position. A reduction of the threshold will also result in more unwanted switching during off-road driving. During the fishhook rollover test (Figure 5.36), dangerous switching to the “ride comfort” setting occurs where the relative roll angle crosses the zero position. This is however also the place where the roll velocity (and therefore kinetic energy due to body roll) is maximum. Switching to “ride” mode under these conditions is highly undesirable.

### 5.6.2 Running RMS vertical acceleration vs. lateral acceleration

The second proposal is to use the running RMS (RRMS) value of lateral acceleration compared to the running RMS of vertical acceleration. This concept will result in an average absolute value of the required parameters and should therefore reduce spurious switching and noise.

The running RMS (RRMS) is calculated determining the RMS value of the last N number of points. The strategy includes hysteresis and will always select the “ride comfort” mode if the RRMS lateral acceleration is less than 0.05g. It also always selects “handling” mode when the RRMS lateral acceleration is greater than 0.3g. Between these two limits, handling mode is selected only when the RRMS lateral acceleration exceeds the RRMS



vertical acceleration. A running RMS of 1 second (or 100 previous data points) has been used for this analysis and seems to successfully remove noise without affecting response time detrimentally.

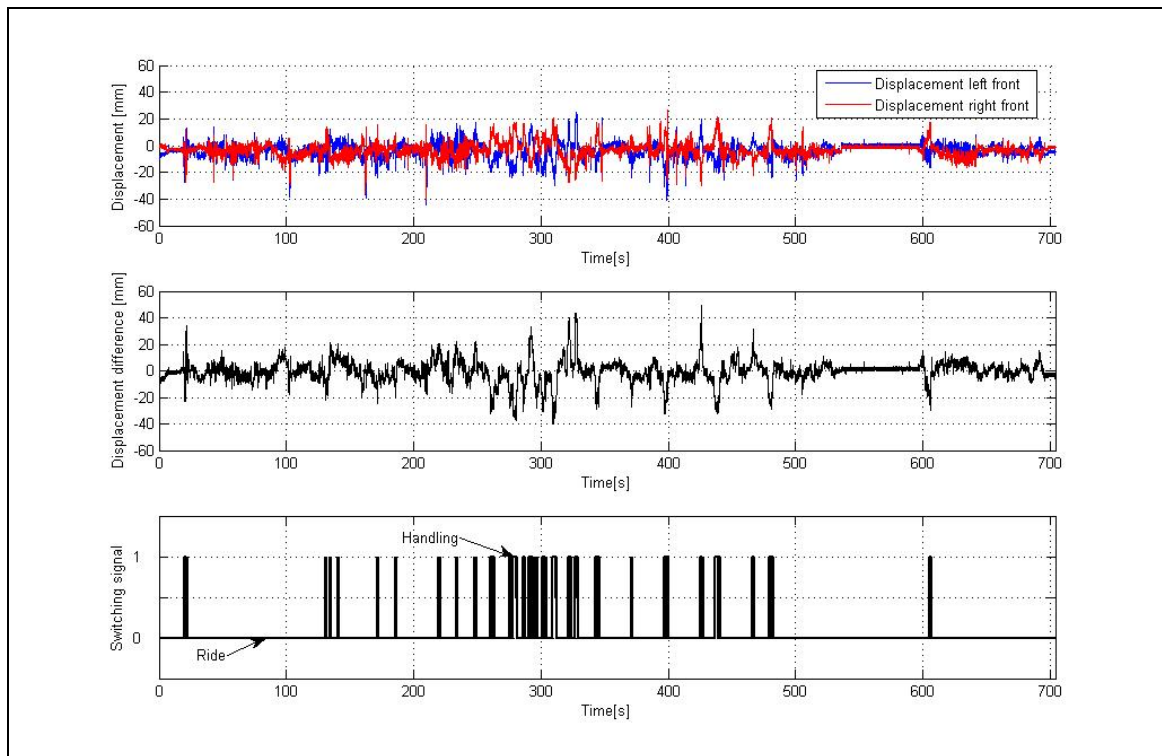


Figure 5.31 – Relative roll angle strategy for city driving

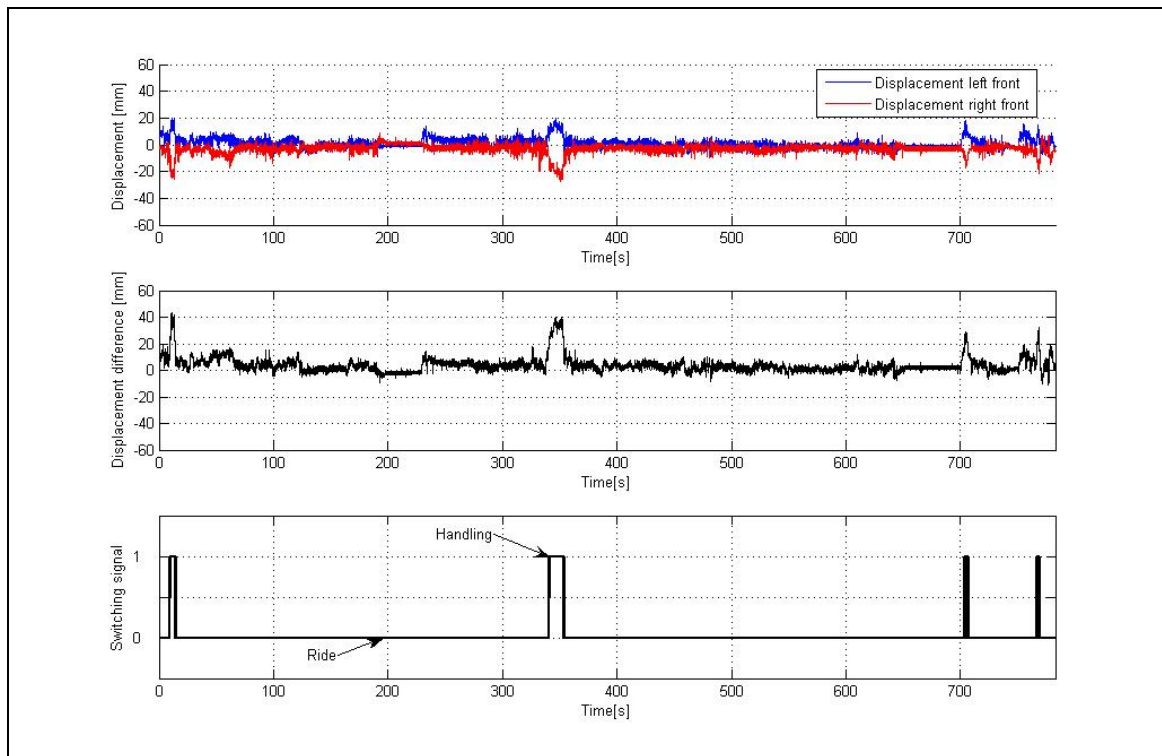


Figure 5.32 – Relative roll angle strategy for highway driving

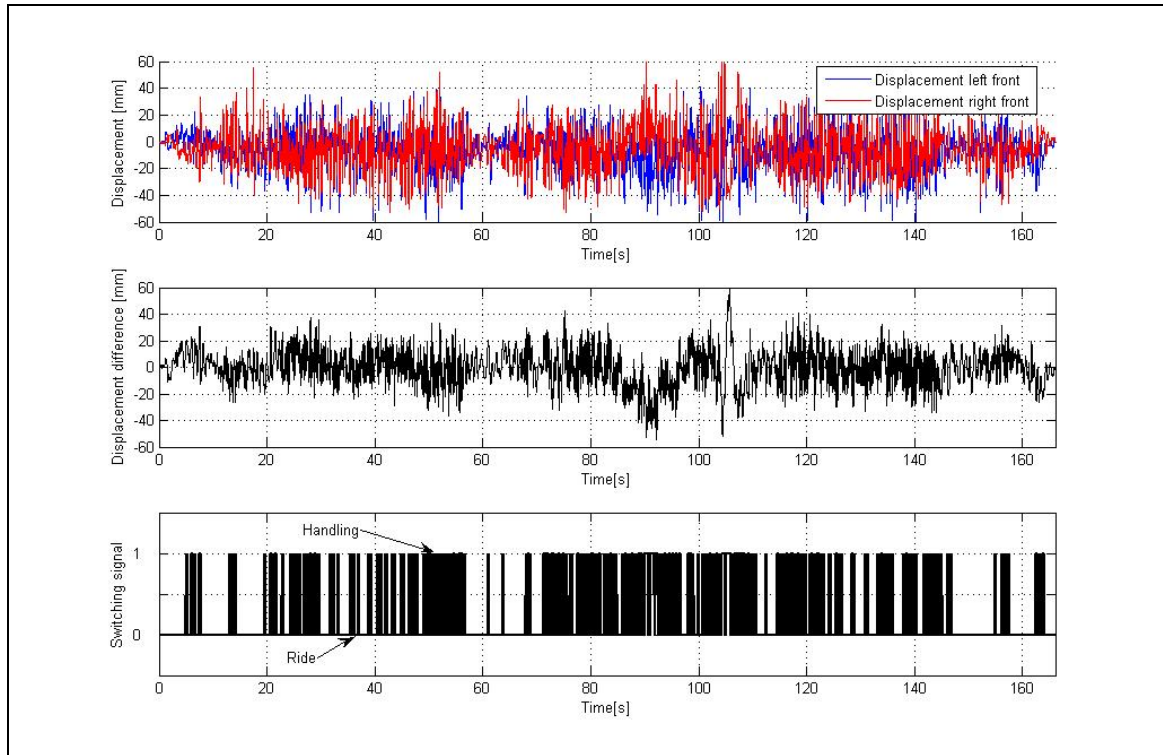


Figure 5.33 – Relative roll angle strategy for off-road driving

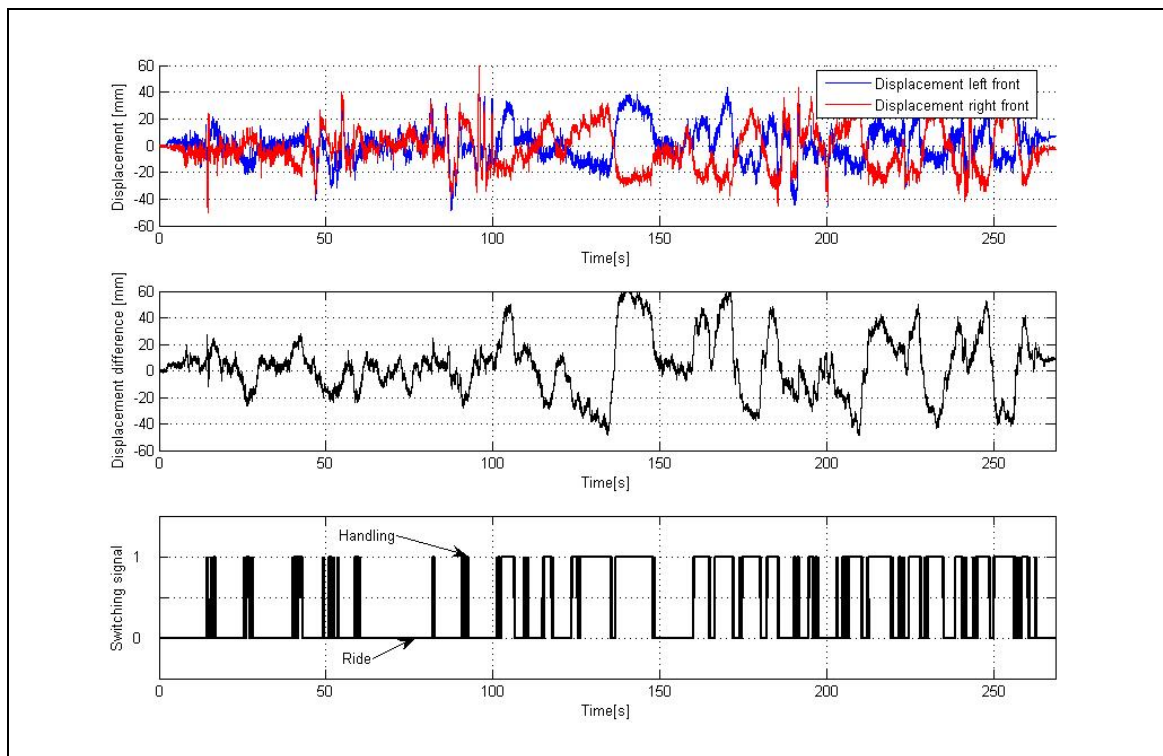


Figure 5.34 – Relative roll angle strategy for mountain pass driving

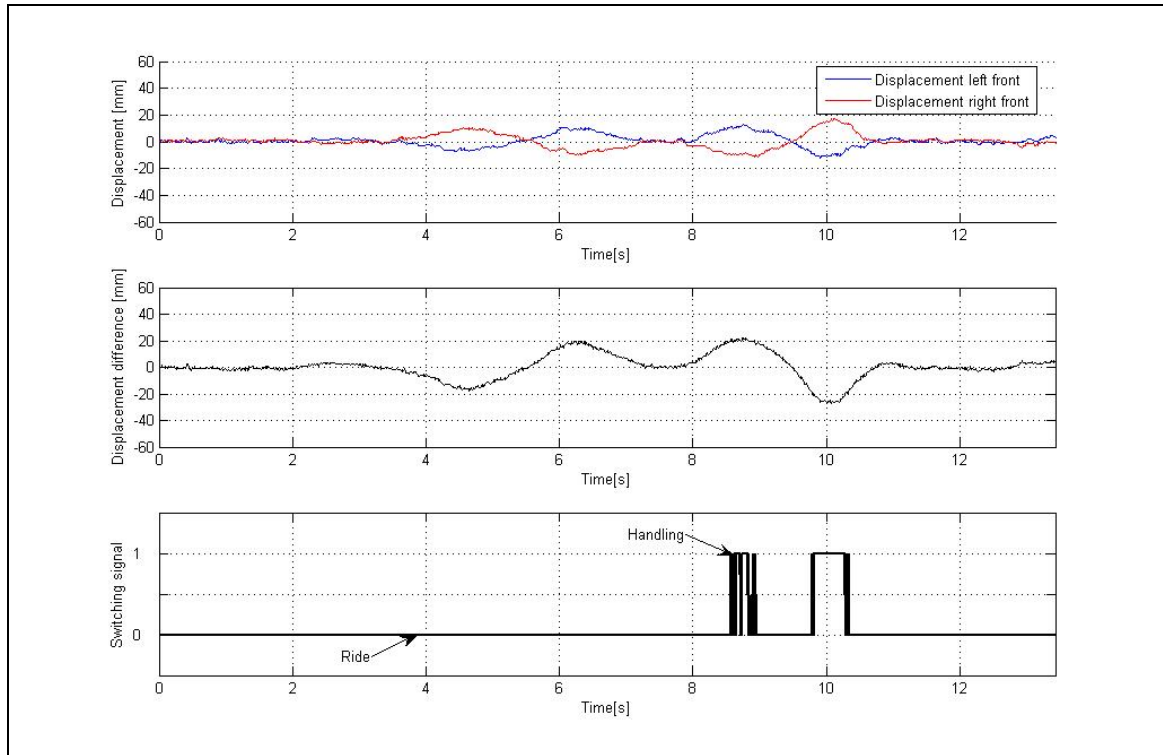


Figure 5.35 – Relative roll angle strategy for handling

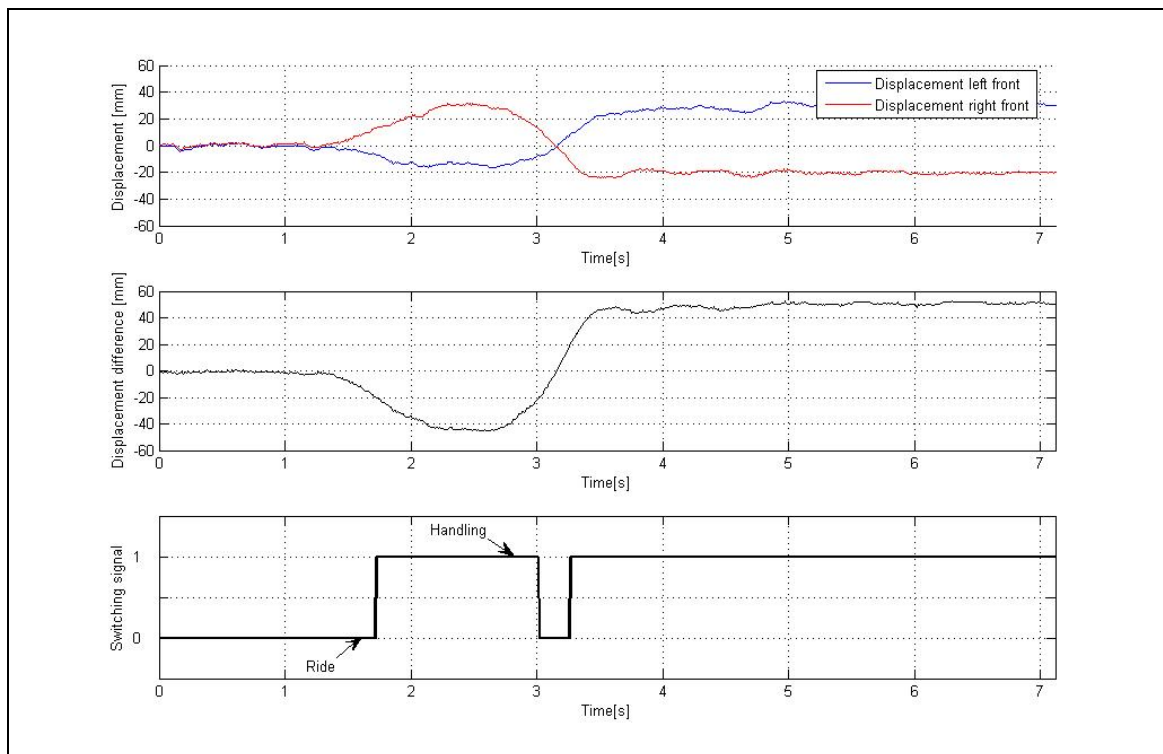


Figure 5.36 – Relative roll angle strategy for rollover

RRMS strategy results are indicated in Figures 5.37 to 5.42. This strategy works well for all conditions except for the double lane change where the “ride comfort” mode is selected about halfway through the test (see Figure 5.41). This is however the point where the vehicle is in the second lane before it starts turning back into the first lane. This should not result in serious problems, as long as the switching back to “handling” mode happens quickly enough.

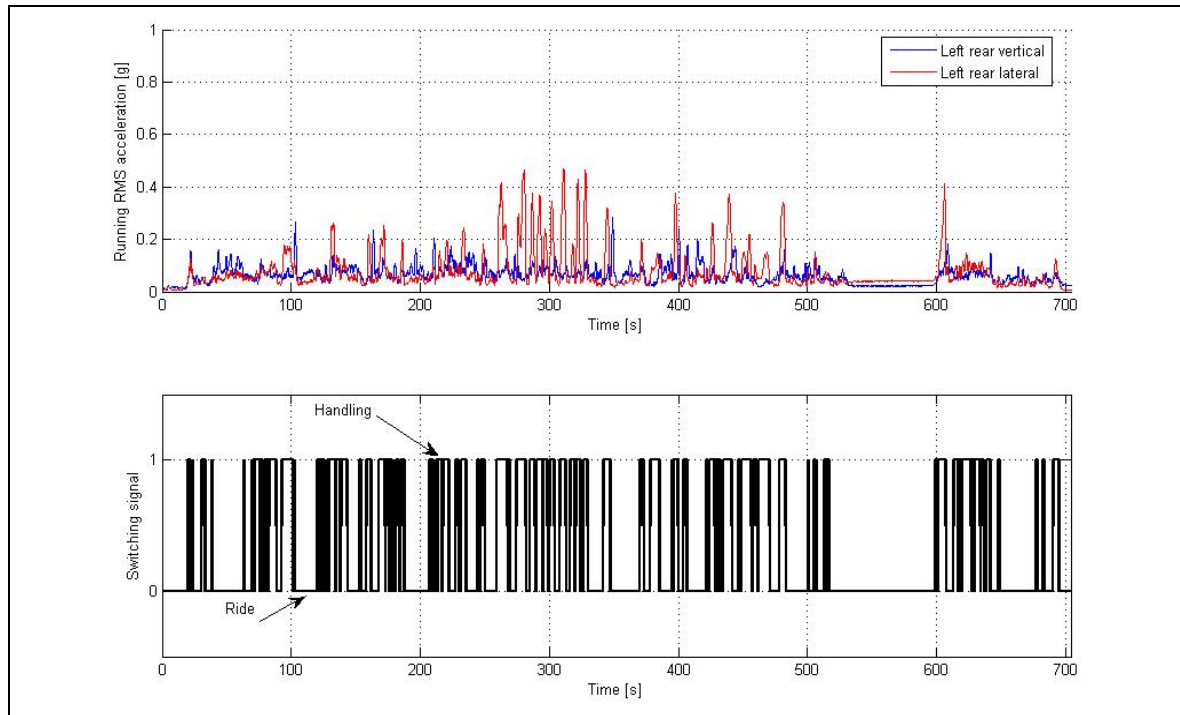


Figure 5.37 – RRMS strategy for city driving

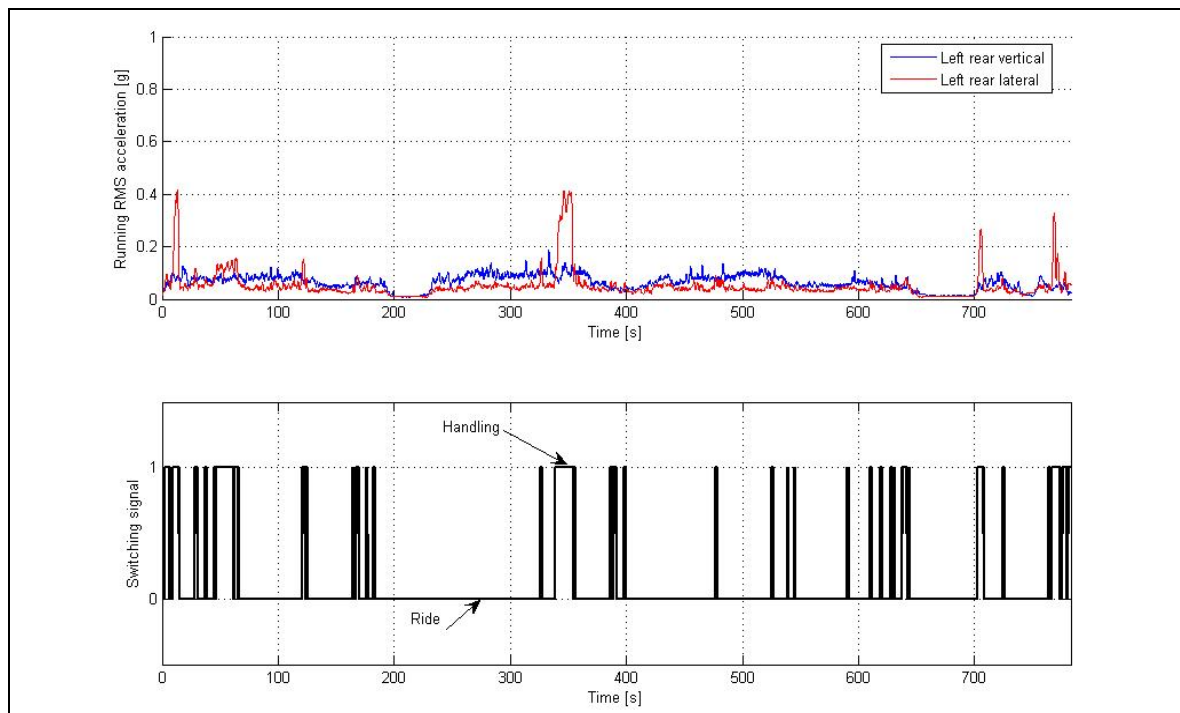


Figure 5.38– RRMS strategy for highway driving

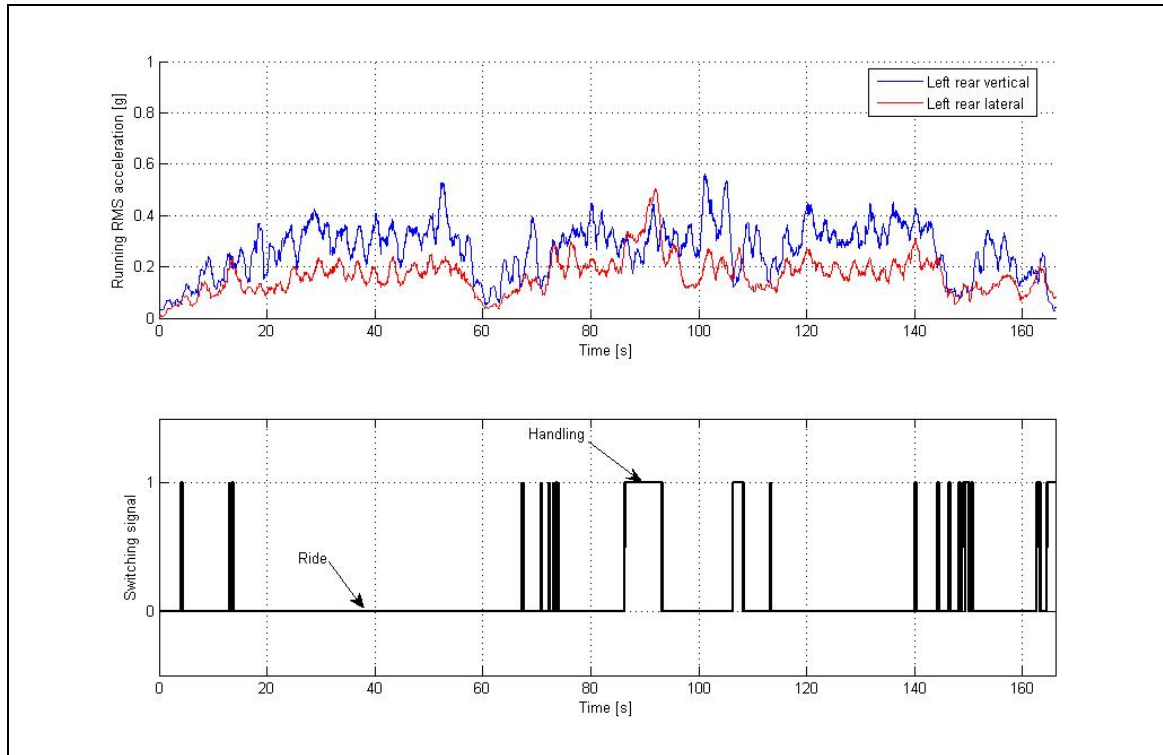


Figure 5.39– RRMS strategy for off-road driving

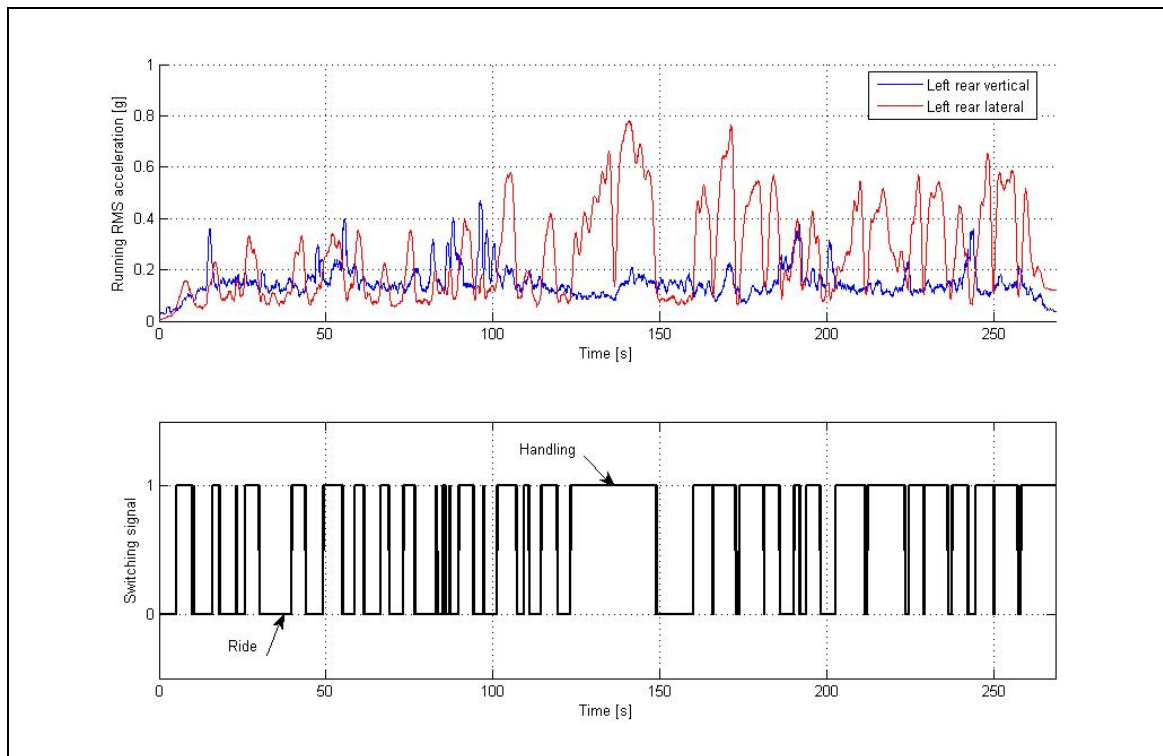


Figure 5.40– RRMS strategy for mountain pass

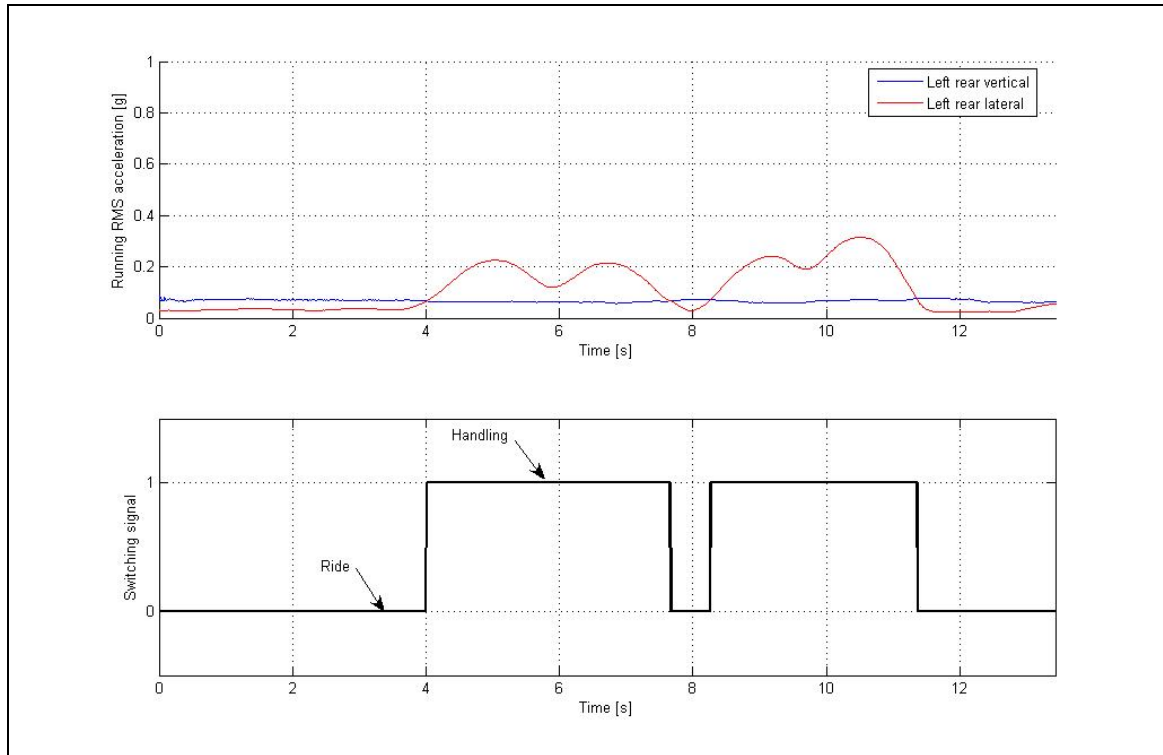


Figure 5.41– RRMS strategy for handling test

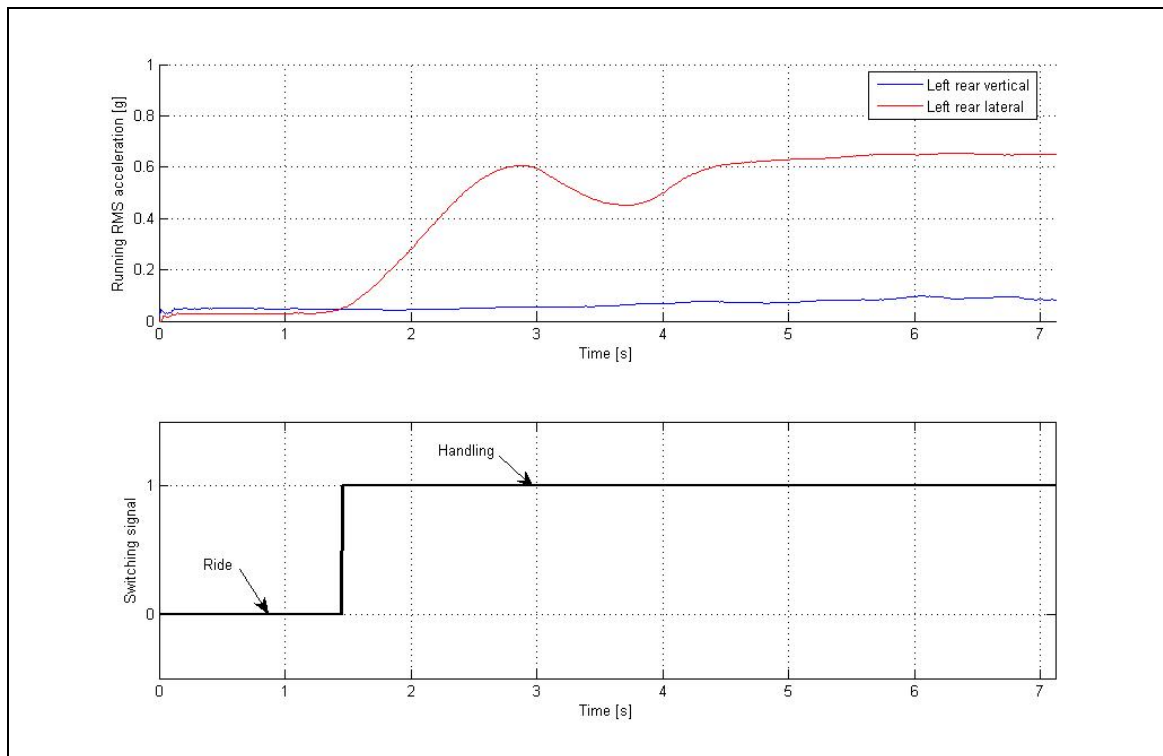


Figure 5.42– RRMS strategy for rollover test

For the analyses discussed above, a 100-point or 1 second RRMS was used. The number of points in the RRMS is expected to influence the response time, threshold levels and rejection of noise for short duration events. Figure 5.43 indicates the effect of the number of points in the RRMS on both the RRMS value and the resultant switching of the system for the handling test. The ideal behaviour would be if the system switches to “handling” mode immediately upon starting the test (*i.e.* at 3.7 seconds), and then remains in “handling” mode for the duration of the test. Figure 5.43(a) indicates the RRMS of the lateral acceleration for number of points from one to 500. The one point RRMS corresponds to the absolute value of the measured acceleration, while the 500 point RRMS corresponds to a five second RRMS. An increase in the number of points results in more “smoothing”. The RRMS magnitude also decreases with an increase in the number of points. This means that the threshold levels should be decreased as the number of points is increased.

The corresponding switching according to the RRMS strategy is indicated in Figure 5.43(b). The y-axis has no units but just indicates the switching pattern for the eight different analyses. For the one point RRMS, switching occurs quickly after the start of the test (at 3.7 seconds). The switching delay as a function of the RRMS duration is indicated in Figure 5.44. As the RRMS duration increases, the switching delay increases accordingly. A one point RRMS does however result in many switchovers between “ride” and “handling” mode. As the RRMS duration is increased, the number of switchovers decreases. RRMS durations of 2 seconds and higher result in the system staying in “handling” mode for the duration of the test. The percentage time spent in the “handling” mode is indicated in Figure 5.45 as a function of the RRMS duration. As the RRMS duration increases above 2 seconds, the initial delay results in a reduction of time spent in the “handling” mode. The choice of RRMS duration is therefore a trade-off between response time and switching behaviour. Values between one and two seconds seem to be a reasonable starting point.

## 5.7 Conclusion

It is concluded that, of all the proposed strategies, only the running RMS (RRMS) appears to work for all the test conditions. Vehicle tests must be performed to validate the strategy.

A combination of strategies may also result in improvements, *e.g.* the steering angle can be used to determine the switching point from “ride comfort” to “handling”, but switching back to “ride comfort” may then be based on the running RMS, or simply delayed by a fixed time to eliminate spurious switching.

If the terrain or driving conditions could be successfully identified, using for example artificial intelligence techniques (self organising maps, neural networks *etc.*), other concepts (*e.g.* steering angle *vs.* vehicle speed) may be successfully implemented by adapting thresholds according to operating conditions.

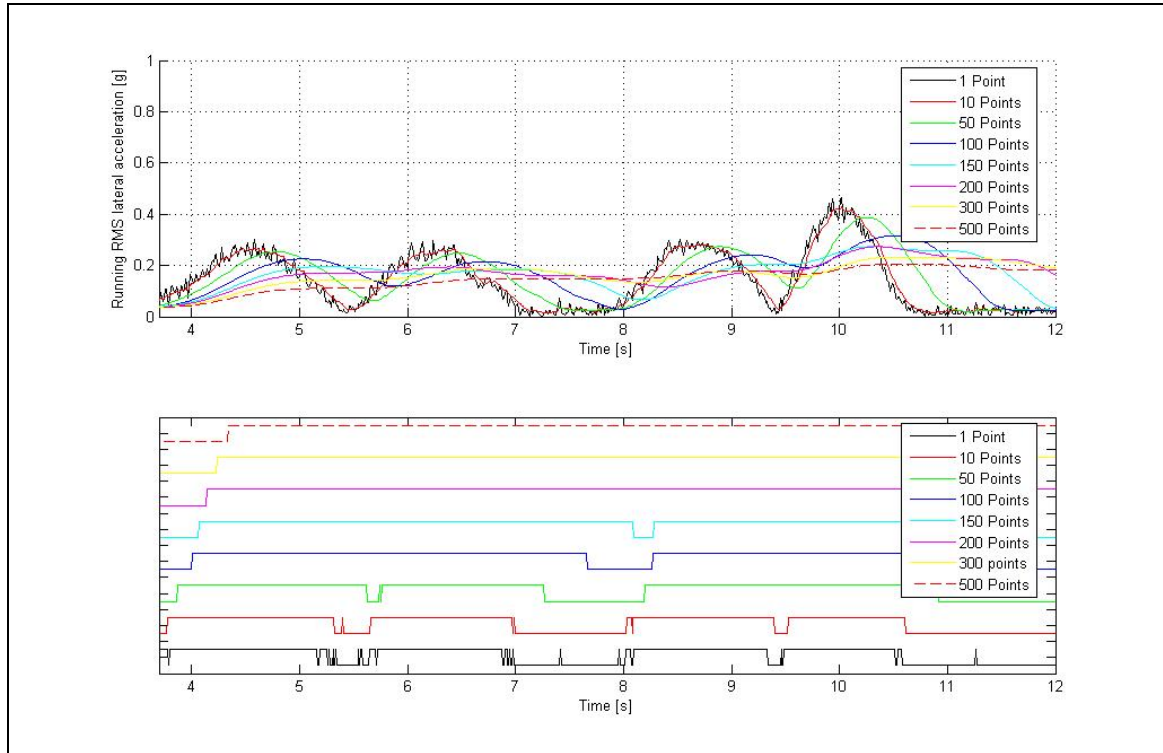


Figure 5.43 – Effect of number of points in the RRMS on switching for handling test

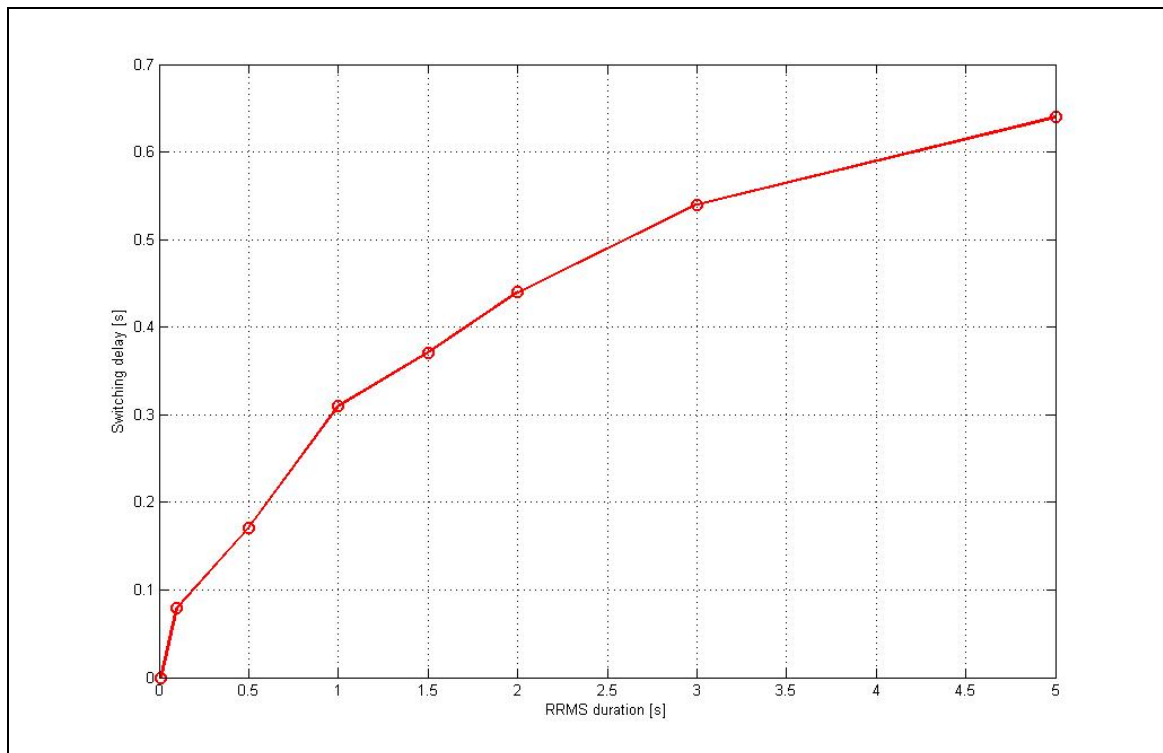
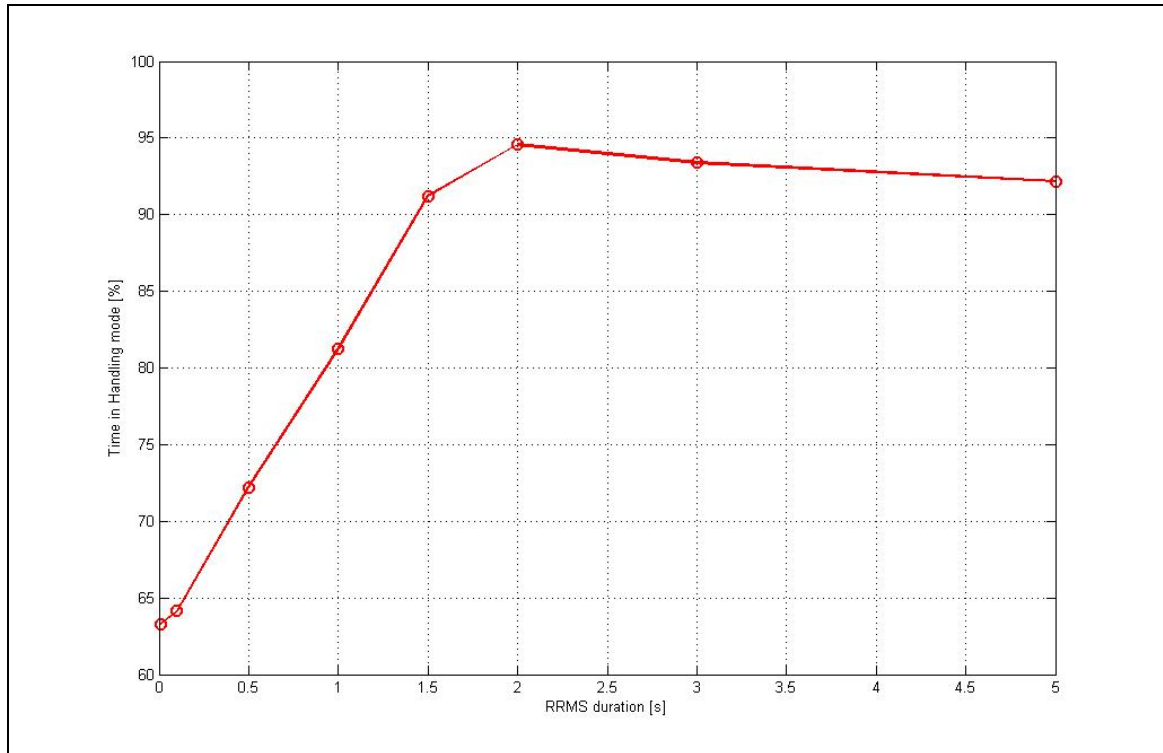


Figure 5.44 – Effect of number of points in the RRMS on the switching delay for handling test





**Figure 5.45** – Effect of number of points in the RRMS on time spent in “handling” mode for handling test

---

### *VEHICLE IMPLEMENTATION*

---

The integration of the 4S<sub>4</sub> suspension hardware, associated hydraulics and electronics on the test vehicle is discussed in this chapter. Ride comfort and handling test results, performed on the vehicle with the 4S<sub>4</sub> system fitted, are quantified, discussed and compared to baseline values obtained from testing of the baseline vehicle. Results are interpreted to determine whether the system works as intended and if the proposed “ride comfort vs. handling” decision strategy performs as predicted.

#### **6.1 Installation of 4S<sub>4</sub> hardware on test vehicle**

Mounting of the new suspension system to the test vehicle required relatively minor modifications to the chassis and axle mounting points. Mudguards on the inside had to be cut to make provision for the units. The struts are mounted on the same centerline as the baseline suspension system. One notable change is the absence of any rubber elements in the mounting arrangement compared to the baseline suspension system, where the dampers were mounted to the chassis and axles with rubber bushes. The original rubber bump stops and axle-locating links were not modified. This results in exactly the same suspension travel and suspension kinematics as the baseline suspension system.

The prototype 4S<sub>4</sub> units, as fitted to the right hand side of the test vehicle, are illustrated in Figures 6.1 to 6.5. Purpose-made top and bottom mounting brackets can be seen in Figure 6.1. The required wiring to the solenoid valves, as well as the hydraulic pipe for height adjustment is visible in Figure 6.5.

The pressure transducers, used to measure strut pressure, can be seen on top of the aluminium valve blocks in the figures.

Ride height adjustment capability was also incorporated on the test vehicle. The requirement for the ride height adjustability is that the system should be able to raise or lower the vehicle body up to the maximum or minimum elevation in 30 seconds. The minimum required oil flow for all four struts was calculated to be 1.57 l/min. The pump used has a volumetric displacement of 1.0 cm<sup>3</sup>/rev and delivers 3.0 litres per minute at a motor speed of 3000 r.p.m. The required oil reservoir should hold sufficient oil to guarantee functionality during lowering or raising of the vehicle. In order to have a sufficient reserve, a reservoir with a usable capacity of 5.9 litres was selected. The hydraulic power pack consists of a 12 Volt direct current (DC) electric motor, hydraulic gear pump and oil reservoir supplied by SPX Stone (Anon, 2005c). The assembled DC power pack is shown in Figure 6.6. The power pack is driven from a supplementary 12 Volt battery that is connected in parallel to the vehicle’s 12 Volt battery.

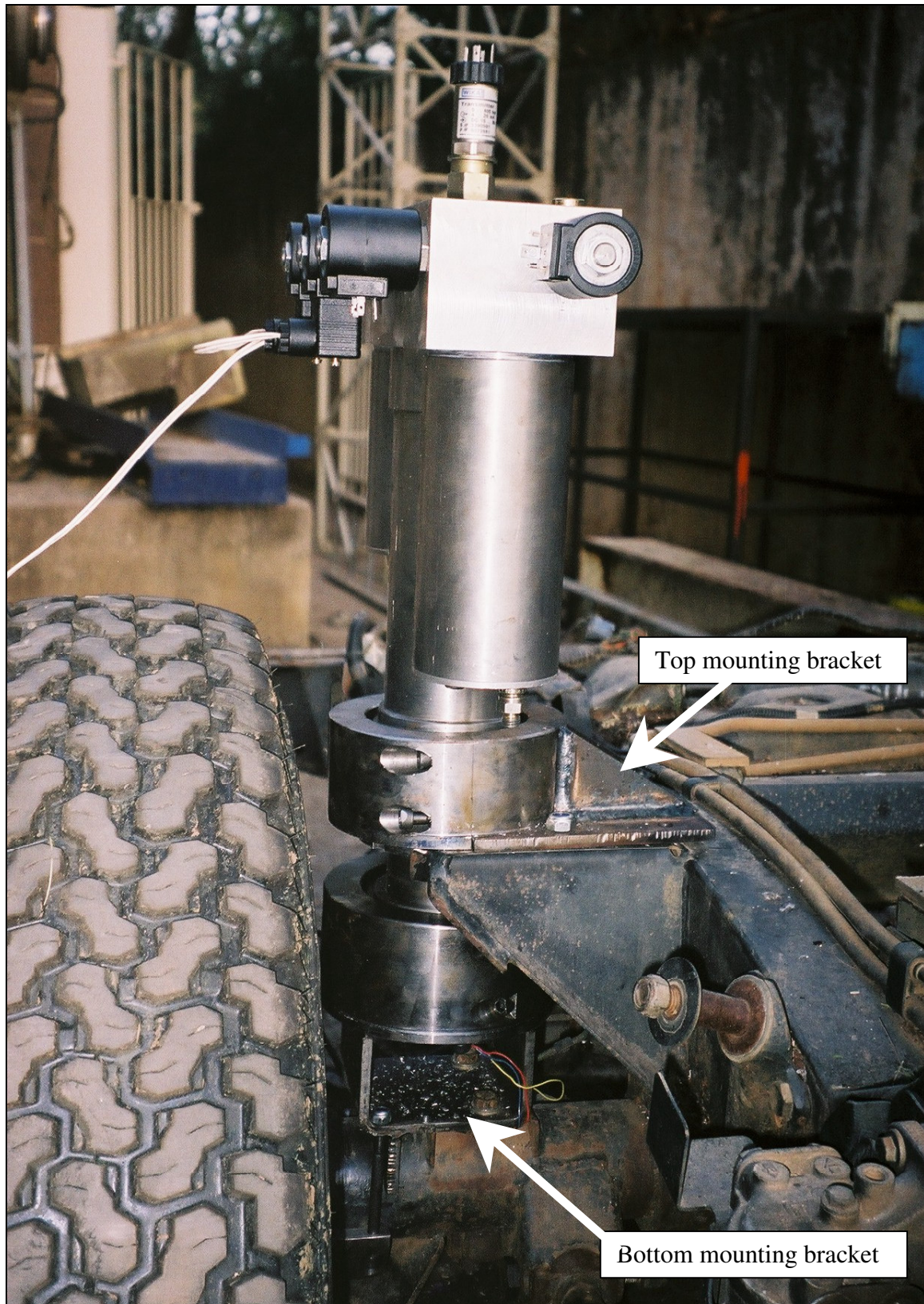


**Figure 6.1** - Right rear suspension fitted to chassis – front view



**Figure 6.2** - Right rear suspension fitted to chassis – inside view



**Figure 6.3** - Right front and right rear suspension fitted to chassis

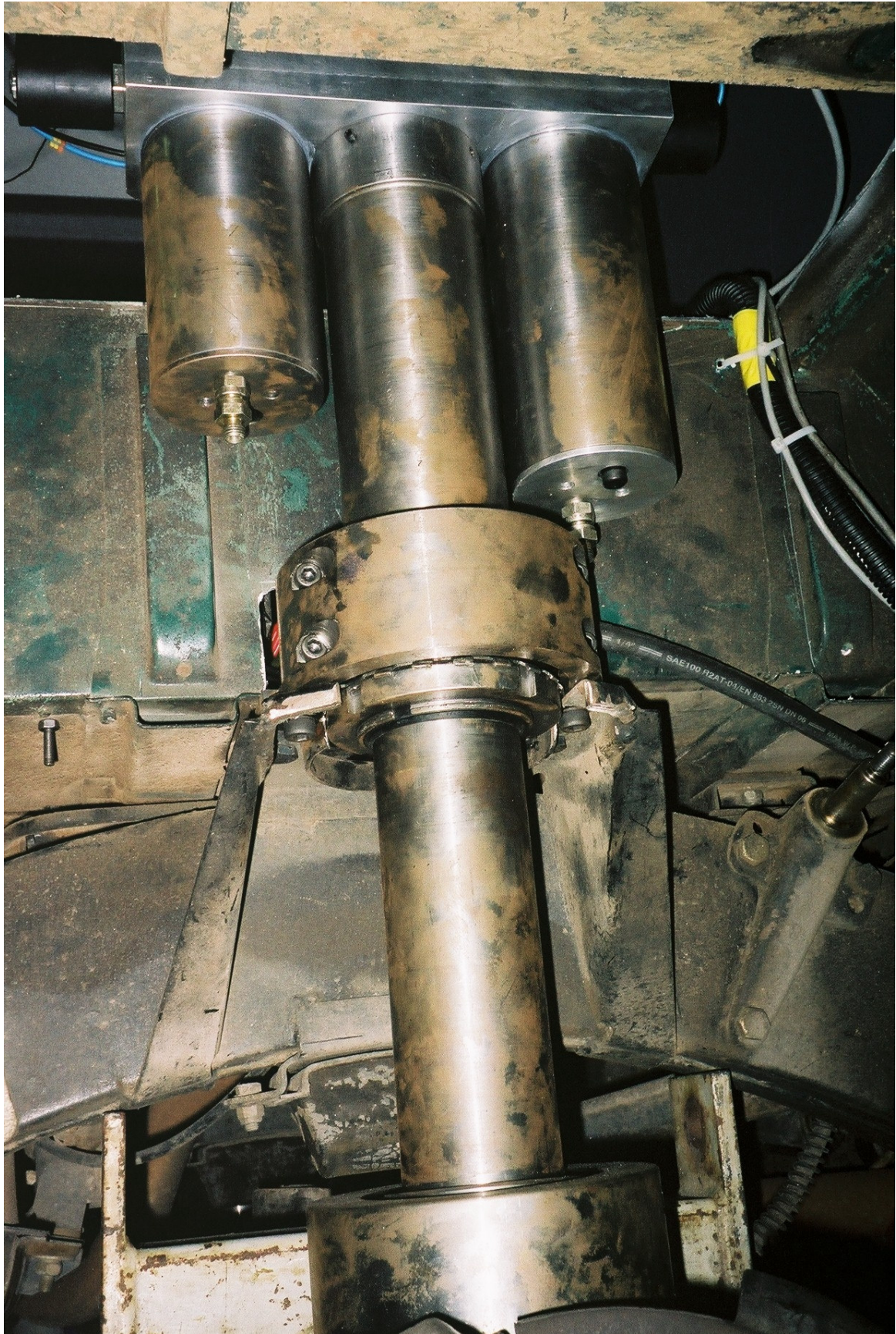


**Figure 6.4** - Right rear suspension fitted to test vehicle – side view

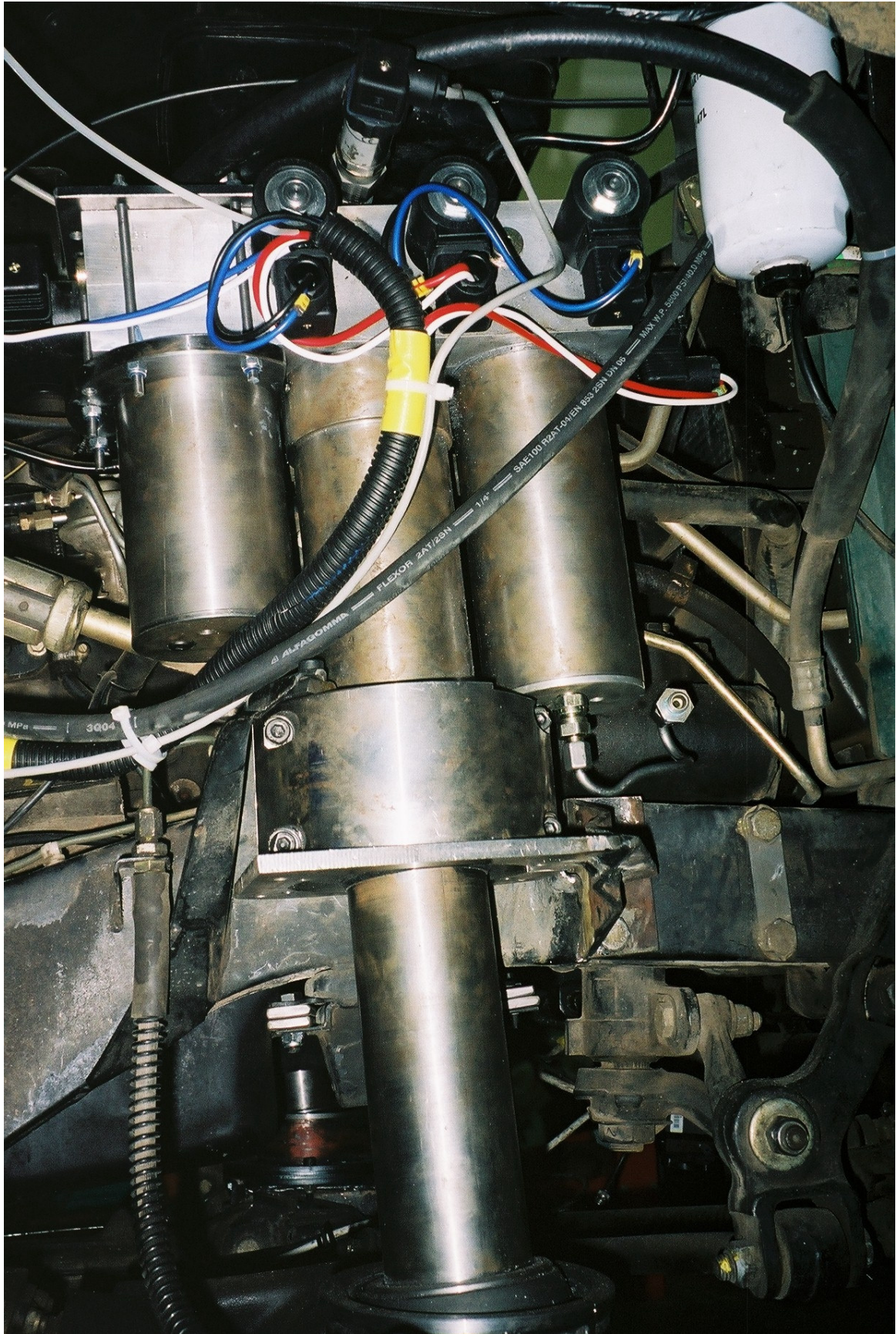


Figure 6.5 - Right front suspension fitted to test vehicle – side view



**Figure 6.6** - Assembled hydraulic power pack

A control manifold (Figure 6.7) is used to regulate the oil flow from the power pack to the individual struts, or to let the oil flow back to the oil reservoir.

Figure 6.8 indicates the hydraulic pump and associated reservoir and valves used for height adjustment, mounted in the load area of the vehicle. The solid-state relays used to switch the solenoid valves are also shown.

## 6.2 Control electronics

The 4S<sub>4</sub> control system controls ride height as well as the different spring and damper settings by means of solenoid valves. For this purpose it is necessary for the controller to process analog signals, from sensors measuring the vehicle's current operating conditions, to switch the solenoid valves and hydraulic power pack.

The control unit is based on a Coremodule 420 computer (PC-104 form factor) from AMPRO. Analog inputs are measured with a Diamond Systems MM-16-AT 16-bit analog to digital convertor card. The digital outputs, controlling the solid-state relays, are provided by a Diamond Systems Onyx-MM-DIO card. A schematic diagram of the control unit is provided in Figure 6.9.



Figure 6.7 - Control manifold for ride height adjustment

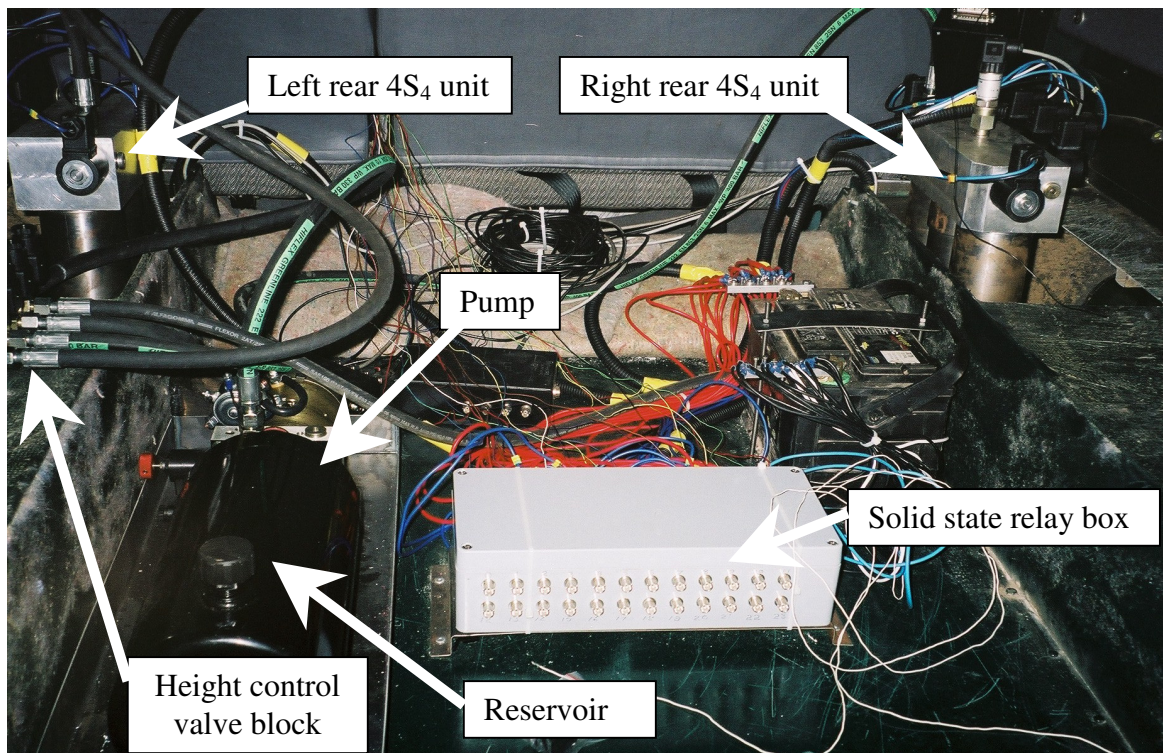


Figure 6.8 – Piping, wiring and electronics



The four relative strut displacements (one for each 4S<sub>4</sub> strut) as well as lateral and vertical accelerations are digitised by the analog to digital converter card. The ride height adjustment algorithms use the relative strut displacements while the “ride vs. handling” decision uses only the vertical and lateral body accelerations. After computing the required settings for all the valves, the valves are switched via the digital output card and solid state relays.

The control algorithm used for the “ride vs. handling decision” is the running RMS (RRMS) strategy proposed in chapter 5. The control loop runs at 100 Hz and employs a 100-point (or 1 second) RRMS. Both lateral and vertical accelerations are measured using a single Crossbow CXL04LP3 tri-axial accelerometer with built-in signal conditioning.

There are several issues that require special attention including zero positions, signal drift and noise. Initially the aim was to mount the accelerometers on the test vehicle in the vicinity of the center of mass. This mounting position resulted in high noise content from presumably the engine or drivetrain vibration. Although the mean signal was zero, the RMS resulted in an unacceptably high value. The accelerometer was subsequently moved to a position under the rear seat, where the engine vibration levels were significantly reduced. As an additional precaution, these accelerations were filtered with a 6<sup>th</sup> order analog low-pass Butterworth filter, with a 50 Hz cut-off frequency, to prevent aliasing and to filter out engine related vibration. The software also recorded measurements before each test in order to obtain the zero values on all sensors.

Relative strut displacements are measured using ICS-100 In-Cylinder Sensors from Penny & Giles. The linear potentiometer positioning sensors are mounted inside the struts, surrounded by the hydraulic oil. They offer low hysteresis, low electrical noise, stable output under temperature extremes and good dither vibration performance. No signal conditioning is necessary and the sensors only require a stable supply voltage to operate reliably.

All the valves are normally closed *i.e.* in the event of power failure (*e.g.* due to a flat battery, cable breaking or control computer that reboots), the 4S<sub>4</sub> system will revert to the “handling” mode (*i.e.* stiff spring and high damping with no height adjustment). This adds a failsafe capability to the system. Due to the required reverse logic, the switching signals indicated in the rest of this chapter have the opposite meaning to those in Chapter 5, *i.e.* a logic “1” now means “ride” mode (all valves open) and a logic “0” indicates handling mode (all valves closed).

### 6.3 Steady state handling

The steady state handling characteristics of the vehicle were tested using a constant radius test. In this test, the vehicle was driven around a circle of 25-meter radius starting at crawl speed and gradually increasing speed until the vehicle reached its handling limit (based on either sliding out or impending rollover). Data is represented as a graph of steering link displacement against lateral acceleration. A zero slope on this graph indicates neutral steer. A positive slope (steering angle increases as lateral acceleration increases) indicates understeer while a negative slope (steering angle decreases as lateral acceleration increases) indicates oversteer.

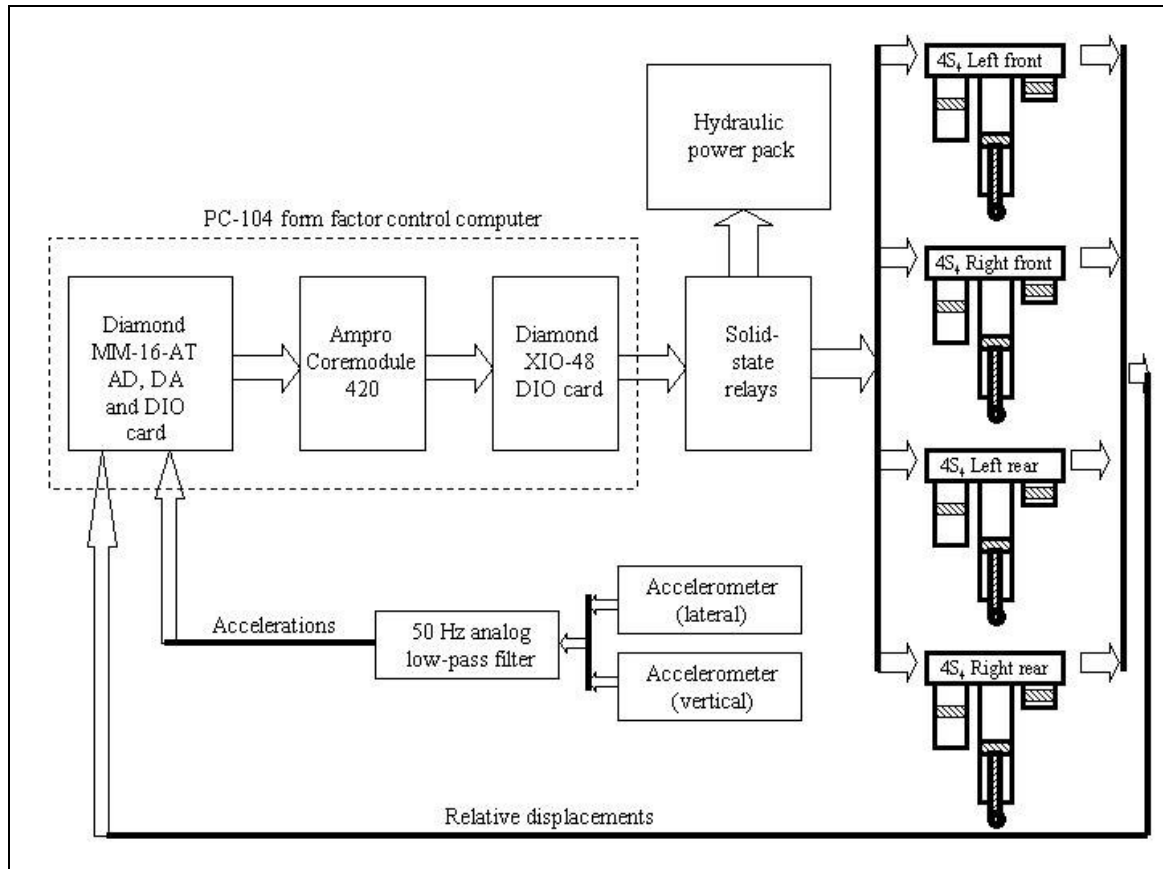


**Figure 6.9** - Control computer schematic

The effect of front:rear roll-stiffness balance was determined experimentally by performing preliminary tests without any control applied, but just switching the valves manually.

Measured characteristics are indicated in Figure 6.10 for the “handling” (all springs hard) mode, front suspension hard (rear soft) and rear suspension hard (front soft). All three settings steer neutrally up to 0.3 g after which oversteer develops for “all springs hard” and “rear springs hard”. In the case where the front suspension is hard, the vehicle steers neutrally up to 0.4 g and thereafter understeers. This indicates that switching the front suspension to the hard setting can induce understeer. The opposite scenario is probably also valid (*e.g.* switching the rear to hard will result in oversteer) although this is not as evident from the data in Figure 6.10. A possible handling strategy then is to switch the front suspension to hard when oversteer is detected and *vice versa* to counter understeer.

Figures 6.11 to 6.14 indicate the relative roll angle between the body and axle against lateral acceleration for different combinations of spring stiffness and ride height. It is clear that stiffening the suspension, as well as lowering the ride height, considerably reduces the body roll angle.

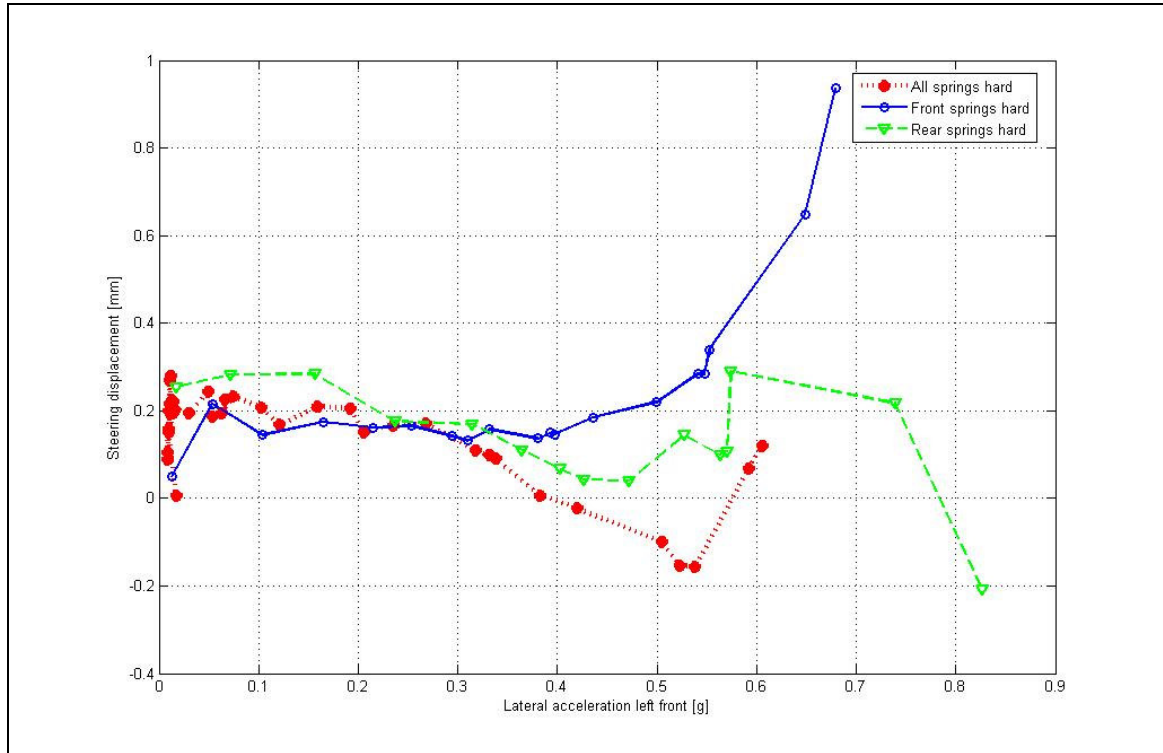


**Figure 6.10** – Constant radius test results

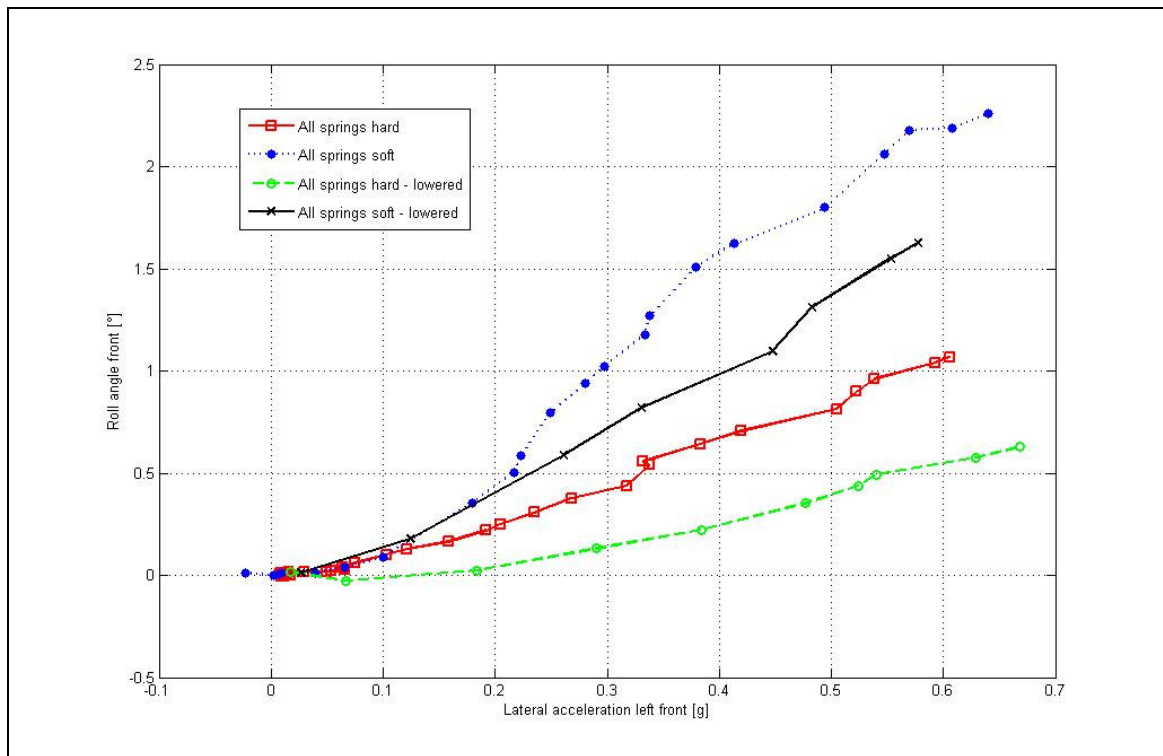


**Figure 6.11** – Relative roll angle front – effect of ride height

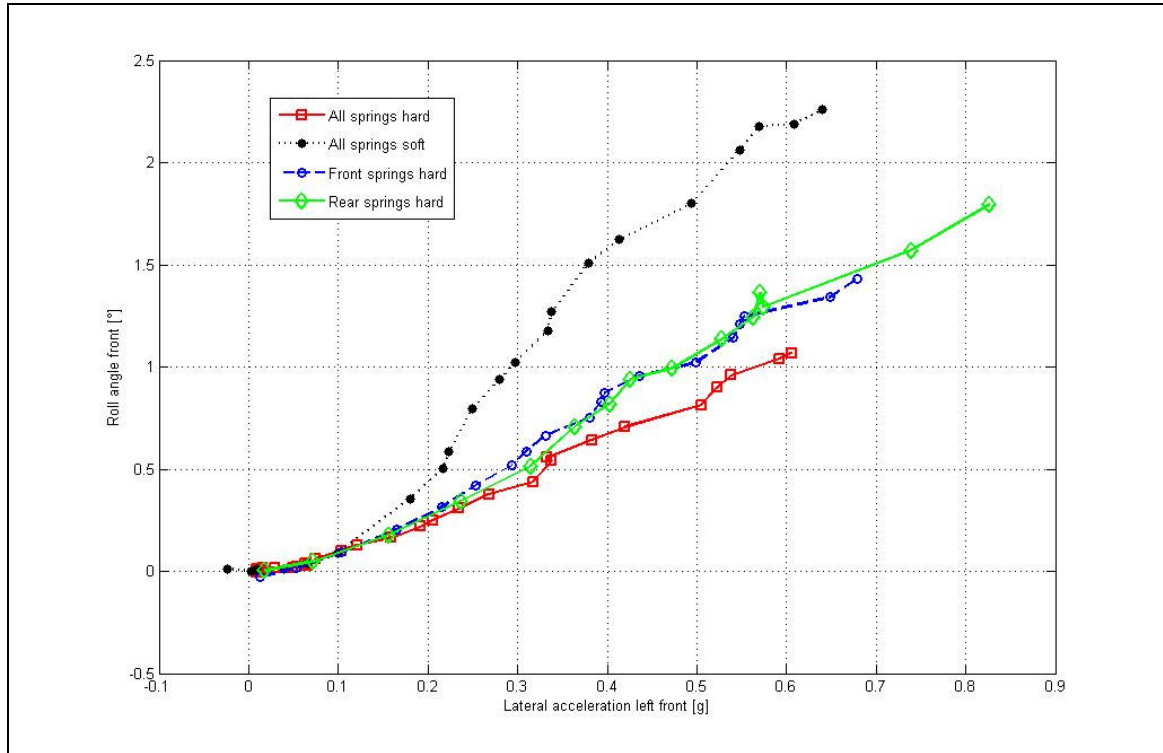


**Figure 6.12** – Relative roll angle front – effect of stiffness

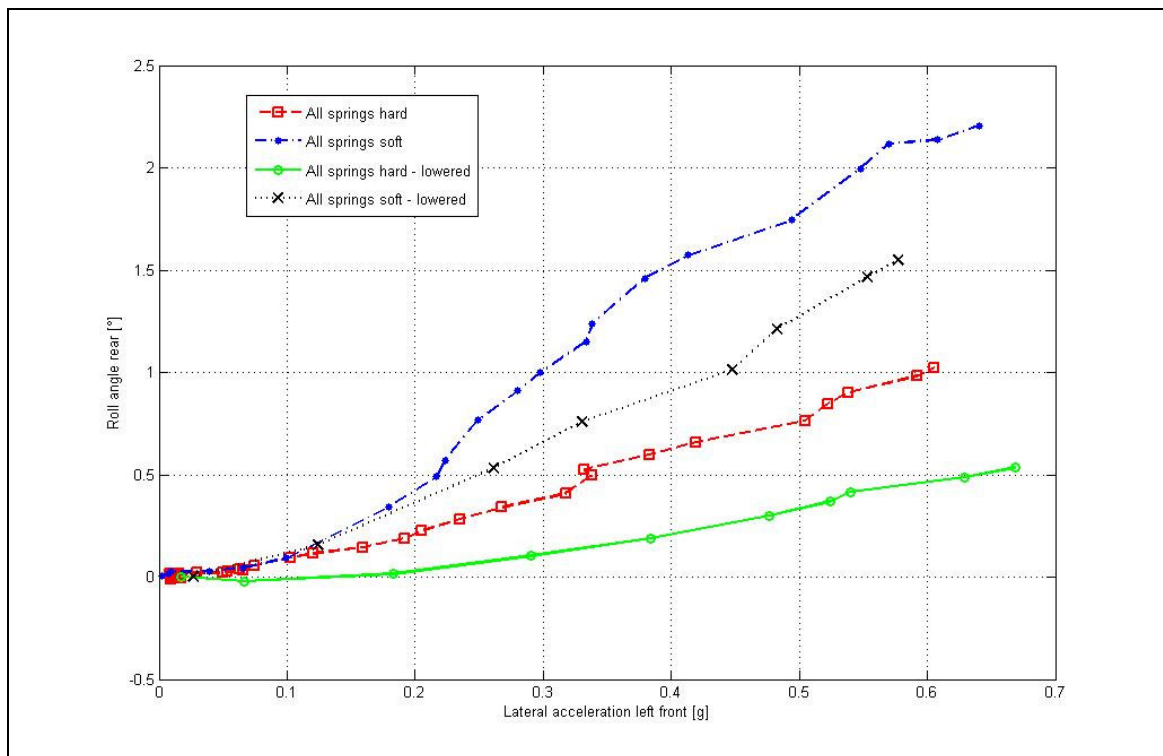


**Figure 6.13** – Relative roll angle rear – effect of ride height

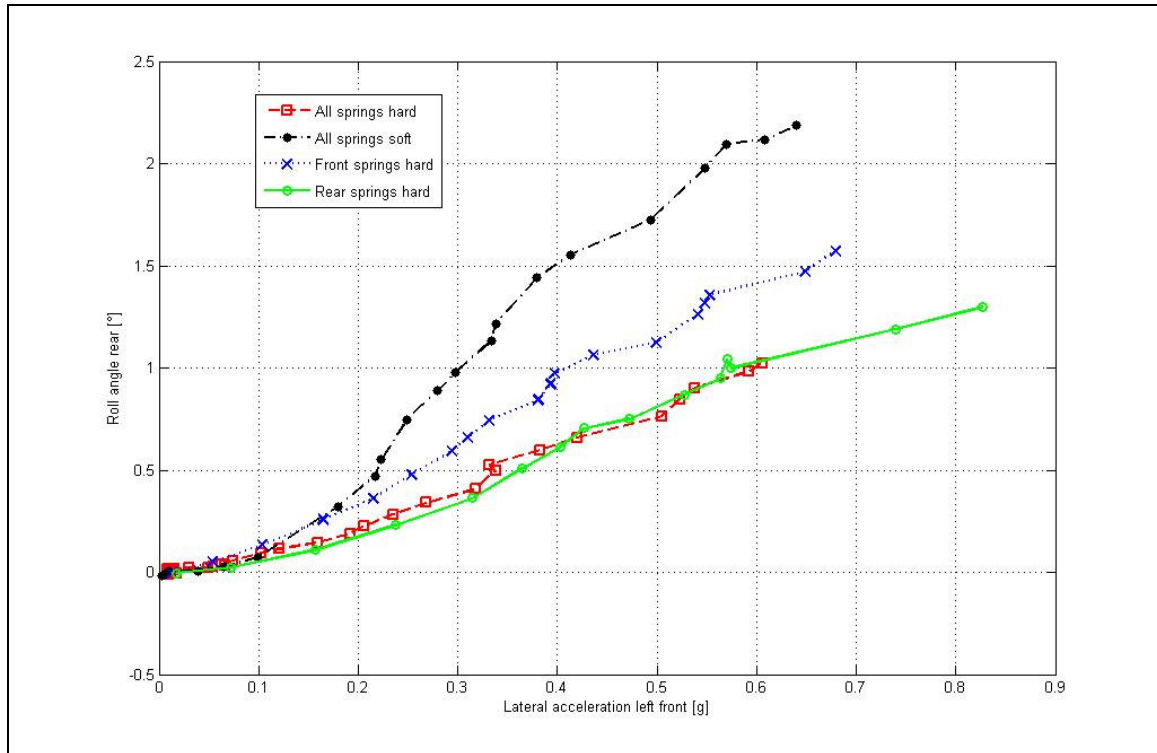


**Figure 6.14** – Relative roll angle rear – effect of stiffness

It is concluded that the hard suspension setting results in a considerable decrease in body roll. Further improvements might be obtained by switching the roll stiffness balance between front and rear to counter over- or understeer.

## 6.4 Dynamic handling

In order to evaluate the dynamic handling characteristics of the vehicle, the ISO 3888 double lane change test was performed. The vehicle body roll angle is used as a measure of handling.

Handling test results through the ISO 3888 double lane change at a vehicle speed of 58 km/h is indicated in Figure 6.15. At first valve selection was performed manually without any control applied. The vehicle was driven in a specific gear against the diesel engine’s governor in an attempt to keep the vehicle speed as constant as possible, and to ensure the same speed for different test runs. Test speeds did however vary slightly *e.g.* between 57 and 61 km/h, 70 and 75 km/h and 82 to 84 km/h respectively for the three gear ratios used for testing. The “ride” setting (soft spring and low damping), “handling” setting (stiff spring and high damping) and baseline vehicle is compared to each other at the same vehicle speed. It is observed that the “handling” setting results in significant improvements in roll angle (between 61 and 78 %) compared to the baseline vehicle. The “ride” setting is, however, very soft and results in unsatisfactory handling as expected. Roll angle was determined in two ways. The top graph indicates the body roll angle obtained by integrating the roll velocity measurement and correcting for drift. The bottom graph indicates the relative roll angle between the vehicle body and the axle, calculated from the measured relative displacement on the left and right hand struts. The values for all four peaks, based on the relative roll angle between the body and the axle, are

summarised in table 6.1. The “handling mode” results in significant improvements in roll angle, compared to the baseline vehicle.

**Table 6.1** – Comparison between baseline and 4S<sub>4</sub> relative roll angles through double lane change at 57 to 61 km/h

Peak	Baseline roll angle [°]	“Handling mode” roll angle [°]	“Ride mode” roll angle [°]	Improvement of “Handling mode” over baseline [%]
1	1.6	0.6	3.0	63
2	-2.1	-0.8	-4.5	62
3	-2.3	-0.9	-3.7	61
4	1.8	0.4	4.0	78

Figure 6.16 illustrates the effect of a 50 mm reduction in ride height on the body roll angle at 58 km/h. There is a slight improvement in roll angle for the “handling mode”. The major advantage is, however, seen in the “ride comfort mode” where the body roll angle is reduced substantially to the same levels as for the baseline suspension system. Note that the vehicle speed for the soft suspension with lowered ride height is marginally lower than for the other three test runs.

With these large differences between the “handling mode” and the “ride comfort” mode, it is imperative to investigate whether the RRMS control strategy will switch the 4S<sub>4</sub> system to “handling mode” for the duration of the manoeuvre. Figure 6.17 indicates results for RRMS control at 61 km/h. After a delay of 0.8 seconds, the system switches to “handling mode”. It does however switch back to “ride mode” between 3.1 and 4.2 seconds. Figures 6.18 and 6.19 indicate that at speeds in the region of 75 km/h, the system switches back to “ride mode” in some of the tests (Figure 6.19) but remains in the “handling mode” for others (Figure 6.18). At higher speeds (above 80 km/h) the system stays in “handling mode” as indicated in Figures 6.20 and 6.21. The switching between settings at the lower speeds is not regarded as a problem as the vehicle is still far from the handling limits. When approaching the handling limits at higher speeds, the RRMS control functions correctly by switching to “handling mode” and remaining in “handling mode” until the manoeuvre is completed. The initial switching delay is also reduced from 0.8 seconds at 61 km/h to 0.5 seconds at 75 and 0.4 seconds at 84 km/h. The vehicle will therefore travel 13.5 m at 61 km/h and 9.2 m at 83 km/h before the 4S<sub>4</sub> system switches from the “ride mode” to the “handling mode”. In actual fact the valve response time of between 0.04 and 0.09 seconds (see paragraph 4.7.6 in Chapter 4) should be added to this initial switching delay of the control strategy.

The comparison between roll angle for the “handling mode” and RRMS control is indicated in Figures 6.22 and 6.23. Both figures indicate that the RRMS control does not perform as well as the “handling mode” with a definite offset noticeable in the data. This is attributed to the delay from the start of the test until the RRMS strategy selects the handling mode. This switching delay results in an initial roll angle on the soft suspension. Once switching takes place, the large accumulator, and the oil in it, is isolated from the rest of the system. The portion of oil removed, results in a differential change in ride height between left and right and therefore an initial body roll angle. After switching takes place, the resulting roll angle corresponds to the “handling mode”, with an offset equal to the initial roll on the soft suspension. This offset in body roll angle is eliminated when the system switches back to “ride comfort mode”. The roll angles at 70 and 82 km/h however still compare favourably with the baseline roll angle at 57 km/h.

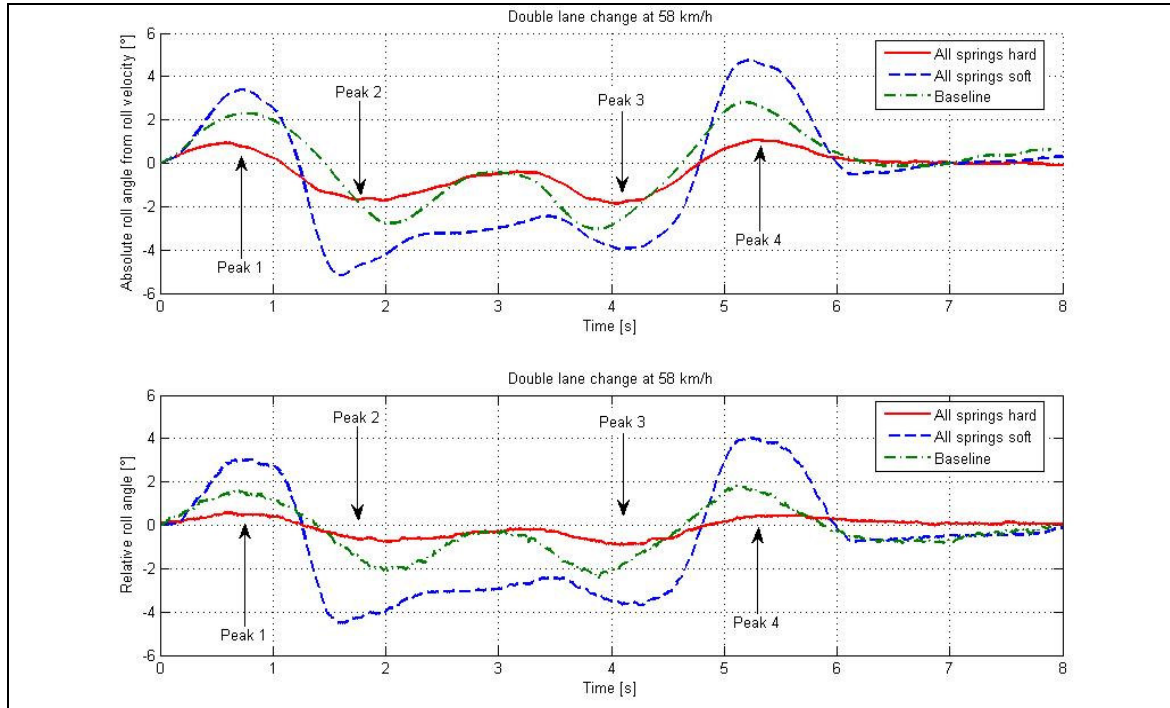


**Figure 6.15** – Body roll with 4S<sub>4</sub> settings compared to baseline at 58 km/h

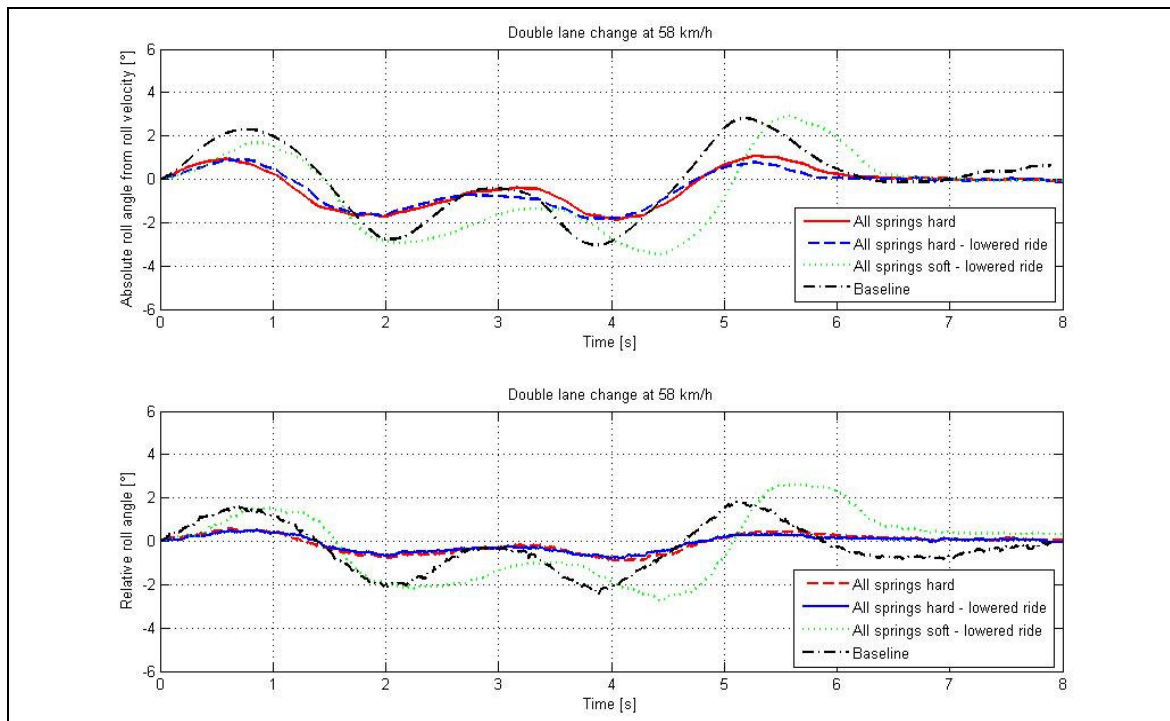


**Figure 6.16** - effect of ride height on body roll at 58 km/h

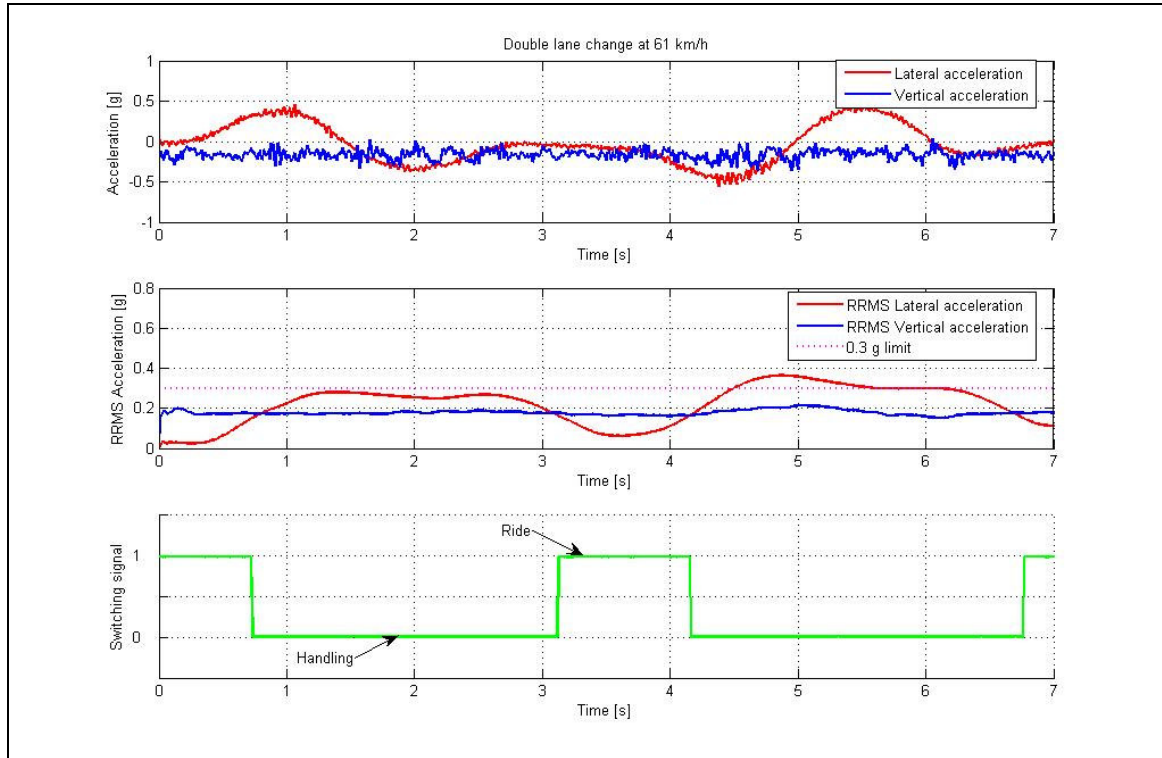


**Figure 6.17** - RRMS control at 61 km/h

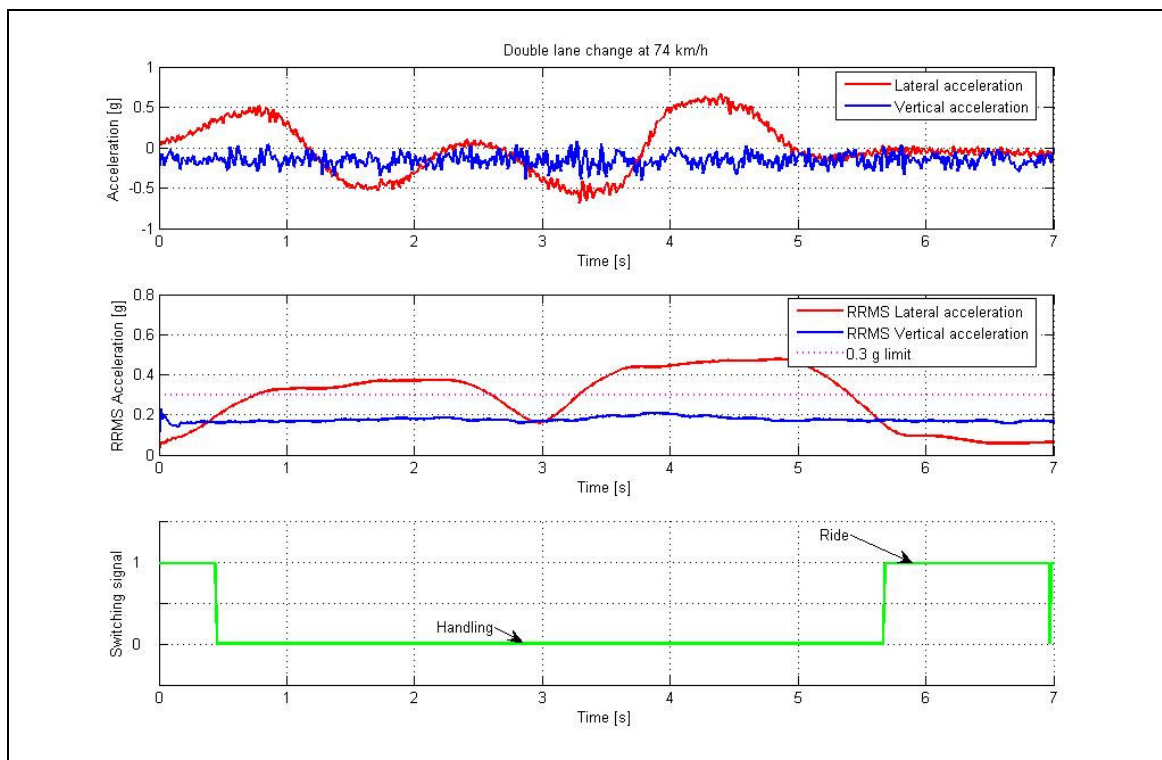


**Figure 6.18** - RRMS control at 74 km/h



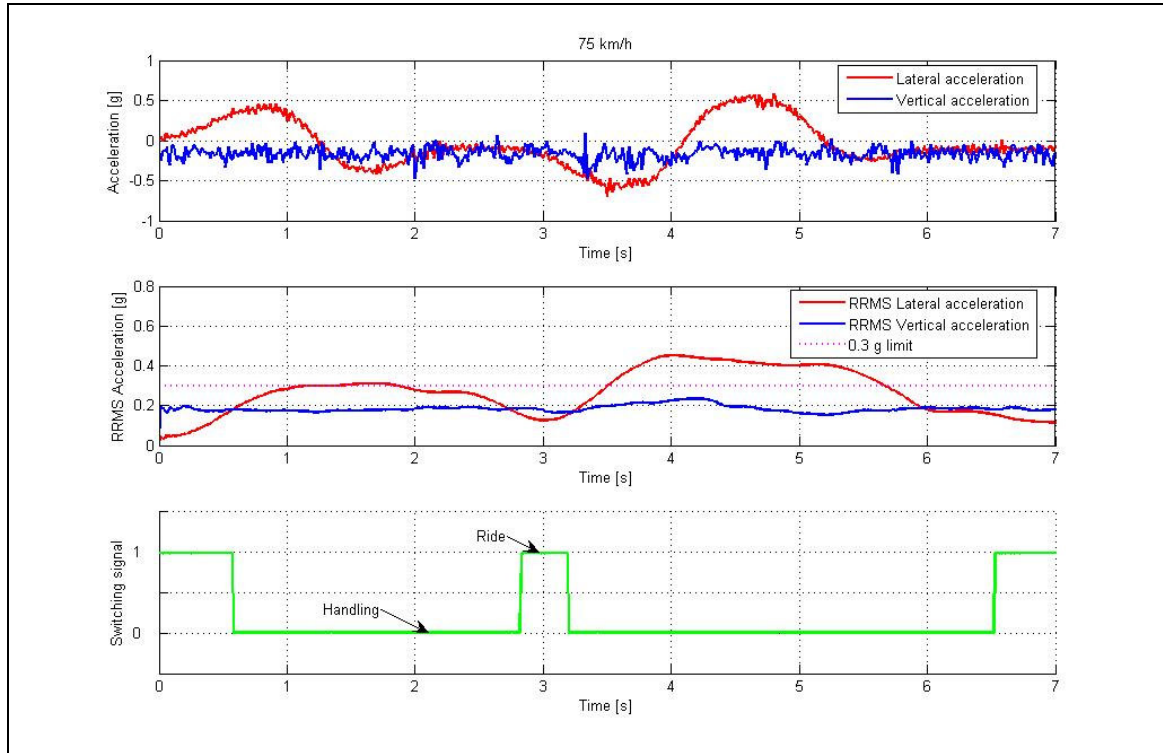


Figure 6.19 - RRMS control at 75 km/h

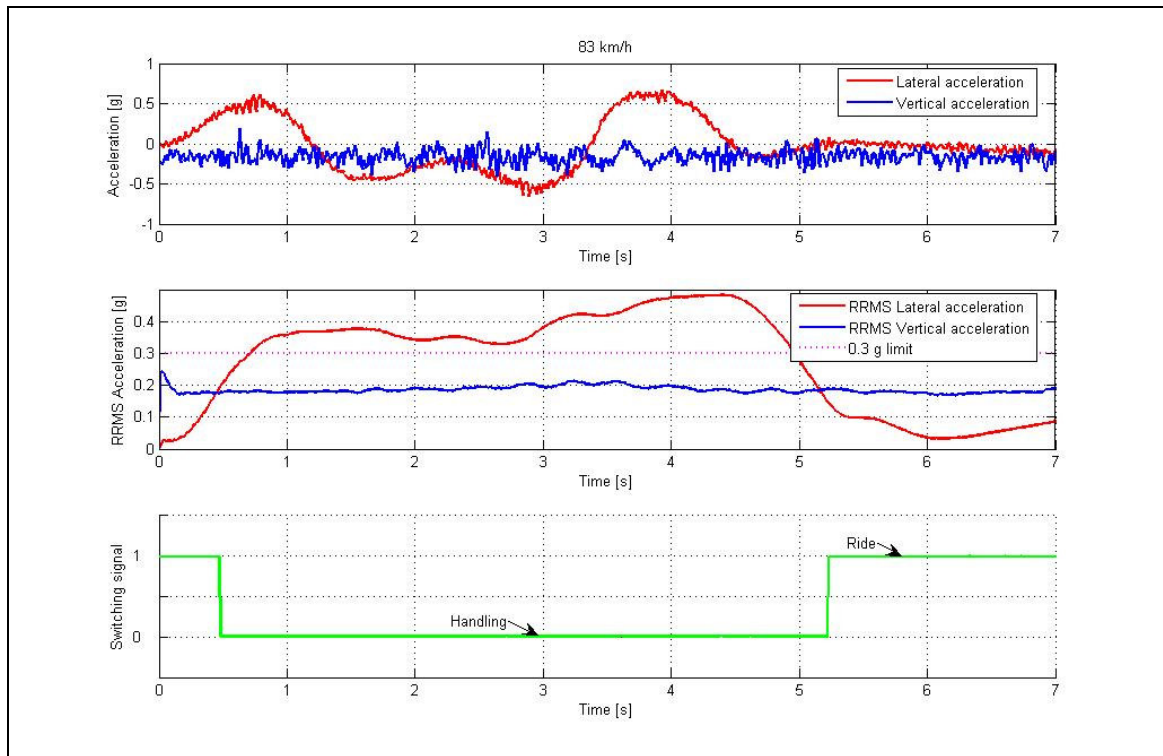
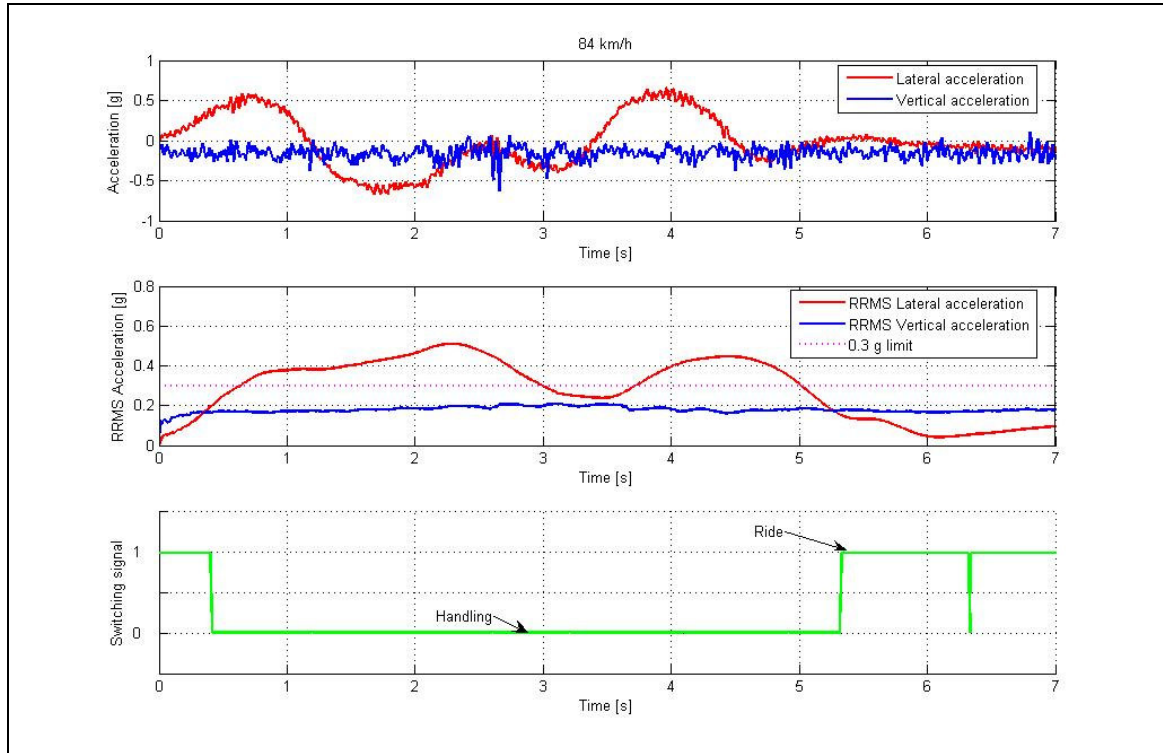
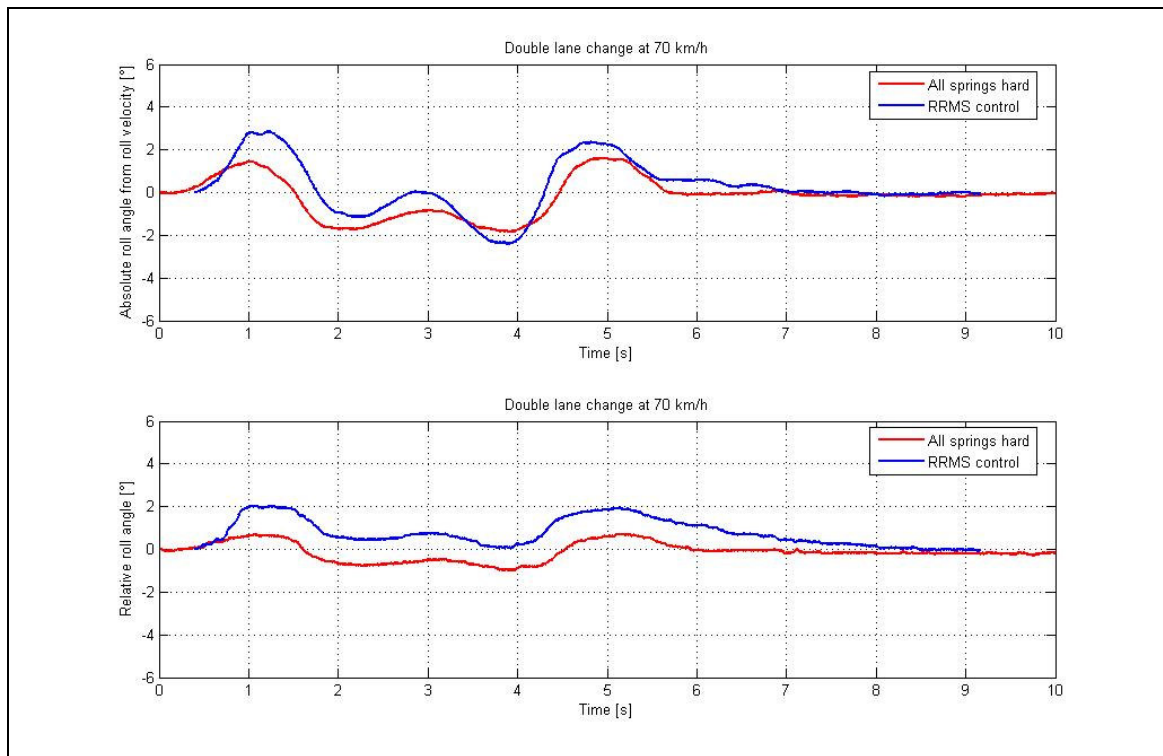


Figure 6.20 - RRMS control at 83 km/h



**Figure 6.21** - RRMS control at 84 km/h



**Figure 6.22** - RRMS control compared to “handling mode” at 70 km/h

As a final comparison, Figures 6.24 and 6.25 indicate the roll angle for the handling mode at three different speeds (Figure 6.24) and the corresponding roll angle for the RRMS control mode (Figure 6.25). The peak-to-peak roll angles of the RRMS strategy at 73 and 83 km/h are significantly lower than at 60 km/h, primarily due to the fact that the strategy does not switch between “handling” and “ride” modes during the manoeuvre, as it tends to do at 60 km/h. This is favourable as it will improve ride comfort at lower speeds but, at the onset of a handling manoeuvre, switch to handling as the vehicle speed increases, improving high-speed vehicle stability.

## 6.5 Ride comfort

For the evaluation of ride comfort, the vehicle is driven over the Belgian paving (see Figure 2.21 in Chapter 2) at five speeds. The vertical accelerations, measured at three positions on the vehicle body and weighed according to the BS6841 standard, is used as a measure of ride comfort.

In order to test if the RRMS control strategy performs correctly, the vehicle was driven over the Belgian paving track at different speeds in both the “ride comfort” mode (all soft) and the RRMS control mode. Figure 6.26 indicates that the strategy indeed switches to the soft setting on the Belgian paving. At 4.8 seconds the driver changes direction to avoid the very rough test track following the Belgian paving. During this manoeuvre the RRMS control strategy switches the suspension to “handling” mode. Figure 6.27 confirms that there is no significant difference in the ride comfort, at the three measuring positions and five speeds, when the “ride mode” is compared to the RRMS control. The data points for “handling mode” are only indicated for the lowest speed of 17 km/h.

The RRMS strategy performs correctly for driving in a straight line over a rough road. The “ride comfort mode” results in an improvement in ride comfort, of between 50 and 80%, compared to the “handling mode”. A significant improvement in ride comfort with respect to the baseline values is however not experienced due to the following reasons:

- i) The current 4S<sub>4</sub> hardware has the same damper setting front and rear while on the baseline vehicle, front damping is considerably lower than rear damping.
- ii) The low damping characteristic on the current 4S<sub>4</sub> hardware has more or less the same characteristics as the rear dampers on the baseline vehicle due to pressure drops in the bypass valves and valve block channels. Significant improvements in ride comfort are only expected for damper characteristics less than 50% of the baseline values.
- iii) The baseline vehicle’s rear dampers are installed at an angle while the 4S<sub>4</sub> dampers are vertical, thus exerting greater damper force even though the force-velocity characteristics are similar.

Refinement of the 4S<sub>4</sub> damper settings for the low damping characteristic is necessary before ride comfort improvements will be noticed. This will mean enlarging the diameter of the existing ports and channels, and fitting valves with a lower pressure drop or higher capacity.

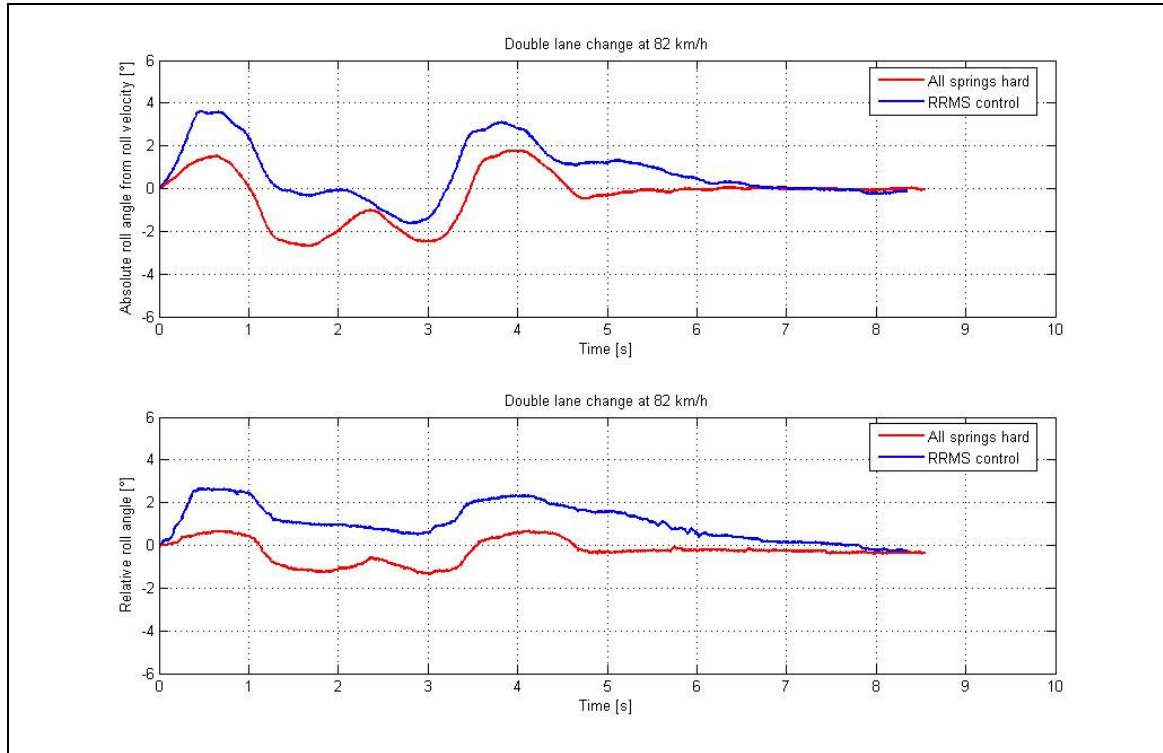


**Figure 6.23** - RRMS control compared to “handling mode” at 82 km/h

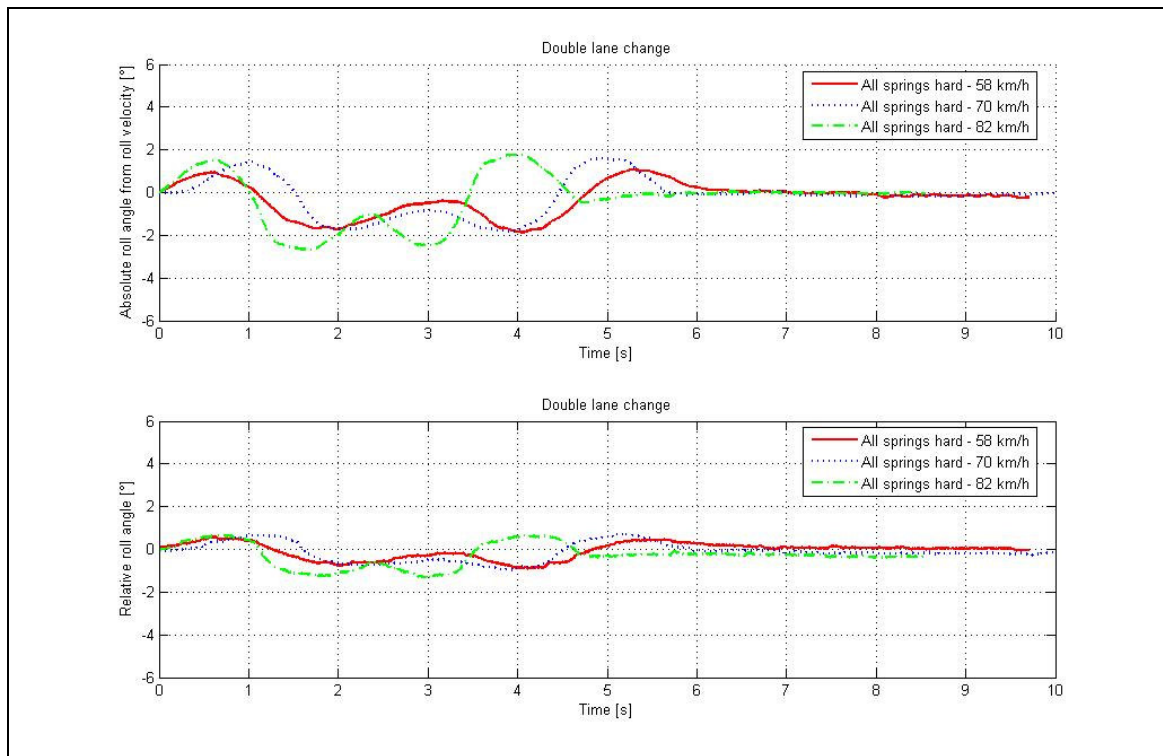


**Figure 6.24** - Body roll for “handling mode” at different speeds

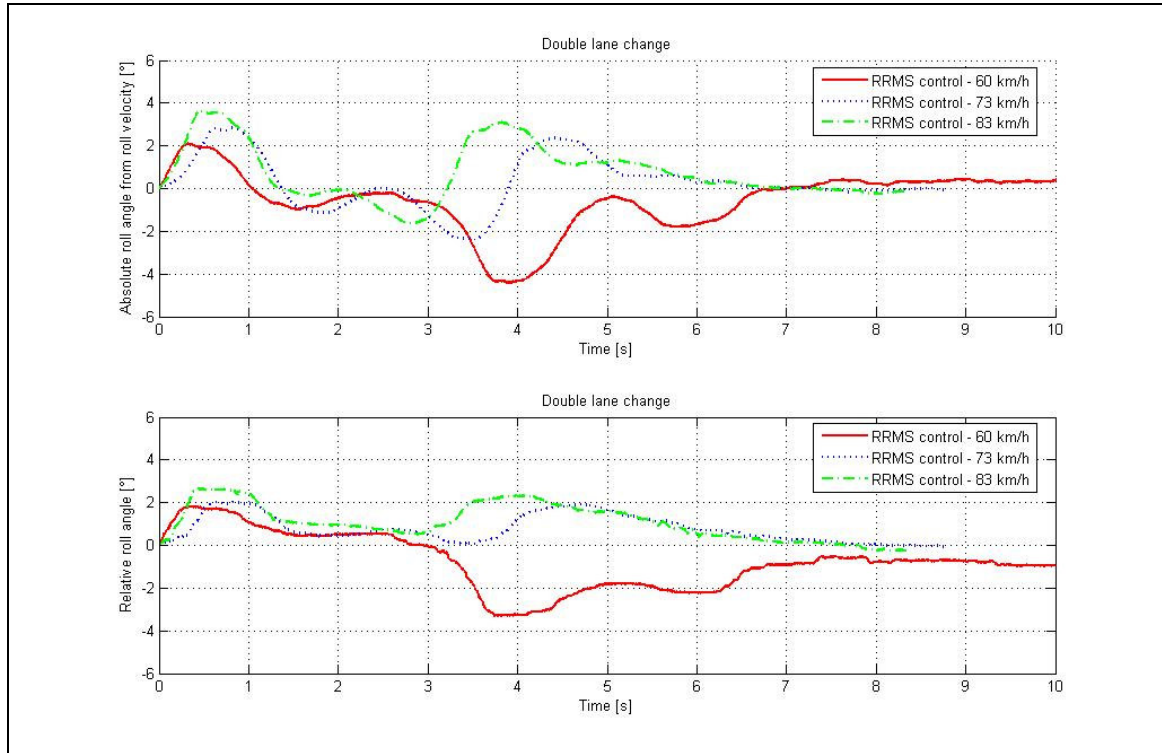


**Figure 6.25** - Body roll for RRMS control at different speeds

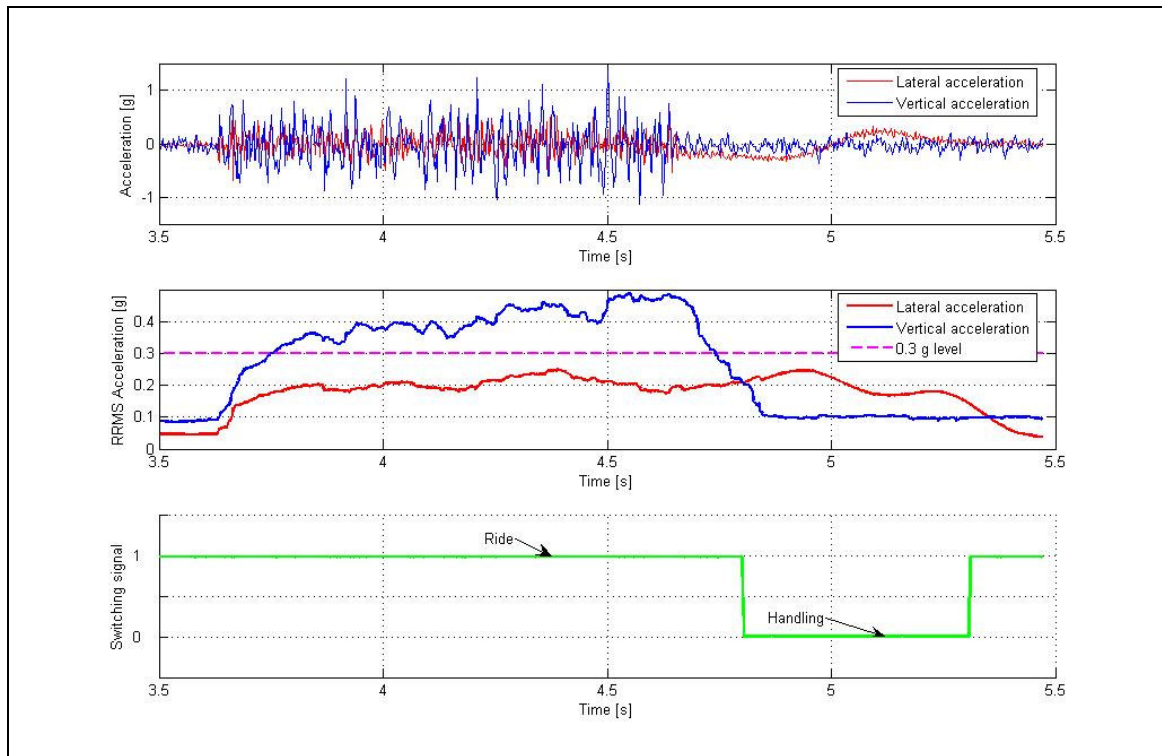


**Figure 6.26** - RRMS control over Belgian paving at 74 km/h

### 6.6 Mountain pass driving

Performance of the RRMS strategy during mountain pass driving is shown in Figure 6.28. The RRMS control switches to “handling mode” whenever the RRMS lateral acceleration exceeds the vertical acceleration. Subjectively the vehicle feels very stable. The subjective improvement in ride comfort is considerable compared to “handling” mode.

### 6.7 City and highway driving

Results for city driving and highway driving are indicated in Figures 6.29 and 6.30 respectively. Switching to “handling mode” occurs rarely and only when cornering or changing lanes. Again subjectively the system performs as expected with a very noticeable improvement in ride comfort compared to “handling” mode, but also inspiring confidence when performing handling manoeuvres.

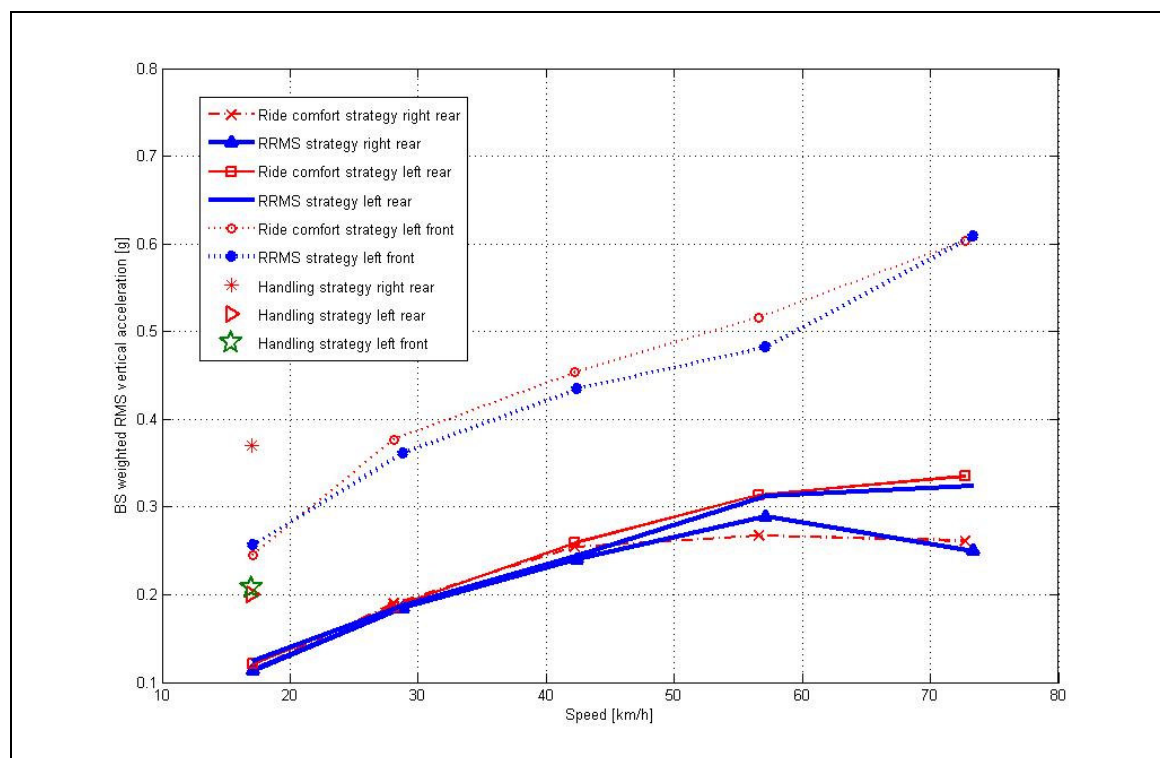


**Figure 6.27** - Ride comfort of RRMS control compared to “ride mode”

### 6.8 Conclusions

The 4S<sub>4</sub> suspension system performs according to expectations. Ride comfort in the “ride” setting, is a 50 to 80 % improvement over the “handling” setting. Body roll angle in the “handling” setting, is a 61 to 78 % improvement over the baseline vehicle and a 47 to 90 % improvement over the “ride comfort” setting.

The RRMS control strategy performs well under most circumstances, the only drawback being the time taken to switch to “handling” mode during the double lane change manoeuvre. Switching between “ride comfort mode” and “handling mode” occurs seamlessly, without the driver noticing the switching. The low damper characteristic is not sufficiently low enough to improve the ride comfort compared to the baseline vehicle.

The differences between “ride comfort mode” and “handling mode” are significant, illustrating that the principle works according to expectation.

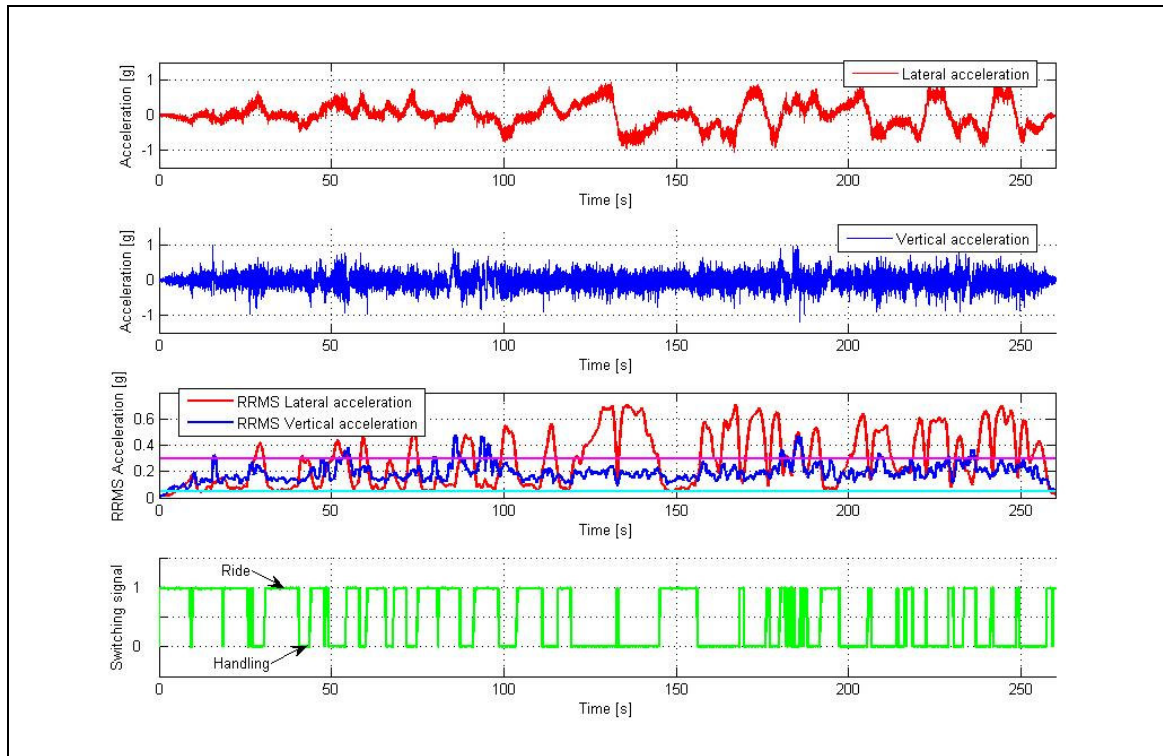


**Figure 6.28** - RRMS control during mountain pass driving

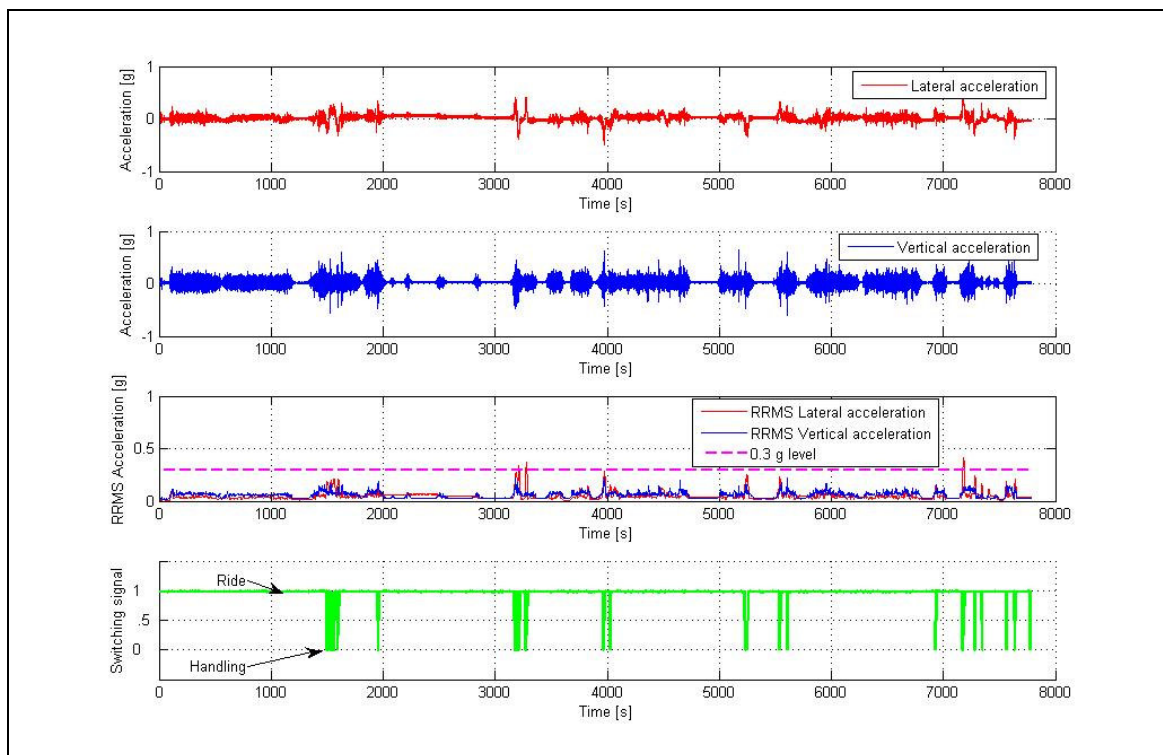


**Figure 6.29** – City driving

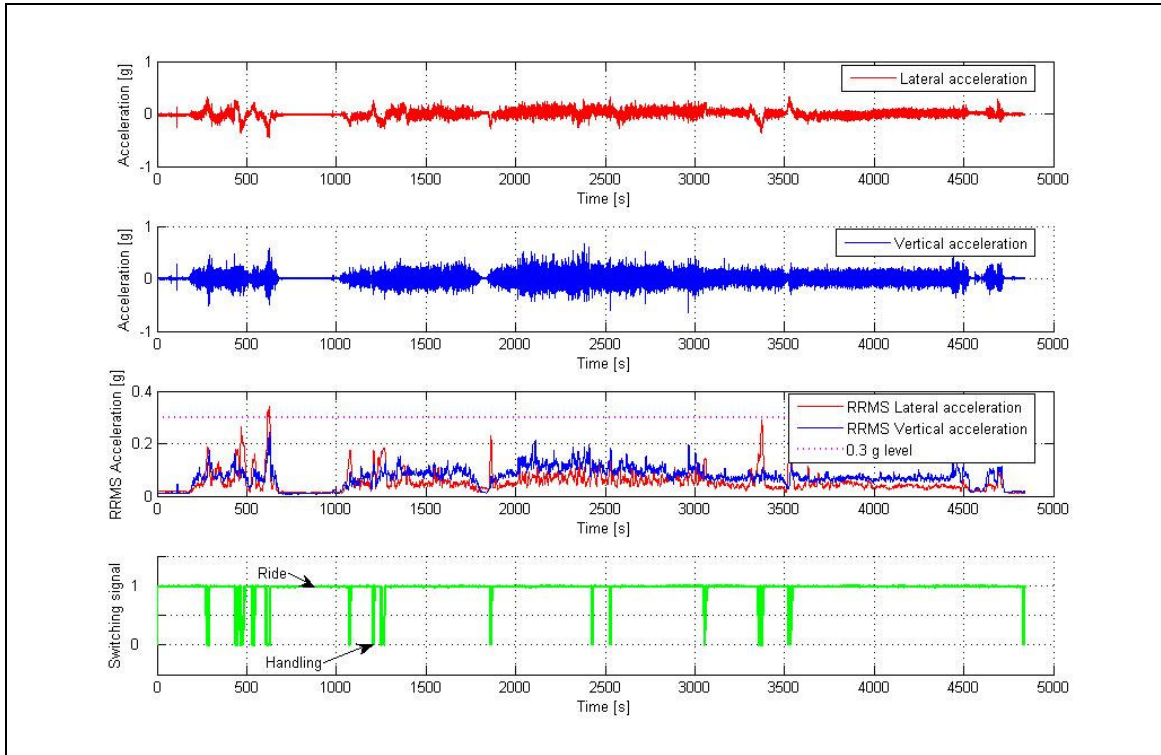


**Figure 6.30** – Highway driving



---

---

## CONCLUSIONS AND RECOMMENDATIONS

---

---

### 7.1. Conclusions

Controllable suspension systems have been implemented successfully in top-end passenger cars and are regarded by industry specialists as the development trend of the future. Basic systems employ a “mode switch” where the driver manually selects a suspension setting *e.g.* “comfort” or “sport”. More advanced systems react quicker and use some form of control to determine suspension settings.

Application of controllable suspension systems to vehicles that require good off-road capability (high ground clearance, large suspension travel and soft springs), but also good handling and stability on smooth roads at high speeds (low centre of gravity and stiff springs) are rare. Military wheeled vehicles, Sports utility vehicles (SUV’s) and Crossover utility vehicles (CUV’s) all fall within this category. This thesis attempts to fill this gap.

For off-road vehicles, a “mode switch” where the driver manually selects a suspension setting *e.g.* “off-road” or “on-road” can be used, but if the design in any case offers “ride comfort” and “handling” settings, automatic switching may just as well be employed to get the best possible benefit from the system. This also relieves the driver from making this decision. Furthermore, good handling is often required during off-road driving and good ride comfort is desirable when driving on bad roads. A successful “ride comfort” *vs.* “handling” decision can automatically select the required suspension settings according to the prevailing driving conditions. An important point worth noting is that current production systems still employ compromised characteristics, *i.e.* the “low” and “high” characteristics are often not optimised for ride comfort and handling respectively. The “low” setting is merely biased towards ride comfort but still results in acceptable handling. The “high” setting is biased towards handling, but still gives tolerable ride comfort. The suspension settings used in the present study are at the limits of the design space, *i.e.* the “low” setting gives the best possible ride comfort, but with unacceptable handling. The opposite holds for the “high” setting, *i.e.* best possible handling with intolerable ride comfort. This configuration results in large improvements in both ride comfort and handling respectively, but its successful application in vehicles rely on the “ride comfort *vs.* handling decision”

### 7.1.1 The ride comfort vs. handling compromise

Although no clear-cut answer is available for a metric that quantifies vehicle handling, the body roll angle was used in this research as an indication of handling.

The following hypotheses were made:

- i) Ride comfort and handling have opposing requirements in terms of spring and damper characteristics.
- ii) Suspension requirements for off-road use differ substantially from requirements for high-speed on-road use.
- iii) A set of passive spring and damper characteristics, called the “ride comfort characteristic” can be obtained that results in excellent ride comfort over prescribed off-road terrains at prescribed speeds. Additional improvements may be possible by using “control”, but is not considered for the purposes of this research.
- iv) A set of passive spring and damper characteristics, called the “handling characteristic”, can be obtained that results in excellent handling for prescribed high-speed maneuvers on good roads. Additional improvements may be possible by the use of “control” but is not considered for the purposes of this research.
- v) Advanced suspension system hardware that can switch between the passive “ride comfort” and “handling” spring and damper characteristics, can be feasibly implemented. Response time must be rapid enough to enable control of the sprung mass natural frequencies.
- vi) A robust decision can be made whether “ride comfort” or “handling” is required for the prevailing conditions.

A validated, non-linear full vehicle model was used to investigate the “optimal” characteristics for both ride comfort and handling. The conflicts between these requirements were investigated and analysed using simulation. The following conclusions are made based on the evidence presented:

- i) A passive suspension system is a compromise between ride comfort and handling, as the respective requirements for ride comfort and handling are at opposite ends of the design space.
- ii) To eliminate the “ride comfort vs. handling” compromise the following is required:
  - a. At least two discrete spring characteristics are required namely:
    - A stiff spring for excellent handling.
    - A soft spring for excellent ride comfort.
  - b. At least two discrete damper characteristics are required namely:
    - High damping for excellent handling.
    - Low damping for excellent ride comfort.
  - c. The capability to rapidly switch between the two spring and two damper characteristics.
  - d. A control strategy that can switch between “ride comfort” mode and “handling” mode in a safe and predictable way.

### **7.1.2 Possible solutions to the ride comfort vs. handling compromise**

The solution proposed to solve the “ride comfort vs. handling” compromise, is to use a twin accumulator hydropneumatic spring (two-state) combined with a two-state (on-off) semi-active hydraulic damper. Although more than two spring and/or damper characteristics can be incorporated, two is considered sufficient based on the simulation results presented. The pre-requisite is however that a successful ride comfort vs. handling decision-making strategy can be developed that will switch automatically between the “ride comfort” and “handling” modes. This switching must be safe and quick enough to prevent accidents, but not disturbing to the driver.

Preliminary investigation indicates that further improvements in ride comfort using control techniques are unlikely, especially when the spring and damper characteristics have been determined by optimising for ride comfort.

The proposed solution to the “ride comfort vs. handling” compromise is the 4 State Semi-active Suspension System or 4S<sub>4</sub>.

### **7.1.3 The four-state semi-active suspension system (4S<sub>4</sub>)**

A possible solution was formulated and investigated in greater detail in Chapter 4 where the design, manufacturing, testing and mathematical modelling of the proposed prototype four-state semi-active hydropneumatic spring-damper system (4S<sub>4</sub>) system was described.

The design meets all the initial design specifications and can be fitted to the proposed test vehicle with minor modifications to the test vehicle. The manufactured prototypes have been extensively tested and characterised. Although several problems were identified on the first prototype, these have been addressed and eliminated on the second prototype. Prototype 2 meets all the dynamic requirements, except that the low damping characteristic is too high to achieve the maximum ride comfort benefit.

A mathematical model of the suspension unit was developed and implemented in SIMULINK. Agreement between the model predictions and the measurements was generally good. Some aspects where the model or the quantification of its parameters needs improvement were identified. In particular, the tests to date clearly identified the need for a better method of quantifying the mass of gas loaded into the accumulators.

### **7.1.4 The ride comfort vs. handling decision**

The crucial “ride comfort” vs. “handling” decision was investigated in chapter 5. Numerous tests were performed for different driving conditions and the data thoroughly analysed. Based on this analysis, different decision-making ideas were investigated. It is concluded that of all the proposed strategies, only the running RMS (RRMS) strategy appeared to work for all the test conditions.

A combination of strategies may also result in improvements, *e.g.* the steering angle can be used to determine the switching point from “ride comfort” to “handling”, but switching back to “ride comfort” might then be based on the running RMS, or simply delayed by a fixed time to eliminate spurious switching.

### **7.1.5 Vehicle implementation**

The implementation of the proposed hardware and decision-making strategy in the vehicle, as well as final test results is discussed in Chapter 6.

The 4S<sub>4</sub> suspension system performs according to expectations. Switching between “ride comfort mode” and “handling mode” occurs seamlessly without the driver being aware of the switching. Ride comfort with the “ride” setting is 50 to 80 % better than with the “handling” setting. The “ride comfort mode” does not present an improvement in ride comfort compared to the baseline vehicle, because the low damping characteristic on the 4S<sub>4</sub> prototypes is too high. Body roll angle on the “handling” setting is improved by 61 to 78 % compared to the baseline vehicle and 47 to 90 % compared to the “ride comfort” setting.

The RRMS control strategy performs well under most circumstances, with the only drawback being the time taken to switch to “handling” mode during the double lane change manoeuvre.

### **7.1.6 Final comments**

The proposed solution successfully eliminates the “ride comfort vs. handling” compromise when designing vehicles for both on- and off-road use. The 4S<sub>4</sub> suspension system can be successfully implemented in hardware form, as this research has proven. The “ride comfort vs. handling” decision can be made using easily measurable parameters from freely available sensors.

## **7.2 Recommendations**

Several recommendations to improve the system, and aspects that warrant further investigation have been identified.

### **7.2.1 The ride comfort vs. handling compromise**

The handling study, presented in chapter 2, should be expanded to include more vehicles (especially off-road vehicles) and more drivers. This should enable better limits to be obtained.

For the present study, suspension characteristics for optimal ride comfort were obtained by simulating the vehicle driving over the Belgian paving at a speed of 60 km/h. Optimal characteristics for handling were obtained by performing a double lane change at 60 km/h on a smooth level road. The issue of combined ride comfort and handling was briefly investigated by performing the double lane change over the Belgian paving.

Before a final verdict can be reached with respect to the optimal suspension characteristics for ride comfort and handling respectively, it is necessary to investigate the effects of the following aspects in greater detail:

- i. Different terrain roughnesses
- ii. Different vehicle speeds
- iii. Different handling manoeuvres

- iv. Combined ride comfort and handling over a rough terrain *e.g.* performing the double lane change manoeuvre over the Belgian paving
- v. More design variables such as the low speed and high speed damping characteristics, different compression and rebound characteristics, as well as the transition point between the low- and high speed characteristic.
- vi. Effect of ride height
- vii. Different vehicle loading conditions
- viii. Improving vehicle handling compared to passive “handling” setting by applying control.

### **7.2.2 Possible solutions to the ride comfort vs. handling compromise**

The effect of ride height, on the ride comfort and handling of the vehicle, should be investigated in more detail. Limited test results discussed in chapter 6 indicate that handling, with the soft suspension, can be considerably improved by lowering the ride height. A control strategy to change ride height, while the vehicle is moving, should be investigated.

### **7.2.3 The four-state semi-active suspension system (4S<sub>4</sub>)**

The current 4S<sub>4</sub> system can be improved in several ways namely:

- i. The “off “ characteristic for the damper is currently too high and compares to the baseline damper value. This characteristic should be lowered significantly to between 20% and 50% of the baseline value before substantial improvements in ride comfort will be realized. This should be achievable by enlarging the ports and channels in the valve block or replacing the valve with a valve of larger flow capacity.
- ii. The low-speed “on” characteristic for the damper needs to be increased.
- iii. The gas charging procedure needs to be improved to ensure that the correct mass of gas is initially charged into the unit.
- iv. Weight and cost should be reduced before the system can be commercially viable.
- v. The 4S<sub>4</sub> simulation model should be further verified to determine if the transient response, during valve opening and closing, is correctly simulated.

### **7.2.4 The ride comfort vs. handling decision**

For further improvement of the “ride comfort vs. handling” decision, the use of artificial intelligence techniques (self organising maps, neural networks, fuzzy logic *etc.*) to identify the terrain and operating conditions is suggested. If the terrain or driving conditions can be successfully identified, then other concepts such as the steering angle vs. vehicle speed limit values can be implemented and thresholds adapted according to operating conditions. Possible reduction of the delay time caused by the length of the RRMS calculation, using additional information, should be investigated.

The SIMULINK model, comprising four of these units, should be incorporated into the ADAMS vehicle dynamics model of the sport utility vehicle in question. This will enable investigation of control strategies using simulation instead of vehicle testing.

The possibility of controlling vehicle over- and understeer by altering the front:rear roll stiffness balance should be investigated.

The capability of the 4S<sub>4</sub> system to reduce rollover propensity has not been investigated. Suspension characteristics required to prevent rollover, and the effect of ride height and control, must be determined. Early rollover warning systems might be beneficial in this application because ride height and suspension characteristics can be adapted to operating conditions. It might for example be possible to reduce ride height rapidly by dumping oil in the reservoir and prevent rollover. Reduction in centre of gravity height of up to 150 mm may be achieved in this manner.

### **7.2.5 Vehicle implementation**

Concerning implementation of the 4S<sub>4</sub> system on a vehicle, the measuring position for the two accelerometers needs to be investigated. If the lateral accelerometer is mounted at the front, it might react earlier during a handling manoeuvre. The installation of a steering angle sensor should also be investigated.

### **7.2.6 Additional possibilities**

Additional improvements may be possible using integrated chassis control, where the ABS braking system and automatic stability control is linked to the 4S<sub>4</sub> suspension control. Not only can sensors be shared, but additional information can be used *e.g.* the system pressure in the 4S<sub>4</sub> gives vertical wheel load (not true when bump or rebound stops are in contact). This could be used as input to the brake or stability control system to determine which wheels should be braked. This early warning could improve the performance of the other systems.

Installation of a higher capacity hydraulic pump could facilitate slow-active control, such as active body control or active anti-rollbars, without need for additional suspension hardware. The suspension system can then be used as an actuator or force generator instead of the current application as an adaptive element.

Reduced rollover propensity might require a third set of spring and damper characteristics or a different combination *e.g.* soft springs with high damping. The effect of front:rear stiffness balance has been indicated, but not used in the control yet. Switching spring and damper characteristics individually for each wheel might also have possible benefits in other driving scenarios that were not investigated.

Many other driving scenarios (other than the six investigated) should be investigated to ensure that the switching strategy works under all conditions, or otherwise adapt the strategy accordingly.

---

## ***BIBLIOGRAPHY / REFERENCES***

---

### **Bibliography / References**

#### **A**

Abd El-Tawwab, A.M. and Crolla, D.A., 1996, **An Experimental and Theoretical Study of a Switchable Damper**, SAE Technical Paper 960937, Society of Automotive Engineers, Warrendale, 1996.

Abd El-Tawwab, 1997, **Twin-Accumulator Suspension System**, SAE Technical Paper 970384, Reprinted from Steering and Suspension Technology, SP-1223, Society of Automotive Engineers, Warrendale, 1997, pp. 257-264.

Alanoly, J. and Sankar, S., 1987, **A New Concept in Semi-Active Vibration Isolation**, Transactions of the ASME, Volume 109, June 1987, pp. 242-247.

Alexander, D., 2003, **Cadillac SRX**, Automotive Engineering International, November 2003, pp. 58-61.

Alexander, D., 2004a, **Performance Air Suspension**, Automotive Engineering International, May 2004, p. 32.

Alexander, D., 2004b, **Global Viewpoints – North America: Chassis Integration Keeps Rubber on the Road**, Automotive Engineering International, May 2004, p. 32.

Anon., 1998, **High performance hydraulic cartridge valves and manifold systems**, HydraForce catalog 1998/99.

Anon, 2002, **Getting Started Using ADAMS/View, Version 12**, Mechanical Dynamics.

Anon, 2004, **ZF Sachs Goes Mainstream with Active Damping**, Automotive Engineering International, December 2004, p. 44.

Anon, 2005a, **Active suspension Iltis**, [http://www.suffield.drdc-rddc.gc.ca/ResearchTech/Products/MilEng\\_Products/RD95010/index\\_e.html](http://www.suffield.drdc-rddc.gc.ca/ResearchTech/Products/MilEng_Products/RD95010/index_e.html), accessed on 11 August 2005.

Anon, 2005b, **The Bose Suspension System- Resolving the conflict between Comfort and control**, [http://www.bose.com/controller?event=VIEW\\_STATIC\\_PAGE\\_EVENT&url=/learning/project\\_sound/suspension\\_challenge.jsp](http://www.bose.com/controller?event=VIEW_STATIC_PAGE_EVENT&url=/learning/project_sound/suspension_challenge.jsp).

Anon, 2005c, [www.stonehydraulics.com/PickAPackframe.html](http://www.stonehydraulics.com/PickAPackframe.html) , accessed on 14 May 2005.

Anon, 2005d, **Busak and Shamban Seal Catalogues**, <http://www.busakshamban.com/> accessed on 21 September 2005.

## **B**

Besinger, F.H., Cebon, D. and Cole, D.J., 1991, **An Experimental Investigation Into the use of Semi-active Dampers on Heavy Lorries**, Proceedings of the 12th IAVSD Symposium, Lyoun, France, 26-30 August 1991.

Birch, S., 1998, **Mercedes and the “Moose Test”**, Global Viewpoints, Automotive Engineering International, April 1998, pp. 11-13.

Birch, S., Yamaguchi, J. and Demmler, A., 1990, **Tech Briefs – Concepts: Citroen’s Activa 2**, Automotive Engineering, Vol. 98, No. 12, pp. 55-56.

Birch, S., 1999, **Actively Suspended Mercedes**, Automotive Engineering International, May 1999, pp. 38-40.

Birch, S., 2001a, **Global Viewpoints – Europe embraces the AT-factor: Land Rover introducing new technologies through Range Rover**, Automotive Engineering International, June 2001, pp. 58-60.

Birch, S., 2002a, **Global vehicles: 2002 Paris Mondial De L’Automobile, Tech highlights**, Automotive Engineering International, November 2002, pp. 22-24.

Birch, S., 2002b, **Global vehicles: 2002 Paris Mondial De L’Automobile, Tech highlights**, Automotive Engineering International, November 2002, p. 26.

Birch, S., 2002c, **Global vehicles: Audi A8 and RS6**, Automotive Engineering International, September 2002, pp. 18-24.

Birch, S., 2003a, **Global Viewpoints – Europe: Chassis systems integration** Automotive Engineering International, June 2003, pp. 58-62.

Birch, S., 2003b, **Global vehicles: Frankfurt Motor Show concepts 2003**, Automotive Engineering International, November 2003, pp. 8-22.

Birch, S., 2003c, **Automotive Manufacturing: Aluminium and the XJ**, Automotive Engineering International, April 2003, pp. 97-100.

Birch, S., 2003d, **Global vehicles: Geneva Motor Show technical highlights**, Automotive Engineering International, May 2003, pp. 10-23.



Birch, S., 2004a, **Global vehicles: Audi Makes A6 Sportier**, Automotive Engineering International, July 2004, p. 14.

Birch, S., 2004b, **Global vehicles: Mercedes-Benz CVT for new A-Class**, Automotive Engineering International, September 2004, pp. 13-16.

Böcker, M. and Neuking, R., 2001, **Development of TRW's Active Roll Control**, 16<sup>th</sup> European Mechanical Dynamics User's Conference, 14-15 November 2001, Berchtesgaden, Germany,  
[http://www.mscsoftware.com/support/library/conf/adams/euro/2001/proceedings/papers/pdf/Paper\\_6.pdf](http://www.mscsoftware.com/support/library/conf/adams/euro/2001/proceedings/papers/pdf/Paper_6.pdf) accessed on 18 May 2005 at 14:50.

British Standards Institution, 1987, **British Standard Guide to Measurement and Evaluation of Human Exposure to Whole Body Mechanical Vibration and Repeated Shock**, BS 6841, 1987.

Broge, J.L., 1999, **Interactive Vehicle Dynamics**, Automotive Engineering International, December 1999, pp. 47.

Buchholz, K., 2003a, **Another smart truck for the U.S. Army**, Automotive Engineering International, April 2003, pp. 14-15.

Buchholz, K., 2003b, **Sachs levels at the curbside**, Automotive Engineering International, December 2003, pp. 37-38.

Buchholz, K., 2003c, **Global Viewpoints – North America: Body and chassis developments**, Automotive Engineering International, May 2003, pp. 65-70.

Buckner, G.D., Schuetze, K.T. and Beno, J.H., 2000, **Active vehicle suspension control using intelligent feedback linearization**, Proceedings of the American Control Conference, Chicago, Illinois, June 2002, pp. 4014-4018.

## C

Carney, D., 2003a, **Ferrari 360 takes up challenge**, Automotive Engineering International, October 2003, p.12.

Carney, D., 2003b, **Maserati Coupe and Spyder evolve**, Automotive Engineering International, October 2003, p.14.

Carney, D., 2004b, **New Vehicle Technology Highlights: Grand Ride for Grand Cherokee**, Automotive Engineering International, November 2004, pp. 54-60.

Cebon, D., (1999), **Handbook of Vehicle-Road Interaction**, 629.231CEBON, ISBN 9026515545, Swets and Zeitlinger.

Choi, S.B., Lee, H.K. and Chang, E.G., 2001, **Field results of a semi-active ER suspension system associated with skyhook controller**, *Mechatronics* Vol. 11, pp. 345-353.

Chou, J.-H., Chen, S.-H. and Lee, F.-Z., 1998, **Grey-Fuzzy Control for Active Suspension Design**, *International Journal of Vehicle Design*, Volume 19, Number 1, 1998, pp. 65-77.

Cooper, H.W. and Goldfrank, J.C., 1967, **B-W-R constants and new correlations**, *Hydrocarbon Processing*, Vol. 46, No. 12, December 1967, pp. 141-146.

Crolla, D.A., Chen, D.C., Whitehead, J.P. and Alstead, C.J., 1998, **Vehicle Handling Assessment Using a Combined Subjective-Objective Approach**, SAE Technical Paper No. 980226.

Crolla, D.A. and Abdel-Hady, M.B.A., 1991, **Semi-Active Suspension Control for a Full Vehicle Model**, SAE Technical Paper 911904, Society of Automotive Engineers, Warrendale, 1991.

## **D**

Dahlberg, E., 2000, **A Method Determining the Dynamic Roll over Threshold of Commercial Vehicles**, SAE paper 2000-01-3492.

Darling, J. and Hickson, H.R., 1998, **An experimental study of a prototype active anti-roll suspension system**, *Vehicle System Dynamics*, 29 (1998), pp. 309-329.

Data, S. and Frigero, F., 2002, **Objective evaluation of handling quality**, *Proceedings of the Institution of Mechanical Engineers*, Vol. 216, Part D, *Journal of Automobile Engineering*, pp. 297-305.

Decker, H., Schramm, W. and Kallenbach, R., 1988, **A practical approach towards advanced semi-active suspension systems**, *IMEchE*, 1988, C430/88.

De Wet, G.J., 2000, **Semi-aktiewe voertuigdemper: Modelling en eksperimentele bevestiging van solenoïde klep, "Semi-active vehicle damper: modelling and experimental verification of solenoid valve"**, Unpublished final year project, Department of Mechanical and Aeronautical Engineering, University of Pretoria.

## **E**

Eberle, W.R. and Steele, M.M., 1975, **Investigation of Fluidically Controlled Suspension Systems for Tracked Vehicles – Final Report**, Technical Report No. 12072, TACOM Mobility Systems Laboratory, US Army Tank Automotive Command, Warren, Michigan, September 1975.

ElBeheiry, E.M., Karnopp, D.C., Elaraby, M.E. and Abdelraaouf, A.M., 1995a, **Advanced Ground Vehicle Suspension Systems - A Classified Bibliography**, Vehicle System Dynamics, Volume 24, Number 3, April 1995, pp. 231-258, Swets and Zeitlinger.  
El Gindy, M. and Mikulcik, E.C., 1993, **Sensitivity of a Vehicle's Yaw Rate Response: Application to a Three-axle Truck**, International Journal of Vehicle Design, Vol. 14, no. 4, pp. 325-352.

EL Gindy, M. and Ilosvai, L., 1983, **Computer simulation study on a vehicle's directional response in some severe manoeuvres. Part 2: Steering and braking manoeuvres**, International Journal of Vehicle Dynamics, Vol. 4, No. 5, pp. 501-510.

El Gindy, M. and Mikulcik, E.C., 1993, **Sensitivity of a vehicle's yaw rate response: application to a three-axle truck**, International Journal of Vehicle Design, Vol. 14, No. 4, pp. 325-352.

Els, P.S., 1993, **Die Hitteprobleem op Hidropneumatiese Veer-en-Demperstelsels "The overheating problem on hydropneumatic spring-damper systems"**, Unpublished M.Eng Dissertation, Department of Mechanical and Aeronautical Engineering, University of Pretoria, South Africa.

Els, P.S. and Grobbelaar, B., 1993, **Investigation of the Time- and Temperature Dependency of Hydropneumatic Suspension Systems**, SAE Technical Paper Series no. 930265, Published in Vehicle Suspension and Steering Systems, SAE Special Publication SP-256, 1993, pp. 55-65.

Els, P.S. and Grobbelaar, B., 1999, **Heat Transfer Effects on Hydropneumatic Suspension Systems**, Journal of Terramechanics, Vol. 36, pp. 197-205.

Els, P.S. and Holman, T.J., 1999, **Semi-Active Rotary Damper for a Heavy Off-Road Wheeled Vehicle**, Journal of Terramechanics, Volume 36, 1999, pp. 51-60.

Els, P.S. and Van Niekerk, J.L., 1999, **Dynamic Modelling of an Off-Road Vehicle for the Design of a Semi-Active, Hydropneumatic Spring-Damper System**, Proceedings of the 16th International Association for Vehicle System Dynamics (IAVSD) Symposium: Dynamics of Vehicles on roads and Tracks, Pretoria, South Africa, August 30 to September 3, 1999.

Els, P.S., and Uys, P.E., 2003, **Investigation Of The Applicability Of The Dynamic-Q Optimisation Algorithm To Vehicle Suspension Design**, Mathematical and Computer Modeling, Vol. 37, pp. 1029-1046.

Els, P.S., 2005, **The Applicability of Ride Comfort Standards to Off-Road Vehicles**, Journal of Terramechanics, Vol. 42, pp. 47-64.

Els, P.S., Uys, P.E., Snyman, J.A. and Thoresson, M.J., 2003, **Obtaining Vehicle Spring and Damper Characteristics for Improved Ride Comfort and Handling, Using Mathematical Optimisation**, 18<sup>th</sup> IAVSD Symposium, Dynamics of Vehicles on Roads and Tracks, Extensive Summaries, IAVSD 2003, August 24-30, Kanagawa Institute of Technology, Japan.

Esmailzadeh, E., 1979, **Servo-valve-controlled Pneumatic Suspensions**, Journal of Mechanical Engineering Science, Vol. 21, No. 1.

## F

Fodor, M. and Redfield, R.C., 1996, **Experimental Verification of Resistance Control, Semi-Active Damping**, Vehicle System Dynamics, Volume 26, Number 2, August 1996, pp. 143-159, Swets and Zeitlinger.

Forkenbrock, G.J. and Garrot, W. R., 2001, **Light Vehicle Dynamic Roll over Propensity Phases IV, V and VI**, NHTSA Power Point Presentation, NHTSA 2001-01-0128, [http://www-nrd.nhtsa.dot.gov/pdf/nrd-01/SAE/SAE2002/RGarrott\\_rollover.pdf](http://www-nrd.nhtsa.dot.gov/pdf/nrd-01/SAE/SAE2002/RGarrott_rollover.pdf), accessed on 18 May 2005, 16:40.

## G

Garrot, W.R., Howe, J.G. and Forkenbrock, G., 2001, **Results from NHTSA's experimental examination of selected manoeuvres that may induce on road untripped light vehicle rollover**, NHTSA 2001-01-0131.

Gehm, R., 2003, **Chrysler Pacifica**, Automotive Engineering International, October 2003, p. 62-64.

Gehm, R., 2004, **Tech Briefs – ZF Sachs goes mainstream with active damping**, Automotive Engineering International, June 2004, p. 20-22.

Ghazi Zadeh, A., Fahim, A. and El-Gindy, M., 1997, **Neural Network and Fuzzy Logic Applications to Vehicle Systems: Literature Survey**, International Journal of Vehicle Design, Volume 18, Number 2, 1997, ISSN 0143-3369.

Giliomee, C.L. and Els, P.S., 1998, **Semi-Active Hydropneumatic Spring and Damper System**, Journal of Terramechanics, Volume 35, 1998, pp. 109-117.

Giliomee, C.L., Els, P.S. and Van Niekerk, J.L., 2005, **Anelastic Model of a Twin Accumulator Hydro-pneumatic Suspension System**, R&D Journal, South African Institution of Mechanical Engineering, Vol. 21, No. 2, July 2005.

Gillespie, T.D., 1992, **Fundamentals of Vehicle Dynamics**, Society of Automotive Engineers, Inc., Warrendale, PA.

## H

Hall, B.B. and Gill, K.F., 1987, **Performance Evaluation of Motor Vehicle Active Suspensions Systems**, Proceedings of the Institution of Mechanical Engineers, Volume 201, Number D2, IMechE, 1987.

Hamilton, J.M., 1985, **Computer-Optimized Adaptive Suspension Technology (COAST)**, IEEE Transactions on Industrial Electronics, Volume IE-32, No 4, November 1985, pp. 355-363.

Harada, H., 1997, **Stability criteria of a driver-vehicle system and objective evaluation of vehicle handling performance**, International Journal of vehicle Design, Vol. 18, No. 6., pp. 597-615.

Harty, D., 2003, **Branding vehicle dynamics**, Automotive Engineering International, July 2003, pp. 53-60.

Harty, D., 2005, **A review of dynamic intervention technologies and a method to choose between them**, Vehicle Dynamics Expo 2005, Open Technology Forum, 31 May - 2 June 2005, Stuttgart Messe, Stuttgart, Germany.

Hashiyama, T., Furuhashi, T. and Uchikawa, Y. 1995, **A Study on Finding Fuzzy Rules for Semi-Active Suspension Controllers with Genetic Algorithm**, In Proc. Second IEEE Conference on Evolutionary Computation (EC-IEEE'95), volume 1, pages 279-282. Perth

Hedrick, J.K., Rajamani, R. and Yi, K., 1994, **Observer Design for Electronic Suspension Applications**, Vehicle System Dynamics, Volume 23, Number 6, September 1994.

Hedrick, J.K. and Wormley, D.N., 1975, **Active Suspensions for Ground Transport Vehicles - A State of the Art Review**, Mechanics of Transportation Suspension Systems, ASME AMD, Volume 15, 1975, pp. 21-40.

Hennecke, D. and Zieglmeier, F.J., 1988, **Frequency Dependent Variable Suspension Damping - Theoretical Background and Practical Success**, IMechE, 1988, C431/88, pp. 101-111.

Hine, P.J. and Pearce, P.T., 1988, **A Practical Intelligent Damping System**, IMechE, 1988, C436/88, pp. 141-147.

Hirose, M., Matsushige, S., Buma, S. and Kamiya, K., 1988, **Toyota Electronic Modulated Suspension System for the 1986 Soarer**, IEEE Transactions on Industrial Electronics, Volume 35, Number 2, May 1988.

Hohl, G.H., 1984, **Ride Comfort of Off-Road Vehicles**, In Proceedings of the 8th International Conference of the ISTVS, Vol. I of III, Cambridge, England, August 5-11, 1984.

Holdmann, P. and Holle, M., 1999, **Possibilities to improve the ride and handling performance of delivery trucks by modern mechatronic systems**, JSAE Review, Vol. 20, pp. 505-510.

Holscher, R. and Huang, Z., 1991, **Das komfortorientierte semiaktive dampfungssystem**, Aktive Fahrwerkstechnik, Fortschritte der Fahrzeugtechnik 10, Vieweg and Sohn Verlagsgesellschaft, Braunschweig.

Horiuchi, S., Yuhara, N. and Takeda, H., 1989, **Identification of driver/vehicle multiloop properties for handling quality evaluation**, 11<sup>th</sup> IAVSD Symposium, 21-25 Aug 1989, Supplement to Vehicle System Dynamics, Vol. 18.

Hrovat, D., 1997, **Survey of Advanced Suspension Developments and Related Optimal Control Applications** Automatica, Vol 33, No. 10, pp. 1781-1817, Elsevier Science.

Hrovat D. and Margolis, D.L., 1981, **An Experimental Comparison Between Semi-Active and Passive Suspensions for Air-Cushion Vehicles**, International Journal of Vehicle Design, Volume 2, Number 3, 1981, pp. 308-321.

## I

Ikenaga, S., Lewis, F.L., Campos, J. and Davis, L., 2000, **Active Suspension Control of Ground Vehicle Based on Full-Vehicle Model**, Proceedings of the American Control Conference, Chicago, Illinois, June 2000, pp. 4019-4024.

International Standards Organisation, 1982, **International Standard ISO 4138: Road vehicles – Steady state circular test procedure**, ISO 7401:1988(E).

International Standards Organisation, 1988, **International Standard ISO 7401: Road vehicles – Lateral transient response test methods**, ISO 7401:1988(E).

International Standards Organisation, 1995, **International Standard ISO 8608: Mechanical vibration – Road surface profiles – Reporting of measured data**, ISO 8608:1995(E).

International Standards Organisation, 1997, **Mechanical Vibration and Shock - Evaluation of Human Exposure to Whole-Body Vibration, Part 1: General Requirements**, ISO 2631-1, Second Edition, The International Organisation for Standardisation, 15 July 1997.

International Standards Organisation, 1999, **International Standard ISO 3888-1: Passenger cars – Test track for a severe lane-change manoeuvre – Part 1: Double lane-change**, ISO 3888-1:1999(E).

International Standards Organisation, 2002, **International Standard ISO 3888-2: Passenger cars – Test track for a severe lane-change manoeuvre – Part 2: Obstacle avoidance**, ISO 3888-2:2002(E).

Ivers, D.E. and Miller, L.R., 1989, **Experimental Comparison of Passive, Semi-Active On/Off, and Semi-Active Continuous Suspensions**, SAE Technical Paper 892484, Society of Automotive Engineers, Warrendale, 1989. (Reprinted from “Advanced Truck Suspensions”, SP-802).

## J

Janse van Rensburg, N., Steyn, J.L. and Els, P.S., 2002, **Time delay in a semi-active damper: modeling the bypass valve**, Journal of Terramechanics, Volume 39, 2002, pp. 35-45.

Jolly, M.R. and Miller, L.R., 1989, **The Control of Semi-Active Dampers Using Relative Feedback Systems**, SAE Technical Paper 892483, Society of Automotive Engineers, Warrendale, 1989. (Reprinted from “Advanced Truck Suspensions”, SP-802)

Jost, K., 2002a, **Continental gives Phaeton a lift**, Automotive Engineering International, November 2002, p. 49.

Jost, K., 2002b, **Top technologies of the year: Delphi improves Cadillac’s ride**, Automotive Engineering International, December 2002, p. 40.

Jost, K., 2004, **Segment firsts for Opel Astra**, Automotive Engineering International, January 2004, p. 12.

Jost, K., 2005, **Audi Allroad Quattro**, Automotive Engineering International, February 2005, p. 28-30.

## K

Karnopp, D., 1968, **Applications of Random Process Theory to the Design and Testing of Ground Vehicles**, Transportation Research, Vol. 2, pp. 269-278, Pergamon Press.

Karnopp, D.C., Crosby, M.J. and Harwood, R.A., 1973, **Vibration Control using Semi-active Force Generators**, ASME paper 73-DET-122.

Karnopp, D., 1983, **Active Damping in Road Vehicle Suspension Systems**, Vehicle System Dynamics, Volume 12, 1983, pp. 291-316.

Karnopp, D., 1990, **Design Principles for Vibration Control Systems Using Semi-Active Dampers**, Transactions of the ASME, Volume 112, September 1990, pp. 448-455.

Karnopp, D. and Margolis, D., 1984, **Adaptive Suspension Concepts for Road Vehicles**, Vehicle System Dynamics, Volume 13, 1984, pp. 145-160.

Karnopp, D., Crosby, M.J. and Harwood, R.A., 1974, **Vibration Control Using Semiactive Force Generators**, ASME Journal of Engineering for Industry, Vol. 98, pp. 914-918.

Kelly, K., 2001, **Spyder of a different stripe – Maserati’s ragtop lives up to its Italian heritage**, Ward’s Autoworld, December 2001, pp. 65-66.

Kizu, R., Saito, R., Matsumura, S. and Yokoya, Y., 1989, **Technical Note: Suspension Technology capable of reconciling handling stability and ride comfort**, International Journal of Vehicle Design, Vol. 10, No. 4, pp. 497-501.

Kim, H-J. and Park, Y-P., 2004, **Investigation of robust roll motion control considering varying speed and actuator dynamics**, Mechatronics, Vol. 14, pp. 35-54.

Kornhuaser, A.A., 1994, **Dynamic modelling of gas springs**, Transactions of the ASME, Vol. 116, September 1994. pp. 414-418.

Kojima, H., Nakano, J., Nakayama, H., Kawashima, N. and Fujimoto, H., 1991, **Development of Toyota Electronic Modulated Suspension - Two Concepts for Semi-Active Suspension Control**, SAE Technical Paper 911900, Society of Automotive Engineers, Warrendale, 1991. (Reprinted from "Car Suspension Systems and Vehicle Dynamics", SP-878).

Krasnicki, E.J., 1981, **The Experimental Performance of an "On-Off" Active Damper**, Shock and Vibration Bulletin, Number 50, May 1981, pp. 125-131.

## L

Lieh, J., 1996, **Development of Active Suspensions Using Velocity Feedback**, SAE Technical Paper 960935, Society of Automotive Engineers, Warrendale, 1995. (Reprinted from "Suspension and Steering Technology", SP-1136).

Lizell, M., 1988, **Semi-Active Damping**, IMechE, 1988, C429/88, pp. 83-91.

Lord Corporation, 2005, **Magneto-Rheological (MR) Technology**, <http://www.lord.com/defaultt.aspx?tabid=762&pid=3> accessed on 23 May 2005.

## M

Margolis, D.L., 1982a, **The Response of Active and Semi-Active Suspensions to Realistic Feedback Signals**, Vehicle System Dynamics, Volume 11, Number 5-6, December 1982.

Margolis, D.L., 1982b, **Semi-Active Heave and Pitch Control for Ground Vehicles**, Vehicle System Dynamics, Volume 11, Number 1, February 1982.

Masato, A., 1989, **Handling characteristics of four-wheel active steering vehicles over full manoeuvring range of lateral and longitudinal accelerations**, 11<sup>th</sup> IAVSD Symposium, 21-25 Aug 1989, Supplement to Vehicle System Dynamics, Vol. 18.

Mayne, E., 2002, **Land Rover Innovation Goes From Paper to Practice**, [www.wardsauto.com](http://www.wardsauto.com), accessed on 08 Jan 2002 at 07:53.

Miller, L.R., 1988a, **The Effect of Hardware Limitations on an On/Off Semi-Active Suspension**, IMechE Paper number C442/88, 1988, pp. 199-206.



Miller, L.R., 1988b, **Tuning Passive, Semi-Active and Fully Active Suspension Systems**, Proceedings of the 27th Conference on Decision and Control, Austin, Texas, 7-9 December 1988.

Miller, L.R. and Nobles, C.M., 1988, **The Design and Development of a Semi-Active Suspension for a Military Tank**, SAE Technical Paper 881133, Society of Automotive Engineers, Warrendale, 1988.

Misselhorn, W.E., Theron, N.J. and Els, P.S., 2006, **Investigation of Hardware-in-the-Loop for use in suspension development**, Vehicle System Dynamics, Vol. 44, No.1, January 2006, pp. 65-81.

Mizuguchi, M., Chikamari, S., Suda, T. and Kobayashi, K., 1984, **Electronic Controlled Suspension (ECS)**, SAE Technical Paper 845051, Society of Automotive Engineers, Warrendale, 1984.

Murphy, R.W., 1984, **Further Development in Ride Quality**, In Proceedings of the 8th International Conference of the ISTVS, Vol I of III, Cambridge, England, August 5-11, 1984.

## N

Nastasić, Ž. and Jahn, G.D., 2005, **The Citroën Technical Guide**, [http://www.club\\_xm.com/files/citroen%20guide.pdf](http://www.club_xm.com/files/citroen%20guide.pdf), Accessed on 29 April 2005.

National Highway Traffic Safety Administration, 2000, **Roll over prevention Docket No. NHTSA-2000-6859 RIN 2127-AC64**, [www.nhtsa.dot.gov/cars/rules/rulings/Roll over/Chapt03.html](http://www.nhtsa.dot.gov/cars/rules/rulings/Roll%20over/Chapt03.html). Accessed September 2002.

Nell, S., 1993, **‘n Algemene Strategie vir die Beheer van Semi-Aktiewe Dempers in ‘n Voertuigsuspensiestelsel**, “A general strategy for the control of semi-active dampers in a vehicle suspension system”, Unpublished PhD Thesis, Department of Mechanical and Aeronautical Engineering, Faculty of Engineering, University of Pretoria, November 1993.

Nell, S. and Steyn, J.L., 1994, **Experimental Evaluation of an Unsophisticated Two State Semi-Active Damper**, Journal of Terramechanics, Volume 31, Number 4, pp. 227-238, 1994, Elsevier Science Ltd.

Nell, S. and Steyn J.L., 1998, **An alternative control strategy for semi-active dampers on off-road vehicles**. Journal of Terramechanics, Vol. 35, 1998, pp 25-40.

Nell, S. and Steyn J.L., 2003, **Development and experimental evaluation of translational semi-active dampers on a high mobility off-road vehicle**. Journal of Terramechanics, Vol. 40, pp. 25-32.

## O

Ouellette, J., 2005, **Smart Fluids Move into the Marketplace**, <http://www.aip.org/tip/INPHFA/vol-9/iss-6/p14.html> , accessed on 23 May 2005.

## P

Palmeri, P.S., Moschetti, A. and Gortan, L., 1995, **H-Infinity Control for Lancia Thema Full Active Suspension System**, SAE Technical Paper 950583, Society of Automotive Engineers, Warrendale, 1995. (Reprinted from “New Developments in Vehicle Dynamics, Simulation, and Suspension Systems”, SP-1074).

Petek, N.K., Romstadt, D.J., Lizell, M.B. and Weyenberg, T.R., 1995, **Demonstration of an Automotive Semi-Active Suspension Using Electrorheological Fluid**, SAE Technical Paper 950586, Society of Automotive Engineers, Warrendale, 1995. (Reprinted from “New Developments in Vehicle Dynamics, Simulation, and Suspension Systems”, SP-1074).

Pinkos, A., Shtarkman, E. and Fitzgerald, T., 1993, **An Actively Damped Passenger Car Suspension System with Low Voltage Electro-Rheological Magnetic Fluid**, SAE Technical Paper 930268, Society of Automotive Engineers, Warrendale, 1993. (Reprinted from Special Publication SP-952), pp. 87-93).

Poley, R., 2005, **DSP Control of Electro-hydraulic Servo Actuators**, Texas Instruments Application Report, SPRAA76 – January 2005 from: [www.eetchina.com/ARTICLES/2005MAR/PDF/2005MAR21\\_DSP\\_CTRLD\\_ANONLINE35.PDF](http://www.eetchina.com/ARTICLES/2005MAR/PDF/2005MAR21_DSP_CTRLD_ANONLINE35.PDF), accessed on 11 January 2006.

Pollard, M.G., 1983, **Active Suspensions Enhance Ride Quality**, Railway Gazette International, November 1983.

Ponticel, P., 2002, **New magnetorheological fluids from Lord**, Automotive Engineering International, August 2002, p. 13.

Poyser, J., 1987, **Development of a Computer Controlled Suspension System**, International Journal of Vehicle Design, Volume 8, Number 1, 1987, pp. 74-86.

Pradko, F. and Lee, R.A., 1966, **Vibration Comfort Criteria**, SAE Technical Paper 660139, Society of Automotive Engineers, Warrendale.

## R

Rajamani, R. and Hedrick, J.K., 1991, **Semi-Active Suspensions - A Comparison Between Theory and Experiments**, The Dynamics of Vehicles on Roads and on Tracks, Proceedings of the 12<sup>th</sup> IAVSD-Symposium held in Lyon, France, 26-30 August 1991, Supplement to Vehicle System Dynamics, Volume 20, Swets & Zeitlinger.

Rakheja, S. and Sankar, S., 1985, **Vibration and Shock Isolation Performance of a Semi-Active “On-Off” Damper**, Transactions of the ASME, Volume 107, October 1985, pp. 398-403.

Reichardt, W., 1991, **Correlation Analysis of Open/Closed Loop Data for Objective Assessment of Handling Characteristics of Cars**, SAE Technical Paper No. 910238.

## S

Salemka, R.M. and Beck, R.R., 1975, **Feasibility Analysis and Evaluation of an Adaptive Tracked Vehicle Suspension and Control System**, TACOM, Technical Report Number 11893(LL-146), June 1975.

Sharp, R.S. and Crolla, D.A., 1987, **Road Vehicle Suspension System Design - A Review**, Vehicle System Dynamics, Volume 16, number 3, 1987, Swets and Zeitlinger, pp. 167-192.

Sharp, R.S. and Hassan, S.A., 1987, **Performance and Design Considerations for Dissipative Semi-Active Suspension Systems for Automobiles**, Proceedings of the IMechE, Volume 201, Number D2, 1987, pp. 149-153.

Sharp, R.S. and Pan, D., 1991, **On active control for automobiles**, 12<sup>th</sup> IAVSD Symposium, Aug 26-30, 1991, Supplement to Vehicle System Dynamics, Vol. 20.

Silani, E., Savaresi, S.M. and Bittanti, S., 2003, **Semi-active Suspensions: an Optimal Control Strategy for a Quarter-car Model**, Dipartimento di Elettronica e Informazione, Politecnico di Milano.

Simon, D.E., 2001, **An Investigation of the Effectiveness of Skyhook Suspensions for Controlling Roll Dynamics of Sport Utility Vehicles Using Magneto-Rheological Dampers**, PhD Dissertation. Virginia Polytechnic Institute and State University.

Soliman, A.M.A., Abd El-Tawwab, A.M. and Crolla, D.A., 1996a, **Adaptive Control Strategies for a Switchable Damper Suspension System**, SAE Technical Paper 960939, Society of Automotive Engineers, Warrendale, 1996. (Reprinted from “Suspension and Steering Technology”, SP-1136.

Soliman, A.M.A. and Crolla, D.A., 1996b, **Preview Control for a Semi-Active Suspension System**, International Journal of Vehicle Design, Volume 17, Number 4, 1996.

Speckhart, F.A. and Harrison, E., 1968, **The Design of a Shock Absorber to Improve Ride Comfort by Reducing Jerk**, SAE Technical Paper 680472, Society of Automotive Engineers, Warrendale, 1968.

Starkey, J.M., 1993, **The effects of vehicle design parameters on handling frequency response characteristics**, International Journal of Vehicle Design, Vol. 14, No. 5/6, pp. 497-510.

Stone, E. and Cebon, D., 2002, **A preliminary investigation of semi-active roll control**, [http://www.cvdc.org/recent\\_papers/StoneCebon\\_avec02.pdf](http://www.cvdc.org/recent_papers/StoneCebon_avec02.pdf), accessed on 19 May 2005, 07:45.

## T

Temple, N.L. and Hoogterp, F.B., 1992, **Semi-Active Suspension: A Mobility Enhancement for Combat Vehicles**, Proceedings of the ISTVS/FISITA 92, Seminar on Off-road Vehicles, Institution of Mechanical Engineers, London, 9-11 June 1992.

Theron, N.J. and Els, P.S., 2005, **Modelling of a Semi-active Hydropneumatic Spring-damper Unit**, Accepted for publication in International Journal of Vehicle Design (IJVD), Inderscience Publishers, 3 March 2005.

Thoreson, M.J., 2003, **Mathematical optimisation of the suspension system of an off-road vehicle for ride comfort and handling**, Unpublished M.Eng Thesis, University of Pretoria, Pretoria, South Africa.

Tomizuka, M. and Hedrick, J.K., 1995, **Advanced Control Methods for Automotive Applications**, Vehicle System Dynamics, Volume 24, 1995, pp. 449-468, Swets and Zeitlinger.

Trent, V. and Greene, M., 2002, **A Genetic Algorithms Predictor for Vehicular Rollover**, 0-7803-7474-6/02/\$17.00, IEEE, 2002

Truscott, A.J., 1994, **Composite Active Suspension for Automotive Vehicles**, Computing and Control Engineering Journal, June 1994, pp. 149-154.

Tseng, H.E. and Hedrick, J.K., 1994, **Semi-Active Control Laws - Optimal and Sub-optimal**, Vehicle System Dynamics, Volume 23, Number 7, October 1994, pp. 545-569, Swets and Zeitlinger.

## U

Uffelman, F., 1983, **Automotive Stability and Handling Dynamics in Cornering and Braking Manoeuvres**, Vehicle System Dynamics, Vol. 12, pp. 203-223.

Uys, P.E., Els, P.S. and Thoreson, M.J., 2006, **Criteria for Handling Measurement**, Journal of Terramechanics, Vol. 43, pp. 43-67.

Uys, P.E., Els, P.S., Thoreson, M.J., Voigt, K.G. and Combrinck, W.C., 2005, **Experimental determination of moments of inertia for an off-road vehicle in a regular engineering laboratory**, Accepted for publication in the International Journal of Mechanical Engineering Education.

## V

Vlk. F., 1985, **Handling performance of truck-trailer vehicles: A state-of-the-art-survey**, International Journal of Vehicle Design, Vol. 6, No. 3, pp. 323-361.

Voigt, K.G., 2006, **Semi-active spring and damper control for ride comfort**, Draft copy of Masters degree thesis at University of Pretoria submitted to study leaders, Prof. N.J. Theron and Mr. P.S. Els, for review.

## W

Wallentowitz, H. and Holdman, P., 1997, **Hardware and Software Demands on Adjustable Shock Absorbers for Trucks and Passenger Cars**, Internet - <http://www.ika.rwth-aachen.de/vortrag/ph-hdt> accessed on 26 August 1997.

Weeks, D.A., Bresie, D.A., Beno, J.H. and Guenin, A.M., 1999, **The Design of an Electromagnetic Linear Actuator for an Active Suspension**, SAE Technical paper 1999-01-0730.

Weissler, P., 2003, **Continuously Controlled Chassis from Volvo**, Automotive Engineering International, August 2003, pp. 10-13 .

Williams, R.A., 1994, **Electronically Controlled Automotive Suspensions**, Computing and Control Engineering Journal, June 1994, pp. 143-148.

Wright, P., 2001, **Formula 1 Technology**, Society of Automotive Engineers, pp. 325-335.

## Y

Yoshimura, T., Nakaminami, K. and Hino, J., 1997, **A Semi-Active Suspension with Dynamic Absorbers of Ground Vehicles Using Fuzzy Reasoning**, International Journal of Vehicle Design, Volume 18, Number 1, 1997.

Youn, I., 1991, **Optimal Preview Control Design of Active and Semi-Active Suspension Systems Including Jerk**, SAE Technical Paper 960936, Society of Automotive Engineers, Warrendale, 1991. (Reprinted from "Suspension and Steering Technology", SP-1136).



# Appendix **A**

---

---

## ***HANDLING CRITERIA***

---

---

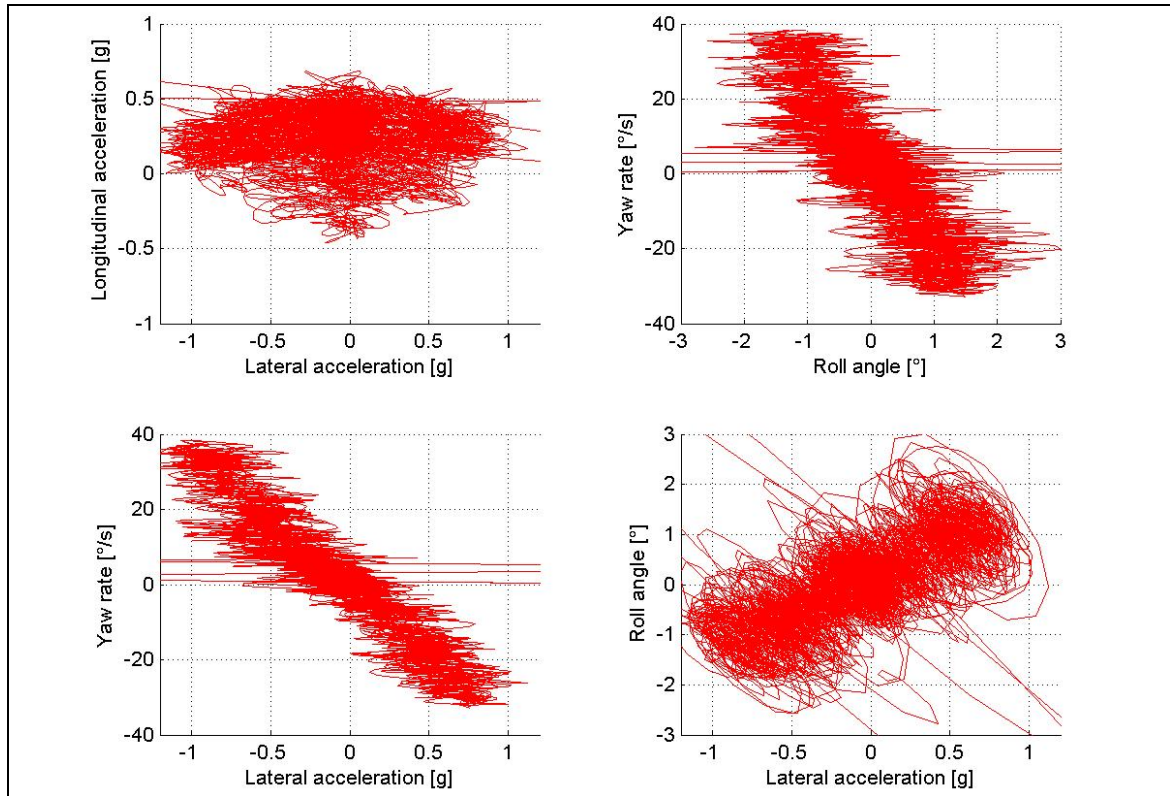


**Figure A-1** - Performance related to driver A – Volkswagen Golf 4 GTI on ride and handling track

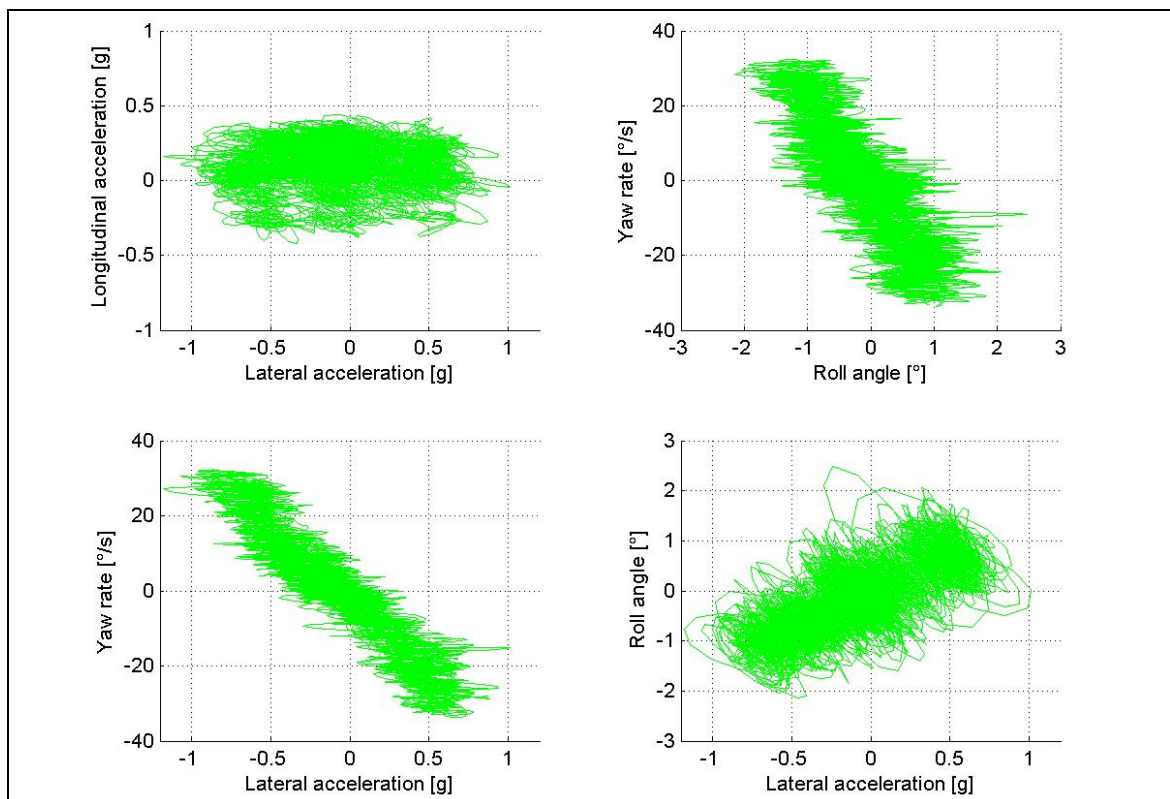


**Figure A-2** - Performance related to driver B – Volkswagen Golf 4 GTI on ride and handling track

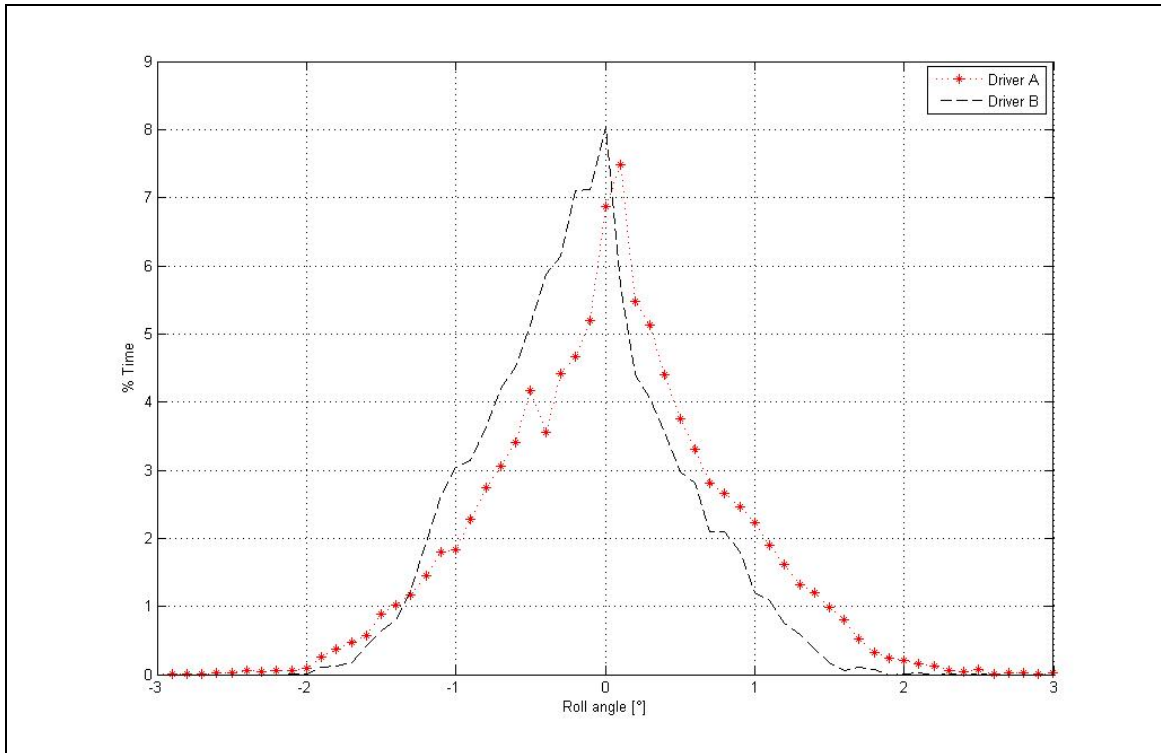


**Figure A-3** - Roll angle histograms for Drivers A and B – Volkswagen Golf 4 GTI on ride and handling track

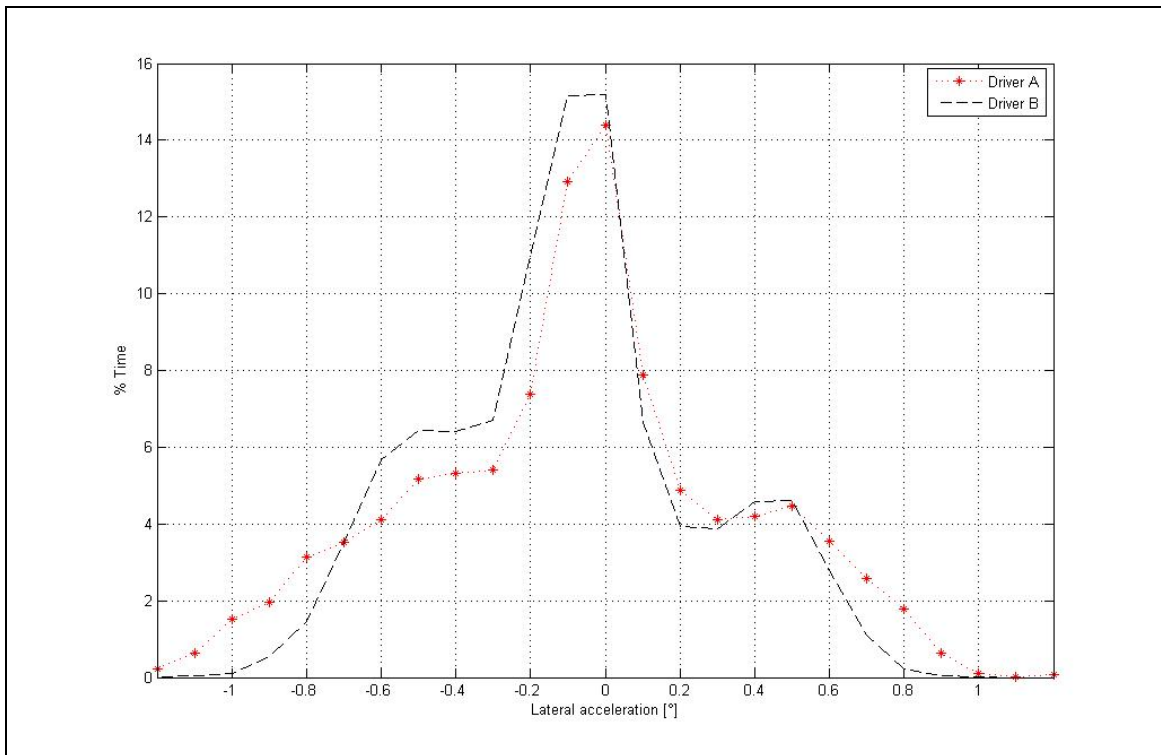


**Figure A-4** - Lateral acceleration histogram for Drivers A and B – Volkswagen Golf 4 GTI on ride and handling track



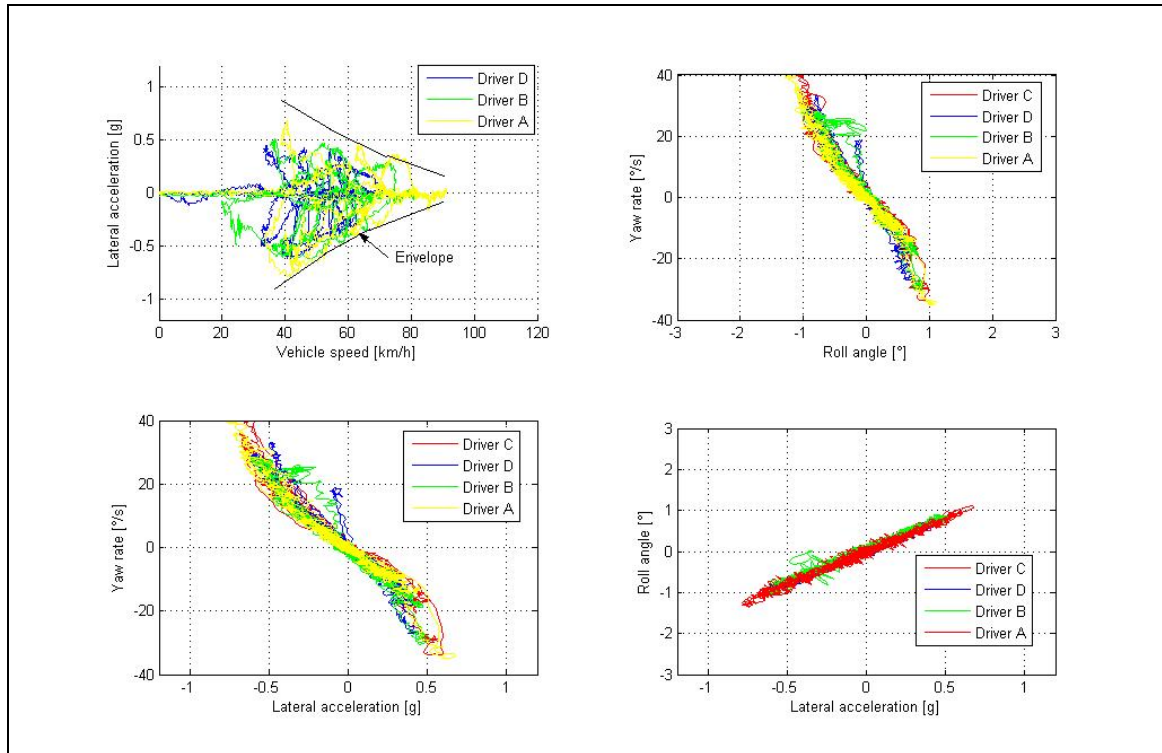


**Figure A-5** - Lateral acceleration, yaw rate and roll angle performance of a Ford Courier on a dynamic handling track

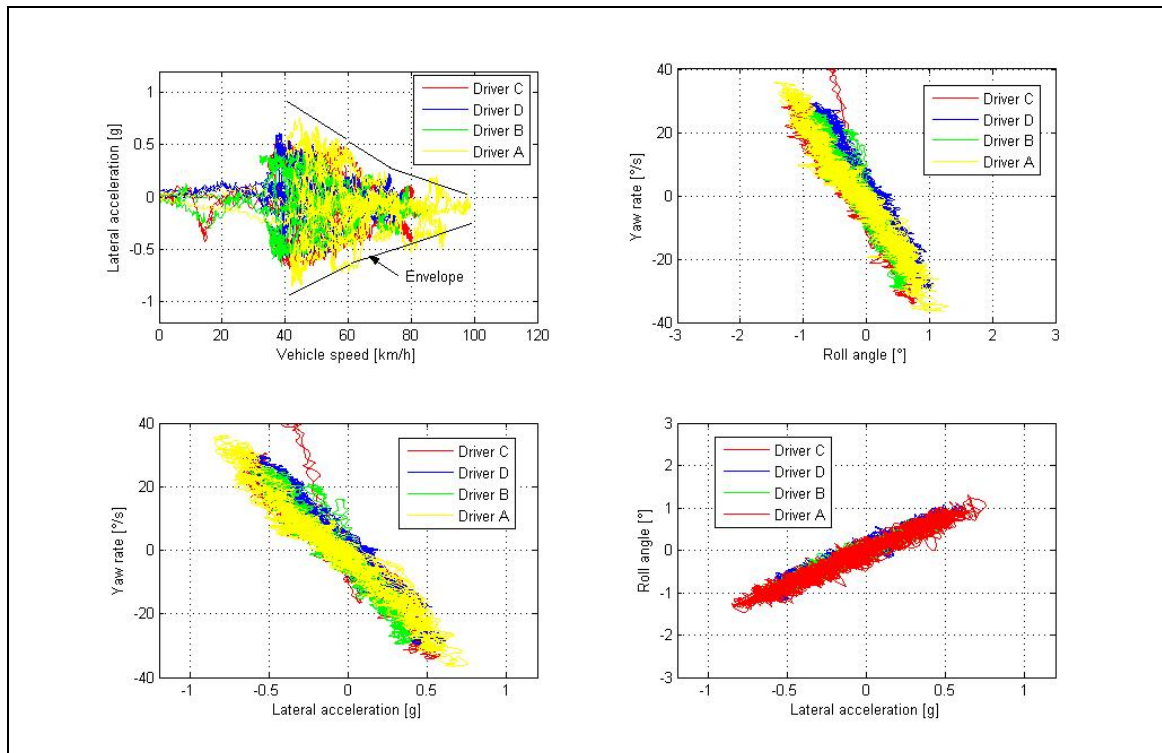


**Figure A-6** - Lateral acceleration, yaw rate and roll angle performance of a Ford Courier on a ride and handling track

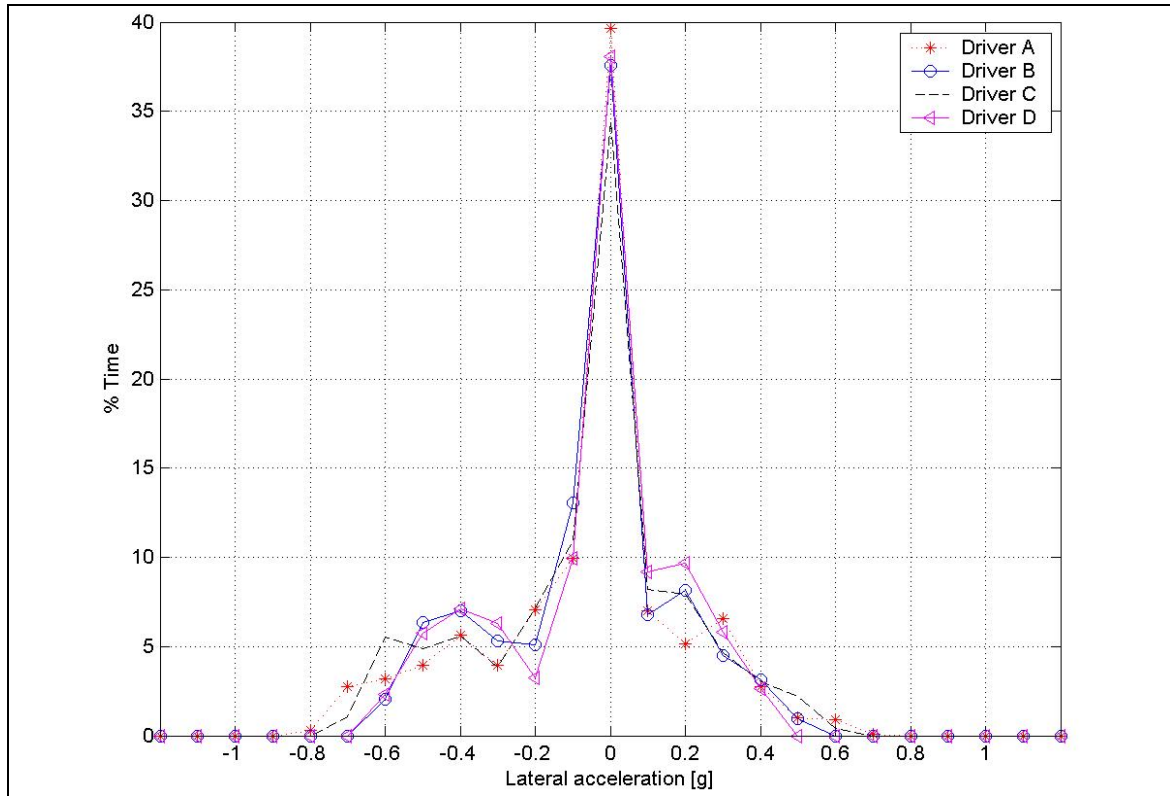


**Figure A-7** – Lateral acceleration histogram for a Ford Courier on the dynamic handling track

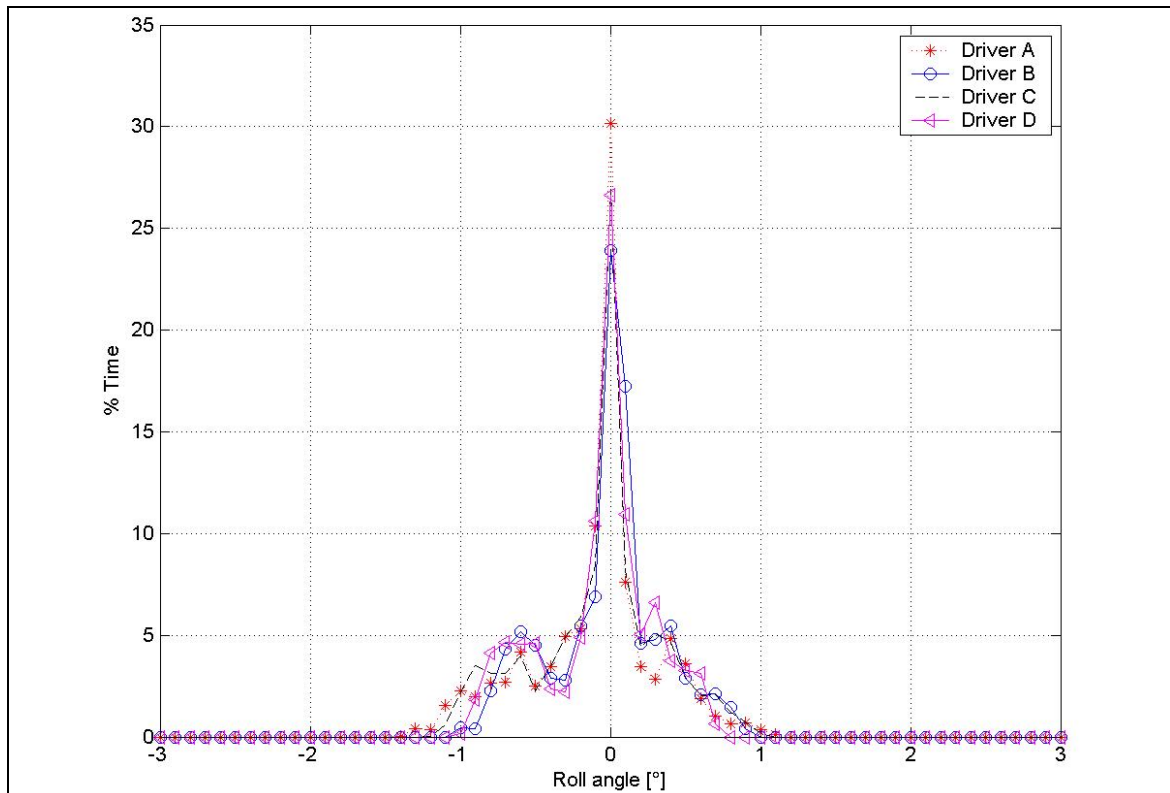


**Figure A-8** - Roll angle histograms for a Ford Courier on a dynamic handling track

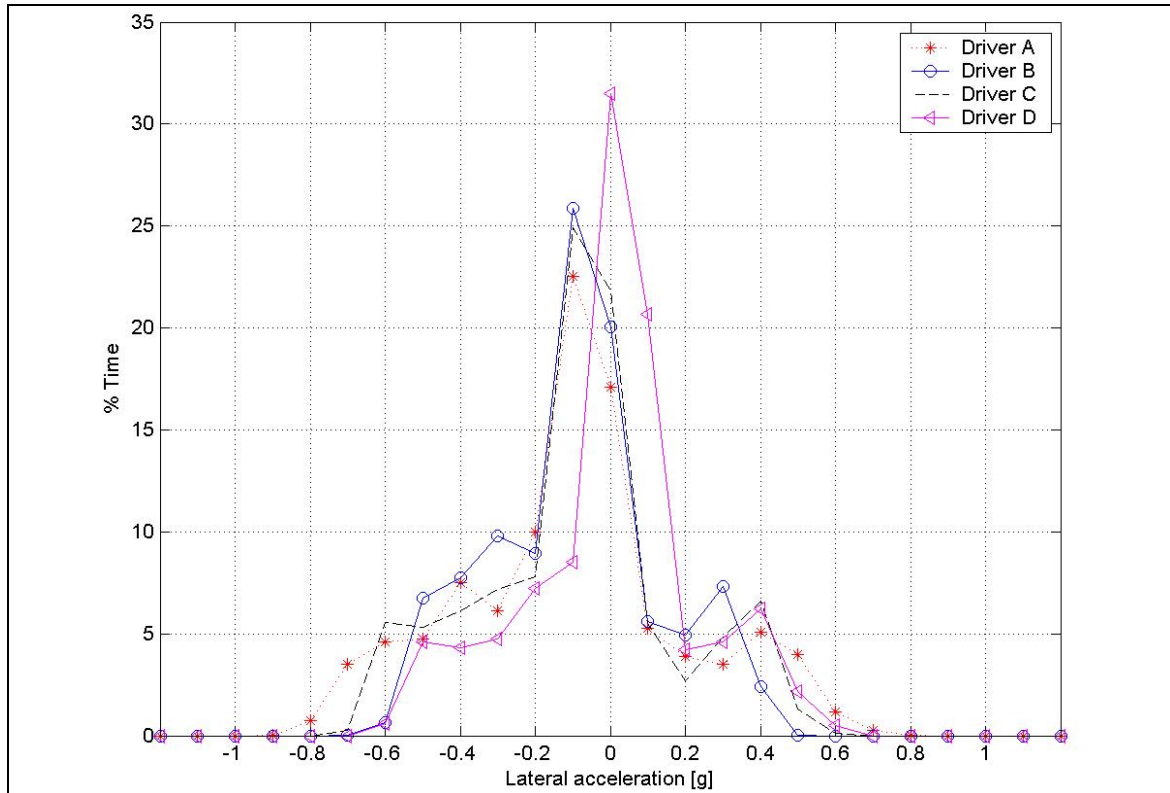


**Figure A-9** - Lateral acceleration histogram of a Ford Courier on the ride and handling track

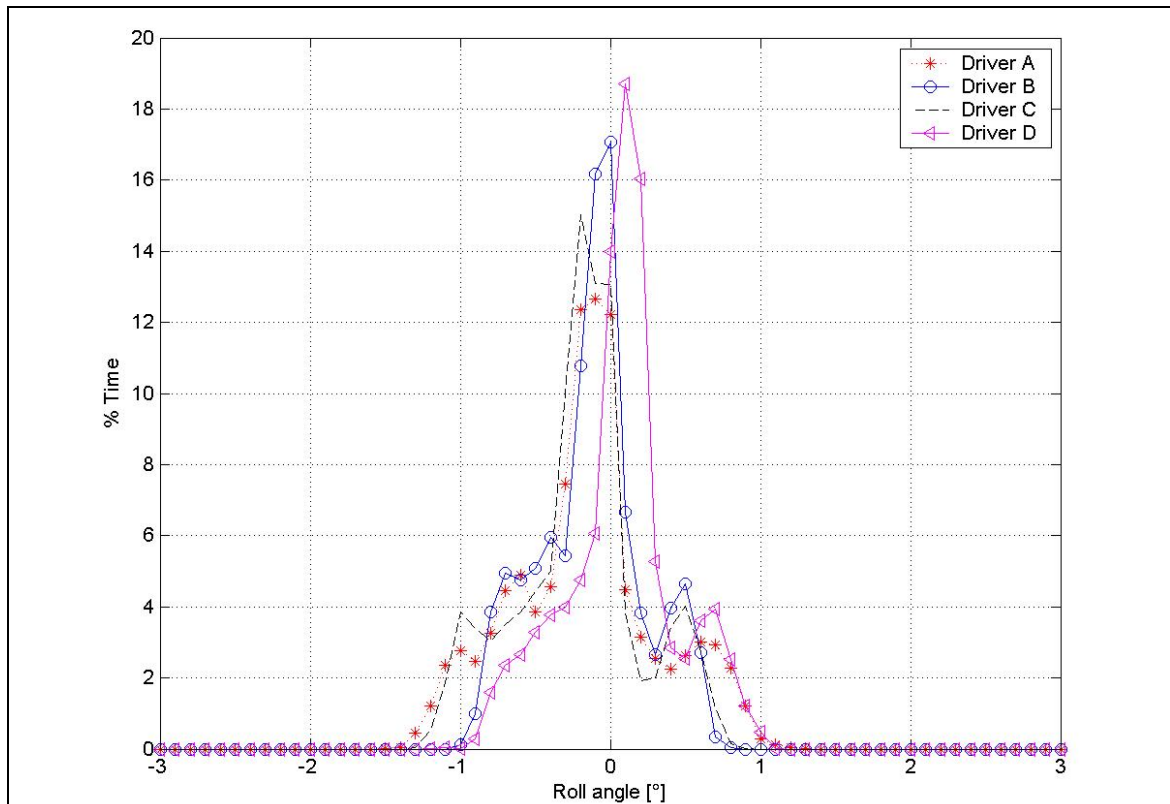


**Figure A-10** - Roll angle histogram of a Ford Courier on a ride and handling track

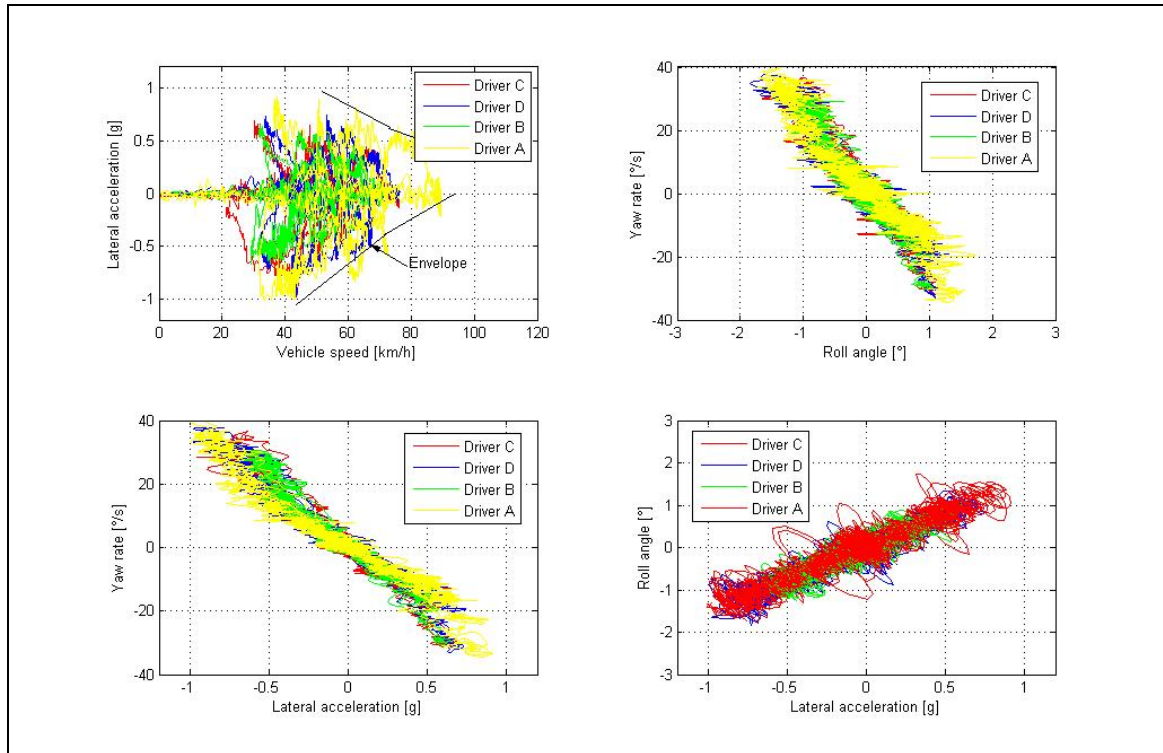


**Figure A-11** - Lateral acceleration, yaw rate and roll angle performance of a VW Golf 4 GTI on a dynamic handling track

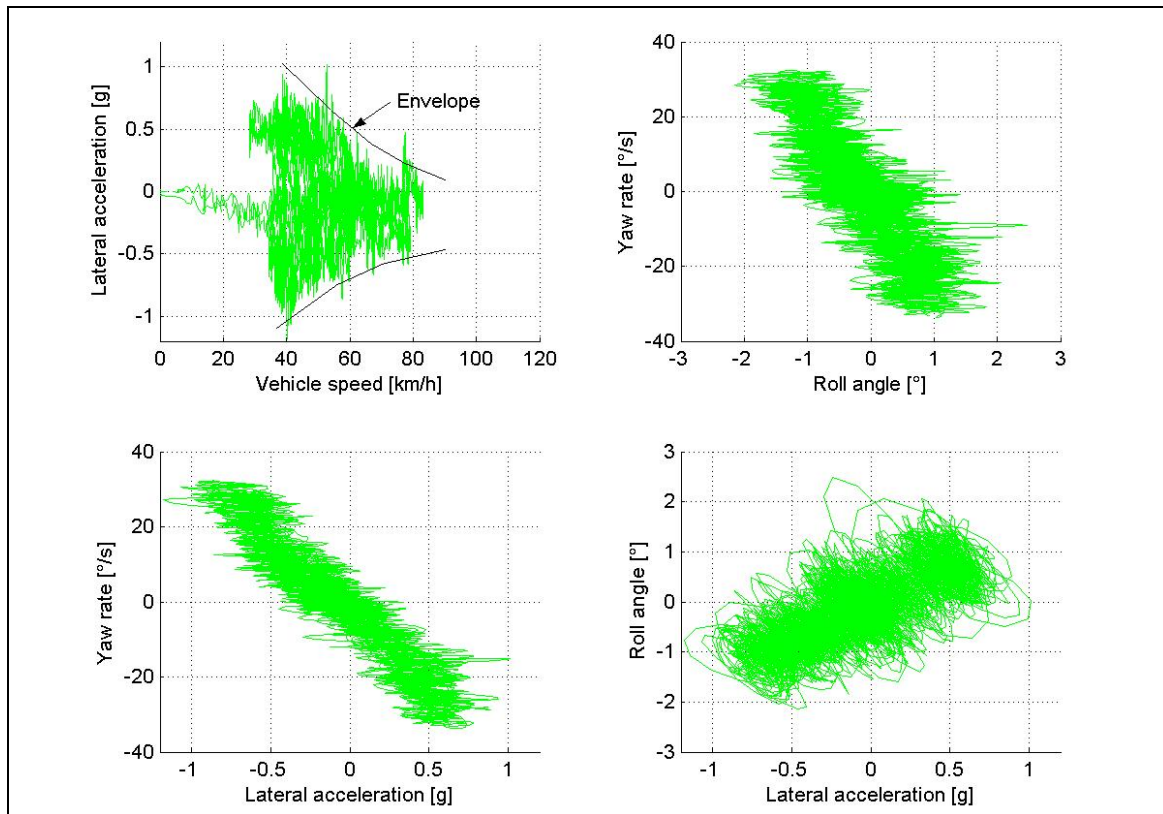


**Figure A-12** - Lateral acceleration, yaw rate and roll angle performance of a VW Golf 4 GTI on a ride and handling track

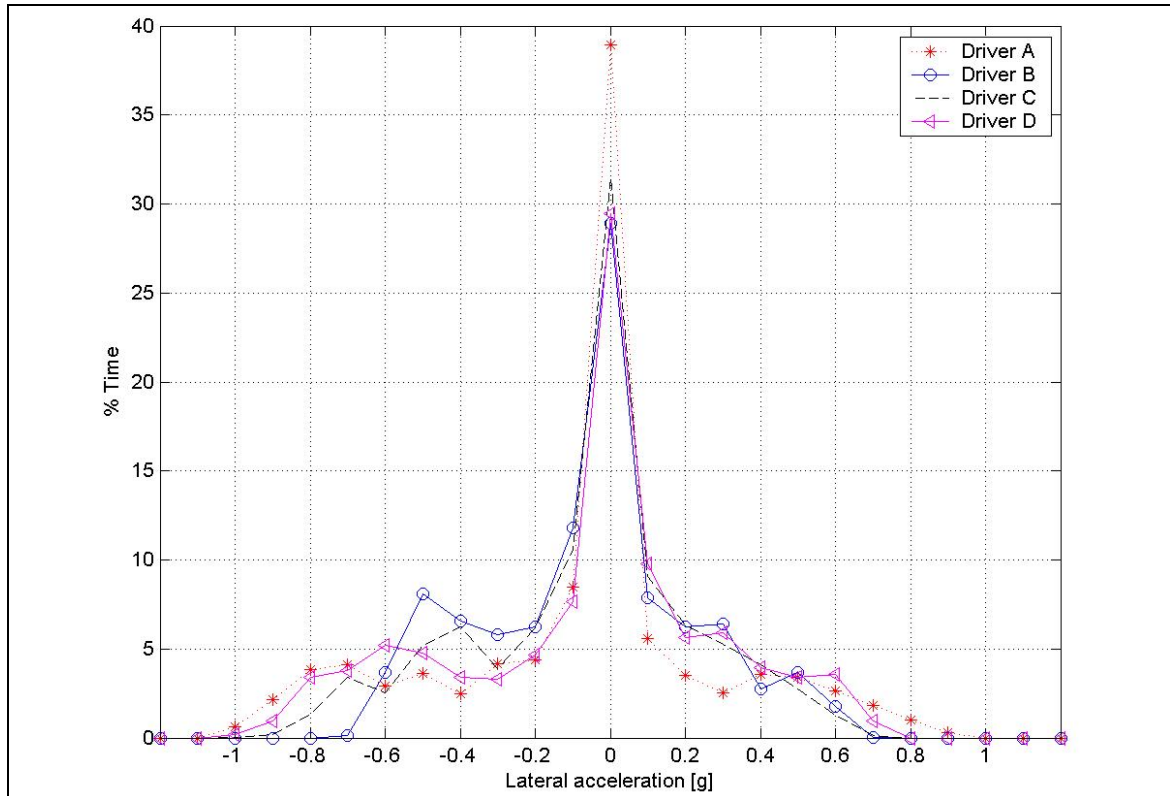


**Figure A-13** - Lateral acceleration histogram for a VW Golf 4 GTI on a dynamic handling track

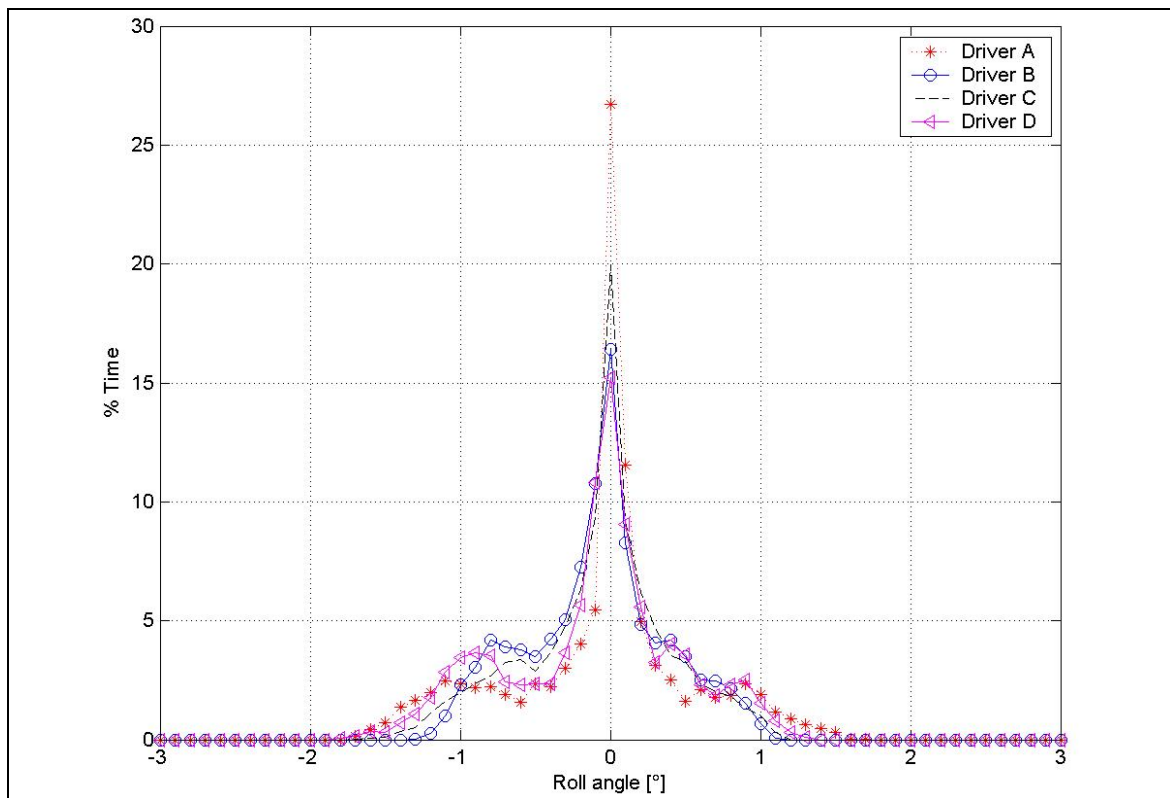


**Figure A-14** - Roll angle histogram for a VW Golf 4 GTI on a dynamic handling track

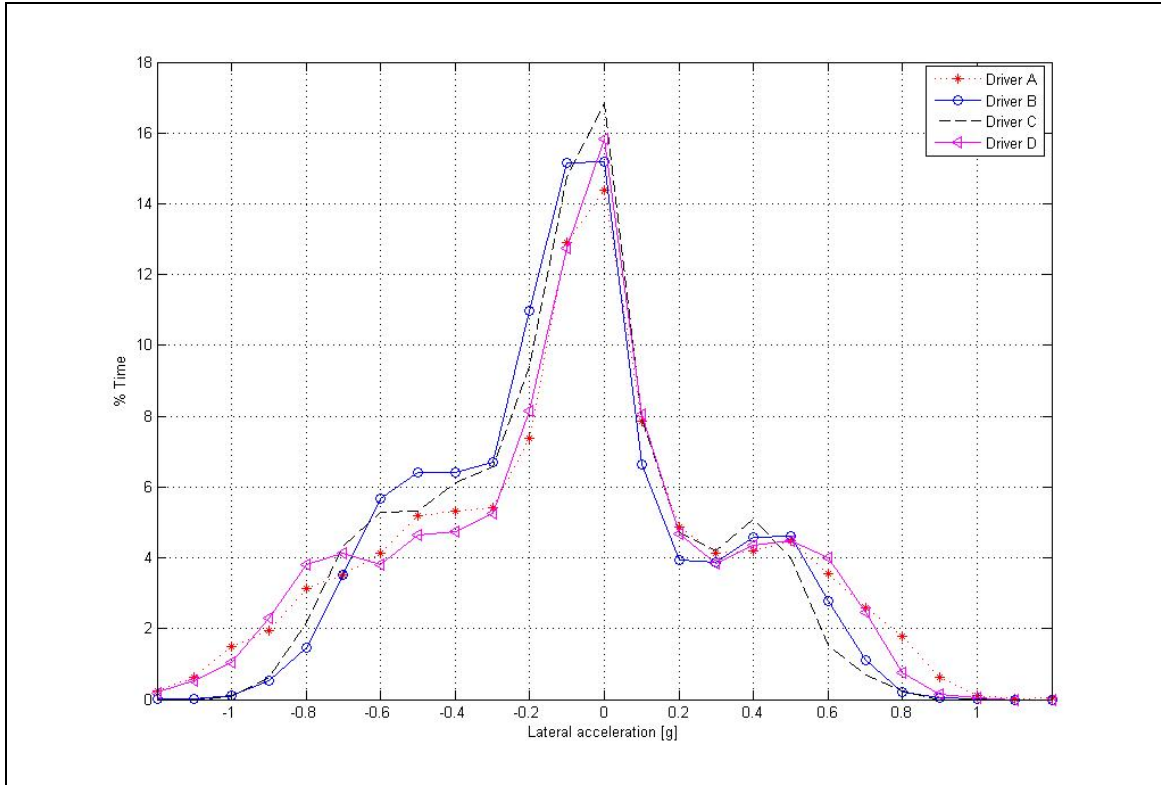


**Figure A-15** - Lateral acceleration histogram for a VW Golf 4 GTI on a ride and handling track

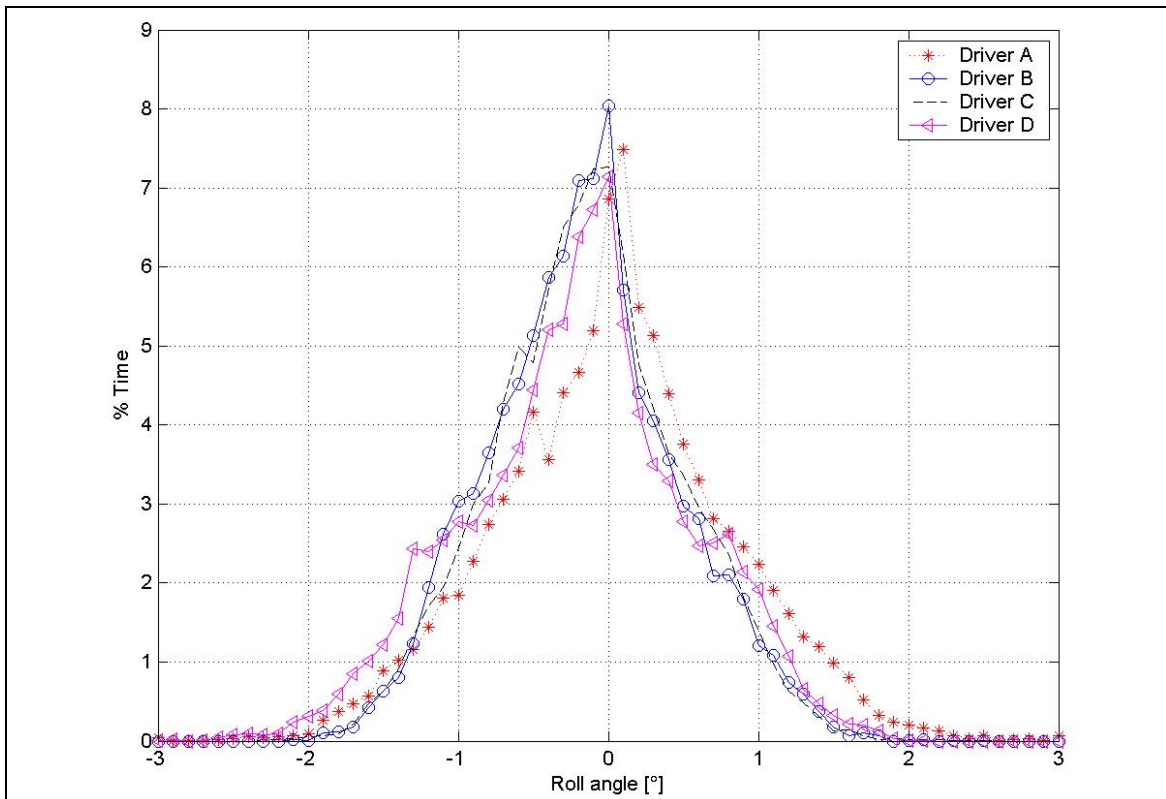


**Figure A-16** - Roll angle histogram for a VW Golf 4 GTI on a ride and handling track

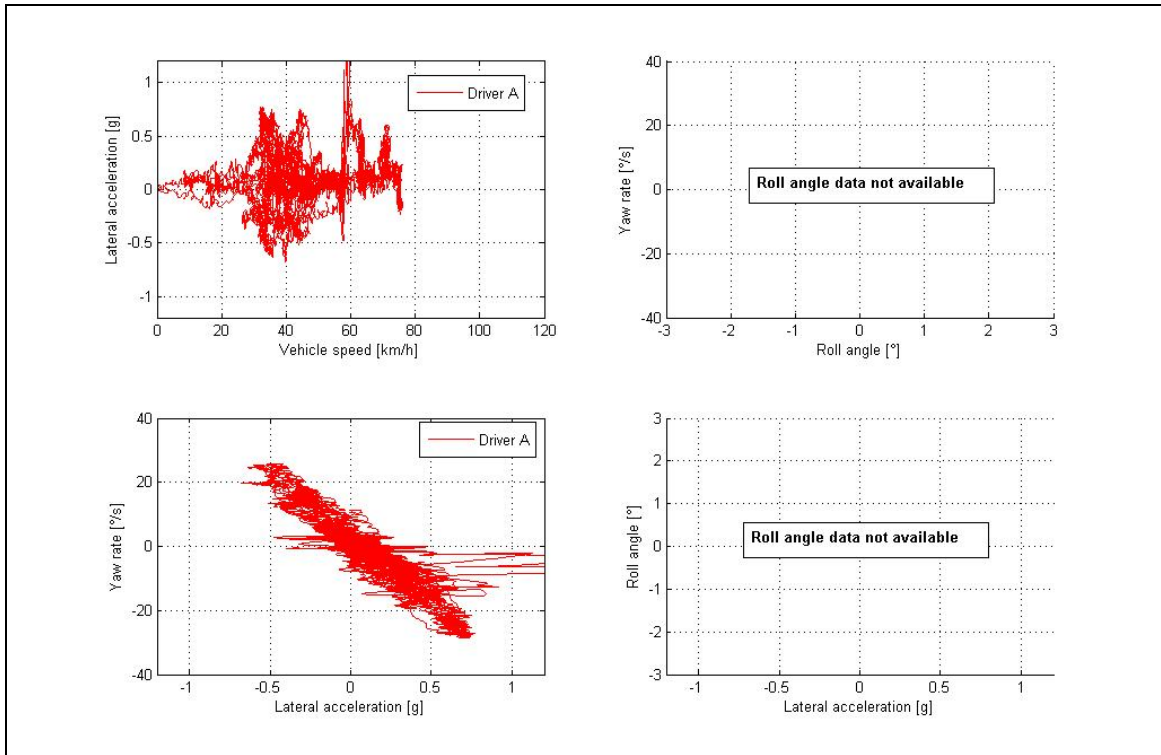


**Figure A-17** - Lateral acceleration and yaw rate performance of a Land Rover Defender 110 on the ride and handling track (roll angle data not available)

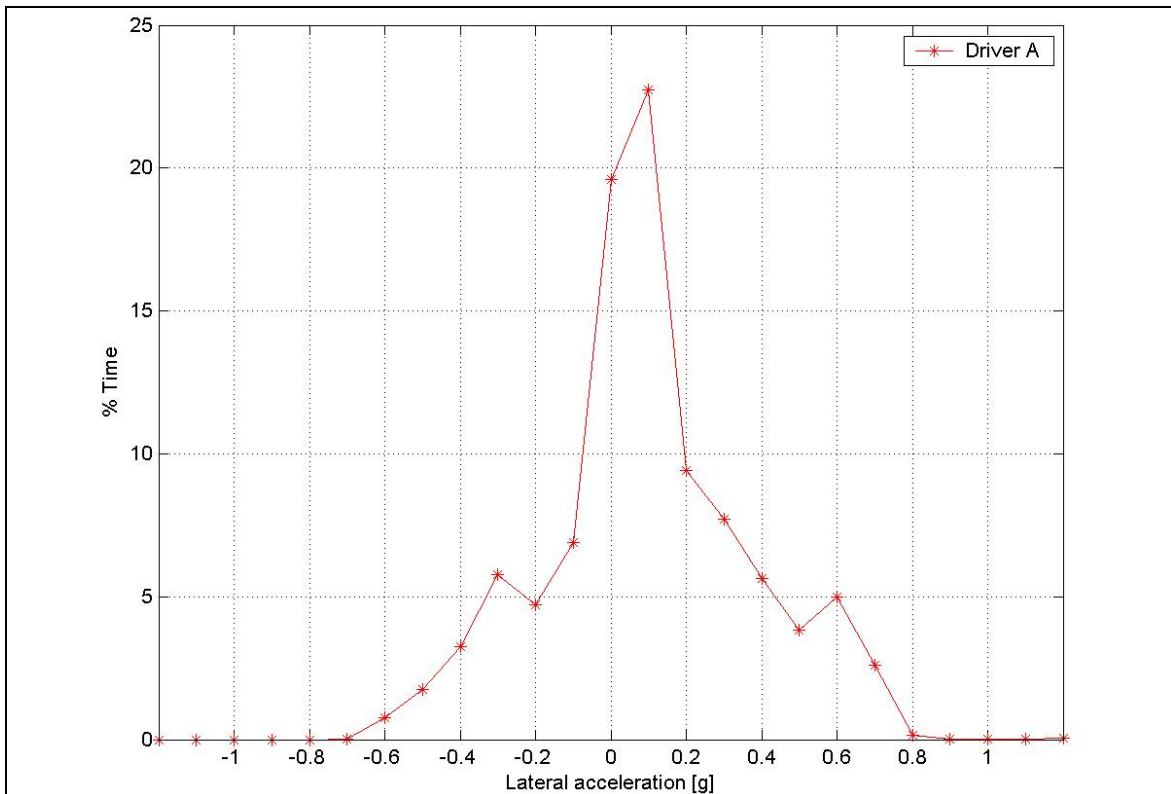


**Figure A-18** – Lateral acceleration histogram for a Land Rover Defender 110 on the ride and handling track